frontiers | Research Topics

Coronavirus: Broad-spectrum anti-viral targets and treatments

Edited by
Jian Shang, Wanbo Tai, Yushun Wan and Yang Yang

Published in
Frontiers in Microbiology

ISSN 1664-8714
ISBN 978-2-8325-2393-3
DOI 10.3389/978-2-8325-2393-3

About Frontiers

Frontiers is more than just an open access publisher of scholarly articles: it is a pioneering approach to the world of academia, radically improving the way scholarly research is managed. The grand vision of Frontiers is a world where all people have an equal opportunity to seek, share and generate knowledge. Frontiers provides immediate and permanent online open access to all its publications, but this alone is not enough to realize our grand goals.

Frontiers journal series

The Frontiers journal series is a multi-tier and interdisciplinary set of open-access, online journals, promising a paradigm shift from the current review, selection and dissemination processes in academic publishing. All Frontiers journals are driven by researchers for researchers; therefore, they constitute a service to the scholarly community. At the same time, the *Frontiers journal series* operates on a revolutionary invention, the tiered publishing system, initially addressing specific communities of scholars, and gradually climbing up to broader public understanding, thus serving the interests of the lay society, too.

Dedication to quality

Each Frontiers article is a landmark of the highest quality, thanks to genuinely collaborative interactions between authors and review editors, who include some of the world's best academicians. Research must be certified by peers before entering a stream of knowledge that may eventually reach the public - and shape society; therefore, Frontiers only applies the most rigorous and unbiased reviews. Frontiers revolutionizes research publishing by freely delivering the most outstanding research, evaluated with no bias from both the academic and social point of view. By applying the most advanced information technologies, Frontiers is catapulting scholarly publishing into a new generation.

What are Frontiers Research Topics?

Frontiers Research Topics are very popular trademarks of the *Frontiers journals series*: they are collections of at least ten articles, all centered on a particular subject. With their unique mix of varied contributions from Original Research to Review Articles, Frontiers Research Topics unify the most influential researchers, the latest key findings and historical advances in a hot research area.

Find out more on how to host your own Frontiers Research Topic or contribute to one as an author by contacting the Frontiers editorial office: frontiersin.org/about/contact

Coronavirus: Broad-spectrum anti-viral targets and treatments

Topic editors

Jian Shang — Zhengzhou University, China
Wanbo Tai — Shenzhen Bay Laboratory, China
Yushun Wan — Chongqing Medical University, China
Yang Yang — Iowa State University, United States

Citation

Shang, J., Tai, W., Wan, Y., Yang, Y., eds. (2023). *Coronavirus: Broad-spectrum anti-viral targets and treatments*. Lausanne: Frontiers Media SA.
doi: 10.3389/978-2-8325-2393-3

Table of contents

frontiers | Frontiers in Microbiology

TYPE Original Research
PUBLISHED 12 August 2022
DOI 10.3389/fmicb.2022.895695

OPEN ACCESS

EDITED BY
Wanbo Tai,
Shenzhen Bay Laboratory,
China

REVIEWED BY
Andrei Lobiuc,
Ștefan cel Mare University of Suceava,
Romania
J. Shawn Goodwin,
Meharry Medical College, United States

*CORRESPONDENCE
Eun-Min Seo
seoem@hallym.or.kr
Chiranjib Chakraborty
drchiranjib@yahoo.com

†These authors have contributed equally to this work

SPECIALTY SECTION
This article was submitted to Virology, a section of the journal Frontiers in Microbiology

RECEIVED 14 March 2022
ACCEPTED 25 July 2022
PUBLISHED 12 August 2022

CITATION
Bhattacharya M, Sharma AR, Mallick B, Lee S-S, Seo E-M and Chakraborty C (2022) B.1.1.7 (Alpha) variant is the most antigenic compared to Wuhan strain, B.1.351, B.1.1.28/triple mutant and B.1.429 variants. *Front. Microbiol.* 13:895695. doi: 10.3389/fmicb.2022.895695

B.1.1.7 (Alpha) variant is the most antigenic compared to Wuhan strain, B.1.351, B.1.1.28/triple mutant and B.1.429 variants

Manojit Bhattacharya[1†], Ashish Ranjan Sharma[2†], Bidyut Mallick[3], Sang-Soo Lee[2], Eun-Min Seo[2*] and Chiranjib Chakraborty[4*†]

[1]Department of Zoology, Fakir Mohan University, Balasore, Odisha, India, [2]Institute for Skeletal Aging and Orthopedic Surgery, Hallym University-Chuncheon Sacred Heart Hospital, Chuncheon, Gangwon-do, South Korea, [3]Department of Applied Science, Galgotias College of Engineering and Technology, Greater Noida, Uttar Pradesh, India, [4]Department of Biotechnology, School of Life Science and Biotechnology, Adamas University, Kolkata, West Bengal, India

The rapid spread of the SARS-CoV-2 virus and its variants has created a catastrophic impact worldwide. Several variants have emerged, including B.1.351 (Beta), B.1.1.28/triple mutant (P.1), B.1.1.7 (Alpha), and B.1.429 (Epsilon). We performed comparative and comprehensive antigenicity mapping of the total S-glycoprotein using the Wuhan strain and the other variants and identified 9-mer, 15-mer, and 20-mer CTL epitopes through *in silico* analysis. The study found that 9-mer CTL epitope regions in the B.1.1.7 variant had the highest antigenicity and an average of the three epitope types. Cluster analysis of the 9-mer CTL epitopes depicted one significant cluster at the 70% level with two nodes (KGFNCYFPL and EGFNCYFPL). The phage-displayed peptides showed mimic 9-mer CTL epitopes with three clusters. CD spectra analysis showed the same band pattern of S-glycoprotein of Wuhan strain and all variants other than B.1.429. The developed 3D model of the superantigen (SAg)-like regions found an interaction pattern with the human TCR, indicating that the SAg-like component might interact with the TCR beta chain. The present study identified another partial SAg-like region (ANQFNSAIGKI) from the S-glycoprotein. Future research should examine the molecular mechanism of antigen processing for $CD8^+$ T cells, especially all the variants' antigens of S-glycoprotein.

KEYWORDS

emerging variants, CTL epitopes, B.1.1.7, antigenicity, cluster, phage-displayed peptides, CD spectra, SAg-like region

Introduction

The COVID-19 has affected the global population, and a surge of the SARS-CoV-2 has been noted in many countries (Chakraborty et al., 2020; Dinesh et al., 2020; Li and Liu, 2020). Due to this COVID-19 wave, high peaks of daily infection and death occurred in these countries. One of the most significant causes of surges in different countries is the

emergence of new variants, developing because of mutations (Brüssow, 2021).

Several significant variants of concern/interest (VOCs/VOIs) of this virus [B.1.351, (Beta), B.1.1.28/triple mutant (P.1), B.1.1.7 (Alpha), and B.1.429 (Epsilon)] have been determined in South Africa, Brazil, United Kingdom, and the United States and have mushroomed to many other countries (Chakraborty et al., 2021a,b; Focosi et al., 2021; Harvey et al., 2021). These newly evolved variants with significant mutations have developed from the original Wuhan strain in different regions worldwide. The ongoing evolution of the SARS-CoV-2 virus is due to the region-wise adaptive changes and multiple mutations during the evolutionary process (Chakraborty et al., 2021c; Rochman et al., 2021). Diverse variants of this virus have developed over time due to the several mutations (Figure 1A). However, four significant variants (B.1.351, B.1.1.28/triple mutant, B.1.1.7, and B.1.429) have been identified in different regions worldwide. All four variants have mutations within the spike (S) protein, which change the attachment site of the virus, human cell entry, and strong binding affinity with VOC/VOI and receptor compared to the Wuhan strain. The UK variant (B.1.1.7) steadily surged in just a few months and is now found in at least 114 countries worldwide (Davies et al., 2021). Several significant mutations have been identified in the B.1.1.7 lineage. One significant mutation (N501Y) was observed in the viral S-glycoprotein of the receptor-binding domain (RBD). Similarly, four mutations were observed in the S1-domain (del144Y, del69–70 HV, D614G, and A570D), and four mutations were noted in the S2 domain (P681H, S982A, T761I, and D1118H) (Li et al., 2021; Meng et al., 2021; Shen et al., 2021). The B.1.351 lineage consists of three significant mutations in the RBD region of the S-glycoprotein. These mutations are noted as K417N, E484K, and N501Y. Five important mutations have been observed in the N-terminal domain: R246I, D215G, L18F, D80A, and a deletion mutation at amino acid positions 242–244. Another mutation (A701V) in the S2 subunit has also been observed (Cele et al., 2021; Wang et al., 2021b). The P.1 (B.1.1.28.1) lineage has three significant mutations (K417T, E484K, and N501Y) in the RBD region of the S-glycoprotein, and eight other significant amino acid changes have been found (D138Y, T20N, L18F, R190S, P26S, T1027I, H655Y, and V1176F). The B.1.429 lineage has four mutations, two mutations (L452R and D614G) reside within the RBD, and two mutations (S13I and W152C) are found in the NTD (N-terminal domain) segment of the S-glycoprotein. These mutational changes exhibit augmented neutralization resistance (Faria et al., 2021; Wang et al., 2021a). The present study has explored the antigenicity of B.1.1.28/triple mutant along with two VOCs (B.1.1.7 and B.1.351). Similarly, several mutations have been noted in the S-glycoprotein of these variants (Naveca et al., 2021).

Abbreviations: SARS-CoV-2, Severe acute respiratory syndrome coronavirus 2; COVID-19, Coronavirus disease 2019; RBD, Receptor-binding domain; S-protein, Spike glycoprotein; CTL, Cytotoxic T lymphocytes; CD, Circular dichroism; TCR, T-cell antigen receptor; VOC, Variants of concern.; VOI, Variants of interest; MSA, Multiple sequence alignment; SAg, Superantigen; RMSD, Root-mean-square deviation; MHC, Major histocompatibility complex; HLA, Human leukocyte antigens; PDB, Protein Data Bank; HMMs, Hidden Markov models.

Antigenicity mapping is a powerful technique for understanding the antigenic properties of any virus and can be analyzed using epitope mapping (Sun et al., 2013; Anderson et al., 2018). Antigenicity mapping can help to understand different characteristics such as antigenic sites and immune escape mechanisms (Peacock et al., 2016). $CD8^+$ T cells epitopes are also called cytotoxic T lymphocytes (CTL) epitopes and are one of the critical determinants for understanding the $CD8^+$ T cell response and antigenic properties (Feliu et al., 2013; Tscharke et al., 2015). Recently, Gangaev et al. (2021) attempted to map the immunodominant and immunogenic epitopes of this virus to illustrate the role of $CD8^+$ T cells in host defense (Gangaev et al., 2021). Understanding CTL epitopes with antigenic properties can assist in vaccine design (Wong et al., 2019; Bhattacharya et al., 2020a,b, 2021). Therefore, CTL epitope mapping plays a vital role in determining the antigenicity of a pathogen. Researchers have examined 9-mer, 15-mer, and 20-mer CTL epitopes to understand the antigenicity of pathogens and designed vaccines against these pathogens (Doi et al., 2009; Bhatnager et al., 2020; Rencilin et al., 2021; Shey et al., 2021). The 9-mer CTL epitopes determine the viral antigenicity (Raza et al., 2021). Several researchers have used 9-mer CTL epitopes to assess the antigenic peptides from S-glycoprotein, and this 9-mer CTL epitope has been used for vaccine development against SARS CoV-2 (Kar et al., 2020; Rencilin et al., 2021).

Epitope clustering strategies might help capture the diversity of pathogens' epitopes and understand highly similar or overlapping sequences. Previous studies have examined CTL epitope clustering for different pathogens (Liu et al., 2010; Rist et al., 2015; Vujovic et al., 2020). In the present study, the epitope clustering method was used to understand the clustering of CTL epitopes of the S-glycoprotein of the Wuhan strain (wild type) and mutant variants of SARS-CoV-2. Circular dichroism (CD) spectra provide information on the molecular structure of proteins at a quantitative level (Micsonai et al., 2015). The CD spectra can also provide information on the molecular structure of a mutant protein (Huai et al., 2021). We analyzed the CD spectra of the Wuhan strain and mutant variants of the S-glycoprotein of this virus.

In patients with severe cases, toxic shock syndrome has been observed, which causes hyperinflammation. Cheng et al. (2020) observed a superantigenic insert, which is a unique S-glycoprotein, in SARS-CoV-2, and concluded that the insert might be responsible for causing hyper inflammation in patients with severe COVID-19 (Cheng et al., 2020). SAgs can excessively activate the immune system. Previous studies have identified SAgs from viruses (Lafon, 2000). A SAg-like region (PRRA) was recently detected in this virus S-glycoprotein of the Wuhan strain (Cheng et al., 2020). We attempted to analyze the superantigenic insert in the Wuhan strain and mutant variants further.

In this study, our objective was to perform a comprehensive *in silico* analysis of the total S-glycoprotein of the Wuhan strain, B.1.351, B.1.1.28/triple mutant, B.1.1.7, and B.1.429 variants to understand the antigenicity using the CTL epitopes or SAg-like region of S-glycoprotein and the interaction between the SAg-like area within the and the T-cell antigen receptor (TCR).

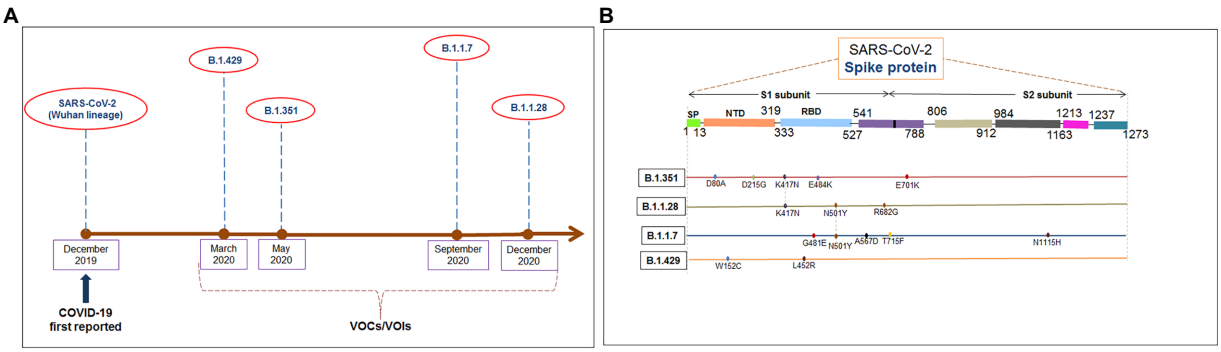

FIGURE 1
The figure depicted the timeline and mutations of newly significant emerging variants and Wuhan strain. **(A)** Timeline showing the origin time of some newly significant emerging variants (B.1.351, B.1.1.28/triple mutant, B.1.1.7, and B.1.429) and Wuhan strain. **(B)** The schematic diagram shows the significant mutations present in the CTL antigenic regions of newly emerging SARS-CoV-2 variants S-protein.

Materials and methods

Data acquisition of the S-glycoprotein of the Wuhan strain and B.1.351, B.1.1.28/ triple mutant, B.1.1.7, and B.1.429 variants

The sequences of amino acids within the S protein of the Wuhan strain and the four significant mutant variants were retrieved from the NCBI/PDB (protein database) in FASTA format. The accession numbers of the Wuhan strain and the B.1.351, B.1.1.28/triple mutant, B.1.1.7, and B.1.429 variants are QHR63290.2, 7LYL_A, 7LWW_A, 7LWV_A, and 7N8H_A, respectively. Similarly, we collected PDB files from the PDB database for the Wuhan strain and the B.1.351, B.1.1.28/triple mutant, B.1.1.7, and B.1.429 variants, 6VXX 7LYL, 7LWW, 7LWV, and 7N8H, respectively. We started our work with the PDB immediately at that time of deposition of the structure for 7LWW. We found that the 7LWW was mentioned as structure S-glycoprotein of the B.1.1.28 in the PDB database.

Afterward, we found that the PDB is mentioned as a triple mutant in some pieces of literature. In this study, we have used both the two parameters ("B.1.1.28" and "triple mutant") at the same time for describing the 7LWW and mentioning it as B.1.1.28/ triple mutant.

Identification of 9-mer, 15-mer, and 20-mer CTL epitopes of total S-glycoprotein and RBD region of S-glycoprotein of the Wuhan strain and the B.1.351, B.1.1.28/triple mutant, B.1.1.7, and B.1.429 variants

We identified the 9-mer, 15-mer, and 20-mer CTL epitopes of S-glycoprotein from the Wuhan strain and all four variants (B.1.351, B.1.1.28/triple mutant, B.1.1.7, and B.1.429) and analyzed their antigenic sequences. To identify any promising MHC-I (Major Histocompatibility Complex class I) binding epitopes, we used ProPred-I, which is an online web server for predicting 9-mer, 15-mer, and 20-mer peptide binding to MHC-I alleles (Singh and Raghava, 2003). Finally, we calculated the average number of epitopes in the five variants.

Antigenicity predictions of the identified epitopes of the S-glycoprotein of the Wuhan strain and the B.1.351, B.1.1.28/triple mutant, B.1.1.7, and B.1.429 variants

In the present study, we employed the VaxiJen server, which uses a unique algorithm comprising an auto cross-covariance-based machine-learning server and an alignment-based prediction process (Doytchinova and Flower, 2007). This server uses a default parameter and threshold to calculate the antigenicity of pathogens. Here, we applied 0.4 as the threshold value for the viral peptide.

Comprehensive and comparative analysis of significant 9-mer CTL epitopic landscape of S-glycoprotein of the Wuhan strain and the B.1.351, B.1.1.28/triple mutant, B.1.1.7, and B.1.429 variants

We performed a comprehensive comparative analysis of the Wuhan strain's significant 9-mer CTL epitopic landscape and significant VOCs/VOI/others. We attempted to determine the different essential mutations present in the 9-mer CTL epitopes in the B.1.351, B.1.1.28/triple mutant, B.1.1.7, and B.1.429 variants. Finally, we hypothesized that the epitopes mutated from the Wuhan strain evolved into different significant VOCs/ VOI/others.

MSA using the identified CTL epitopes (9-mer, 15-mer, and 20-mer) of the S-glycoprotein of the Wuhan strain and B.1.351, B.1.1.28/triple mutant, B.1.1.7, and B.1.429 variants

The 9-mer, 15-mer, and 20-mer CTL epitopes of the S-glycoprotein of the Wuhan strain and the B.1.351, B.1.1.28/triple mutant, B.1.1.7, and B.1.429 variants were used to perform MSA. MSA was used to undertake sequence alignment with Clustal Omega (Sievers and Higgins, 2018, 2021). The tool applied the HHalign technique to align the landscape of HMMs (Hidden Markov models).

Cluster analysis of CTL epitopes (9-mer, 15-mer, and 20-mer) of S-glycoprotein of the Wuhan strain and the B.1.351, B.1.1.28/triple mutant, B.1.1.7, and B.1.429 variants

The clustering of peptides is a well-known problem in biological science. The analysis of the clustering of epitopes informs us of the epitope homology. It also helps us to generate a precise consensus sequence, which is essential to understanding a group of sequences sharing a defined level of identity. We performed cluster analysis at the different threshold levels (10 to 80%).

The clustering tool resolves the similarity between peptide sequences in separate and specific clusters. It is also ideal for analyzing sequences that may cluster together, even though they are derived explicitly from distinct antigenic sequences. It also specifies and identifies regions of homology between unrelated peptide sequences linked with several critical biological phenomena (allergen cross-reactivity, molecular mimicry, modulation of adaptive immune responses). Researchers also identified the epitopes in a large-scale screen of overlapping peptides that frequently share substantial sequence similarities, usually complicating the analysis of epitope-related data (Stufano et al., 2010). Therefore, clustering algorithms are often used to simplify these analyses. However, existing approaches are commonly inadequate in their capacity to define the biologically meaningful epitope clusters in the advanced framework of the immune response. Therefore, this algorithm-based IEDB epitope cluster analysis tool is applied to generate epitope clusters based on consensus or representative sequences (Vita et al., 2015). This specialized tool also allows the researchers to cluster the target peptide sequences based on a specified level of identity by selecting among changed method options (Dhanda et al., 2018). From a computational standpoint and advanced phase of immunoinformatics, the clustering tool is flexible enough to consider diverse strategies to address different immunological queries using B cell and T cell epitopes (Vivona et al., 2008).

We performed cluster analysis of the CTL epitopes (9-mer, 15-mer, and 20-mer) of S-glycoprotein of the Wuhan strain and the B.1.351, B.1.1.28/triple mutant, B.1.1.7, and B.1.429 variants. We used the IEDB epitope cluster analysis tool (Zhang et al., 2008; Dhanda et al., 2018). This tool graph visualizes the generated network using Python networks.

Exploration of the CD spectra and different components of the secondary structure of S-glycoprotein of the Wuhan strain and the B.1.351, B.1.1.28/triple mutant, B.1.1.7, and B.1.429 variants

CD spectroscopy is a significant parameter for understanding the protein structure. A CD spectrum is an essential component that can help rapidly determine the secondary structure of proteins (Greenfield, 2006). We can understand different secondary structure elements using the CD spectra *via* MD simulations (Rogers et al., 2019; Drew and Janes, 2020). The PDBMD2CD is a server that can generate CD spectra using PDB files. Using this server, we analyzed the CD spectra of the S-glycoprotein of the Wuhan strain and significant VOCs/VOIs (Drew and Janes, 2020). The analysis illustrated information on the wavelength of the CD signal. The server produces a result with an RMSD smaller or equivalent to 0.5, the utmost away from the investigational spectrum. We used this server to analyze the secondary structural features such as the helix, antiparallel sheet, parallel sheet, and turn of the S-glycoprotein of the Wuhan strain and the B.1.351, B.1.1.28/triple mutant, B.1.1.7, and B.1.429 variants.

Tertiary or 3D model generation of the 9-mer CTL epitopic regions

We developed the tertiary structure of 9-mer CTL epitopes from the S-glycoprotein of the Wuhan strain and significant VOCs/VOIs/others using the DISTILL 2.0 server (Baú et al., 2006). This tool adopts an algorithm based on recursive neural network architectures. The algorithm can predict through a specific architecture of a neural network (single-or dual-layer) and directs an acyclic graph (Li et al., 2019). Different epitopes were marked in the tertiary structure, generated from the PDB file. The 3D structure of the PDB was developed using chimera visualization software (Pettersen et al., 2004).

Phage-displayed peptides that mimic SARS-CoV-2 9-mer CTL epitopic peptides

A peptide library for phage-displayed was applied for epitope mapping (Wu et al., 2016). We analyzed the SARS-CoV-2 9-mer CTL epitopic peptides that mimic phage-displayed peptides' epitopes. We used a routine technique to map the location of the epitope using a phage-display library. We used the Pepitope server to perform this analysis, which applied the PepSurf algorithm. This algorithm is based on a specific amino acid similarity matrix (Mayrose et al., 2007).

Identification of the SAg-like region from the S-glycoprotein of SARS-CoV-2 of the Wuhan strain and B.1.351, B.1.1.28/triple mutant, B.1.1.7, and B.1.429 variants, and their tertiary or 3D model generation

We have identified the SAg-like region from the S-glycoprotein of SARS-CoV-2 of the Wuhan strain and B.1.351, B.1.1.28/triple mutant, B.1.1.7, and B.1.429 variants. We developed a 3D structure model using the same SAg-like region from the S-glycoprotein of Wuhan strain and the B.1.351, B.1.1.28/triple mutant, B.1.1.7, and B.1.429 variants using the DISTILL 2.0 server (Baú et al., 2006).

Interaction between SAg-like part of S-glycoprotein of SARS-CoV-2 and TCR

A 3D structural model of the SAg-like region of the S-glycoprotein of this virus and TCR interaction was illustrated with the HADDOCK server (PDB ID: 4WW1; De Vries et al., 2010), which was used for protein–protein docking. The docking analysis was further validated using the ClusPro server (Kozakov et al., 2017).

Identification of the partial SAg-like part of this virus S-glycoprotein of the Wuhan strain and the B.1.351, B.1.1.28/triple mutant, B.1.1.7, and B.1.429 variants

The SAgs used in the present study were: α-cobra toxin (*Naja naja*), α-bungarotoxin, rabies virus G protein (189–199), α-cobra toxin (*Naja kaouthia*), and HIV-1 gp120 (164–174). We utilized the entire sequence of the S-glycoprotein of the Wuhan strain and B.1.351, B.1.1.28/triple mutant, B.1.1.7, and B.1.429 variants during the present study. We found another SAg-like part from the S-glycoprotein of the Wuhan strain and B.1.351, B.1.1.28/triple mutant, B.1.1.7, and B.1.429 variants. The peptide sequence of the SAg-like part of all these SARS-CoV-2 virus sequences (both wild and mutant type) was used for cluster formation.

Finally, we have depicted a flowchart of the materials and methods to provide a bird's eye view of the current study (Figure 2).

Results

Total number of CTL epitopes (9-mer, 15-mer, and 20-mer) in the S-glycoprotein of the Wuhan strain and B.1.351, B.1.1.28/triple mutant, B.1.1.7, and B.1.429 variants

We identified 9-mer, 15-mer, and 20-mer CTL epitopes in the S-glycoprotein of the Wuhan strain and B.1.351, B.1.1.28/triple mutant, B.1.1.7, and B.1.429 variants. We found that B.1.1.7 contained a maximum number of 9-mer CTL epitopes (approximately six), whereas the B.1.429 variant had a minimum number of 9-mer CTL epitopes (approximately three; Figure 3A). We noted a maximum number of 15-mer CTL epitopes in the S-glycoprotein in B.1.1.7 and B.1.351 (approximately five), whereas the Wuhan strain and B.1.1.28/triple mutant variant contained a minimum number of 15-mer CTL epitopes in the S-glycoprotein (approximately three; Figure 3A; Supplementary Table S1). However, the 20-mer CTL epitopes in the S-glycoprotein showed slightly different results. We found a maximum number of 20-mer CTL epitopes in the S-glycoprotein in B.1.351 (approximately four). In contrast, the Wuhan strain and the B.1.1.28/triple mutant, B.1.1.7, and B.1.429 variants contained a minimum number of 20-mer CTL epitopes in the S-glycoprotein (approximately three; Figure 3A; Supplementary Table S2). Calculating the average number of epitopes found that the average number of epitopes was the same in B.1.1.7 and B.1.351 (Figure 3A).

Total number of CTL epitopes (9-mer, 15-mer, and 20-mer) in the RBD region of S-glycoprotein of the Wuhan strain and the B.1.351, B.1.1.28/triple mutant, B.1.1.7, and B.1.429 variants

We identified 9-mer, 15-mer, and 20-mer CTL epitopes in the RBD region of the S-glycoprotein of the Wuhan strain and the B.1.351, B.1.1.28/triple mutant, B.1.1.7, and B.1.429 variants. We found that the B.1.1.7, B.1.351, and B.1.1.28/triple mutant variants contained a maximum number of 9-mer CTL epitopes (approximately two). In contrast, the Wuhan strain and B.1.429 variant had a minimum number of 9-mer CTL epitopes (approximately one; Figure 3B).

We noted a maximum number of 15-mer CTL epitopes in the RBD region of the S-glycoprotein in the B.1.1.7 variant (approximately two). In contrast, the Wuhan strain and B.1.351, B.1.1.28/triple mutant, and B.1.429 variants contained no 15-mer CTL epitopes (Figure 3B).

However, the 20-mer CTL epitopes in the RBD region showed slightly different results. We found one 20-mer CTL epitope in the RBD region in B.1.351 and B.1.1.7. The other two variants (Wuhan strain and the B.1.1.28/triple mutant) contained no 20-mer CTL epitopes in the RBD region of this virus (Figure 3B).

By calculating the average number of epitopes in the RBD region, we found that highest average number of epitopes was contained in the B.1.1.7 variant (Figure 3A).

Comprehensive analysis of significant 9-mer CTL epitopic landscape of S-glycoprotein of the Wuhan strain and the B.1.351, B.1.1.28/triple mutant, B.1.1.7, and B.1.429 variants

We performed comparative antigenicity mapping of the S-glycoprotein on the Wuhan strain and B.1.351, B.1.1.28/triple

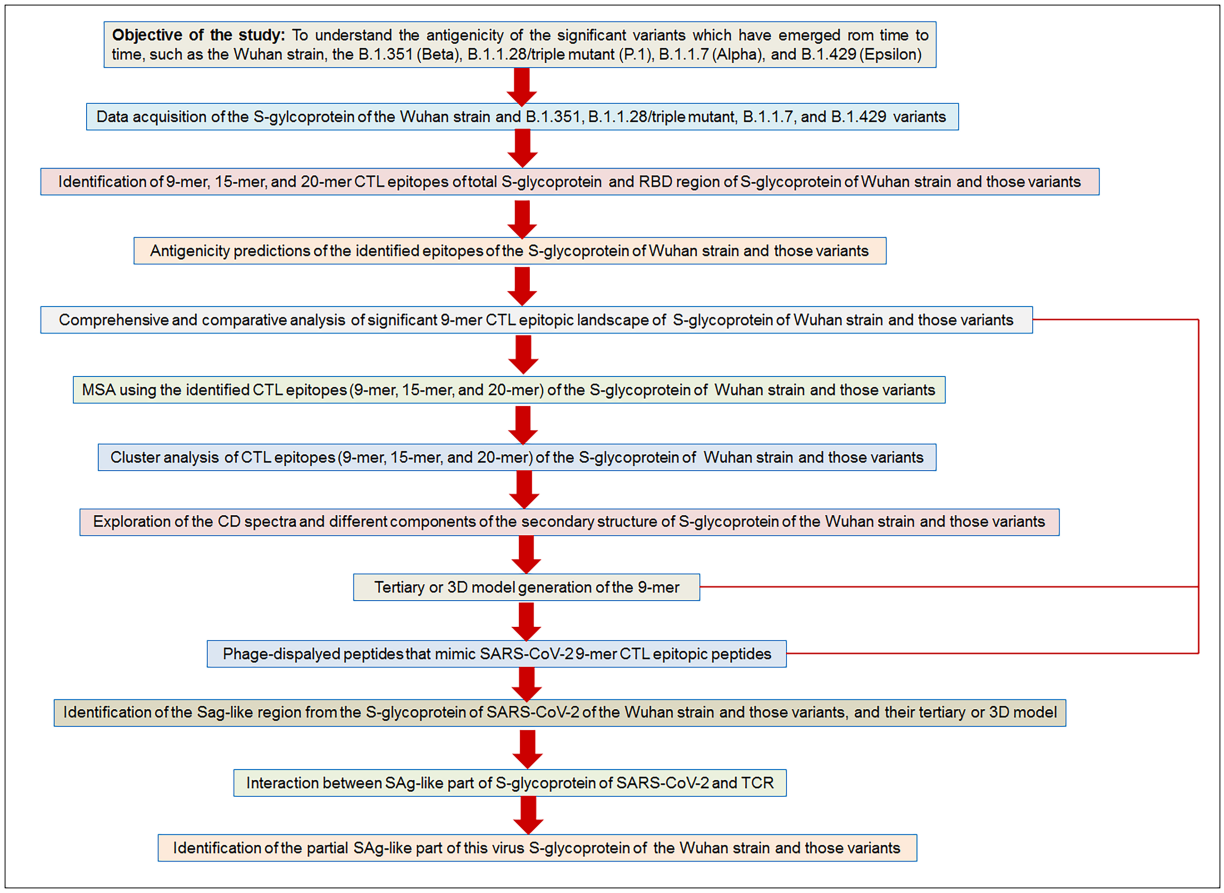

FIGURE 2
The flow diagram illustrates our used methodologies to test the objective of the study hypothesis. Our aim/objective of this research is to understand the antigenicity of the significant variants which have emerged from time to time, such as the Wuhan strain, the B.1.351 (Beta), B.1.1.28/triple mutant (P.1), B.1.1.7 (Alpha), and B.1.429 (Epsilon).

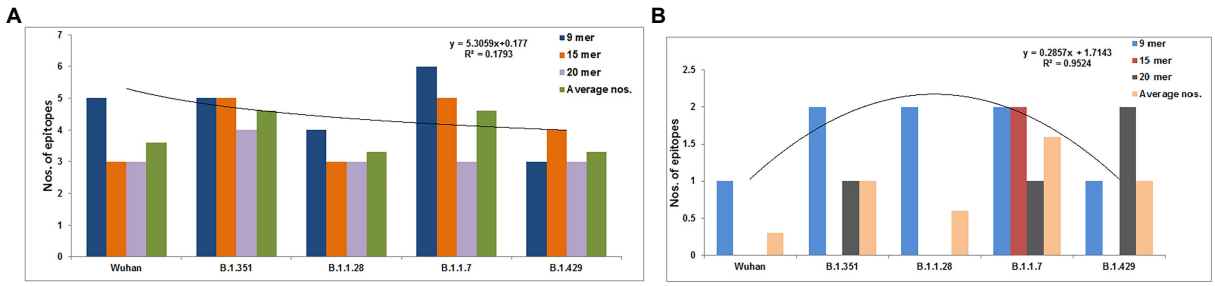

FIGURE 3
Comparison of the number of the 9 mer, 15 mer, 20 mer CTL antigenic epitopes of total S-glycoprotein and RBD region of S-glycoprotein of Wuhan strain and B.1.351, B.1.1.28/triple mutant, B.1.1.7, and B.1.429 variant. **(A)** Comparison of the number of the 9 mer, 15 mer, 20 mer, and an average number of CTL antigenic epitopes of total S-glycoprotein. **(B)** Comparison of the number of 9 mer, 15 mer, 20 mer, and the average number of CTL antigenic epitopes of RBD region of S-glycoprotein. We develop the polynomial (order 2) relationships for the two graphs (**A**; R^2 = 0.1793 and **B**; R^2 = 0.9524).

mutant, B.1.1.7, and B.1.429 variants, with 23 epitopes identified. Four epitopes were non-antigenic based on their VaxiJen score (> 0.4). The significant mutations in the variants containing the 9-mer epitope played a crucial role in viral antigenicity (Figure 1B). Five 9-mer antigenic CTL epitopes were identified from the S-glycoprotein of the Wuhan strain. Similarly, the

S-glycoprotein of B.1.351 contained five 9-mer CTL antigenic epitopes covering the mutagenic regions. Among these five epitopes, three were highly antigenic, as predicted by the VaxiJen server. The S-glycoprotein of the B.1.1.28/triple mutant variant contained four 9-mer CTL antigenic epitopes. We found the highest number of 9-mer CTL antigenic epitopes in the B.1.1.7 variant (approximately six), with all six antigenic epitopes showing a significant VaxiJen score (highest score = 1.5485 and lowest score = 0.4551). We found the lowest number of 9-mer CTL antigenic epitopes in B.1.429 (approximately three), with all showing a significant to mild antigen-related VaxiJen score (highest score = 0.4587 and lowest score = 0.6465; Figure 3A).

We performed a comparative assessment and characterization of the 9-mer CTL antigenic epitopes in the S-glycoprotein chain of the Wuhan strain and the B.1.351, B.1.1.28/triple mutant, B.1.1.7, and B.1.429 variants (Table 1). However, during the comparative assessment and characterization, we found that some of the 9-mer CTL antigenic epitopes of the Wuhan strain were also found in particular parts of the S-glycoprotein in the other four variants.

Our study observed that the Wuhan strain contained five 9-mer CTL epitopes. One epitope with residue positions 1,060–1,068 showed the highest antigenic score (1.5122; Figure 4A). Similarly, the B.1.351 variant showed five significant mutation 9-mer CTL epitopes. The 9-mer CTL epitope with residue positions 417–425 showed the highest antigenic score (1.5325) and contained the K417N mutation (Figure 4B). This mutation might play a crucial role in providing the highest antigenicity for this particular epitope.

We found four 9-mer CTL epitopes in B.1.1.28/triple mutant. Among the epitopes, the highest antigenic score was 1.5476 in the 9-mer CTL epitope, where no mutations were observed (Figure 4C). The other three epitopes had significant mutations. The second 9-mer CTL epitope (epitopic residue positions 680–688) contained the R682G mutation, and the third epitope (epitopic residue positions 497–505) contained the N501Y mutation. The last one (epitopic residue positions 417–425) had a K417N mutation.

The B.1.1.7 variant contained six 9-mer CTL epitopes. The epitope with residue positions 497–505 showed the highest antigenicity (antigenic score 1.5485). This CTL epitope contained the N501Y mutation (Figure 4D), which might substantially provide the antigenicity for this CTL epitope. Other epitopes included different mutations [G481E (epitopic residue positions 481–489), A567D (epitopic residue positions 564–572), T715F (epitopic residue positions 715–723), and N1115H (epitopic residue positions 1,111–1,119)].

The 9-mer CTL epitopes analysis found that the B.1.429 variant contained one significant antigenic CTL epitope (antigenic score 0.4587). This epitope, with residue positions 152–160, consisted of a substantial mutation (W152C). In this variant, we also found two non-antigenic epitopes: the first one with residue positions 452–460 (antigenic score−0.6465) and the second one with residue positions 132–149 (antigenic

TABLE 1 Identification and comparative analysis of 9 mer CTL epitopes of Wuhan strain and B.1.351, B.1.1.28/triple mutant, B.1.1.7, B.1.429 variant.

Variants name	Epitopes	Epitopes position		VaxiJen score
		S-protein domain	S-protein chain	
B.1.351	FANPVLPFN	NTD	79–87	0.2328 (Non-antigen)
	GLPQGFSAL	NTD	215–223	0.1868 (Non-antigen)
	NIADYNYKL	RBD	417–425	1.5325 (Antigenic)
	KGFNCYFPL	RBD	484–492	0.5711 (Antigenic)
	VENSVAYSN	SD2	701–709	0.4171 (Antigenic)
B.1.1.28/ triple mutant	SQCVNLTTR	NTD	13–21	1.5476 (Antigenic)
	SPGSASSVA	SD1	680–688	0.4280 (Antigenic)
	FQPTYGVGY	RBD	497–505	0.4935 (Antigenic)
	NIADYNYKL	RBD	417–425	1.0536 (Antigenic)
B.1.1.7	EILDITPCS	SD1	583–591	0.4935 (Antigenic)
	FQPTYGVGY	RBD	497–505	1.5485 (Antigenic)
	EGFNCYFPL	RBD	481–489	0.5453 (Antigenic)
	RDIDDTTDA	SD1	564–572	0.7902 (Antigenic)
	FTISVTTEI	SD2	715–723	0.8535 (Antigenic)
	IITTHNTFV	CD	1,111–1,119	0.4551 (Antigenic)
B.1.429	CMESEFRVY	NTD	152–160	0.4587 (Antigenic)
	RYRLFRKSN	RBD	452–460	−0.6465 (Non-antigen)
	FQFCNDPFL	NTD	132–140	−0.2493 (Non-antigen)
Wuhan	VVFLHVTYV	HR2	1,060–1,068	1.5122 (Antigenic)
	GKQGNFKNL	NTD	181–189	1.0607 (Antigenic)
	GIYQTSNFR	NTD	311–319	0.5380 (Antigenic)
	VSPTKLNDL	RBD	382–390	1.4610 (Antigenic)
	FKNHTSPDV	CD	1,156–1,164	0.4846 (Antigenic)

score−0.2493; Figure 4E). The CTL epitope with residue positions 452–460 contained the L452R mutation, which might help generate a negative score for the epitope. Therefore, in this variant, antigenicity loss was noted in the 9-mer CTL epitopes.

Comparative mapping of significant 9-mer CTL epitope of the S-glycoprotein of the Wuhan strain and the B.1.351, B.1.1.28/triple mutant, B.1.1.7, and B.1.429 variants

Comparative sequence homology analysis of the 9-mer CTL epitopes using S-glycoprotein from the Wuhan strain and B.1.351, B.1.1.28/triple mutant, B.1.1.7, and B.1.429 variants showed some epitopic homology among significant VOCs/VOI/others. Sequence homology was observed between the epitopic regions of the S-glycoprotein in the two variants such as B.1.351 and B.1.1.7. We found epitopic homology between the 481–489 residues in epitopic part of the B.1.1.7 variant and the 484–492 residues in epitopic part of the B.1.351 variant. Similarly, we also found high sequence homology between the 497–505 epitopic part of the B.1.1.7 variant and 497–505 residues in epitopic part of the B.1.1.28/triple mutant variant. A substantial epitopic homology was observed between the 417–525 epitopic region of the B.1.351 variant and the 417–525 epitopic part of the B.1.1.28/triple mutant variant (Figure 5A). The evolutionary process is attributed to creating the epitopic homology of variants, which determines their antigenicity. However, epitopic homology was not observed in the Wuhan strain and B.1.429 variant (Figure 5B).

MSA using the identified CTL epitopes (9-mer, 15-mer, and 20-mer) of S-glycoprotein of the Wuhan strain and B.1.351, B.1.1.28/triple mutant, B.1.1.7, and B.1.429 variants

Sequence alignment of 9-mer, 15-mer, and 20-mer CTL epitopes of the S-glycoprotein of the Wuhan strain and B.1.351, B.1.1.28/triple mutant, B.1.1.7, and B.1.429 variants were examined. The 9-mer CTL epitopes showed four blocks (Figure 6A), whereas the 15-mer CTL epitopes showed two blocks (Figure 6B) and the 20-mer CTL epitopes showed one block (Figure 6C).

Cluster analysis of 9-mer CTL epitopes of S-glycoprotein of the Wuhan strain and B.1.351, B.1.1.28/triple mutant, B.1.1.7, and B.1.429 variants

We performed a cluster analysis of the 9-mer CTL epitopes of the S-glycoprotein of the Wuhan strain and B.1.351, B.1.1.28/triple mutant, B.1.1.7, and B.1.429 variants at different threshold levels (10 to 80% level). We used 23 of the 9-mer CTL epitopes for cluster formation. We found that one dense cluster was formed at the 10% level (Figure 7A), which had a circular shape, and approximately 23 nodes were visible.

We found that three clusters formed at the 20% level, containing one, seven, and 13 nodes (Figure 7B). We observed five prominent cluster formations at the 30% level, which had two, three, three, three, and four nodes (Figure 7C). We found one significant cluster at the 40% level that contained two nodes (Figure 7D), with the other nodes individually scattered. We found one crucial cluster creation at the 50% level, including two nodes (Figure 7E), and the other nodes were individually scattered. We observed one significant cluster at the 60% level, containing two nodes, with the other nodes individually scattered (Figure 7F). We evaluated the cluster formation at the 70% level, which showed one significant cluster, containing two nodes and several nodes individually scattered (Figure 7G). Finally, we evaluated the cluster formation at the 80% level, which showed one significant cluster containing two nodes and several nodes positioned in a scattered manner (Figure 7H).

Cluster analysis of 15-mer CTL epitopes of the Wuhan strain and B.1.351, B.1.1.28/triple mutant, B.1.1.7, and B.1.429 variants

We performed a cluster analysis of the 15-mer CTL epitopes of the S-glycoprotein of the Wuhan strain and B.1.351, B.1.1.28/triple mutant, B.1.1.7, and B.1.429 variants at different threshold levels (10 to 80% level). We examined 19 numbers of the 15-mer CTL epitopes for cluster formation. We found a dense cluster formation at the 10% level, with a circular shape, and approximately 16 nodes were visible (Supplementary Figure S1A).

We found one significant cluster at the 20% level, containing 15 nodes, and observed another single cluster with one node (Supplementary Figure S1B). We found three prominent clusters at the 30% level, containing three, three, and four nodes (Supplementary Figure S1C). We found four significant clusters at the 40% level, having three, three, three, and two, and the other nodes were individually scattered (Supplementary Figure S1D). At the 50% level, we identified four critical clusters containing three, three, two, and two nodes and several nodes individually scattered (Supplementary Figure S1E). We observed four major clusters at the 60% level, containing two, two, three, and three nodes and several other nodes were independently scattered (Supplementary Figure S1F). We evaluated the cluster formation at the 70% level, which showed four significant clusters containing three, two, two, and two nodes, and several nodes individually scattered (Supplementary Figure S1G). Finally, we evaluated the cluster formation at the 80% level, which showed four significant clusters, containing two, two, two, and three nodes, and numerous nodes separately situated in a scattered manner (Supplementary Figure S1H).

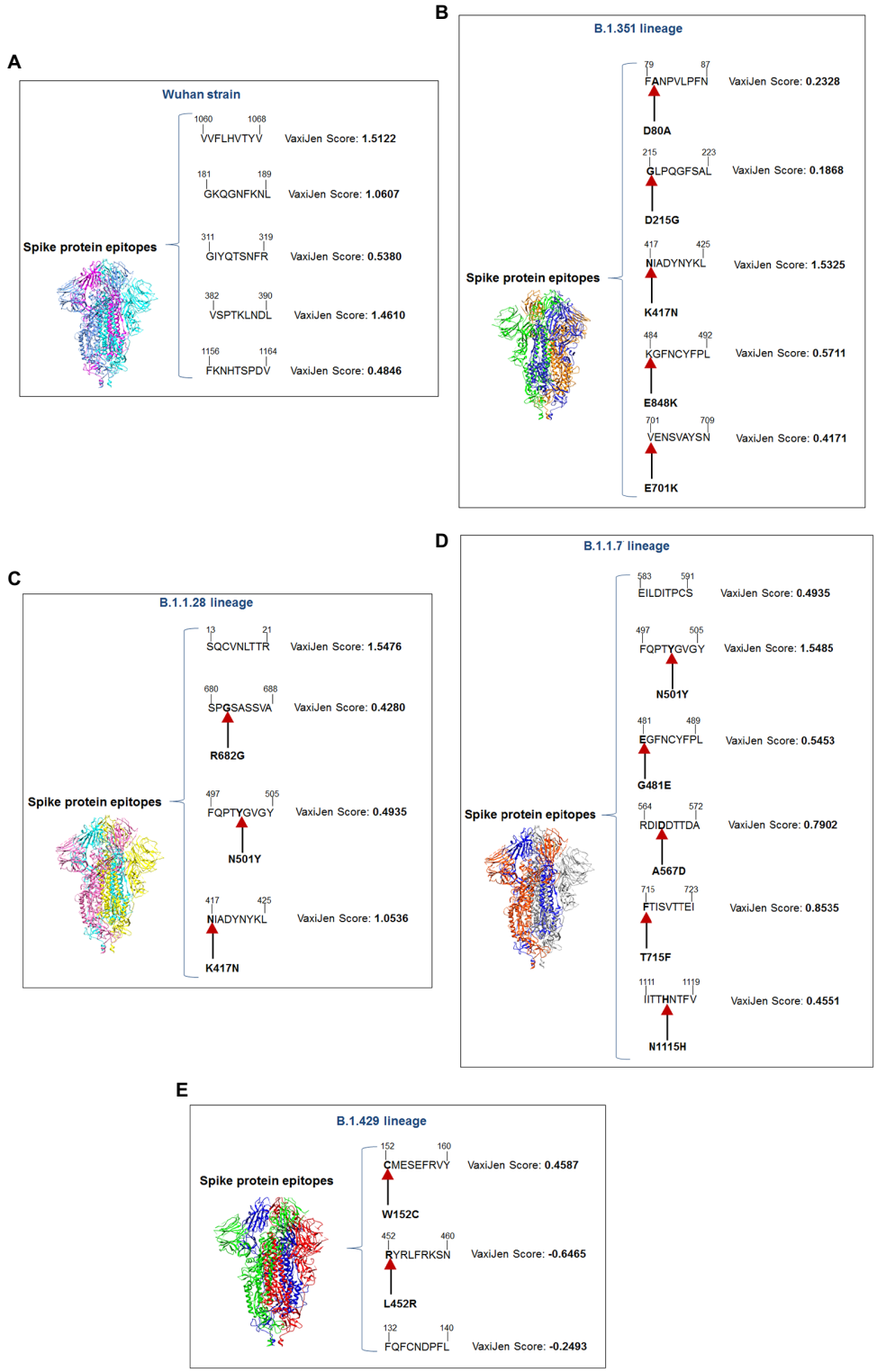

FIGURE 4
A schematic diagram of significant 9 mer CTL epitopic landscape of S-glycoprotein of Wuhan strain and B.1.351, B.1.1.28/triple mutant, B.1.1.7, and B.1.429 variant. The figure also shows the significant mutations present in the 9 mer CTL epitopic regions. **(A)** A schematic diagram of 9 mer CTL antigenic epitopes identified of S-glycoprotein in Wuhan strain. **(B)** A schematic diagram of 9 mer CTL antigenic epitopes recognized of S-glycoprotein in the B.1.351 variant with significant mutations in the epitopic regions. **(C)** A schematic diagram of 9 mer CTL antigenic epitopes identified of S-glycoprotein in B.1.1.28/triple mutant variant with substantial mutations in the epitopic areas. **(D)** A schematic diagram of 9 mer CTL antigenic epitopes recognized of S-glycoprotein in B.1.1.7 variant with significant mutations in the epitopic regions. **(E)** A schematic diagram of 9 mer CTL antigenic epitopes identified of S-glycoprotein in B.1.429 variant with substantial mutations in the epitopic regions.

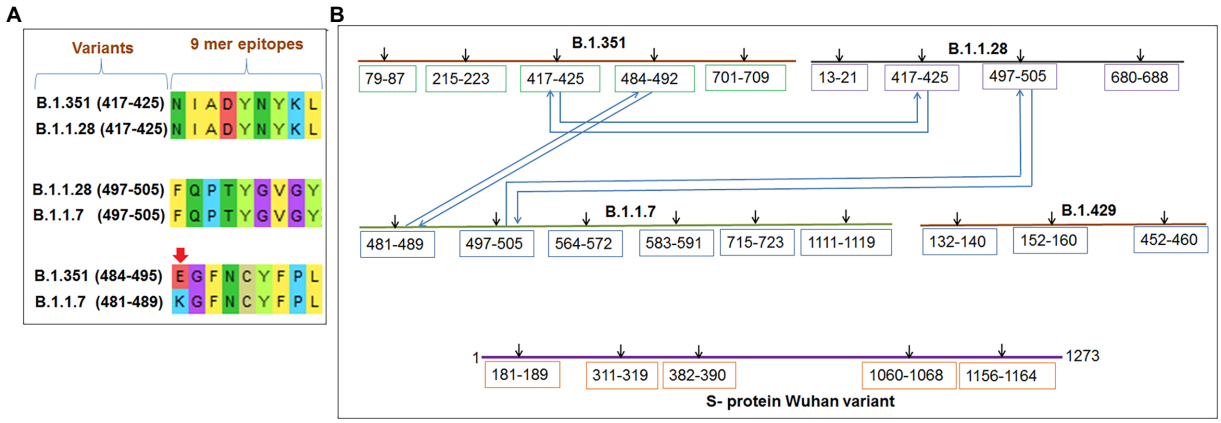

FIGURE 5
Comparative mapping of significant 9 mer CTL epitope of S-glycoprotein of Wuhan strain and B.1.351, B.1.1.28/triple mutant, B.1.1.7, and B.1.429 variant. **(A)** Epitopes homology of Wuhan strain and B.1.351, B.1.1.28/triple mutant, B.1.1.7, and B.1.429 variant. **(B)** A schematic diagram shows the similarity between the epitopes among B.1.351, B.1.1.28/triple mutant, B.1.1.7, and B.1.429 variant.

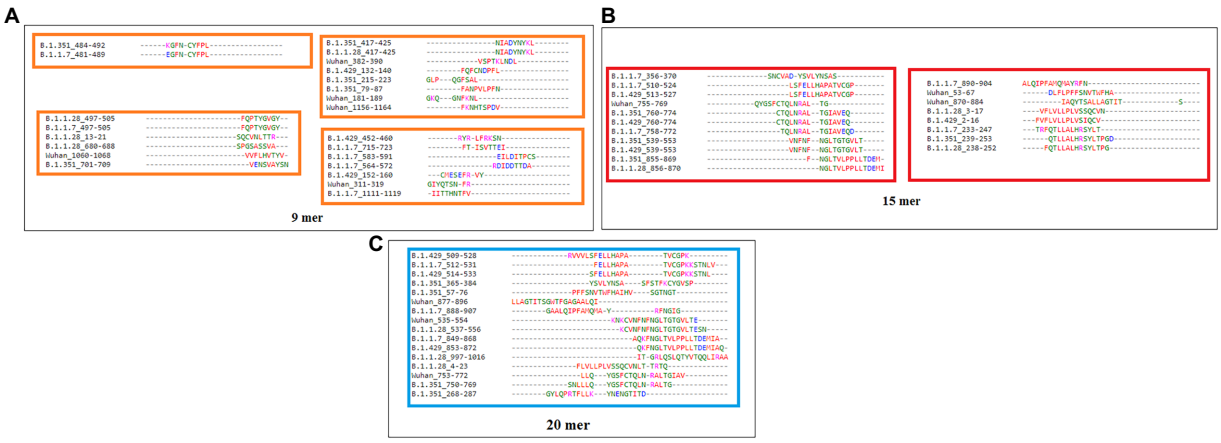

FIGURE 6
Epitope alignment of 9 mer, 15 mer, 20 mer CTL antigenic epitopes present in the S-glycoprotein of Wuhan strain and B.1.351, B.1.1.28/triple mutant, B.1.1.7, and B.1.429 variant. **(A)** Epitope alignment shows four significant blocks from 9 mer CTL antigenic epitopes. **(B)** Epitope alignment shows two significant blocks from 15 mer CTL antigenic epitopes. **(C)** Epitope alignment shows one significant block from 20 mer CTL antigenic epitopes.

Cluster analysis of the 20-mer CTL epitopes of S-glycoprotein of the Wuhan strain and B.1.351, B.1.1.28/triple mutant, B.1.1.7, and B.1.429 variants

We performed cluster analysis of the 20-mer CTL epitopes of S-glycoprotein of the Wuhan strain and B.1.351, B.1.1.28/triple mutant, B.1.1.7, and B.1.429 variants at different threshold levels (minimum sequence identity threshold 10 to 80% level). We examined 16 numbers of the 20-mer CTL epitopes for cluster formation. We found one dense cluster formation at the 10% level, which had a circular shape, and approximately 16 nodes were visible (Supplementary Figure S2A). All 20-mer CTL epitopes participated in the cluster formation.

We found two significant clusters at the 20% level, containing four and 12 nodes (Supplementary Figure S2B). We found four prominent clusters at the 30% level, including four, two, two, and three nodes, and the other nodes were individually scattered (Supplementary Figure S2C).

We found four significant clusters that were generated at the 40% level, containing two, two, two, and three nodes and some other nodes were individually scattered (Supplementary Figure S2D). We observed four significant clusters created at the 50% level, containing three, two, two, and two nodes and several nodes positioned individually in a scattered manner (Supplementary Figure S2E). We observed four major clusters at the 60% level, containing two, two, two, and three nodes and some other nodes were located independently in a scattered manner

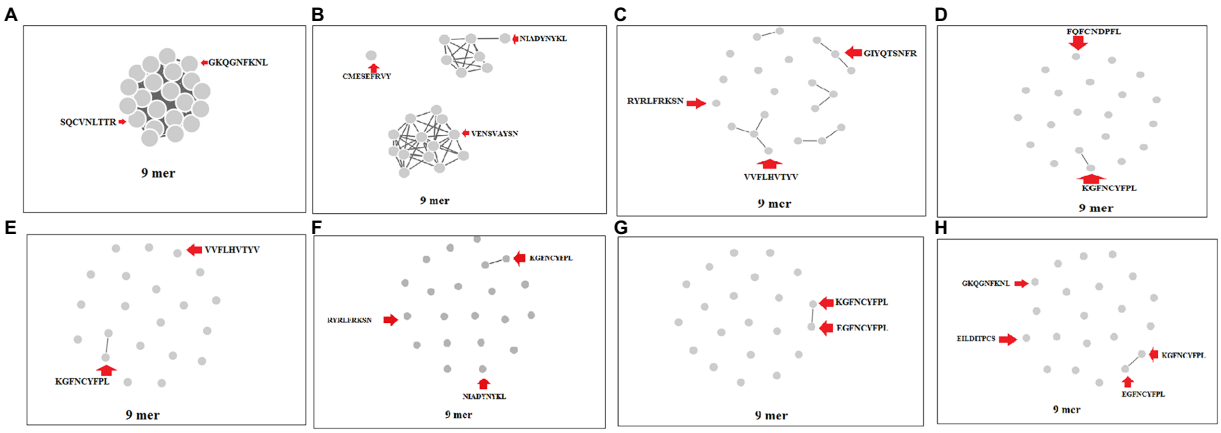

FIGURE 7
Cluster formation of 9 mer CTL epitopes of S-glycoprotein of Wuhan strain and B.1.351, B.1.1.28/triple mutant, B.1.1.7, and B.1.429 variant using the threshold 10% level to 80% level. **(A)** Cluster formation at 10% level. **(B)** Cluster formation at 20% level. **(C)** Cluster formation at 30% level. **(D)** Cluster formation at 40% level. **(E)** Cluster formation at 50% level. **(F)** Cluster formation at 60% level. **(G)** Cluster formation at 70% level. **(H)** Cluster formation at 80% level.

(Supplementary Figure S2F). We evaluated the cluster formation at the 70% level, which showed four significant clusters, containing two, two, two, and three nodes and several nodes were individually scattered (Supplementary Figure S2G). We evaluated the cluster formation at the 80% level, which showed four significant clusters, containing two, two, two, and two nodes and numerous single nodes were situated in a scattered manner (Supplementary Figure S2H).

Analysis of the CD spectra of S-glycoprotein of the Wuhan strain and B.1.351, B.1.1.28/triple mutant, B.1.1.7, and B.1.429 variants

A CD spectrum is essential for analyzing the proper secondary structure and fold detection of a protein (Micsonai et al., 2015). We generated the computer-simulated CD spectra of S-glycoprotein of the Wuhan strain and B.1.351, B.1.1.28/triple mutant, B.1.1.7, and B.1.429 variants. The spectrum of the viral glycoprotein of the Wuhan strain showed both positive and negative bands. The CD spectra showed a positive band at approximately 198 nm, comprising a maximum positive peak at about 190 nm, and showed a negative band from 198 nm to 225 nm with a maximum negative peak at 207–210 nm (Figure 8A). We analyzed the CD spectra of the B.1.351 variant, where we used the Wuhan strain as a control or the closest CD spectrum to the experimental protein (green spectra). Here, we used the S-glycoprotein of the B.1.351 variant as the experimental protein, and the generated spectrum is shown in red (Figure 8B). Both CD spectra showed the same pattern, with the maximum positive peak greater for the B.1.351 variant than for the Wuhan strain. The study evaluated the root-mean-square deviation (RMSD) variation of the control or closest CD spectrum and experimental CD spectrum (B.1.351 variant), which was 0.12 (Figure 9A; Supplementary Table S3). We analyzed the CD spectrum of the B.1.1.28/triple mutant variant using the same methodology as described above (Figure 8C). Both CD spectra (Wuhan strain and B.1.1.28/triple mutant variant) showed a similar pattern. The maximum positive peak was slightly more remarkable in the B.1.1.28/triple mutant variant than in the Wuhan strain, with an RMSD variation of 0.17 (Figure 9B). We generated the CD spectrum of the B.1.1.7 variant and compared it to the Wuhan strain (Figure 8D), and both CD spectra showed identical patterns. Maximum positive and maximum negative peaks were the same. The RMSD variation was 0.14 (Figure 9C). Finally, we generated the CD spectrum of the B.1.429 variant and compared it to the Wuhan strain (Figure 8E), with both CD spectra showing identical patterns. A lower negative peak was observed for the CD signal of the B.1.429 variant than the Wuhan strain, and the RMSD variation was 0.45 (Figure 9D). We also analyzed the secondary structure pattern of the Wuhan strain, B.1.351, B.1.1.28/triple mutant, B.1.1.7, and B.1.429 variants to calculate the beta-sheet (β-sheet) percentages, which were 26.21% (Supplementary Figure S3A), 24.84% (Supplementary Figure S3B), 24.84% (Supplementary Figure S3C), 24.46% (Supplementary Figure S3D), and 32.19%, respectively (Supplementary Figure S3E; Supplementary Table S4). Therefore, all proteins were β-sheet-rich. However, more β-sheets were found in B.1.429 than in the Wuhan strain and the B.1.351, B.1.1.28/triple mutant, and B.1.1.7 variants (Supplementary Figure S4A). In addition, more β turns (9.71%) were found in B.1.429 than in the Wuhan strain and the B.1.351, B.1.1.28/triple mutant, and B.1.1.7 variants (Supplementary Figure S4B).

The CD spectra of proteins were applied to evaluate proteins' secondary structure pattern, binding properties, and folding shape. It is one of the rapid methods for assessing proteins' secondary structure pattern, binding properties, and folding shape.

Parsons et al. (2019) have evaluated the RBD protein secondary structure of avian coronavirus by CD spectra analysis (Parsons et al., 2019). In this analysis, the spectral bandwidth has shown diverse

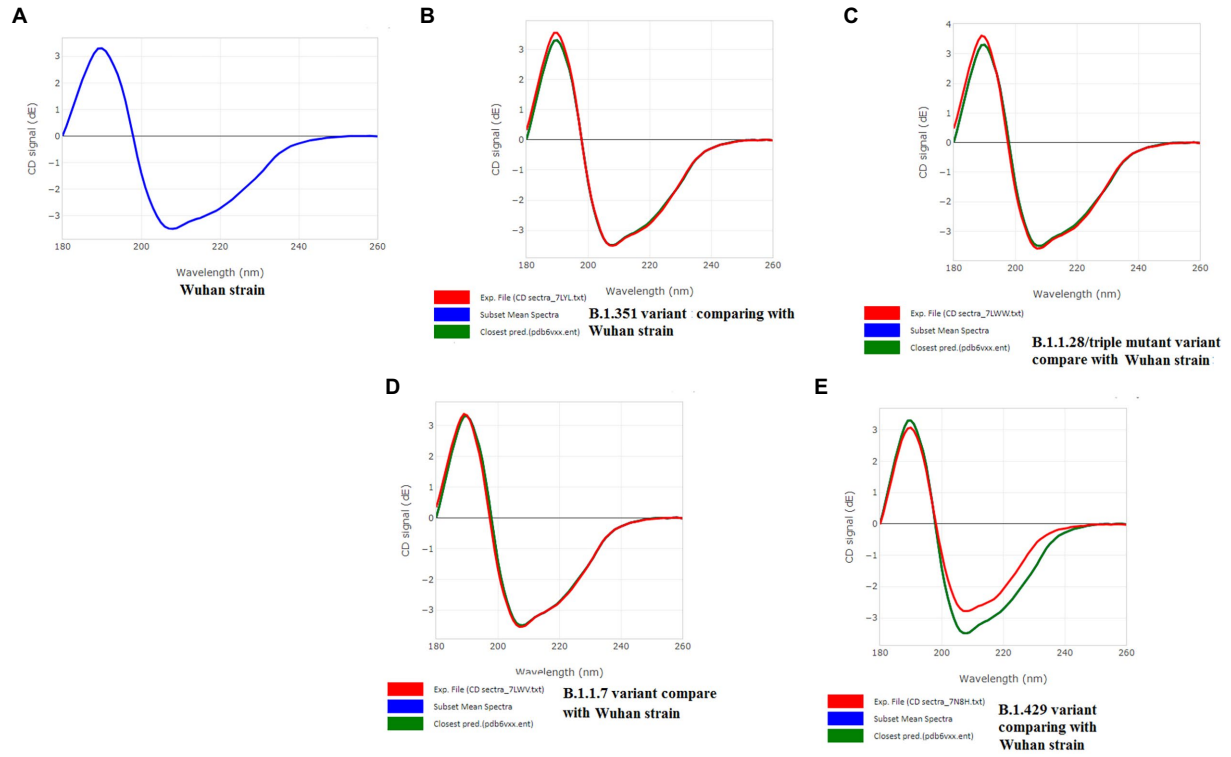

FIGURE 8
CD spectra of S-glycoprotein of the Wuhan variant and B.1.351, B.1.1.28/triple mutant, B.1.1.7, B.1.429 variants. **(A)** CD spectra of S-glycoprotein of the Wuhan strain **(B)** Resemblance of CD spectra of S-glycoprotein of the Wuhan strain and B.1.351. **(C)** The resemblance of CD spectra of S-glycoprotein of the Wuhan strain and B.1.1.28/triple mutant. **(D)** The resemblance of CD spectra of S-glycoprotein of the Wuhan strain and B.1.1.7. **(E)** The resemblance of CD spectra of S-glycoprotein of the Wuhan strain and B.1.429.

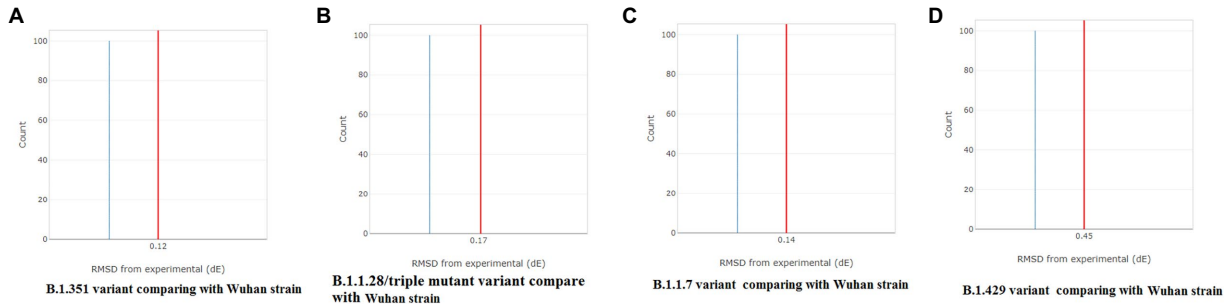

FIGURE 9
Comparison of RMSD between the CD spectra of the S-glycoprotein Wuhan variant and other variants. **(A)** The resemblance of RMSD between the CD spectra of S-glycoprotein Wuhan strain and B.1.351. **(B)** The resemblance of RMSD between the CD spectra of S-glycoprotein Wuhan strain and B.1.1.28/triple mutant. **(C)** The resemblance of RMSD between the CD spectra of the S-glycoprotein Wuhan strain and B.1.1.7. **(D)** The resemblance of RMSD between the CD spectra of S-glycoprotein Wuhan strain and B.1.429.

values regarding nanometer scale, specific temperature, etc., of RBD proteins of glycosylation-site and non-glycosylation-site variants.

In our study, we applied the PDBMD2CD server to generate the *in silico* CD spectra (wavelength of the CD signal) using PDB files of S-glycoprotein of the Wuhan strain and significant variants.

The secondary structure pattern of S-glycoprotein of studied SARS-CoV-2 (Wuhan strain and other variants) features are stabilized by the amino acid residues turn tendencies as well as the cross-strand interactions among the sequences flanking the beta-turns. Researchers also showed that the specific β-turns of protein have a crucial role in interacting with the T-cell receptor (TCR), leading the MHCII-peptide-TCR complex to induce a suitable immune response (Bermudez et al., 2018). Subsequently, the beta-sheets also significantly impact on the managing the affinity of MHC class II binding sites in superantigens (Al-Shangiti et al., 2004). However, in the case of SARS-CoV-2 S-glycoprotein, no

such work has been reported. But, our bioinformatics tools have shown the proper interactions of epitopic peptides (9-mer) from S-glycoprotein with TCR. These tools have established the vital role of beta-sheets and beta-turns in forming the SAg-like region.

3D model generation of the 9-mer CTL epitopic regions

3D models were created for all 9-mer CTL epitopes, and their epitopic regions were located in the S-glycoprotein. We generated four 3D models for the 9-mer CTL epitopes of the Wuhan strain: G181-L189, G311-R319, V382-L390, and V1060-1068 (Figure 10A); four 3D models for the B.1.351 variant: F79-N87, G215-L223, N417-L425, K484-L492, and V701-N709 (Figure 10B); two 3D models for the B.1.1.28/triple mutant variants: N417-L425 and F497-Y505 (Figure 10C); six 3D models for the B.1.1.7 variant: E481-L489, F497-Y505, R564-A572, E583-S591, F715-I723, and I1111-V1119 (Figure 10D); and three 3D models for the B.1.429 variant: F132-L140, C152-Y160, and R452-N460 (Figure 10E).

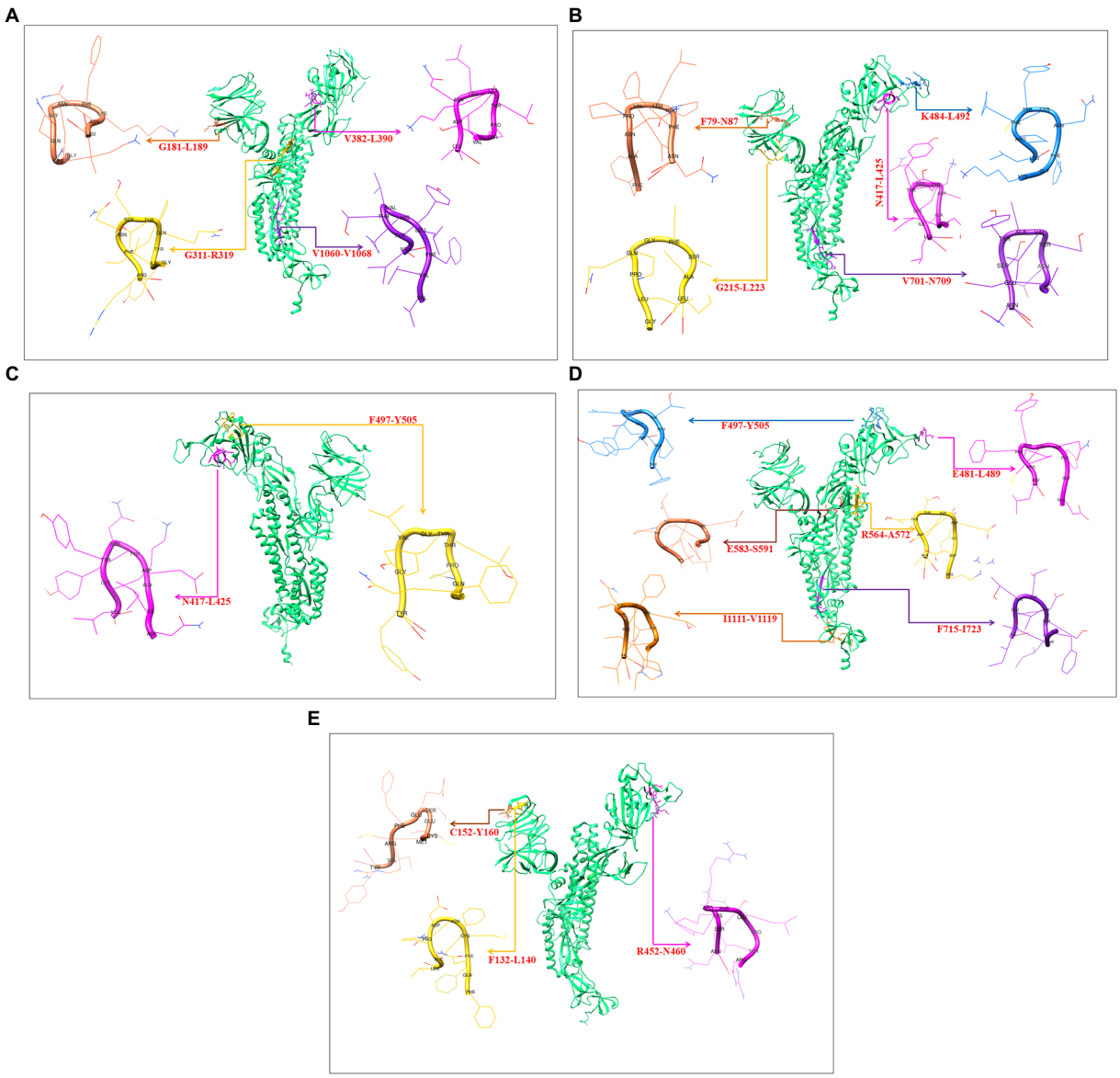

FIGURE 10
Generated three-dimensional (3D) model of 9 mer CTL epitopic regions of the Wuhan strain and B.1.351, B.1.1.28/triple mutant, B.1.1.7, B.1.429 variants and their position in 3D model of S-glycoprotein. **(A)** 3D model of 9 mer CTL epitopic regions of the Wuhan strain and their position in 3D model of S-glycoprotein. **(B)** 3D model of 9 mer CTL epitopic regions of the B.1.351 variant and their position in 3D model of S-glycoprotein. **(C)** 3D model of 9 mer CTL epitopic regions of the B.1.1.28/triple mutant variant and their position in 3D model of S-glycoprotein. **(D)** 3D model of 9 mer CTL epitopic regions of the B.1.1.7 variant and their position in 3D model of S-glycoprotein. **(E)** 3D model of 9 mer CTL epitopic regions of the B.1.429 variant and their position in the 3D model of S-glycoprotein.

Mimic phage-displayed peptides for 9-mer CTL epitopes of SARS-CoV-2S-glycoprotein

Previous studies have identified unique phage-displayed peptides that mimic different pathogen epitopes, such as *Mycobacterium tuberculosis* (Wang et al., 2016) and the hepatitis E virus (Larralde and Petrik, 2017). The present study aimed to determine the mimic 9-mer CTL epitopes from the S-glycoprotein of SARS-CoV-2 from phage-displayed peptides. A random peptide library was scanned, and the selected peptides were supposed to mimic the 9-mer CTL epitopes of S-glycoprotein of this virus, which showed a list of clusters in the Wuhan, B.1.351, B.1.1.28/triple mutant, and B.1.1.7 variants. The Wuhan strain showed three mimic clusters with four different 9-mer epitopes (Figure 11A). The first mimic cluster was formed with two 9-mer epitopes (VVFLHVTYV and GIYQTSNFR), the second mimic cluster was formed with one 9-mer epitope (VSPTKLNDL), and the third mimic cluster was formed with one 9-mer epitope (GKQGNFKNL).

The B.1.351 variant showed three mimic clusters with four 9-mer epitopes (Figure 11B). The first mimic cluster consisted of two 9-mer epitopes (GLPQGFSAL and KGFNCYFP), the second was formed with one 9-mer epitope (VENSVAYSN), and the third included one 9-mer epitope (FANPVLPFN).

The B.1.1.28/triple mutant variant showed three mimic clusters with three different 9-mer epitopes (Figure 11C). The first mimic cluster consisted of one 9-mer epitope (FQPTYGVGY), the second was formed with one 9-mer epitope (SQCVNLTTR), and the third was formed with one 9-mer epitope (SPGSASSVA).

Finally, the B.1.1.7 variant showed three mimic clusters with four 9-mer epitopes (Figure 11D). The first mimic cluster had two 9-mer epitopes (EILDITPCS and RDIDDTTDA), the second was formed with one 9-mer epitope (FQPTYGVGY), and the third consisted of one 9-mer epitope (IITTHNTFV).

SAg-like region from S-glycoprotein of SARS-CoV-2 of the Wuhan strain and B.1.351, B.1.1.28/triple mutant, B.1.1.7, and B.1.429 variants

Following Cheng et al. (2020) study, we developed a 3D structural model of the SAg-like part of the S-glycoprotein of

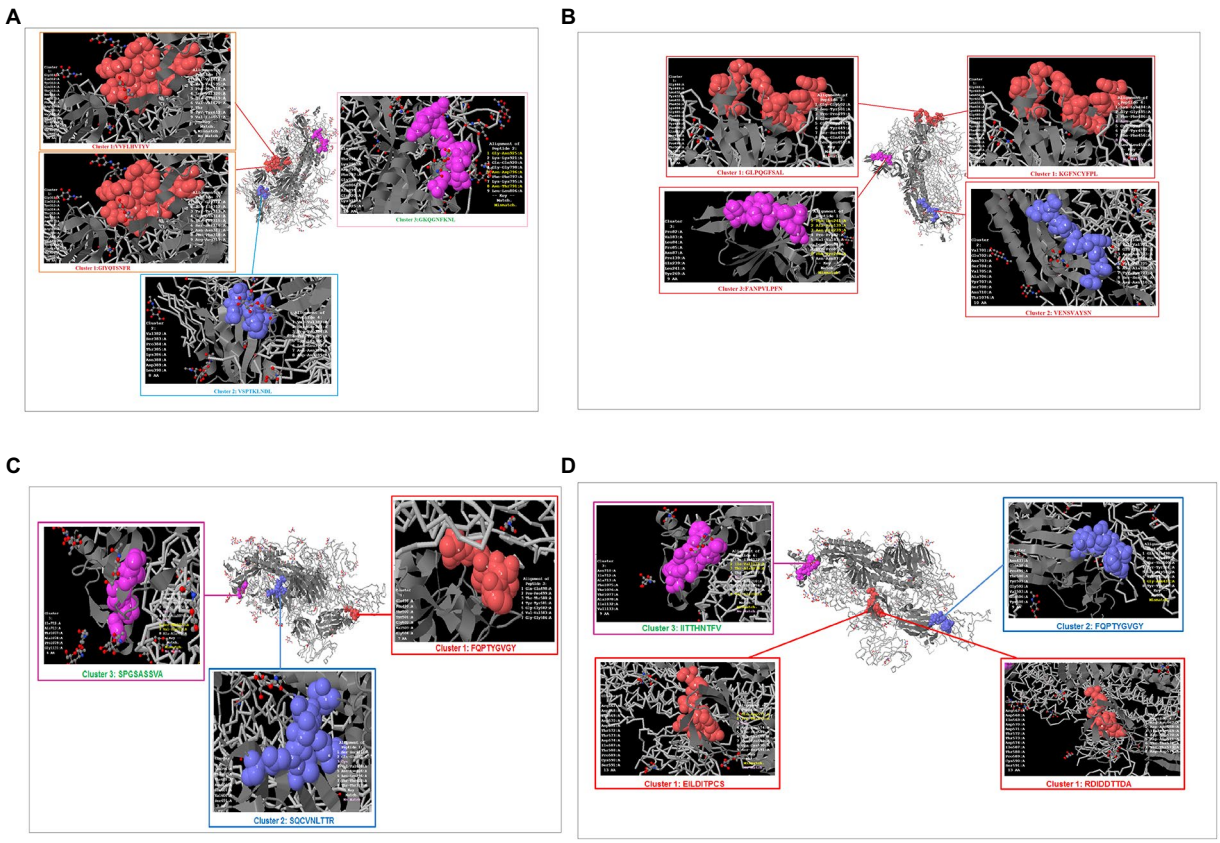

FIGURE 11
Phage-displayed peptides that mimic S-glycoprotein of SARS-CoV-2 9 mer CTL epitopes of the Wuhan strain and B.1.351, B.1.1.28/triple mutant, B.1.1.7, B.1.429 variants. **(A)** Phage-displayed peptides that mimic S-glycoprotein of 9 mer CTL epitopes of the Wuhan strain and the cluster epitopes. **(B)** Phage-displayed peptides that mimic S-glycoprotein of 9 mer CTL epitopes of the B.1.351 variant and the cluster epitopes. **(C)** Phage-displayed peptides that mimic S-glycoprotein of 9 mer CTL epitopes of the B.1.1.28/triple mutant variant and the cluster epitopes. **(D)** Phage-displayed peptides that mimic S-glycoprotein of 9 mer CTL epitopes of B.1.1.7 and the cluster epitopes.

SARS-CoV-2 of the Wuhan strain (Figure 12A; Baú et al., 2006; Cheng et al., 2020). We also developed a 3D structure model using the same region (SAg-like region) from the S-glycoprotein of this virus of the different variants, i.e., B.1.351 (Figure 12B), B.1.1.28/triple mutant (Figure 12C), B.1.1.7 (Figure 12D), and B.1.429 (Figure 12E).

Interaction between SAg-like region of the viral glycoprotein and T cell receptor (TCR)

The present study illustrated the interaction with our developed 3D structural model of the SAg-like region of the S-glycoprotein of

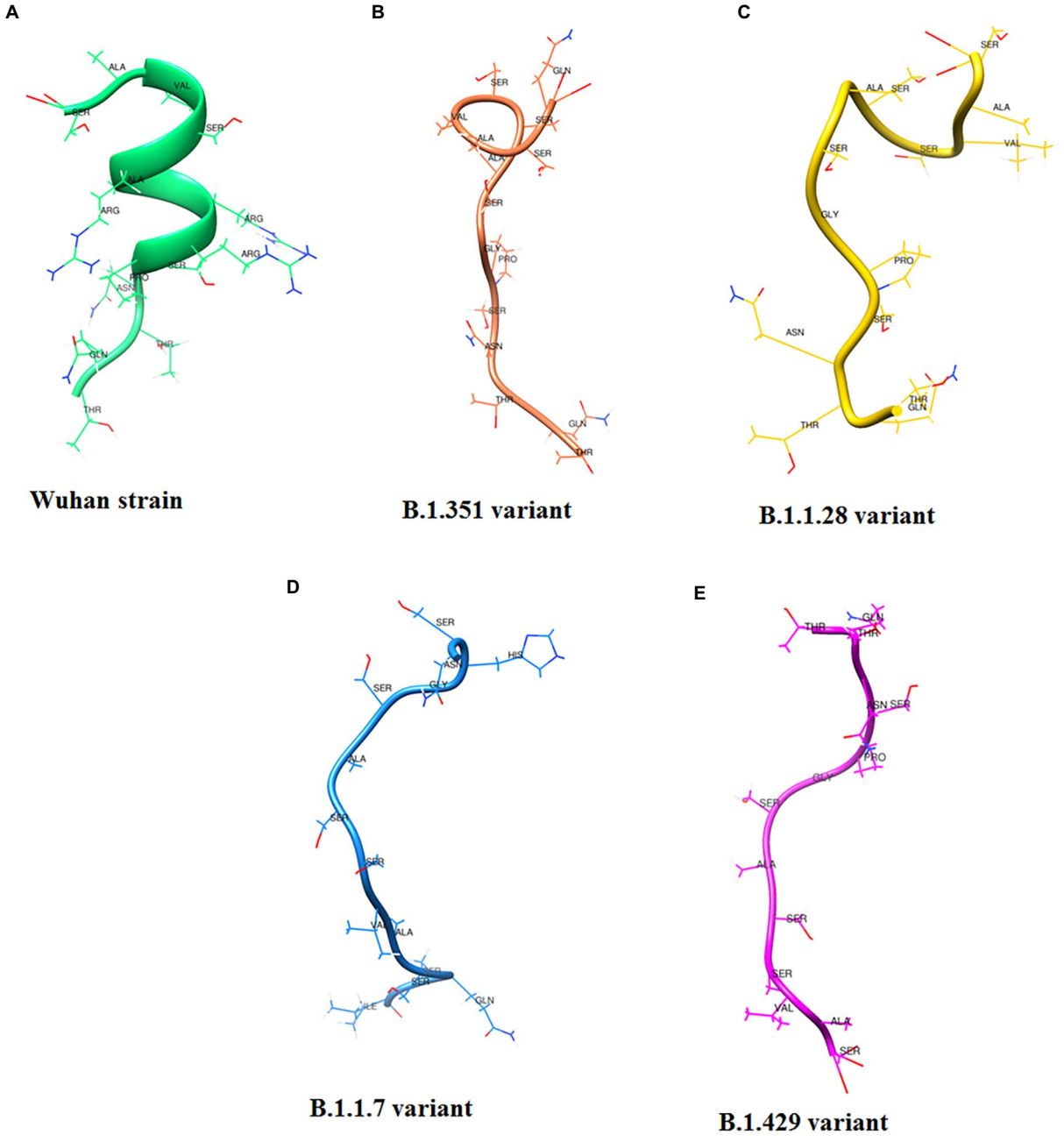

FIGURE 12
3D model of SAg-like region from S-glycoprotein of Wuhan strain and B.1.351, B.1.1.28/triple mutant, B.1.1.7 and B.1.429 variants. **(A)** 3D model of SAg-like region from S-glycoprotein of Wuhan strain. **(B)** 3D model of SAg-like region from S-glycoprotein of the B.1.351 variant which was generated same SAg-like region from S-glycoprotein of Wuhan strain. **(C)** 3D model of SAg-like region from S-glycoprotein of the B.1.1.28/triple mutant variant which was generated same SAg-like region from S-glycoprotein of Wuhan strain. **(D)** 3D model of SAg-like region from S-glycoprotein of the B.1.1.7 variant which was generated same SAg-like region from S-glycoprotein of Wuhan strain. **(E)** 3D model of SAg-like region from S-glycoprotein of the B.1.429 variant which was generated same SAg-like region from S-glycoprotein of Wuhan strain.

the Wuhan strain and B.1.351, B.1.1.28/triple mutant, B.1.1.7, and B.1.429 variants with human TCR. These interactions can be seen in Figures 13A–E and showed that the SAg-like region interacted with the beta chain of the human TCR.

Identification of the partial SAg-like part of the viral S-glycoprotein of the Wuhan strain and B.1.351, B.1.1.28/triple mutant, B.1.1.7, and B.1.429 variants

Sequence alignment was performed using significant SAgs [α-cobra toxin (*N. naja*), α-bungarotoxin, rabies virus G protein (189–199), and α-cobra toxin (*N. kaouthia*)], and HIV-1 gp120 (164–174), Wuhan strain and B.1.351, B.1.1.28/triple mutant, B.1.1.7, and B.1.429 variants. We observed a partial SAg-like part (ANQFNSAIGKI) of the S-glycoprotein of this virus in the Wuhan strain and B.1.351, B.1.1.28/triple mutant, B.1.1.7, and B.1.429 variants, as depicted in Figure 14A.

We developed a cluster with these MSA sequences at the 30, 40, and 70% levels. We found one cluster with all sequences at the 30% level (Figure 14B). However, the SAg-like region was detached from the central cluster at 40% (Figure 14C) and 70% levels (Figure 14D).

Discussion

MHC-I-restricted CTLs play a significant role in controlling viral infections. $CD8^+$ T cells perform a crucial role in the clearance of infections of this virus (acute model) in the lungs (Schmidt and Varga, 2018) and are activated and differentiated in patients with severe COVID-19 (Chen and Wherry, 2020). Bange et al. (2021) concluded that $CD8^+$ T cells might help with the survival of patients with COVID-19 (Bange et al., 2021). Therefore, identifying CTL epitopes is essential for understanding the T cell activation mechanism and assisting epitope-driven vaccine design.

The identification and characterization of the CTL 9-mer epitope have a substantial importance in medical immunology. The identification of peptide epitopes can be helpful in the production of vaccines against microorganisms that have very little growth in the medium, as well as microorganisms whose antigenic regions are not precisely detected during the typical immune system infection (Andreatta and Nielsen, 2018; Rencilin et al., 2021). Therefore, finding considerable numbers of CTL epitopes is a necessary process for vaccine design, and those CTL epitopes consist of the binding motifs of the known class I MHC. Still, even the epitopes do not conform precisely to consensus motifs or vary in length. To do this with conventional peptide synthesizers is costly and impractical because of the large number of peptides, and a considerable amount of testing is required. Therefore, these advanced strategies for epitope mapping offer a more precise solution than the initial CTL epitope screening experiments rather than other aspects (Soria-Guerra et al., 2015).

In the present study, CTL epitopic regions of S protein were analyzed using antigenic scores. We assessed the antigenicity of the wild type (Wuhan strain) and mutant S-glycoprotein of four variants (B.1.351, B.1.1.28/triple mutant, B.1.1.7, and B.1.429). The analysis of 9-mer CTL epitope regions of S-glycoprotein showed

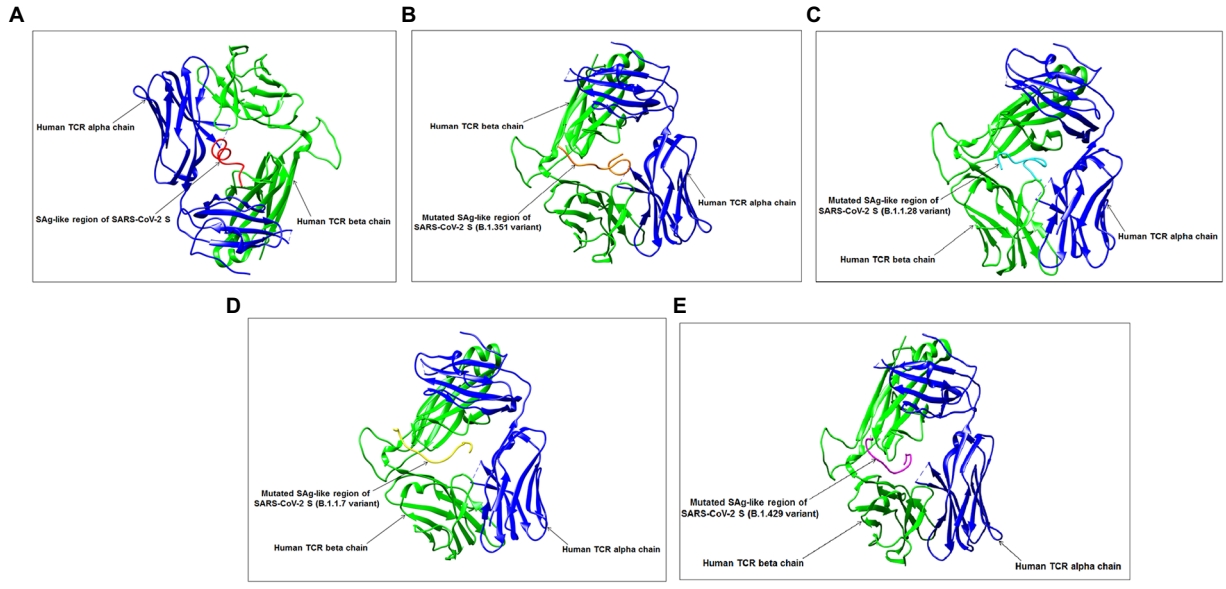

FIGURE 13
Interaction between SAg-like region from S-glycoprotein of Wuhan strain, B.1.351, B.1.1.28/triple mutant, B.1.1.7, B.1.429 variants and TCR. **(A)** Interaction between SAg-like region of Wuhan strain and TCR. **(B)** Interaction between SAg-like part of B.1.351 variant and TCR. **(C)** Interaction between SAg-like part of the B.1.1.28/triple mutant variant and TCR. **(D)** Interaction between the SAg-like part of the B.1.1.7 variant and TCR. **(E)** Interaction between the SAg-like part of the B.1.429 variant and TCR.

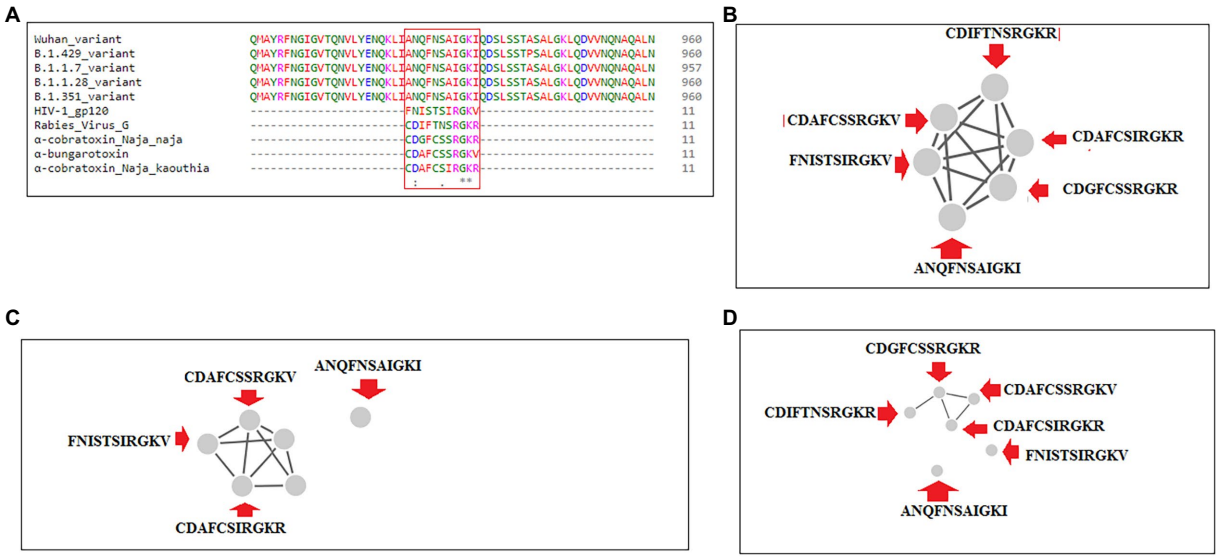

FIGURE 14
Another partial SAg-like region from S-glycoprotein of SARS-CoV-2 of Wuhan strain, B.1.351, B.1.1.28/triple mutant, B.1.1.7, B.1.429 variants shows the sequence similarity with an α-cobra toxin (*Naja naja*),α-bungarotoxin, Rabies Virus G Protein (189–199), α-cobra toxin (*Naja kaouthia*), and HIV-1 gp120 (164–174) and their cluster formation. **(A)** Sequence similarity of superantigens (α-cobra toxin (*Naja naja*),α-bungarotoxin, Rabies Virus G Protein (189–199), α-cobra toxin (*N. kaouthia*), and HIV-1 gp120 (164–174)), Wuhan variant, and significant VOCs/VOI (B.1.351, B.1.1.28/triple mutant, B.1.1.7, B.1.429) shows a partial super SAg-like region. **(B)** Cluster (with these MSA sequences) at 30% level. **(C)** Cluster (with these MSA sequences) at 40% level. **(D)** Cluster (with these MSA sequences) at 70% level.

that the B.1.1.7 variant had an elevated antigenicity compared to other variants and the Wuhan strain for the 9-mer CTL epitopes and average CTL epitopes (average number of three epitope types). The RBD region also showed the highest numbers of 9-mer CTL epitope and 15-mer CTL epitope and an average number of CTL epitopes for the B.1.1.7 variant.

CTL 9-mer epitope sequences in the viral protein can be identified using the IEDB server. This is a standard method (Islam et al., 2020). The selected peptide size (9 amino acids) has a potential binding capacity to MHC-I rather than the 15-mer and 20-mer epitopes because these are optimal stimulators for CD8 response and can interact with several HLA-A alleles, which has a considerable binding affinity (Li Pira et al., 2010; Shi et al., 2015). Therefore, our study performed the identification and characterization of the CTL 9-mer epitope of the Wuhan strain and four mutative variants, which has immense importance.

We have used the IEDB epitope cluster analysis tool (Dhanda et., 2018) for the cluster analysis of CTL epitopes (9-mer, 15-mer, and 20-mer) of S-glycoprotein of the Wuhan strain and the B.1.351, B.1.1.28/triple mutant, B.1.1.7, and B.1.429 variants. This tool groups epitopes into clusters based on sequence identity. A cluster is a group of sequences with a sequence similarity more incredible than the minimum sequence identity threshold specified. Our manuscript represents the CTL epitopic peptides as circles, and the solid line connecting two peptides is identified above the specified threshold. All the connected peptides are in a cluster. Here, all the peptides homologous to a certain pre-specified level are clustered together, for example, at the 20% level. In this case, any member of the cluster will be at least 20% homologous to at least one member. However, the approach's shortcoming is that cluster members might and often are related by levels of homology much lower than 20%. As a result, the cluster provides a clear consensus sequence. Conversely, the singletons are isolated peptides, and those do not share any sequence identity with any other peptides in the given data. However, using this approach, in our work, we have analyzed and offered from a 10% threshold level of sequence identity to the 80% level of CTL epitopes (9-mer, 15-mer, and 20-mer) of mentioned SARS-CoV-2 Wuhan strain and other significant variants.

During cluster formation of 9-mer CTL epitopes, we found one significant cluster formation at the 70% level with two nodes (KGFNCYFPL and EGFNCYFPL), and the other nodes were scattered. Consequently, they did not form a dense cluster at the 70% level and showed a high level of diversity. We found four significant clusters in the 15-mer CTL epitopes and four multiple clusters formed in the 20-mer CTL epitopes at the 70% level. Considering the cluster formation of the 9-mer, 15-mer, and 20-mer CTL epitopes, the 9-mer CTL epitopes showed uniqueness in their cluster formation pattern. These epitopes, which have formed the clusters in higher percentage levels (such as 70% or 80%), might have a similar kind of nature regarding antigenicity and their antigen processing. However, we need to confirm the hypothesis through further experiments. Therefore, understanding the method of cluster formation is of enormous medical significance. Recently, Meckiff et al. (2020) used the cluster

formation technique and the epitope mega pool of peptide design for this virus during the COVID-19 infection (Meckiff et al., 2020).

The CD spectra of the S-glycoprotein of the Wuhan strain and B.1.351, B.1.1.28/triple mutant, and B.1.1.7 variants showed almost the same band pattern. On the other hand, we have found a slight difference in the CD spectra of S-glycoprotein of the B.1.429 variant compared to the Wuhan strain. This difference occurred because of the spectral contrast of the B.1.429 variant and Wuhan strain. After comparing the closest and experimental CD spectra, the RMSD variation was calculated. The Wuhan strain and the B.1.351, B.1.1.28/triple mutant, and B.1.1.7 variants had minor differences (0.12–0.17 range). However, the RMSD variation was 0.45 for the B.1.429 variant. A higher RMSD variation occurred because of more spectral differences than the control. This result is in corroboration with the results of Li and Hirst (Li and Hirst, 2020), who attempted to develop a model of SARS-CoV-2 proteins using CD spectra analysis.

The present study found three phage-displayed peptides that mimicked the 9-mer CTL epitopes from the S-glycoprotein of SARS-CoV-2 (Wuhan strain, and B.1.351, B.1.1.28/triple mutant, and B.1.1.7 variants). Previous studies have identified mimic phage-displayed peptides similar to CTL epitopes of SARS-CoV-2, which have immense importance for epitope-based immunotherapy, diagnostics, and vaccine development (Bazan et al., 2012; Wu et al., 2016). Recently, Guo et al. (2021) characterized different B cell epitopes from this virus using a peptide library (phage-displayed; Guo et al., 2021).

Finally, we attempted to understand the interaction pattern of the SAg-like region within the Wuhan strain and TCR, following Cheng et al. (Cheng et al., 2020). An identical portion of the SAg-like part of the Wuhan strain was searched from the B.1.351, B.1.1.28/triple mutant, B.1.1.7, and B.1.429 variants. The hyperinflammatory response in COVID-19 patients is a significant area of research. We developed a 3D model of these SAg-like regions and determined their interaction pattern with TCR. A proper understanding of hyper inflammation in severe COVID-19 cases may help solve the mystery of the death of these patients (García, 2020; Tay et al., 2020). Our study allows us to illustrate the TCR and downstream regulatory pathways for the hyperinflammatory response in COVID-19 patients. Our MSA analysis found another partial super SAg-like region (ANQFNSAIGKI) from the S-glycoprotein of SARS-CoV-2 in the Wuhan strain and B.1.351, B.1.1.28/triple mutant, B.1.1.7, and B.1.429 variants.

The study of the insight into the antigenicity of SARS-CoV-2 variants has fundamental importance. It helps us illustrate the dynamic interaction between SARS-CoV-2 variants with humans or other hosts and also allows us to understand the immunopathogenesis of SARS-CoV-2 variants. Understanding the antigenic variations has immense importance. Antigenic variation might be a significant factor in comparing the antigenicity among the virus variants. Antigenic variation can help us to understand the virus fitness. At the same time, it can also explain how a virus can reinfect hosts by escaping the immune memory. Antigenic variations, diversification, conservation, and the total number of antigens in a particular virus protein need to be studied. However, antigenic variations have been studied in different viruses from time to time (Zost et al., 2019). The antigenic variations have also been studied in all human coronaviruses and SARS-CoV-2 (Kumar et al., 2020). Researchers have also investigated antigenic variations in spike protein in SARS-CoV-2 (Harvey et al., 2021). Some researchers have tried to illustrate the antigenic variations in SARS-CoV-2 variants (Mittal et al., 2022).

However, the total number of epitopes in a spike protein might be one criterion to determine the antigenicity comparing the SARS-COV-2 and SARS-CoV (Zheng and Song, 2020). Here we compared the total number of CTL epitopes in variants of SARS-CoV-2. Our study showed that B.1.1.7 (Alpha) of spike protein displayed the highest number of CTL epitopes compared to Wuhan strain, B.1.351 (Beta), B.1.1.28/triple mutant (P.1), and B.1.429 (epsilon). However, the surface accessibility of those epitopes is also a significant factor in interacting nAb (neutralizing antibody), and a need of further study for these variants. At the same time, there is also a need to understand how antigenic epitopes are presented to the T cell by MHC (major histocompatibility complex) molecules (both class I and class II molecules; Forni et al., 2021).

Limitations of the study

The study has performed a comprehensive analysis of the CTL epitopes or SAg-like region of the total S-glycoprotein of the Wuhan strain, B.1.351, B.1.1.28/triple mutant, B.1.1.7, and B.1.429 variants and predicted the antigenicity through computational biology. The analyses were performed in various directions. Every data accumulated through the bioinformatics methods for Wuhan strain and emerging mutant variants is essential for future researchers and society. The arrival of emerging variants during the pandemic made the pandemic period more critical. At this point of urgency, our data predicting the potent antigenicity through bioinformatics tools which is very significant and highly beneficial for society. However, data acquired by us needs further validation through *in vitro* and *in vivo* methods, which is a limitation of this study. Therefore, we urgently urge future researchers to validate our data to end the pandemic crisis and prepare for a future pandemic.

Conclusion

Several studies have focused on the identification and characterization of immunogenic $CD8^+$ T cell epitopes. MHC-I molecules naturally contain 8-aa to 11-aa length peptide chains, which is the main consequence of the proteasomal degradation of antigens. This antigen is derived from infection or self-peptides (Blum et al., 2013). Our 9-mer CTL epitopic study helped identify

the primary mechanism of antigen processing of the S-glycoprotein of SARS-CoV-2 *via* the MHC-I molecules of $CD8^+$ T cells.

This study initiated several questions regarding the antigen processing of the S-glycoprotein of this virus *via* MHC-I molecules for $CD8^+$ T cells. The researcher should solve these questions. We should also know about the antigen processing of the S-glycoprotein of the Wuhan strain and other emerging VOCs/VOIs such as B.1.351, B.1.1.28/triple mutant, B.1.1.7, and B.1.429 variants. At the same time, it is also necessary to understand more about the peptide–MHC-I complexes formation for the Wuhan strain and other emerging VOCs/VOIs such as B.1.351, B.1.1.28/triple mutant, B.1.1.7, and B.1.429 variants.

Different scientists have developed immunogenicity models for CTL epitopes (Harndahl et al., 2012; Calis et al., 2013). However, specific immunogenicity models for CTL epitopes of SARS-CoV-2 S-glycoprotein remain to be developed.

We identified the highest virulent epitopes with a significant mutation within the S-glycoprotein of SARS-CoV-2 emerging VOCs/VOIs (B.1.351, B.1.1.28/triple mutant, B.1.1.7, and B.1.429 variants) and the Wuhan strain. Our results showed that the mutations might be responsible for the high antigenicity identified in the B.1.1.7 variant. This variant might help activate more $CD8^+$ T cells *via* the MHC-I pathway than in the South African, Brazilian, and Wuhan variants. It might help activate more $CD4^+$ T cells *via* the MHC-II pathway and cytokine signaling. In the future, the molecular mechanism by which $CD8^+$ T cells distinguish antigens from immunogenic property antigens of S-glycoprotein of wild strain and their variants should be evaluated.

Data availablity statement

The original contributions presented in the study are included in the article/Supplementary material, further inquiries can be directed to the corresponding authors.

Author contributions

CC: conceptualization, data acquisition, and writing–original draft. MB and ARS: formal analysis, validation, and reviewing and editing. BM and S-SL: formal analysis and validation. CC and E-MS: supervision and funding. All authors contributed to the article and approved the submitted version.

Funding

This study was supported by the Hallym University Research Fund and the Basic Science Research Program through the National Research Foundation of Korea (NRF), funded by the Ministry of Education (NRF-2020R1C1C1008694 and NRF-2020R1I1A3074575).

Conflict of interest

The authors declare that the research was conducted in the absence of any commercial or financial relationships that could be construed as a potential conflict of interest.

Publisher's note

Supplementary material

The Supplementary material for this article can be found online at: https://www.frontiersin.org/articles/10.3389/fmicb.2022.895695/full#supplementary-material

SUPPLEMENTARY FIGURE S1
Cluster formation of 15 mer CTL epitopes of S-glycoprotein of Wuhan strain and B.1.351, B.1.1.28/triple mutant, B.1.1.7, and B.1.429 variant using the threshold 10% level to 80% level. **(A)** Cluster formation at 10% level. **(B)** Cluster formation at 20% level. **(C)** Cluster formation at 30% level. **(D)** Cluster formation at 40% level. **(E)** Cluster formation at 50% level. **(F)** Cluster formation at 60% level. **(G)** Cluster formation at 70% level. **(H)** Cluster formation at 80% level.

SUPPLEMENTARY FIGURE S2
Cluster formation of 20 mer CTL epitopes of S-glycoprotein of Wuhan strain and B.1.351, B.1.1.28/triple mutant, B.1.1.7, and B.1.429 variant using the threshold 10% level to 80% level. **(A)** Cluster formation at 10% level. **(B)** Cluster formation at 20% level. **(C)** Cluster formation at 30% level. **(D)** Cluster formation at 40% level. **(E)** Cluster formation at 50% level. **(F)** Cluster formation at 60% level. **(G)** Cluster formation at 70% level. **(H)** Cluster formation at 80% level.

SUPPLEMENTARY FIGURE S3
Percentage of secondary structure component (α-helix and β-sheet) calculated from CD spectra of S-glycoprotein of the Wuhan strain and B.1.351, B.1.1.28/triple mutant, B.1.1.7, B.1.429 variants. **(A)** Percentage of α-helix and β-sheet of S-glycoprotein of the Wuhan variant. **(B)** Percentage of α-helix and β-sheet of S-glycoprotein of the B.1.351 variant. **(C)** Percentage of α-helix and β-sheet of S-glycoprotein of the B.1.1.28/triple mutant variant. **(D)** Percentage of α-helix and β-sheet of S-glycoprotein of the B.1.1.7 variant. **(E)** Percentage of α-helix and β-sheet of S-glycoprotein of the B.1.429 variant.

SUPPLEMENTARY FIGURE S4
Comparison of α-helix and β-sheet and β turns of S-glycoprotein of the Wuhan strain and B.1.351, B.1.1.28/triple mutant, B.1.1.7, B.1.429 variants. **(A)** Comparison of α-helix and β-sheet of S-glycoprotein among Wuhan strain and B.1.351, B.1.1.28/triple mutant, B.1.1.7, B.1.429 variants. **(B)** Comparison of β turns of S-glycoprotein among Wuhan strain and B.1.351, B.1.1.28/triple mutant, B.1.1.7, B.1.429 variants.

References

Al-Shangiti, A. M., Naylor, C. E., Nair, S. P., Briggs, D. C., Henderson, B., and Chain, B. M. (2004). Structural relationships and cellular tropism of staphylococcal superantigen-like proteins. *Infect. Immun.* 72, 4261–4270. doi: 10.1128/IAI.72.7.4261-4270.2004

Anderson, C. S., McCall, P. R., Stern, H. A., Yang, H., and Topham, D. J. (2018). Antigenic cartography of H1N1 influenza viruses using sequence-based antigenic distance calculation. *BMC Bioinformatics* 19, 1–11. doi: 10.1186/s12859-018-2042-4

Andreatta, M., and Nielsen, M. (2018). Bioinformatics tools for the prediction of T-cell epitopes. *Methods Mol. Biol.* 1785, 269–281. doi: 10.1007/978-1-4939-7841-0_18

Bange, E. M., Han, N. A., Wileyto, P., Kim, J. Y., Gouma, S., Robinson, J., et al. (2021). $CD8^+$ T cells contribute to survival in patients with COVID-19 and hematologic cancer. *Nat. Med.* 27, 1280–1289. doi: 10.1038/s41591-021-01386-7

Baú, D., Martin, A. J., Mooney, C., Vullo, A., Walsh, I., and Pollastri, G. (2006). Distill: a suite of web servers for the prediction of one-, two-and three-dimensional structural features of proteins. *BMC Bioinformatics* 7, 1–8. doi: 10.1186/1471-2105-7-402

Bazan, J., Całkosiński, I., and Gamian, A. (2012). Phage display—A powerful technique for immunotherapy: 1. Introduction and potential of therapeutic applications. *Hum. Vaccin. Immunother.* 8, 1817–1828. doi: 10.4161/hv.21703

Bermudez, A., Alba, M. P., Vanegas, M., Patarroyo, M. A., and Patarroyo, M. E. (2018). Specific β-turns precede PPIIL structures binding to allele-specific HLA-DRβ1* PBRs in fully-protective malaria vaccine components. *Front. Chem.* 6:106. doi: 10.3389/fchem.2018.00106

Bhatnager, R., Bhasin, M., Arora, J., and Dang, A. S. (2020). Epitope based peptide vaccine against SARS-COV2: an immune-informatics approach. *J. Biomol. Struct. Dyn.* 39, 5690–5705. doi: 10.1080/07391102.2020.1787227

Bhattacharya, M., Sharma, A. R., Ghosh, P., Lee, S.-S., and Chakraborty, C. (2021). A next-generation vaccine candidate using alternative epitopes to protect against Wuhan and all significant mutant variants of SARS-CoV-2: an immunoinformatics approach. *Aging Dis.* 12, 2173–2195. doi: 10.14336/AD.2021.0518

Bhattacharya, M., Sharma, A. R., Patra, P., Ghosh, P., Sharma, G., Patra, B. C., et al. (2020a). Development of epitope-based peptide vaccine against novel coronavirus 2019 (SARS-COV-2): immunoinformatics approach. *J. Med. Virol.* 92, 618–631. doi: 10.1002/jmv.25736

Bhattacharya, M., Sharma, A. R., Patra, P., Ghosh, P., Sharma, G., Patra, B. C., et al. (2020b). A SARS-CoV-2 vaccine candidate: In-silico cloning and validation. *Inform. Med. Unlocked* 20:100394. doi: 10.1016/j.imu.2020.100394

Blum, J. S., Wearsch, P. A., and Cresswell, P. (2013). Pathways of antigen processing. *Annu. Rev. Immunol.* 31, 443–473. doi: 10.1146/annurev-immunol-032712-095910

Brüssow, H. (2021). COVID-19: emergence and mutational diversification of SARS-CoV-2. *Microb. Biotechnol.* 14, 756–768. doi: 10.1111/1751-7915.13800

Calis, J. J., Maybeno, M., Greenbaum, J. A., Weiskopf, D., De Silva, A. D., Sette, A., et al. (2013). Properties of MHC class I presented peptides that enhance immunogenicity. *PLoS Comput. Biol.* 9:e1003266. doi: 10.1371/journal.pcbi.1003266

Cele, S., Gazy, I., Jackson, L., Hwa, S.-H., Tegally, H., Lustig, G., et al. (2021). Escape of SARS-CoV-2 501Y. V2 from neutralization by convalescent plasma. *Nature* 593, 142–146. doi: 10.1038/s41586-021-03471-w

Chakraborty, C., Bhattacharya, M., and Sharma, A. R. (2021a). Present variants of concern and variants of interest of severe acute respiratory syndrome coronavirus 2: their significant mutations in S-glycoprotein, infectivity, re-infectivity, immune escape and vaccines activity. *Rev. Med. Virol.* 32:e2270. doi: 10.1002/rmv.2270

Chakraborty, C., Bhattacharya, M., Sharma, A. R., Lee, S.-S., and Agoramoorthy, G. (2021b). SARS-CoV-2 Brazil variant in Latin America: more serious research urgently needed on public health and vaccine protection. *Ann. Med. Sur.* 66:102428. doi: 10.1016/j.amsu.2021.102428

Chakraborty, C., Sharma, A. R., Bhattacharya, M., Agoramoorthy, G., and Lee, S.-S. (2021c). Evolution, mode of transmission, and mutational landscape of newly emerging SARS-CoV-2 variants. *MBio* 12, e01140–e01121. doi: 10.1128/mBio.01140-21

Chakraborty, C., Sharma, A., Sharma, G., Bhattacharya, M., and Lee, S. (2020). SARS-CoV-2 causing pneumonia-associated respiratory disorder (COVID-19): diagnostic and proposed therapeutic options. *Eur. Rev. Med. Pharmacol. Sci.* 24, 4016–4026. doi: 10.26355/eurrev_202004_20871

Chen, Z., and Wherry, E. J. (2020). T cell responses in patients with COVID-19. *Nat. Rev. Immunol.* 20, 529–536. doi: 10.1038/s41577-020-0402-6

Cheng, M. H., Zhang, S., Porritt, R. A., Rivas, M. N., Paschold, L., Willscher, E., et al. (2020). Superantigenic character of an insert unique to SARS-CoV-2 spike supported by skewed TCR repertoire in patients with hyperinflammation. *Proc. Natl. Acad. Sci. U. S. A* 117, 25254–25262. doi: 10.1073/pnas.2010722117

Davies, N. G., Abbott, S., Barnard, R. C., Jarvis, C. I., Kucharski, A. J., Munday, J. D., et al. (2021). Estimated transmissibility and impact of SARS-CoV-2 lineage B. 1.1.7 in England. *Science* 372, eabg3055. doi: 10.1126/science.abg3055

De Vries, S. J., Van Dijk, M., and Bonvin, A. M. (2010). The HADDOCK web server for data-driven biomolecular docking. *Nat. Protoc.* 5, 883–897. doi: 10.1038/nprot.2010.32

Dhanda, S. K., Vaughan, K., Schulten, V., Grifoni, A., Weiskopf, D., Sidney, J., et al. (2018). Development of a novel clustering tool for linear peptide sequences. *Immunology* 155, 331–345. doi: 10.1111/imm.12984

Dinesh, D. C., Chalupska, D., Silhan, J., Koutna, E., Nencka, R., Veverka, V., et al. (2020). Structural basis of RNA recognition by the SARS-CoV-2 nucleocapsid phosphoprotein. *PLoS Pathog.* 16:e1009100. doi: 10.1371/journal.ppat.1009100

Doi, H., Hiroishi, K., Shimazaki, T., Eguchi, J., Baba, T., Ito, T., et al. (2009). Magnitude of $CD8^+$ T-cell responses against hepatitis C virus and severity of hepatitis do not necessarily determine outcomes in acute hepatitis C virus infection. *Hepatol. Res.* 39, 256–265. doi: 10.1111/j.1872-034X.2008.00459.x

Doytchinova, I. A., and Flower, D. R. (2007). VaxiJen: a server for prediction of protective antigens, tumour antigens and subunit vaccines. *BMC Bioinformatics* 8, 1–7. doi: 10.1186/1471-2105-8-4

Drew, E. D., and Janes, R. W. (2020). PDBMD2CD: providing predicted protein circular dichroism spectra from multiple molecular dynamics-generated protein structures. *Nucleic Acids Res.* 48, W17–W24. doi: 10.1093/nar/gkaa296

Faria, N. R., Claro, I. M., Candido, D., Moyses Franco, L., Andrade, P. S., Coletti, T. M., et al. (2021). Genomic characterisation of an emergent SARS-CoV-2 lineage in manaus: preliminary findings. Version 1. medRxiv [Preprint]. doi: 10.1101/2021.02.26.21252554

Feliu, V., Vasseur, V., Grover, H. S., Chu, H. H., Brown, M. J., Wang, J., et al. (2013). Location of the CD8 T cell epitope within the antigenic precursor determines immunogenicity and protection against the toxoplasma gondii parasite. *PLoS Pathog.* 9:e1003449. doi: 10.1371/journal.ppat.1003449

Focosi, D., Tuccori, M., Baj, A., and Maggi, F. (2021). SARS-CoV-2 variants: a synopsis of In vitro efficacy data of convalescent plasma, currently marketed vaccines, and monoclonal antibodies. *Viruses* 13, 1211. doi: 10.3390/v13071211

Forni, D., Cagliani, R., Pontremoli, C., Mozzi, A., Pozzoli, U., Clerici, M., et al. (2021). Antigenic variation of SARS-CoV-2 in response to immune pressure. *Mol. Ecol.* 30, 3548–3559. doi: 10.1111/mec.15730

Gangaev, A., Ketelaars, S. L., Isaeva, O. I., Patiwael, S., Dopler, A., Hoefakker, K., et al. (2021). Identification and characterization of a SARS-CoV-2 specific $CD8^+$ T cell response with immunodominant features. *Nat. Commun.* 12, 1–14. doi: 10.1038/s41467-021-22811-y

García, L. F. (2020). Immune response, inflammation, and the clinical spectrum of COVID-19. *Front. Immunol.* 11:1441. doi: 10.3389/fimmu.2020.01441

Greenfield, N. J. (2006). Using circular dichroism spectra to estimate protein secondary structure. *Nat. Protoc.* 1, 2876–2890. doi: 10.1038/nprot.2006.202

Guo, J.-Y., Liu, I.-J., Lin, H.-T., Wang, M.-J., Chang, Y.-L., Lin, S.-C., et al. (2021). Identification of COVID-19 B-cell epitopes with phage-displayed peptide library. *J. Biomed. Sci.* 28, 1–13. doi: 10.1186/s12929-021-00740-8

Harndahl, M., Rasmussen, M., Roder, G., Dalgaard Pedersen, I., Sørensen, M., Nielsen, M., et al. (2012). Peptide-MHC class I stability is a better predictor than peptide affinity of CTL immunogenicity. *Eur. J. Immunol.* 42, 1405–1416. doi: 10.1002/eji.201141774

Harvey, W. T., Carabelli, A. M., Jackson, B., Gupta, R. K., Thomson, E. C., Harrison, E. M., et al. (2021). SARS-CoV-2 variants, spike mutations and immune escape. *Nat. Rev. Microbiol.* 19, 409–424. doi: 10.1038/s41579-021-00573-0

Huai, Z., Tong, Z., Mei, Y., and Mo, Y. (2021). Theoretical study of the spectral differences of the Fenna–Matthews–Olson protein from different species and their mutants. *J. Phys. Chem. B* 125, 8313–8324. doi: 10.1021/acs.jpcb.1c01686

Islam, M. S. B., Miah, M., Hossain, M. E., and Kibria, K. K. (2020). A conserved multi-epitope-based vaccine designed by targeting hemagglutinin protein of highly pathogenic avian H5 influenza viruses. *3 Biotech* 10, 1–16. doi: 10.1007/s13205-020-02544-3

Kar, T., Narsaria, U., Basak, S., Deb, D., Castiglione, F., Mueller, D. M., et al. (2020). A candidate multi-epitope vaccine against SARS-CoV-2. *Sci. Rep.* 10, 1–24. doi: 10.1038/s41598-020-67749-1

Kozakov, D., Hall, D. R., Xia, B., Porter, K. A., Padhorny, D., Yueh, C., et al. (2017). The ClusPro web server for protein–protein docking. *Nat. Protoc.* 12, 255–278. doi: 10.1038/nprot.2016.169

Kumar, S., Maurya, V. K., Prasad, A. K., Bhatt, M. L., and Saxena, S. K. (2020). Structural, glycosylation and antigenic variation between 2019 novel coronavirus

(2019-nCoV) and SARS coronavirus (SARS-CoV). *Virus* 31, 13–21. doi: 10.1007/s13337-020-00571-5

Lafon, M. (2000). Les superantigènes viraux. *Rev. Med. Interne* 21, 713–716. doi: 10.1016/S0248-8663(00)80034-X

Larralde, O., and Petrik, J. (2017). Phage-displayed peptides that mimic epitopes of hepatitis E virus capsid. *Med. Microbiol. Immunol.* 206, 301–309. doi: 10.1007/s00430-017-0507-0

Li, Z., and Hirst, J. D. (2020). Computed optical spectra of SARS-CoV-2 proteins. *Chem. Phys. Lett.* 758:137935. doi: 10.1016/j.cplett.2020.137935

Li, J., Li, X., and He, D. (2019). A directed acyclic graph network combined with CNN and LSTM for remaining useful life prediction. *IEEE Access* 7, 75464–75475. doi: 10.1109/ACCESS.2019.2919566

Li, J., and Liu, W. (2020). Puzzle of highly pathogenic human coronaviruses (2019-nCoV). *Protein Cell* 11, 235–238. doi: 10.1007/s13238-020-00693-y

Li, R., Ma, X., Deng, J., Chen, Q., Liu, W., Peng, Z., et al. (2021). Differential efficiencies to neutralize the novel mutants B. 1.1.7 and 501Y. V2 by collected sera from convalescent COVID-19 patients and RBD nanoparticle-vaccinated rhesus macaques. *Cell. Mol. Immunol.* 18, 1058–1060. doi: 10.1038/s41423-021-00641-8

Li Pira, G., Ivaldi, F., Moretti, P., and Manca, F. (2010). High throughput T epitope mapping and vaccine development. *J. Biomed. Biotechnol.* 2010:325720. doi: 10.1155/2010/325720

Liu, J., Sun, Y., Qi, J., Chu, F., Wu, H., Gao, F., et al. (2010). The membrane protein of severe acute respiratory syndrome coronavirus acts as a dominant immunogen revealed by a clustering region of novel functionally and structurally defined cytotoxic T-lymphocyte epitopes. *J. Infect. Dis.* 202, 1171–1180. doi: 10.1086/656315

Mayrose, I., Penn, O., Erez, E., Rubinstein, N. D., Shlomi, T., Freund, N. T., et al. (2007). Pepitope: epitope mapping from affinity-selected peptides. *Bioinformatics* 23, 3244–3246. doi: 10.1093/bioinformatics/btm493

Meckiff, B. J., Ramírez-Suástegui, C., Fajardo, V., Chee, S. J., Kusnadi, A., Simon, H., et al. (2020). Imbalance of regulatory and cytotoxic SARS-CoV-2-reactive $CD4^+$ T cells in COVID-19. *Cell* 183, 1340–1353.e16. doi: 10.1016/j.cell.2020.10.001

Meng, B., Kemp, S. A., Papa, G., Datir, R., Ferreira, I. A., Marelli, S., et al. (2021). Recurrent emergence of SARS-CoV-2 spike deletion H69/V70 and its role in the Alpha variant B.1.1.7. *Cell Reports* 35:109292. doi: 10.1016/j.celrep.2021.109292

Micsonai, A., Wien, F., Kernya, L., Lee, Y.-H., Goto, Y., Réfrégiers, M., et al. (2015). Accurate secondary structure prediction and fold recognition for circular dichroism spectroscopy. *Proc. Natl. Acad. Sci.* 112, E3095–E3103. doi: 10.1073/pnas.1500851112

Mittal, A., Khattri, A., and Verma, V. (2022). Structural and antigenic variations in the spike protein of emerging SARS-CoV-2 variants. *PLoS Pathog.* 18:e1010260. doi: 10.1371/journal.ppat.1010260

Naveca, F., Nascimento, V., Souza, V., Corado, A., Nascimento, F., Silva, G., et al. (2021). Phylogenetic relationship of SARS-CoV-2 sequences from Amazonas with emerging Brazilian variants harboring mutations E484K and N501Y in the Spike protein. *Virological. Org.* 1, 1–8.

Parsons, L.M., Bouwman, K.M., Azurmendi, H., De Vries, R.P., and Cipollo, J.F. MH Verheije. (2019). Glycosylation of the viral attachment protein of avian coronavirus is essential for host cell and receptor binding. *J. Biol. Chem.* 294, 7797–7809, doi: 10.1074/jbc.RA119.007532

Peacock, T., Reddy, K., James, J., Adamiak, B., Barclay, W., Shelton, H., et al. (2016). Antigenic mapping of an H9N2 avian influenza virus reveals two discrete antigenic sites and a novel mechanism of immune escape. *Sci. Rep.* 6, 1–12. doi: 10.1038/srep18745

Pettersen, E. F., Goddard, T. D., Huang, C. C., Couch, G. S., Greenblatt, D. M., Meng, E. C., et al. (2004). UCSF Chimera—a visualization system for exploratory research and analysis. *J. Comput. Chem.* 25, 1605–1612. doi: 10.1002/jcc.20084

Raza, M. T., Mizan, S., Yasmin, F., Akash, A.-S., and Shahik, S. M. (2021). Epitope-based universal vaccine for Human T-lymphotropic virus-1 (HTLV-1). *PLoS One* 16:e0248001. doi: 10.1371/journal.pone.0248001

Rencilin, C. F., Rosy, J. C., Mohan, M., Coico, R., and Sundar, K. (2021). Identification of SARS-CoV-2 CTL epitopes for development of a multivalent subunit vaccine for COVID-19. *Infect. Genet. Evol.* 89:104712. doi: 10.1016/j.meegid.2021.104712

Rist, M. J., Neller, M. A., Burrows, J. M., and Burrows, S. R. (2015). T cell epitope clustering in the highly immunogenic BZLF1 antigen of Epstein-Barr virus. *J. Virol.* 89, 703–712. doi: 10.1128/JVI.02642-14

Rochman, N. D., Wolf, Y. I., Faure, G., Mutz, P., Zhang, F., and Koonin, E. V. (2021). Ongoing global and regional adaptive evolution of SARS-CoV-2. *Proc. Natl. Acad. Sci. U. S. A.* 118, –e2104241118. doi: 10.1073/pnas.2104241118

Rogers, D. M., Jasim, S. B., Dyer, N. T., Auvray, F., Réfrégiers, M., and Hirst, J. D. (2019). Electronic circular dichroism spectroscopy of proteins. *Chem* 5, 2751–2774. doi: 10.1016/j.chempr.2019.07.008

Schmidt, M. E., and Varga, S. M. (2018). The CD8 T cell response to respiratory virus infections. *Front. Immunol.* 9:678. doi: 10.3389/fimmu.2018.00678

Shen, X., Tang, H., McDanal, C., Wagh, K., Fischer, W., Theiler, J., et al. (2021). SARS-CoV-2 variant B. 1.1.7 is susceptible to neutralizing antibodies elicited by ancestral spike vaccines. *Cell Host Microbe* 29, 529–539.e523. doi: 10.1016/j.chom.2021.03.002

Shey, R. A., Ghogomu, S. M., Shintouo, C. M., Nkemngo, F. N., Nebangwa, D. N., Esoh, K., et al. (2021). Computational design and preliminary serological analysis of a novel multi-epitope vaccine candidate against Onchocerciasis and related filarial diseases. *Pathogens* 10, 99. doi: 10.3390/pathogens10020099

Shi, J., Zhang, J., Li, S., Sun, J., Teng, Y., Wu, M., et al. (2015). Epitope-based vaccine target screening against highly pathogenic MERS-CoV: an in silico approach applied to emerging infectious diseases. *PLoS One* 10:e0144475. doi: 10.1371/journal.pone.0144475

Sievers, F., and Higgins, D. G. (2018). Clustal Omega for making accurate alignments of many protein sequences. *Protein Sci.* 27, 135–145. doi: 10.1002/pro.3290

Sievers, F., and Higgins, D. G. (2021). The clustal omega multiple alignment package. *Methods Mol. Biol.* 2231, 3–16. doi: 10.1007/978-1-0716-1036-7_1

Singh, H., and Raghava, G. J. B. (2003). ProPred1: prediction of promiscuous MHC class-I binding sites. *Bioinformatics* 19, 1009–1014. doi: 10.1093/bioinformatics/btg108

Soria-Guerra, R. E., Nieto-Gomez, R., Govea-Alonso, D. O., and Rosales-Mendoza, S. (2015). An overview of bioinformatics tools for epitope prediction: implications on vaccine development. *J. Biomed. Inform.* 53, 405–414. doi: 10.1016/j.jbi.2014.11.003

Stufano, A., Capone, G., Pesetti, B., Polimeno, L., and Kanduc, D. (2010). Clustering of rare peptide segments in the HCV immunome. *Self* 1, 154–162. doi: 10.4161/self.1.2.11391

Sun, H., Yang, J., Zhang, T., Long, L.-P., Jia, K., Yang, G., et al. (2013). Using sequence data to infer the antigenicity of influenza virus. *MBio* 4, e00230–e00213. doi: 10.1128/mBio.00230-13

Tay, M. Z., Poh, C. M., Rénia, L., MacAry, P. A., and Ng, L. F. (2020). The trinity of COVID-19: immunity, inflammation and intervention. *Nat. Rev. Immunol.* 20, 363–374. doi: 10.1038/s41577-020-0311-8

Tscharke, D. C., Croft, N. P., Doherty, P. C., and La Gruta, N. L. (2015). Sizing up the key determinants of the $CD8^+$ T cell response. *Nat. Rev. Immunol.* 15, 705–716. doi: 10.1038/nri3905

Vita, R., Overton, J. A., Greenbaum, J. A., Ponomarenko, J., Clark, J. D., Cantrell, J. R., et al. (2015). The immune epitope database (IEDB) 3.0. *Nucleic Acids Res.* 43, D405–D412. doi: 10.1093/nar/gku938

Vivona, S., Gardy, J. L., Ramachandran, S., Brinkman, F. S., Raghava, G. P. S., Flower, D. R., et al. (2008). Computer-aided biotechnology: from immuno-informatics to reverse vaccinology. *Trends Biotechnol.* 26, 190–200. doi: 10.1016/j.tibtech.2007.12.006

Vujovic, M., Degn, K. F., Marin, F. I., Schaap-Johansen, A.-L., Chain, B., Andresen, T. L., et al. (2020). T cell receptor sequence clustering and antigen specificity. *Comput. Struct. Biotechnol. J.* 18, 2166–2173. doi: 10.1016/j.csbj.2020.06.041

Wang, P., Casner, R. G., Nair, M. S., Wang, M., Yu, J., Cerutti, G., et al. (2021a). Increased resistance of SARS-CoV-2 variant P. 1 to antibody neutralization. *Cell Host Microbe* 29, 747–751.e4. doi: 10.1016/j.chom.2021.04.007

Wang, L., Deng, X., Liu, H., Zhao, L., You, X., Dai, P., et al. (2016). The mimic epitopes of Mycobacterium tuberculosis screened by phage display peptide library have serodiagnostic potential for tuberculosis. *Pathog. Dis.* 74, ftw091. doi: 10.1093/femspd/ftw091

Wang, P., Nair, M. S., Liu, L., Iketani, S., Luo, Y., Guo, Y., et al. (2021b). Antibody resistance of SARS-CoV-2 variants B. 1.351 and B. 1.1. 7. *Nature* 593, 130–135. doi: 10.1038/s41586-021-03398-2

Wong, Y. C., Croft, S., Smith, S. A., Lin, L. C., Cukalac, T., La Gruta, N. L., et al. (2019). Modified vaccinia virus Ankara can induce optimal $CD8^+$ T cell responses to directly primed antigens depending on vaccine design. *J. Virol.* 93, e01154–e01119. doi: 10.1128/JVI.01154-19

Wu, C.-H., Liu, I.-J., Lu, R.-M., and Wu, H.-C. (2016). Advancement and applications of peptide phage display technology in biomedical science. *J. Biomed. Sci.* 23, 1–14. doi: 10.1186/s12929-016-0223-x

Zhang, Q., Wang, P., Kim, Y., Haste-Andersen, P., Beaver, J., Bourne, P. E., et al. (2008). Immune epitope database analysis resource (IEDB-AR). *Nucleic Acids Res.* 36, W513–W518. doi: 10.1093/nar/gkn254

Zheng, M., and Song, L. (2020). Novel antibody epitopes dominate the antigenicity of spike glycoprotein in SARS-CoV-2 compared to SARS-CoV. *Cell. Mol. Immunol.* 17, 536–538. doi: 10.1038/s41423-020-0385-z

Zost, S. J., Wu, N. C., Hensley, S. E., and Wilson, I. A. (2019). Immunodominance and antigenic variation of influenza virus hemagglutinin: implications for design of universal vaccine immunogens. *J. Infect. Dis.* 219, S38–S45. doi: 10.1093/infdis/jiy696

frontiers | Frontiers in Microbiology

TYPE Original Research
PUBLISHED 08 September 2022
DOI 10.3389/fmicb.2022.975632

OPEN ACCESS

EDITED BY
Yang Yang,
Iowa State University, United States

REVIEWED BY
Hualei Wang,
Jilin University, China
Guigen Zhang,
Sun Yat-sen University, China

*CORRESPONDENCE
Suttipun Sungsuwan
suttipun.sun@biotec.or.th

SPECIALTY SECTION
This article was submitted to Frontiers in Microbiology | Virology, a section of the journal Frontiers in Microbiology

RECEIVED 22 June 2022
ACCEPTED 15 August 2022
PUBLISHED 08 September 2022

CITATION
Sungsuwan S, Kadkanklai S, Mhuantong W, Jongkaewwattana A and Jaru-Ampornpan P (2022) Zinc-finger antiviral protein-mediated inhibition of porcine epidemic diarrhea virus growth is antagonized by the coronaviral nucleocapsid protein. *Front. Microbiol.* 13:975632. doi: 10.3389/fmicb.2022.975632

Zinc-finger antiviral protein-mediated inhibition of porcine epidemic diarrhea virus growth is antagonized by the coronaviral nucleocapsid protein

Suttipun Sungsuwan[1]*, Supasek Kadkanklai[1], Wuttichai Mhuantong[2], Anan Jongkaewwattana[1] and Peera Jaru-Ampornpan[1]

[1]Virology and Cell Technology Laboratory, National Center for Genetic Engineering and Biotechnology (BIOTEC), National Science and Technology Development Agency (NSTDA), Khlong Nueng, Pathum Thani, Thailand, [2]Enzyme Technology Laboratory, National Center for Genetic Engineering and Biotechnology (BIOTEC), National Science and Technology Development Agency (NSTDA), Khlong Nueng, Pathum Thani, Thailand

Coronaviruses have long posed a major threat not only to human health but also to agriculture. Outbreaks of an animal coronavirus such as porcine epidemic diarrhea virus (PEDV) can cause up-to-100% mortality in suckling piglets, resulting in devastating effects on the livestock industry. Understanding how the virus evades its host's defense can help us better manage the infection. Zinc-finger antiviral protein (ZAP) is an important class of host antiviral factors against a variety of viruses, including the human coronavirus. In this study, we have shown that a representative porcine coronavirus, PEDV, can be suppressed by endogenous or porcine-cell-derived ZAP in VeroE6 cells. An uneven distribution pattern of CpG dinucleotides in the viral genome is one of the factors contributing to suppression, as an increase in CpG content in the nucleocapsid (N) gene renders the virus more susceptible to ZAP. Our study revealed that the virus uses its own nucleocapsid protein (pCoV-N) to interact with ZAP and counteract the activity of ZAP. The insights into coronavirus-host interactions shown in this work could be used in the design and development of modern vaccines and antiviral agents for the next pandemic.

KEYWORDS

coronavirus, virus–host interaction, porcine epidemic diarrhea virus, zinc-finger antiviral protein, nucleocapsid protein

Introduction

Porcine epidemic diarrhea virus (PEDV) is an enveloped virus in the family *Coronaviridae*. The virus infects swine intestinal epithelial cells and causes severe watery diarrhea, vomiting, and dehydration. The high mortality rate due to the infection, especially in suckling piglets, causes severe economic losses in pig production worldwide. Despite continued development, available PEDV vaccines are still suboptimal in their efficacy, making the epidemic a long-term threat to the swine industry. Understanding how a virus antagonizes antiviral factors in a host could provide insights into the innovative design of an effective vaccine as well as a therapeutic intervention for current and emerging outbreaks.

In response to viral infection, hosts have evolved sensing systems that recognize foreign components to trigger innate immune defenses. Zinc-finger antiviral protein (ZAP), also known as Zinc-finger CCCH-type containing antiviral 1 (PARP13 or ZC3HAV1), is a part of the host immune system that acts as a restriction factor against a variety of RNA and DNA viruses (Ficarelli et al., 2021). As products of alternative RNA splicing, the short and long isoforms of ZAP (ZAPS and ZAPL, respectively) share the N-terminal domain, which contains a highly conserved zinc finger domain. The long isoform has an additional C-terminal portion with an inactive poly-(ADP-ribose) polymerase (PARP)-like domain that has been shown to contribute to increased antiviral activity (Schwerk et al., 2019; Kmiec et al., 2021). In general, ZAPS is upregulated as one of the interferon (IFN)-stimulated genes (ISGs) during the type I IFN response, whereas ZAPL is constitutively expressed and less dependent on stimulation by interferon or ISGs (Schwerk et al., 2019; Kmiec et al., 2021).

Zinc-finger antiviral protein selectively binds viral or non-proprietary RNAs with high CpG content, which is abundant in some viruses but underrepresented in the host genome, and recruits cellular endonucleases to degrade the bound viral RNAs (Takata et al., 2017; Ficarelli et al., 2019; Luo et al., 2020). As a result, the amount of viral RNA species decreases significantly, hindering viral protein production and viral replication. To escape detection and subsequent restriction by ZAP, many viruses evolve to suppress CpG dinucleotide content in their own genome (Rima and McFerran, 1997; Cheng et al., 2013). Alternatively, some viruses evolve an effector that counteracts the antiviral function of ZAP. For instance, the NS1 protein of influenza A virus antagonizes the antiviral function of ZAP by preventing ZAP from binding to its viral mRNA target (Tang et al., 2017). Porcine reproductive and respiratory syndrome virus (PRRSV) uses its nsp4 protease to degrade ZAP (Zhao et al., 2020), while enterovirus A71 uses its 3C protease (Xie et al., 2018). Among coronaviruses, only SARS-CoV-2 has been reported to be suppressed by ZAP in a host (Nchioua et al., 2020). However, it remains unclear whether the restriction generally affects all coronaviruses and if the pressure drives them to evolve antagonistic mechanisms against ZAP. The interplay between coronaviruses and ZAP still awaits further investigation.

As a coronavirus, PEDV has a single-stranded positive-sense ∼28-kb RNA genome encoding four structural proteins: spike (S), membrane (M), envelope (E), and nucleocapsid (N). The N protein is one of the most abundant structural proteins produced in infected host cells. Its main function is to oligomerize to form a scaffold associated with viral genomic RNA. This forms the RNA-protein complex that constitutes the inner core of virions. In addition to its main function, N also suppresses host immunity, facilitates viral assembly, and promotes viral genome replication (McBride et al., 2014). We have previously shown that nucleocapsid proteins of porcine alpha-coronaviruses, including PEDV and Transmissible gastroenteritis virus (TGEV), can increase viral RNA content and promote PEDV replication. However, it is not yet clear whether nucleocapsid proteins increase viral RNA production or protect it from degradation.

In this work, the susceptibility of PEDV to ZAP was investigated. We showed that local CpG-rich clusters in the PEDV genome could contribute to suppression by ZAP. We also demonstrated how the virus can use its own nucleocapsid protein to counteract the activity of ZAP. This study altogether demonstrated an alternative function of the nucleocapsid protein in maintaining high viral titers in a host expressing ZAP.

Materials and methods

Cell line and plasmid construction

Human embryonic kidney (HEK) 293T (ATCC CRL-3216), African green monkey (VeroE6) cells (ATCC CRL-1586), and their derivatives were grown and maintained in Opti-MEM^{TM} (Gibco^{TM}, Thermo Scientific, Waltham, MA, United States) at 37°C and 5% CO_2. All culture media were supplemented with 10% fetal bovine serum (FBS) and 1% antibiotic-antimycotic solution.

The plasmids for the expression of C-terminal Myc-tagged PEDV-N, TGEV-N, and SADS-CoV-N have been described previously (Jaru-Ampornpan et al., 2017; Sungsuwan et al., 2020). Porcine ZAP (pZAP) genes were PCR-amplified from cDNA reverse transcribed from cellular RNA extracted from porcine alveolar macrophages (PAMs). The forward primer for pZAPL/S (pZAP-F), the reverse primer for pZAPL (pZAPL-R), and the reverse primer for pZAPS (pZAPS-R) are listed in the primer list (**Supplementary Table 1**). By In-Fusion ligation (Takara Bio, Shiga, Japan), the amplified PCR products were ligated into the pre-digested pCAGGS vector at *Mlu*I and *Kpn*I restriction sites with an indicated C-terminal tag. The virus PEDV-AVCT12-mCherry and their infectious clones (pSMART-BAC- mCherry-PEDVAVCT12 [pPEDV-mCh]) were

described previously (Jengarn et al., 2015; Jaru-Ampornpan et al., 2017).

Generation of zinc-finger antiviral protein-KO cell lines

Zinc-finger antiviral protein-KO HEK293T or VeroE6 ZAP-KO cell pools were generated by the CRISPR-Cas9 approach using a guide RNA (5′-GGCCGGGATCACCCGATCGG-3′). ZAP targeting guide RNA was cloned downstream of the U6 promoter into the lentiCRISPR v2 vector, a gift from Feng Zhang (Addgene plasmid # 52961; RRID:Addgene_52961)[1] (The resulting plasmid is referred to as lentiCRISPRv2-gZAP-Cas9-P2A-GFP). Wild-type cells were transiently transfected with the lentiCRISPRv2-gZAP-Cas9-P2A-GFP plasmid using FuGENE HD (Promega, Madison, WI, United States), according to the manufacturer's instructions. At 48 hpt, the transfected cells were sorted based on GFP expression using a fluorescence-activated cell sorter (BD FACSAria^{TM} Fusion, Singapore) to isolate the pool of GFP expressing cells into single isolated cells. Single cell clones that continued to grow were selected for verification of gene knockout. The absence of ZAP expression in the sorted cells was verified by SDS-PAGE/western blot analysis compared to wild-type cells.

Generation of VeroE6 cell lines stably expressing HA-tagged pZAPL

The ZAP-KO VeroE6 cell line expressing HA-tagged pZAPL was constructed by lentivirus transduction. Lentiviruses carrying the C-terminal HA-tagged pZAPL gene were prepared by co-transfection of pSIN-CSGW-UbEM carrying the inserted pZAPL-HA gene with a packaging plasmid encoding Gag, Pol, Rev, and Tat (pCMV-ΔR8.91) and a plasmid expressing the lentiviral VSV envelope glycoprotein (pMD2.G) into HEK293T cells. At 48 hpt, the supernatants containing the lentiviruses were harvested and filtered through a 0.45-μm filter. The filtered supernatants were then used for transduction of the ZAP-KO VeroE6 cells. A single clone of the transduced cells expressing pZAP was sorted based on GFP expression using a fluorescence-activated cell sorter (BD FACSAria^{TM} Fusion, Singapore) and verified by SDS-PAGE/western blot analysis.

Viral infection

VeroE6-derived cell lines (5×10^5 cells/ml) plated in a six-well plate were inoculated with 1 ml of the virus at the indicated multiplicity of infection (MOI) for an hour. The inoculum was then removed, and the cells were washed once with PBS and replaced with 2 ml of fresh OptiMEM containing 0.1% TrypLE. The extent of PEDV infection was monitored by mCherry fluorescence under a fluorescence microscope. Cell lysates or supernatants were harvested at the indicated time points for further analysis. To study porcine CoV-N's ability to rescue ZAP-mediated suppression (**Figure 8**), VeroE6 cells were transfected with 2 μg of the pCAGGS-plasmid expressing the protein and incubated for 24 h to allow protein expression. Cells were then infected with the virus. To image cytopathic effect (CPE), the infected cells were washed twice with Phosphate-buffered saline (PBS) and fixed with cold 70% acetone and stained with crystal-violet-based plaque staining solution for 20 min. After the staining solution was removed, the plates were washed several times with water and dried before imaging.

Western blot analysis

Virus-infected or plasmid-transfected cells were harvested and lysed with RIPA lysis buffer (25 mM Tris–HCl pH 7.4, 150 mM NaCl, 1 mM EDTA, 1% NP-40, and 5% glycerol, supplemented with a protease inhibitor cocktail (Halt^{TM} Protease Inhibitor Cocktail, Thermo Fisher Scientific, MA, United States). The mixture was centrifuged at 12,000 g, 4°C for 10 min and the resulting supernatants were mixed with sodium dodecyl sulfate polyacrylamide gel electrophoresis (SDS-PAGE) loading buffer and boiled for 5 min. Proteins from the cell lysates were separated using SDS-PAGE, and then transferred to nitrocellulose membranes (Bio-Rad Laboratories, CA, United States). The membrane was blocked with 5% skim milk prior to incubation with the indicated primary antibodies. Horseradish peroxidase (HRP)-conjugated goat anti-mouse IgG (Biolegend, CA, United States) or (HRP)-conjugated donkey anti-rabbit IgG (Biolegend, CA, United States) were used as secondary antibodies. Primary antibodies used in this study included mouse-anti-Myc (Thermo Fisher Scientific, MA, United States), rabbit-anti-FLAG (ab1162, abcam, Cambridge, United Kingdom), rabbit-anti-HA (ab9110, abcam, Cambridge, United Kingdom), and mouse-anti-PEDV-N (SD 6–29, Medgene labs, SD, United States), rabbit polyclonal anti-Zinc finger antiviral protein (ab154680, abcam, Cambridge, United kingdom).

Virus titration ($TCID_{50}$ assay)

VeroE6 cells stably expressing TGEV-N-FLAG (Sungsuwan et al., 2020) were plated overnight in 96-well plates to obtain monolayers of the cells. The culture media were removed, and the cells were washed once with PBS. Supernatants obtained from infected cells were prepared at 10-fold serial dilutions

1 http://n2t.net/addgene:52961

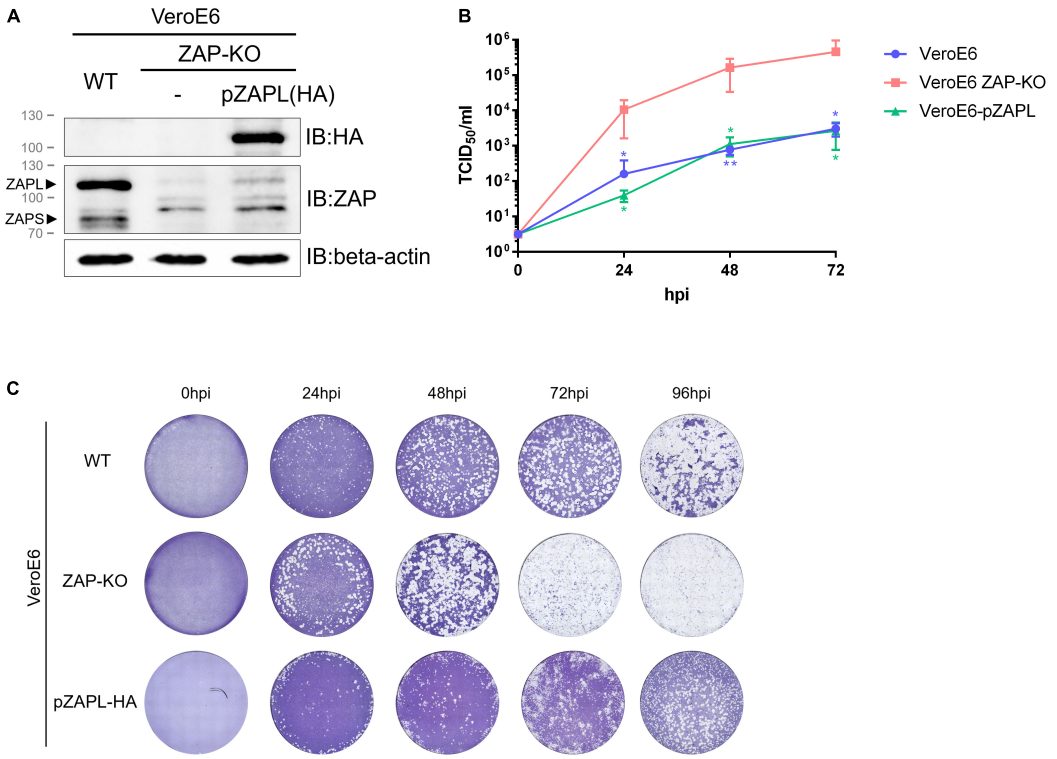

FIGURE 1
Replication of porcine epidemic diarrhea virus (PEDV) is suppressed in VeroE6 cells by an endogenous or porcine cell-derived long isoform of zinc-finger antiviral protein (ZAP). **(A)** The VeroE6 ZAP-KO cell line was verified by western blot analysis. To generate a stable VeroE6 cell expressing only the HA-tagged long isoform of pZAP (VeroE6-pZAPL), VeroE6 ZAP-KO cells were transduced using the lentiviral transduction method. SDS-PAGE/western against the HA tag confirmed expression of HA-tagged pZAPL in the transduced cells. **(B)** VeroE6, VeroE6 ZAP-KO, or VeroE6-pZAPL cells were infected with PEDV (AVCT12 strain) at MOI = 0.0001. PEDV growth kinetics were monitored at the indicated time points using the $TCID_{50}$ assay. Values shown are averages ± SEM of three independent experiments (Student's *t*-test, $^{**}p < 0.05$, $^{**}p < 0.005$). **(C)** Representative images showing the spread of virus at different time points post-infection were visualized with cytopathic effect (CPE) by crystal violet staining.

in OptiMEM containing 0.1% TrypLE. The diluted virus was added to the pre-seeded cells (eight wells for each dilution). At 72 h post-infection (hpi), the infected cells were examined by mCherry expression under a fluorescence microscope. The $TCID_{50}$ of the viral titers was determined using the Reed-Muench method (Reed and Muench, 1938).

Generation of sequences encoding the porcine epidemic diarrhea virus-N gene with varied CpG content

To generate PEDV-N sequences with high CpG content, an in-house algorithm was developed based on the concept of codon pair bias deoptimization introduced by Coleman et al. (2008) via python3,[2] to recode a gene by replacing native codon pairs with synonymous codon pairs and obtain a sequence with an expected codon-paired bias (CPB) value. The generated codon-paired bias deoptimized (CPD) sequences were further analyzed using SSE software (Simmonds, 2012) and sorted according to the difference in RNA folding energy compared to the original sequence. Selected sequences with the highest similarity in RNA folding energy profile compared to that of the native N gene sequence were finally selected. The selected sequences were chemically synthesized *de novo* by an oligonucleotide synthesis service provider (Integrated DNA Technologies, Inc.; IDT, Singapore), and used for subsequent experiments.

Construction of infectious clones with CPD-N genes and rescues of reverse genetics-derived CPD-porcine epidemic diarrhea virus

Oligonucleotide fragments extending from the early S gene to the 3′ end of the M gene and fused to the full length of

2 http://citebay.com/how-to-cite/python/

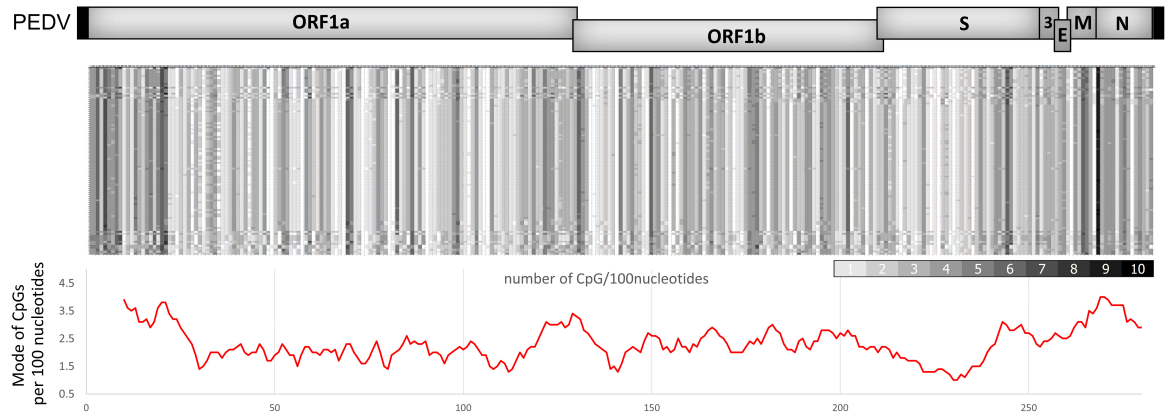

FIGURE 2
CpG dinucleotide distribution in porcine epidemic diarrhea virus (PEDV) genomes. **(top)** Representative complete genome sequences of various PEDV strains were aligned (NCBI accession numbers are listed in the **Supplementary material**). The number of CpGs per 100 nucleotides of each segment was analyzed. Results were shown in a heat map (white = 0 CpGs/100-bp, black = 10 CpGs/100-bp). **(Bottom)** Mode of CpGs per 100-bp from the aligned sequences in each region of the PEDV genomes. The graph below the heat map was plotted by a moving average trend line for every 1,000-bp (10 values of CpGs/100-bp) showing high CpG regions in the early 5′ region of ORF1a, the frameshift region between ORF1a and ORF1b, and the structural genes downstream of the spike gene.

various CPD-N genes were obtained by overlap PCR extension of the S-mCherry-E-M fragments and the corresponding full length CPD-N (**Figure 3D**). The purified PCR product was inserted by In-Fusion ligation into a pre-digested vector of pPEDV.mCh.*Mlu*I.3UTR at *Pac*I and *Mlu*I restriction sites. To rescue the virus from the infectious clone, HEK293T cells were transfected with 3 μg of the infectious clone plasmid carrying the indicated CPD-N sequence and 0.5 μg of PEDV N expressing plasmid in order to enhance virus production (Liwnaree et al., 2019). FuGENE® HD (Promega, Madison, WI, United States) was used as a transfection reagent, according to the manufacturer's instructions. At 72 hpt, supernatants were transferred to adsorb onto VeroE6-PEDV N cells for 1 h at 37°C. The inocula were then removed, and the cells were washed twice with PBS. 2 ml OptiMEM containing 0.1% TrypLE (Thermo Fisher Scientific, MA, United States) was added, and the cells were kept in the incubator at 37°C and 5% CO_2 for 72 h. The rescued viruses were harvested by the freeze-thaw method and titrated by the $TCID_{50}$ method. The harvested viruses were kept in −80°C until use.

Co-immunoprecipitation

HEK293T cells in 6-well plates were transfected with 0.5–1.0 μg of plasmids using FuGENE HD (Promega, Madison, WI, United States), according to the manufacturer's instructions. The cells were lysed on ice in lysis buffer (50 mM Tris–HCl pH 8.0, 150 mM NaCl, 5 mM EDTA, 1% NP-40 supplemented with a protease inhibitor cocktail). The lysates or mixed lysates were centrifuged at 20,000 g for 10 min at 25°C. The lysates were aliquoted into 50 μl for immunoblot and 150 μl for co-immunoprecipitation. Co-immunoprecipitated lysates were incubated with 25 μg of agarose beads conjugated to the indicated antibody (Pierce™ anti-c-Myc or HA-Epitope Tag Antibody agarose, Thermo Fisher Scientific, IL, United States) overnight at 4°C under rotation. The lysates were washed three times with wash buffer (50 mM Tris–HCl pH 8.0, 550 mM NaCl, 5 mM EDTA, 1% NP-40), and then eluted with 25 μl 2X non-reducing dye then boiled for 5 min and supplemented with 5 μL 0.5M DTT. Proteins were analyzed by SDS-PAGE/western blot analysis.

Immuno-fluorescence imaging

VeroE6 ZAP-KO cells plated on glass coverslips were transfected with the indicated plasmids. At 48 hpt, cells were fixed with 4% paraformaldehyde at 4°C for 20 min and washed three times with PBS. The fixed cells were permeabilized and blocked for 1 h with 1% BSA, 1% FBS, and 0.1% Triton-X in PBS. Then, cells were stained with rabbit anti-HA (pZAPL) (1:500) and mouse anti-PEDV-N (1:500) diluted in 1% BSA in PBS for 1 h. After washing three times with PBS, cells were stained with AlexaFluor-488 goat anti-mouse IgG antibody (1:500) or AlexaFluor-568 goat anti-rabbit IgG antibody (Invitrogen, Thermo Fisher Scientific, OR, United States) (1:500) diluted in 1% BSA in PBS for 1 h and then washed with PBS three times. Glass coverslips were mounted on slides using ProLong™ Diamond Antifade Mountant with DAPI (Invitrogen, Thermo Fisher Scientific, OR, United States). Protein localization was observed and analyzed using Olympus Fluoview-1000 confocal microscopy.

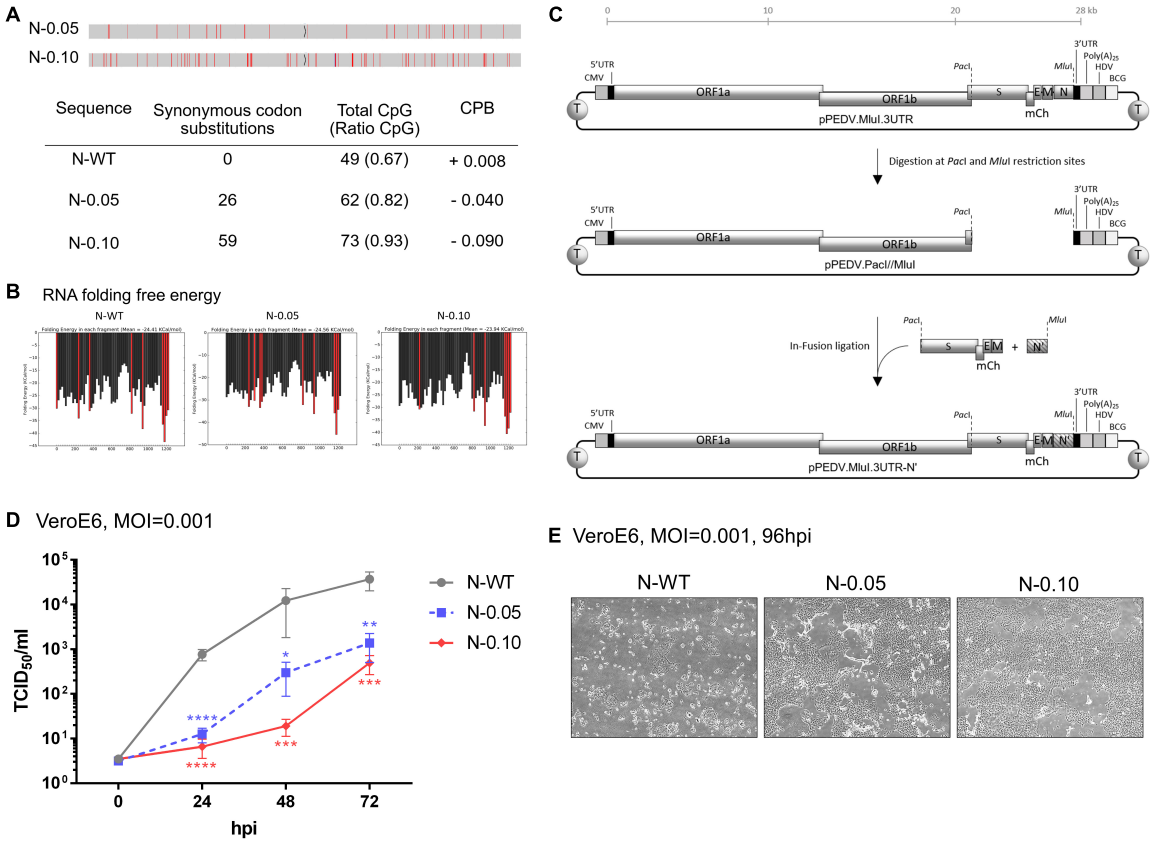

FIGURE 3
Increasing CpG content in the N gene results in slower growth of porcine epidemic diarrhea virus (PEDV) in VeroE6 cells. **(A)** Analysis of generated nucleotide sequences encoding PEDV-N protein with varied CpG dinucleotides. Red lines in a sequence bar display silent mutations where the original nucleotides are replaced to increase CpG content. Synonymous codon substitutions, CpG dinucleotide compositions, and codon-paired bias (CPB) values of each sequence are listed in the Table. **(B)** RNA folding free energy profiles for each 100- and 20-base window of the generated CPD-N sequences compared to the native N gene sequence. The red bars indicate the high (<−30 Kcal/mol) free energy of RNA folding. **(C)** Construction of infectious clones using the N genes with high CpG content. PCR-amplified products of an oligonucleotide fragment from the S gene to the M gene (S-mCherry-E-M) and another fragment of various N genes (N′) were inserted into a pre-cut vector containing the rest of the viral genes (pPEDV.mCh.*MluI*.3UTR) by the In-Fusion ligation method. **(D)** VeroE6 cells were infected with each recombinant PEDV (MOI = 0.001) and virus replication was monitored at the indicated time points by the $TCID_{50}$ assay. Values shown are averages ± SEM of three independent experiments. **(E)** Representative images of virus spread in the infected cells at 96 hpi are shown.

Luciferase assays measuring zinc-finger antiviral protein activity

Synthetic oligonucleotides of each ZAP-responsive sequence (ZRS) were inserted into the pGL3-SV40-Luc (Promega, Madison, WI, United States) plasmid as a 3′UTR downstream of the Luciferase encoding gene as described previously (Guo et al., 2004a; Chen et al., 2012). A ZAP-sensitive sequence derived from Sindbid virus, Na, was used as a positive control (Guo et al., 2004a). For the experiment to determine ZAP activity in the presence of the various pCoV-N, a reporter plasmid carrying N-0.10 as ZRS was used as it showed the highest ZAP sensitivity in our study. Each construct was co-transfected with plasmids carrying pZAPL or pZAPS and the empty vector- or pCoV-N expressing plasmid as indicated into ZAP-KO HEK293T cells. A plasmid expressing Renilla luciferase, pRL-TK, was used to normalize transfection efficiency. At 48 hpt, cells were lysed, and luciferase activity was measured using the Dual-Luciferase Reporter Assay System (Promega, Madison, WI, United States) according to the manufacturer's instructions with an EnVision plate reader (PerkinElmer, MA, United States). Fold inhibition was calculated as the normalized luciferase activity in ZAP-KO HEK293T cells divided by the normalized luciferase activity in ZAP-expressing cells.

Statistical analysis

All data with statistical analysis were analyzed with GraphPad Prism 7.0 (GraphPad Software Inc., La Jolla, CA, United States). All results were

presented as means ± standard errors of the means (SEM); p values of <0.05 were considered statistically significant.

Results

Porcine epidemic diarrhea virus replication was suppressed by zinc-finger antiviral protein in VeroE6 cells

We first determined whether PEDV was sensitive to ZAP. The ZAP gene (ZC3HAV1) was knocked out in VeroE6 cells by a CRISPR-Cas9-based approach. The selected knockout clone of the cell line (designated VeroE6 ZAP-KO) was confirmed by western blot and ZAP-encoding RNA expression (**Figure 1A** and **Supplementary Figure 1**). Because PEDV normally infects pigs, we also wanted to determine the degree of inhibition by a more biologically relevant porcine host factor. A porcine-derived ZAP gene (pZAP) was cloned from porcine alveolar macrophage cells (PAMs) and transduced into VeroE6 ZAP-KO cells to generate a stable VeroE6 cell line expressing only the HA-tagged long isoform of pZAP (designated as VeroE6-pZAPL). Since pZAPL cannot be recognized by anti-human-ZAP antibodies, expression of HA-tagged pZAPL in the transduced VeroE6 cells was confirmed by SDS-PAGE/western blot analysis against the HA tag (**Figure 1A**). PEDV was inoculated into wild-type VeroE6, VeroE6 ZAP-KO, or VeroE6-pZAPL cells at MOI = 0.0001. The growth rate of PEDV determined by $TCID_{50}$ (**Figure 1B**) and viral spread at different time points by plaque imaging (**Figure 1C**) showed that the virus replicated significantly faster in VeroE6 ZAP-KO cells than in the wild-type or VeroE6-pZAPL cells. These results suggest that PEDV can be suppressed by ZAP derived from either the African green monkey host (VeroE6) or a porcine host (PAMs).

The porcine epidemic diarrhea virus genome contains an uneven distribution pattern of CpG dinucleotides similar to other human coronaviruses

Coronaviruses generally contain low levels of CpG, considering the average of their genomes (Xia, 2020). However, SARS-CoV-2 replication has been reported to be suppressed by endogenous ZAP (Nchioua et al., 2020). Therefore, we hypothesized that the suppression of coronaviruses, including PEDV, might be due to an uneven distribution of CpG clusters in the viral genome. We analyzed the CpG distribution in the genomes of various PEDV strains. The analysis shows that there are common areas where a high density of CpG content is clustered. These areas include the early 5′region of ORF1a, the frameshift region between ORF1a and ORF1b, and the structural genes downstream of the spike gene, particularly in the N gene (**Figure 2**). The result shows a similar pattern of distribution of CpG content in their genomes as in SARS-CoV-2 (Nchioua et al., 2020; Zimmer et al., 2021). This led us to speculate that these highly localized CpG contents could be targeted by ZAP.

Modulation of CpG content in the N gene affects growth rates of recombinant porcine epidemic diarrhea virus in wild-type host cells

Based on the above analysis, we hypothesized that altering the CpG cluster in the viral genome would affect viral growth in wild-type cells in a ZAP-dependent manner. For instance, increasing CpG clusters would further attenuate the mutant virus. We chose to increase CpG content in the N gene because it could affect viral transcriptional regulatory sequences in other suspected areas of high CpG content, such as the 5′UTR or ribosomal frameshift region (TRS). Nucleotide sequences encoding the viral N gene with increased CpG content without changing its amino acid sequence were generated with controlled RNA folding energy to avoid the effects of RNA folding on protein expression (**Figures 3A,B**). Two sequences were selected, as shown in **Figure 3A**. While the native sequence contains 49 CpG (67%) with a codon-paired bias (CPB) value (Moura et al., 2007) = +0.008, the generated sequences, N-0.05 and N-0.10, contain 62 CpG (82%, CPB = −0.04) and 73 CpG (93%, CPB = −0.09), respectively.

To determine how increasing CpG density in the N gene affects viral growth in wild-type cells, we generated recombinant PEDVs carrying these synthetic sequences and measured their replication kinetics. The oligonucleotides carrying the generated sequences were cloned into the PEDV infectious clone according to the method shown in **Figure 3C**. The infectious clone plasmids were transfected into HEK293T cells to generate infectious particles. The recombinant viruses were passaged and verified by RT-PCR sequencing of viral RNA (data not shown). We inoculated the resulting viruses at MOI = 0.001 onto VeroE6 cells to determine the replication rate of each virus by $TCID_{50}$ assay. The generated viruses grew at varied rates that were inversely correlated with the level of CpG content in the N gene (**Figures 3D,E**). The results in this section suggest that increasing the CpG content in the N gene of PEDV can suppress viral growth in a susceptible cell line.

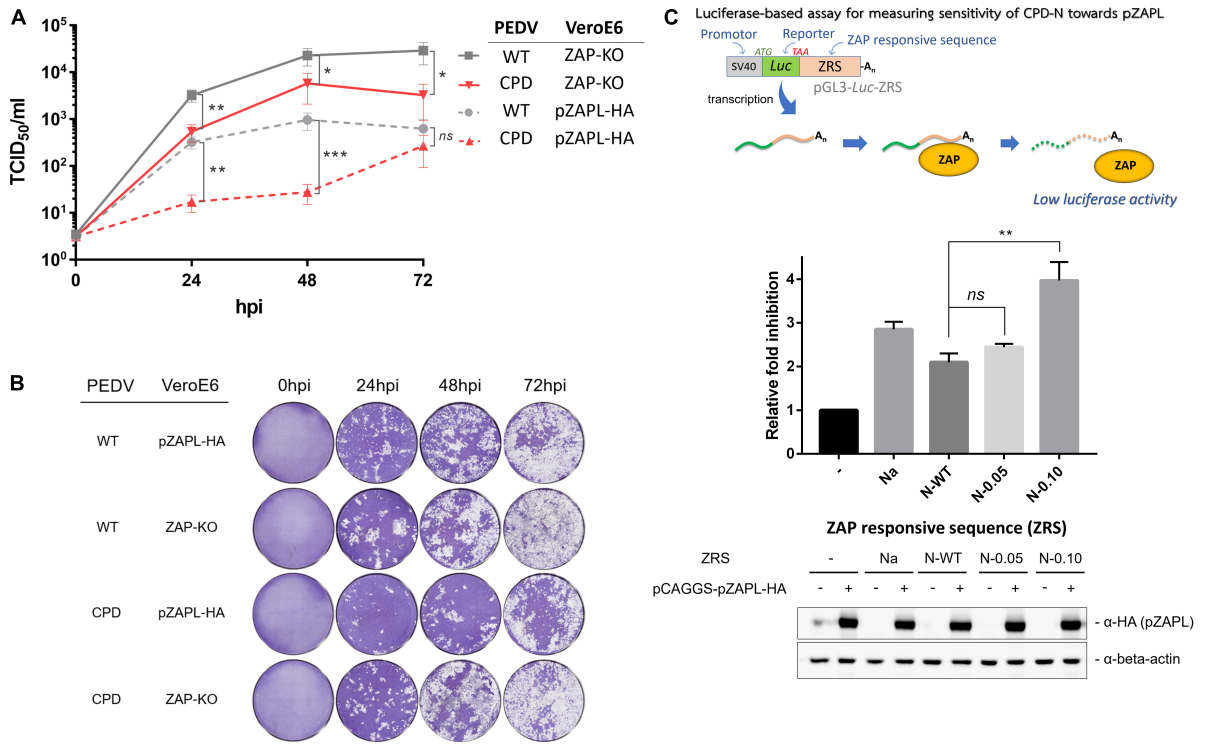

FIGURE 4

The growth of CPD-porcine epidemic diarrhea virus (PEDV) is suppressed by porcine zinc-finger antiviral protein (ZAP). **(A)** VeroE6 ZAP-KO or VeroE6-pZAPL cells were infected with CPD-PEDV at MOI = 0.001. Viral growth kinetics in VeroE6 ZAP-KO or VeroE6-pZAPL were monitored at the indicated time points using the $TCID_{50}$ assay. Values shown are averages ± SEM of three independent experiments (Student's *t*-test, $^{**}p < 0.05$, $^{**}p < 0.005$, $^{***}p < 0.0005$). **(B)** Representative viral spread at varied time points from A) was shown as images of CPE. **(C) (Top)** Schematic representation of the luciferase-based assay used to measure the sensitivity of each ZRS to pZAPL. **(Middle)** Each reporter plasmid containing ZRS was transfected into the ZAP-KO-293T cells along with a transfection normalizing plasmid, pRL-TK, and an empty control plasmid or a pZAPL-expressing plasmid. At 48 hpt, the transfected cells were lysed and luciferase activity was measured using the dual-luciferase reporter assay. The sensitivity of each ZRS to pZAPL was compared as the inhibition fold, which was calculated as described in methods. Inhibition data shown are the means ± SD of three independent measurements (Student's *t*-test, $^{**}p < 0.005$). **(Bottom)** SDS-PAGE/western blot showing expression of pZAPL in each condition.

Growth of porcine epidemic diarrhea virus carrying high-CpG content in the N gene is suppressed by porcine zinc-finger antiviral protein

Based on the above results, PEDV with N-0.10 (designated as CPD-PEDV) was selected as it grew the slowest in WT-VeroE6 to further investigate the sensitivity of increased CpG content in the N gene on viral growth against the corresponding porcine ZAP. To test whether the suppressed growth of CPD-PEDV is caused by ZAP in the host, we compared the growth of CPD-PEDV and WT-PEDV in cells lacking or expressing ZAP. CPD-PEDV or WT-PEDV (MOI = 0.001) were inoculated onto either VeroE6 ZAP-KO or VeroE6-pZAPL. Supernatants of infected cells were collected to determine the virus titers at varied time points by $TCID_{50}$ (**Figure 4A**), and the spread of viruses was shown by images of the CPE (**Figure 4B**). The results show that, while WT-PEDV was suppressed by pZAPL by 1–1.5 logs (**Figure 4A**, gray lines), CPD-PEDV is even more sensitive to pZAPL, resulting in 1.5–2.5 log decrease in titers (**Figure 4A**, red lines). In ZAP-KO cells, only a small viral growth difference (~0.5–1.0 logs) is observed between the two viruses (**Figure 4A**, solid lines), possibly due to ZAP-independent effects (e.g., different translation efficiency or RNA stability). However, in cells expressing pZAPL, the growth difference is significantly greater, especially at early time points (~1.5 logs) (**Figure 4A**, dashed lines), indicating a ZAP-dependent effect on the CPD-virus at early time points in the viral replication process. These results suggest that the reduced replication of PEDV with a high CpG content in the N gene is affected by ZAP-mediated suppression.

To provide additional evidence that the selected sequences in CPD-PEDV are targeted according to the increased CpG content of ZAP, we applied a luciferase-based assay previously used to determine the sensitivity of RNA sequences to ZAP (Guo et al., 2004a; Chen et al., 2012). The assay is based on a reporter plasmid encoding a luciferase gene fused to

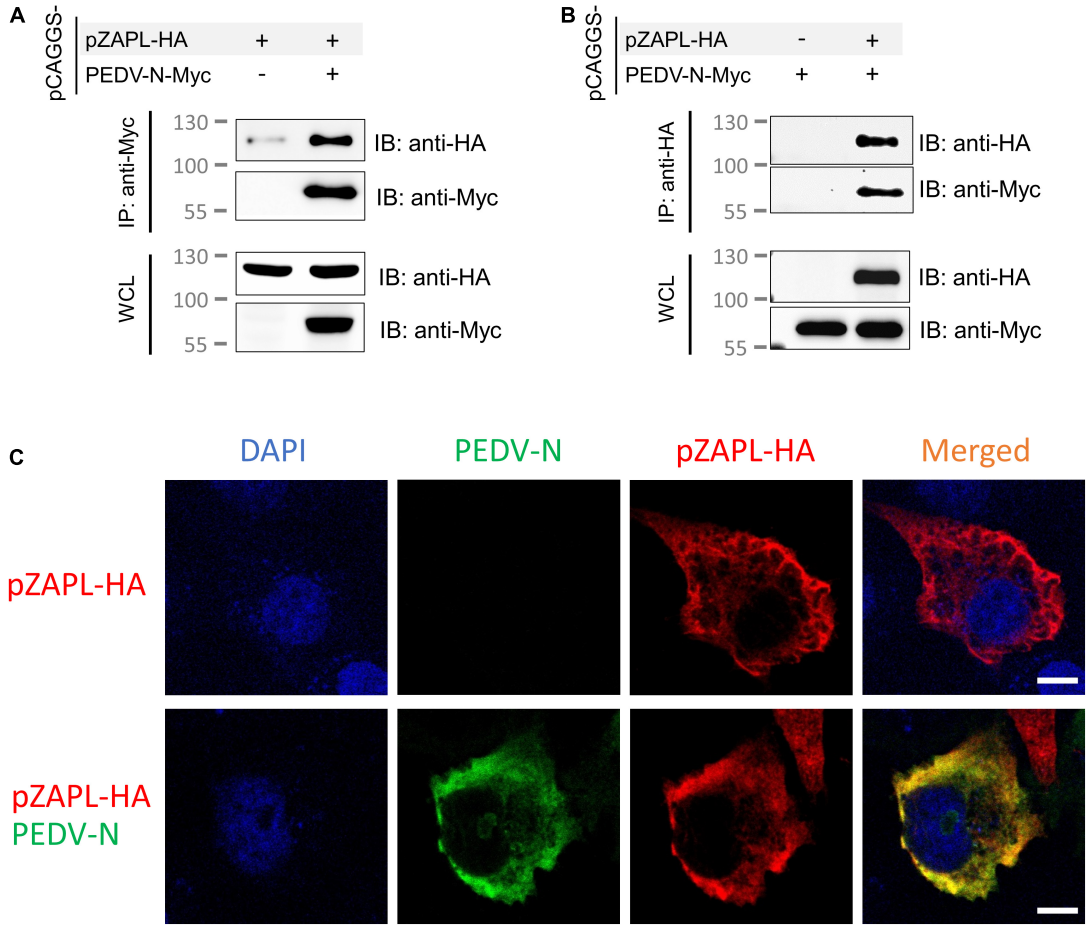

FIGURE 5
pZAPL interacts with PEDV-N. **(A,B)** Cell lysates from ZAP-KO HEK293T transfected with pCAGGS-pZAPL-HA or pCAGGS-PEDV-N-Myc were mixed as indicated. A co-IP experiment was performed with agarose beads conjugated with anti-Myc- **(A)** or anti-HA **(B)** antibodies. Prey proteins were analyzed by western blot with the indicated antibodies. **(C)** Co-localization of PEDV-N with pZAPL. VeroE6 cells were co-transfected with pCAGGS-PEDV-N and pCAGGS-pZAPL-HA. Confocal microscopy images of the transfected cells were taken at 48 hpt to examine the localization of the indicated proteins (scale bar = 10 μm).

an untranslated region containing a ZAP-responsive sequence (ZRS) (**Figure 4C**). In this assay, ZAP targets the ZRS and subsequently degrades total RNA, resulting in inhibition of luciferase signaling. The more ZAP-sensitive the sequences are, the stronger the luciferase inhibition will be. The synthesized N gene with varied CpGs was cloned into a non-translated region downstream of the luciferase gene in the pGL3-Luc plasmid as was done previously (Guo et al., 2004a; Chen et al., 2012; **Figure 4C**). The resulting Luciferase-based reporter plasmids (pGL3-Luc-ZRS) with various CpG-containing sequences were transfected into ZAP-KO HEK293T cells with a transfection normalization plasmid expressing Renilla luciferase (pRL-TK) and an empty pCAGGS vector or a pCAGGS plasmid expressing HA-tagged pZAPL (pCAGGS-pZAPL-HA). A previously reported ZAP-sensitive sequence, Na, was used as a positive control (Guo et al., 2004a). At 48 hpt, the cells were lysed, and luciferase activities were measured by the Dual-Luciferase Reporter Assay. The ZAP sensitivity of each generated sequence is presented as the inhibition fold as done previously in other studies (Guo et al., 2004b; Chen et al., 2012). Intermediate increase in CpG dinucleotides in N-0.05 slightly increases ZAP sensitivity, while the reporter plasmid with the highest CpGs, N-0.10, highly enhances the sensitivity toward pZAPL (**Figure 4C**). This result supports the hypothesis that the increased CpG dinucleotides in the N gene of CPD-PEDV are correlated with the higher ZAP-sensitivity of the virus.

Porcine epidemic diarrhea virus nucleocapsid protein interacts with pZAPL

From the above results, we observed delayed replication of the CPD-virus in a host expressing pZAPL at an early time

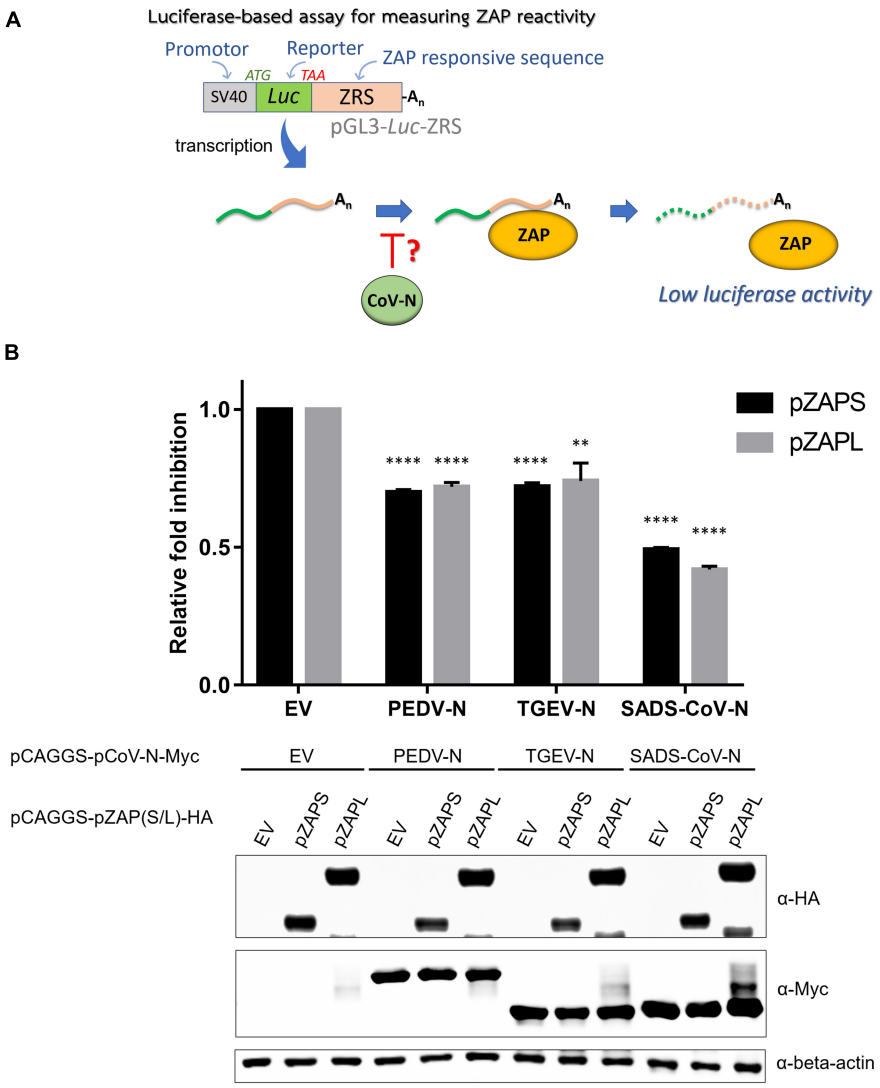

FIGURE 6
Nucleocapsid proteins of porcine alpha-coronaviruses suppress the function of porcine cell-derived zinc-finger antiviral protein (ZAP). **(A)** Schematic representation of the procedure of a luciferase-based assay to measure the activities of pZAPL and -S in the presence of the various pCoV-N. **(B)** To assess the ability of pCoV-N to antagonize ZAP activity, pGL3-Luc-ZRS was co-transfected with pZAPS or -L and the indicated pCoV-N expressing plasmids. A plasmid expressing Renilla luciferase, pRL-TK, was used to normalize transfection efficiency, and an empty pCAGGS vector (EV) was used as a control plasmid. At 48 hpt, cells were lysed, and luciferase activity was measured. Relative fold inhibition is fold inhibition (described in "Materials and methods") in the presence of the respective pCoV-N divided by fold inhibition of cells with EV. Data shown are the means ± SD of three independent measurements (Student's *t*-test, $^{**}p < 0.005$, $^{****}p < 0.00005$). **(Bottom)** SDS-PAGE/western blot showing expression of pZAPL in each condition.

point (24–48 hpi) (**Figures 4A,B**) compared with the ZAP-KO cells. However, the virus accelerated its growth at the late stage of replication (72 hpi). We next asked whether PEDV could use its own viral factors, which accumulate during prolonged replication, to counteract the suppression exerted by ZAP.

Among viral structural proteins, nucleocapsid protein (N) is the most likely candidate, as an interactome study by Zheng et al. (2021) showed that N of SARS-CoV-2 can interact with ZAP. Moreover, several studies have shown that N from human coronaviruses can interact with TRIM25, an essential co-factor to promote the function of ZAP (Hu et al., 2017; Li et al., 2017; Chang et al., 2020). We now aimed to determine whether PEDV N has an antagonistic function against ZAP.

First, we examined the interaction between PEDV-N and pZAPL. A co-IP experiment was performed to determine whether they interact with each other. Cell lysates from ZAP-KO HEK293T transfected with pCAGGS-pZAPL-HA or pCAGGS-PEDV-N-Myc were mixed and incubated. By pulling PEDV-N-Myc in the co-IP setup, we found that PEDV-N can pull pZAPL-HA (**Figure 5A**) and vice versa when pZAPL-HA is used as bait

(Figure 5B). The co-IP result indicated that PEDV-N can be associated with pZAPL. Co-localization between these proteins in cells was demonstrated by confocal imaging (Figure 5C).

Nucleocapsid proteins of porcine alpha-coronaviruses suppress the function of porcine cell-derived zinc-finger antiviral protein

Next, we investigated how nucleocapsid proteins from porcine coronaviruses affect the function of ZAP. In this experiment, we used a luciferase-based assay using the reporter plasmid described above [pGL3-Luc-ZRS(N-0.10)] (Figure 4C). To test how different ZAP isoforms behave, short and long isoforms of ZAP, derived from porcine cells, were cloned from porcine alveolar macrophage cells (PAMs). Both isoforms showed ZAP activity in this assay setup, with pZAPL exerting stronger inhibition than pZAPS (Supplementary Figure 2).

To investigate the effect of pCoV-N on the activity of ZAP, ZAP-KO HEK293T cells were co-transfected with the reporter plasmid [pGL3-luc-ZRS(N-0.10)], the pCAGGS plasmid expressing HA-tagged pZAPL (pCAGGS-pZAPL-HA) and the plasmids expressing various pCoV-N in the presence of the plasmid expressing Renilla luciferase (pRL-TK) to normalize transfection. At 48 hpt, cells were lysed, and luciferase activities were measured by the Dual-Luciferase reporter assay (Figure 6A). The antagonistic effects of pCoV-N on pZAP were compared based on the relative fold of inhibition. The result showed that PEDV-N and TGEV-N can reduce the inhibition of luciferase signal by ZAP by about 25%, whereas SADS-CoV-N can reduce the relative inhibition up to 50% (Figure 6B). The antagonistic effects of these pCoV-Ns against pZAPL or pZAPS are comparable. Overall, the results showed the conserved antagonizing function of pCoV-Ns against both isoforms of pZAP.

pCoV-Ns can alleviate zinc-finger antiviral protein-mediated suppression of influenza virus PB2 expression

To demonstrate that pCoV-Ns can suppress the function of pZAP, we performed another assay based on the previous finding that influenza virus polybasic protein 2 (PB2) expression can be suppressed by ZAP via a viral mRNA reduction-dependent mechanism (Tang et al., 2017). HEK293T cells were co-transfected with a plasmid expressing Flag-tagged PB2 protein and the indicated pZAP variants in the absence or presence of a plasmid expressing various pCoV-N. The pCAGGS-empty vector was used as a mock control. SDS-PAGE/western blot analysis of the transfected cell lysates showed that PB2 expression was substantially reduced in the presence of pZAPL (Lane 2 in Figure 7A), consistent with the previous reports (Liu et al., 2015; Tang et al., 2017). However, in the presence of nucleocapsid proteins from PEDV, TGEV, or SADS-CoV, PB2 expression was restored to the same level as in the absence of ZAP (cf. Lanes 3-5 and 1, Figure 7A). To rule out the possibility that CoV-Ns contribute to enhancing PB2 expression independently of the ZAP-regulatory pathway, we replaced ZAP with a ZAP mutant [pZAPL(Y108A)] lacking the essential residue for RNA binding, rendering it non-functional (Luo et al., 2020; Figure 7B). The result showed that PB2 expression was not affected by the non-functional mutant [pZAPL(Y108A)] (Lane 2, Figure 7B) and that CoV-N only slightly increased the expression of PB2 compared to that with pZAPL (Lanes 3–5, Figure 7B). These results support the notion that the nucleocapsid proteins of porcine alpha-coronaviruses, at least of PEDV, TGEV, or SADS-CoV, have a conserved function in antagonizing the function of pZAP and are able to restore the expression of a ZAP-responsive protein such as PB2.

Growth suppression of CPD-porcine epidemic diarrhea virus by pZAPL can be reversed by pCoV-Ns

We next examined whether pCoV-Ns expressed *in-trans* can reverse the growth suppressive effect of ZAP on CPD-PEDV. VeroE6 ZAP-KO were co-transfected with HA-tagged pZAPL or empty vector and Myc-tagged PEDV-N or TGEV-N. At 24 hpt, transfected cells were inoculated with CPD-PEDV (MOI = 0.001). Supernatants containing viruses at 48 and 72 hpi were collected for viral titer analysis by $TCID_{50}$. At 48 hpi, virus titers from cells expressing only pZAPL-HA were significantly lower than those from the mock-transfected cells indicating viral suppression by pZAPL (Figure 8). In the absence of pZAPL-HA expression, transfection of either PEDV-N-Myc or TGEV-N-Myc slightly but not statistically significantly increased viral titers. However, in the presence of pZAPL-HA, co-transfection with pCoV-Ns can significantly reverse the viral suppression induced by pZAPL-HA (Figure 8, left). Similar to the titers observed at 48 hpi, expression of pCoV-N without the suppressive effect of pZAPL-HA did not show significantly increased viral titers at 72 hpi. At 72 hpi, the effect of transient expression of pZAPL-HA did not significantly decrease viral titer compared with mock transfection, possibly because the virus produced sufficient N at this stage to target ZAP. However, both pCoV-Ns can still slightly increase viral titers in the presence of pZAPL compared with the condition where no additional pCoV-N was present. This result suggests that both PEDV-N and TGEV-N expressed *in-trans* may antagonize the function of pZAPL in suppressing the growth of CPD-PEDV.

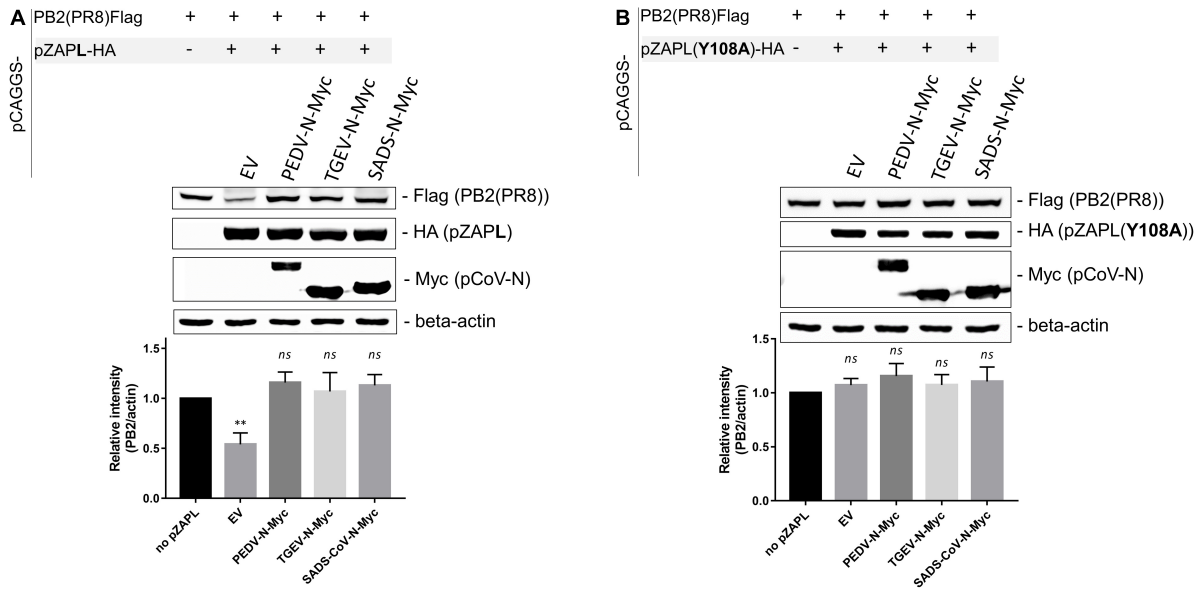

FIGURE 7
pCoV-Ns reverses the repression of PB2 expression by zinc-finger antiviral protein (ZAP). **(A,B)** A pCAGGS plasmid expressing Flag-tagged PB2 was co-transfected into HEK293T cells with a plasmid expressing HA-tagged pZAPL **(A)** or the non-functional ZAP mutant, ZAP (Y108A) **(B)**, and a plasmid encoding the indicated pCoV-N protein. An empty vector plasmid served as a control. At 48 hpt, cells were lysed, and protein expression was analyzed by SDS-PAGE/western blotting. The western blotting results shown are representative of three independent experiments. The relative band intensities of PB2-FLAG and beta-actin under each lane were analyzed using Image Lab software (Bio-Rad Laboratories, CA, United States). Values shown are the means ± SD of three independent measurements (Student's *t*-test, $^{**}p < 0.005$).

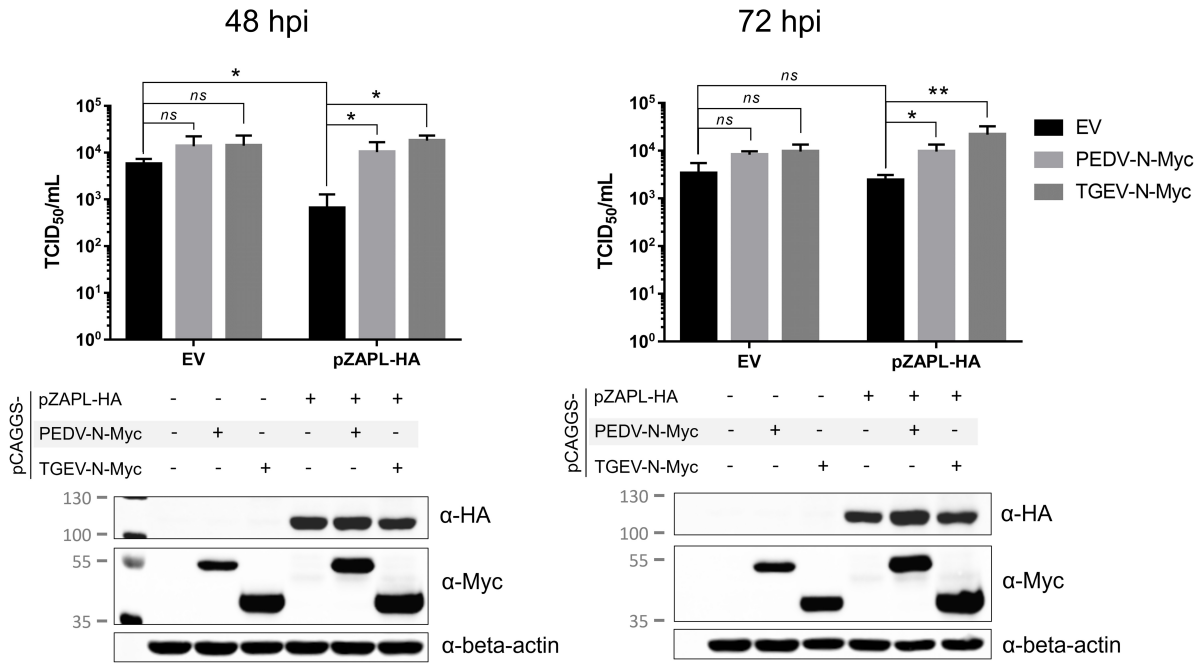

FIGURE 8
Suppression of CPD-porcine epidemic diarrhea virus (PEDV) growth by pZAPL can be reversed by pCoV-Ns. VeroE6 ZAP-KO cells were transfected with the indicated plasmids. At 24 hpt, transfected cells were infected with CPD-PEDV (MOI = 0.001). Supernatants were collected at 48 and 72 hpi to determine viral titers using the $TCID_{50}$ assay. Expression of the indicated proteins is shown by SDS-PAGE/western blot results below. Values shown are averages ± SEM of three independent experiments (Student's *t*-test, $^{*}p < 0.05$, $^{**}p < 0.005$).

Discussion

The global threat posed by SARS-CoV-2 again underscores the need for a better understanding of coronavirus-host interaction. As an example, insights gained from previous SARS-CoV research can make a critical leap in the development of therapeutic and preventive approaches to alleviate the global suffering of COVID-19. A comprehensive understanding of how a host defends itself against viral infection and how viruses counteract this defense would better prepare us for the next pandemic.

Among various host antiviral factors, ZAP plays an important role in inhibiting the growth of many RNA viruses (Ficarelli et al., 2021), including SARS-CoV-2 (Nchioua et al., 2020), by suppressing the production of genomic or subgenomic viral RNA during viral infection. In this study, we demonstrated that the growth of PEDV can be suppressed by endogenous or porcine cell-derived ZAP in VeroE6 cells. The conserved function of ZAPs from both cell lines may be due to the conserved RNA-binding domain in the N-terminal part of ZAP in mammalian hosts (Gonçalves-Carneiro et al., 2021).

Two major isoforms of ZAP (short and long isoforms) contribute to viral restriction function. Despite sharing a common RNA-binding domain, the long isoform exerts stronger viral inhibition due to the extended C-terminal domain containing the inactive poly-(ADP-ribose) polymerase (PARP)-like domain, which has been shown to aid in RNA binding, interact with its cofactor (Kmiec et al., 2021) and recruit an endonuclease protein to degrade bound RNA (Ficarelli et al., 2019). Moreover, the long isoform is constitutively expressed, while the short isoform is dependent on IFN response (Ryman et al., 2005; Wang et al., 2010; Hayakawa et al., 2011; Schwerk et al., 2019). Considering that the VeroE6 cell line is IFN gene deficient (Emeny and Morgan, 1979; Chew et al., 2009), the long isoform, which is expressed at a much higher level (**Figure 1A**), would play a dominant role in virus inhibition in our experimental setup. Therefore, our study focused on the interplay between the virus and the long isoform of ZAP, with the IFN-dependent response playing a minor role. However, the contribution of pZAPS could not be excluded in a native host in which the IFN response functions normally.

Our analysis of the PEDV genomes revealed high CpG clusters in the 5′UTR, the ribosomal frameshift region and the structural gene region, particularly in the N gene. This pattern of CpG distribution is similar to that of the SARS-CoV-2 genome (Nchioua et al., 2020; Zimmer et al., 2021). This suggests that ZAP targets these regions of high CpG content and mediates the degradation of viral RNA, leading to suppression of viral growth, as found in SARS-CoV-2. We have shown that increasing CpG content only in the N gene can make viral RNA more visible to ZAP and thus more susceptible to degradation. Given that all coronaviral genomic and subgenomic RNA species share the N gene at the 3′-terminal segment, any change in the N gene could affect all species of viral RNAs. Therefore, a subtle effect of small CpG changes in the N gene could accumulate to cause sufficient suppression by ZAP, resulting in decreased replicative viral fitness of CPD-PEDV. This is supported by another study showing that SARS-CoV-2 containing a partial fragment with high CpG in its genome was attenuated in animal experiments (Trimpert et al., 2021). Therefore, the increased density of CpG in a specific genomic region rather than the CpG number in the whole genome could alter the ZAP susceptibility of PEDV. Our results have shown that the attenuation of CPD virus is mainly due to ZAP, as the suppressed viral replication can be reversed in ZAP-KO cells, but is evident in VeroE6 with exogenous pZAPL reconstitution. The attenuation shown here by designing CPD-PEDV could be applied based on the concept of *synthetic attenuated virus engineering* (SAVE) (Coleman et al., 2008) to generate an attenuated live vaccine candidate.

We have previously shown that PEDV-N or TGEV-N can promote PEDV replication by increasing the level of viral RNA in the viral replication process compared to the state without exogenous N-protein expression (Sungsuwan et al., 2020). Our findings from this work reveal an alternative factor that contributes to our previous observation that the additional CoV-N antagonizes ZAP and protects viral RNA from degradation. This novel function of pCoV-N has been shown to be conserved among porcine alpha-coronaviruses, including PEDV, TGEV, and SADS-CoV and likely among other human coronaviruses. We have also shown that the host expressing PEDV-N or TGEV-N *in-trans* can recover the slow replication of the CPD-virus. It could be argued that the extra PEDV-N supplements the delayed production of PEDV-N from the CPD-N gene and restores slow virus replication by participating in virion assembly. However, TGEV-N, which was previously shown to be unable to replace PEDV-N in the production of PEDV virions (Sungsuwan et al., 2020), also showed a similar effect. Together with the demonstration that these pCoV-Ns can restore normal expression of IAV-PB2, an unrelated protein known to be suppressed by ZAP, these results suggest a novel function of pCoV-Ns that antagonizes the pZAP function in a universal and non-pCoV-specific manner.

Our results showed that PEDV can grow faster in the ZAP-KO cells compared to the wild-type cells in the early phase of infection (24–48 hpi), while it reaches a plateau thereafter (**Figures 1**, **4**). In the transient expression experiment, the suppression by ZAP is less significant in the late phase of virus replication (at 72 hpi, **Figure 8**). This may suggest that novel function of pCoV-N in antagonizing the function of ZAP may be an auxiliary role in addition to its primary functions of initiating or modulating viral genome replication (McBride et al., 2014). These primary functions of virus-derived N could be of high priority during the early phase of replication, when N production cannot catch up to antagonize the active ZAP in the

host. However, once CoV-N produced either by the virus or by the host (*in-trans*) is excessive, ZAP inhibition may be observed. On the other hand, given that a primary function of CoV-N is to bind the viral RNA, it is also possible that the excess CoV-N may be sufficient to cover and protect the viral RNA from being recognized by ZAP as well.

Regarding the interaction between pZAPL and PEDV-N shown in this study, we could not exclude that it is direct or mediated by an intermediary. On the one hand, several works have shown that CoV-N proteins have myriads of interaction partners (McBride et al., 2014). On the other hand, two independent studies have shown that nucleocapsid proteins of coronaviruses (MERS- and SARS-CoVs) can interact with TRIM25, an essential ZAP co-factor (Li et al., 2017), preventing it from interacting with RIG-I for IFN production (Hu et al., 2017; Chang et al., 2020). This led us to hypothesize that PEDV-N might interact with pZAPL possibly via TRIM25 (Li et al., 2017; Zheng et al., 2017; Ficarelli et al., 2019). Whether pCoV-N interacts with TRIM25 and affects its cofactor function for ZAP requires further investigation.

In summary, PEDV can be suppressed by ZAP. Increasing CpG content only in the N gene makes the virus more susceptible to ZAP. Our study revealed an alternative function of the nucleocapsid protein (pCoV-N) that targets and counteracts the antiviral activity of ZAP. The insights into the interplay between coronavirus and host demonstrated in this work could be used to develop therapeutic and preventive agents to combat the impending pandemic.

Data availability statement

The original contributions presented in this study are included in the article/**Supplementary material**, further inquiries can be directed to the corresponding author.

Author contributions

SS: conceptualization, investigation, and methodology. SS and SK: validation. WM: bioinformatic analysis. SS and PJ-A: writing – original draft preparation. SS, PJ-A, and AJ: writing – review and editing. All authors have read and approved the manuscript.

Funding

This study was financially supported by National Center for Genetic Engineering and Biotechnology [BIOTEC Young Fellow's Research Grant (P-21-50128)].

Acknowledgments

We would like to thank Nanchaya Wanasen for providing PAM cells for porcine-derived cellular RNA.

Conflict of interest

The authors declare that the research was conducted in the absence of any commercial or financial relationships that could be construed as a potential conflict of interest.

Publisher's note

All claims expressed in this article are solely those of the authors and do not necessarily represent those of their affiliated organizations, or those of the publisher, the editors and the reviewers. Any product that may be evaluated in this article, or claim that may be made by its manufacturer, is not guaranteed or endorsed by the publisher.

Supplementary material

The Supplementary Material for this article can be found online at: https://www.frontiersin.org/articles/10.3389/fmicb.2022.975632/full#supplementary-material

References

Chang, C.-Y., Liu, H. M., Chang, M.-F., and Chang, S. C. (2020). Middle East Respiratory Syndrome Coronavirus Nucleocapsid Protein Suppresses Type I and Type III Interferon Induction by Targeting RIG-I Signaling. *J Virol.* 94, e00099–20. doi: 10.1128/JVI.00099-20

Chen, S., Xu, Y., Zhang, K., Wang, X., Sun, J., Gao, G., et al. (2012). Structure of N-terminal domain of ZAP indicates how a zinc-finger protein recognizes complex RNA. *Struct. Mol. Biol.* 19, 430–435. doi: 10.1038/nsmb.2243

Cheng, X., Virk, N., Chen, W., Ji, S., Ji, S., Sun, Y., et al. (2013). CpG usage in RNA viruses: Data and hypotheses. *PLoS One* 8:e74109. doi: 10.1371/journal.pone.0074109

Chew, T., Noyce, R., Collins, S. E., Hancock, M. H., and Mossman, K. L. (2009). Characterization of the interferon regulatory factor 3-mediated antiviral response in a cell line deficient for IFN production. *Mol. Immunol.* 46, 393–399. doi: 10.1016/j.molimm.2008.10.010

Coleman, J. R., Papamichail, D., Skiena, S., Futcher, B., Wimmer, E., and Mueller, S. (2008). Virus Attenuation by Genome-Scale Changes in Codon Pair Bias. *Science* 320:1784.

Emeny, J. M., and Morgan, M. J. (1979). Regulation of the Interferon System: Evidence that Vero Cells have a Genetic Defect in Interferon Production. *J. Gen. Virol.* 43, 247–252. doi: 10.1099/0022-1317-43-1-247

Ficarelli, M., Neil, S. J. D., and Swanson, C. M. (2021). Targeted Restriction of Viral Gene Expression and Replication by the ZAP Antiviral System. *Annu. Rev. Virol.* 8, 265–283.

Ficarelli, M., Wilson, H., Pedro Galao, R., Mazzon, M., Antzin-Anduetza, I., Marsh, M., et al. (2019). KHNYN is essential for the zinc finger antiviral protein (ZAP) to restrict HIV-1 containing clustered CpG dinucleotides. *elife* 8:e46767. doi: 10.7554/eLife.46767

Gonçalves-Carneiro, D., Takata, M. A., Ong, H., Shilton, A., and Bieniasz, P. D. (2021). Origin and evolution of the zinc finger antiviral protein. *PLoS Pathogens* 17:e1009545. doi: 10.1371/journal.ppat.1009545

Guo, X., Carroll, J. W., Macdonald, M. R., Goff, S. P., and Gao, G. (2004). The zinc finger antiviral protein directly binds to specific viral mRNAs through the CCCH zinc finger motifs. *J. Virol.* 78, 12781–12787.

Hayakawa, S., Shiratori, S., Yamato, H., Kameyama, T., Kitatsuji, C., Kashigi, F., et al. (2011). ZAPS is a potent stimulator of signaling mediated by the RNA helicase RIG-I during antiviral responses. *Nat. Immunol.* 12, 37–44. doi: 10.1038/ni.1963

Hu, Y., Li, W., Gao, T., Cui, Y., Jin, Y., Li, P., et al. (2017). The Severe Acute Respiratory Syndrome Coronavirus Nucleocapsid Inhibits Type I Interferon Production by Interfering with TRIM25-Mediated RIG-I Ubiquitination. *J. Virol.* 91, e2143–e2116.

Jaru-Ampornpan, P., Jengarn, J., Wanitchang, A., and Jongkaewwattana, A. (2017). Porcine Epidemic Diarrhea Virus 3C-Like Protease-Mediated Nucleocapsid Processing: Possible Link to Viral Cell Culture Adaptability. *J. Virol.* 91:2. doi: 10.1128/JVI.01660-16

Jengarn, J., Wongthida, P., Wanasen, N., Frantz, P. N., Wanitchang, A., and Jongkaewwattana, A. (2015). Genetic manipulation of porcine epidemic diarrhoea virus recovered from a full-length infectious cDNA clone. *J. Gen. Virol.* 96, 2206–2218. doi: 10.1099/vir.0.000184

Kmiec, D., Lista, M. J., Ficarelli, M., Swanson, C. M., and Neil, S. J. D. (2021). S-farnesylation is essential for antiviral activity of the long ZAP isoform against RNA viruses with diverse replication strategies. *PLoS Pathogens* 17:e1009726. doi: 10.1371/journal.ppat.1009726

Li, M. M. H., Lau, Z., Cheung, P., Aguilar, E. G., Schneider, W. M., Bozzacco, L., et al. (2017). TRIM25 Enhances the Antiviral Action of Zinc-Finger Antiviral Protein (ZAP). *PLoS Pathogens* 13:e1006145. doi: 10.1371/journal.ppat.1006145

Liu, C.-H., Zhou, L., Chen, G., and Krug, R. M. (2015). Battle between influenza A virus and a newly identified antiviral activity of the PARP-containing ZAPL protein. *Proc. Natl. Acad. Sci. U.S.A.* 112:14048. doi: 10.1073/pnas.1509745112

Liwnaree, B., Narkpuk, J., Sungsuwan, S., Jongkaewwattana, A., and Jaru-Ampornpan, P. (2019). Growth enhancement of porcine epidemic diarrhea virus (PEDV) in Vero E6 cells expressing PEDV nucleocapsid protein. *PLoS One* 14:e0212632. doi: 10.1371/journal.pone.0212632

Luo, X., Wang, X., Gao, Y., Zhu, J., Liu, S., Gao, G., et al. (2020). Molecular Mechanism of RNA Recognition by Zinc-Finger Antiviral Protein. *Cell Rep.* 30, 46–52.e4.

McBride, R., van Zyl, M., and Fielding, B. (2014). The Coronavirus Nucleocapsid Is a Multifunctional Protein. *Viruses* 6:2991.

Moura, G., Pinheiro, M., Arrais, J., Gomes, A. C., Carreto, L., Freitas, A., et al. (2007). Large Scale Comparative Codon-Pair Context Analysis Unveils General Rules that Fine-Tune Evolution of mRNA Primary Structure. *PLoS One* 2:e847. doi: 10.1371/journal.pone.0000847

Nchioua, R., Kmiec, D., Müller, J. A., Conzelmann, C., Groß, R., Swanson, C. M., et al. (2020). SARS-CoV-2 Is Restricted by Zinc Finger Antiviral Protein despite Preadaptation to the Low-CpG Environment in Humans. *mBio* 11, e1930–e1920. doi: 10.1128/mBio.01930-20

Reed, L. J., and Muench, H. A. (1938). A SIMPLE METHOD OF ESTIMATING FIFTY PER CENT ENDPOINTS. *Am. J. Epidemiol.* 27, 493–497. doi: 10.1016/j.jviromet.2005.05.005

Rima, B. K., and McFerran, N. V. (1997). Dinucleotide and stop codon frequencies in single-stranded RNA viruses. *J. Gen. Virol.* 78, 2859–2870. doi: 10.1099/0022-1317-78-11-2859

Ryman, K. D., Meier, K. C., Nangle, E. M., Ragsdale, S. L., Korneeva, N. L., Rhoads, R. E., et al. (2005). Sindbis virus translation is inhibited by a PKR/RNase L-independent effector induced by alpha/beta interferon priming of dendritic cells. *J. Virol.* 79, 1487–1499. doi: 10.1128/JVI.79.3.1487-1499.2005

Schwerk, J., Soveg, F. W., Ryan, A. P., Thomas, K. R., Hatfield, L. D., Ozarkar, S., et al. (2019). RNA-binding protein isoforms ZAP-S and ZAP-L have distinct antiviral and immune resolution functions. *Nat. Immunol.* 20, 1610–1620. doi: 10.1038/s41590-019-0527-6

Simmonds, P. (2012). SSE: A nucleotide and amino acid sequence analysis platform. *BMC Res. Notes* 5:50. doi: 10.1186/1756-0500-5-50

Sungsuwan, S., Jongkaewwattana, A., and Jaru-Ampornpan, P. (2020). Nucleocapsid proteins from other swine enteric coronaviruses differentially modulate PEDV replication. *Virology* 540, 45–56. doi: 10.1016/j.virol.2019.11.007

Takata, M. A., Goncalves-Carneiro, D., Zang, T. M., Soll, S. J., York, A., Blanco-Melo, D., et al. (2017). CG dinucleotide suppression enables antiviral defence targeting non-self RNA. *Nature* 550, 124–127. doi: 10.1038/nature24039

Tang, Q., Wang, X., and Gao, G. (2017). The Short Form of the Zinc Finger Antiviral Protein Inhibits Influenza A Virus Protein Expression and Is Antagonized by the Virus-Encoded NS1. *J. Virol.* 91, e01909–16. doi: 10.1128/JVI.01909-16

Trimpert, J., Dietert, K., Firsching, T. C., Ebert, N., Thi Nhu Thao, T., Vladimirova, D., et al. (2021). Development of safe and highly protective live-attenuated SARS-CoV-2 vaccine candidates by genome recoding. *Cell Rep.* 36:109493. doi: 10.1016/j.celrep.2021.109493

Wang, N., Dong, Q., Li, J., Jangra, R. K., Fan, M., Brasier, A. R., et al. (2010). Viral induction of the zinc finger antiviral protein is IRF3-dependent but NF-kappaB-independent. *J. Biol. Chem.* 285, 6080–6090. doi: 10.1074/jbc.M109.054486

Xia, X. (2020). Extreme Genomic CpG Deficiency in SARS-CoV-2 and Evasion of Host Antiviral Defense. *Mol. Biol. Evol.* 37, 2699–2705.

Xie, L., Lu, B., Zheng, Z., Miao, Y., Liu, Y., Zhang, Y., et al. (2018). The 3C protease of enterovirus A71 counteracts the activity of host zinc-finger antiviral protein (ZAP). *J. Gen. Virol.* 99, 73–85. doi: 10.1099/jgv.0.000982

Zhao, Y., Song, Z., Bai, J., Liu, X., Nauwynck, H., and Jiang, P. (2020). Porcine reproductive and respiratory syndrome virus Nsp4 cleaves ZAP to antagonize its antiviral activity. *Vet. Microbiol.* 250:108863. doi: 10.1016/j.vetmic.2020.108863

Zheng, X., Sun, Z., Yu, L., Shi, D., Zhu, M., Yao, H., et al. (2021). Interactome Analysis of the Nucleocapsid Protein of SARS-CoV-2 Virus. *Pathogens* 10:1155.

Zheng, X., Wang, X., Tu, F., Wang, Q., Fan, Z., and Gao, G. (2017). TRIM25 Is Required for the Antiviral Activity of Zinc Finger Antiviral Protein. *J. Virol.* 91, e88–e17.

Zimmer, M. M., Kibe, A., Rand, U., Pekarek, L., Ye, L., Buck, S., et al. (2021). The short isoform of the host antiviral protein ZAP acts as an inhibitor of SARS-CoV-2 programmed ribosomal frameshifting. *Nat. Commun.* 12:7193. doi: 10.1038/s41467-021-27431-0

frontiers | Frontiers in Microbiology

TYPE Original Research
PUBLISHED 28 September 2022
DOI 10.3389/fmicb.2022.988298

OPEN ACCESS

EDITED BY
Jian Shang,
Zhengzhou University, China

REVIEWED BY
Xiaoli Xiong,
Guangzhou Institutes of Biomedicine and Health (CAS), China
Elena Criscuolo,
Vita-Salute San Raffaele University, Italy

*CORRESPONDENCE
Haixia Zhou
haixia_zhou@hms.harvard.edu
Linqi Zhang
zhanglinqi@mail.tsinghua.edu.cn
Xinquan Wang
xinquanwang@mail.tsinghua.edu.cn

†PRESENT ADDRESSES
Wenxv Jia,
Institute of Education, Teaching Center for Writing and Communication, Tsinghua University, Beijing, China

Jianwei Zeng,
Department of Biochemistry and Molecular Biophysics, School of Medicine, Washington University in St. Louis, St. Louis, MO, United States

Haixia Zhou,
Department of Biological Chemistry and Molecular Pharmacology, Blavatnik Institute and Harvard Medical School, Boston, MA, United States

‡These authors have contributed equally to this work

SPECIALTY SECTION
This article was submitted to Virology, a section of the journal Frontiers in Microbiology

RECEIVED 07 July 2022
ACCEPTED 31 August 2022
PUBLISHED 28 September 2022

CITATION
Zhang S, Jia W, Zeng J, Li M, Wang Z, Zhou H, Zhang L and Wang X (2022) Cryoelectron microscopy structures of a human neutralizing antibody bound to MERS-CoV spike glycoprotein.
Front. Microbiol. 13:988298.
doi: 10.3389/fmicb.2022.988298

Cryoelectron microscopy structures of a human neutralizing antibody bound to MERS-CoV spike glycoprotein

Shuyuan Zhang[1‡], Wenxv Jia[2,3†‡], Jianwei Zeng[1†‡], Mingxi Li[2,3], Ziyi Wang[1], Haixia Zhou[1*†], Linqi Zhang[2,3*] and Xinquan Wang[1*]

[1]The Ministry of Education Key Laboratory of Protein Science, Beijing Advanced Innovation Center for Structural Biology, Beijing Frontier Research Center for Biological Structure, School of Life Sciences, Tsinghua University, Beijing, China, [2]Comprehensive AIDS Research Center and Beijing Advanced Innovation Center for Structural Biology, School of Medicine, Tsinghua University, Beijing, China, [3]NexVac Research Center, Tsinghua University, Beijing, China

Neutralizing monoclonal antibodies (mAbs) against highly pathogenic coronaviruses represent promising candidates for clinical intervention. Here, we isolated a potent neutralizing monoclonal antibody, MERS-S41, from a yeast displayed scFv library using the S protein as a bait. To uncover the neutralization mechanism, we determined structures of MERS-S41 Fab in complex with the trimeric spike glycoprotein by cryoelectron microscopy (cryo-EM). We observed four distinct classes of the complex structure, which showed that the MERS-S41 Fab bound to the "up" receptor binding domain (RBD) with full saturation and also bound to an accessible partially lifted "down" RBD, providing a structural basis for understanding how mAbs bind to trimeric spike glycoproteins. Structure analysis of the epitope and cell surface staining assays demonstrated that virus entry is blocked predominantly by direct competition with the host receptor, dipeptidyl peptidase-4 (DPP4).

KEYWORDS

neutralizing antibody, MERS-CoV, spike glycoprotein, cryo-EM structures, neutralization mechanism

Introduction

The outbreak of coronavirus disease 2019 (COVID-19), caused by the severe acute respiratory syndrome coronavirus 2 (SARS-CoV-2), has been declared by the World Health Organization (WHO) as a global health emergency that, at the time of writing, has been responsible for more than 6 million deaths.[1] Unfortunately, it is just the latest in a line of lethal respiratory diseases spread by coronaviruses to cause worldwide

1 https://covid19.who.int/

epidemics. SARS-CoV-1 emerged in 2002, resulting in 8,000 infections and nearly 800 deaths in 37 countries (Peiris et al., 2003). In 2012, Middle East respiratory syndrome coronavirus (MERS-CoV), emerged in the Arabian peninsula and caused numerous outbreaks in humans, with a fatality rate of 35%.[2] MERS-CoV likely originated from bats, with camels functioning as a nature reservoir (Azhar et al., 2014; Mohd et al., 2016). Small clusters of infections without camel exposure in several countries suggested that human-to-human transmission can occur through close contact (Zumla et al., 2015). Due to the high pathogenicity, significant lethality and verified capability of human-to-human transmission, there has been a persistent concern that MERS-CoV could cause a disruptive pandemic.

Coronavirus trimeric spike (S) glycoproteins mediate viral entry. The MERS-CoV S protein undergoes protease cleavage into two subunits (Millet and Whittaker, 2014), leading to non-covalently associated S1 and S2 subunits, whereby a trimer of S1 sits atop a trimer of S2 subunits. S1 is responsible for binding to the host receptor, and contains the N-terminal domain (NTD), the receptor binding domain (RBD), and subdomain 1 and 2 (SD1 and SD2). S1 adopts dynamic conformations in cryo-EM structures of prefusion MERS-CoV (Pallesen et al., 2017; Yuan et al., 2017), SARS-CoV (Gui et al., 2017; Yuan et al., 2017), and SARS-CoV-2 (Walls et al., 2020; Wrapp et al., 2020), wherein RBDs adopt either a "down" conformation that buries the receptor-binding surface, or an "up" conformation that facilitates binding with host-cell receptors. The binding of S1 RBD to the host receptor DPP4 (Lu et al., 2013; Raj et al., 2013; Wang et al., 2013) likely initiates the fully receptor-binding capable state in which all three RBDs adopt the "up" conformation, resulting in conformational change of S2, which mediates the fusion of the viral and host-cell membranes (Pallesen et al., 2017; Yuan et al., 2017; Walls et al., 2019). As the S protein decorates the viral surface and is vital for its infectivity, it is the main target of neutralizing antibodies. Numerous monoclonal antibodies (mAbs) against the S protein of MERS-CoV have been reported, isolated from single chain fragment variable (scFv) libraries (Jiang et al., 2014; Tang et al., 2014; Ying et al., 2014), generated from immunized animals (Li et al., 2015; Wang et al., 2015; Chen et al., 2017) or based on B cell cloning from convalescent individuals (Corti et al., 2015). Most neutralizing antibodies were isolated using the RBD as a bait. Structural studies have revealed that RBD-targeting mAbs directly or indirectly disrupt the interaction between RBD and DPP4 (Li et al., 2015; Wang et al., 2015, 2018; Ying et al., 2015; Yu et al., 2015; Chen et al., 2017; Niu et al., 2018; Zhang et al., 2018). The trimeric spike glycoprotein has also used as a bait for selection from phage displayed scFv libraries or to inoculate mice. Successful examples are antibody 3B11 isolated from a scFv library (Tang et al., 2014) and mAb 7D10 generated from S protein immunized mice (Zhou et al., 2019). Since the trimeric S protein has the potential to isolate mAbs targeting various sites including the RBD, NTD, S2, or structural elements of the trimer, it could be a more effective antigen to select mAbs than the RBD.

Here, we report the isolation of a potent neutralizing monoclonal antibody, MERS-S41, from a yeast displayed scFv library using the S protein as the bait. To determine the neutralization mechanism and further explore the interactions between MERS-S41 and S protein, we resolved the structures of the trimeric spike glycoprotein in complex with the MERS-S41 Fab by cryoelectron microscopy (cryo-EM). The structures showed that MERS-S41 can bind the MERS-CoV spike with different stoichiometries, in which MERS-S41 Fab was able to bind "up" RBD and partially lifted "down" RBD, whereas MERS-S41 Fab was unable to bind fully "down" RBD. As a result of structure analysis of the epitope and cell surface staining assay, the main neutralization mechanism for MERS-S41 is demonstrated to be direct competition with DPP4.

Results

Neutralizing mAb MERS-S41 isolated from non-immune human antibody library

To generate neutralizing mAbs against the MERS-CoV glycoprotein spike, we first expressed and purified the ectodomain of the spike as described before (Gui et al., 2017; **Supplementary Figure 1**). The bait was then used to select antibodies from a non-immune human scFv library displayed on the surface of the yeast, *Saccharomyces cerevisiae* (Jiang et al., 2014). The selection procedure is shown in **Figure 1A**. We performed two rounds of magnetic bead–activated cell sorting (MACS) followed by three rounds of florescence-activated cell sorting (FACS). Plasmids containing the coding sequences for scFv were then extracted from the sorted yeast population, and proliferated in *Escherichia coli* for sequence analysis.

Among the 119 plasmid sequences analyzed, 13 distinct scFv sequences were identified (**Supplementary Table 1**). Interestingly, one of the scFv sequences, MERS-S111, was identical to the MERS-27 sequence which we isolated previously using RBD as the bait (Yu et al., 2015). Subsequently, we grafted the scFv sequences onto constant region sequences to generate full-length IgG1s which possess better thermal stability than the scFv or Fab forms. To assess the binding of the selected antibodies to the MERS-CoV spike, 13 pairs of plasmids were co-transfected into HEK293T cells respectively and the supernatants containing mAbs were used. Six mAbs were confirmed to specifically bind to MERS-CoV Spike by the enzyme-linked immunosorbent assay (ELISA) (**Supplementary Figure 2**). We further expressed and purified each antibody

2 http://www.who.int/emergencies/mers-cov/en/

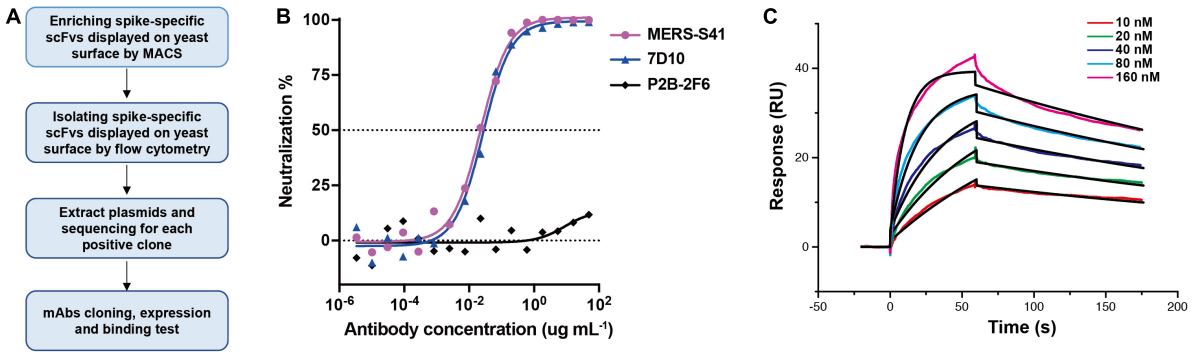

FIGURE 1
Antibody MERS-S41, isolated from a scFv yeast display library, has potent neutralizing activity. **(A)** The selection flowchart. **(B)** Neutralization of the MERS-S41 IgG against pseudotyped MERS-CoV. Antibody 7D10 IgG targets NTD of MERS-CoV S and P2B-2F6 targets RBD of SARS-CoV-2, as positive and negative controls, respectively. **(C)** Surface plasmon resonance curves showing binding of MERS-CoV spike glycoprotein to immobilized MERS-S41 IgG. Data are shown as different colored lines and the best fit of the data to a 1:1 binding model is shown in black.

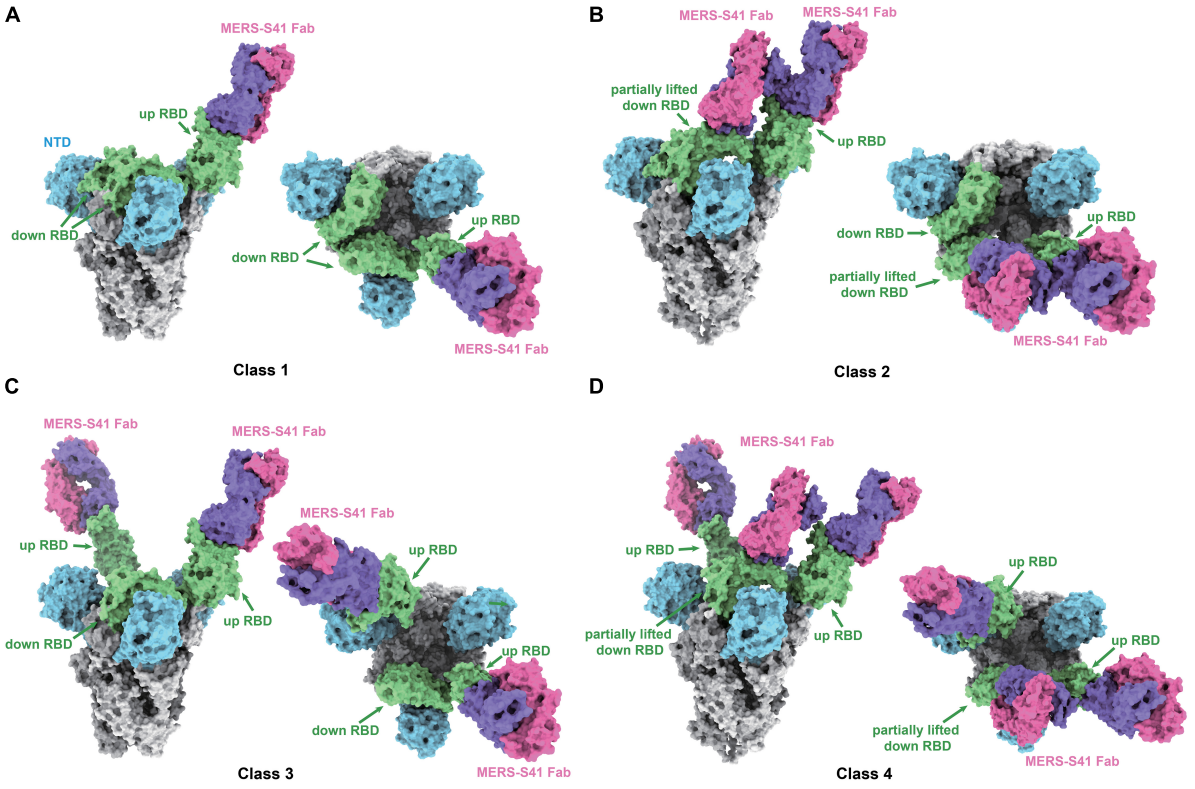

FIGURE 2
Cryo-EM structures of the MERS-S41 Fab bound to MERS-CoV spike trimer. **(A)** Class 1 shows MERS-S41 Fab bound to one "up" RBD. **(B)** Class 2 shows one "up" RBD bound by two MERS-S41 Fabs. **(C)** Class 3 shows two "up" RBDs bound by two MERS-S41 Fabs. **(D)** Class 4 shows two "up" RBDs bound by three MERS-S41 Fabs. In panels **(A–D)**, the MERS-CoV spike trimer NTDs are colored in blue, RBDs in green and other domains in gray. The light chain and heavy chain of MERS-S41 are colored in magenta and purple. The representations are models, shown as surface using Chimera X.

in FreeStyle 293F cells. The purified antibodies were used to evaluate the neutralizing activity against cell entry with pseudotyped MERS-CoV. In addition to MERS-S111 (MERS-27), antibody MERS-S41 was able to inhibit pseudotyped MERS-CoV entry into susceptible Huh7 cells, with an IC_{50} of approximately 0.022 μg/mL (Figure 1B). Surface plasmon resonance (SPR) demonstrated that purified MERS-S41 could bind the spike with an affinity of approximately 4.6 nM

(Figure 1C). MERS-S41 therefore has potent neutralizing activity and high affinity for the MERS-CoV spike glycoprotein.

Structure determination

To determine the complex structure of MERS-S41 with the MERS-CoV spike trimer, we first digested recombinant MERS-S41 IgG to obtain the Fab (Supplementary Figure 1). We then incubated the MERS-S41 Fab with the S protein at a molar ratio of 3.6:1. The complex was visualized by cryo-EM, and the resulting images were processed using single-particle analysis methods (Supplementary Figures 3, 4 and Supplementary Table 2). The nominal resolution of the resolved spike trimer is 2.5Å (Supplementary Figure 4). To obtain better resolution of each RBD-Fab interaction, we performed focused three-dimensional classification and refinement. The resolution of each RBD-Fab ranged from 3.7 to 4.3Å, allowing us to build atomic models with sidechain accuracy (Supplementary Figure 4). In total, we identified four distinct classes (Figure 2; Supplementary Figure 3).

MERS-S41 binds to different conformational states of the spike trimer

As we and others have previously demonstrated, coronavirus RBDs can sample "up" or "down" conformational states (Gui et al., 2017; Pallesen et al., 2017; Yuan et al., 2017). At least one RBD in the "up" position is necessary for the spike trimer to be in an activated, receptor-binding capable state, while all three RBDs in the "down" position keep the S protein in an inactive, receptor-binding incapable state (Song et al., 2018). The four different classes we identified showed that MERS-S41 bound to two distinct conformational states of the spike trimer (Figure 2). State 1 represented a conformation in which just one of the RBDs was "up" (42%) (Figures 2A,B), whereas State 2 corresponded to two "up" RBDs (58%) (Figures 2C,D). We did not observe MERS-S41 bound to spike trimers in which all RBDs were simultaneously "up" or "down."

The MERS-S41 Fabs showed full saturation with one Fab bound to each "up" RBD (Figure 2) regardless of the state of the spike glycoprotein. This observation provided the first indication that MERS-S41 could potentially disrupt receptor binding (see below) by occupying the "up" RBDs required to bind DPP4 (Pallesen et al., 2017; Yuan et al., 2017). Besides binding to "up" RBDs, we also observed two classes in which MERS-S41 Fabs were bound to a partially lifted "down" RBD (Figures 2B,D). The Fab-bound "down" RBDs slightly lifted up with an additional angle of about 25.4° in class 2 and 27.7° in class 4 between the long axes (yellow lines) of the partially lifted "down" RBD and the horizontal plane, comparing to the corresponding non-Fab-bound "down" RBD in class 1 or class 3 (with an angle of about −13.7°) (Supplementary Figure 5). Notably, the partially lifted RBDs are incompatible with DPP4 binding (Supplementary Figures 5c,d). In this binding manner, MERS-S41 could potentially prevent further conformational changes to a fully activated, receptor-binding capable state with all three RBDs "up" rather than only inhibiting receptor binding.

The MERS-S41 epitope overlaps with the DPP4 binding interface

The binding interface between MERS-S41 and the RBD consists of 12 residues from the RBD and 15 residues mainly from MERS-S41 heavy chain (Figure 3). Specifically, the RBD residues L506, Y540, R542, and W553 interact with S30, S31, and Y32 from the heavy chain HCDR1. The RBD residues K502, L506, E513, G538, D539, Y540, V555, and S557 interact with R50, I52, I54, L55, I57, and R59 from the heavy chain HCDR2. The RBD residues Y540, Y541, and R542 interact with G100, G101, and S102 from the heavy chain HCDR3. Residue K74 of the MERS-S41 heavy chain outside the CDRs interacts with residues L506, R511, and E513 of RBD. Only one residue S95 from the light chain LCDR1 interacts with E536 of RBD. Thus, a prominent feature of the interface is that recognition is mainly mediated by the heavy chain. Comparison of the MERS-S41 epitope with the DPP4 binding motif of RBD (Figures 3B,D) shows that there is an overlap with 10 of the 12 epitope residues, suggesting that MERS-S41 binds to the RBD from almost the same direction as DPP4. As expected, superposition of the RBD/MERS-S41 structure with the crystal structure of the MERS-CoV RBD in complex with DPP4 (PDB: 4L72) (Wang et al., 2013) showed severe steric clashes between the variable domain of the heavy chain and the β-propeller domain of DPP4 (Figure 3E). To further confirm that MERS-S41 can inhibit the binding of the spike trimer to DPP4, we performed a cell-surface staining assay by FACS. The results showed that MERS-S41 potently inhibited the binding of the spike trimer to Huh7 cells (Supplementary Figure 6).

Neutralizing activity of MERS-S41 against pseudotyped MERS-CoV bearing naturally changing residues on the S glycoprotein

There are 22 natural variant mutants of the MERS-CoV EMC strain S glycoproteins and we have generated all the pseudotyped MERS-CoV EMC strain mutants (Zhou et al., 2019), including V26F, V26I, V26A, D158Y, L411F, T424I, A482Y, L506F, D509G, V530L, V534A, E536K, D537E, V810I, Q833R, Q914H, R1020H, R1020Q, A1193S, T1202I, G1224S, and V1314A. Among these mutations, we expected that E536K

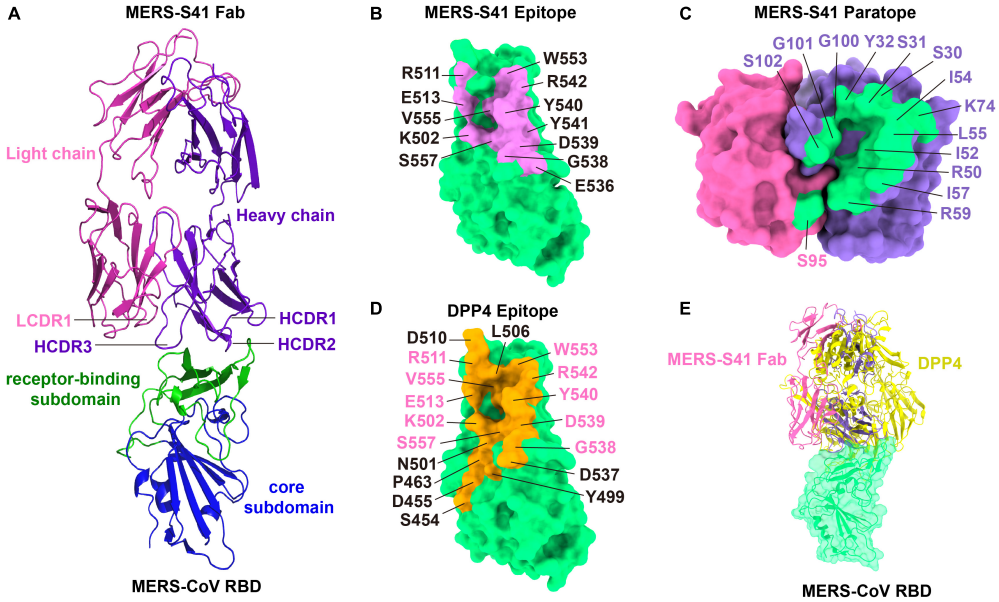

FIGURE 3
The binding interface of the MERS-S41 Fab and MERS-CoV RBD. **(A)** Structure of the MERS-S41 Fab bound to RBD. The RBD core subdomain is colored in blue, the receptor-binding subdomain in green, the MERS-S41 light chain in magenta, and the MERS-S41 heavy chain in purple. **(B)** The MERS-S41 epitope. The MERS-CoV RBD is shown in green surface with residues within 4Å of MERS-S41 Fab labeled and colored pink. **(C)** The MERS-S41 paratope. The MERS-S41 light and heavy chain surfaces are shown in magenta and purple, respectively. Residues within 4Å of the RBD are colored green and labeled in either magenta or purple, depending on whether they are from the light or heavy chain. **(D)** The DPP4 binding site. The MERS-CoV RBD is shown in green surface with residues within 4Å of DPP4 colored orange and labeled. Residues labeled in pink are also in the MERS-S41 epitope. **(E)** The RBD/MERS-S41 Fab structure superposed on the RBD-DPP4 structure (PDB 4L72). The MERS-CoV RBD is shown in green surface, DPP4 shown in yellow cartoon, and MERS-S41 Fab in pink cartoon.

would enable MERS-CoV to escape neutralization by MERS-S41 as E536 is within the epitope. To confirm the binding and test its neutralizing activity against pseudotyped MERS-CoV bearing naturally changing residues, we performed the neutralizing analysis of MERS-S41 against MERS-CoV wild-type (WT) and its mutants. Indeed, E536K increased the IC_{50} value by more than 3000-fold and significantly reduced the activity of MERS-S41 (**Figure 4**). Three others RBD mutations, L506F, D509G and V534A, also increased the IC_{50} value by more than 100-fold (**Figure 4**). The results are consistent with the previous observation that MERS-CoV escaped the neutralization of RBD-targeting antibodies (Wang et al., 2015, 2018) when residue changes occurred on D506, D509, and E536.

Discussion

Here, we have identified a MERS-CoV mAb, MERS-S41, that exhibits potent neutralizing activity. By combining cell surface staining assays with cryo-EM structural analysis of MERS-S41 in complex with the MERS-CoV spike trimer, we have demonstrated that MERS-S41 inhibits MERS-CoV entry by blocking binding to the receptor DPP4.

Based on the epitopes revealed by structural studies, we previously classified MERS-CoV RBD antibodies into three Groups (Xu et al., 2019). Group 1 and 2 antibodies directly compete with the receptor DPP4 but with different approach angles to the RBD, whereas Group 3 antibodies indirectly prevent DPP4 binding by inducing a conformation change of the RBD β5-β6 loop (Zhang et al., 2018) (**Supplementary Figure 7**). Group 2 antibodies typically have more potent neutralizing activity than those in Group 1 (**Supplementary Table 3**), as the approach angles of Group 2 antibodies are closer to that of DPP4. MERS-S41 binds an epitope almost fully overlapping with the receptor binding motif on the RBD (**Figures 3B,D**) and thus blocks attachment to DPP4 *via* direct competition. This observation explained its potent neutralizing activity and led us to classify it into the Group 2 MERS-CoV RBD antibodies (**Supplementary Figure 7**). MERS-S41 with IC_{50} at 0.053 μg/mL and K_D at 4.6 nM is stronger than most antibodies in Group 1 and at equal level with MERS-4 at Group 3. MERS-S41 is not as good as other antibodies among group 2, in terms of pseudoviruses neutralization activity and binding affinity. However, it is the one that was structurally analyzed with trimeric spike, not only just RBD domain. Of note, a structure of LCA60 in complex with trimeric spike was also determined, and it showed that LCA60 can bind both "up" and "down" RBDs in two states of spike. One state of spike was one "up" RBD and two "down" RBDs, another state was two "up" RBDs and one "down" RBD (Walls et al., 2019). Our MERS-S41

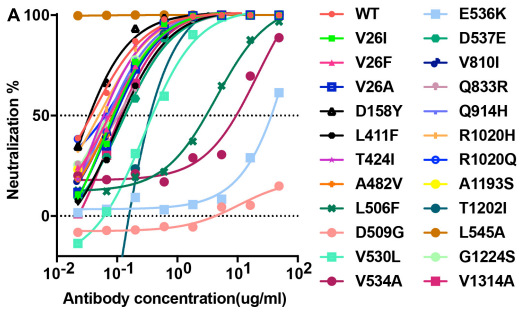

B

Mutation	IC50	Fold	Mutation	IC50	Fold
WT	0.041	1.0	E536K	131	3162.7
V26I	0.059	1.4	D537E	0.119	2.9
V26F	0.077	1.9	L545A	0.073	0.4
V26A	0.069	1.7	V810I	0.138	1.8
D158Y	0.018	0.4	Q833R	0.055	3.3
L411F	0.096	2.3	Q914H	0.056	1.3
T424I	0.036	0.9	R1020H	0.111	1.4
A482V	0.074	1.8	R1020Q	0.073	2.7
L506F	4.457	107.6	A1193S	0.069	1.8
D509G	10.470	252.7	T1202I	0.018	1.7
V530L	0.279	6.7	G1224S	0.068	1.7
V534A	21.410	516.9	V1314A	0.072	1.7

FIGURE 4
Breadth of MERS-S41 neutralization. **(A)** Neutralizing analysis of MERS-S41 IgG against MERS-CoV wild-type (WT) and its variant mutants. Site-directed mutations were introduced into the EMC strain to create 23 variant mutants according to natural mutations of MERS-CoV S. **(B)** Summary of MERS-S41 IgG mediated inhibition of infection by all pseudotyped viruses. IC_{50} neutralization titers for mutant EMC S variants are presented relative to wild-type S.

can bind to the MERS-CoV spike at different stoichiometries and the Fab-bound "down" RBDs were lifted up.

In our complex structures, MERS-S41 Fab can bind to "up" or partially lifted "down" RBDs, indicating that the neutralization mechanism is not only the direct competition with DPP4 but also potentially able to stop the conformation change of RBD from "down" to "up." However, this speculated ability of trapping the RBD of S protein in the "down" conformation is limited. Based on our observations, MERS-S41 Fab binding to the non-"up" RBDs in the presence of excessive Fabs requires two conditions. First, MERS-S41 Fab only binds to the partially lifted "down" RBDs (**Figure 2**; **Supplementary Figure 5**). If we dock our Fab onto the "down" RBD in class 1 (**Supplementary Figure 5a**), class 2 (**Supplementary Figure 8a**), or class 3 (**Supplementary Figure 5b**), severe steric clashes occur. This analysis suggests that fully "down" RBDs are not accessible to MERS-S41. We therefore think that MERS-S41 recognizes an intermediate state between "down" and "up" although we cannot rule out that the Fab would induce this transformation. Second, the partially lifted "down" RBD requires an "up" RBD that sits at its pointing side (**Figures 2B,D**; **Supplementary Figure 8a**). The epitope of MERS-S41 is inaccessible in the inactivated state without "up" RBDs. We superimposed MERS-S41 Fab-RBD structure onto the structure of inactive MERS-CoV spike trimer (PDB 5W9J). Severe steric clashes would be expected between the MERS-S41 Fab and the "down" RBD of the neighboring S monomer (**Supplementary Figure 8b**).

Materials and methods

Cell lines

Vero E6, 293T, 293F, and Huh7 cell lines were bought from ATCC (Manassas, VA, USA) and cultured in Dulbecco's Modified Eagle medium (DMEM) supplemented with 10% fetal bovine serum (FBS) and incubated at 37°C in a humidified atmosphere comprising 5% CO_2.

Protein expression and purification

The coding sequence of the MERS-CoV spike glycoprotein ectodomain (EMC strain, spike residues 1-1290) was ligated into the pFastBac-Dual vector (Invitrogen, Carlsbad, CA, USA) with a C-terminal T4 fibritin trimerization domain and a hexa-His-strep tap tag to facilitate purification. Briefly, the protein was expressed using the Bac-to-Bac baculovirus expression system and purified by sequentially applying Strep-Tactin and Superose 6 column (GE Healthcare, Chicago, IL, USA) with HBS buffer (10 mM HEPES, pH 7.2, 150 mM NaCl). Fractions containing MERS-CoV S glycoprotein were pooled and concentrated for subsequent biochemical analyses and EM studies.

The sequence encoding the MERS-S41 VL and VH were separately cloned into the backbone of antibody expression vectors containing the constant regions of human IgG1. The antibody MERS-S41 was expressed in FreeStyle 293-F cells by transient transfection and purified by affinity chromatography using Protein A Sepharose and size-exclusion chromatography. Purified MERS-S41 was exchanged into PBS and digested with papain protease (Sigma, St. Louis, MO, USA) overnight at 37°C. The digested antibody was then passed back over Protein A Sepharose to remove the Fc fragment, and the unbound Fab in the flow through was additionally purified using a Superdex 200 High Performance column (GE Healthcare).

Selection of yeast library for MERS-CoV spike-specific scFvs

Human non-immune scFv library (~1×10^9), constructed from spleen and lymph node polyadenylated RNA pooled from

58 naïve humans, was provided by C. Baird (Pacific Northwest National Laboratory) (Feldhaus et al., 2003). Purified soluble S protein was used as a bait to select 2×10^9 yeast cells by two rounds of MACS followed by three rounds of FACS with a BD FACSAria II sorter (San Jose, CA, USA). Between each round of selection, the sorted yeast cells were grown in SD-CAA and induced in SG-CAA medium as previously reported (Chao et al., 2006). After the second round of FACS, DNA plasmids were extracted from the sorted yeast population and transformed into *E. coli* DH5α for producing sufficient amounts of DNA for sequencing and sequence analysis.

The heavy and light chain genes of MERS-CoV spike–specific scFvs were separately cloned into backbone of antibody expression vectors containing the constant regions of IgG1. Whole-human IgG1 was expressed in 293T cells by transient transfection. The supernatants were serially diluted in PBS and applied on the IgG coated 96-well plates to confirm the IgG expression by a human IgG quantification kit (Abcam, Cambridge, UK). Then, MERS-CoV S glycoprotein at 1 μg/mL were used to coat plates overnight at 4°C, and the successfully expressed mAbs in each supernatant were serially diluted in PBS and assessed for binding affinity to the MERS-CoV spike by ELISA.

Neutralizing assay of pseudotyped MERS-CoV

HEK293T cells cultured in 100 mm dish were co-transfected with 6 μg of pcDNA3.1-MERS-Spike-2p or its mutants and 24 μg of pNL4-3.luc.RE. The supernatants containing sufficient pseudotyped MERS-CoV were harvested 48–72 h post-transfection. Subsequently, the 50% tissue culture infectious dose ($TCID_{50}$) was determined by infection of Huh7 cells. For the neutralization assay, 100 $TCID_{50}$ per well of pseudotyped virus were incubated with 16 serial 1:3 dilutions of purified antibodies, Fabs or scFvs for 1 h at 37°C, after which Huh7 cells (about 1.5×10^4 per well) were added. After incubation for 72 h at 37°C, the neutralizing activities of antibodies were determined by luciferase activity and presented as IC_{50}, calculated using the dose-response inhibition function in GraphPad Prism 5 (GraphPad Software Inc.).

Surface plasmon resonance experiments

Running buffer composed of 10 mM HEPES pH 7.2, 150 mM NaCl and 0.05% (v/v) Tween-20 was used during the analysis and all proteins were exchanged to the same buffer. The purified MERS-S41 IgG was covalently immobilized to a CM5 sensor chip (GE Healthcare) using Biacore T200 (GE Healthcare). The blank channel of the chip was used as the negative control. Serial dilutions of MERS-CoV Spike proteins were flowed through the chip sequentially. The resulting data were analyzed using Biacore T200 Evaluation Software 3.1 (GE Healthcare) by fitting to a 1:1 binding model.

Florescence-activated cell sorting analysis of cell-surface staining

The binding between recombinant soluble MERS-CoV spike trimer (S) and human DPP4 expressed on the surface of Huh7 cells was measured using fluorescence-activated cell sorting (FACS). All cell-surface staining experiments were performed at room temperature. Soluble S protein with strep-tag (1 μg) was incubated with monoclonal antibodies (mAbs) in advance at molar ratios of 1:1, 1:3, 1:9, and 1:27 for 1 h. Huh7 cells were trypsinized and then incubated with S or S and mAbs mixtures for 1 h. After washing the un-bound S with PBS 3 times, the Huh7 cells were then stained with streptavidin APC (BD eBioscience, Franklin Lakes, NJ, USA) for another 45 min. Cells were subsequently washed with PBS 5 times and analyzed by flow cytometry on a FACS Aria III machine (BD eBiosciences).

Cryoelectron microscopy data collection and image processing

Images for MERS-CoV spike ectodomains with MERS-S41 Fab were recorded using FEI Titan Krios microscope (Thermo Fisher Scientific, Waltham, MA, USA) operating at 300 kV with a Gatan K3 Summit direct electron detector (Gatan Inc., Pleasanton, CA, USA) at Tsinghua University. The automated software [AutoEMation2 (Scheres, 2012)] was used to collect 5,010 movies in super-resolution mode at a nominal magnification of 81,000× and at a defocus range between −1.5 and −2.0 μm. Each movie has a total accumulated exposure of 50 $e^-/Å^2$ fractionated in 32 frames of 175 ms exposure. The final image was binned 2-fold to a pixel size of 1.0825Å. Motion Correction (MotionCor2) (Zheng et al., 2017) and CTF-estimation (GCTF) (Zhang, 2016) were automatically executed by TsinghuaTitan.py program (developed by Dr. Fang Yang) during data collection. Data collection statistics are summarized in **Supplementary Table 2**.

The image processing procedures are presented in **Supplementary Figure 3**. Initially, 5,010 micrographs (3,360 Quantifoil micrographs and 1,650 Lacey carbon micrographs) were inspected and selected using the TsinghuaTitan.py program, followed by particle auto-picking using Gautomatch (developed by Kai Zhang[3]) or Relion 3.0 (Scheres, 2012;

3 https://www2.mrc-lmb.cam.ac.uk/download/gautomatch-056/

Zivanov et al., 2018). Multiple rounds of 2D classification were performed to eliminate bad particles, followed by 3D classification. 644,359 particles belonging to the best class were expanded with C3 symmetry, resulting in 1,933,007 particles, and followed by local 3D classification. Three classes had the same conformation but belonged to three different orientations around the C3 symmetry axis. Particles from the three classes were reorientated into the same orientation and duplicates removed, which yielded 424,969 particles. Refinement of these particles resulted in a map with a nominal resolution of 3.2Å. To improve the resolution further, CTF refinement, C3 symmetry and Bayesian Polishing were applied, which improved the overall resolution to 3.0, 2.8, and 2.5Å, successively. To improve the map density of RBD-Fab complex region, different masks of RBD-Fab complex were applied in focused 3D classification and subsequent refinement, which produced reconstructions of 4.3Å (RBD1-Fab, 118,198 particles), 4.2Å (RBD2-Fab, 88,100 particles), and 4.2Å (RBD3-Fab, 72,803 particles). Similarly, CTF refinement and Bayesian Polishing were applied to the RBD3-Fab complex, which improved the overall resolution to 3.7Å. To further classify different conformations, particle subtraction with a mask focused on all three RBD-Fab regions were applied, followed by 3D classification without alignment, which obtained four distinct conformations. Maps of the spike and three RBD-Fab regions were combined according to the classified distinct four classes to generate the final combined maps of the MERS-CoV spike-MERS-S41 complexes. All classification and refinement jobs were performed in Relion 3.0 or Relion 3.1. CTF refinement, Bayesian polishing, and particle subtraction were done in Relion 3.1.

Model building and refinement

The atomic model of the MERS-CoV spike was built in Coot (Emsley et al., 2010) using PDB 5 × 58 as a starting model. The initial model of the MERS-S41 Fab was generated by SWISS-MODEL (Waterhouse et al., 2018) and fitted into the map using UCSF Chimera (Pettersen et al., 2004), followed by manual rebuilding in Coot. The atomic models were refined in real space using Phenix (Afonine et al., 2018), and validated using the Molprobity web application (Williams et al., 2018). UCSF Chimera and PyMol (Janson et al., 2017) were used for map segmentation and figure generation. Model refinement statistics are summarized in **Supplementary Table 2**.

Figures

Figure panels depicting cryo-EM maps or atomic models were generated using Chimera (Pettersen et al., 2004) or ChimeraX (Pettersen et al., 2020). Maps colored by local resolution were generated using RELION 3.1 (Zivanov et al., 2018).

Data availability statement

Publicly available datasets were analyzed in this study. This data can be found here: https://www.ncbi.nlm.nih.gov/igblast/.

Author contributions

HZ and WJ isolated and characterized MERS-S41 and performed cell surface staining assays. SZ and HZ prepared proteins. SZ collected cryo-EM data and performed binding and neutralizing assays. JZ and SZ processed the cryo-EM data and built the model. HZ, LZ, and XW supervised the research. HZ and XW wrote the manuscript with input from SZ, WJ, JZ, ML, ZW, and LZ. All authors contributed to the article and approved the submitted version.

Acknowledgments

We thank the Tsinghua University Branch of China National Center for Protein Sciences (Beijing) for the cryo-EM facility. We also thank Alan Brown (BCMP at Harvard Medical School) for comments on the manuscript.

Conflict of interest

The authors declare that the research was conducted in the absence of any commercial or financial relationships that could be construed as a potential conflict of interest.

Publisher's note

Supplementary material

The Supplementary Material for this article can be found online at: https://www.frontiersin.org/articles/10.3389/fmicb.2022.988298/full#supplementary-material

References

Afonine, P. V., Poon, B. K., Read, R. J., Sobolev, O. V., Terwilliger, T. C., Urzhumtsev, A., et al. (2018). Real-space refinement in PHENIX for cryo-EM and crystallography. *Acta Crystallogr. D Struct. Biol.* 74, 531–544. doi: 10.1107/S2059798318006551

Azhar, E. I., El-Kafrawy, S. A., Farraj, S. A., Hassan, A. M., Al-Saeed, M. S., Hashem, A. M., et al. (2014). Evidence for camel-to-human transmission of MERS coronavirus. *N. Engl. J. Med.* 370, 2499–2505. doi: 10.1056/NEJMoa1401505

Chao, G., Lau, W. L., Hackel, B. J., Sazinsky, S. L., Lippow, S. M., and Wittrup, K. D. (2006). Isolating and engineering human antibodies using yeast surface display. *Nat. Protoc.* 1, 755–768. doi: 10.1038/nprot.2006.94

Chen, Y., Lu, S., Jia, H., Deng, Y., Zhou, J., Huang, B., et al. (2017). A novel neutralizing monoclonal antibody targeting the N-terminal domain of the MERS-CoV spike protein. *Emerg. Microbes Infect.* 6:e60. doi: 10.1038/emi.2017.50

Corti, D., Zhao, J., Pedotti, M., Simonelli, L., Agnihothram, S., Fett, C., et al. (2015). Prophylactic and postexposure efficacy of a potent human monoclonal antibody against MERS coronavirus. *Proc. Natl. Acad. Sci. U.S.A.* 112, 10473–10478. doi: 10.1073/pnas.1510199112

Emsley, P., Lohkamp, B., Scott, W. G., and Cowtan, K. (2010). Features and development of Coot. *Acta Crystallogr. D Biol. Crystallogr.* 66, 486–501. doi: 10.1107/S0907444910007493

Feldhaus, M. J., Siegel, R. W., Opresko, L. K., Coleman, J. R., Feldhaus, J. M., Yeung, Y. A., et al. (2003). Flow-cytometric isolation of human antibodies from a nonimmune *Saccharomyces cerevisiae* surface display library. *Nat. Biotechnol.* 21, 163–170. doi: 10.1038/nbt785

Gui, M., Song, W., Zhou, H., Xu, J., Chen, S., Xiang, Y., et al. (2017). Cryo-electron microscopy structures of the SARS-CoV spike glycoprotein reveal a prerequisite conformational state for receptor binding. *Cell Res.* 27, 119–129. doi: 10.1038/cr.2016.152

Janson, G., Zhang, C., Prado, M. G., and Paiardini, A. (2017). PyMod 2.0: improvements in protein sequence-structure analysis and homology modeling within PyMOL. *Bioinform.* 33, 444–446. doi: 10.1093/bioinformatics/btw638

Jiang, L., Wang, N., Zuo, T., Shi, X., Poon, K. M., Wu, Y., et al. (2014). Potent neutralization of MERS-CoV by human neutralizing monoclonal antibodies to the viral spike glycoprotein. *Sci. Transl. Med.* 6:234ra259. doi: 10.1126/scitranslmed.3008140

Li, Y., Wan, Y., Liu, P., Zhao, J., Lu, G., Qi, J., et al. (2015). A humanized neutralizing antibody against MERS-CoV targeting the receptor-binding domain of the spike protein. *Cell Res.* 25, 1237–1249. doi: 10.1038/cr.2015.113

Lu, G., Hu, Y., Wang, Q., Qi, J., Gao, F., Li, Y., et al. (2013). Molecular basis of binding between novel human coronavirus MERS-CoV and its receptor CD26. *Nature* 500, 227–231. doi: 10.1038/nature12328

Millet, J. K., and Whittaker, G. R. (2014). Host cell entry of Middle East respiratory syndrome coronavirus after two-step, furin-mediated activation of the spike protein. *Proc. Natl. Acad. Sci. U.S.A.* 111, 15214–15219. doi: 10.1073/pnas.1407087111

Mohd, H. A., Al-Tawfiq, J. A., and Memish, Z. A. (2016). Middle east respiratory syndrome coronavirus (MERS-CoV) origin and animal reservoir. *Virol. J.* 13:87. doi: 10.1186/s12985-016-0544-0

Niu, P., Zhang, S., Zhou, P., Huang, B., Deng, Y., Qin, K., et al. (2018). Ultrapotent human neutralizing antibody repertoires against Middle East respiratory syndrome coronavirus from a recovered patient. *J. Infect. Dis.* 218, 1249–1260. doi: 10.1093/infdis/jiy311

Pallesen, J., Wang, N., Corbett, K. S., Wrapp, D., Kirchdoerfer, R. N., Turner, H. L., et al. (2017). Immunogenicity and structures of a rationally designed prefusion MERS-CoV spike antigen. *Proc. Natl. Acad. Sci. U.S.A.* 114, E7348–E7357. doi: 10.1073/pnas.1707304114

Peiris, J. S., Lai, S. T., Poon, L. L., Guan, Y., Yam, L. Y., Lim, W., et al. (2003). Coronavirus as a possible cause of severe acute respiratory syndrome. *Lancet* 361, 1319–1325. doi: 10.1016/s0140-6736(03)13077-2

Pettersen, E. F., Goddard, T. D., Huang, C. C., Couch, G. S., Greenblatt, D. M., Meng, E. C., et al. (2004). UCSF Chimera–a visualization system for exploratory research and analysis. *J. Comput. Chem.* 25, 1605–1612. doi: 10.1002/jcc.20084

Pettersen, E. F., Goddard, T. D., Huang, C. C., Meng, E. C., and Ferrin, T. E. (2020). UCSF ChimeraX: structure visualization for researchers, educators, and developers. *Protein Sci.* 30, 70–82. doi: 10.1002/pro.3943

Raj, V. S., Mou, H., Smits, S. L., Dekkers, D. H., Muller, M. A., Dijkman, R., et al. (2013). Dipeptidyl peptidase 4 is a functional receptor for the emerging human coronavirus-EMC. *Nature* 495, 251–254. doi: 10.1038/nature12005

Scheres, S. H. (2012). A Bayesian view on cryo-EM structure determination. *J. Mol. Biol.* 415, 406–418. doi: 10.1016/j.jmb.2011.11.010

Song, W., Gui, M., Wang, X., and Xiang, Y. (2018). Cryo-EM structure of the SARS coronavirus spike glycoprotein in complex with its host cell receptor ACE2. *PLoS Pathog.* 14:e1007236. doi: 10.1371/journal.ppat.1007236

Tang, X. C., Agnihothram, S. S., Jiao, Y., Stanhope, J., Graham, R. L., Peterson, E. C., et al. (2014). Identification of human neutralizing antibodies against MERS-CoV and their role in virus adaptive evolution. *Proc. Natl. Acad. Sci. U.S.A.* 111, E2018–E2026. doi: 10.1073/pnas.1402074111

Walls, A. C., Park, Y. J., Tortorici, M. A., Wall, A., McGuire, A. T., and Veesler, D. (2020). Structure, function, and antigenicity of the SARS-CoV-2 spike glycoprotein. *Cell* 181, 281.e6–292.e6. doi: 10.1016/j.cell.2020.02.058

Walls, A. C., Xiong, X., Park, Y. J., Tortorici, M. A., Snijder, J., Quispe, J., et al. (2019). Unexpected receptor functional mimicry elucidates activation of coronavirus fusion. *Cell* 176, 1026–1039. doi: 10.1016/j.cell.2018.12.028

Wang, L., Shi, W., Chappell, J. D., Joyce, M. G., Zhang, Y., Kanekiyo, M., et al. (2018). Importance of neutralizing monoclonal antibodies targeting multiple antigenic sites on the Middle East respiratory syndrome coronavirus spike glycoprotein to avoid neutralization escape. *J. Virol.* 92:10. doi: 10.1128/JVI.02002-17

Wang, L., Shi, W., Joyce, M. G., Modjarrad, K., Zhang, Y., Leung, K., et al. (2015). Evaluation of candidate vaccine approaches for MERS-CoV. *Nat. Commun.* 6:7712. doi: 10.1038/ncomms8712

Wang, N., Shi, X., Jiang, L., Zhang, S., Wang, D., Tong, P., et al. (2013). Structure of MERS-CoV spike receptor-binding domain complexed with human receptor DPP4. *Cell Res.* 23, 986–993. doi: 10.1038/cr.2013.92

Waterhouse, A., Bertoni, M., Bienert, S., Studer, G., Tauriello, G., Gumienny, R., et al. (2018). SWISS-MODEL: homology modelling of protein structures and complexes. *Nucleic Acids Res.* 46, W296–W303. doi: 10.1093/nar/gky427

Williams, C. J., Headd, J. J., Moriarty, N. W., Prisant, M. G., Videau, L. L., Deis, L. N., et al. (2018). MolProbity: more and better reference data for improved all-atom structure validation. *Protein Sci.* 27, 293–315. doi: 10.1002/pro.3330

Wrapp, D., Wang, N., Corbett, K. S., Goldsmith, J. A., Hsieh, C. L., Abiona, O., et al. (2020). Cryo-EM structure of the 2019-nCoV spike in the prefusion conformation. *Science* 367, 1260–1263. doi: 10.1126/science.abb2507

Xu, J., Jia, W., Wang, P., Zhang, S., Shi, X., Wang, X., et al. (2019). Antibodies and vaccines against Middle East respiratory syndrome coronavirus. *Emerg. Microbes Infect.* 8, 841–856. doi: 10.1080/22221751.2019.1624482

Ying, T., Du, L., Ju, T. W., Prabakaran, P., Lau, C. C., Lu, L., et al. (2014). Exceptionally potent neutralization of Middle East respiratory syndrome coronavirus by human monoclonal antibodies. *J. Virol.* 88, 7796–7805. doi: 10.1128/JVI.00912-14

Ying, T., Prabakaran, P., Du, L., Shi, W., Feng, Y., Wang, Y., et al. (2015). Junctional and allele-specific residues are critical for MERS-CoV neutralization by an exceptionally potent germline-like antibody. *Nat. Commun.* 6:8223. doi: 10.1038/ncomms9223

Yu, X., Zhang, S., Jiang, L., Cui, Y., Li, D., Wang, D., et al. (2015). Structural basis for the neutralization of MERS-CoV by a human monoclonal antibody MERS-27. *Sci. Rep.* 5:13133. doi: 10.1038/srep13133

Yuan, Y., Cao, D., Zhang, Y., Ma, J., Qi, J., Wang, Q., et al. (2017). Cryo-EM structures of MERS-CoV and SARS-CoV spike glycoproteins reveal the dynamic receptor binding domains. *Nat. Commun.* 8:15092. doi: 10.1038/ncomms15092

Zhang, K. (2016). Gctf: real-time CTF determination and correction. *J. Struct. Biol.* 193, 1–12. doi: 10.1016/j.jsb.2015.11.003

Zhang, S., Zhou, P., Wang, P., Li, Y., Jiang, L., Jia, W., et al. (2018). Structural definition of a unique neutralization epitope on the receptor-binding domain of MERS-CoV spike glycoprotein. *Cell Rep.* 24, 441–452. doi: 10.1016/j.celrep.2018.06.041

Zheng, S. Q., Palovcak, E., Armache, J. P., Verba, K. A., Cheng, Y., and Agard, D. A. (2017). MotionCor2: anisotropic correction of beam-induced motion for improved cryo-electron microscopy. *Nat. Methods* 14, 331–332. doi: 10.1038/nmeth.4193

Zhou, H., Chen, Y., Zhang, S., Niu, P., Qin, K., Jia, W., et al. (2019). Structural definition of a neutralization epitope on the N-terminal domain of MERS-CoV spike glycoprotein. *Nat. Commun.* 10:3068. doi: 10.1038/s41467-019-10897-4

Zivanov, J., Nakane, T., Forsberg, B. O., Kimanius, D., Hagen, W. J., Lindahl, E., et al. (2018). New tools for automated high-resolution cryo-EM structure determination in RELION-3. *Elife* 7:e42166. doi: 10.7554/eLife.42166

Zumla, A., Hui, D. S., and Perlman, S. (2015). Middle East respiratory syndrome. *Lancet* 386, 995–1007. doi: 10.1016/S0140-6736(15)60454-8

frontiers | Frontiers in Microbiology

TYPE Review
PUBLISHED 06 October 2022
DOI 10.3389/fmicb.2022.979719

OPEN ACCESS

EDITED BY
Wanbo Tai,
Shenzhen Bay Laboratory,
China

REVIEWED BY
Lihui Guo,
University of Amsterdam,
Netherlands
Sanchita Hati,
University of Wisconsin–Eau Claire,
United States

*CORRESPONDENCE
Carlos A. Labarrere
clabarrere@sbcglobal.net

SPECIALTY SECTION
This article was submitted to Virology, a section of the journal Frontiers in Microbiology

RECEIVED 27 June 2022
ACCEPTED 14 September 2022
PUBLISHED 06 October 2022

CITATION
Labarrere CA and Kassab GS (2022) Glutathione deficiency in the pathogenesis of SARS-CoV-2 infection and its effects upon the host immune response in severe COVID-19 disease.
Front. Microbiol. 13:979719.
doi: 10.3389/fmicb.2022.979719

Glutathione deficiency in the pathogenesis of SARS-CoV-2 infection and its effects upon the host immune response in severe COVID-19 disease

Carlos A. Labarrere* and Ghassan S. Kassab

California Medical Innovations Institute, San Diego, CA, United States

Severe acute respiratory syndrome coronavirus 2 (SARS-CoV-2) that causes coronavirus disease 19 (COVID-19) has numerous risk factors leading to severe disease with high mortality rate. Oxidative stress with excessive production of reactive oxygen species (ROS) that lower glutathione (GSH) levels seems to be a common pathway associated with the high COVID-19 mortality. GSH is a unique small but powerful molecule paramount for life. It sustains adequate redox cell signaling since a physiologic level of oxidative stress is fundamental for controlling life processes *via* redox signaling, but excessive oxidation causes cell and tissue damage. The water-soluble GSH tripeptide (γ-L-glutamyl-L-cysteinyl-glycine) is present in the cytoplasm of all cells. GSH is at 1–10mM concentrations in all mammalian tissues (highest concentration in liver) as the most abundant non-protein thiol that protects against excessive oxidative stress. Oxidative stress also activates the Kelch-like ECH-associated protein 1 (Keap1)-Nuclear factor erythroid 2-related factor 2 (Nrf2)-antioxidant response element (ARE) redox regulator pathway, releasing Nrf2 to regulate the expression of genes that control antioxidant, inflammatory and immune system responses, facilitating GSH activity. GSH exists in the thiol-reduced and disulfide-oxidized (GSSG) forms. Reduced GSH is the prevailing form accounting for >98% of total GSH. The concentrations of GSH and GSSG and their molar ratio are indicators of the functionality of the cell and its alteration is related to various human pathological processes including COVID-19. Oxidative stress plays a prominent role in SARS-CoV-2 infection following recognition of the viral S-protein by angiotensin converting enzyme-2 receptor and pattern recognition receptors like toll-like receptors 2 and 4, and activation of transcription factors like nuclear factor kappa B, that subsequently activate nicotinamide adenine dinucleotide phosphate (NADPH) oxidase (NOX) expression succeeded by ROS production. GSH depletion may have a fundamental role in COVID-19 pathophysiology, host immune response and disease severity and mortality. Therapies enhancing GSH could become a cornerstone to reduce severity and fatal outcomes of COVID-19 disease and increasing GSH levels may prevent and subdue the disease. The life value of GSH makes for a paramount research field in biology and medicine and may be key against SARS-CoV-2 infection and COVID-19 disease.

KEYWORDS

Glutathione, SARS-CoV-2, COVID-19, reactive oxygen species, oxidative stress, acute respiratory distress syndrome, atherosclerosis, atherothrombosis

Introduction

The coronavirus disease 2019 (COVID-19) pandemic affected more than 602.8 million cases with more than 6.4 million deaths reported globally (The New York Times, 2022). Several risk factors including age, hypertension, ischemic heart disease, diabetes, and chronic respiratory disease (Khanfar and Al Qaroot, 2020) increase the fatality rate (Ruan et al., 2020; O'Driscoll et al., 2021) which is directly related with the cytokine storm (Fajgenbaum and June, 2020; Mehta et al., 2020) that can cause acute respiratory distress syndrome, lung injury, respiratory insufficiency, endothelial cell dysfunction, thrombosis, cardiovascular disease and end-organ damage (Klok et al., 2020; Teuwen et al., 2020; Yang L. et al., 2020; Chang et al., 2021; Kaklamanos et al., 2021; Stenmark et al., 2021). All these risk factors have a common characteristic, they are associated with a continuous state of oxidative stress and inflammation, excessive production of free radicals (reactive oxygen and nitrogen species) and endothelial cell dysfunction leading to cardiovascular disease and respiratory failure.

A common pathway affecting all these risk factors involves a low measure of reduced glutathione (i.e., GSH) level (Khanfar and Al Qaroot, 2020; Polonikov, 2020; Silvagno et al., 2020). SARS-CoV-2-infected patients with COVID-19 disease show alterations in the glucose–insulin axis leading to hyperglycemia, hyperinsulinemia and insulin resistance, increased oxidative/nitrosative stress, and significantly decreased vitamin D, thiols, total-antioxidant-capacity, GSH and selenium (Soto et al., 2022). In-depth knowledge of the pathophysiology causing COVID-19-mediated GSH depletion, tissue damage, and acute respiratory distress syndrome is urgently needed. Moreover, the way GSH depletion can lead to immune system failure and make the end organs in danger of oxidative stress-mediated damage needs to be explained. The disturbed redox homeostasis leading to accumulation of reactive oxygen species (ROS) is a common feature in all conditions associated with COVID-19 (Miripour et al., 2020; Pérez de la Lastra et al., 2021). Interestingly, all patients with severe COVID-19 disease and high mortality risk have low basal GSH levels (Khanfar and Al Qaroot, 2020) that could explain an ominous outcome. Several studies pointed out that GSH and the enzymes associated with the GSH pathway are involved in SARS-CoV-2 infection and COVID-19 disease. Recent studies demonstrated that individuals with glutathione transferase omega polymorphisms, genotype variants GSTO1*AA (rs4925) and GSTO2*GG (rs156697), showed significant propensity towards development of clinical manifestations in COVID-19 supporting the significance of these enzymes in the regulation of redox homeostasis and immune response, especially NACHT, LRR, and PYD domains-containing protein 3 (NLRP3) inflammasome activation (Zhao and Zhao, 2020; Djukic et al., 2022). Combined glutathione S-transferase (GST)P1 (rs1138272 and rs1695) and GSTM3 genotypes showed cumulative risk regarding both occurrence and severity of COVID-19 (Coric et al., 2021). COVID-19 patients with the GSTT1-null genotype experience higher mortality (Saadat, 2020; Abbas et al., 2021). Diabetic COVID-19 patients have high cellular oxidative stress, evidenced by decreased extracellular superoxide dismutase 3 levels (Kumar D.S. et al., 2022). Low glutathione S-transferase P1 levels are associated with higher mortality in COVID-19 patients, and high levels of glutathione S-transferase P1 possibly offer protection for cellular redox reactions in severe COVID-19 infection, preventing deterioration especially in patients with co-morbidities like diabetes (Kumar D.S. et al., 2022).

Acute respiratory distress syndrome (ARDS) is considered as a decisive cause of death in COVID-19 disease (Gralinski and Baric, 2015; Quan et al., 2021). Cytokine storm and oxidative stress are the main participants in the development of ARDS during respiratory virus infections (Meftahi et al., 2021). SARS-CoV-2 infection generates massive ROS production and the excessive oxidative damage is responsible for cytokine storm, undermined immunity, tissue damage and severe lung disease causing ARDS and death (Silvagno et al., 2020). Therefore, augmenting tissue GSH levels may lower COVID-19 severity and mortality rates.

Old age, a consequence of aging, is one of the most important risk factors for SARS-CoV-2 infection and development of COVID-19 disease. Aging is directly related to the damage caused by free radicals, particularly ROS causing oxidative stress (Sies, 2015; Baş, 2018). Endothelial cells play a fundamental role in chronic oxidative stress and the development of atherosclerosis, thrombosis and lung injury, principal complications of SARS-CoV-2-mediated tissue and organ dysfunction (Chang et al., 2021). Excess mitochondrial ROS production, causes cellular

Abbreviations: SARS-CoV-2, Severe acute respiratory syndrome coronavirus 2; COVID-19, coronavirus disease 19; ROS, reactive oxygen species; GSH, glutathione; Keap1, Kelch-like ECH-associated protein 1; Nrf2, Nuclear factor erythroid 2-related factor 2; ARE, antioxidant response element; GSSG, GSH disulfide; NADPH, nicotinamide adenine dinucleotide phosphate; NOX, NADPH oxidase; ARDS, Acute respiratory distress syndrome; NFκB, nuclear factor-κB; ACE2, angiotensin converting enzyme-2; NETs, neutrophil extracellular traps; rTEM, reverse trans-endothelial migration; NAC, N-acetylcysteine; CRP, C-reactive protein; HSPGs, heparan sulfate proteoglycans; GCS, glutamyl-cysteine synthetase; TMPRSS2, transmembrane protease serine 2; TLRs, Toll-like receptors.

oxidative stress, sustains mitochondrial dysfunction and ROS production and perpetuates inflammation (Chang et al., 2021). SARS-CoV-2 can activate mitochondrial ROS production, especially in older individuals having ROS overproduction, enhancing oxidative stress and promoting endothelial dysfunction, cardiovascular disease and lung injury. The ROS-mediated damage is further enhanced in older individuals since during aging, GSH levels appear to diminish in numerous tissues, thereby placing cells at increased risk of stress-related death (Maher, 2005). Low GSH in aging is associated with lower intake of GSH precursors, mainly cysteine, and lower GSH synthesis evidencing diminished function of nuclear factor erythroid 2–related factor 2 (Nrf2)-dependent inductive mechanisms that enhance glutamate cysteine ligase expression, rate limiting factor for the synthesis of GSH (McCarty and DiNicolantonio, 2015).

All COVID-19 risk factors are associated with reduced GSH levels (Figure 1). As noted previously, increasing age is linked to reduced GSH levels (Dröge, 2002a,b), which can be the result of extensive GSH oxidation and/or reduced pool of cell thiols, and cysteine (whey protein) administration enhances GSH levels and increases longevity (Bounous et al., 1989; Dröge, 2002a,b; Andriollo-Sanchez et al., 2005). Hypertension, ischemic heart disease, patients with atherosclerosis and coronary artery disease, diabetes, chronic lung diseases, smoking and obesity are associated with low baseline GSH levels and reduced GSH/oxidized glutathione (GSSG) ratios (Khanfar and Al Qaroot, 2020; Polonikov, 2020). We will discuss the life-sustaining importance of GSH, its relationship with oxidative stress, as well as its synthesis and catabolism, its biological functions and the paramount relevance of GSH in the immune system (especially the innate immune system), in reducing COVID-19 severity and mortality, and the antiviral capabilities of GSH to reduce SARS-CoV-2 infectivity and multiorgan failure secondary to a cytokine storm in COVID-19 disease.

Oxidative stress and antioxidants in SARS-CoV-2

Small increase in ROS cellular levels act as signaling molecules in the preservation of cell's physiological functions — a process known as redox biology; while excessively high levels of ROS causing lipid, protein and DNA cell damage are known as oxidative stress (Schieber and Chandel, 2014). Oxidative stress is a fundamental concept in biology introduced by the first time by Sies (2015). "Oxidative stress is an imbalance between oxidants and antioxidants in favor of the oxidants, leading to a disruption of redox signaling and control and/or molecular damage" (Sies, 2015) that harm lipids, proteins and DNA (Schieber and Chandel, 2014). The prooxidant oxidative stress imbalance needs an antioxidant system able to balance it and the principal role in antioxidant defense is carried out by antioxidant enzymes, with the paramount involvement of small-molecule antioxidant

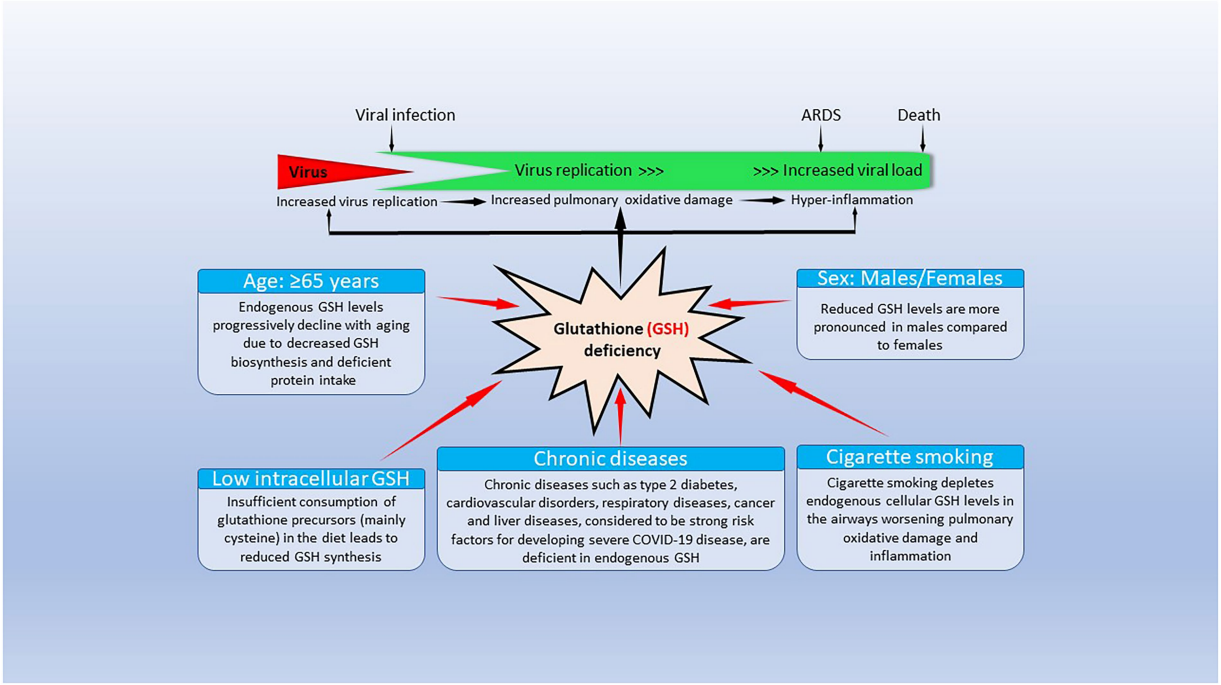

FIGURE 1
Factors causing endogenous glutathione (GSH) deficiency and GSH deficiency-mediated mechanisms contributing to coronavirus disease 19 (COVID-19) pathogenesis and outcomes. The bottom part of the figure shows that risk factors for severe COVID-19 infection lead to decrease/depletion of intracellular GSH. The top part of the figure shows potential GSH deficiency-mediated mechanisms that could influence clinical manifestations and outcomes in COVID-19 disease. Modified from Polonikov (2020).

compounds like GSH. Oxidative stress responses clarified the functioning of central principal switches like nuclear factor (NF)-κB (NFκB) or the Kelch-like ECH-associated protein 1 (Keap1)-Nuclear factor erythroid 2-related factor2 (Nrf2)-antioxidant response element (ARE) redox regulator pathway (Sies, 2015; Yamamoto et al., 2018; Cuadrado et al., 2019; Herengt et al., 2021). Under oxidative stress and induced by excessive ROS generation, Nrf2 is released from its inhibitor Keap1, allowing its translocation into the nucleus (Kasprzak et al., 2020), where it binds to the antioxidant response element (ARE) present in the DNA sequence of numerous antioxidant enzymes like glutathione-S-transferase, γ-glutamyl cysteine synthetase (glutamate cysteine ligase), heme oxygenase 1, and paraoxonase-1 inducing their transcription, managing the phase II response to oxidative stress (Kasprzak et al., 2020). Nrf2 also regulates the expression of genes that control inflammatory and immune system responses (Kasprzak et al., 2020). The presence of Nrf2 and its inhibitor Keap1 in plasma is associated with damaged vascular endothelial cell-, macrophage-and other cell-associated leakage secondary to the loss of cell membrane integrity due to lipid peroxidation following chronic inflammation and oxidative stress (Kasprzak et al., 2020), and Nrf2 and Keap1 in circulation are markers of severe inflammation and oxidative stress (Tu et al., 2019). Continuous oxidative stress can lead to chronic inflammation, intense cytokine release and a cytokine storm as seen in SARS-CoV-2 infection in COVID-19 disease, and the viral infection enhances oxidative stress creating a fatal vicious circle between oxidative stress and cytokine storm during COVID-19 infection (Delgado-Roche and Mesta, 2020; Meftahi et al., 2021).

Oxidative stress plays a prominent role in innate immunity being closely involved in SARS-CoV-2 infection (Kozlov et al., 2021). The role of oxidative stress in the COVID-19 disease may involve recognition of the viral S-protein by angiotensin converting enzyme-2 (ACE2) receptor and pattern recognition receptors like toll-like receptors 2 and 4, and activation of transcription factors like nuclear factor kappa B, that subsequently activate nicotinamide adenine dinucleotide phosphate (NADPH) oxidase (NOX) expression succeeded by ROS production (Kozlov et al., 2021). Interestingly, excessive ROS production and oxidative stress raises the binding affinity of the spike protein for the human ACE2 receptor (Hati and Bhattacharyya, 2020; Fossum et al., 2022), suggesting that restoring GSH levels would reduce viral entry and SARS-CoV-2 cellular infection. Thus, excessive production of ROS mediates hyper-inflammation and generation of cytokine storm that directly determine both ARDS development and ARDS course severity. ROS are a necessary defense system to combat microbial respiratory infections (Lambeth, 2004), but oxidative stress and the excessive production of ROS by numerous cells including monocytes and macrophages, neutrophils, as well as pulmonary endothelial and epithelial cells play a major role in the development of ARDS and its complications during COVID-19 infections (Meftahi et al., 2021). The high neutrophil to lymphocyte ratio in critically ill patients, the intense neutrophil infiltration in pulmonary capillaries and into pulmonary alveoli, and the increased levels of circulating neutrophil extracellular traps (NETs) clearly show neutrophil involvement/activation favoring intense ROS production and oxidative damage caused by lipid peroxidation, and protein and DNA oxidation (Komaravelli and Casola, 2014; Laforge et al., 2020; Veras et al., 2020; Ng et al., 2021). SARS-CoV-2-mediated NET release can promote lung epithelial cell death unravelling a detrimental role of NETs in the pathophysiology of COVID-19 disease (Veras et al., 2020; Ouwendijk et al., 2021). Extensive persistent inflammation even when SARS-CoV-2-infected cells are only sporadically present at late stages of COVID-19 (Schurink et al., 2020) could also justify low GSH levels in association with over-abundance of cellular ROS, cellular oxidative damage, increased inflammation and cell death pathways activation seen in inflammaging (Zuo et al., 2019; Bharath and Nikolajczyk, 2020; Cunha et al., 2020). Neutrophilia causes excessive ROS production that aggravates the host immunopathological response, leading to a more severe disease (Laforge et al., 2020). In addition to the neutrophil infiltration and ROS release, viral infections decrease antioxidant defenses. They inhibit Nrf2 translocation into the nucleus and enhance NFκB activation promoting inflammation and oxidative damage (Laforge et al., 2020). Nrf2 is the principal transcription factor in charge of protecting cells from oxidative stress through the regulation of cytoprotective genes, including the antioxidant GSH pathway, that controls GSH homeostasis by affecting *de novo* synthesis. It has been shown that Nrf2 modulates the GSH redox state *via* glutathione reductase regulation. Overall, Nrf2 is fundamental for the sustenance of the GSH redox state through glutathione reductase transcriptional regulation and for cell protection against oxidative stress (Harvey et al., 2009).

The overwhelming dominance of ROS generated by enzymes like NADPH oxidases and xanthine oxidase over antioxidants like superoxide dismutase causes cell injury and tissue damage through direct injury, lipid peroxidation and protein oxidation leading to protease release and antioxidant and antiprotease enzyme inactivation as well as alteration of transcription factors activator protein-1 and NFκB. Exposure to pro-oxidant stimuli usually induces Nrf2 activation and upregulation of antioxidant enzyme expression through binding to the antioxidant response element (ARE), localized in the antioxidant enzyme gene promoters; while respiratory viral infections cause antioxidant enzyme expression/activity inhibition associated with reduced Nrf2 nuclear localization, decreased cellular levels and reduced ARE-dependent gene transcription (Komaravelli and Casola, 2014). All these changes lead to cytokine storm characterized by increased expression and release of proinflammatory cytokines that participate in the pathogenesis of ARDS during virus respiratory infections like COVID-19. Proinflammatory cytokines further stimulate ROS overproduction aggravating ARDS and lung damage causing a vicious circle between oxidative stress and cytokine storm. In response to a viral infection, activated cells have enhanced production of the NOX family of NADPH oxidases (Brandes et al., 2014; Panday et al., 2015). NOX family members normally regulate cellular physiological functions, but under abnormal circumstances

contribute to the pathogenesis of cell/tissue damage associated with infections and vascular disorders (Panday et al., 2015). The presence of oxidative stress markers like lipid peroxidation, neutrophil reverse trans-endothelial migration (rTEM) and high neutrophil to lymphocyte ratio in patients with COVID-19, facilitates identification of high-risk individuals early in the course of the disease preventing their sudden deterioration (Laforge et al., 2020). Furthermore, increased ACE2 expression in alveolar type II pneumocytes and alveolar macrophages of individuals with severe SARS-CoV-2 disease (ARDS with diffuse alveolar damage) requiring mechanical ventilation (Baker et al., 2021) favors a concomitant increase in oxidative stress in those individuals.

Glutathione and immune system enhancement

Glutathione is fundamental to sustain an adequate function of the immune system, particularly affecting the lymphocyte activity since low GSH levels inhibit T-cell proliferation and immune response (Dröge and Breitkreutz, 2000; Ghezzi, 2011; Moro-García et al., 2018; Kelly and Pearce, 2020; Khanfar and Al Qaroot, 2020; Shyer et al., 2020). GSH depletion is strongly associated with impaired immune function and with disease development including viral diseases, cancer, cardiovascular diseases, arthritis and diabetes (Sinha et al., 2018; Sharifi-Rad et al., 2020; Silvagno et al., 2020; Fraternale et al., 2021; Matuz-Mares et al., 2021). GSH is essential for immunomodulation of both innate and adaptive immune system functions, including T-lymphocyte proliferation, polymorphonuclear neutrophil phagocytosis, and dendritic cell functions, and is also important for fine-tuning the innate immune response to infection and for the first step of adaptive immunity involving antigen-presenting cell (macrophages, dendritic cells)-related antigen presentation (Morris et al., 2013; Diotallevi et al., 2017). GSH works to modulate the behavior of many immune cells, augmenting both, innate immunity (and trained innate immunity or innate immune memory; Netea et al., 2020; Chumakov et al., 2021; Ferreira et al., 2021; Gong et al., 2021; Brueggeman et al., 2022), severely affected by SARS-CoV-2 viral infection (Polonikov, 2020; Rodrigues et al., 2020; Forcados et al., 2021; Kozlov et al., 2021; Bellanti et al., 2022; Paludan and Mogensen, 2022), and adaptive immunity (Dröge et al., 1991; Dröge and Breitkreutz, 2000; Dröge, 2002c; Ghezzi, 2011; Morris et al., 2013; Fraternale et al., 2017), as well as conferring protection against oxidative stress caused by microbial, parasitic and viral infections such as SARS-CoV-2 that causes COVID-19 disease (Morris et al., 2013; Diotallevi et al., 2017; Derouiche, 2020; Polonikov, 2020; Silvagno et al., 2020; Suhail et al., 2020; Forcados et al., 2021; Pérez de la Lastra et al., 2021; Bellanti et al., 2022; Kumar P. et al., 2022). Persistent and uncontrolled oxidative stress and exacerbating NLRP3 (NOD-, LRR-, and pyrin domain-containing protein 3) inflammasome activation during severe COVID-19 disease (Lage et al., 2022), induce production of pro-inflammatory cytokines, such as IL-1β and IL-18, that can be explained because of sharply decreased macrophage GSH intracellular levels associated with increased GSH efflux (Zhang T. et al., 2021).

Many antioxidant molecules, such as GSH and N-acetylcysteine (NAC), were found to inhibit viral replication through different mechanisms of action (Fraternale et al., 2006). GSH levels in macrophages, directly affect the Th1/Th2 cytokine response, and more specifically, GSH depletion inhibits Th1-associated cytokine production and/or promotes Th2 associated responses (Fraternale et al., 2006). Cell-mediated immunity primarily needs protein antigen degradation in the endocytic vesicles of antigen presenting cells (macrophages, dendritic cells), to be able to present smaller peptides on the cell surface through major histocompatibility complex antigens to activate antigen-specific T cell proliferation. One of the initial steps in antigen degradation and processing is the reduction of disulfide bonds, that requires GSH; and although GSH inhibits production of most inflammatory cytokines, it is needed to keep an adequate interferon gamma production by dendritic cells, essential for intracellular pathogen host defense (Ghezzi, 2011; Lee and Ashkar, 2018; Calder, 2020; Fraternale et al., 2021). The principal function of endogenous GSH is not to limit inflammation but to fine-tune the innate immune response to infection (Diotallevi et al., 2017; De Flora et al., 2020; Silvagno et al., 2020; Ferreira et al., 2021). GSH is capable of scavenging ROS through Nrf2-mediated heme oxygenase-1 induction and enhancing M1-like macrophage polarization regulation, showing that GSH may be a useful strategy to increase the human defense system (Mittal et al., 2014; Kwon et al., 2019; Funes et al., 2020). Strategies to enhance intracellular GSH levels such as supplementation of additional sources of cysteine (Deneke and Fanburg, 1989; Dröge et al., 1991; Lands et al., 1999; Dröge and Breitkreutz, 2000; Ghezzi et al., 2019; Gould and Pazdro, 2019; Minich and Brown, 2019; Castejon et al., 2021), oral and intravenous GSH (Cazzola et al., 2021), and sublingual and/or oral liposomal GSH administration (Schmitt et al., 2015; Campolo et al., 2017; Sinha et al., 2018; Guloyan et al., 2020; To et al., 2021) will also help to improve the immunological functions. The GSH and NAC digestive degradation occurring during oral treatments lead to consider GSH and NAC nebulization as a viable alternative to manage early stages of COVID-19 disease (Santos Duarte Lana et al., 2021).

GSH increases activation of cytotoxic T cells *in vivo*, and adequate functioning of T lymphocytes and other cells depends upon *cellular supplies of cysteine* (Edinger and Thompson, 2002; Garg et al., 2011; Levring et al., 2015). Cells acquire cysteine mainly by macrophage and lymphocyte uptake, and impaired immune responses are associated with a reduction in GSH concentration (Dröge and Breitkreutz, 2000; Edinger and Thompson, 2002; Garg et al., 2011; Ghezzi, 2011; Diotallevi et al., 2017; Calder, 2020). GSH depletion triggers the lymphocyte's apoptotic cascade leading to lymphopenia that affects for the most part T lymphocytes, and lymphopenia is directly associated with severe disease and high mortality rate in COVID-19 patients (Pallardó et al., 2009; Circu and Aw, 2012; Huang and Pranata, 2020; Ruan et al., 2020; Wang et al., 2021b; Zaboli et al., 2021).

GSH is of paramount importance for the appropriate function of the immune system in general and particularly lymphocytes since low GSH levels inhibit T lymphocytes proliferation and subsequently disturbs the immune response (Hamilos et al., 1989; Dröge and Breitkreutz, 2000; Hadzic et al., 2005; Kesarwani et al., 2013; Fraternale et al., 2017; Moro-García et al., 2018; Khanfar and Al Qaroot, 2020). The decreased immune response could be reversed by the administration of N-acetylcysteine (Atkuri et al., 2007; Rushworth and Megson, 2014; De Flora et al., 2020; Bourgonje et al., 2021; Schwalfenberg, 2021) which elevates tissue GSH levels by providing the amino acid cysteine (Atkuri et al., 2007; Rushworth and Megson, 2014; De Flora et al., 2020; Bourgonje et al., 2021; Schwalfenberg, 2021). Low GSH levels inhibit interleukin-2 production, which induces lymphocyte proliferation (Chang et al., 1999; Hadzic et al., 2005).

T-cell function can be recuperated following administration of GSH precursors like N-acetyl cysteine and cysteine (Dröge and Breitkreutz, 2000; Ghezzi, 2011; Aquilano et al., 2014; De Flora et al., 2020; Guloyan et al., 2020; Pedre et al., 2021). A deepest effect of low GSH levels on the immune system would be the induction of lymphocytes' apoptotic cascade. GSH depletion is needed for apoptosis to be triggered in the lymphocytes regardless of ROS (Franco et al., 2007a; Pallardó et al., 2009; Circu and Aw, 2012; Franco and Cidlowski, 2012; Khanfar and Al Qaroot, 2020). In order to induce T lymphocyte apoptosis, GSH must be pumped out of the cells (Franco and Cidlowski, 2006, 2012; Franco et al., 2007a; Ballatori et al., 2009; Khanfar and Al Qaroot, 2020). The GSH effects on apoptosis and inhibition of T-cell proliferation could explain why patients with SARS-CoV-2 infection and COVID-19 disease develop lymphopenia and subsequent failure of the immune system (Khanfar and Al Qaroot, 2020). A way to explain cell death associated with reduced levels of GSH is ferroptosis, a unique iron-dependent form of non-apoptotic cell death, characterized by lipid peroxidation with ROS accumulation due to GSH peroxidase inactivation and high levels of GSH consumption; ferroptosis has been proposed to be involved in COVID-19-related brain injury (Zhang et al., 2022). Immune system failure could lead to uncontrolled replication of the SARS-CoV-2 virus, secondary infections and continuous shedding of the virus in patients who die from COVID-19 regardless of the time passed from the start of the infection (Ruan et al., 2020; Sharma et al., 2020; Zhou et al., 2020; Proal and Van Elzakker, 2021; Trougakos et al., 2021). GSH is essential for the appropriate function of all components of the immune system, particularly T-lymphocytes, macrophages and neutrophils; and the failure of the immune system combined with the loss of GSH's protective effect as an antioxidant may explain the progression of the disease into acute respiratory distress syndrome/acute lung injury.

Glutathione and SARS-CoV-2

SARS-CoV-2 infection causes intense inflammation which is associated with damaging systemic events that include excessive ROS production, oxidative stress, ROS-mediated apoptosis/cell death, dysregulation of iron homeostasis, hypercoagulability and thrombus formation (Kernan and Carcillo, 2017; Moore and June, 2020; Phua et al., 2020; Vinciguerra et al., 2020; Zhou et al., 2020; Figure 2). Several viral infections, and the progression of virus-induced diseases, especially those associated with COVID-19, are characterized by an alteration in the intracellular redox balance (Polonikov, 2020). Oxidative stress reflects an imbalance between increased ROS production and reduced cellular antioxidant capabilities. This imbalance disallows reactive intermediate detoxification by the cell biological systems. ROS production and associated inflammation are closely related to aging and numerous chronic diseases as diabetes, cardiovascular and respiratory diseases, known risk factors for developing severe illness and death in patients with SARS-CoV-2 and COVID-19 disease.

Atherosclerosis, a chronic inflammatory disease, may be an ideal environment for the high viral replication capabilities of SARS-CoV-2 in human cells, enhancing hyper-inflammation secondary to immune system dysregulation (Figure 3) that leads to adverse outcomes, as shown in patients with cardiovascular risk factors. In a vicious circle, feeding itself, SARS-CoV-2 may aggravate the evolution of atherosclerosis as a result of excessive and aberrant plasmatic concentration of cytokines (Vinciguerra et al., 2020; Labarrere and Kassab, 2021). Atherosclerosis progression, as a chronic inflammatory mechanism, is characterized by immune system dysregulation associated with increased pro-inflammatory cytokine production, including interleukin 6 (IL-6), tumor necrosis factor-α (TNF-α), and IL-1β (Vinciguerra et al., 2020; Labarrere and Kassab, 2021). C-reactive protein (CRP), an active regulator of host innate immunity, is a biomarker of severe COVID-19 disease, including lung and atherosclerotic disease progression; strongly predicts the need for mechanical ventilation; and may guide intensification of treatment of COVID-19-associated uncontrolled inflammation (Potempa et al., 2020; Labarrere and Kassab, 2021; Luan et al., 2021). Macrophage activation and foam cell formation may explain the elevated CRP serum levels and contribute to disease progression (Figure 3). CRP-mediated inflammation in atherosclerosis during SARS-CoV-2 infection may be explained by the presence of monomeric CRP (mCRP) in the lesions (Potempa et al., 2020; Fazal, 2021; Fendl et al., 2021; Labarrere and Kassab, 2021; Luan et al., 2021; Mosquera-Sulbaran et al., 2021). The affinity of SARS-CoV-2 for ACE2 receptors makes the virus prone to cause vascular infection that could explain atherosclerosis progression and arterial and venous thrombosis (Vinciguerra et al., 2020; Labarrere and Kassab, 2021). Endothelial injury generated directly by intracellular viral replication and by ACE2 downregulation, exposing cells to angiotensin II in the absence of the modulator effects of angiotensin 1–7 (Vinciguerra et al., 2020), and vascular chronic inflammation promoting the development of tissue macrophages overloaded by cholesterol (foam cells), both increase the possibility of acquiring a severe COVID-19 infection (Vinciguerra et al., 2020; Labarrere and Kassab, 2021).

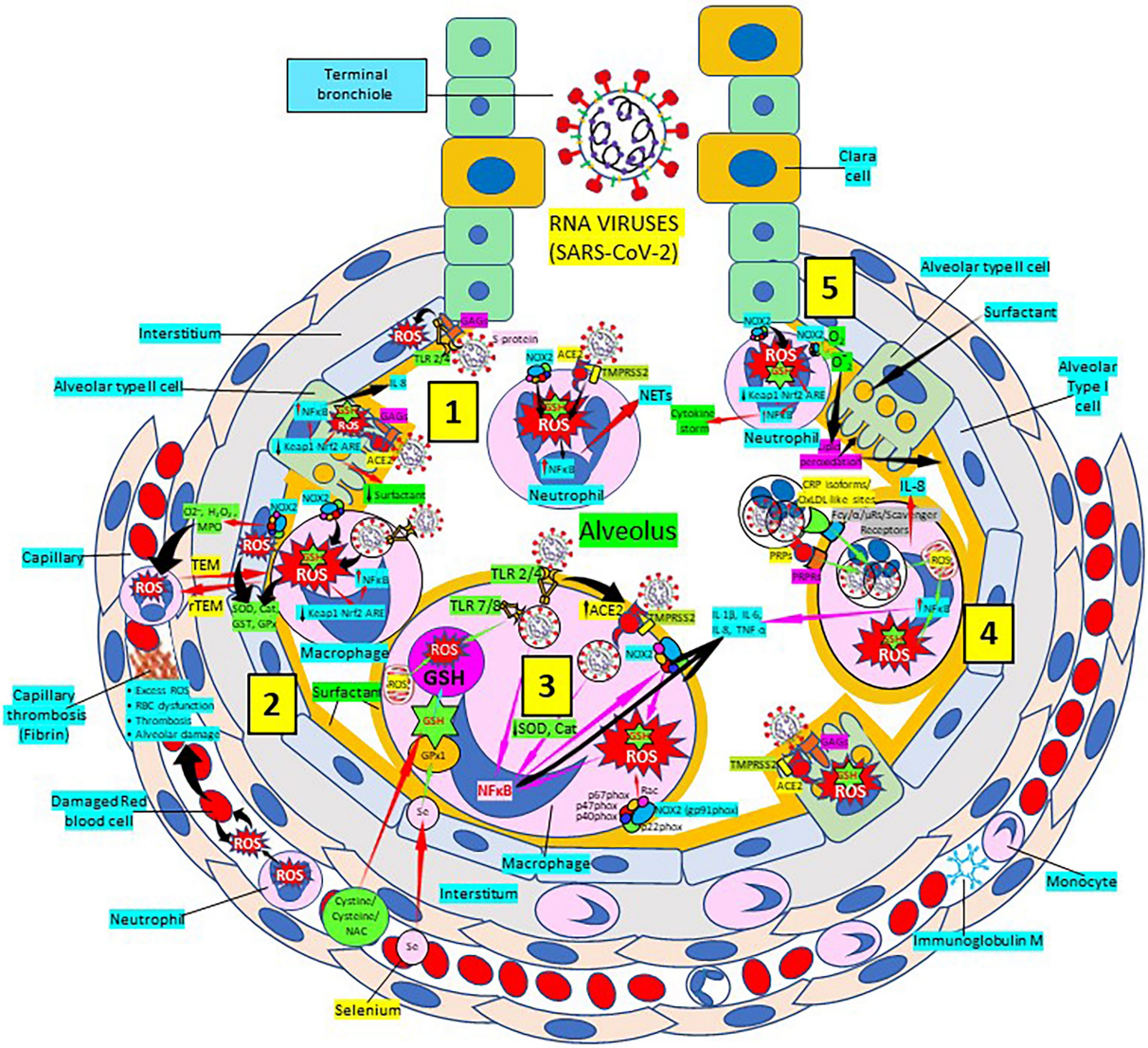

FIGURE 2
Severe acute respiratory syndrome coronavirus 2 (SARS-CoV-2) pulmonary infection, oxidative stress and antioxidant defenses. [1] After entry of SARS-CoV-2 into the alveolus, viruses invade type II alveolar cells through angiotensin-converting enzyme 2 receptors (ACE2) and glycosaminoglycans (GAGs), and infected cells increase reactive oxygen species (ROS) production, reduce Kelch-like ECH-associated protein 1 (Keap1)-Nuclear factor erythroid 2-related factor 2 (Nrf2)-antioxidant response element (ARE) redox regulator pathway and become defective for surfactant production. Infected cells activate nuclear factor (NF)-κB and release cytokines like interleukin (IL)-8. Alveolar type I cells augment ROS production *via* toll-like receptors (TLRs) 2 and 4. SARS-CoV-2 enhances neutrophil extracellular trap (NET) release and increases ROS production [2] SARS-CoV-2 augments macrophage's ROS production, inhibiting Nrf2 activation and enhancing NF-κB upregulation. ROS are counterbalanced by enzymes like superoxide dismutase (SOD), catalase (Cat), glutathione S-transferase (GST) and glutathione peroxidase (GPx) to protect cells from oxidative damage caused by nicotinamide adenine-dinucleotide phosphate (NADPH) oxidase 2 (NOX2), superoxide (O_2^-), hydrogen peroxide (H_2O_2), and myeloperoxidase (MPO). Capillary neutrophils migrate to and from alveoli by trans-endothelial (TEM) and reverse transmigration (rTEM), respectively. SARS-CoV-2 infection can cause excessive ROS production in capillaries, red blood cell (RBC) dysfunction, thrombosis and alveolar damage. [3] SARS-CoV-2-infected macrophages (*via* ACE2 and TLRs) reduce enzymes like SOD and Cat, among others, and activate NF-κB. NOX2 activation increases ROS production that enhance NF-κB activation. Activated alveolar macrophages release increased levels of IL-1β, IL-6, IL-8 and tumor necrosis factor (TNF)-α. Glutathione (GSH) precursors (Cystine, cysteine, N-acetyl cysteine, NAC), and selenium (Se) restore GSH and GPx, respectively, to counteract the effects of ROS. [4] Alveolar macrophages engulf SARS-CoV-2-infected apoptotic cells *via* Fc (γ/α/μ) and scavenger receptors and/or pattern recognition protein receptors (PRPRs) leading to increased ROS production, NFκB activation and cytokine release; and infected alveolar type II cells enhance inflammation. [5] Neutrophils contribute to O_2^- production, lipid peroxidation and increased oxidative stress, Keap-1-Nrf2-ARE signaling pathway reduction and NFκB activation promoting cytokine storm. Abbreviations: TMPRSS2: Transmembrane protease Serine 2; PRPs: pattern recognition proteins.

As mentioned previously, GSH, a tripeptide containing glutamate, cysteine and glycine, (L-γ-glutamyl-L-cysteinyl-glycine) is the master and most potent cellular antioxidant and the most abundant low molecular weight thiol that plays a crucial role in antioxidant defense against cellular ROS/reactive nitrogen species (RNS)-mediated oxidative damage and in the

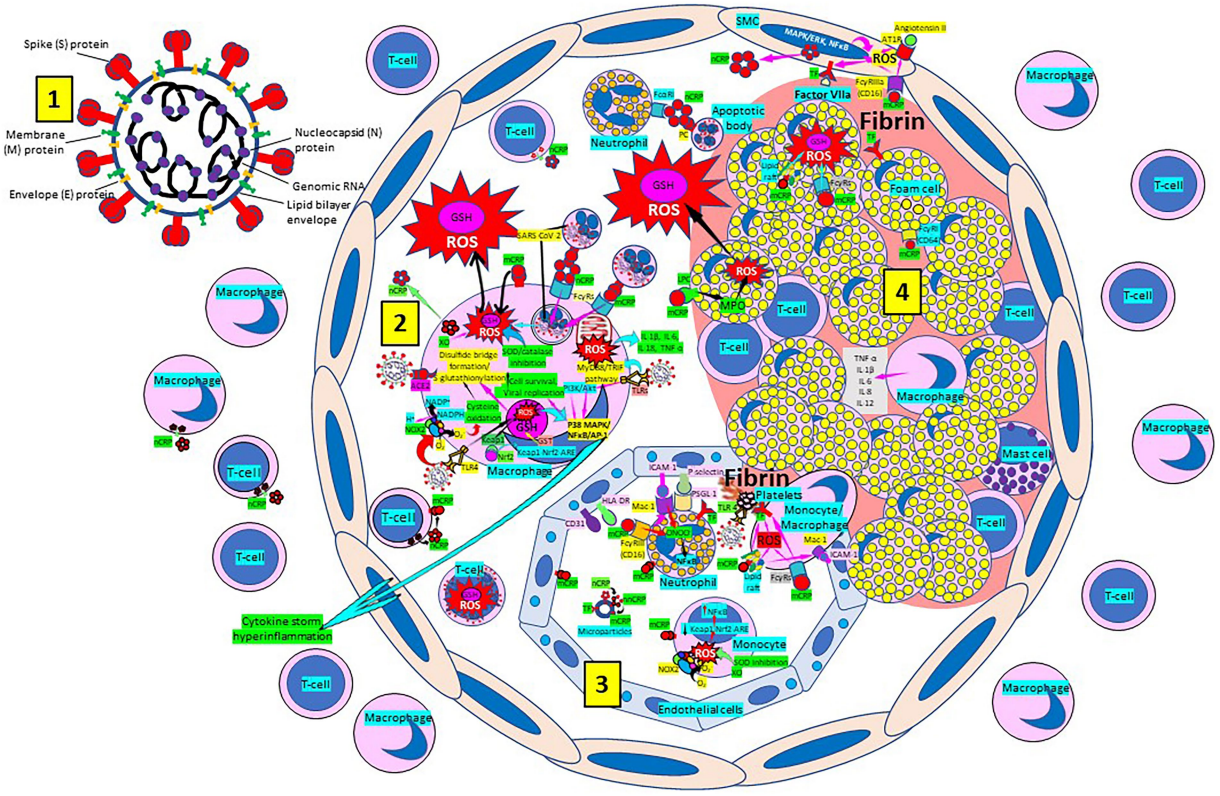

FIGURE 3
Severe acute respiratory syndrome coronavirus-2 (SARS-CoV-2) enhances oxidative stress and atherosclerosis progression. [1] SARS-CoV-2 structure. [2] SARS-CoV-2 viruses facilitate oxidative stress and inflammation in the arterial intima. Native C-reactive protein (nCRP), a marker of severe SARS-CoV-2 produced in liver, macrophages, lymphocytes, smooth muscle cells (SMC) and other cells, promotes inflammation through monomeric CRP (mCRP) enhancing intimal oxidative stress. SARS-CoV-2 binds macrophage toll-like receptor (TLR) 4 and facilitates nicotinamide adenine dinucleotide phosphate (NADP) H oxidase 2 (Nox2) activity and superoxide (O_2^-) production causing cysteine oxidation, disulfide bridge formation and S-glutathionylation. Xanthine oxidase (XO) and inhibition of superoxide dismutase (SOD)/catalase further facilitate O_2^- cellular activity and ROS generation. SARS-CoV-2 can bind TLRs 2 and 4 and activate transcription factors like nuclear factor (NF)-κB facilitating cytokine storm and hyperinflammation. Excessive mitochondrial reactive oxygen species (ROS) generation further enhances cytokine production. CRP (nCRP, mCRP) can facilitate macrophage and neutrophil uptake of SARS-CoV-2-infected apoptotic cells through Fcγ and Fcα receptors, respectively (FcRs). Oxidative stress also activates the Kelch-like ECH-associated protein 1 (Keap1)-Nuclear factor erythroid 2-related factor2 (Nrf2)-antioxidant response element (ARE) redox regulator pathway in monocytes (see [3] and macrophages, releasing Nrf2 to regulate the expression of genes that control antioxidant enzymes like glutathione S-transferase (GST)), facilitating glutathione (GSH) activity. Macrophages, Tlymphocytes, neutrophils and SMCs can generate mCRP increasing inflammation. [3] Monocytes, macrophages, neutrophils, endothelial cells and microparticles can generate mCRP, increase O_2^- and ROS formation and reactive nitrogen species like peroxinitrite ($ONOO^-$), and tissue factor (TF) expression enhancing oxidation, inflammation and thrombosis. TLR 4-mediated SARS-CoV-2-binding to platelets promotes thrombosis, mCRP binding to lipid rafts and FcγRs enhances inflammation and endothelial activation allows intimal cell migration. [4] Foam cells and smooth muscle cells associated with atherosclerotic plaques enhance ROS formation, cytokine release and tissue factor (TF)-mediated fibrin deposition. MAPK/ERK, mitogen-activated protein kinase/extracellular signal-regulated kinase; AT1R, Angiotensin II type 1 receptor; PC, phosphorylcholine; LPC, lysophosphatidylcholine; MPO, myeloperoxidase; nnCRP, non-native CRP; TNF, tumor necrosis factor; IL, interleukin; ACE, angiotensin converting enzyme; MyD88/TRIF, myeloid differentiation primary response88/TIR-domain-containing adapter-inducing interferon-β; PI3K/Akt, phosphatidylinositol-3-kinase/protein kinase B; AP-1, activator protein 1; CD31, cluster of differentiation 31; ICAM-1, intercellular adhesion molecule-1; Mac-1, macrophage-1 antigen; PSGL-1, P-selectin glycoprotein ligand-1; HLA-DR, Human Leukocyte Antigen – DR isotype.

regulation of numerous metabolic pathways essential for maintaining whole body homeostasis. GSH synthesis catalyzed sequentially by two cytosolic enzymes, γ-glutamyl-cysteine synthetase (GCS) and GSH synthetase is part of virtually all cell types, and the liver is the major GSH producer and exporter. Preservation of the highest (millimolar) concentrations of reduced GSH in most cell types highlights GSH vital and multifunctional roles in controlling various biological processes like detoxification of foreign and endogenous compounds, protein folding, regeneration of vitamins C and E, maintenance of mitochondrial function, regulation of cell cycle and cell proliferation, apoptosis, immune response, and multiple other cellular and biological functions, particularly important, antiviral defense (Meister and Anderson, 1983; Townsend et al., 2003; Sastre et al., 2005; Franco et al., 2007b; Valko et al., 2007; Forman et al., 2009; Diaz-Vivancos et al., 2010; Lushchak, 2012; Denzoin Vulcano et al., 2013; García-Giménez et al., 2013; Lu, 2013; Giustarini et al., 2016; Scirè et al., 2019; Marí et al., 2020;

Polonikov, 2020; Sestili and Fimognari, 2020; Silvagno et al., 2020; Bartolini et al., 2021). SARS-CoV-2 markedly decreases the levels of cellular thiols, essentially lowering the reduced form of GSH; and the use of antivirals that enhance activation of the Nrf2 transcription factor together with N-acetylcysteine administration restore GSH levels correcting the SARS-CoV-2-mediated impaired GSH metabolism (Aquilano et al., 2014; Khanfar and Al Qaroot, 2020; Sestili and Fimognari, 2020; Silvagno et al., 2020; Bartolini et al., 2021; Bourgonje et al., 2021; Fraternale et al., 2021; Kumar P. et al., 2022; Figure 4).

Alterations in the intracellular redox status are often associated with GSH depletion (Polonikov, 2020) and endogenous GSH deficiency, due either to decreased biosynthesis and/or increased consumption, is a marked contributor to the pathogenesis of numerous diseases *via* mechanisms including oxidative stress and inflammation. GSH deficiency is associated with age, a major risk factor for SARS-CoV-2 infection's outcome (Grigoletto Fernandes et al., 2020; Polonikov, 2020; Sestili and Fimognari, 2020; Suhail et al., 2020; Yang X. et al., 2020; Yang J. et al., 2020; Schwalfenberg, 2021), sex, low intracellular GSH, cigarette smoking and presence of chronic diseases, among other factors, and GSH deficiency caused by any or all these factors may contribute to severe COVID-19 disease pathogenesis (Polonikov, 2020; Sestili and Fimognari, 2020; Silvagno et al., 2020; Suhail et al., 2020; Yang J. et al., 2020; Yang X. et al., 2020; Figure 1). Individuals 65 years and older with comorbidities, are more susceptible to become infected with SARS-CoV-2 and become critically ill and are more prone to develop ARDS and require mechanical ventilation, having a high 28-day mortality rate (Yang X. et al., 2020).

COVID-19 is clinically mild in most cases, severe cases develop pneumonia, and critical cases end with ARDS, sepsis, and multiple organ failure (Yang X. et al., 2020). COVID-19 sepsis is a serious problem in critically ill patients infected with SARS-CoV-2 (Beltrán-García et al., 2020; Coz Yataco and Simpson, 2020; De Candia et al., 2021). Sepsis is a systemic inflammatory response caused by excessive cytokine secretion, such as interleukin (IL)-6, IL-10, IL1β and TNF-α. Severe SARS-CoV-2 infection with high cytokine levels causes T-cell exhaustion characterized by high levels of programmed cell death protein 1 and low numbers of $CD4^+$ and $CD8^+$ cells (Diao et al., 2020; Lin et al., 2020; Poe and Corn, 2020). ROS may be important mediators of cellular injury during COVID-19 sepsis (Silvagno et al., 2020), either following macromolecular damage or by hindering extracellular and intracellular regulatory processes. Multiple organ failure including sepsis-induced cardiac dysfunction seem to be the result of numerous factors as overwhelming inflammation and nitric oxide synthesis impairment associated with mitochondrial dysfunction and increased oxidative stress (Cecchini and Cecchini, 2020). Excessive ROS production, associated with inflammation, induces oxidative stress. Oxidative stress is a major contributor to the high mortality rates associated with SARS-CoV-2 infections (Poljsak et al., 2013; Forcados et al., 2021; Lage et al., 2022). Immune cells use ROS to sustain their functions and need adequate levels of antioxidant defenses to avoid harmful effects caused by excessive ROS production, since accurate balance between ROS and intracellular antioxidants is essential for a normal function of the cell (Banjac et al., 2008; Liu et al., 2018).

L-cysteine is the rate-limiting substrate in the synthesis of intracellular GSH (Raftos et al., 2007; Whillier et al., 2009; Radtke et al., 2012). Although N-acetylcysteine (NAC) directly influences the pool of extracellular cystine and intracellular cysteine *via* a series of plasmatic redox reactions, in order to be effective, intracellular cysteine precursors must be designed to enter erythrocytes rapidly and use high activity enzymes within erythrocytes to liberate cysteine (Whillier et al., 2009; Radtke et al., 2012). NAC enhances extracellular cysteine and by using transport channels increases intracellular cysteine (Franco and Cidlowski, 2009; Aldini et al., 2018; Liu et al., 2018; Ulrich and Jakob, 2019; Pedre et al., 2021; Schwalfenberg, 2021). During oxidative stress, NAC will increase GSH synthesis (Franco and Cidlowski, 2009; Rushworth and Megson, 2014; Campolo et al., 2017). Without oxidative stress, cysteine and cystine appear to essentially mediate cellular stress *via* thiols other than GSH (Rahman and MacNee, 2000; Ashfaq et al., 2008; Sekhar et al., 2011a; Liu et al., 2018).

Individuals 60 years and older have lower plasma GSH levels and increased oxidative stress (Samiec et al., 1998). Individuals with diabetes have lower GSH levels compared to control subjects (Samiec et al., 1998; Sekhar et al., 2011b). Supplementation of cysteine and glycine in the diet can increase GSH levels and reduce oxidative stress in the elderly and persons with diabetes (Sekhar et al., 2011b; Tan et al., 2018). Elderly adults may also have reduced redox potential due to lower GSH levels (Samiec et al., 1998; Maher, 2005; Trachootham et al., 2008; Aquilano et al., 2014; McCarty and DiNicolantonio, 2015; Baş, 2018; Hajjar et al., 2018; Polonikov, 2020; Sestili and Fimognari, 2020). Lowered cellular redox status increases susceptibility to oxidative stress that may lead to cell death and virus release (Raftos et al., 2007; Hotchkiss et al., 2009; Circu and Aw, 2010; Kesarwani et al., 2013; He et al., 2017; Khomich et al., 2018; Chen et al., 2020; Sharifi-Rad et al., 2020; Zhang et al., 2020). The potential clinical use of antioxidants and antioxidant precursors in the treatment of COVID-19 needs to be seriously considered. GSH is paramount with respect to disease pathogenesis and individual response to COVID-19 infection; and enhancement of GSH levels can be a means for treating and preventing COVID-19 disease (Polonikov, 2020). As it was recently suggested, GSH depletion could be the Trojan horse of COVID-19 severity and mortality and elevating GSH levels in tissues may decrease COVID-19 severity and mortality rates (Khanfar and Al Qaroot, 2020).

SARS-CoV-2 new therapeutic approaches

The prominence of the coronavirus disease 2019 (COVID-19) pandemic urges multidisciplinary strategies to control disease

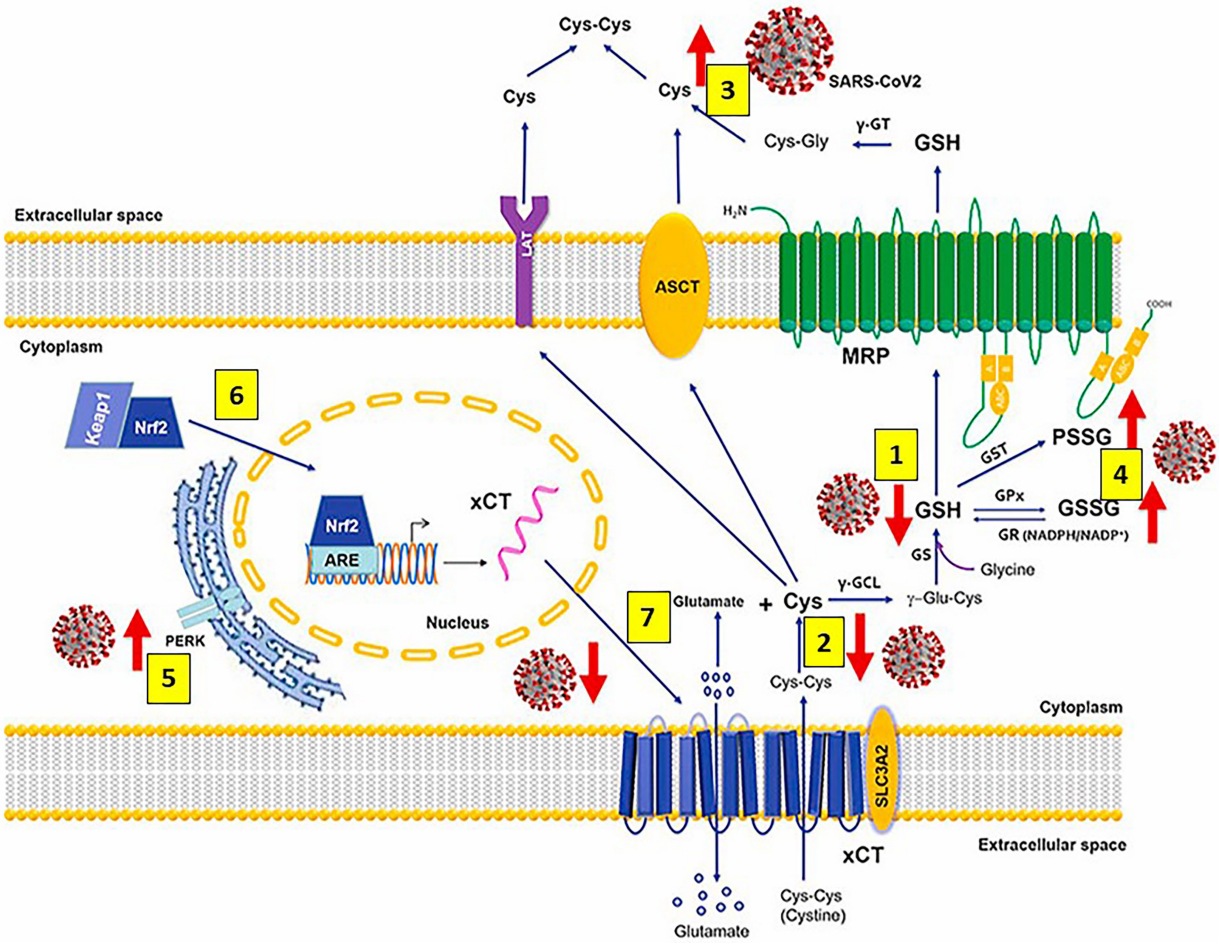

FIGURE 4
Severe acute respiratory syndrome coronavirus 2 (SARS-CoV-2) infection alters metabolism and redox function of cellular glutathione (GSH). SARS-CoV-2 markedly decreases GSH levels [1], that could be explained by lower intake of the GSH precursor cysteine (Cys) [2] and increased efflux of cellular thiols [3]. Increased levels of oxidized glutathione (GSSG) and protein glutathionylation [4] along with upregulation of endoplasmic reticulum stress marker protein kinase R (PKR)-like endoplasmic reticulum kinase (PERK) [5] are also observed. Antivirals activate the Kelch-like ECH-associated protein 1 (Keap1)-Nuclear factor erythroid 2-related factor2 (Nrf2)-antioxidant response element (ARE) redox regulator pathway, releasing Nrf2 [6] to regulate the expression of genes that control antioxidant, inflammatory and immune system responses (including the cystine (cys-cys)/glutamate transporter xCT and the membrane transporter multidrug resistance protein [MRP], which are decreased and markedly upregulated, respectively, during infection); restoring GSH levels in the infected cells and facilitating GSH synthesis [7] and activity. Abbreviations: γ-GT: γ-glutamyl transferase; ASCT: alanine-serine-cysteine transporter; LAT: L-type amino acid transporter; PSSG: S-glutathionylated Proteins; GST: glutathione-S-transferase; γ-GCL: γ-glutamate cysteine ligase; γ-glutamyl cysteine; GST: glutathione-S-transferase; GPx: glutathione peroxidase; GR: glutathione reductase; NADPH: reduced NADP+; NADP+: Nicotinamide adenine dinucleotide phosphate; GS: glutathione synthetase; xCT (SLC7A11)/SLC3A2: cystine/glutamate transporter light (xCT [SLC7A11]) and heavy (SLC3A2) chains. Modified from Bartolini et al. (2021).

spread and prevent its complications (Labarrere and Kassab, 2021). SARS-CoV-2 and its massive cytokine storm primarily compromises the lungs causing acute respiratory distress syndrome also affecting the cardiovascular system aggravating atherosclerotic lesions leading to thromboembolic events and cell and tissue death (Ryu and Shin, 2021; Taoufik et al., 2021; Yuan et al., 2021). SARS-CoV-2 infects pulmonary type II alveolar cells because these cells express angiotensin-converting enzyme 2 (ACE2; Ryu and Shin, 2021; Taoufik et al., 2021; Yuan et al., 2021). SARS-CoV-2 ACE2-mediated host cell invasion is enhanced by the presence of heparan sulfate proteoglycans (HSPGs) consisting of a core protein bearing glycosaminoglycan carbohydrate chains (Souza-Fernandes et al., 2006; Davis and Parish, 2013; Kang et al., 2018; Clausen et al., 2020; De Pasquale et al., 2021). Virus protein ligands, like trimeric spike glycoprotein interact with cellular receptors, such as ACE2, and host proteases, like transmembrane protease serine 2 (TMPRSS2), participate in virus entry by proteolytically activating virus ligands (Sallenave and Guillot, 2020; Kalra and Kandimalla, 2021; Zhang Q. et al., 2021; Jackson et al., 2022). In the lungs, after entering in type II alveolar cells, SARS-CoV-2 infected cells become defective for surfactant production (Ghati et al., 2021) and release cytokines, like IL-8

among others, which in turn activate alveolar macrophages to release IL-1, IL-6, and TNF-α, that induce natural killer and dendritic cell differentiation and macrophage M1 polarization, enhancing the proinflammatory response with increased vasodilation causing neutrophil and activated T cell influx from the capillaries into the alveolus, all leading to the cytokine storm (Carcaterra and Caruso, 2021; Figure 2).

Alveolar macrophages, due to their polarization state toward M1 or M2 phenotypes, provoke different effects following SARS-CoV-2 infection. Hyperactivated M1 alveolar macrophages are taken over by SARS-CoV-2 allowing for viral infection and spread, while M2 alveolar macrophages can degrade the virus and limit its spread (Knoll et al., 2021; Lv et al., 2021). Neutrophils produce ROS and proteinases, causing further destruction of healthy type II cells; as a result, surfactant production decreases markedly, which in turn causes alveolar fluid accumulation leading to alveolar collapse and ARDS (Matthay and Zemans, 2011; Carcaterra and Caruso, 2021). Due to the exhaustion of cellular and extracellular GSH caused by numerous GSH-consuming pathways the severe inflammation and oxidative stress triggered by the viral infection steals GSH from crucial functions like NO-dependent vasodilatation, disallowing the patient of being protected from an inflammation that can become fatal. Based on the previous discussion, administration of antioxidants or Nrf2 inducers are potential viable therapies for viral-induced diseases, like respiratory infections and infections associated with reduced cellular antioxidant capacity (Komaravelli and Casola, 2014). A high neutrophil to lymphocyte ratio found in critically ill patients with COVID-19 is associated with excessive ROS levels, that promote a cascade of biological events driving pathological host responses. Since ROS induce tissue damage, thrombosis and red blood cell dysfunction that contribute to COVID-19 disease severity, administration of free radical scavengers could be beneficial for the most vulnerable patients (Laforge et al., 2020).

Toll-like receptors (TLRs) play a key role in microorganism and viral particle recognition and activation of the innate immune system (Sasai and Yamamoto, 2013; Kawasaki and Kawai, 2014; McClure and Massari, 2014; Sartorius et al., 2021; Manik and Singh, 2022). TLR pathway activation leads to secretion of pro-inflammatory cytokines, like interleukin (IL)-1, IL-6, and tumor necrosis factor-α, as well as type 1 interferon. TLRs can be localized either on the cell surface (TLR-1, -2, -4, -5, -6, -10) or in the endosome compartment (TLR-3, -7, -8, -9; Sasai and Yamamoto, 2013; Kawasaki and Kawai, 2014; Sartorius et al., 2021). TLRs-2, -3, -4, -6, -7, -8, and -9 are potentially important in COVID-19 infection (Onofrio et al., 2020; Khanmohammadi and Rezaei, 2021; Sariol and Perlman, 2021). TLR1/2/6 activation and subsequent signal transduction may be in part responsible for clinical immunopathological manifestations found in patients infected with COVID-19 (Gadanec et al., 2021). Interactions between TLR1/6 and the S-protein may participate in immunopathology as a result of unregulated TLR activation (Kawasaki and Kawai, 2014; Gadanec et al., 2021). SARS-CoV-2 may activate TLR4 in the heart and lungs causing aberrant TLR4 signaling favoring the proinflammatory MyD88-dependent (canonical) pathway instead of the alternative TRIF/TRAM-dependent anti-inflammatory and interferon pathway (Aboudounya and Heads, 2021). TLR4-mediated recognition of S protein may initiate receptor dependent internalization and explain SARS-CoV-2 infection in patients and cells lacking or deficient in ACE2 expression (Aboudounya and Heads, 2021; Gadanec et al., 2021). Viral proteins as well as host damage-associated molecular patterns, that accumulate following cellular stress during viral infection, were linked to TLR4 activation, with uncontrolled TLR4 activation being associated with severe disease (Olejnik et al., 2018). TLR4 activation in platelets whether by pathogen- (viremia) or damage-associated molecular patterns induces a prothrombotic and proinflammatory state (Schattner, 2019). SARS-CoV-2 spike glycoprotein binds TLR4 and activates TLR4 signaling increasing cell surface expression of ACE2 facilitating entry (Aboudounya and Heads, 2021). Activation of endosomal TLR7/8 during SARS-CoV-2 may increase the inflammatory response resulting in severe and potentially lethal immunopathological effects in COVID-19 patients as consequence of the simultaneous release of pro-inflammatory cytokines and chemokines. TLR signaling molecules, like mitogen-activated protein kinases (MAPK) and phosphoinositide 3-kinase (PI3K)/protein kinase B (Akt), play fundamental roles in TLR-mediated cell proliferation and survival *via* reducing apoptosis and increasing time for viral replication (Li et al., 2010; Aboudounya and Heads, 2021) and could facilitate increased viral replication. The expression of CD14, TLR2 and 4 in human alveolar type I and II cells (Thorley et al., 2011) suggests that they most probably participate in SARS-CoV-2 infection and COVID-19 disease. Ten human TLRs that signal *via* 4 adaptor proteins and 2 initial kinases activate distal kinases that subsequently regulate transcription factors such as NFκB and activator protein 1 (AP-1), that control gene expression. Posttranslational modifications of ROS-mediated kinase activity most probably contribute to the diversity and intensity of gene expression following microbial activation of innate immunity (Kolls, 2006).

SARS-CoV-2 mainly destroys pulmonary surfactant-secreting type II alveolar cells (Wang et al., 2021a), that normally decrease the air/tissue surface tension and block TLR4 in the lungs, promoting ARDS and inflammation. TLR4 activation, aberrant TLR4 signaling, and hyperinflammation may explain SARS-CoV-2-induced myocarditis and multiple-organ injury in COVID-19 patients (Aboudounya and Heads, 2021). Augmented activation of TLR4 increases oxidative stress and the generated ROS participate in signaling events downstream of TLRs. TLR4 activation may lead to ROS signaling *via* direct interaction between TLR4 and NADPH oxidase (Gill et al., 2010; Pushpakumar et al., 2017). TLR1, TLR2 and TLR4 activation results in augmented mitochondrial ROS production following recruitment of mitochondria to macrophage phagosomes, leading the way to increased mitochondrial and cellular ROS generation (West et al., 2011). ROS can oxidize cysteine residues allowing formation of disulfide bridges with one another or with GSH

leading to S-glutathionylation. ROS can be inactivated by antioxidants such as GSH. The link between oxidation and inflammation is complex, going from fine-tuned signaling by ROS during TLR4 activation that leads to active mobilization of damaged-associated molecular patterns, to cellular injury from redox stress that leads to damaged-associated molecular patterns release triggering TLR4-mediated inflammation and organ injury (Gill et al., 2010; Pushpakumar et al., 2017). Neutralization of oxidation radicals becomes paramount in SARS-CoV-2-mediated cellular and tissue damage.

As we previously published, a multiweapon approach is needed to successfully combat SARS-CoV-2 and COVID-19 disease (Labarrere and Kassab, 2021), involving vaccines (Jin et al., 2022) especially vaccines that selectively and efficiently induce antibodies that target the SARS-CoV-2 receptor binding domain (Robbiani et al., 2020), pattern recognition proteins such as surfactant proteins A and D (Arroyo et al., 2021; Ghati et al., 2021; Wang et al., 2021a; DePietro and Salzberg, 2022; Labarrere and Kassab, 2022), modulators of mannose binding lectin, C1q, C-reactive protein (Tang et al., 2011; Torzewski et al., 2020; Labarrere and Kassab, 2021; Ringel et al., 2021), and IgM natural antibodies, TLR inhibitors, modulators of cellular components (neutrophils, basophils, eosinophils, mast cells, monocytes, macrophages, dendritic cells, regulatory T cells, natural killer cells) of innate immunity, cellular components of both innate and adaptive immune systems (γδ T cells, natural killer T cells), soluble constituents of adaptive immunity (polyreactive IgM antibodies to the viral disease, among others), and cellular components of adaptive immunity (T cell subsets like Th1 CD4+ T cells, cytotoxic CD8+ T cells, Th2 cells, Th17 cells, Th9 cells), viral replication inhibitors, renin-angiotensin system inhibitors (Williams, 2021) and human recombinant soluble ACE2 (Abd El-Aziz et al., 2020), as well as heparin and glycosaminoglycan antithrombotics (Magnani, 2021), among others. Sadly, there are no effective antivirals and vaccines to definitively treat or prevent COVID-19. Globally launched clinical trials like the European study DISCOVERY showed that antiviral drugs (remdesivir, lopinavir and ritonavir in combination, ritonavir given with or without interferon beta and hydroxychloroquine) are unable to efficiently attack COVID-19 progression (Ader et al., 2022). Although a recent trial has shown to be beneficial when antiviral treatment is introduced early during the disease before hospitalization than later in the course of the disease, there is an urgent need for early therapies to reduce the risk of disease progression, prevent transmission, and be widely distributed to meet the worldwide demand (Gottlieb et al., 2022; Heil and Kottilil, 2022). Here we emphasize the role of Nrf2 activators and the vital role of antioxidants like the GSH system in prevention against oxidative stress and cell and tissue damage (Cuadrado et al., 2020) in SARS-CoV-2 infection and COVID-19 disease (Figure 5).

Since oxidative stress plays an important role in the pathogenesis of viral-associated cardiovascular and lung diseases, antioxidant intervention would be a rational approach to use for treating lower respiratory tract infections (Komaravelli and Casola, 2014) and balancing oxidative damage by enhancing antioxidant defense (Banjac et al., 2008; Chen et al., 2020; Sharifi-Rad et al., 2020; Perła-Kaján and Jakubowski, 2022) could be a major strategy for a successful intervention against SARS-CoV-2 infection and COVID-19 disease. Since SARS-CoV-2 activates mitochondrial ROS-mediated feedback loops that produce long-term changes in the redox status and endothelial function of the host, leading to cardiovascular disease and lung injury (Chang et al., 2021), and endothelial cells are key players in inflammatory pathologies, such as acute respiratory distress syndrome, thrombosis, and atherosclerosis; the use of pro-GSH molecules (Fraternale et al., 2006) and/or glutathione precursors like N-acetyl cysteine (NAC), glutamine, cysteine (cystine) and glycine, as well as nuclear factor erythroid 2 p45–related factor 2 (Nrf2) inducers like sulforaphane can enhance glutathione production and increase nuclear Nrf2 translocation and antioxidant response element (ARE) transcription (Komaravelli and Casola, 2014; Atefi et al., 2020; Poe and Corn, 2020; Dominari et al., 2021; Obayan, 2021; Di Marco et al., 2022). Nrf2, a member of the "cap'n'collar" family of basic region–leucine zipper transcription factors involved in transcription of antioxidant genes in response to xenobiotic stress, is also a critical regulator of cellular oxidative stress in sepsis (Kolls, 2006) and a regulator of exacerbated proinflammatory cytokine release (cytokine storm) and loss of T lymphocytes (leukopenia) that characterize the most aggressive presentation of SARS-CoV-2-mediated COVID-19 infection (Kobayashi et al., 2016; Cuadrado et al., 2019; Olagnier et al., 2020; Calabrese et al., 2021; Herengt et al., 2021). By regulating glutathione S-transferase (GST) and intracellular glutathione (GSH) levels, Nrf2 controls the level of ROS in the cell (Kolls, 2006; Lushchak, 2012; Aquilano et al., 2014; Tu et al., 2019; Bartolini et al., 2021); and a multifaceted anti-inflammatory strategy based on pharmacological activation of Nrf2 and enhancement of GSH precursors like bonded cysteine or NAC can be deployed against the virus (Cuadrado et al., 2019; Olagnier et al., 2020; Emanuele et al., 2021; Fratta Pasini et al., 2021; Wong et al., 2021). Since Nrf2 participates in the resolution of inflammation by repressing genes for proinflammatory cytokines IL-6 and IL-1β (Kobayashi et al., 2016; Cuadrado et al., 2020) and pharmacological activation of Nrf2 might also limit NF-κB-mediated pulmonary inflammation caused by SARS-CoV-2 infection (Cuadrado et al., 2019, 2020; Chang et al., 2021; Emanuele et al., 2021; Fratta Pasini et al., 2021). NRF2 inducers, like sulforaphane modify cysteine sensors of Keap1 and inactivate its repressor function. The liberation of Nrf2 from Keap1 allows Nrf2 accumulation and translocation to the nucleus (Cuadrado et al., 2019; McCord et al., 2020; Perła-Kaján and Jakubowski, 2022). In the nucleus, following heterodimer complex formation with transcription factors, like small Maf proteins (G/F/K) and c-Jun, Nrf2 complexes bind to the antioxidant response element (ARE), a regulatory enhancer region within gene promoters that upregulate antioxidant and

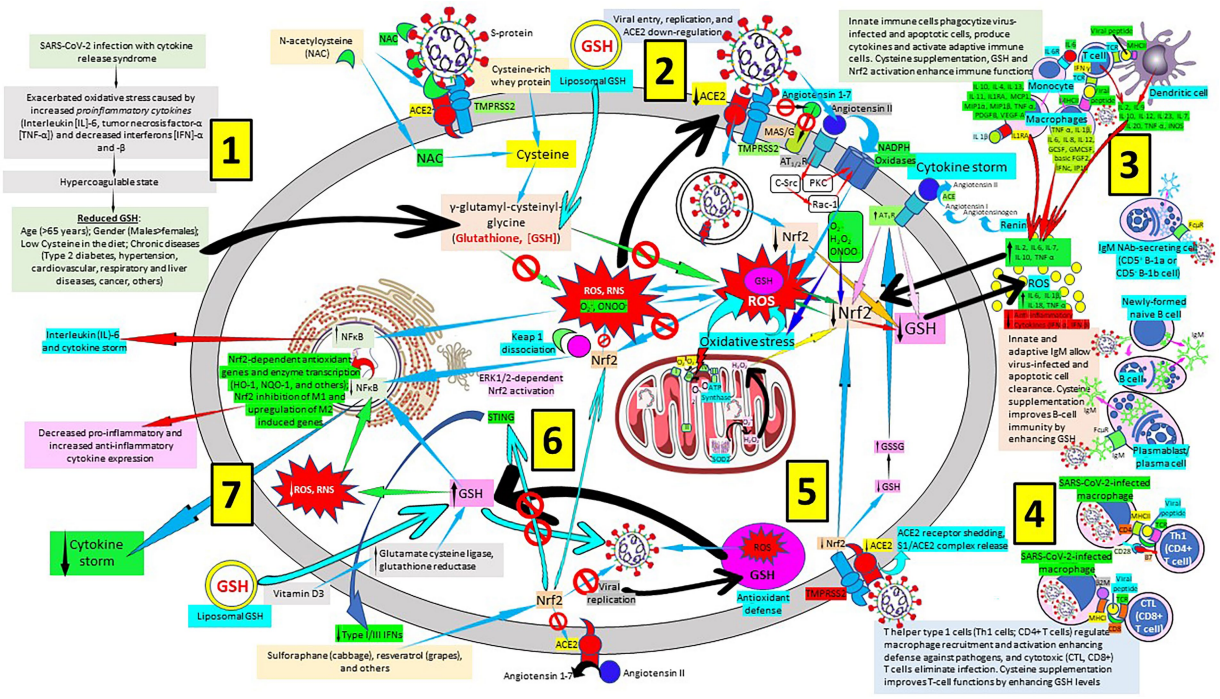

FIGURE 5
Severe acute respiratory syndrome coronavirus 2 (SARS-CoV-2)-related glutathione (GSH) cellular depletion, repletion treatment options and a multiweapon defense approach. [1] SARS-CoV-2 exacerbates oxidative stress, inflammation and coagulation, reducing GSH levels mainly in hosts with added risk factors. [2] SARS-CoV-2 invades host cells through virus protein ligands, like trimeric spike glycoprotein interacting with cellular receptors like angiotensin converting enzyme 2 (ACE2), and host proteases, like transmembrane protease serine 2 (TMPRSS2), that proteolytically activates virus ligands, promoting virus entry, replication and ACE2 down-regulation; N-acetylcysteine (NAC) can block this interaction. SARS-CoV-2-related ACE2 downregulation facilitates angiotensin II/angiotensin types 1 and 2 receptor (AT1/2R)-mediated nicotinamide adenine dinucleotide phosphate (NADPH) oxidase activation and reactive oxygen species (ROS) production; and inhibits interaction of angiotensin 1–7 and MAS1 oncogene/G protein-coupled (MAS/G) receptor. [3] A multiweapon approach includes enhancing host response to viral particles and peptides by monocytes/macrophages and T-cells, as well as innate and adaptive B-cell/plasma cells producing antibodies to reduce cytokine production and the subsequent cytokine storm. Reactive oxygen species (ROS) cell production enhances proinflammatory cytokine release while reducing anti-inflammatory cytokines. [4] Modulation of CD4+ and CD8+ T cells will facilitate SARS-CoV-2 removal. [5] SARS-CoV-2 binding and cleavage of ACE2 receptor leads to shedding of host ACE2 receptor contributing to the loss of ACE2 function and systemic release of S1/ACE2 complex. SARS-CoV-2 reduces Nrf2 and GSH allowing ROS and RNS to damage the cell. [6] Liposomal GSH (see [2], vitamin D3 by increasing glutamate cysteine ligase and glutathione reductase activity), and N acetyl cysteine (NAC), see [2] participate in GSH synthesis. Increased intracellular GSH reduces ROS and reactive nitrogen species (RNS), as well as NF-κB activation. Sulforaphane and resveratrol enhance Nrf2 production and Nrf2 negatively regulates the endoplasmic-reticulum-resident protein stimulator of interferon genes (STING) reducing interferon secretion. Increased antioxidant defense (cystine, cysteine, NAC, liposomal GSH, vitamin D3, sulforaphane, resveratrol, and others) reestablishes cell homeostasis [7]. Increased nuclear factor-κB (NF-κB) activity enhances interleukin (IL)-6 secretion and cytokine storm, while decreased nuclear NF-κB allows activation of nuclear factor erythroid 2-related factor2 (Nrf2)-dependent antioxidant genes and enzyme transcription (HO-1, NQO-1, and others); Nrf2 inhibition of M1 and upregulation of M2 induced genes; decreased pro-inflammatory and increased anti-inflammatory cytokine expression; and decreased cytokine storm. C-Src, proto-oncogene tyrosine-protein kinase sarcoma; PKC, protein kinase C; Rac-1, Ras-related C3 botulinum toxin substrate 1; IL1RA, IL1 receptor antagonist; MCP1, monocyte chemoattractant protein-1; MIP, macrophage inflammatory protein; PDGFB, Platelet Derived Growth Factor B; VEGF-A, vascular endothelial growth factor A; iNOS, inducible nitric oxide synthase; TCR, T-cell receptor; MHCI/II, major histocompatibility complex class I/II; GCSF, granulocyte colony-stimulating factor; GMCSF, granulocyte-macrophage colony-stimulating factor; FGF, fibroblast growth factor; IP10, interferon gamma-induced protein 10; NAb, natural antibody; SOD, superoxide dismutase; HO-1, heme oxygenase-1; NQO1, NAD(P) H quinone dehydrogenase 1; β2M, β2 microglobulin; GSSG, glutathione disulfide; Keap 1, Kelch-like ECH-associated protein 1; ERK, extracellular signal-regulated protein kinase; FcμR, Fcμ receptor; IgM, immunoglobulin M.

anti-inflammatory defense processes (Cuadrado et al., 2019; McCord et al., 2020; Perła-Kaján and Jakubowski, 2022).

Since SARS-CoV-2 mediates Nrf2 suppression and limits host anti-inflammatory response (Cuadrado et al., 2020; McCord et al., 2020; Olagnier et al., 2020; Emanuele et al., 2021; Fratta Pasini et al., 2021), targeting Nrf2 is therefore essential for the treatment of diseases characterized by enhanced oxidative stress and inflammation, such as aging and COVID-19-induced pneumonia and ARDS (Lewis et al., 2010; Lee, 2018; Robledinos-Antón et al., 2019; Schmidlin et al., 2019; Lin and Yao, 2020). Nrf2 activation suppresses ROS in antigen-presenting dendritic cells enhancing their capacity to interact with and promote the transformation of naïve CD8 T cells into cytotoxic T lymphocytes enabling cytotoxic T-cells to eliminate virally infected cells (Kesarwani et al., 2013; Moro-García et al., 2018; Calabrese et al., 2021; Emanuele et al., 2021).

Nrf2 activation regulates antioxidant responses to modify cellular redox states from predominantly pro-oxidant to antioxidant, and, in an antioxidant environment, macrophage phenotypes shift from M1 pro-inflammatory to M2 anti-inflammatory, reducing the probability of cytokine storms, ARDS, and lethality (Tan et al., 2016; Bousquet et al., 2020; Calabrese et al., 2021). Cytoprotective effects against viruses like SARS-CoV-2 could be enhanced by sulforaphane, an isothiocyanate abundant in cruciferous vegetables, since sulforaphane has been found to be a powerful activator of the Nrf2 pathway by increasing Nrf2-regulated cellular antioxidant response such as induction of NAD(P)H: quinone oxidoreductase 1, glutamate-cysteine ligase (γ-glutamyl cysteine synthetase) and glutathione (Theodore et al., 2008; Lewis et al., 2010; Schmidlin et al., 2019; Bousquet et al., 2020; Cuadrado et al., 2020; Mahn and Castillo, 2021). Nrf2 activators like sulforaphane have a potential role with dual antiviral and anti-inflammatory properties in the management of viral pneumonia, a serious complication in COVID-19 disease (Bousquet et al., 2020; Cuadrado et al., 2020; Lin and Yao, 2020; Emanuele et al., 2021; Fratta Pasini et al., 2021). Nrf2-interacting nutrients can equilibrate insulin resistance and have a significant effect upon COVID-19 severity. It is then possible that intake of these nutrients may re-establish an optimal natural balance for the Nrf2 pathway and mitigate COVID-19 severity (Bousquet et al., 2020). The enhancement of Nrf2 transcription with sulforaphane or melatonin could benefit patients with "LONG COVID" (Post-Acute Sequelae of SARS-CoV-2 or Post-COVID-Syndrome), a significant proportion (approximately 40%) of individuals with COVID-19 experiencing a variety of symptoms (loss of smell and/or taste, fatigue, cough, aching pain, "brain fog," insomnia, shortness of breath, and tachycardia) after 12 weeks (Jarrott et al., 2022; Ordonez et al., 2022). Multi-omics studies revealed that SARS-CoV-2 infection provokes significant changes in numerous metabolites including those impacting on virus propagation (one-carbon metabolism) and GSH synthesis (amino acids glutamic acid, cysteine and glycine) that could be used as early prognosis biomarkers in COVID-19 at diagnose to predict severe COVID-19 and "LONG COVID" (Doğan et al., 2021; Li C.-X. et al., 2022; Perła-Kaján and Jakubowski, 2022; Valdés et al., 2022). Therapeutic interventions aimed at normalizing GSH and Nrf2 might provide a promising approach to combat the COVID-19 pandemic.

Augmented oxidative stress secondary to increased levels of interleukin-6 and tumor necrosis factor-α in addition to decreased levels of interferons α and β are primarily believed to be the drivers of the disease process (Guloyan et al., 2020). Since it was shown that glutathione (GSH) inhibits viral replication and decreases IL-6 levels, it was suggested that liposomal GSH could be beneficial in COVID-19 patients characterized by SARS-CoV-2-induced cytokine storm and redox imbalance (Guloyan et al., 2020). SARS-CoV-2 binds to the ACE2 receptor and induces down regulation of NRF2, which leads to inhibition of GSH release. This leads to elevated inflammatory cytokines, elevated ROS, and recruitment of immune cells. The importance of thiol-reactive molecules like NAC and GSH in SARS-CoV-2 infectivity has been shown recently (Murae et al., 2022). NAC and GSH directly suppress spike protein receptor-binding domain-ACE2 binding functions of various SARS-CoV-2 variants. An intramolecular disulfide bridge in the receptor-binding domain of the SARS-CoV-2 spike protein between Cys-488 and Cys-480, considered to be important for ACE2-binding, results directly inhibited by NAC and GSH and these compounds could be used effectively against SARS-CoV-2 cell viral entry and infection (Murae et al., 2022). GSH was shown to be the main inhibitor in the active site of the main protease (M^{pro}), the essential protein for virus invasion, and cysteine (Cys300) glutathionylation inhibits M^{pro} activity by blocking its dimerization supporting the use of GSH in COVID-19 patients (Davis et al., 2021; Linani et al., 2022). GSH deficiency has been associated with increased ROS and more severe clinical COVID-19 (Guillin et al., 2019; Derouiche, 2020; Grigoletto Fernandes et al., 2020; Guloyan et al., 2020; Polonikov, 2020; Sestili and Fimognari, 2020; Silvagno et al., 2020; Suhail et al., 2020; Bourgonje et al., 2021; Forcados et al., 2021; Kozlov et al., 2021; Pérez de la Lastra et al., 2021; Kumar P. et al., 2022). SARS-CoV-2 affects intracellular GSH levels by decreasing intracellular NRF2 function, that plays a key role in protecting cells from oxidative damage by upregulating GSH production (Rahman and MacNee, 2000; Guloyan et al., 2020; Polonikov, 2020; Sharifi-Rad et al., 2020; Silvagno et al., 2020; Bartolini et al., 2021). In stressed cells NRF2 is released and taken from the cytoplasm into the nucleus by karyopherins (Theodore et al., 2008; Sims et al., 2013; Bousquet et al., 2020; Derouiche, 2020; Guloyan et al., 2020). Coronavirus inhibits karyopherin-mediated nuclear import decreasing GSH production (Sims et al., 2013; Guloyan et al., 2020). In the setting of SARS-CoV-2, COVID-19 and oxidative stress, patients with comorbidities may have altered levels of glutamate-cysteine ligase and GSH synthetase, the enzymes participating in GSH synthesis. Therefore, it is reasonable using supplementation of liposomal glutathione, instead of the N-acetylcysteine or bonded cysteine utilized as precursors for GSH cell synthesis, since patients with deficient levels of glutamate-cysteine ligase and GSH synthetase will not be able to use N-acetylcysteine or bonded cysteine as substrates to synthesize their own GSH. Replenishing the nutritional status of the host by increasing vital amino acids such as cysteine to enhance GSH levels and selenium to improve selenium deficiency and facilitate selenoprotein (GSH peroxidases, thioredoxin reductases) expression can inhibit oxidative stress, modulating inflammation, suppressing endothelial dysfunction, and protecting vascular cells against apoptosis and calcification (He et al., 2017; Guillin et al., 2019; Seale et al., 2020; Taylor and Radding, 2020; Martinez et al., 2022). The demonstration that a combination of glycine and N-acetylcysteine supplementation rapidly improves GSH deficiency, oxidative stress and oxidant damage has implications

for considering the GSH importance in combating COVID-19 infected patients warranting further investigations (Kumar P. et al., 2022). Enzymes involved in GSH biosynthesis and function like γ-glutamyl-cysteine ligase and glutathione synthetase are completely dependent on ATP and require magnesium as a cofactor (Bani Younes et al., 2020; Tang et al., 2020; Arancibia-Hernández et al., 2022). Additionally, γ-glutamyl-transpeptidase uses magnesium as an enzyme activator (Arancibia-Hernández et al., 2022). Magnesium supplementation improves mitochondrial function and increases the content of GSH in those organelles (Liu et al., 2019; Mohammadi et al., 2020). Furthermore, magnesium sulfate was effective as a treatment for preeclampsia, significantly promoting GSH production and suppressing ROS generation (Kawasaki et al., 2019; Arancibia-Hernández et al., 2022). Recent studies have suggested that serum magnesium levels of critically ill patients deserve attention (Bani Younes et al., 2020; Iotti et al., 2020) and could not only prevent SARS CoV-2 infection, reduce severity of COVID-19 symptoms and facilitate disease recovery (Trapani et al., 2022) but benefit enzymatic activity of the GSH pathway in COVID-19. Molecules of nutritional value with antioxidant properties besides GSH, like selenium, zinc and polyphenols, are important in the immune response against SARS-CoV-2 that occurs primary in the lungs (Pérez de la Lastra et al., 2021) in critically ill patients with severe COVID-19 acute respiratory distress syndrome (Notz et al., 2021). The value of selenium upon glutathione peroxidase 1 activity and oxidative stress mitigation in SARS-CoV-2 infection and COVID-19 disease has been clearly emphasized recently (Seale et al., 2020; Fakhrolmobasheri et al., 2021) and can prevent atherosclerosis progression in SARS-CoV-2 infection. The recent demonstration of elevated superoxide dismutase, GSH peroxidase, and total antioxidant capacity in COVID-19 outpatients compared to controls could be interpreted as a response to excessive COVID-19-related oxidative stress (Golabi et al., 2022). Adequate levels and function of GSH and selenoproteins can prevent worsening of acute respiratory distress syndrome and atherosclerosis, two main causes of morbimortality in SARS-CoV-2 infection and COVID-19 disease.

Conclusion

COVID-19 is a historic challenge to the fields of research, infectious disease, and global healthcare (Hunter et al., 2022). The demand for detailed analysis of COVID-19 pathogenesis and clinical course is paramount. The unprecedented awareness of a rapidly spreading pandemic disease such as COVID-19 brings an opportunity to enhance international collaboration in the scientific community. As new variants like the omicron (Abdool Karim and Abdool, 2021; Callaway and Ledford, 2021) and others (Markov et al., 2022) appear, besides new vaccine trials continuously ongoing, physicians have been encouraged to utilize various treatments with established efficacy in similar viral or bacterial illnesses that also cause bilateral pneumonia and ARDS, as SARS-CoV-2 does. Here we present the antioxidant GSH as a potential unexplored way for further investigation as intervention for COVID-19, since GSH levels are correlated with disease severity and lung damage supporting the participation of GSH in disease outcome (Kryukov et al., 2021; Singh et al., 2022). Enhancing GSH, mainly through NAC, GSH precursors or pro-GSH compound administration, becomes a potential treatment option for SARS-CoV-2 infection and COVID-19 disease by reducing oxidative stress and cytokine expression especially in diabetic patients at risk of more severe disease (Singh et al., 2022). Whey protein concentrate ameliorates lung damage and inhibits lung furin activity targeting SARS-CoV-2 S1/S2 site cleavage and SARS CoV-2 spike protein-angiotensin converting enzyme binding and could be used to protect against COVID-19 inhibiting SARS-CoV-2 cell entry (Tufan et al., 2022). A combination of vitamin D and L-cysteine administration significantly augmented GSH levels and lowered oxidative stress and inflammation (Jain et al., 2018; Jain and Parsanathan, 2020). Maintaining an adequate GSH redox status and 25-hydroxy-vitamin D levels will have the potential to reduce oxidative stress, enhance immunity and diminish the adverse clinical consequences of COVID-19 especially in African American communities having glucose-6-phosphate dehydrogenase deficiency, enzyme necessary to prevent GSH exhaustion and depletion (Jain and Parsanathan, 2020; Jain et al., 2020). We propose that enhancement of the reduced form of GSH will reduce the body's oxidation and inflammation associated with SARS-CoV-2 infection and COVID-19 disease (Karkhanei et al., 2021). Maintaining GSH levels using therapies that do not deplete the body's GSH (Sestili and Fimognari, 2020) would be the best choice. In a patient that is overloaded with cytokine storm, the best way to fortify the immune system would be to supply it with reduced GSH, since reduced GSH is already able to provide reducing equivalents from its thiol group. This is particularly relevant when we consider GSH pathways, as well as their transcriptional regulator Nrf2, for proliferation, survival and function of T cells, B cells and macrophages (Muri and Kopf, 2021). The value of GSH and nutritional strategies like amino acids, vitamins, minerals, phytochemicals, sulforaphane to enhance cellular Nrf2, and other supplements used to restore GSH levels (Minich and Brown, 2019; Hermel et al., 2021) as adjunct treatments for SARS-CoV-2 infection needs to be further emphasized. Reestablishing the cellular metabolic homeostasis in SARS-CoV-2 infection and COVID-19 disease especially in the lungs, could become paramount to balance altered innate and adaptive immunity and cell function and reduce morbimortality (Hsu et al., 2022; Li S. et al., 2022). COVID-19 of the respiratory system appears to be a complex disease that may resist finding a single silver bullet intervention (Brosnahan et al., 2020). A multi-weaponry approach (Table 1) that

TABLE 1 Multi-weaponry approach involving glutathione (GSH) enhancers, nuclear factor erythroid 2 p45–related factor 2 (Nrf2) activators, toll-like receptor (TLR) inhibitors/immunomodulators, C-reactive protein (CRP) level reduction, natural and immune immunoglobulin M (IgM) enhancement and immune cell function recovery against SARS-CoV-2 infection and COVID-19 disease.

	Proinflammatory effects	Anti-inflammatory effects	Treatment effects on SARS-CoV-2/ COVID-19
GSH Enhancers (N-acetylcysteine [NAC], glutamine, cysteine [cystine], glycine)	GSH is fundamental to sustain an adequate function of the immune system, particularly affecting the lymphocyte activity since low GSH levels inhibit T-cell proliferation and immune response (Dröge and Breitkreutz, 2000; Ghezzi, 2011; Moro-García et al., 2018; Kelly and Pearce, 2020; Khanfar and Al Qaroot, 2020; Shyer et al., 2020). GSH levels in macrophages, directly affect the Th1/Th2 cytokine response (Fraternale et al., 2006). GSH is capable of scavenging ROS through Nrf2-mediated heme oxygenase-1 induction and enhancing M1-like macrophage polarization regulation, showing that GSH may be a useful strategy to increase the human defense system (Mittal et al., 2014; Kwon et al., 2019; Funes et al., 2020). GSH increases activation of cytotoxic T cells *in vivo*, and adequate functioning of T lymphocytes and other cells depends upon cellular supplies of cysteine (Edinger and Thompson, 2002; Garg et al., 2011; Levring et al., 2015)	GSH inhibits production of most inflammatory cytokines, and it is needed to keep an adequate interferon gamma production by dendritic cells, essential for intracellular pathogen host defense (Ghezzi, 2011; Lee and Ashkar, 2018; Calder, 2020; Fraternale et al., 2021). The principal function of endogenous GSH is not to limit inflammation but to fine-tune the innate immune response to infection (Diotallevi et al., 2017; De Flora et al., 2020; Silvagno et al., 2020; Ferreira et al., 2021)	Administration of free radical scavengers could benefit the most vulnerable SARS-CoV-2-infected patients (Laforge et al., 2020). Many antioxidants like *GSH, and NAC* inhibit viral replication (Fraternale et al., 2006). GSH precursors like NAC, glutamine, cysteine (cystine) and glycine, and Nrf2 inducers like sulforaphane can enhance GSH production and increase nuclear Nrf2 translocation and antioxidant response element (ARE) transcription (Komaravelli and Casola, 2014; Atefi et al., 2020; Poe and Corn, 2020; Dominari et al., 2021; Obayan, 2021; Di Marco et al., 2022). Since GSH inhibits viral replication and decreases IL-6 levels, liposomal GSH could benefit COVID-19 patients having SARS-CoV-2-induced cytokine storm and redox imbalance (Guloyan et al., 2020). NAC and GSH directly suppress spike protein receptor-binding domain-ACE2 binding functions of various SARS-CoV-2 variants (Murae et al., 2022)
Nrf2 Activators (Sulforaphane, melatonin)	Nrf2 activation suppresses ROS in antigen-presenting dendritic cells enhancing their capacity to interact with and promote the transformation of naïve CD8 T cells into cytotoxic T lymphocytes enabling cytotoxic T-cells to eliminate virally infected cells (Kesarwani et al., 2013; Moro-García et al., 2018; Calabrese et al., 2021; Emanuele et al., 2021)	Nrf2 activation regulates antioxidant responses to modify cellular redox states from predominantly pro-oxidant to antioxidant, and, in an antioxidant environment, macrophage phenotypes shift from M1 pro-inflammatory to M2 anti-inflammatory, reducing the probability of cytokine storms, ARDS, and lethality (Tan et al., 2016; Bousquet et al., 2020; Calabrese et al., 2021)	Antioxidants (GSH, GSH enhancers) or Nrf2 inducers (sulforaphane, melatonin) are potential viable therapies for viral-induced diseases; Nrf2 activators like sulforaphane have a potential role with dual antiviral and anti-inflammatory properties in the management of COVID-19 pneumonia (Bousquet et al., 2020; Cuadrado et al., 2020; Lin and Yao, 2020; Emanuele et al., 2021; Fratta Pasini et al., 2021) and LONG COVID (Jarrott et al., 2022; Ordonez et al., 2022)
Toll-like receptors (TLRs)	TLR4 in the heart and lungs causing aberrant TLR4 signaling favors the proinflammatory MyD88-dependent (canonical) pathway instead of the alternative TRIF/TRAM-dependent anti-inflammatory and interferon pathway (Aboudounya and Heads, 2021). TLR4 activation in platelets whether by pathogen- (viremia) or damage-associated molecular patterns induces a prothrombotic and proinflammatory state (Schattner, 2019). Activation of endosomal TLR7/8 during SARS-CoV-2 may increase the inflammatory response resulting in severe and potentially lethal immunopathological effects in COVID-19 patients as consequence of the simultaneous release of pro-inflammatory cytokines and chemokines (Dai et al., 2022)	TLRs play a key role in microorganism and viral particle recognition and activation of the innate immune system and although pathogen-associated molecular pattern (PAMP) recognition by TLRs is crucial for host defense responses to pathogen infection, *aberrant activation of TLR signaling* by PAMPs, *mutations of TLR signaling molecules*, and *damage-associated molecular patterns (DAMPs)-mediated TLRs signaling activation* are responsible for the development of chronic inflammatory diseases (Sasai and Yamamoto, 2013; Kawasaki and Kawai, 2014; McClure and Massari, 2014; Sartorius et al., 2021; Manik and Singh, 2022)	GSH and GSH enhancers could neutralize oxidation radicals generated during TLR-mediated mitochondrial ROS production and directly affect SARS-CoV-2-mediated cellular and tissue damage (Aboudounya and Heads, 2021); TLR inhibitors/immunomodulators could become promising treatments for severe COVID-19 (Jung and Lee, 2021; Dai et al., 2022)

(Continued)

TABLE 1 (Continued)

	Proinflammatory effects	Anti-inflammatory effects	Treatment effects on SARS-CoV-2/ COVID-19
C-reactive protein	*Pentameric native (n)CRP*-FcɣRI/FcɣRIIa: increases inflammatory cytokine release; nCRP-FcɣRIIb maintains a predominant anti-inflammatory effect; *non-native (nn)CRP* enhances inflammation and complement activation; induces atherogenesis; mostly proinflammatory; *monomeric (m)CRP* promotes chemotaxis; increases IL-8, MCP-1 and nitric oxide; induces ROS; mCRP-FcɣRIII induce inflammation; promotes adhesion molecule expression, thrombosis and atherogenesis (Labarrere and Kassab, 2021)	*Pentameric nCRP* bound to phosphorylcholine (PC) or lysoPC-apoptotic cells, C1q and factor H: enhance phagocytosis; nCRP-FcɣRs: M2 response; *mnCRP* binds atherogenic LDL, reduces foam cell formation and could also be atheroprotective; *mCRP* is mainly proinflammatory and not anti-inflammatory (Labarrere and Kassab, 2021)	Binding of CRP to SARS-CoV-2 virus and/or the cell membrane can impair subsequent virus attachment and entry into the cell (Labarrere and Kassab, 2021). CRP apheresis could reduce CRP levels and inflammation (Ringel et al., 2021; Torzewski et al., 2020), and reduced GSH, which has the anti-inflammation and anti-oxidation effects, can significantly decrease the plasma concentrations of CRP (Tang et al., 2011)
Natural (innate) and immune (adaptive) immunoglobulin M (IgM)	*Lack of innate and adaptive IgM* allows cell necrosis and inflammation and prevents apoptotic cell clearance (Labarrere and Kassab, 2021)	Non-inflammatory clearance of apoptotic cells; enhances virus and bacteria phagocytosis (Labarrere and Kassab, 2021)	Since IgM NAbs enhance pulmonary alveolar late apoptotic cell clearance (Litvack and Palaniyar, 2010), intravenous administration of IgM NAbs will intensify antiviral protection and late apoptotic cell removal in the lungs by alveolar macrophages (Litvack and Palaniyar, 2010; Labarrere and Kassab, 2021). Cysteine supplementation will improve immunological functions by enhancing GSH levels (Dröge and Breitkreutz, 2000; Ghezzi, 2011)
Innate immune cells (monocytes, macrophages, dendritic cells)	Innate immune cells use pattern recognition receptors to phagocytize microorganisms and apoptotic/ infected cells, produce cytokines and activate adaptive immune cells; they also promote phagocytosis, tissue repair, immunoregulation, antigen presentation, and cytokine production. Excessive cytokine production during cytokine storm in SARS-CoV-2 infection causes macrophage dysregulation, severe tissue damage and organ failure (Labarrere and Kassab, 2021)	Monocyte-derived tissue macrophages are normally involved in phagocytosis, clearance of apoptotic cells, immunoregulation and antigen presentation, and pattern recognition proteins like CRP, innate IgM and complement facilitate phagocytosis of infected apoptotic cells promoting tissue repair. Dendritic cells and macrophages are involved in linking innate and adaptative immunity against viral infections and participate in antigen presentation, cytokine production and immune cell recruitment (Labarrere and Kassab, 2021)	Hyperinflammation in severe COVID-19 infection, causes a dysregulated macrophage response, excessive cytokine production and tissue damage (Labarrere and Kassab, 2021). Dendritic cell dysfunction and dendritic cell depletion during SARS-CoV-2 infection are associated with lower Interferon I response and poorer prognosis. Dendritic cell changes contribute to COVID-19 pathogenesis and increased susceptibility to worst outcomes especially in the elderly (Cerqueira Borges et al., 2021; Labarrere and Kassab, 2021). GSH, enhanced by cysteine supplementation Nrf2 activation, is essential to reestablish innate and adaptive immune functions including T-lymphocyte proliferation, phagocytosis and antigen presentation by macrophages and dendritic cells (Dröge and Breitkreutz, 2000; Ghezzi, 2011)
B lymphocytes, plasma cells	Low affinity high valency IgM antibodies neutralize/ remove virus and bacteria and lack of IgM neutralizing antibodies enhances inflammation (Labarrere and Kassab, 2021)	B-lymphocytes/plasma cells generate innate and adaptive IgM antibodies to neutralize/ remove virus/bacteria (Labarrere and Kassab, 2021)	SARS-CoV-2 infection is characterized by an excessive inflammatory response associated with a cytokine storm and a prominent lymphopenia affecting CD4+ T cells, CD8+ T cells, B cells and natural killer cells. Both lymphopenia and the cytokine storm determine increased COVID-19 disease severity and enhanced mortality. Cysteine supplementation will improve immunological functions by enhancing GSH levels (Dröge and Breitkreutz, 2000; Ghezzi, 2011)

(Continued)

TABLE 1 (Continued)

	Proinflammatory effects	Anti-inflammatory effects	Treatment effects on SARS-CoV-2/ COVID-19
Helper (CD4) T cells, cytotoxic (CD8) T cells	T helper type 1 cells (Th1 cells; CD4+ T cells) regulate macrophage recruitment and activation enhancing defense against pathogens, and cytotoxic CD8+ T cells eliminate infection (Labarrere and Kassab, 2021)	Th2 cells mediate and maintain humoral (antibody-mediated) immune response against pathogens but unsuccessful control of the cytokine storm by Th2 cells in SARS-CoV-2 infection is associated with severe COVID-19 disease (Labarrere and Kassab, 2021)	SARS-CoV-2 infection is characterized by an excessive inflammatory response associated with a cytokine storm and a prominent lymphopenia affecting CD4+ T cells, CD8+ T cells, B cells and natural killer cells (Chen and Wherry, 2020; Labarrere and Kassab, 2021). Both lymphopenia and the cytokine storm determine increased COVID-19 disease severity and enhanced mortality (Labarrere and Kassab, 2021). Cysteine supplementation improves T-cell functions by enhancing GSH levels (Dröge and Breitkreutz, 2000; Ghezzi, 2011)

SARS-CoV-2, severe acute respiratory syndrome coronavirus 2; COVID-19, coronavirus disease 19; MyD88, Myeloid differentiation primary response 88; TRIF/TRAM, TRIF (TLR4 signaling)-related adapter molecule (TRAM).

includes global vaccine availability distributed without the greedy and selfish attitude of pharmaceutical company executives and shareholders or politicians, needs to bear in mind that "no one is safe until everyone is safe" (Hunter et al., 2022).

Author contributions

All authors listed have made a substantial, direct, and intellectual contribution to the work and approved it for publication.

Acknowledgments

Conflict of interest

The authors declare that the research was conducted in the absence of any commercial or financial relationships that could be construed as a potential conflict of interest.

Publisher's note

All claims expressed in this article are solely those of the authors and do not necessarily represent those of their affiliated organizations, or those of the publisher, the editors and the reviewers. Any product that may be evaluated in this article, or claim that may be made by its manufacturer, is not guaranteed or endorsed by the publisher.

Supplementary material

The Supplementary material for this article can be found online at: https://www.frontiersin.org/articles/10.3389/fmicb.2022.979719/full#supplementary-material

References

Abbas, M., Verma, S., Verma, S., Siddiqui, S., Khan, F. H., Raza, S. T., et al. (2021). Association of GSTM1 and GSTT1 gene polymorphisms with COVID-19 susceptibility and its outcome. *J. Med. Virol.* 93, 5446–5451. doi: 10.1002/jmv.27076

Abd El-Aziz, T. M., Al-Sabi, A., and Stockand, J. D. (2020). Human recombinant soluble ACE2 (hrs ACE2) shows promise for treating severe COVID19. *Signal Transduct. Target. Ther.* 5:258. doi: 10.1038/s41392-020-00374-6

Abdool Karim, S. S., and Abdool, K. Q. (2021). Omicron SARS-CoV-2 variant: a new chapter in the COVID-19 pandemic. *Lancet* 398, 2126–2128. doi: 10.1016/S0140-6736(21)02758-6

Aboudounya, M. M., and Heads, R. J. (2021). COVID-19 and toll-like receptor 4 (TLR4): SARS-CoV-2 may bind and activate TLR4 to increase ACE2 expression, facilitating entry and causing hyperinflammation. *Mediat. Inflamm.* 2021:8874339. doi: 10.1155/2021/8874339

Ader, F., Bouscambert-Duchamp, M., Hites, M., Peiffer-Smadja, N., Poissy, J., Belhadi, D., et al. (2022). Remdesivir plus standard of care versus standard of care alone for the treatment of patients admitted to hospital with COVID-19 (dis CoVeRy): a phase 3, randomised, controlled, open-label trial. *Lancet Infect. Dis.* 22, 209–221. doi: 10.1016/S1473-3099(21)00485-0

Aldini, G., Altomare, A., Baron, G., Vistoli, G., Carini, M., Borsani, L., et al. (2018). N-Acetylcysteine as an antioxidant and disulphide breaking agent: the reasons why. *Free Radic. Res.* 52, 751–762. doi: 10.1080/10715762.2018.1468564

Andriollo-Sanchez, M., Hininger-Favier, I., Meunier, N., Venneria, E., O'Connor, J. M., Maiani, G., et al. (2005). Age-related oxidative stress and antioxidant parameters in middle-aged and older European subjects: the ZENITH study. *Eur. J. Clin. Nutr.* 59, S58–S62. doi: 10.1038/sj.ejcn.1602300

Aquilano, K., Baldelli, S., and Ciriolo, M. R. (2014). Glutathione: new roles in redox signaling for an old antioxidant. *Front. Pharmacol.* 5:196. doi: 10.3389/fphar.2014.00196

Arancibia-Hernández, Y. L., Aranda-Rivera, A. K., Cruz-Gregorio, A., and Pedraza-Chaverri, J. (2022). Antioxidant/anti-inflammatory effect of Mg2+ in coronavirus disease 2019 (COVID-19). *Rev. Med. Virol.* 32:e2348. doi: 10.1002/rmv.2348

Arroyo, R., Grant, S. N., Colombo, M., Salvioni, L., Corsi, F., Truffi, M., et al. (2021). Full-length recombinant hSP-D binds and inhibits SARS-CoV-2. *Biomol. Ther.* 11:1114. doi: 10.3390/biom11081114

Ashfaq, S., Abramson, J. L., Jones, D. P., Rhodes, S. D., Weintraub, W. S., Hooper, W. C., et al. (2008). Endothelial function and Aminothiol biomarkers of oxidative stress in healthy adults. *Hypertension* 52, 80–85. doi: 10.1161/HYPERTENSIONAHA.107.097386

Atefi, N., Behrangi, E., Mozafarpoor, S., Seirafianpour, F., Peighambari, S., and Goodarzi, A. (2020). N-acetylcysteine and coronavirus disease 2019: may it work as a beneficial preventive and adjuvant therapy? A comprehensive review study. *J. Res. Med. Sci.* 25:109. doi: 10.4103/jrms.JRMS_777_20

Atkuri, K. R., Mantovani, J. J., Herzenberg, L. A., and Herzenberg, L. A. (2007). N-Acetylcysteine-a safe antidote for cysteine/glutathione deficiency. *Curr. Opin. Pharmacol.* 7, 355–359. doi: 10.1016/j.coph.2007.04.005

Baker, S. A., Kwok, S., Berry, G. J., and Montine, T. J. (2021). Angiotensin-converting enzyme 2 (ACE2) expression increases with age in patients requiring mechanical ventilation. *PLoS One* 16:e0247060. doi: 10.1371/journal.pone.0247060

Ballatori, N., Krance, S., Marchan, R., and Hammond, C. L. (2009). Plasma membrane glutathione transporters and their roles in cell physiology and pathophysiology. *Mol. Asp. Med.* 30, 13–28. doi: 10.1016/j.mam.2008.08.004

Bani Younes, M., Alshawabkeh, A. D., Jadallah, A. R. R., Awwad, E. F., and Al Tarabsheh, T. M. (2020). Magnesium sulfate extended infusion as an adjunctive treatment for complicated COVID-19 infected critically ill patients. *EAS J. Anesthesiol. Crit. Care* 2, 97–101. doi: 10.36349/easjacc.2020.v02i03.001

Banjac, A., Perisic, T., Sato, H., Seiler, A., Bannai, S., Weiss, N., et al. (2008). The cystine/cysteine cycle: a redox cycle regulating susceptibility versus resistance to cell death. *Oncogene* 27, 1618–1628. doi: 10.1038/sj.onc.1210796

Bartolini, D., Stabile, A. M., Bastianelli, S., Giustarini, D., Pierucci, S., Busti, C., et al. (2021). SARS-CoV2 infection impairs the metabolism and redox function of cellular glutathione. *Redox Biol.* 45:102041. doi: 10.1016/j.redox.2021.102041

Baş, H. (2018). The effects of free radicals on aging process. *Curr. Trends Biomedical Eng. Biosci.* 13:555871. doi: 10.19080/CTBEB.2018.13.555871

Bellanti, F., Lo Buglio, A., and Vendemiale, G. (2022). Redox homeostasis and immune alterations in coronavirus Disease-19. *Biology* 11:159. doi: 10.3390/biology11020159

Beltrán-García, J., Osca-Verdegal, R., Pallardó, F. V., Ferreres, J., Rodríguez, M., Mulet, S., et al. (2020). Sepsis and coronavirus disease 2019: common features and anti-inflammatory therapeutic approaches. *Crit. Care Med.* 48, 1841–1844. doi: 10.1097/CCM.0000000000004625

Bharath, L. P., and Nikolajczyk, B. S. (2020). Next steps in mechanisms of inflammaging. *Autophagy* 16, 2285–2286. doi: 10.1080/15548627.2020.1822089

Bounous, G., Gervais, F., Amer, V., Batist, G., and Gold, P. (1989). The influence of dietary whey protein on tissue glutathione and the diseases of aging. *Clin. Invest. Med.* 12, 343–349.

Bourgonje, A. R., Offringa, A. K., van Eijk, L. E., Abdulle, A. E., Hillebrands, J.-L., van der Voort, P. H. J., et al. (2021). N-Acetylcysteine and hydrogen sulfide in coronavirus disease 2019. *Antioxid. Redox Signal.* 35, 1207–1225. doi: 10.1089/ars.2020.8247

Bousquet, J., Cristol, J.-P., Czarlewski, W., Anto, J. M., Martineau, A., Haahtela, T., et al. (2020). Nrf 2-interacting nutrients and COVID-19: time for research to develop adaptation strategies. *Clin. Transl. Allergy* 10:58. doi: 10.1186/s13601-020-00362-7

Brandes, R. P., Weissmann, N., and Schröder, K. (2014). Nox family NADPH oxidases: molecular mechanisms of activation. *Free Radic. Biol. Med.* 76, 208–226. doi: 10.1016/j.freeradbiomed.2014.07.046

Brosnahan, S. B., Jonkman, A. H., Kugler, M. C., Munger, J. S., and Kaufman, D. A. (2020). COVID-19 and respiratory system disorders. Current knowledge, future clinical and translational research questions. *Arterioscler. Thromb. Vasc. Biol.* 40, 2586–2597. doi: 10.1161/ATVBAHA.120.314515

Brueggeman, J. M., Zhao, J., Schank, M., Yao, Z. Q., and Moorman, J. P. (2022). Trained immunity: an overview and the impact on COVID-19. *Front. Immunol.* 13:837524. doi: 10.3389/fimmu.2022.837524

Calabrese, E. J., Kozumbo, W. J., Kapoor, R., Dhawan, G., Lara, P. C., and Giordano, J. (2021). Nrf 2 activation putatively mediates clinical benefits of low-dose radiotherapy in COVID-19 pneumonia and acute respiratory distress syndrome (ARDS): novel mechanistic considerations. *Radiother. Oncol.* 160, 125–131. doi: 10.1016/j.radonc.2021.04.015

Calder, P. C. (2020). Nutrition, immunity and COVID-19. *BMJ Nutr. Prev. Health* 3, 74–92. doi: 10.1136/bmjnph-2020-000085

Callaway, E., and Ledford, H. (2021). How bad is omicron? What scientists know so far. *Nature* 600, 197–199. doi: 10.1038/d41586-021-03614-z

Campolo, J., Bernardi, S., Cozzi, L., Rocchiccioli, S., Dellanoce, C., Cecchettini, A., et al. (2017). Medium-term effect of sublingual l-glutathione supplementation on flow-mediated dilation in subjects with cardiovascular risk factors. *Nutrition* 38, 41–47. doi: 10.1016/j.nut.2016.12.018

Carcaterra, M., and Caruso, C. (2021). Alveolar epithelial cell type II as main target of SARS-CoV-2 virus and COVID-19 development via NF-kb pathway deregulation: a physio-pathological theory. *Med. Hypotheses* 146:110412. doi: 10.1016/j.mehy.2020.110412

Castejon, A. M., Spaw, J. A., Rozenfeld, I., Sheinberg, N., Kabot, S., Shaw, A., et al. (2021). Improving antioxidant capacity in children with autism: a randomized, double-blind controlled study with cysteine-rich whey protein. *Front. Psych.* 12:669089. doi: 10.3389/fpsyt.2021.669089

Cazzola, M., Rogliani, P., Salvi, S. S., Ora, J., and Matera, M. G. (2021). Use of thiols in the treatment of COVID-19: current evidence. *Lung* 199, 335–343. doi: 10.1007/s00408-021-00465-3

Cecchini, R., and Cecchini, A. L. (2020). SARS-CoV-2 infection pathogenesis is related to oxidative stress as a response to aggression. *Med. Hypotheses* 143:110102. doi: 10.1016/j.mehy.2020.110102

Cerqueira Borges, R., Sayuri Hohmann, M., and Marques, B. S. (2021). Dendritic cells in COVID-19 Immunopathogenesis: insights for a possible role in determining disease outcome. *Int. Rev. Immunol.* 40, 108–125. doi: 10.1080/08830185.2020.1844195

Chang, R., Mamun, A., Dominic, A., and Le, N.-T. (2021). SARS-CoV-2 mediated endothelial dysfunction: the potential role of chronic oxidative stress. *Front. Physiol.* 11:605908. doi: 10.3389/fphys.2020.605908

Chang, W. K., Yang, K. D., and Shaio, M. F. (1999). Lymphocyte proliferation modulated by glutamine: involved in the endogenous redox reaction. *Clin. Exp. Immunol.* 117, 482–488. doi: 10.1046/j.1365-2249.1999.01009.x

Chen, K.-K., Minakuchi, M., Wuputra, K., Ku, C.-C., Pan, J.-B., Kuo, K.-K., et al. (2020). Redox control in the pathophysiology of influenza virus infection. *BMC Microbiol.* 20:214. doi: 10.1186/s12866-020-01890-9

Chen, Z., and Wherry, E. J. (2020). T cell responses in patients with COVID-19. *Nat. Rev. Immunol.* 20, 529–536. doi: 10.1038/s41577-020-0402-6

Chumakov, K., Avidan, M. S., Benn, C. S., Bertozzi, S. M., Blatt, L., Chang, A. Y., et al. (2021). Old vaccines for new infections: exploiting innate immunity to control COVID-19 and prevent future pandemics. *Proc. Natl. Acad. Sci.* 118:e2101718118. doi: 10.1073/pnas.2101718118

Circu, M. L., and Aw, T. Y. (2010). Reactive oxygen species, cellular redox systems, and apoptosis. *Free Radic. Biol. Med.* 48, 749–762. doi: 10.1016/j.freeradbiomed.2009.12.022

Circu, M. L., and Aw, T. Y. (2012). Glutathione and modulation of cell apoptosis. *Biochim. Biophys. Acta* 1823, 1767–1777. doi: 10.1016/j.bbamcr.2012.06.019

Clausen, T. M., Sandoval, D. R., Spliid, C. B., Pihl, J., Perrett, H. R., Painter, C. D., et al. (2020). SARS-CoV-2 infection depends on cellular Heparan sulfate and ACE2. *Cells* 183, 1043–1057.e15. doi: 10.1016/j.cell.2020.09.033

Coric, V., Milosevic, I., Djukic, T., Bukumiric, Z., Savic-Radojevic, A., Matic, M., et al. (2021). GSTP1 and GSTM3 variant alleles affect susceptibility and severity of COVID-19. *Front. Mol. Biosci.* 8:747493. doi: 10.3389/fmolb.2021.7

Coz Yataco, A. O., and Simpson, S. Q. (2020). Coronavirus disease 2019 sepsis. A nudge toward antibiotic Stewardship. *Chest* 158, 1833–1834. doi: 10.1016/j.chest.2020.07.023

Cuadrado, A., Pajares, M., Benito, C., Jiménez-Villegas, J., Escoll, M., Fernández-Ginés, , et al. (2020). Can activation of NRF2 be a strategy against COVID-19? *Trends Pharmacol. Sci.* 41, 598–610. doi: 10.1016/j.tips.2020.07.003

Cuadrado, A., Rojo, A. I., Wells, G., Hayes, J. D., Cousin, S. P., Rumsey, W. L., et al. (2019). Therapeutic targeting of the NRF2 and KEAP1 partnership in chronic diseases. *Nat. Rev. Drug Discov.* 18, 295–317. doi: 10.1038/s41573-018-0008-x

Cunha, L. L., Perazzio, S. F., Azzi, J., Cravedi, P., and Riella, L. V. (2020). Remodeling of the immune response with aging: immunosenescence and its potential impact on COVID-19 immune response. *Front. Immunol.* 11:1748. doi: 10.3389/fimmu.2020.01748

Dai, J., Wang, Y., Wang, H., Gao, Z., Wang, Y., Fang, M., et al. (2022). Toll-like receptor signaling in severe acute respiratory syndrome coronavirus 2-induced innate immune responses and the potential application value of toll-like receptor

Immunomodulators in patients with coronavirus disease 2019. *Front. Microbiol.* 13:948770. doi: 10.3389/fmicb.2022.948770

Davis, D. A., Bulut, H., Shrestha, P., Yaparla, A., Jaeger, H. K., Hattori, S.-i., et al. (2021). Regulation of the dimerization and activity of SARS-CoV-2 main protease through reversible glutathionylation of cysteine 300. *mBio* 12, 12:e02094-21. doi: 10.1128/mBio.02094-21

Davis, D. A. S., and Parish, C. R. (2013). Heparan sulfate: a ubiquitous glycosaminoglycan with multiple roles in immunity. *Front. Immunol.* 4:470. doi: 10.3389/fimmu.2013.00470

De Candia, P., Prattichizzo, F., Garavelli, S., and Matarese, G. (2021). T cells: warriors of SARS-CoV-2 infection. *Trends Immunol.* 42, 18–30. doi: 10.1016/j.it.2020.11.002

De Flora, S., Balansky, R., and La Maestra, S. (2020). Rationale for the use of N-acetylcysteine in both prevention and adjuvant therapy of COVID-19. *FASEB J.* 34, 13185–13193. doi: 10.1096/fj.202001807

De Pasquale, V., Quiccione, M. S., Tafuri, S., Avallone, L., and Pavone, L. M. (2021). Heparan sulfate proteoglycans in viral infection and treatment: a special focus on SARS-CoV-2. *Int. J. Mol. Sci.* 22:6574. doi: 10.3390/ijms22126574

Delgado-Roche, L., and Mesta, F. (2020). Oxidative stress as key player in severe acute respiratory syndrome coronavirus (SARS-CoV) infection. *Arch. Med. Res.* 51, 384–387. doi: 10.1016/j.arcmed.2020.04.019

Deneke, S. M., and Fanburg, B. L. (1989). Regulation of cellular glutathione. *Am. J. Phys.* 257, L163–L173. doi: 10.1152/ajplung.1989.257.4.L163

Denzoin Vulcano, L. A., Soraci, A. L., and Tapia, M. O. (2013). Homeostasis del glutatión. *Acta Bioquím Clín Latinoam* 47, 529–539.

DePietro, M., and Salzberg, M. (2022). Commentary: pattern recognition proteins: first line of defense against coronaviruses. *Front. Immunol.* 13:815168. doi: 10.3389/fimmu.2022.815168

Derouiche, S. (2020). Oxidative stress associated with SARS-Cov-2 (COVID-19) increases the severity of the lung disease – a systematic review. *J. Infect. Dis. Epidemiol.* 6:121. doi: 10.23937/2474-3658/1510121

Di Marco, F., Foti, G., and Corsico, A. G. (2022). Where are we with the use of N-acetylcysteine as a preventive and adjuvant treatment for COVID-19? *Eur. Rev. Med. Pharmacol. Sci.* 26, 715–721. doi: 10.26355/eurrev_202201_27898

Diao, B., Wang, C., Tan, Y., Chen, X., Liu, Y., Ning, L., et al. (2020). Reduction and functional exhaustion of T cells in patients with coronavirus disease 2019 (COVID-19). *Front. Immunol.* 11:827. doi: 10.3389/fimmu.2020.00827

Diaz-Vivancos, P., Wolff, T., Markovic, J., Pallardó, F. V., and Foyer, C. H. (2010). A nuclear glutathione cycle within the cell cycle. *Biochem. J.* 431, 169–178. doi: 10.1042/BJ20100409

Diotallevi, M., Checconi, P., Palamara, A. T., Celestino, I., Coppo, L., Holmgren, A., et al. (2017). Glutathione fine-tunes the innate immune response toward antiviral pathways in a macrophage cell line independently of its antioxidant properties. *Front. Immunol.* 8:1239. doi: 10.3389/fimmu.2017.01239

Djukic, T., Stevanovic, G., Coric, V., Bukumiric, Z., Pljesa-Ercegovac, M., Matic, M., et al. (2022). GSTO1, GSTO2 and ACE2 polymorphisms modify susceptibility to developing COVID-19. *J. Pers. Med.* 12:458. doi: 10.3390/jpm12030458

Doğan, H. O., Şenol, O., Bolat, S., Yıldız, Ş. N., Büyüktuna, S. A., Sarıismailoğlu, R., et al. (2021). Understanding the pathophysiological changes via untargeted metabolomics in COVID-19 patients. *J. Med. Virol.* 93, 2340–2349. doi: 10.1002/jmv.26716

Dominari, A., Hathaway Iii, D., Kapasi, A., Paul, T., Makkar, S. S., Castaneda, V., et al. (2021). Bottom-up analysis of emergent properties of N-acetylcysteine as an adjuvant therapy for COVID-19. *World J. Virol.* 10, 34–52. doi: 10.5501/wjv.v10.i2.34

Dröge, W. (2002a). The plasma redox state and ageing. *Ageing Res. Rev.* 1, 257–278. doi: 10.1016/s1568-1637(01)00008-3

Dröge, W. (2002b). Aging-related changes in the thiol/disulfide redox state: implications for the use of thiol antioxidants. *Exp. Gerontol.* 37, 1333–1345. doi: 10.1016/s0531-5565(02)00175-4

Dröge, W. (2002c). Free radicals in the physiological control of cell function. *Physiol. Rev.* 82, 47–95. doi: 10.1152/physrev.00018.2001

Dröge, W., and Breitkreutz, R. (2000). Glutathione and immune function. *Proc. Nutr. Soc.* 59, 595–600. doi: 10.1017/S0029665100000847

Dröge, W., Eck, H. P., Gmünder, H., and Mihm, S. (1991). Modulation of lymphocyte functions and immune responses by cysteine and cysteine derivatives. *Am. J. Med.* 91, S140–S144. doi: 10.1016/0002-9343(91)90297-b

Edinger, A. L., and Thompson, C. B. (2002). Antigen-presenting cells control T cell proliferation by regulating amino acid availability. *Proc. Natl. Acad. Sci. U. S. A.* 99, 1107–1109. doi: 10.1073/pnas.042707999

Emanuele, S., Celesia, A., D'Anneo, A., Lauricella, M., Carlisi, D., De Blasio, A., et al. (2021). The good and bad of Nrf 2: an update in cancer and new perspectives in COVID-19. *Int. J. Mol. Sci.* 22:7963. doi: 10.3390/ijms22157963

Fajgenbaum, D. C., and June, C. H. (2020). Cytokine storm. *N. Engl. J. Med.* 383, 2255–2273. doi: 10.1056/NEJMra2026131

Fakhrolmobasheri, M., Mazaheri-Tehrani, S., Kieliszek, M., Zeinalian, M., Abbasi, M., Karimi, F., et al. (2021). COVID-19 and selenium deficiency: a systematic review. *Biol. Trace Elem. Res.* 200, 3945–3956. doi: 10.1007/s12011-021-02997-4

Fazal, M. (2021). C-reactive protein a promising biomarker of COVID-19 severity. *Korean J. Clin. Lab. Sci.* 53, 201–207. doi: 10.15324/kjcls.2021.53.3.201

Fendl, B., Weiss, R., Eichhorn, T., Linsberger, I., Afonyushkin, T., Puhm, F., et al. (2021). Extracellular vesicles are associated with C−reactive protein in sepsis. *Sci. Rep.* 11:6996. doi: 10.1038/s41598-021-86489-4

Ferreira, A. V., Koeken, V. A. C. M., Matzaraki, V., Kostidis, S., Alarcon-Barrera, J. C., de Bree, L. C. J., et al. (2021). Glutathione metabolism contributes to the induction of trained immunity. *Cells* 10:971. doi: 10.3390/cells10050971

Forcados, G. E., Muhammad, A., Oladipo, O. O., Makama, S., and Meseko, C. A. (2021). Metabolic implications of oxidative stress and inflammatory process in SARS-CoV-2 pathogenesis: therapeutic potential of natural antioxidants. *Front. Cell. Infect. Microbiol.* 11:654813. doi: 10.3389/fcimb.2021.654813

Forman, H. J., Zhang, H., and Rinna, A. (2009). Glutathione: overview of its protective roles, measurement, and biosynthesis. *Mol. Asp. Med.* 30, 1–12. doi: 10.1016/j.mam.2008.08.006

Fossum, C. J., Laatsch, B. F., Lowater, H. R., Narkiewicz-Jodko, A. W., Lonzarich, L., Hati, S., et al. (2022). Pre-existing oxidative stress creates a docking-ready conformation of the SARS-CoV-2 receptor-binding domain. *ACS Bio. Med. Chem. Au.* 2, 84–93. doi: 10.1021/acsbiomedchemau.1c00040

Franco, R., and Cidlowski, J. A. (2006). SLCO/OATP-like transport of glutathione in FASL-induced apoptosis: glutathione efflux is coupled to an organic anion exchange and is necessary for the progression of the execution phase of apoptosis. *J. Biol. Chem.* 281, 29542–29557. doi: 10.1074/jbc.M602500200

Franco, R., and Cidlowski, J. A. (2009). Apoptosis and glutathione: beyond an antioxidant. *Cell Death Differ.* 16, 1303–1314. doi: 10.1038/cdd.2009.107

Franco, R., and Cidlowski, J. A. (2012). Glutathione efflux and cell death. *Antioxid. Redox Signal.* 17, 1694–1713. doi: 10.1089/ars.2012.4553

Franco, R., Panayiotidis, M. I., and Cidlowski, J. A. (2007a). Glutathione depletion is necessary for apoptosis in lymphoid cells independent of reactive oxygen species formation. *J. Biol. Chem.* 282, 30452–30465. doi: 10.1074/jbc.M703091200

Franco, R., Schoneveld, O. J., Pappa, A., and Panayiotidis, M. I. (2007b). The central role of glutathione in the pathophysiology of human diseases. *Arch. Physiol. Biochem.* 113, 234–258. doi: 10.1080/13813450701661198

Fraternale, A., Brundu, S., and Magnani, M. (2017). Glutathione and glutathione derivatives in immunotherapy. *Biol. Chem.* 398, 261–275. doi: 10.1515/hsz-2016-0202

Fraternale, A., Paoletti, M. F., Casabianca, A., Oiry, J., Clayette, P., Vogel, J.-U., et al. (2006). Antiviral and Immunomodulatory properties of new pro-glutathione (GSH) molecules. *Curr. Med. Chem.* 13, 1749–1755. doi: 10.2174/092986706777452542

Fraternale, A., Zara, C., De Angelis, M., Nencioni, L., Palamara, A. T., Retini, M., et al. (2021). Intracellular redox-modulated pathways as targets for effective approaches in the treatment of viral infection. *Int. J. Mol. Sci.* 22:3603. doi: 10.3390/ijms22073603

Fratta Pasini, A. M., Stranieri, C., Cominacini, L., and Mozzini, C. (2021). Potential role of antioxidant and anti-inflammatory therapies to prevent severe SARS-Cov-2 complications. *Antioxidants* 10:272. doi: 10.3390/antiox10020272

Funes, S. C., Rios, M., Fernández-Fierro, A., Covián, C., Bueno, S. M., Riedel, C. A., et al. (2020). Naturally derived heme-oxygenase 1 inducers and their therapeutic application to immune-mediated diseases. *Front. Immunol.* 11:1467. doi: 10.3389/fimmu.2020.01467

Gadanec, L. K., McSweeney, K. R., Qaradakhi, T., Ali, B., Zulli, A., and Apostolopoulos, V. (2021). Can SARS-CoV-2 virus use multiple receptors to enter host cells? *Int. J. Mol. Sci.* 22:992. doi: 10.3390/ijms22030992

García-Giménez, J. L., Markovic, J., Dasí, F., Queval, G., Schnaubelt, D., Foyer, C. H., et al. (2013). Nuclear glutathione. *Biochim. Biophys. Acta* 1830, 3304–3316. doi: 10.1016/j.bbagen.2012.10.005

Garg, S. K., Yan, Z., Vitvitsky, V., and Banerjee, R. (2011). Differential dependence on cysteine from Transsulfuration versus transport during T cell activation. *Antiox Redox Signal* 15, 39–47. doi: 10.1089/ars.2010.3496

Ghati, A., Dam, P., Tasdemir, D., Kati, A., Sellami, H., Sezgin, G. C., et al. (2021). Exogenous pulmonary surfactant: a review focused on adjunctive therapy for severe acute respiratory syndrome coronavirus 2 including SP-A and SP-D as added clinical marker. *Curr. Opin. Colloid Interface Sci.* 51:101413. doi: 10.1016/j.cocis.2020.101413

Ghezzi, P. (2011). Role of glutathione in immunity and inflammation in the lung. *Int. J. Gen. Med.* 4, 105–113. doi: 10.2147/IJGM.S15618

Ghezzi, P., Lemley, K. V., Andrus, J. P., De Rosa, S. C., Holmgren, A., Jones, D., et al. (2019). "Cysteine/glutathione deficiency: a significant and treatable corollary of disease," in *The Therapeutic Use of N-Acetylcysteine (NAC) in Medicine*. eds. R. E. Frye and M. Berk (Springer Nature Singapore Pte Ltd.), 349–386.

Gill, R., Tsung, A., and Billiar, T. (2010). Linking oxidative stress to inflammation: toll-like receptors. *Free Radic. Biol. Med.* 48, 1121–1132. doi: 10.1016/j.freeradbiomed.2010.01.006

Giustarini, D., Tsikas, D., Colombo, G., Milzani, A., Dalle-Donne, I., Fanti, P., et al. (2016). Pitfalls in the analysis of the physiological antioxidant glutathione (GSH) and its disulfide (GSSG) in biological samples: an elephant in the room. *J. Chromatogr. B Analyt. Technol. Biomed. Life Sci.* 1019, 21–28. doi: 10.1016/j.jchromb.2016.02.015

Golabi, S., Ghasemi, S., Adelipour, M., Bagheri, R., Suzuki, K., Wong, A., et al. (2022). Oxidative stress and inflammatory status in COVID-19 outpatients: a health center-based analytical cross-sectional study. *Antioxidants* 11:606. doi: 10.3390/antiox11040606

Gong, W., Aspatwar, A., Wang, S., Parkkila, S., and Wu, X. (2021). COVID-19 pandemic: SARS-CoV-2 specific vaccines and challenges, protection via BCG trained immunity, and clinical trials. *Expert Rev. Vaccines* 20, 857–880. doi: 10.1080/14760584.2021.1938550

Gottlieb, R. L., Vaca, C. E., Paredes, R., Mera, J., Webb, B. J., Perez, G., et al. (2022). Early Remdesivir to prevent progression to severe Covid-19 in outpatients. *N. Engl. J. Med.* 386, 305–315. doi: 10.1056/NEJMoa2116846

Gould, R. L., and Pazdro, R. (2019). Impact of supplementary amino acids, micronutrients, and overall diet on glutathione homeostasis. *Nutrients* 11:1056. doi: 10.3390/nu11051056

Gralinski, L. E., and Baric, R. S. (2015). Molecular pathology of emerging coronavirus infections. *J. Pathol.* 235, 185–195. doi: 10.1002/path.4454

Grigoletto Fernandes, I., Alves de Brito, C., Silva Dos Reis, V. M., Sato, M. N., and Zanete, P. N. (2020). SARS-CoV-2 and other respiratory viruses: what does oxidative stress have to do with it? *Oxidative Med. Cell. Longev.* 2020:8844280. doi: 10.1155/2020/8844280

Guillin, O. M., Vindry, C., Ohlmann, T., and Chavatte, L. (2019). Selenium, selenoproteins and viral infection. *Nutrients* 11:2101. doi: 10.3390/nu11092101

Guloyan, V., Oganesian, B., Baghdasaryan, N., Yeh, C., Singh, M., Guilford, F., et al. (2020). Glutathione supplementation as an adjunctive therapy in COVID-19. *Antioxidants* 9:914. doi: 10.3390/antiox9100914

Hadzic, T., Li, L., Cheng, N., Walsh, S. A., Spitz, D. R., and Knudson, C. M. (2005). The role of low molecular weight thiols in T lymphocyte proliferation and IL-2 secretion. *J. Immunol.* 175, 7965–7972. doi: 10.4049/jimmunol.175.12.7965

Hajjar, I., Hayek, S. S., Goldstein, F. C., Martin, G., Jones, D. P., and Quyyumi, A. (2018). Oxidative stress predicts cognitive decline with aging in healthy adults: an observational study. *J. Neuroinflammation* 15:17. doi: 10.1186/s12974-017-1026-z

Hamilos, D. L., Zelarney, P., and Mascali, J. J. (1989). Lymphocyte proliferation in glutathione-depleted lymphocytes: direct relationship between glutathione availability and the proliferative response. *Immunopharmacology* 18, 223–235. doi: 10.1016/0162-3109(89)90020-9

Harvey, C. J., Thimmulappa, R. K., Singh, A., Blake, D. J., Ling, G., Wakabayashi, N., et al. (2009). Nrf 2-regulated glutathione recycling independent of biosynthesis is critical for cell survival during oxidative stress. *Free Radic. Biol. Med.* 46, 443–453. doi: 10.1016/j.freeradbiomed.2008.10.040

Hati, S., and Bhattacharyya, S. (2020). Impact of Thiol−disulfide balance on the binding of Covid-19 spike protein with angiotensin-converting enzyme 2 receptor. *ACS Omega* 5, 16292–16298. doi: 10.1021/acsomega.0c02125

He, L., He, T., Farrar, S., Ji, L., Liu, T., and Ma, X. (2017). Antioxidants maintain cellular redox homeostasis by elimination of reactive oxygen species. *Cell. Physiol. Biochem.* 44, 532–553. doi: 10.1159/000485089

Heil, E. L., and Kottilil, S. (2022). The goldilocks time for Remdesivir— is any indication just right? *N. Engl. J. Med.* 386, 385–387. doi: 10.1056/NEJMe2118579

Herengt, A., Thyrsted, J., and Holm, C. K. (2021). NRF2 in viral infection. *Antioxidants* 10:1491. doi: 10.3390/antiox10091491

Hermel, M., Sweeney, M., Ni, Y.-M., Bonakdar, R., Triffon, D., Suhar, C., et al. (2021). Natural supplements for COVID19—background, rationale, and clinical trials. *J. Evid. Based Integr. Med.* 26:2515690X211036875. doi: 10.1177/2515690X211036875

Hotchkiss, R. S., Strasser, A., McDunn, J. E., and Swanson, P. E. (2009). Cell death. *N. Engl. J. Med.* 361, 1570–1583. doi: 10.1056/NEJMra0901217

Hsu, R.-J., Yu, W.-C., Peng, G.-R., Ye, C.-H., Hu, S. Y., Chong, P. C. T., et al. (2022). The role of cytokines and chemokines in severe acute respiratory syndrome coronavirus 2 infections. *Front. Immunol.* 13:832394. doi: 10.3389/fimmu.2022.832394

Huang, I., and Pranata, R. (2020). Lymphopenia in severe coronavirus disease-2019 (COVID-19): systematic review and meta-analysis. *J. Intensive Care* 8:36. doi: 10.1186/s40560-020-00453-4

Hunter, D. J., Abdool Karim, S. S., Baden, L. R., Farrar, J. J., Hamel, M. B., Longo, D. L., et al. (2022). Addressing vaccine inequity — Covid-19 vaccines as a global public good. *N. Engl. J. Med.* 386, 1176–1179. doi: 10.1056/NEJMe2202547

Iotti, S., Wolf, F., Mazur, A., and Maier, J. A. (2020). The COVID-19 pandemic: is there a role for magnesium? Hypotheses and perspectives. *Magnes Res.* 33, 21–27. doi: 10.1684/mrh.2020.0465

Jackson, C. B., Farzan, M., Chen, B., and Choe, H. (2022). Mechanisms of SARS-CoV-2 entry into cells. *Nat. Rev. Mol. Cell Biol.* 23, 3–20. doi: 10.1038/s41580-021-00418-x

Jain, S. K., and Parsanathan, R. (2020). Can vitamin D and L-cysteine co-supplementation reduce 25 (OH)-vitamin D deficiency and the mortality associated with COVID-19 in African Americans? *J. Am. Coll. Nutr.* 39, 694–699. doi: 10.1080/07315724.2020.1789518

Jain, S. K., Parsanathan, R., Achari, A. E., Kanikarla-Marie, P., and Bocchini, J. A. (2018). Glutathione stimulates vitamin D regulatory and glucose-metabolism genes, lowers oxidative stress and inflammation, and increases 25-Hydroxy-vitamin D levels in blood: a novel approach to treat 25-Hydroxyvitamin D deficiency. *Antioxid. Redox Signal.* 29, 1792–1807. doi: 10.1089/ars.2017.7462

Jain, S. K., Parsanathan, R., Levine, S. N., Bocchini, J. A., Holick, M. F., and Vanchiere, J. A. (2020). The potential link between inherited G6PD deficiency, oxidative stress, and vitamin D deficiency and the racial inequities in mortality associated with COVID-19. *Free Radic. Biol. Med.* 161, 84–91. doi: 10.1016/j.freeradbiomed.2020.10.002

Jarrott, B., Head, R., Pringle, K. G., Lumbers, E. R., and Martin, J. H. (2022). "LONG COVID"—a hypothesis for understanding the biological basis and pharmacological treatment strategy. *Pharmacol. Res. Perspect.* 10:e00911. doi: 10.1002/prp2.911

Jin, Y., Hou, C., Li, Y., Zheng, K., and Wang, C. (2022). mRNA vaccine: how to meet the challenge of SARS-CoV-2. *Front. Immunol.* 12:821538. doi: 10.3389/fimmu.2021.821538

Jung, H. E., and Lee, H. K. (2021). Current understanding of the innate control of toll-like receptors in response to SARS-CoV-2 infection. *Viruses* 13:2132. doi: 10.3390/v13112132

Kaklamanos, A., Belogiannis, K., Skendros, P., Gorgoulis, V. G., Vlachoyiannopoulos, P. G., and Tzioufas, A. G. (2021). COVID-19 Immunobiology: lessons learned, new questions arise. *Front. Immunol.* 12:719023. doi: 10.3389/fimmu.2021.719023

Kalra, R. S., and Kandimalla, R. (2021). Engaging the spikes: heparan sulfate facilitates SARS-CoV-2 spike protein binding to ACE2 and potentiates viral infection. *Signal Transduct. Target. Ther.* 6:39. doi: 10.1038/s41392-021-00470-1

Kang, I., Chang, M. Y., Wight, T. N., and Frevert, C. W. (2018). Proteoglycans as Immunomodulators of the innate immune response to lung infection. *J. Histochem. Cytochem.* 66, 241–259. doi: 10.1369/0022155417751880

Karkhanei, B., Talebi Ghane, E., and Mehri, F. (2021). Evaluation of oxidative stress level: total antioxidant capacity, total oxidant status and glutathione activity in patients with COVID-19. *New Microbes New Infect* 42:100897. doi: 10.1016/j.nmni.2021.100897

Kasprzak, M. P., Olasińska-Wiśniewska, A., Gryszczyńska, B., Budzyń, M., Lesiak, M., Trojnarska, O., et al. (2020). Changes in the Nrf 2/Keap 1 ratio and PON1 concentration in plasma of patients undergoing the left main coronary artery stenting. *Oxidative Med. Cell. Longev.* 2020, 1–9. doi: 10.1155/2020/8249729

Kawasaki, T., and Kawai, T. (2014). Toll-like receptor signaling pathways. *Front. Immunol.* 5:461. doi: 10.3389/fimmu.2014.00461

Kawasaki, K., Kondoh, E., Chigusa, Y., Kawamura, Y., Mogami, H., Takeda, S., et al. (2019). Metabolomic profiles of placenta in preeclampsia. Antioxidant effect of magnesium sulfate on Trophoblasts in early-onset preeclampsia. *Hypertension* 73, 671–679. doi: 10.1161/HYPERTENSIONAHA.118.12389

Kelly, B., and Pearce, E. L. (2020). Amino assets: how amino acids support immunity. *Cell Metab.* 32, 154–175. doi: 10.1016/j.cmet.2020.06.010

Kernan, K. F., and Carcillo, J. A. (2017). Hyperferritinemia and inflammation. *Int. Immunol.* 29, 401–409. doi: 10.1093/intimm/dxx031

Kesarwani, P., Murali, A. K., Al-Khami, A. A., and Mehrotra, S. (2013). Redox regulation of T-cell function: from molecular mechanisms to significance in human health and disease. *Antiox Redox Signal* 18, 1497–1534. doi: 10.1089/ars.2011.4073

Khanfar, A., and Al Qaroot, B. (2020). Could glutathione depletion be the Trojan horse of COVID-19 mortality? *Eur. Rev. Med. Pharmacol. Sci.* 24, 12500–12509. doi: 10.26355/eurrev_202012_24046

Khanmohammadi, S., and Rezaei, N. (2021). Role of toll-like receptors in the pathogenesis of COVID-19. *J. Med. Virol.* 93, 2735–2739. doi: 10.1002/jmv.26826

Khomich, O. A., Kochetkov, S. N., Bartosch, B., and Ivanov, A. V. (2018). Redox biology of respiratory viral infections. *Viruses* 10:392. doi: 10.3390/v10080392

Klok, F. A., Kruip, M. J. H. A., van der Meer, N. J. M., Arbous, M. S., Gommers, D. A. M. P. J., Kant, K. M., et al. (2020). Incidence of thrombotic complications in critically ill ICU patients with COVID-19. *Thromb. Res.* 191, 145–147. doi: 10.1016/j.thromres.2020.04.013

Knoll, R., Schultze, J. L., and Schulte-Schrepping, J. (2021). Monocytes and macrophages in COVID-19. *Front. Immunol.* 12:720109. doi: 10.3389/fimmu.2021.720109

Kobayashi, E. H., Suzuki, T., Funayama, R., Nagashima, T., Hayashi, M., Sekine, H., et al. (2016). Nrf 2 suppresses macrophage inflammatory response by blocking proinflammatory cytokine transcription. *Nat. Commun.* 7:11624. doi: 10.1038/ncomms11624

Kolls, J. K. (2006). Oxidative stress in sepsis: a redox redux. *J. Clin. Invest.* 116, 860–863. doi: 10.1172/JCI28111

Komaravelli, N., and Casola, A. (2014). Respiratory viral infections and subversion of cellular antioxidant defenses. *J. Pharmacogenomics Pharmacoproteomics* 5:5. doi: 10.4172/2153-0645.1000141

Kozlov, E. M., Ivanova, E., Grechko, A. V., Wu, W.-K., Starodubova, A. V., and Orekhov, A. N. (2021). Involvement of oxidative stress and the innate immune system in SARS-CoV-2 infection. *Diseases* 9:17. doi: 10.3390/diseases9010017

Kryukov, E. V., Ivanov, A. V., Karpov, V. O., Vasil'evich Alexandrin, V., Dygai, A. M., Kruglova, M. P., et al. (2021). Association of low molecular weight plasma aminothiols with the severity of coronavirus disease 2019. *Oxidative Med. Cell. Longev.* 2021:9221693. doi: 10.1155/2021/9221693

Kumar, D. S., Hanumanram, G., Suthakaran, P. K., Mohanan, J., Nair, L. D. V., and Rajendran, K. (2022). Extracellular oxidative stress markers in COVID-19 patients with diabetes as co-morbidity. *Clin. Pract.* 12, 168–176. doi: 10.3390/clinpract12020021

Kumar, P., Osahon, O., Vides, D. B., Hanania, N., Minard, C. G., and Sekhar, R. V. (2022). Severe glutathione deficiency, oxidative stress and oxidant damage in adults hospitalized with COVID-19: implications for Gly NAC (glycine and N-Acetylcysteine) supplementation. *Antioxidants* 11:50. doi: 10.3390/antiox11010050

Kwon, D. H., Lee, H., Park, C., Hong, S.-H., Hong, S. H., Kim, G.-Y., et al. (2019). Glutathione induced immune-stimulatory activity by promoting M1-like macrophages polarization via potential ROS scavenging capacity. *Antioxidants* 8:413. doi: 10.3390/antiox8090413

Labarrere, C. A., and Kassab, G. S. (2021). Pattern recognition proteins: first line of defense against coronaviruses. *Front. Immunol.* 12:652252. doi: 10.3389/fimmu.2021.652252

Labarrere, C. A., and Kassab, G. S. (2022). Response: commentary: pattern recognition proteins: first line of defense against coronaviruses. *Front. Immunol.* 13:853015. doi: 10.3389/fimmu.2022.853015

Laforge, M., Elbim, C., Frère, C., Hémadi, M., Massaud, C., Nuss, P., et al. (2020). Tissue damage from neutrophil-induced oxidative stress in COVID-19. *Nat. Rev. Immunol.* 20, 515–516. doi: 10.1038/s41577-020-0407-1

Lage, S. L., Pinheiro Amaral, E., Hilligan, K. L., Laidlaw, E., Rupert, A., Namasivayan, S., et al. (2022). Persistent oxidative stress and Inflammasome activation in $CD14^{high}CD16^{-}$ monocytes from COVID-19 patients. *Front. Immunol.* 12:799558. doi: 10.3389/fimmu.2021.799558

Lambeth, J. D. (2004). NOX enzymes and the biology of reactive oxygen. *Nat. Rev. Immunol.* 4, 181–189. doi: 10.1038/nri1312

Lands, L. C., Grey, V. L., and Smountas, A. A. (1999). Effect of supplementation with a cysteine donor on muscular performance. *J. Appl. Physiol.* 87, 1381–1385. doi: 10.1152/jappl.1999.87.4.1381

Lee, C. (2018). Therapeutic modulation of virus-induced oxidative stress via the Nrf 2-dependent antioxidative pathway. *Oxidative Med. Cell. Longev.* 2018:6208067. doi: 10.1155/2018/6208067

Lee, A. J., and Ashkar, A. A. (2018). The dual nature of type I and type II interferons. *Front. Immunol.* 9:2061. doi: 10.3389/fimmu.2018.02061

Levring, T. B., Kongsbak, M., Rode, A. K. O., Woetmann, A., Ødum, N., Menné Bonefeld, C., et al. (2015). Human CD4+ T cells require exogenous cystine for glutathione and DNA synthesis. *Oncotarget* 6, 21853–21864. doi: 10.18632/oncotarget.5213

Lewis, K. N., Mele, J., Hayes, J. D., and Buffenstein, R. (2010). Nrf 2, a guardian of healthspan and gatekeeper of species longevity. *Integ. Comp. Biol.* 50, 829–843. doi: 10.1093/icb/icq034

Li, C.-X., Gao, J., Zhang, Z., Chen, L., Li, X., Zhou, M., et al. (2022). Multiomics integration-based molecular characterizations of COVID-19. *Brief. Bioinform.* 23:bbab 485. doi: 10.1093/bib/bbab485

Li, X., Jiang, S., and Tapping, R. I. (2010). Toll-like receptor signaling in cell proliferation and survival. *Cytokine* 49, 1–9. doi: 10.1016/j.cyto.2009.08.010

Li, S., Zhao, F., Ye, J., Li, K., Wang, Q., Du, Z., et al. (2022). Cellular metabolic basis of altered immunity in the lungs of patients with COVID-19. *Med. Microbiol. Immunol.* 211, 49–69. doi: 10.1007/s00430-021-00727-0

Lin, Y., Xu, Y., and Zhang, Z. (2020). Sepsis-induced myocardial dysfunction (SIMD): the pathophysiological mechanisms and therapeutic strategies targeting mitochondria. *Inflammation* 43, 1184–1200. doi: 10.1007/s10753-020-01233-w

Lin, C.-Y., and Yao, C.-A. (2020). Potential role of Nrf 2 activators with dual antiviral and anti-inflammatory properties in the management of viral pneumonia. *Infect. Drug Resist.* 13, 1735–1741. doi: 10.2147/IDR.S256773

Linani, A., Benarous, K., Bou-Salah, L., Yousfi, M., and Goumri-Said, S. (2022). Exploring structural mechanism of COVID-19 treatment with glutathione as a potential peptide inhibitor to the Main protease: molecular dynamics simulation and MM/PBSA free energy calculations study. *Int. J. Pept. Res. Ther.* 28:55. doi: 10.1007/s10989-022-10365-6

Litvack, M. L., and Palaniyar, N. (2010). Review: soluble innate immune pattern-recognition proteins for clearing dying cells and cellular components: implications on exacerbating or resolving inflammation. *Innate Immun.* 16, 191–200. doi: 10.1177/1753425910369271

Liu, M., Jeong, E.-M., Liu, H., Xie, A., So, E. Y., Shi, G., et al. (2019). Magnesium supplementation improves diabetic mitochondrial and cardiac diastolic function. *JCI Insight* 4:e123182. doi: 10.1172/jci.insight.123182

Liu, Z., Ren, Z., Zhang, J., Chuang, C.-C., Kandaswamy, E., Zhou, T., et al. (2018). Role of ROS and Nutritional antioxidants in human diseases. *Front. Physiol.* 9:477. doi: 10.3389/fphys.2018.00477

Lu, S. C. (2013). Glutathione synthesis. *Biochim. Biophys. Acta* 1830, 3143–3153. doi: 10.1016/j.bbagen.2012.09.008

Luan, Y.-y., Yin, C.-h., and Yao, Y.-m. (2021). Update advances on C-reactive protein in COVID-19 and other viral infections. *Front. Immunol.* 12:720363. doi: 10.3389/fimmu.2021.720363

Lushchak, V. I. (2012). Glutathione homeostasis and functions: potential targets for medical interventions. *J. Amino Acids* 2012:736837. doi: 10.1155/2012/736837

Lv, J., Wang, Z., Qu, Y., Zhu, H., Zhu, Q., Tong, W., et al. (2021). Distinct uptake, amplification, and release of SARS-CoV-2 by M1 and M2 alveolar macrophages. *Cell Discov.* 7:24. doi: 10.1038/s41421-021-00258-1

Magnani, H. N. (2021). Rationale for the role of heparin and related GAG Antithrombotics in COVID-19 infection. *Clin. Appl. Thromb. Hemost.* 27:1076029620977702. doi: 10.1177/1076029620977702

Maher, P. (2005). The effects of stress and aging on glutathione metabolism. *Ageing Res. Rev.* 4, 288–314. doi: 10.1016/j.arr.2005.02.005

Mahn, A., and Castillo, A. (2021). Potential of Sulforaphane as a natural immune system enhancer: a review. *Molecules* 26:752. doi: 10.3390/molecules26030752

Manik, M., and Singh, R. K. (2022). Role of toll-like receptors in modulation of cytokine storm signaling in SARS-CoV-2-induced COVID-19. *J. Med. Virol.* 94, 869–877. doi: 10.1002/jmv.27405

Marí, M., de Gregorio, E., de Dios, C., Roca-Agujetas, V., Cucarull, B., Tutusaus, A., et al. (2020). Mitochondrial glutathione: recent insights and role in disease. *Antioxidants* 9:909. doi: 10.3390/antiox9100909

Markov, P. V., Katzourakis, A., and Stilianakis, N. I. (2022). Antigenic evolution will lead to new SARS-CoV-2 variants with unpredictable severity. *Nat. Rev. Microbiol.* 20, 251–252. doi: 10.1038/s41579-022-00722-z

Martinez, S. S., Huang, Y., Acuna, L., Laverde, E., Trujillo, D., Barbieri, M. A., et al. (2022). Role of selenium in viral infections with a major focus on SARS-CoV-2. *Int. J. Mol. Sci.* 23:280. doi: 10.3390/ijms23010280

Matthay, M. A., and Zemans, R. L. (2011). The acute respiratory distress syndrome: pathogenesis and treatment. *Annu. Rev. Pathol. Mech. Dis.* 6, 147–163. doi: 10.1146/annurev-pathol-011110-130158

Matuz-Mares, D., Riveros-Rosas, H., Vilchis-Landeros, M. M., and Vázquez-Meza, H. (2021). Glutathione participation in the prevention of cardiovascular diseases. *Antioxidants* 10:1220. doi: 10.3390/antiox10081220

McCarty, M. F., and DiNicolantonio, J. J. (2015). An increased need for dietary cysteine in support of glutathione synthesis may underlie the increased risk for mortality associated with low protein intake in the elderly. *Age* 37:96. doi: 10.1007/s11357-015-9823-8

McClure, R., and Massari, P. (2014). TLR-dependent human mucosal epithelial cell responses to microbial pathogens. *Front. Immunol.* 5:386. doi: 10.3389/fimmu.2014.00386

McCord, J. M., Hybertson, B. M., Cota-Gomez, A., Geraci, K. P., and Gao, B. (2020). Nrf 2 activator PB125® as a potential therapeutic agent against COVID-19. *Antioxidants* 9:518. doi: 10.3390/antiox9060518

Meftahi, G. H., Bahari, Z., Jangravi, Z., and Iman, M. (2021). A vicious circle between oxidative stress and cytokine storm in acute respiratory distress syndrome pathogenesis at COVID-19 infection. *Ukr. Biochem. J.* 93, 18–29. doi: 10.15407/ubj93.01.018

Mehta, P., McAuley, D. F., Brown, M., Sanchez, E., Tattersall, R. S., and Manson, J. J. (2020). HLH across Speciality collaboration, UK. COVID-19: consider cytokine storm syndromes and immunosuppression. *Lancet* 395, 1033–1034. doi: 10.1016/S0140-6736(20)30628-0

Meister, A., and Anderson, M. E. (1983). Glutathione. *Annu. Rev. Biochem.* 52, 711–760. doi: 10.1146/annurev.bi.52.070183.003431

Minich, D. M., and Brown, B. I. (2019). A review of dietary (phyto) nutrients for glutathione support. *Nutrients* 11:2073. doi: 10.3390/nu11092073

Miripour, Z. S., Sarrami-Forooshani, R., Sanati, H., Makarem, J., Taheri, M. S., Shojaeian, F., et al. (2020). Real-time diagnosis of reactive oxygen species (ROS) in fresh sputum by electrochemical tracing; correlation between COVID-19 and viral-induced ROS in lung/respiratory epithelium during this pandemic. *Biosens. Bioelectron.* 165:112435. doi: 10.1016/j.bios.2020.112435

Mittal, M., Siddiqui, M. R., Tran, K., Reddy, S. P., and Malik, A. B. (2014). Reactive oxygen species in inflammation and tissue injury. *Antiox Redox Signal* 20, 1126–1167. doi: 10.1089/ars.2012.5149

Mohammadi, H., Shamshirian, A., Eslami, S., Shamshirian, D., and Ebrahimzadeh, M. A. (2020). Magnesium sulfate attenuates lethality and oxidative damage induced by different models of hypoxia in mice. *Bio Med. Res. Int.* 2020, 1–8. doi: 10.1155/2020/2624734

Moore, J. B., and June, C. H. (2020). Cytokine release syndrome in severe COVID-19. Lessons from arthritis and cell therapy in cancer patients point to therapy for severe disease. *Science* 368, 473–474. doi: 10.1126/science.abb8925

Moro-García, M. A., Mayo, J. C., Sainz, R. M., and Alonso-Arias, R. (2018). Influence of inflammation in the process of T lymphocyte differentiation: proliferative, metabolic, and oxidative changes. *Front. Immunol.* 9:339. doi: 10.3389/fimmu.2018.00339

Morris, D., Khurasany, M., Nguyen, T., Kim, J., Guilford, F., Mehta, R., et al. (2013). Glutathione and infection. *Biochim. Biophys. Acta* 1830, 3329–3349. doi: 10.1016/j.bbagen.2012.10.012

Mosquera-Sulbaran, J. A., Pedreañez, A., Carrero, Y., and Callejas, D. (2021). C-reactive protein as an effector molecule in Covid-19 pathogenesis. *Rev. Med. Virol.* 31:e2221. doi: 10.1002/rmv.2221

Murae, M., Shimizu, Y., Yamamoto, Y., Kobayashi, A., Houri, M., Inoue, T., et al. (2022). The function of SARS-CoV-2 spike protein is impaired by disulfide-bond disruption with mutation at cysteine-488 and by thiol-reactive N-acetyl-cysteine and glutathione. *Biochem. Biophys. Res. Commun.* 597, 30–36. doi: 10.1016/j.bbrc.2022.01.106

Muri, J., and Kopf, M. (2021). Redox regulation of immunometabolism. *Nat. Rev. Immunol.* 21, 363–381. doi: 10.1038/s41577-020-00478-8

Netea, M. G., Giamarellos-Bourboulis, E. J., Domínguez-Andrés, J., Curtis, N., van Crevel, R., van de Veerdonk, F. L., et al. (2020). Trained immunity: a tool for reducing susceptibility to and the severity of SARS-CoV-2 infection. *Cells* 181, 969–977. doi: 10.1016/j.cell.2020.04.042

Ng, H., Havervall, S., Rosell, A., Aguilera, K., Parv, K., von Meijenfeldt, F. A., et al. (2021). Circulating markers of neutrophil extracellular traps are of prognostic value in patients with COVID-19. *Arterioscler. Thromb. Vasc. Biol.* 41, 988–994. doi: 10.1161/ATVBAHA.120.315267

Notz, Q., Herrmann, J., Schlesinger, T., Helmer, P., Sudowe, S., Sun, Q., et al. (2021). Clinical significance of micronutrient supplementation in critically ill COVID-19 patients with severe ARDS. *Nutrients* 13:2113. doi: 10.3390/nu13062113

O'Driscoll, M., Ribeiro Dos Santos, G., Wang, L., Cummings, D. A. T., Anzman, A. S., Paireau, J., et al. (2021). Age-specific mortality and immunity patterns of SARS-CoV-2. *Nature* 590, 140–145. doi: 10.1038/s41586-020-2918-0

Obayan, A. O. E. (2021). Overview of the rationale for L-glutamine treatment in moderate-severe COVID-19 infection. *J. Infect. Dis. Epidemiol.* 7:187. doi: 10.23937/2474-3658/1510187

Olagnier, D., Farahani, E., Thyrsted, J., Blay-Cadanet, J., Herengt, A., Idorn, M., et al. (2020). SARS-CoV2 mediated suppression of NRF2-signaling reveals potent antiviral and anti-inflammatory activity of 4-octyl-itaconate and dimethyl fumarate. *Nat. Commun.* 11:4938. doi: 10.1038/s41467-020-18764-3

Olejnik, J., Hume, A. J., and Mühlberger, E. (2018). Toll-like receptor 4 in acute viral infection: too much of a good thing. *PLoS Pathog.* 14:e1007390. doi: 10.1371/journal.ppat.1007390

Onofrio, L., Caraglia, M., Facchini, G., Margherita, V., De Placido, S., and Buonerba, C. (2020). Toll-like receptors and COVID-19: a two-faced story with an exciting ending. *Future Sci. OA* 6:FSO605. doi: 10.2144/fsoa-2020-0091

Ordonez, A. A., Bullen, C. K., Villabona-Rueda, A. F., Thompson, E. A., Turner, M. L., Merino, V. F., et al. (2022). Sulforaphane exhibits antiviral activity against pandemic SARS-CoV-2 and seasonal HCoV-OC43 coronaviruses in vitro and in mice. *Commun. Biol.* 5:242. doi: 10.1038/s42003-022-03189-z

Ouwendijk, W. J. D., Raadsen, M. P., van Kampen, J. J. A., Verdijk, R. M., von der Thusen, J. H., Guo, L., et al. (2021). High levels of neutrophil extracellular traps persist in the lower respiratory tract of critically ill patients with coronavirus disease 2019. *J. Infect. Dis.* 223, 1512–1521. doi: 10.1093/infdis/jiab050

Pallardó, F. V., Markovic, J., García, J. L., and Viña, J. (2009). Role of nuclear glutathione as a key regulator of cell proliferation. *Mol. Asp. Med.* 30, 77–85. doi: 10.1016/j.mam.2009.01.001

Paludan, S. R., and Mogensen, T. H. (2022). Innate immunological pathways in COVID-19 pathogenesis. *Sci Immunol* 7:eabm5505. doi: 10.1126/sciimmunol.abm5505

Panday, A., Sahoo, M. K., Osorio, D., and Batra, S. (2015). NADPH oxidases: an overview from structure to innate immunity-associated pathologies. *Cell. Mol. Immunol.* 12, 5–23. doi: 10.1038/cmi.2014.89

Pedre, B., Barayeu, U., Ezeriņa, D., and Dick, T. P. (2021). The mechanism of action of N-acetylcysteine (NAC): the emerging role of H2S and sulfane sulfur species. *Pharmacol. Ther.* 228:107916. doi: 10.1016/j.pharmthera.2021.107916

Pérez de la Lastra, J. M., Andrés-Juan, C., Plou, F. J., and Pérez-Lebeña, E. (2021). Impact of zinc, glutathione, and polyphenols as antioxidants in the immune response against SARS-CoV-2. *PRO* 9:506. doi: 10.3390/pr9030506

Perła-Kaján, J., and Jakubowski, H. (2022). COVID-19 and one-carbon metabolism. *Int. J. Mol. Sci.* 23:4181. doi: 10.3390/ijms23084181

Phua, J., Weng, L., Ling, L., Egi, M., Lim, C.-M., Divatia, J. V., et al. (2020). Intensive care management of coronavirus disease 2019 (COVID-19): challenges and recommendations. *Lancet Respir. Med.* 8, 506–517. doi: 10.1016/S2213-2600(20)30161-2

Poe, F. L., and Corn, J. (2020). N-Acetylcysteine: a potential therapeutic agent for SARS-CoV-2. *Med. Hypotheses* 143:109862. doi: 10.1016/j.mehy.2020.109862

Poljsak, B., Šuput, D., and Milisav, I. (2013). Achieving the balance between ROS and Antioxidants: when to use the synthetic Antioxidants. *Oxidative Med. Cell. Longev.* 2013:956792. doi: 10.1155/2013/956792

Polonikov, A. (2020). Endogenous deficiency of glutathione as the most likely cause of serious manifestations and death in COVID-19 patients. *ACS Infect. Dis.* 6, 1558–1562. doi: 10.1021/acsinfecdis.0c00288

Potempa, L. A., Rajab, I. M., Hart, P. C., Bordon, J., and Fernandez-Botran, R. (2020). Insights into the use of C-reactive protein as a diagnostic index of disease severity in COVID-19 infections. *Am. J. Trop. Med. Hyg.* 103, 561–563. doi: 10.4269/ajtmh.20-0473

Proal, A. D., and Van Elzakker, M. B. (2021). Long COVID or post-acute Sequelae of COVID-19 (PASC): an overview of biological factors that may contribute to persistent symptoms. *Front. Microbiol.* 12:698169. doi: 10.3389/fmicb.2021.698169

Pushpakumar, S., Ren, L., Kundu, S., Gamon, A., Tyagi, S. C., and Sen, U. (2017). Toll-like receptor 4 deficiency reduces oxidative stress and macrophage mediated inflammation in hypertensive kidney. *Sci. Rep.* 7:6349. doi: 10.1038/s41598-017-06484-6

Quan, C., Li, C., Ma, H., Li, Y., and Zhang, H. (2021). Immunopathogenesis of coronavirus induced acute respiratory distress syndrome (ARDS): potential infection-associated hemophagocytic lymphohistiocytosis. *Clin. Microbiol. Rev.* 34, e00074–e00020. doi: 10.1128/CMR.00074-20

Radtke, K. K., Coles, L. D., Mishra, U., Orchard, P. J., Holmay, M., and Cloyd, J. C. (2012). Interaction of n-acetylcysteine and cysteine in human plasma. *J. Pharm. Sci.* 101, 4653–4659. doi: 10.1002/jps.23325

Raftos, J. E., Whillier, S., Chapman, B. E., and Kuchel, P. W. (2007). Kinetics of uptake and deacetylation of N-acetylcysteine by human erythrocytes. *Int. J. Biochem. Cell Biol.* 39, 1698–1706. doi: 10.1016/j.biocel.2007.04.014

Rahman, I., and MacNee, N. W. (2000). Oxidative stress and regulation of glutathione in lung inflammation. *Eur. Respir. J.* 16:534. doi: 10.1034/j.1399-3003.2000.016003534.x

Ringel, J., Ramlow, A., Bock, C., and Sheriff, A. (2021). Case report: C-reactive protein apheresis in a patient with COVID-19 and fulminant CRP increase. *Front. Immunol.* 12:708101. doi: 10.3389/fimmu.2021.708101

Robbiani, D. F., Gaebler, C., Muecksch, F., Lorenzi, J. C. C., Wang, Z., Cho, A., et al. (2020). Convergent antibody responses to SARS-CoV-2 in convalescent individuals. *Nature* 584, 437–442. doi: 10.1038/s41586-020-2456-9

Robledinos-Antón, N., Fernández-Ginés, R., Manda, G., and Cuadrado, A. (2019). Activators and inhibitors of NRF2: a review of their potential for clinical development. *Oxid. Med. Cell Long* 2019:9372182. doi: 10.1155/2019/9372182

Rodrigues, P. R. S., Alrubayyi, A., Pring, E., Bart, V. M. T., Jones, R., Coveney, C., et al. (2020). Innate immunology in COVID-19—a living review. Part II: dysregulated inflammation drives immunopathology. *Oxford Open Immunol.* 1:iqaa005. doi: 10.1093/oxfimm/iqaa005

Ruan, Q., Yang, K., Wang, W., Jiang, L., and Song, J. (2020). Clinical predictors of mortality due to COVID-19 based on an analysis of data of 150 patients from Wuhan, China. *Intensive Care Med.* 46, 846–848. doi: 10.1007/s00134-020-05991-x

Rushworth, G. F., and Megson, I. L. (2014). Existing and potential therapeutic uses for N-acetylcysteine: the need for conversion to intracellular glutathione for antioxidant benefits. *Pharmacol. Ther.* 141, 150–159. doi: 10.1016/j.pharmthera.2013.09.006

Ryu, G., and Shin, H.-W. (2021). SARS-CoV-2 infection of airway epithelial cells. *Immune Netw* 21:e3. doi: 10.4110/in.2021.21.e3

Saadat, M. (2020). An evidence for correlation between the glutathione S-transferase T1 (GSTT1) polymorphism and outcome of COVID-19. *Clin. Chim. Acta* 508, 213–216. doi: 10.1016/j.cca.2020.05.041

Sallenave, J.-M., and Guillot, L. (2020). Innate immune signaling and proteolytic pathways in the resolution or exacerbation of SARS-CoV-2 in Covid-19: key therapeutic targets? *Front. Immunol.* 11:1229. doi: 10.3389/fimmu.2020.01229

Samiec, P., Drews-Botsch, C., Flagg, E., Kurtz, J., Sternberg, J., Reed, R., et al. (1998). Glutathione in human plasma: decline in association with aging, age-related macular degeneration, and diabetes. *Free Radic. Biol. Med.* 24, 699–704. doi: 10.1016/s0891-5849(97)00286-4

Santos Duarte Lana, J. F., Santos Duarte Lana, A. V., Souza Rodrigues, Q., Silva Santos, G., Navani, R., Navani, A., et al. (2021). Nebulization of glutathione and N-Acetylcysteine as an adjuvant therapy for COVID-19 onset. *Adv. Redox Res.* 3:100015. doi: 10.1016/j.arres.2021.100015

Sariol, A., and Perlman, S. (2021). SARS-CoV-2 takes its toll. *Nat. Immunol.* 22, 801–802. doi: 10.1038/s41590-021-00962-w

Sartorius, R., Trovato, M., Manco, R., D'Apice, L., and De Berardinis, P. (2021). Exploiting viral sensing mediated by toll-like receptors to design innovative vaccines. *NPJ Vaccines* 6:127. doi: 10.1038/s41541-021-00391-8

Sasai, M., and Yamamoto, M. (2013). Pathogen recognition receptors: ligands and signaling pathways by toll-like receptors. *Int. Rev. Immunol.* 32, 116–133. doi: 10.3109/08830185.2013.774391

Sastre, J., Pallardo, F. V., and Viña, J. (2005). Glutathione. *Handb Environ. Chem.* 2, 91–108. doi: 10.1007/b101148

Schattner, M. (2019). Platelet TLR4 at the crossroads of thrombosis and the innate immune response. *J. Leukoc. Biol.* 105, 873–880. doi: 10.1002/JLB.MR0618-213R

Schieber, M., and Chandel, N. S. (2014). ROS function in redox signaling and oxidative stress. *Curr. Biol.* 24, R453–R462. doi: 10.1016/j.cub.2014.03.034

Schmidlin, C. J., Dodson, M. B., Madhavan, L., and Zhang, D. D. (2019). Redox regulation by NRF2 in aging and disease. *Free Rad. Biol. Med.* 134, 702–707. doi: 10.1016/j.freeradbiomed.2019.01.016

Schmitt, B., Vicenzi, M., Garrel, C., and Denis, F. M. (2015). Effects of N-acetylcysteine, oral glutathione (GSH) and a novel sublingual form of GSH on oxidative stress markers: a comparative crossover study. *Redox Biol.* 6, 198–205. doi: 10.1016/j.redox.2015.07.012

Schurink, B., Roos, E., Radonic, T., Barbe, E., Bouman, C. S. C., de Boer, H. H., et al. (2020). Viral presence and immunopathology in patients with lethal COVID-19: a prospective autopsy cohort study. *Lancet Microbe* 1, e290–e299. doi: 10.1016/S2666-5247(20)30144-0

Schwalfenberg, G. K. (2021). N-Acetylcysteine: a review of clinical usefulness (an old drug with new tricks). *J. Nutr. Metab.* 2021:9949453. doi: 10.1155/2021/9949453

Scirè, A., Cianfruglia, L., Minnelli, C., Bartolini, D., Torquato, P., Principato, G., et al. (2019). Glutathione compartmentalization and its role in glutathionylation and other regulatory processes of cellular pathways. *Biofactors* 45, 152–168. doi: 10.1002/biof.1476

Seale, L. A., Torres, D. J., Berry, M. J., and Pitts, M. W. (2020). A role for selenium-dependent GPX1 in SARS-CoV-2 virulence. *Am. J. Clin. Nutr.* 112, 447–448. doi: 10.1093/ajcn/nqaa177

Sekhar, R. V., McKay, S. V., Patel, S. G., Guthikonda, A. P., Reddy, V. T., Balasubramanyam, A., et al. (2011a). Glutathione synthesis is diminished in patients with uncontrolled diabetes and restored by dietary supplementation with cysteine and glycine. *Diabetes Care* 34, 162–167. doi: 10.2337/dc10-1006

Sekhar, R. V., Patel, S. G., Guthikonda, A. P., Reid, M., Balasubramanyam, A., Taffet, G. E., et al. (2011b). Deficient synthesis of glutathione underlies oxidative stress in aging and can be corrected by dietary cysteine and glycine supplementation. *Am. J. Clin. Nutr.* 94, 847–853. doi: 10.3945/ajcn.110.003483

Sestili, P., and Fimognari, C. (2020). Paracetamol-induced glutathione consumption: is there a link with severe COVID-19 illness? *Front. Pharmacol.* 11:579944. doi: 10.3389/fphar.2020.579944

Sharifi-Rad, M., Kumar, N. V. A., Zucca, P., Varoni, E. M., Dini, L., Panzarini, E., et al. (2020). Lifestyle, oxidative stress, and antioxidants: back and forth in the pathophysiology of chronic diseases. *Front. Physiol.* 11:694. doi: 10.3389/fphys.2020.00694

Sharma, A., Tiwari, S., Deb, M. K., and Marty, J. L. (2020). Severe acute respiratory syndrome coronavirus-2 (SARS-CoV-2): a global pandemic and treatment strategies. *Int. J. Antimicrob. Agents* 56:106054. doi: 10.1016/j.ijantimicag.2020.106054

Shyer, J. A., Flavell, R. A., and Bailis, W. (2020). Metabolic signaling in T cells. *Cell Res.* 30, 649–659. doi: 10.1038/s41422-020-0379-5

Sies, H. (2015). Oxidative stress: impact in redox biology and medicine. *Arch. Med. Biomed. Res.* 2, 146–150. doi: 10.4314/ambr.v2i4.6

Silvagno, F., Vernone, A., and Pescarmona, G. P. (2020). The role of glutathione in protecting against the severe inflammatory response triggered by COVID-19. *Antioxidants* 9:624. doi: 10.3390/antiox9070624

Sims, A. C., Tilton, S. C., Menachery, V. D., Gralinski, L. E., Schäfer, A., Matzke, M. M., et al. (2013). Release of severe acute respiratory syndrome coronavirus nuclear import block enhances host transcription in human lung cells. *J. Virol.* 87, 3885–3902. doi: 10.1128/JVI.02520-12

Singh, M., Barrera Adame, O., Nickas, M., Robison, J., Khatchadourian, C., and Venketaraman, V. (2022). Type 2 diabetes contributes to altered adaptive immune responses and vascular inflammation in patients with SARS-CoV-2 infection. *Front. Immunol.* 13:833355. doi: 10.3389/fimmu.2022.833355

Sinha, R., Sinha, I., Calcagnotto, A., Trushin, N., Haley, J. S., Schell, T. D., et al. (2018). Oral supplementation with liposomal glutathione elevates body stores of glutathione and markers of immune function. *Eur. J. Clin. Nutr.* 72, 105–111. doi: 10.1038/ejcn.2017.132

Soto, M. E., Guarner-Lans, V., Díaz-Díaz, E., Manzano-Pech, L., Palacios-Chavarría, A., Valdez-Vázquez, R. R., et al. (2022). Hyperglycemia and loss of redox homeostasis in COVID-19 patients. *Cells* 11:932. doi: 10.3390/cells11060932

Souza-Fernandes, A. B., Pelosi, P., and Rocco, P. R. M. (2006). Bench-to-bedside review: the role of glycosaminoglycans in respiratory disease. *Crit. Care* 10:237. doi: 10.1186/cc5069

Stenmark, K. R., Frid, M. G., Gerasimovskaya, E., Zhang, H., McCarthy, M. K., Thurman, J. M., et al. (2021). Mechanisms of SARS-CoV-2-induced lung vascular disease: potential role of complement. *Pulm. Circ.* 11:20458940211015799. doi: 10.1177/20458940211015799

Suhail, S., Zajac, J., Fossum, C., Lowater, H., McCracken, C., Severson, N., et al. (2020). Role of oxidative stress on SARS-CoV (SARS) and SARS-CoV-2 (COVID-19) infection: a review. *Protein J.* 39, 644–656. doi: 10.1007/s10930-020-09935-8

Tan, B. L., Norhaizan, M. E., Liew, W.-P.-P., and Rahman, H. S. (2018). Antioxidant and oxidative stress: a mutual interplay in age-related diseases. *Front. Pharmacol.* 9:1162. doi: 10.3389/fphar.2018.01162

Tan, H.-Y., Wang, N., Li, S., Hong, M., Wang, X., and Feng, Y. (2016). The reactive oxygen species in macrophage polarization: reflecting its dual role in progression and treatment of human diseases. *Oxidative Med. Cell. Longev.* 2016:2795090. doi: 10.1155/2016/2795090

Tang, C.-F., Ding, H., Jiao, R.-Q., Wu, X.-X., and Kong, L.-D. (2020). Possibility of magnesium supplementation for supportive treatment in patients with COVID-19. *Eur. J. Pharmacol.* 886:173546. doi: 10.1016/j.ejphar.2020.173546

Tang, Z., Song, T., and Su, H.-X. (2011). Effects of reduced glutathione on plasma levels of C-reactive protein in elderly patients with acute cerebral infarction. *J. Shanghai Jiaotong Univ. (Med. Sci.)* 31, 1489–1491. doi: 10.3969/j.issn.1674-8115.2011.10.029

Taoufik, Y., de Goër de Herve, M.-G., Corgnac, S., Durrbach, A., and Mami-Chouaib, F. (2021). When immunity kills: the lessons of SARS-CoV-2 outbreak. *Front. Immunol.* 12:692598. doi: 10.3389/fimmu.2021.6

Taylor, E. W., and Radding, W. (2020). Understanding selenium and glutathione as antiviral factors in COVID-19: does the viral M^{pro} protease target host Selenoproteins and glutathione synthesis? *Front. Nutr.* 7:143. doi: 10.3389/fnut.2020.00143

Teuwen, L.-A., Geldhof, V., Pasut, A., and Carmeliet, P. (2020). COVID-19: the vasculature unleashed. *Nat. Rev. Immunol.* 20, 389–391. doi: 10.1038/s41577-020-0343-0

The New York Times (2022). *The coronavirus pandemic. Coronavirus World Map: Tracking the Global Outbreak. Covid-19 World Map: Cases, Deaths and Global Trends*. Available at https://www.nytimes.com

Theodore, M., Kawai, Y., Yang, J., Kleshchenko, Y., Reddy, S. P., Villalta, F., et al. (2008). Multiple nuclear localization signals function in the nuclear import of the transcription factor Nrf 2. *J. Biol. Chem.* 283, 8984–8994. doi: 10.1074/jbc.M709040200

Thorley, A. J., Grandolfo, D., Lim, E., Goldstraw, P., Young, A., and Tetley, T. D. (2011). Innate immune responses to bacterial ligands in the peripheral human lung–role of alveolar epithelial TLR expression and Signalling. *PLoS One* 6:e21827. doi: 10.1371/journal.pone.0021827

To, K., Cao, R., Yegiazaryan, A., Owens, J., Nguyen, T., Sasaninia, K., et al. (2021). Effects of oral liposomal glutathione in altering the immune responses against mycobacterium tuberculosis and the Mycobacterium bovis BCG strain in individuals with type 2 diabetes. *Front. Cell. Infect. Microbiol.* 11:657775. doi: 10.3389/fcimb.2021.657775

Torzewski, J., Heigl, F., Zimmermann, O., Wagner, F., Schumann, C., Hettich, R., et al. (2020). First-in-man: case report of selective C-reactive protein apheresis in a patient with SARS-CoV-2 infection. *Am. J. Case Rep.* 21:e925020. doi: 10.12659/AJCR.925020

Townsend, D. M., Tew, K. D., and Tapiero, H. (2003). The importance of glutathione in human disease. *Biomed. Pharmacother.* 57, 145–155. doi: 10.1016/s0753-3322(03)00043-x

Trachootham, D., Lu, W., Ogasawara, M. A., Rivera-Del Valle, N., and Huang, P. (2008). Redox regulation of cell survival. *Antiox Redox Signal* 10, 1343–1374. doi: 10.1089/ars.2007.1957

Trapani, V., Rosanoff, A., Baniasadi, S., Barbagallo, M., Castiglioni, S., Guerrero-Romero, F., et al. (2022). The relevance of magnesium homeostasis in COVID-19. *Eur. J. Nutr.* 61, 625–636. doi: 10.1007/s00394-021-02704-y

Trougakos, I. P., Stamatelopoulos, K., Terpos, E., Tsitsilonis, O. E., Aivalioti, E., Paraskevis, D., et al. (2021). Insights to SARS-CoV-2 life cycle, pathophysiology, and

rationalized treatments that target COVID-19 clinical complications. *J. Biomed. Sci.* 28:9. doi: 10.1186/s12929-020-00703-5

Tu, W., Wang, H., Li, S., Liu, Q., and Sha, H. (2019). The anti-inflammatory and anti-oxidant mechanisms of the Keap 1/Nrf 2/ARE signaling pathway in chronic diseases. *Aging Dis.* 10, 637–651. doi: 10.14336/AD.2018.0513

Tufan, E., Göksun Sivas, G., Gürel-Gökmen, B., Yılmaz-Karaoğlu, S., Ercan, D., Özbeyli, D., et al. (2022). Inhibitory effect of whey protein concentrate on SARS-CoV-2-targeted furin activity and spike protein-ACE2 binding in methotrexate-induced lung damage. *J. Food Biochem.* 46:e14039. doi: 10.1111/jfbc.14039

Ulrich, K., and Jakob, U. (2019). The role of thiols in antioxidant systems. *Free Radic. Biol. Med.* 140, 14–27. doi: 10.1016/j.freeradbiomed.2019.05.035

Valdés, A., Ortega Moreno, L., Rojo Rello, S., Orduña, A., Bernardo, D., and Cifuentes, A. (2022). Metabolomics study of COVID-19 patients in four different clinical stages. *Sci. Rep.* 12:1650. doi: 10.1038/s41598-022-05667-0

Valko, M., Leibfritz, D., Moncol, J., Cronin, M. T. D., Mazur, M., and Telser, J. (2007). Free radicals and antioxidants in normal physiological functions and human disease. *Int. J. Biochem. Cell Biol.* 39, 44–84. doi: 10.1016/j.biocel.2006.07.001

Veras, F. P., Pontelli, M. C., Silva, C. M., Toller-Kawahisa, J. E., de Lima, M., Nascimento, D. C., et al. (2020). SARS-CoV-2-triggered neutrophil extracellular traps mediate COVID-19 pathology. *J. Exp. Med.* 217:e20201129. doi: 10.1084/jem.20201129

Vinciguerra, M., Romiti, S., Fattouch, K., De Bellis, A., and Greco, E. (2020). Atherosclerosis as pathogenetic substrate for Sars-Cov 2 cytokine storm. *J. Clin. Med.* 9:2095. doi: 10.3390/jcm9072095

Wang, S., Li, Z., Wang, X., Zhang, S., Gao, P., and Shi, Z. (2021a). The role of pulmonary surfactants in the treatment of acute respiratory distress syndrome in COVID-19. *Front. Pharmacol.* 12:698905. doi: 10.3389/fphar.2021.698905

Wang, S., Sheng, Y., Tu, J., and Zhang, L. (2021b). Association between peripheral lymphocyte count and the mortality risk of COVID-19 inpatients. *BMC Pulm. Med.* 21:55. doi: 10.1186/s12890-021-01422-9

West, A. P., Brodsky, I. E., Rahner, C., Woo, D. K., Erdjument-Bromage, H., Tempst, P., et al. (2011). TLR signalling augments macrophage bactericidal activity through mitochondrial ROS. *Nature* 472, 476–480. doi: 10.1038/nature09973

Whillier, S., Raftos, J. E., Chapman, B., and Kuchel, P. W. (2009). Role of N-acetylcysteine and cystine in glutathione synthesis in human erythrocytes. *Redox Rep.* 14, 115–124. doi: 10.1179/135100009X392539

Williams, B. (2021). Renin angiotensin system inhibition as treatment for Covid-19? *EClinicalMedicine* 37:101023. doi: 10.1016/j.eclinm.2021.101023

Wong, K. K., Lee, S. W. H., and Kua, K. P. (2021). N-Acetylcysteine as adjuvant therapy for COVID-19 – a perspective on the current state of the evidence. *J. Inflamm. Res.* 14, 2993–3013. doi: 10.2147/JIR.S306849

Yamamoto, M., Kensler, T. W., and Motohashi, H. (2018). The Keap 1-Nrf 2 system: a thiol-based sensor-effector apparatus for maintaining redox homeostasis. *Physiol. Rev.* 98, 1169–1203. doi: 10.1152/physrev.00023.2017

Yang, L., Liu, S., Zhang, Z., Wan, X., Huang, B., Chen, Y., et al. (2020). COVID-19: immunopathogenesis and Immunotherapeutics. *Sig. Transduct. Target Ther.* 5:128. doi: 10.1038/s41392-020-00243-2

Yang, X., Yu, Y., Xu, J., Shu, H., Xia An, J., Liu, H., et al. (2020). Clinical course and outcomes of critically ill patients with SARS-CoV-2 pneumonia in Wuhan, China: a single-centered, retrospective, observational study. *Lancet Respir. Med.* 8, 475–481. doi: 10.1016/S2213-2600(20)30079-5

Yang, J., Zheng, Y., Gou, X., Pu, K., Chen, Z., Guo, Q., et al. (2020). Prevalence of comorbidities and its effects in coronavirus disease 2019 patients: a systematic review and meta-analysis. *Int. J. Infect. Dis.* 94, 91–95. doi: 10.1016/j.ijid.2020.03.017

Yuan, S., Jiang, S.-C., Zhang, Z.-W., Fu, Y.-F., Hu, J., and Li, Z.-L. (2021). The role of alveolar edema in COVID-19. *Cells* 10:1897. doi: 10.3390/cells10081897

Zaboli, E., Majidi, H., Alizadeh-Navaei, R., Hedayatizadeh-Omran, A., Asgarian-Omran, H., Larijani, L. V., et al. (2021). Lymphopenia and lung complications in patients with coronavirus disease-2019 (COVID-19): a retrospective study based on clinical data. *J. Med. Virol.* 93, 5425–5431. doi: 10.1002/jmv.27060

Zhang, Y., Geng, X., Tan, Y., Li, Q., Xu, C., Xu, J., et al. (2020). New understanding of the damage of SARS-CoV-2 infection outside the respiratory system. *Biomed. Pharmacother.* 127:110195. doi: 10.1016/j.biopha.2020.110195

Zhang, R., Sun, C., Chen, X., Han, Y., Zang, W., Jiang, C., et al. (2022). COVID-19-related brain injury: the potential role of Ferroptosis. *J. Inflamm. Res.* 15, 2181–2198. doi: 10.2147/JIR.S353467

Zhang, T., Tsutsuki, H., Islam, W., Ono, K., Takeda, K., Akaike, T., et al. (2021). ATP exposure stimulates glutathione efflux as a necessary switch for NLRP3 inflammasome activation. *Redox Biol.* 41:101930. doi: 10.1016/j.redox.2021.101930

Zhang, Q., Xiang, R., Huo, S., Zhou, Y., Jiang, S., Wang, Q., et al. (2021). Molecular mechanism of interaction between SARS-CoV-2 and host cells and interventional therapy. *Sig. Transduct. Target Ther.* 6:233. doi: 10.1038/s41392-021-00653-w

Zhao, C., and Zhao, W. (2020). NLRP3 Inflammasome—a key player in antiviral responses. *Front. Immunol.* 11:211. doi: 10.3389/fimmu.2020.00211

Zhou, F., Yu, T., Du, R., Fan, G., Liu, Y., Liu, Z., et al. (2020). Clinical course and risk factors for mortality of adult inpatients with COVID-19 in Wuhan, China: a retrospective cohort study. *Lancet* 395, 1054–1062. doi: 10.1016/S0140-6736(20)30566-3

Zuo, L., Prather, E. R., Stetskiv, M., Garrison, D. E., Meade, J. R., Peace, T. I., et al. (2019). Inflammaging and oxidative stress in human diseases: from molecular mechanisms to novel treatments. *Int. J. Mol. Sci.* 20:4472. doi: 10.3390/ijms20184472

frontiers | Frontiers in Microbiology

TYPE Original Research
PUBLISHED 11 October 2022
DOI 10.3389/fmicb.2022.1022006

OPEN ACCESS

EDITED BY
Wanbo Tai,
Shenzhen Bay Laboratory, China

REVIEWED BY
Fei Yu,
Hebei Agricultural University, China
Tianlei Ying,
Fudan University, China
Jun Ma,
Shenzhen Bay Laboratory, China
Weijin Huang,
National Institutes for Food and Drug Control, China

*CORRESPONDENCE
Yuxian He
yhe@ipb.pumc.edu.cn

†These authors have contributed equally to this work

SPECIALTY SECTION
This article was submitted to Virology, a section of the journal Frontiers in Microbiology

RECEIVED 18 August 2022
ACCEPTED 30 August 2022
PUBLISHED 11 October 2022

CITATION
Wu T, Zhu Y, Liu N, Hu Y, Chong H and He Y (2022) Resistance profile and mechanism of severe acute respiratory syndrome coronavirus-2 variants to LCB1 inhibitor targeting the spike receptor-binding motif. *Front. Microbiol.* 13:1022006. doi: 10.3389/fmicb.2022.1022006

Resistance profile and mechanism of severe acute respiratory syndrome coronavirus-2 variants to LCB1 inhibitor targeting the spike receptor-binding motif

Tong Wu†, Yuanmei Zhu†, Nian Liu, Yue Hu, Huihui Chong and Yuxian He*

NHC Key Laboratory of Systems Biology of Pathogens, Center for AIDS Research, Institute of Pathogen Biology, Chinese Academy of Medical Sciences and Peking Union Medical College, Beijing, China

LCB1 is a 56-mer miniprotein computationally designed to target the spike (S) receptor-binding motif of SARS-CoV-2 with potent *in vitro* and *in vivo* inhibitory activities. However, the rapid emergence and epidemic of viral variants have greatly impacted the effectiveness of S protein-targeting vaccines and antivirals. In this study, we chemically synthesized a peptide-based LCB1 inhibitor and characterized the resistance profile and underlying mechanism of SARS-CoV-2 variants. Among five variants of concern (VOCs), we found that pseudoviruses of Beta, Gamma, and Omicron were highly resistant to the LCB1 inhibition, whereas the pseudoviruses of Alpha and Delta as well as the variant of interest (VOI) Lambda only caused mild resistance. By generating a group of mutant viruses carrying single or combination mutations, we verified that K417N and N501Y substitutions in RBD critically determined the high resistance phenotype of VOCs. Furthermore, a large panel of 85 pseudoviruses with naturally occurring RBD point-mutations were generated and applied to LCB1, which identified that E406Q, K417N, and L455F conferred high-levels of resistance, when Y505W caused a ~6-fold resistance fold-change. We also showed that the resistance mutations could greatly weaken the binding affinity of LCB1 to RBD and thus attenuated its blocking capacity on the interaction between RBD and the cell receptor ACE2. In conclusion, our data have provided crucial information for understanding the mechanism of SARS-CoV-2 resistance to LCB1 and will guide the design strategy of novel LCB1-based antivirals against divergent VOCs and evolutionary mutants.

KEYWORDS

SARS-CoV-2, variants of concern, entry inhibitor, LCB1, drug resistance

Introduction

Severe acute respiratory syndrome coronavirus-2 (SARS-CoV-2) caused the global pandemic of coronavirus disease 2019 (COVID-19), which has recently resulted in more than 551 million confirmed cases with about 6.4 million deaths.[1] During the spread of the virus, many variants of concern (VOCs) emerged with significantly changed infectivity and pathogenicity, leading to new waves of infection that have posed daunting challenges (Callaway, 2021; Garcia-Beltran et al., 2021; He et al., 2021; Hoffmann et al., 2021; Kuzmina et al., 2021). The previous four VOCs are Alpha (B.1.1.7), Beta (B.1.351), Gamma (P.1), and Delta (B.1.617.2); the fifth one, Omicron (B.1.1.529), was first reported from Southern Africa in late November 2021. Genome-sequencing data indicate that Omicron variant evolves with the largest number of mutations, including 32 mutations located within spike (S) protein that cover the key mutations in the receptor binding domain (RBD) or motif (RBM), such as K417N, E484A, and N501Y (Callaway, 2021; He et al., 2021; Tao et al., 2021; Yamasoba et al., 2022). Significantly, Omicron is highly transmissible and can spread several times faster than any previous variants; thus, it has quickly outcompeted Delta variant to dominate the epidemic, caused a large number of breakthrough infection or re-infection, and seriously impaired the clinical efficacies of preventive vaccines and therapeutic antibodies (He et al., 2021; Guo et al., 2022; Markov et al., 2022).

Since the outbreak of COVID-19, many efforts have been devoted to the development of antivirals that block different steps of SARS-CoV-2 life-cycle, including viral entry, replication, assembly, budding, and releasing (Yang and Rao, 2021; Yan et al., 2022). Notably, virus entry inhibitors that can inhibit the interaction between S protein and the human cellular receptor angiotensin-converting enzyme 2 (ACE2) are considered a promising strategy (Plavec et al., 2021; Sabbah et al., 2021; Xiang et al., 2021). By applying computational *de novo* design approaches, Cao and coworkers developed a group of miniproteins, which bound the spike RBD with affinities ranging from 100 pM to 10 nM and inhibited SARS-CoV-2 infection with 50% inhibitory concentration (IC_{50}) values between 24 pM and 35 nM (Cao et al., 2020). LCB1, a lead miniprotein designed with 56 amino acids, showed the potent *in vitro* antiviral activity, and its modified versions efficiently blocked SARS-CoV-2 infection in human ACE2 (hACE2)-expressing transgenic mice when administrated as both pre-exposure prophylaxis (PrEP) and post-exposure therapy, providing an ideal candidate for drug development (Case et al., 2021). Considering the COVID-19 epidemic caused by divergent VOCs and still ongoing evolutionary mutations, it is fundamentally important to characterize LCB1 for its drug resistance and underlying mechanism. In this report, we describe our data to specifically address this question, which can guide the design strategy of novel LCB1-based antivirals against divergent VOCs and evolutionary mutants.

1 https://covid19.who.int

Materials and methods

Peptide, plasmids, and cell lines

A 56-mer LCB1 peptide was synthesized on rink amide 4-methylbenzhydrylamine (MBHA) resin using a standard solid-phase 9-flurorenylmethoxycarbonyl (FMOC) protocol as described previously (Yu et al., 2021a). Plasmids encoding the mutant S proteins of SARS-CoV-2 (Alpha, Beta, Gamma, Delta, Lambda, and Omicron) were a kind gift from Linqi Zhang at the Tsinghua University (Beijing, China). HEK293T and Huh-7 cells were purchased from the American type culture collection (ATCC) (Rockville, MD, USA); 293T/ACE2 cells stably expressing human ACE2 were generated and preserved in our laboratory. Cells were cultured in complete growth medium consisting of Dulbecco's minimal essential medium (DMEM) supplemented with 10% fetal bovine serum (FBS), 100 U/ml of penicillin-streptomycin, 2 mM L-glutamine, and 1mM sodium pyruvate under 37^{o}C and 5% CO2.

Circular dichroism spectroscopy

Circular dichroism (CD) spectroscopy was applied to determine the secondary structure and thermostability of LCB1 peptide as described previously (Zhu et al., 2020). Briefly, LCB1 was dissolved in phosphate-buffered saline (PBS; pH 7.2) with a final concentration of 20 μM and incubated at 37^{o}C for 30 min. CD spectra were obtained on Jasco spectropolarimeter (model J-815) a using a 1 nm bandwidth with a 1 nm step resolution from 195 to 270 nm at room temperature. The spectra were corrected by subtracting a solvent blank, and the α-helical content was calculated from the CD signal by dividing the mean residue ellipticity [θ] at 222 nm by with a value of −33,000 deg cm^2 dmol^{-1}, corresponding to a 100% helix. Thermal denaturation was done by monitoring the ellipticity change at 222 nm from 20 to 98^{o}C at a rate of 2^{o}C/min, and the melting temperature (T_m) was defined as the midpoint of the thermal unfolding transition.

Site-directed mutagenesis

Spike mutants were generated by site-directed mutagenesis as described previously (Yu et al., 2021a). In brief, the forward and reverse primers with 16∼28 nucleotides were designed with specific mutations and occupied the same starting and ending positions on the opposite strands of a codon-optimized S gene cloned in a pcDNA3.1 vector. DNA synthesis was

conducted by PCR in a 50-μl reaction volume using 100 ng of denatured plasmid template, 50 pM upper and lower primers, and 5 U of the high-fidelity polymerase PrimeStar (TaKaRa, Dalian, China). PCR amplification was done for one cycle of denaturation at 98°C for 5 min, followed by 25 cycles of 98°C for 10 s and 68°C for 9 min, with a final extension at 72°C for 10 min. The amplicons were treated with restriction enzyme *Dpn*I for 3 h at 37°C, and *Dpn*I-resistant molecules were recovered by transforming *E. coli* stable3 competent cells with antibiotic resistance. The required mutations were confirmed by DNA sequencing of a single clone.

Single-cycle infection assay

Infectivity of various SARS-CoV-2 pseudoviruses on 293T/ACE2 or Huh-7 cells was measured by a single-cycle infection assay as described previously (Yu et al., 2021a). Briefly, pseudoviruses were packaged by cotransfecting HEK293T cells with a wild-type (WT) or mutant S protein-expressing plasmid and pNL4-3.luc.RE plasmid that encodes an Env-defective HIV-1_{NL4-3} genome with luciferase as a reporter. Cell supernatants containing virions were collected after transfection 48 h and stored at -80^{o}C. To determine the inhibitory activity of LCB1 inhibitor, a serially three-fold diluted peptide was incubated with an equal volume of pseudoviruses at 37^{o}C for 1 h, and the peptide-virus mixture was then added to 293T/ACE2 or Huh-7 target cells at a density of 10^4 cells/100 μl per well in a 96-well culture plate. After incubation at 37^{o}C for 48 h, cells were harvested, lysed in reporter lysis buffer, and measured for luciferase activity using luciferase assay reagents and a luminescence counter (Promega, Madison, WI, USA).

Biolayer interferometry

Biolayer interferometry (BLI) was used to measure the binding and blocking activities of LCB1 peptide. In brief, a recombinant His-tagged RBD protein (Sino Biological, Beijing, China) was loaded on a NTA biosensor (ForteBio, San Francisco, CA, USA) at a concentration of 10 μg/ml for 120 s in phosphate buffer saline (PBS), and LCB1 peptide was gradient-diluted in PBST buffer (PBS plus 0.2% Tween 20). The binding kinetics was guided by associating in analyte substrates for 120s and disassociating in PBST alone for 300s.

Flow cytometry assay

The blocking activity of LCB1 peptide on the interaction of ACE2 and RBD proteins was also determined by flow cytometry. Briefly, an RBD protein at 2 μg/ml was mixed with serially diluted LCB1 and incubated at 4°C for 1 h. The mixture was then added to 5×10^5 of 293T/ACE2 cells and incubated at 4°C for 1 h. After being washed twice with PBS, the cells were incubated with 1:500 diluted Alexa Fluor 488-labeled rabbit anti-His tag antibody (Cell Signaling Technology, Danvers, MA, USA) at 4°C for 1 h. After two washes with PBS, cells were resuspended by FACS buffer and analyzed with a FACS CantoII instrument (Becton-Dickinson, Mountain View, CA, USA).

Statistical analysis

The percent inhibition of virus infection and 50% inhibitory concentration (IC_{50}) of LCB1 inhibitor were calculated using GraphPad Prism 6 software (GraphPad Software Inc., San Diego, CA, USA). Statistical comparison of divergent pseudovirus infections were conducted by one-way ANOVA with Dunnett's multiple comparisons test ($^{*}P < 0.05$; $^{**}P < 0.01$; $^{***}P < 0.001$; $^{****}P < 0.0001$; ns, not significant).

Results

Synthesis and characterization of LCB1 peptide

The previously reported LCB1 miniprotein was recombinantly expressed and purified from *E. coli*. Herein, we chemically synthesized a 56-mer LCB1 peptide using a standard solid-phase FMOC protocol. The peptide was acetylated at the N terminus and amidated at the C terminus, purified to a 95.15% homogeneity by reverse-phase high-performance liquid chromatography (HPLC) and characterized for amino acids with mass spectrometry (**Supplementary Figure 1**). The concentration of LCB1 peptide was determined by UV absorbance and a theoretically calculated molar extinction coefficient based on the tryptophan and tyrosine residues. We first characterized the structural properties of LCB1 by CD spectroscopy. As shown in **Figures 1A,B**, CD spectra of LCB1 displayed typical double minima at 208 and 222 nm, which indicated an α-helical content of ∼82%; however, its thermal unfolding transition could not be precisely determined due to a greater than 95^{o}C melting temperature (T_m). Next, the antiviral activity of LCB1 was measured by a pseudovirus-based single-cycle infection assay. To this end, pseudoviruses carrying wild-type (WT) S protein of the original SARS-CoV-2 Wuhan-Hu-1 strain or a single D614G mutation (B1 strain) were packaged and characterized. As shown in **Figures 1C,D**, LCB1 potently inhibited infections of the WT and D614G pseudoviruses with mean IC_{50} values of 0.191 and of 0.062 nM, respectively, on 293T/ACE2 cells and of 0.22 and 0.073 nM, respectively, on Huh-7 cells. In comparison, LCB1 was ∼3-fold more active in inhibiting the D614G mutant relative to its inhibition on WT strain. Taken together, these results

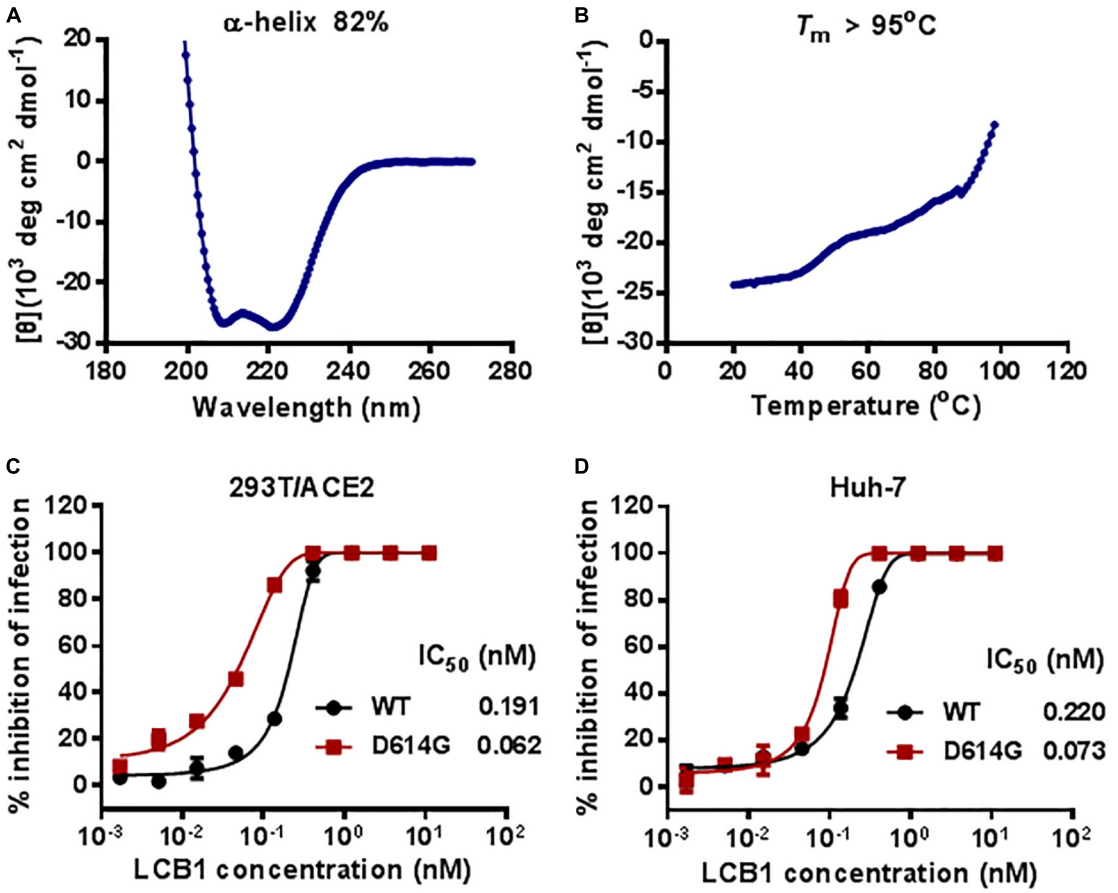

FIGURE 1
Structural and functional characterization of LCB1 peptide. The α-helicity **(A)** and thermostability **(B)** of LCB1 peptide at a concentration of 20 μM were determined by Circular dichroism (CD) spectroscopy. The inhibitory activities of LCB1 against infections of wild-type (WT) SARS-CoV-2 and its D614G mutant on 293T/ACE2 cells **(C)** and Huh-7cells **(D)** were measured by a single-cycle infection assay. Samples were tested in triplicate and repeated, and data are presented as means.

validated the structural integrity and functionality of LCB1 as a peptide-based inhibitor.

Resistance profiles of diverse variants of concerns and variant of interest to LCB1 inhibitor

We recently reported the functionalities of S proteins derived from divergent SARS-CoV-2 variants to mediated cell-cell fusion and infectivity, as well as their susceptibility to the inhibition of fusion-inhibitory lipopeptides. Herein, we sought to characterize LCB1 peptide for its inhibitory activity on five VOCs and one VOI (Lambda, C.37). The corresponding pseudoviruses were therefore generated and used in the single-cycle infection assay. As shown in Figures 2A,B and Table 1, LCB1 infected Alpha, Beta, Gamma, Delta, Lambda, and Omicron variants with mean IC_{50} values of 0.899, 901.8, 204.367, 0.569, 0.301, and 956.5 nM, respectively, on 293T/ACE2 cells and of 0.69, 447.083, 70.405, 0.958, 0.47, and 761.217 nM, respectively, on Huh-7 cells. Because all the VOCs were evolved with a D614G background, here we used D614G virus as a reference strain for calculating the fold-changes of resistance. As shown, Alpha, Beta, Gamma, Delta, Lambda, and Omicron displayed about 15-, 14, 545-, 3, 296-, 9-, 5-, and 15,427-fold resistance on 293T/ACE2 cells and about 9-, 6, 124-, 964-, 13-, 6-, and 10,428-fold resistance on Huh-7 cells, respectively. Therefore, the Beta, Gamma, and Omicron variants had very high levels of resistance to the LCB1 inhibition, whereas the Alpha, Delta, and Lambda variants exhibited mild resistance.

Identification of K417N/T mutation as a key determinant of LCB1 resistance

In order to identify the mutations responsible for the VOC resistance, we further generated a panel of S protein mutants

10.3389/fmicb.2022.1022006

TABLE 1 Resistance profile of SARS-CoV-2 VOCs and related mutants to LCB1 inhibitor[a].

Pseudovirus	PV infection on 293T/ACE2		PV infection on Huh-7	
	IC_{50} ± SD (nM)	Fold change	IC_{50} ± SD (nM)	Fold change
D614G	0.062 ± 0.001	1	0.073 ± 0.008	1
Alpha	0.899 ± 0.139	14.500	0.69 ± 0.075	9.452
Beta	901.8 ± 68.826	14545.161	447.083 ± 1.061	6124.425
Gamma	204.367 ± 0.189	3296.242	70.405 ± 17.067	964.452
Delta	0.569 ± 0.133	9.177	0.958 ± 0.319	13.123
Lamda	0.301 ± 0.078	4.855	0.47 ± 0.029	6.438
Omicron	956.5 ± 43.982	15427.419	761.217 ± 69.367	10427.630
Δ69-70	0.101 ± 0.011	1.629	0.137 ± 0.005	1.877
K417N	2.774 ± 0.191	44.742	4.898 ± 0.357	67.096
E484K	0.059 ± 0.001	0.952	0.07 ± 0.013	0.959
N501Y	0.228 ± 0.022	3.677	0.282 ± 0.037	3.863
P681H	0.071 ± 0.002	1.145	0.069 ± 0.011	0.945
Δ69-70/N501Y	0.209 ± 0.004	3.371	0.392 ± 0.032	5.370
E484K/N501Y	0.579 ± 0.069	9.339	0.525 ± 0.15	7.192
N501Y/P681H	0.199 ± 0.014	3.210	0.31 ± 0.048	4.247
Δ69-70/N501Y/P681H	0.148 ± 0.03	2.387	0.293 ± 0.052	4.014
K417N/E484K/N501Y	250.634 ± 26.257	4042.484	323.017 ± 5.775	4424.890
K417T/E484K/N501Y	59.937 ± 2.497	966.726	68.525 ± 8.03	938.699
L452R/T478K/P681R	0.146 ± 0.003	2.355	0.113 ± 0.021	1.548

[a]The experiments were performed in triplicate and repeated three times, and data are expressed as the means ± SD.

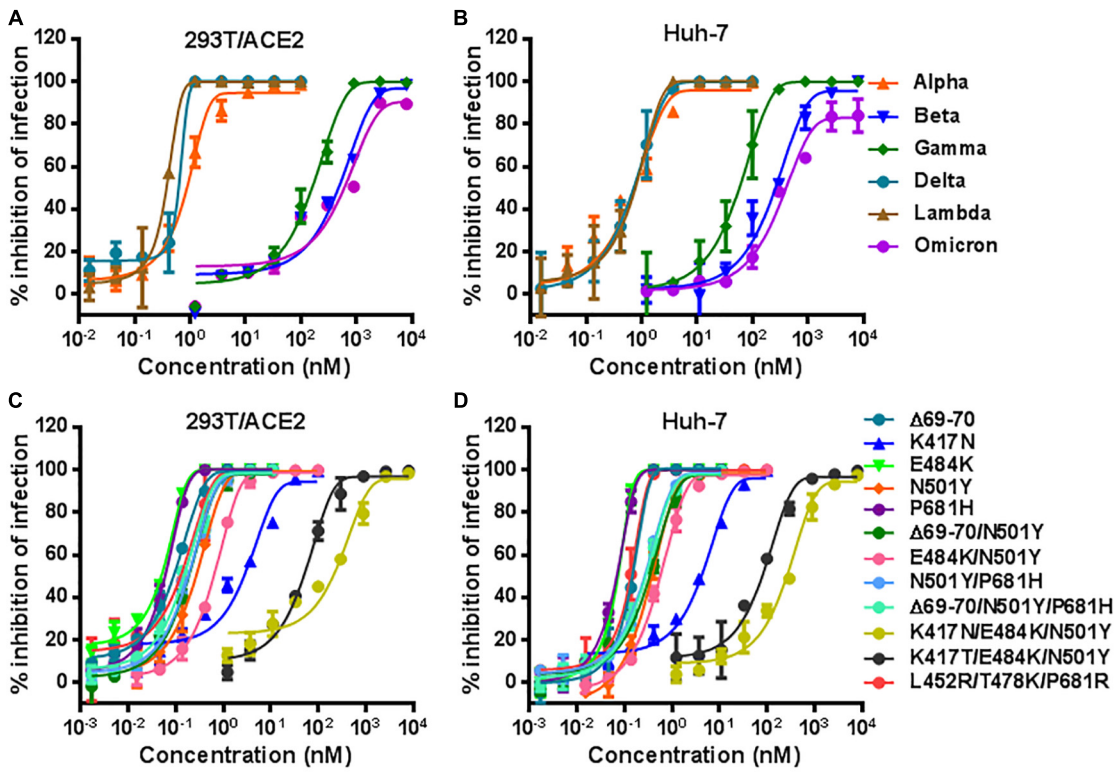

FIGURE 2
Inhibitory activity of LCB1 against divergent SARS-CoV-2 variants. The activities of LCB1 peptide in inhibiting VOCs and VOI **(A,B)** as well as the panel of mutant pseudoviruses carrying single or combined mutations **(C,D)** were measured by the single-cycle infection assay. Samples were tested in triplicate, the experiments were repeated three times, and data are expressed as the means with standard deviations (SD) and presented in **Table 1**.

carrying the key mutations by VOCs. The corresponding pseudoviruses were generated and their infectivity was characterized on both 293T/ACE2 and Huh-7 cells by a single-cycle infection assay (**Supplementary Figure 2**). In the inhibition of pseudoviruses with single mutations, we found that LCB1 inhibited the infection of K417N mutant with IC_{50} of 2.774 nM on 293T/ACE2 and 4.898 nM on Huh-7 cells, which indicated 45-fold or 67-fold resistance changes over D614G reference (**Figures 2C,D**). While N501Y mutant showed mild resistance (∼4-fold), the single mutation of E484K or P681H and the mutant with Δ69-70 deletion did not confer resistance, which were also supported by the IC_{50} fold-changes of three combination mutations (Δ69-70/N501Y, N501Y/P681H, and Δ69-70/N501Y/P681H). Significantly, the E484K/N501Y mutant was more resistant than the N501Y mutant and its combination with K417N or K417T sharply enhanced the resistance phenotype, as evidenced by the fold-changes of two triple mutations (K417N/E484K/N501Y and K417T/E484K/N501Y). In contrast, the triple mutant L452R/T478K/P681R had no obvious resistance to the LCB1 inhibition. These results demonstrated that K417N or K417T mutation in RBD plays a key role in the resistance profiles of SARS-CoV-2 VOCs to LCB1 inhibitor. In line with this conclusion, the Beta, Gamma, and Omicron variants contain K417N or K417T, whereas the Alpha, Delta, and Lambda variants lack this mutation.

Identification of naturally occurring receptor binding domain mutations that confer the LCB1 resistance

Considering the ongoing mutations of SARS-CoV-2 variants, we are interested in characterizing the effects of naturally occurring mutations on the inhibitory activity of LCB1. Thus, a total of 85 substitutions, which naturally occurred in the spike RBD sequence with relatively higher frequencies, were selected and the corresponding S protein mutants were generated. First, we analyzed the functionality of the S protein mutants to mediate pseudovirus infections on both 293T/ACE2 and Huh-7 cells. As shown in **Supplementary Figure 3**, many of the mutants displayed significantly decreased infectivity, whereas several mutations resulted in enhanced infections (L452M, I468T, Y505W, and Y508H). Herein, we determined the susceptibility of 81 pseudoviruses to the LCB1 inhibition on Huh-7 cells by the single-cycle infection assay. As indicated by the IC_{50} values in **Table 2**, there were three mutants (E406Q, K417T, and L455F) displaying high-levels of resistance with the fold-changes of IC_{50} at ∼31, ∼25, and ∼121, respectively, whereas the Y505W mutant conferred a mild resistance with a ∼6-fold increased IC_{50} value. In this experiment, we also verified that L452R and T478K mutations, which appeared in the L452R/T478K/P681R mutant above, had no resistance to LCB1, whereas some mutants (P463S, V483F, A520V, and P521R) behaved with certain degrees of increased susceptibility.

The resistance mutations greatly impair the binding affinity of LCB1

To explore the mechanism underlying the LCB1 resistance, we applied biolayer interferometry (BLI) to analyze the binding affinity of LCB1 to the RBD proteins with or without resistance mutations (**Figure 3**). Comparing to the equilibrium dissociation constant (Kd) of wild-type RBD (WT-RBD) at 3.397 nM, only the RBD proteins carrying a single K417N or double L452R/T478K mutations exhibited slightly reduced binding affinities with Kd values of 6.805 and 6.77 nM, respectively, none of other single mutations (E406Q, K417T, L455F, and N501Y) significantly impaired the LCB1 binding. Notably, the RBD proteins with the combination mutations of K417N/E484K/N501Y or K417T/E484K/N501 had dramatically decreased binding capacities as indicated by their Kd values at 49.11 and 15.83 nM, respectively.

We next determined the blocking activity of LCB1 on the binding of RBD protein with ACE2 expressed on 293T/ACE2 cells by flow cytometry. Consistent with its binding affinity above, LCB1 could effectively blocked the binding of RBD proteins with single or double mutations, but it exhibited a dramatically decreased blocking activity on the RBD with K417N/E484K/N501Y or K417T/E484K/N501Y (**Figure 4**).

Discussion

In this study, we focused on characterizing LCB1 inhibitor for its antiviral activities against divergent SARS-CoV-2 variants and achieved significant findings. First, we successfully synthesized and purified a 56-mer LCB1 peptide, which exhibited high α-helicity, thermostability and antiviral activity. Second, we found that while the Alpha, Delta, and Lambda variants only caused mild resistance to LCB1, the Beta, Gamma, and Omicron variants were highly resistant to the LCB1 inhibition, giving the resistance fold-changes greater than 15,000 or 3,000. Third, with a panel of SARS-CoV-2 mutants carrying the single, double or triple mutations contained in VOCs, K417N, and N501Y in the spike RBD were verified to be critical determinants for the observed resistance phenotype. Fourth, we further generated a large panel of 85 naturally occurring RBD point-mutations, which identified E406Q, K417T and L455F conferring high-levels of resistance, whereas Y505W was responsible for a mild resistance. Moreover, the results by BLI and flow cytometry demonstrated that the resistance mutations could greatly impair the RBD-binding affinity of LCB1 and thus attenuated its blocking function on the

RBD-ACE2 interaction. In conclusion, our studies highlight the resistance profiles of divergent SARS-CoV-2 VOCs and natural RBD mutants as well as the underlying mechanisms, which would facilitate the development of LCB1-based antiviral drugs.

Since its first report, LCB1 inhibitor has specially attracted our attention due to its computer-aided design strategy as a miniprotein and high inhibitory potency on SARS-CoV-2 infection by targeting the spike RBD to block virus entrance (Cao et al., 2020). We are also encouraged by the preventive and therapeutic efficacies of modified LCB1 proteins in animal infection models (Case et al., 2021). Unfortunately, SARS-CoV-2 spread with persistent mutations, resulting in the emergence of divergent VOCs and VOIs that caused new waves of worldwide epidemic. Significantly, many of evolved mutations in RBD can shape the binding conformation and interacting affinity of S protein with the cell receptor ACE2 and thus affect virus's biological properties, e.g., transmission ability and disease severity. The mutations have also affected the performances of vaccines, therapeutic drugs, and diagnostic tools significantly (Garcia-Beltran et al., 2021; Hoffmann et al., 2021; Kuzmina et al., 2021; Fan et al., 2022; Guo et al., 2022; Sun et al., 2022; Zhu et al., 2022). Omicron has emerged as the fifth VOC after Alpha, Beta, Gamma, and Delta, and it has evolved into distinct lineages: BA.1 (B.1.1.529) was responsible for the initial surge but almost replaced by BA.2 in April 2022; while BA.3 remains at low frequency, BA.4 and BA.5 have currently

TABLE 2 Characterization of naturally occuring RBD mutations that mediate LCB1 resistance.

Pseudovirus	IC_{50} ± SD (nM)	Fold change	Pseudovirus	IC_{50} ± SD (nM)	Fold change
D614G	0.081 ± 0.025	1.000	G446V	0.039 ± 0.015	0.485
P330S	0.100 ± 0.014	1.250	L452M	0.084 ± 0.024	1.695
P337S	0.058 ± 0.019	0.714	L452R	0.136 ± 0.014	1.052
F338L	0.081 ± 0.026	1.013	Y453F	0.114 ± 0.026	1.424
G339D	0.035 ± 0.021	0.350	**L455F**	**9.802 ± 0.686**	**121.012**
V341I	0.116 ± 0.026	1.448	S459Y	0.039 ± 0.003	0.489
A344S	0.077 ± 0.021	0.964	P463S	0.018 ± 0.015	0.219
A348S	0.042 ± 0.006	1.752	I468T	0.068 ± 0.019	0.843
A352S	0.114 ± 0.012	1.419	T470A	0.044 ± 0.006	0.552
N354D	0.083 ± 0.021	1.032	E471Q	0.042 ± 0.007	0.519
N354K	0.066 ± 0.039	0.828	I472V	0.063 ± 0.015	0.784
N354S	0.077 ± 0.012	0.956	A475V	0.061 ± 0.017	0.764
S359N	0.077 ± 0.019	0.959	G476S	0.092 ± 0.014	1.152
V367F	0.088 ± 0.028	1.103	S477I	0.060 ± 0.015	0.748
V367L	0.098 ± 0.008	1.590	S477N	0.092 ± 0.023	1.155
N370S	0.077 ± 0.012	0.956	S477R	0.049 ± 0.004	0.609
A372T	0.082 ± 0.038	1.022	T478I	0.078 ± 0.008	0.974
S373L	0.082 ± 0.036	1.021	T478K	0.078 ± 0.009	0.975
F377L	0.050 ± 0.003	0.630	P479S	0.070 ± 0.017	0.880
K378N	0.086 ± 0.009	1.070	G482S	0.057 ± 0.007	0.716
V382L	0.054 ± 0.026	0.675	V483A	0.066 ± 0.005	0.823
P384A	0.084 ± 0.015	1.046	V483F	0.016 ± 0.007	0.199
P384L	0.088 ± 0.014	1.105	V483I	0.084 ± 0.005	1.044
P384S	0.049 ± 0.024	0.617	G485S	0.083 ± 0.013	1.043
T385A	0.096 ± 0.011	1.231	G485R	0.045 ± 0.014	0.560
T385I	0.092 ± 0.003	1.145	F486L	0.096 ± 0.026	1.200
T393P	0.082 ± 0.011	1.157	F490S	0.041 ± 0.009	0.512
V395I	0.091 ± 0.018	1.134	F490L	0.049 ± 0.010	0.617
I402V	0.088 ± 0.052	1.097	Q493L	0.046 ± 0.013	0.580
E406Q	**2.489 ± 0.299**	**31.125**	S494P	0.083 ± 0.019	1.043
R408I	0.096 ± 0.033	1.200	N501T	0.105 ± 0.009	1.306
Q409E	0.077 ± 0.020	0.956	V503F	0.064 ± 0.005	0.798
A411S	0.042 ± 0.006	0.527	**Y505W**	**0.479 ± 0.030**	**5.914**
Q414R	0.029 ± 0.002	0.361	Y508H	0.101 ± 0.011	1.263
K417T	**1.988 ± 0.558**	**24.543**	E516Q	0.070 ± 0.005	0.879
D427Y	0.080 ± 0.040	0.998	A520S	0.076 ± 0.006	0.954
A435S	0.045 ± 0.011	0.565	A520V	0.013 ± 0.006	0.167
N439K	0.033 ± 0.008	0.416	P521R	0.023 ± 0.003	0.289
N440K	0.069 ± 0.012	0.860	P521S	0.053 ± 0.017	0.657
K444N	0.042 ± 0.013	0.528	A522S	0.039 ± 0.004	0.488
K444R	0.046 ± 0.013	0.570	A522V	0.032 ± 0.016	0.404

[a]The experiments were performed in triplicate and repeated three times, and data are expressed as the means ± SD. The resistance mutations are highlighted in bold.

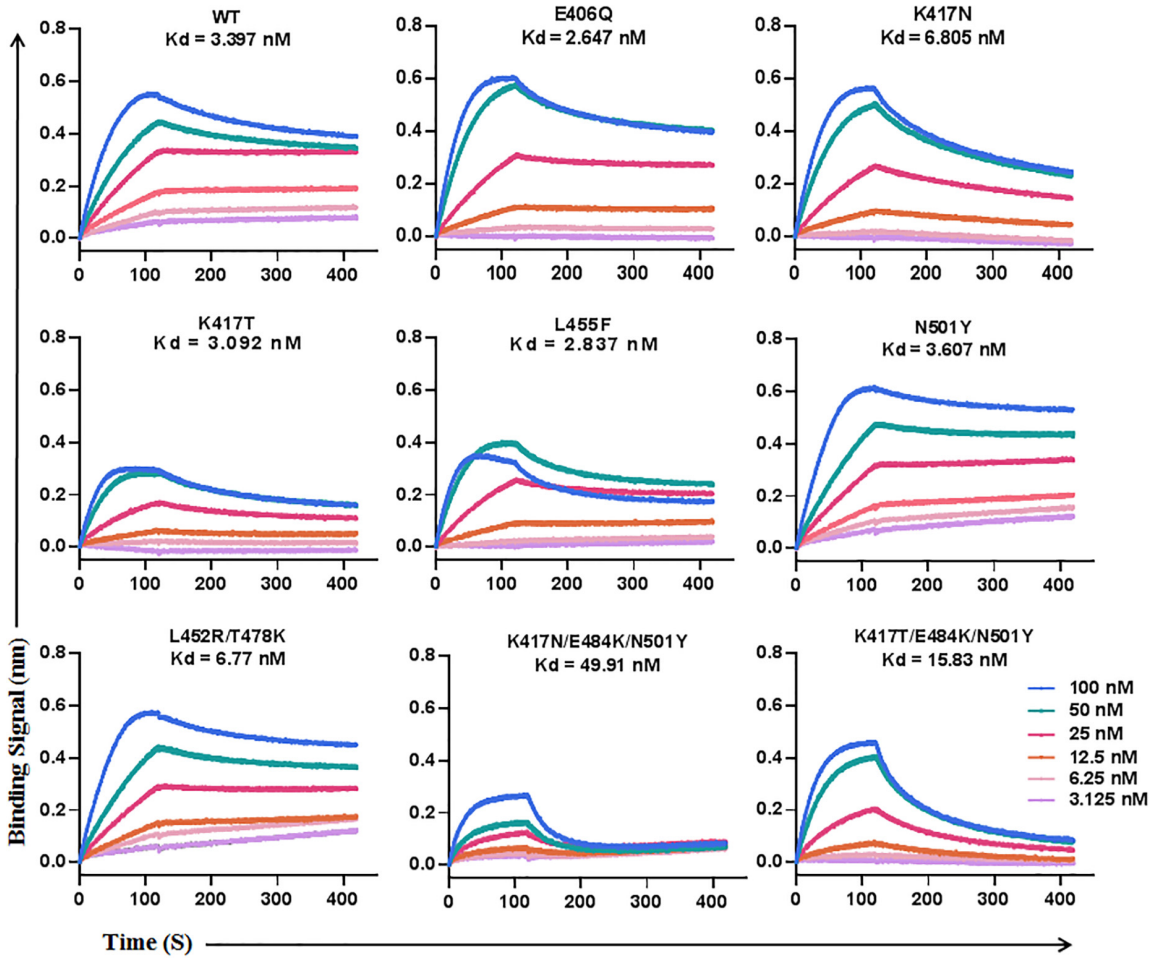

FIGURE 3
The binding affinity of LCB1 with RBD proteins determined by biolayer interferometry. A recombinant His-tagged RBD protein with wild-type sequence or mutations was loaded onto an NTA biosensors and equilibrated before the baseline was set to zero at t = 0. The binding kinetics was guided by associating in different concentrations of LCB1 for 120 s and disassociating for 300 s. The equilibrium dissociation constant (Kd) was calculated.

replaced BA.2 and are becoming prevalent globally (Qu et al., 2022; Tegally et al., 2022). In protein level, BA.4 and BA.5 bear identical S proteins, being most comparable to BA.2 but have additional mutations (Δ67-70, L452R, F486V) and wild type amino acid at position Q493, which critically determine their increased fitness and immune evasion than the earlier BA.1 and BA.2 lineages (Cao et al., 2022). In this study, we identified that single K417N or K417T mutation is a key determinant to the resistance, which occurred in Beta, Gamma and Omicron (VOCs highly resistant to LCB1) but not in Alpha, Delta, and Lambda variants (VOCs or VOI mildly resistant to LCB1). Except for Delta, other four VOCs have an N501Y mutation, which is responsible for a low resistance level when being presented in the Alpha variant alone but can markedly boost the resistance levels of three highly resistant VOCs as a combined mutation with K417N/T. The Delta variant evolved with two RBD mutations (T478K and L452R); while T478K was not associated with the LCB1 resistance, L452R did rendered the virus slightly resistant, as evidenced by ∼2-fold IC_{50} changes (**Table 2**). L452R also appeared in Delta, Omicron, and many other variants, such as Kappa (B.1.617.1), Epsilon (B.1.429), and B.1.617.3. Our studies with the large panel of naturally occurring RBD mutants also found E406Q, L455F, and Y505W being resistant to LCB1, which are not present in the current VOCs. Given that all the characterized mutations in LCB1-resistant VOCs, including K417N, K417T, T478K, L452R, and N501Y, naturally emerged during the evolution process, whether E406Q, L455F, and Y505W mutations will appear in future VOCs to cause LCB1 resistance is an intriguing question.

In order to overcome the resistance problem by LCB1, the same group of authors continued their efforts to design multivalent proteins by using a cell-free expression workflow, which combines an *in vitro* DNA assembly step followed by polymerase chain reaction (PCR) to generate linear expression

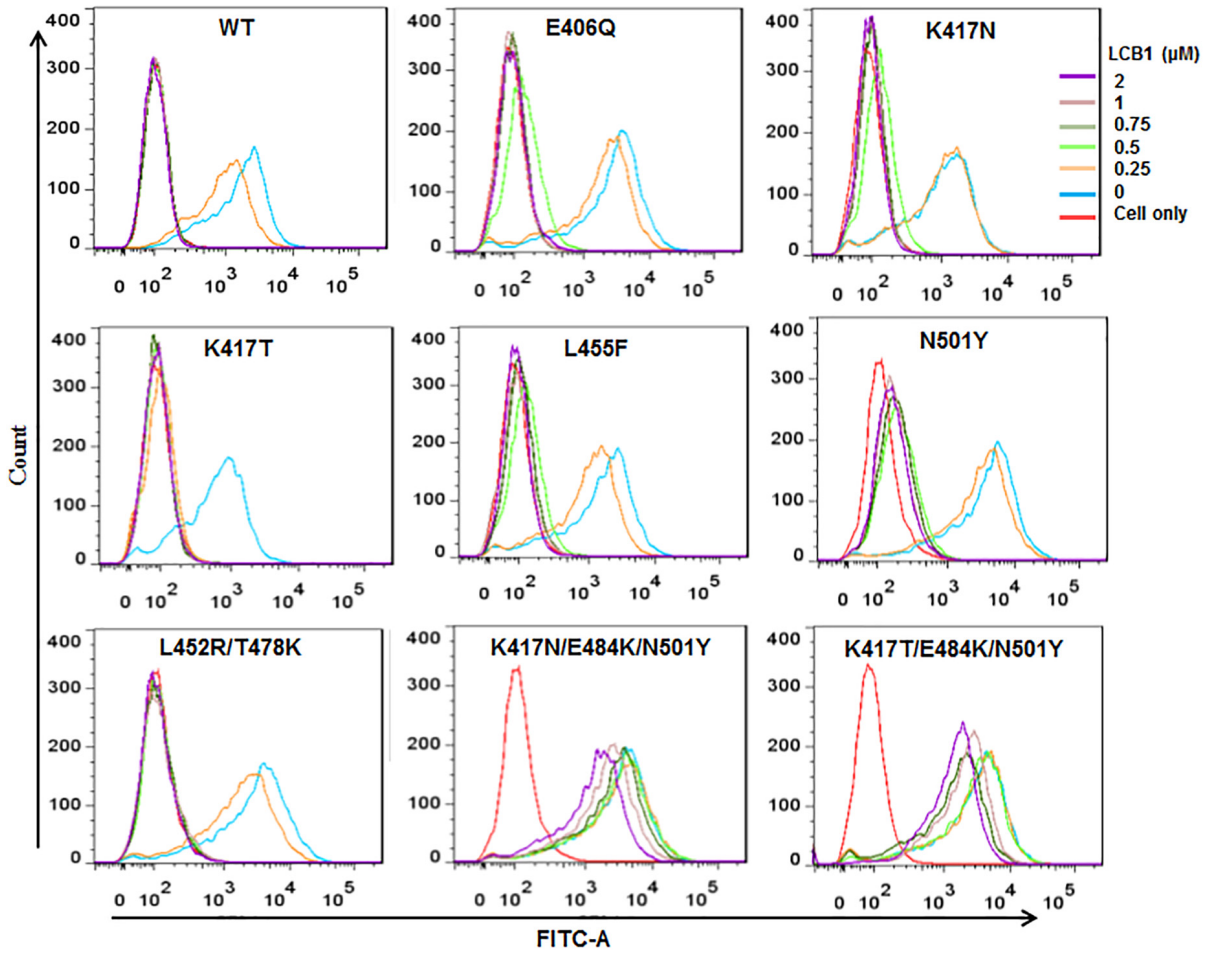

FIGURE 4
The blocking activity of LCB1 on the binding of RBD protein with the cell receptor ACE2. An His-tagged RBD protein was incubated with serially diluted LCB1 and then added to 293T/ACE2 cells for incubation. The bound RBD was detected by an Alexa Fluor 488-labeled rabbit anti-His tag antibody with FACS analysis.

templates that are used to drive cell-free protein synthesis and enable rapid prototyping of new minibinder designs (Hunt et al., 2022). Promisingly, a number of constructs containing LCB1 or other miniproteins displayed dramatically increased binding and inhibitory activities against divergent VOCs and related mutant viruses, and of them a homo-trimeric version of 75-residue ACE2 mimic AHB2 (TRI2-2), which was designed to geometrically match the trimeric spike architecture, conferred prophylactic and therapeutic protection against SARS-CoV-2 challenge when administered intranasally in mice, providing evidence to support LCB1-based drug development with high and broad-spectrum antiviral activities (Hunt et al., 2022). In addition to developing viral entry inhibitors that target membrane fusion step (Zhu et al., 2019, 2020, 2021, 2022; Yu et al., 2021a,b; Xue et al., 2022), our research team is also working to rationally construct LCB1-based inhibitors that have resistance to viral escape and antigenic drift, and several bispecific fusion proteins have been validated with highly potent activity against diverse SARS-CoV-2 VOCs and mutants (unpublished data). Very recently, it was also reported that the length of LCB1 could be reduced to 35 amino acids without interfering its inhibitory capacity, providing a flexible template for LCB1-based design strategies (Weissenborn et al., 2022).

Data availability statement

The original contributions presented in this study are included in the article/**Supplementary material**, further inquiries can be directed to the corresponding author.

Author contributions

TW, YZ, NL, YH, and HC performed the experiments. TW, YZ, and YXH analyzed the data. YH supervised the study and

wrote the manuscript with TW and YZ. All authors read and approved the submitted version.

Funding

This work was supported by grants from the CAMS Innovation Fund for Medical Sciences (2021-I2M-1037) and the National Natural Science Foundation of China (82002150 and 81630061).

Acknowledgments

We thank Linqi Zhang at the Tsinghua University (Beijing, China) for providing the plasmids encoding the mutant S proteins of SARS-CoV-2 VOCs.

Conflict of interest

The authors declare that the research was conducted in the absence of any commercial or financial relationships that could be construed as a potential conflict of interest.

Publisher's note

All claims expressed in this article are solely those of the authors and do not necessarily represent those of their affiliated organizations, or those of the publisher, the editors and the reviewers. Any product that may be evaluated in this article, or claim that may be made by its manufacturer, is not guaranteed or endorsed by the publisher.

Supplementary material

The Supplementary Material for this article can be found online at: https://www.frontiersin.org/articles/10.3389/fmicb.2022.1022006/full#supplementary-material

SUPPLEMENTARY FIGURE 1
Synthesis and characterization of LCB1 peptide. **(A)** LCB1 was chemically synthesized on rink amide 4-methylbenzhydrylamine (MBHA) resin using a standard solid-phase 9-flurorenylmethoxycarbonyl (FMOC) and its purity was determined by reverse-phase HPLC. **(B)** The peptide was characterized by mass spectrometry, indicating a molecular weight of 6,852.5Da.

SUPPLEMENTARY FIGURE 2
Infectivity of divergent SARS-CoV-2 variants. The infectivity of SARS-CoV-2 pseudoviruses with single or multiple mutations on 293T/ACE **(A)** or Huh-7 **(B)** cells was determined by a single-cycle infection assay. D614G mutant was treated as a reference, thus its luciferase activity (RLU) was standard as 100% and the relative infectivity of various mutants was calculated accordingly. The experiments were repeated at least three times and columns are expressed as the means ± SD. Statistical analysis was conducted to compare the differences between the D614G reference and diverse mutants.

SUPPLEMENTARY FIGURE 3
Infectivity of naturally occurring SARS-CoV-2 mutants. The infectivity of 85 SARS-CoV-2 pseudoviruses carrying natural RBD point-mutations was determined on 293T/ACE **(A)** or Huh-7 **(B)** cells by a single-cycle infection assay. Similarly, D614G mutant was treated as a reference, thus its luciferase activity (RLU) was standard as 100% and the relative infectivity of various mutants was calculated accordingly. The experiments were repeated at least three times and columns are expressed as the means ± SD. Statistical analysis was conducted to compare the differences between the D614G reference and diverse mutants.

References

Callaway, E. (2021). Heavily mutated Omicron variant puts scientists on alert. *Nature* 600:21. doi: 10.1038/d41586-021-03552-w

Cao, L., Goreshnik, I., Coventry, B., Case, J. B., Miller, L., Kozodoy, L., et al. (2020). De novo design of picomolar SARS-CoV-2 miniprotein inhibitors. *Science* 370, 426–431. doi: 10.1126/science.abd9909

Cao, Y., Yisimayi, A., Jian, F., Song, W., Xiao, T., Wang, L., et al. (2022). BA.2.12.1, BA.4 and BA.5 escape antibodies elicited by Omicron infection. *Nature* 608, 593–602. doi: 10.1038/s41586-022-04980-y

Case, J. B., Chen, R. E., Cao, L., Ying, B., Winkler, E. S., Johnson, M., et al. (2021). *Ultrapotent miniproteins* targeting the SARS-CoV-2 receptor-binding domain protect against infection and disease. *Cell Host Microbe* 29, 1151–1161e1155. doi: 10.1016/j.chom.2021.06.008

Fan, Y., Li, X., Zhang, L., Wan, S., Zhang, L., and Zhou, F. (2022). SARS-CoV-2 Omicron variant: recent progress and future perspectives. *Signal Transduct Target Ther.* 7:141. doi: 10.1038/s41392-022-00997-x

Garcia-Beltran, W. F., Lam, E. C., St Denis, K., Nitido, A. D., Garcia, Z. H., Hauser, B. M., et al. (2021). Multiple SARS-CoV-2 variants escape neutralization by vaccine-induced humoral immunity. *Cell* 184, 2372–2383e2379. doi: 10.1016/j.cell.2021.03.013

Guo, Y., Han, J., Zhang, Y., He, J., Yu, W., Zhang, X., et al. (2022). SARS-CoV-2 Omicron Variant: Epidemiological Features, Biological Characteristics, and Clinical Significance. *Front. Immunol.* 13:877101. doi: 10.3389/fimmu.2022.877101

He, X., Hong, W., Pan, X., Lu, G., and Wei, X. (2021). SARS-CoV-2 Omicron variant: Characteristics and prevention. *MedComm* 2, 838–845. doi: 10.1002/mco2.110

Hoffmann, M., Arora, P., Gross, R., Seidel, A., Hornich, B. F., Hahn, A. S., et al. (2021). SARS-CoV-2 variants B.1.351 and P.1 escape from neutralizing antibodies. *Cell* 184, 2384–2393e2312. doi: 10.1016/j.cell.2021.03.036

Hunt, A. C., Case, J. B., Park, Y. J., Cao, L., Wu, K., Walls, A. C., et al. (2022). Multivalent designed proteins neutralize SARS-CoV-2 variants of concern and confer protection against infection in mice. *Sci. Transl. Med.* 14:eabn1252. doi: 10.1126/scitranslmed.abn1252

Kuzmina, A., Khalaila, Y., Voloshin, O., Keren-Naus, A., Boehm-Cohen, L., Raviv, Y., et al. (2021). SARS-CoV-2 spike variants exhibit differential infectivity and neutralization resistance to convalescent or post-vaccination sera. *Cell Host Microbe* 29, 522–528e522. doi: 10.1016/j.chom.2021.03.008

Markov, P. V., Katzourakis, A., and Stilianakis, N. I. (2022). Antigenic evolution will lead to new SARS-CoV-2 variants with unpredictable severity. *Nat. Rev. Microbiol.* 20, 251–252. doi: 10.1038/s41579-022-00722-z

Plavec, Z., Pohner, I., Poso, A., and Butcher, S. J. (2021). Virus structure and structure-based antivirals. *Curr. Opin. Virol.* 51, 16–24.

Qu, P., Faraone, J., Evans, J. P., Zou, X., Zheng, Y. M., Carlin, C., et al. (2022). Neutralization of the SARS-CoV-2 Omicron BA.4/5 and BA.2.12.1 Subvariants. *N. Engl. J. Med.* 386, 2526–2528. doi: 10.1056/NEJMc2206725

Sabbah, D. A., Hajjo, R., Bardaweel, S. K., and Zhong, H. A. (2021). An Updated Review on Betacoronavirus viral entry inhibitors: Learning from past discoveries to Advance COVID-19 drug discovery. *Curr. Top. Med. Chem.* 21, 571–596. doi: 10.2174/1568026621666210119111409

Sun, C., Xie, C., Bu, G. L., Zhong, L. Y., and Zeng, M. S. (2022). Molecular characteristics, immune evasion, and impact of SARS-CoV-2 variants. *Signal Transduct. Target. Ther.* 7, 202. doi: 10.1038/s41392-022-01039-2

Tao, K., Tzou, P. L., Nouhin, J., Gupta, R. K., de Oliveira, T., Kosakovsky Pond, S. L., et al. (2021). The biological and clinical significance of emerging SARS-CoV-2 variants. *Nat. Rev. Genet.* 22, 757–773.

Tegally, H., Moir, M., Everatt, J., Giovanetti, M., Scheepers, C., Wilkinson, E., et al. (2022). Emergence of SARS-CoV-2 Omicron lineages BA.4 and BA.5 in South Africa. *Nat. Med.* [Online ahead of print] doi: 10.1038/s41591-022-01911-2

Weissenborn, L., Richel, E., Huseman, H., Welzer, J., Beck, S., Schafer, S., et al. (2022). Smaller, Stronger, More Stable: Peptide Variants of a SARS-CoV-2 neutralizing miniprotein. *Int. J. Mol. Sci.* 23:6309. doi: 10.3390/ijms23116309

Xiang, Y., Wang, M., Chen, H., and Chen, L. (2021). Potential therapeutic approaches for the early entry of SARS-CoV-2 by interrupting the interaction between the spike protein on SARS-CoV-2 and angiotensin-converting enzyme 2 (ACE2). *Biochem. Pharmacol.* 192:114724. doi: 10.1016/j.bcp.2021.114724

Xue, J., Chong, H., Zhu, Y., Zhang, J., Tong, L., Lu, J., et al. (2022). Efficient treatment and pre-exposure prophylaxis in rhesus macaques by an HIV fusion-inhibitory lipopeptide. *Cell* 185, 131–144e118. doi: 10.1016/j.cell.2021.11.032

Yamasoba, D., Kimura, I., Nasser, H., Morioka, Y., Nao, N., Ito, J., et al. (2022). Virological characteristics of the SARS-CoV-2 Omicron BA.2 spike. *Cell* 185, 2103–2115e2119. doi: 10.1016/j.cell.2022.04.035

Yan, W., Zheng, Y., Zeng, X., He, B., and Cheng, W. (2022). Structural biology of SARS-CoV-2: open the door for novel therapies. *Signal Transduct. Target Ther.* 7:26. doi: 10.1038/s41392-022-00884-5

Yang, H., and Rao, Z. (2021). Structural biology of SARS-CoV-2 and implications for therapeutic development. *Nat. Rev. Microbiol.* 19, 685–700. doi: 10.1038/s41579-021-00630-8

Yu, D., Zhu, Y., Jiao, T., Wu, T., Xiao, X., Qin, B., et al. (2021a). Structure-based design and characterization of novel fusion-inhibitory lipopeptides against SARS-CoV-2 and emerging variants. *Emerg. Microbes Infect.* 10, 1227–1240. doi: 10.1080/22221751.2021.1937329

Yu, D., Zhu, Y., Yan, H., Wu, T., Chong, H., and He, Y. (2021b). Pan-coronavirus fusion inhibitors possess potent inhibitory activity against HIV-1, HIV-2, and simian immunodeficiency virus. *Emerg. Microbes Infect.* 10, 810–821. doi: 10.1080/22221751.2021.1917309

Zhu, Y., Chong, H., Yu, D., Guo, Y., Zhou, Y., and He, Y. (2019). Design and Characterization of Cholesterylated Peptide HIV-1/2 Fusion Inhibitors with Extremely Potent and Long-Lasting Antiviral Activity. *J. Virol.* 93, e02312–e02318. doi: 10.1128/JVI.02312-18

Zhu, Y., Dong, X., Liu, N., Wu, T., Chong, H., Lei, X., et al. (2022). SARS-CoV-2 fusion-inhibitory lipopeptides maintain high potency against divergent variants of concern (VOCs) including Omicron. *Emerg. Microbes Infect.* 11, 1819–1827. doi: 10.1080/22221751.2022.2098060

Zhu, Y., Yu, D., Hu, Y., Wu, T., Chong, H., and He, Y. (2021). SARS-CoV-2-derived fusion inhibitor lipopeptides exhibit highly potent and broad-spectrum activity against divergent human coronaviruses. *Signal Transduct. Target. Ther.* 6:294. doi: 10.1038/s41392-021-00698-x

Zhu, Y., Yu, D., Yan, H., Chong, H., and He, Y. (2020). Design of Potent Membrane Fusion Inhibitors against SARS-CoV-2, an emerging coronavirus with high fusogenic activity. *J. Virol.* 94:e00635-20. doi: 10.1128/JVI.00635-20

frontiers | Frontiers in Microbiology

TYPE Opinion
PUBLISHED 12 October 2022
DOI 10.3389/fmicb.2022.998287

OPEN ACCESS

EDITED BY
Yushun Wan,
Chongqing Medical University, China

REVIEWED BY
Masaud Shah,
Ajou University, South Korea

*CORRESPONDENCE
Alexandra Calmy
Alexandra.calmy@hcuge.ch

SPECIALTY SECTION
This article was submitted to Virology, a section of the journal Frontiers in Microbiology

RECEIVED 19 July 2022
ACCEPTED 26 September 2022
PUBLISHED 12 October 2022

CITATION
Hentzien M, Owen A, Strub-Wourgaft N, Pérez-Casas C, Trøseid M and Calmy A (2022) Rethinking treatment paradigms for the deployment of SARS-CoV-2 antiviral drugs on the shifting landscape of new variants. *Front. Microbiol.* 13:998287. doi: 10.3389/fmicb.2022.998287

Rethinking treatment paradigms for the deployment of SARS-CoV-2 antiviral drugs on the shifting landscape of new variants

Maxime Hentzien[1], Andrew Owen[2], Nathalie Strub-Wourgaft[3], Carmen Pérez-Casas[4], Marius Trøseid[5] and Alexandra Calmy[1]*

[1]HIV/AIDS Unit, Infectious Diseases Division, Geneva University Hospitals, Geneva, Switzerland, [2]Centre of Excellence in Long-acting Therapeutics (CELT), University of Liverpool, Liverpool, United Kingdom, [3]COVID Response and Pandemic Preparedness Director, Drugs for Neglected Diseases Initiative (DNDi), Geneva, Switzerland, [4]Strategy, Unitaid, Geneva, Switzerland, [5]Section of Clinical Immunology and Infectious Diseases, Oslo University Hospital, Oslo, Norway

KEYWORDS

COVID-19, direct-acting antivirals, immunocompromised, resistance, variant emergence, monoclonal antibodies, omicron, variants

Introduction

Monoclonal antibodies targeting the anti-SARS-CoV-2 spike (S) protein are prescribed in high-income countries to prevent severe disease in at-risk patients. Although studies report efficacy as between 50–85% (Weinreich et al., 2021; Gupta et al., 2022; Montgomery et al., 2022), global access is currently largely inequitable (Wiltz et al., 2022). Multivariant omicron (B.1.1.529) and subvariant (BA.2 followed by BA.4 and BA.5) dominance has challenged the treatment landscape for mild-to-moderate disease, introducing considerable uncertainty on the efficacy of monoclonal antibodies (Cao et al., 2022; Yamasoba et al., 2022) and leading to changes to initial recommendations for some of them (United States Food Drug Administration, 2022). Contemporaneously, oral, direct-acting antivirals with a reported efficacy ranging from 30% (molnupiravir) (Jayk Bernal et al., 2022) to 89–90% (nirmatrelvir/ritonavir) (United States Food Drug Administration, 2021) have recently received conditional or emergency approval in some countries and been recommended in international guidelines such as the World Health Organization guidelines (World Health Organization, 2022). S-217622, also known as ensitrelvir, a 3CL protease inhibitor that has been shown to significantly reduce the infectious viral load (Mukae et al., 2022a,b), is currently in phase 3 trials and waiting for emergency approval in Japan (Otake, 2022) and should be submitted soon in China (Notice Regarding the Initiation of the Submission of Preparation Materials for a New Drug Application for S-217622, a Therapeutic Drug for COVID-19, in China, 2022). The main purpose of this opinion paper is to highlight the possible strategies to optimize and protect current and future therapeutic options to treat the most vulnerable patients.

Protecting emerging treatment options

Several crucial issues warrant urgent attention to optimize the use of these emerging treatment options (Figure 1). First, as proven to be transformational for HIV, rapid, affordable access to early antiviral treatment to slow the tide of new variants is critical to effective "test-and-treat" strategies to protect the most fragile patients and avoid a severe and/or persistent infection. After more than 2 years of pandemic, progress has been slow (Hasan et al., 2022) and public health attention has recently been attracted by the low-profile agreement during the (World Trade Organization, 2022) in Geneva in May 2022 (Financial Times, 2022). Together with vaccination, early diagnosis and treatment have the ability to reduce disease worsening, to reduce transmission and to constrain variability in viral sequences (United Kingdom Scientific Advisory Group for Emergencies, 2021).

Second, although the combined effect of omicron and increasing vaccine deployment in some regions has shifted the demand response from hospital to outpatient care, considerable uncertainty exists about who is now at risk for severe omicron disease (Skarbinski et al., 2022). While the risk/benefit ratio across at-risk subpopulations has unquestionably changed in vaccinated populations, gains made can only be preserved if those at highest risk are rapidly diagnosed and receive treatment in less than one week.

Third, high levels of antiviral efficacy will be critically important, especially in immunocompromised patients who are grossly underrepresented in registrational trials (John and John, 2020; Trøseid et al., 2022). Causes of immunosuppression are diverse (including organ/stem cell transplants, cancer, immunosuppressive medications or uncontrolled HIV) and these patients represent a significant proportion of the population, e.g., 7 million adults in the USA (Harpaz et al., 2016), but also in low- and middle-income countries due to the high prevalence of uncontrolled HIV. Overall, the mortality risk with omicron is still unclear, but protection of those who cannot be effectively vaccinated or protected by a prior SARS-CoV-2 infection remains imperative (Overvad et al., 2022). Importantly, in regions where HIV is highly prevalent, there is a clear need and opportunity to reinforce HIV epidemic control by prompt diagnosis and sustained viral suppression with antiretrovirals, key factors to also enable the control of SARS COV-2 spread in this group (Msomi et al., 2021; Meiring et al., 2022).

Although there are many other causes for variant emergence (host jump or adaptation, vaccine exposure, to name the most frequent), data confirm that immunocompromised patients with long-term SARS-CoV-2 replication are particularly susceptible to resistance and transmissible variant emergence (Clark et al., 2021; Destras et al., 2022; Quaranta et al., 2022; Sabin et al., 2022). The emergence of resistance mutation thus impacting treatment efficacy is more likely if a patient has been exposed to specific antiviral drugs. In addition, it remains unclear if the small percent rebound occurrence (2%) observed with nirmatrelvir/r in the EPIC-HR (Evaluation of Protease Inhibition for COVID-19 in High-Risk Patients) trial, performed in the delta variant era, is underestimating a risk (Boucau et al., 2022; Rubin, 2022) that would be particularly of concern in patients harboring an impaired immune system and in the omicron era. In one recent case series, one out of 7 patients who had a virologic rebound also had an immunosuppressing condition (Boucau et al., 2022). Another recent case series (Coulson et al., 2022) revealed that all three patients with viral rebound were highly immunocompromised. This potentially raises concerns about the need of longer antiviral courses, especially in these patients.

Preclinical data have clearly demonstrated that virological efficacy is higher for combinations of existing antiviral drugs than single agents (Abdelnabi et al., 2021; Jeong et al., 2022; Li et al., 2022). To achieve the goal of changing the treatment guidelines in SARS-CoV-2-infected immunocompromised individuals, independent and academic clinical trials for drug combinations should be considered as an urgent, unmet research priority. Today, collaboration with industry to allow early access to antiviral drugs to be combined has been an objective still to be achieved (Bloomberg (Europe Edition), 2022). Certain potent monoclonal antibodies, such as bebtelovimab, cannot even be accessed for research or for routine care outside of the USA (Hentzien et al., 2022).

Expert opinion

Treatment optimization has been truly transformational for other viral diseases [e.g., HIV/hepatitis C virus (Cohen et al., 2011)] and was only achieved when antiviral drug combinations became the mainstay. With few drugs currently available, the opportunity must be seized prior to the emergence of resistance to drugs deployed widely as monotherapies. Combinations of polymerase inhibitors and polymerase/protease inhibitors have proven highly successful for other viruses and in animal models for SARS-CoV-2 (Abdelnabi et al., 2021; Jeong et al., 2022). Thus, as drugs that are appropriate to combine are available, there is no good reason not to study them clinically. In addition to the opportunities that combinations present for a more potent antiviral response (individual benefit), there can be no doubt that the rate at which resistance emerges will also be reduced (public health benefit). Higher potency will result in a lower variability in sequences through a lower degree of replication. In addition, the probability of the occurrence of multiple mutations to drive resistance to multiple antivirals simultaneously is much lower than for a

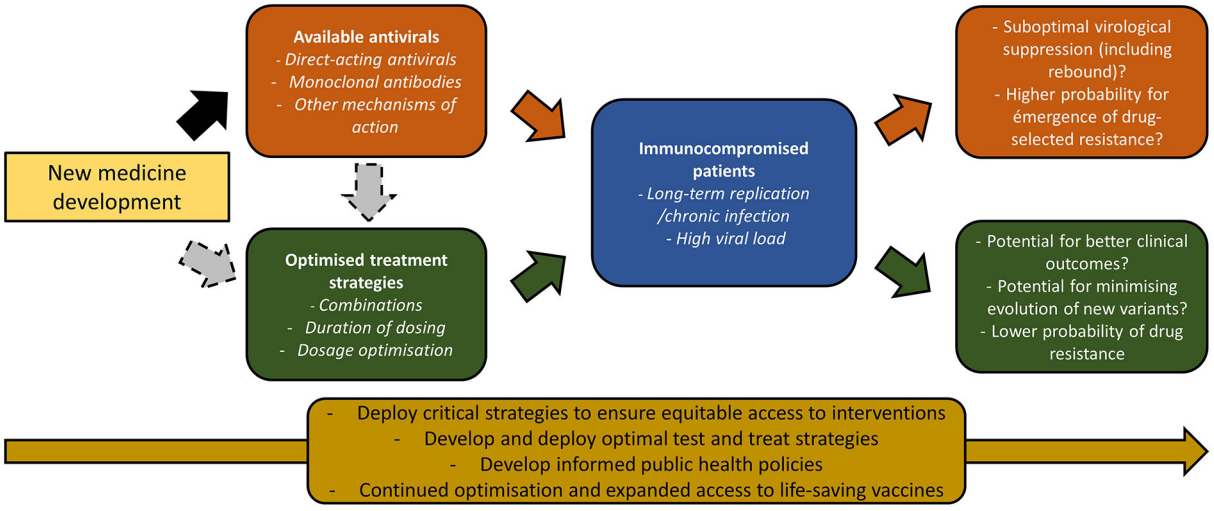

FIGURE 1
Potential impact of SARS-CoV-2 antiviral drugs optimization in protecting available antivirals in the shifting landscape of new variants.

single agent (United States Food Drug Administration, 2021). This is particularly the case where concentrations achieved are close to the therapeutic efficacy threshold or in the case of low compliance.

It is incumbent upon the international research community and the pharmaceutical industry to pool knowledge and provide the critical information that the World Health Organization and country-level authorities so urgently require, as well as early diagnosis and increased access to vaccines and antiviral therapy. The resistance risk for existing drugs has been woefully understudied throughout development, making it extremely challenging to rationalize during policy development. Looking beyond efficacy, drug combinations will unquestionably reduce the rate at which resistance and new variants impacting treatment options emerge and could be made available and accessible to those in need if timely efforts are made.

In conclusion, we call for combination therapies to be tested in adequately powered clinical trials in the target population of immunocompromised patients, both in wealthy and in low-income countries where HIV-driven immunosuppression is prevalent. If higher efficacy is confirmed, the diversity of possible combinations will enable the tailoring of therapeutic options to individual patient needs (e.g., avoiding drug-drug interactions in transplant patients) as well as their specific regional context (e.g., oral-only combinations).

Author contributions

MH and AC wrote the first manuscript draft. All authors critically reviewed the manuscript, validated the final version, and agreed to be accountable for the content of the work.

Acknowledgments

We thank Rosemary Sudan for revision of the English.

Conflict of interest

The authors declare that the research was conducted in the absence of any commercial or financial relationships that could be construed as a potential conflict of interest.

Publisher's note

All claims expressed in this article are solely those of the authors and do not necessarily represent those of their affiliated organizations, or those of the publisher, the editors and the reviewers. Any product that may be evaluated in this article, or claim that may be made by its manufacturer, is not guaranteed or endorsed by the publisher.

References

Abdelnabi, R., Foo, C. S., Kaptein, S. J. F., Zhang, X., Do, T. N. D., Langendries, L., et al. (2021). The combined treatment of Molnupiravir and Favipiravir results in a potentiation of antiviral efficacy in a SARS-CoV-2 hamster infection model. *eBioMedicine* 72, 103595. doi: 10.1016/j.ebiom.2021.103595

Bloomberg (Europe Edition) (2022). Pfizer's Grip on Paxlovid Thwarts Research on Covid Treatment. Bloomberg.com. Available online at: https://www.bloomberg.com/news/articles/2022-05-18/pfizer-s-tight-paxlovid-rein-stymies-drug-combination-research (accessed July 14, 2022).

Boucau, J., Uddin, R., Marino, C., Regan, J., Flynn, J. P., Choudhary, M. C., et al. (2022). Characterization of virologic rebound following nirmatrelvir-ritonavir treatment for COVID-19. *Clin. Infect. Dis.* doi: 10.1101/2022.05.24.22275326

Cao, Y., Yisimayi, A., Jian, F., Song, W., Xiao, T., Wang, L., et al. (2022). BA.2.12.1, BA.4 and BA.5 escape antibodies elicited by Omicron infection. *Nature*. 608, 593–602. doi: 10.1101/2022.04.30.489997

Clark, S. A., Clark, L. E., Pan, J., Coscia, A., McKay, L. G. A., Shankar, S., et al. (2021). SARS-CoV-2 evolution in an immunocompromised host reveals shared neutralization escape mechanisms. *Cell*. 184, 2605–2617.e18. doi: 10.1016/j.cell.2021.03.027

Cohen, M. S., Chen, Y. Q., McCauley, M., Gamble, T., Hosseinipour, M. C., Kumarasamy, N., et al. (2011). Prevention of HIV-1 infection with early antiretroviral therapy. *N. Engl. J. Med*. 365, 493–505. doi: 10.1056/NEJMoa1105243

Coulson, J. M., Adams, A., Gray, L. A., and Evans, A. (2022). COVID-19 "Rebound" associated with nirmatrelvir/ritonavir pre-hospital therapy. *J. Infect*. 85, 436–480 doi: 10.1016/j.jinf.2022.06.011

Destras, G., Bal, A., Simon, B., Lina, B., and Josset, L. (2022). Sotrovimab drives SARS-CoV-2 omicron variant evolution in immunocompromised patients. *Lancet Microbe*. 3, e559. doi: 10.1016/S2666-5247(22)00120-3

Financial Times (2022). WTO agrees partial patent waiver for Covid-19 vaccines [Internet]. June 17. Available online at: https://www.swissinfo.ch/eng/business/wto-agrees-partial-patent-waiver-for-covid-19-vaccines/47681524 (accessed July 7, 2022).

Gupta, A., Gonzalez-Rojas, Y., Juarez, E., Crespo Casal, M., Moya, J., Rodrigues Falci, D., et al. (2022). Effect of sotrovimab on hospitalization or death among high-risk patients with mild to moderate COVID-19: a randomized clinical trial. *JAMA* 327, 1236–1246. doi: 10.1001/jama.2022.2832

Harpaz, R., Dahl, R. M., and Dooling, K. L. (2016). Prevalence of immunosuppression among US adults, 2013. *JAMA* 316, 2547. doi: 10.1001/jama.2016.16477

Hasan, Q., Elfakki, E., Fahmy, K., Mere, O., Ghoniem, A., Langar, H., et al. (2022). Inequities in the deployment of COVID-19 vaccine in the WHO Eastern Mediterranean Region, 2020-2021. *BMJ Glob. Health.* 7 (Suppl 4), e008139.

Hentzien, M., Autran, B., Piroth, L., Yazdanpanah, Y., and Calmy, A. (2022). A monoclonal antibody stands out against omicron subvariants: a call to action for a wider access to bebtelovimab. *Lancet Infect. Dis*. 22, 1278. doi: 10.1016/S1473-3099(22)00495-9

Jayk Bernal, A., Gomes da Silva, M. M., Musungaie, D. B., Kovalchuk, E., Gonzalez, A., Delos Reyes, V., et al. (2022). Molnupiravir for oral treatment of Covid-19 in nonhospitalized patients. *N. Engl. J. Med.* 386, 509–520. doi: 10.1056/NEJMoa2116044

Jeong, J. H., Chokkakula, S., Min, S. C., Kim, B. K., Choi, W.-S., Oh, S., et al. (2022). Combination therapy with nirmatrelvir and molnupiravir improves the survival of SARS-CoV-2 infected mice. *BioRxiv*. doi: 10.1101/2022.06.27.497875

John, N. A., and John, J. E. (2020). Implications of COVID-19 infections in sickle cell disease. *Pan. Afr. Med. J.* 36, 81. doi: 10.11604/pamj.2020.36.158.24011

Li, P., Wang, Y., Lavrijsen, M., Lamers, M. M., de Vries, A. C., Rottier, R. J., et al. (2022). SARS-CoV-2 Omicron variant is highly sensitive to molnupiravir, nirmatrelvir, and the combination. *Cell Res.* 32, 322–324. doi: 10.1038/s41422-022-00618-w

Meiring, S., Tempia, S., Bhiman, J. N., Buys, A., Kleynhans, J., Makhasi, M., et al. (2022). Prolonged shedding of SARS-CoV-2 at high viral loads amongst hospitalised immunocompromised persons living with HIV, South Africa. *Clin. Infect. Dis*. 116, S25. doi: 10.1093/cid/ciac077

Montgomery, H., Hobbs, F. D. R., Padilla, F., Arbetter, D., Templeton, A., Seegobin, S., et al. (2022). Efficacy and safety of intramuscular administration of tixagevimab–cilgavimab for early outpatient treatment of COVID-19 (TACKLE): a phase 3, randomised, double-blind, placebo-controlled trial. *Lancet Respir. Med*. 10, 985–996. doi: 10.1016/S2213-2600(22)00180-1

Msomi, N., Lessells, R., Mlisana, K., and de Oliveira, T. (2021). Africa: tackle HIV and COVID-19 together. *Nature* 600, 33–36. doi: 10.1038/d41586-021-03546-8

Mukae, H., Yotsuyanagi, H., Ohmagari, N., Doi, Y., Imamura, T., Sonoyama, T., et al. (2022a). A randomized phase 2/3 study of ensitrelvir, a novel oral SARS-CoV-2 3C-like protease inhibitor, in japanese patients with mild-to-moderate COVID-19 or asymptomatic SARS-CoV-2 infection: results of the phase 2a part. *Antimicrob. Agents Chemother*. doi: 10.1128/aac.00697-22. [Epub ahead of print].

Mukae, H., Yotsuyanagi, H., Ohmagari, N., Doi, Y., Sakaguchi, H., Sonoyama, T., et al. (2022b). Efficacy and safety of ensitrelvir in patients with mild-to-moderate COVID-19: the phase 2b part of a randomized, placebo-controlled, phase 2/3 study. *MedRxiv [Preprint]*. doi: 10.1101/2022.06.22.22276792

Notice Regarding the Initiation of the Submission of Preparation Materials for a New Drug Application for S-217622, a Therapeutic Drug for COVID-19, in China. (2022). [Internet] 4 July. Available online at: https://www.shionogi.com/global/en/news/2022/07/e220704.html (accessed July 7, 2022).

Otake, T. (2022). Japanese panel postpones verdict on Shionogi's COVID pill until July. *The Japan Times*. 23 June. Available online at: https://www.japantimes.co.jp/news/2022/06/23/national/science-health/shionogi-covid19-pill-verdict-delay/ (accessed July 7, 2022).

Overvad, M., Koch, A., Jespersen, B., Gustafsson, F., Krause, T. G., Hansen, C. H., et al. (2022). Outcomes following SARS-CoV-2 infection in individuals with and without solid organ transplantation; a Danish nationwide cohort study. *Am. J. Transplant*. doi: 10.1111/ajt.17142. [Epub ahead of print].

Quaranta, E. G., Fusaro, A., Giussani, E., D'Amico, V., Varotto, M., Pagliari, M., et al. (2022). SARS-CoV-2 intra-host evolution during prolonged infection in an immunocompromised patient. *Int. J. Infect. Dis.* 122, 444–448. doi: 10.1016/j.ijid.2022.06.023

Rubin, R. (2022). From positive to negative to positive again-the mystery of why COVID-19 rebounds in some patients who take paxlovid. *JAMA* 327, 2380–2382. doi: 10.1001/jama.2022.9925

Sabin, A. P., Richmond, C. S., and Kenny, P. A. (2022). Emergence and onward transmission of a SARS-CoV-2 E484K variant among household contacts of a bamlanivimab-treated patient. *Diagn. Microbiol. Infect. Dis.* 103, 115656. doi: 10.1016/j.diagmicrobio.2022.115656

Skarbinski, J., Wood, M. S., Chervo, T. C., Schapiro, J. M., Elkin, E. P., Valice, E., et al. (2022). Risk of severe clinical outcomes among persons with SARS-CoV-2 infection with differing levels of vaccination during widespread Omicron (B.1.1.529) and Delta (B.1.617.2) variant circulation in Northern California: A retrospective cohort study. *Lancet Reg. Health Am.* 12, 100297. doi: 10.1016/j.lana.2022.100297

Trøseid, M., Hentzien, M., Ader, F., Cardoso, S. W., Arribas, J. R., Molina, J.-M., et al. (2022). Immunocompromized patients have been neglected in Covid-19 trials: A call for action. *Clin. Microbiol. Infect*. 28, 1182–1183. doi: 10.1016/j.cmi.2022.05.005

United Kingdom Scientific Advisory Group for Emergencies (2021). NERVTAG: Antiviral drug resistance and the use of directly acting antiviral drugs (DAAs) for COVID-19, 8 December 2021 [Internet]. Available online at: https://www.gov.uk/government/publications/nervtag-antiviral-drug-resistance-and-the-use-of-directly-acting-antiviral-drugs-daas-for-covid-19-8-december-2021/nervtag-antiviral-drug-resistance-and-the-use-of-directly-acting-antiviral-drugs-daas-for-covid-19-8-december-2021 (accessed February 11, 2022).

United States Food and Drug Administration (2021). Coronavirus (COVID-19) Update: FDA Authorizes First Oral Antiviral for Treatment of COVID-19. *FDA*. Available online at: https://www.fda.gov/news-events/press-announcements/coronavirus-covid-19-update-fda-authorizes-first-oral-antiviral-treatment-covid-19 (accessed February 11, 2022).

United States Food and Drug Administration (2022). FDA updates Sotrovimab emergency use authorization. FDA. Available online at: https://www.fda.gov/drugs/drug-safety-and-availability/fda-updates-sotrovimab-emergency-use-authorization (accessed May 15, 2022).

Weinreich, D. M., Sivapalasingam, S., Norton, T., Ali, S., Gao, H., Bhore, R., et al. (2021). REGEN-COV antibody combination and outcomes in outpatients with Covid-19. *New Engl. J. Med.* 38, e8. doi: 10.1056/NEJMoa2035002

Wiltz, J. L., Feehan, A. K., Molinari, N. M., Ladva, C. N., Truman, B. I., Hall, J., et al. (2022). Racial and ethnic disparities in receipt of medications for treatment of COVID-19 — United States, March 2020–August 2021. *Morb. Mortal. Wkly. Rep.* 71, 96–102. doi: 10.15585/mmwr.mm7103e1

World Health Organization (2022). Therapeutics and COVID-19: living guideline Available online at: https://app.magicapp.org/#/guideline/nBkO1E (accessed July 18, 2022).

World Trade Organization (2022). Draft texts on WTO response to pandemic, IP response sent to ministers for decision [Internet]. 10 June. Available online at: https://www.wto.org/english/news_e/news22_e/covid_10jun22_e.htm (accessed July 7, 2022).

Yamasoba, D., Kosugi, Y., Kimura, I., Fujita, S., Uriu, K., Ito, J., et al. (2022). Neutralisation sensitivity of SARS-CoV-2 omicron subvariants to therapeutic monoclonal antibodies. *Lancet Infect. Dis.* 22, 942–943. doi: 10.1016/S1473-3099(22)00365-6

frontiers | Frontiers in Microbiology

TYPE Review
PUBLISHED 28 November 2022
DOI 10.3389/fmicb.2022.1042200

OPEN ACCESS

EDITED BY
Jian Shang,
Zhengzhou University, China

REVIEWED BY
Kirsty Pringle,
The University of Newcastle, Australia
Dulce Elena Casarini,
Federal University of São Paulo, Brazil

*CORRESPONDENCE
Christian A. Devaux
christian.devaux@
mediterranee-infection.com

SPECIALTY SECTION
This article was submitted to Virology, a section of the journal Frontiers in Microbiology

RECEIVED 12 September 2022
ACCEPTED 07 November 2022
PUBLISHED 28 November 2022

CITATION
Devaux CA and Camoin-Jau L (2022) An update on angiotensin-converting enzyme 2 structure/functions, polymorphism, and duplicitous nature in the pathophysiology of coronavirus disease 2019: Implications for vascular and coagulation disease associated with severe acute respiratory syndrome coronavirus infection. *Front. Microbiol.* 13:1042200. doi: 10.3389/fmicb.2022.1042200

An update on angiotensin-converting enzyme 2 structure/functions, polymorphism, and duplicitous nature in the pathophysiology of coronavirus disease 2019: Implications for vascular and coagulation disease associated with severe acute respiratory syndrome coronavirus infection

Christian A. Devaux[1,2]* and Laurence Camoin-Jau[1,3]

[1]Aix-Marseille Université, IRD, APHM, MEPHI, IHU–Méditerranée Infection, Marseille, France, [2]Center National de la Recherche Scientifique, Marseille, France, [3]Laboratoire d'Hématologie, Hôpital de La Timone, APHM, Boulevard Jean-Moulin, Marseille, France

It has been known for many years that the angiotensin-converting enzyme 2 (ACE2) is a cell surface enzyme involved in the regulation of blood pressure. More recently, it was proven that the severe acute respiratory syndrome coronavirus (SARS-CoV-2) interacts with ACE2 to enter susceptible human cells. This functional duality of ACE2 tends to explain why this molecule plays such an important role in the clinical manifestations of coronavirus disease 2019 (COVID-19). At the very start of the pandemic, a publication from our Institute (entitled "ACE2 receptor polymorphism: susceptibility to SARS-CoV-2, hypertension, multi-organ failure, and COVID-19 disease outcome"), was one of the first reviews linking COVID-19 to the duplicitous nature of ACE2. However, even given that COVID-19 pathophysiology may be driven by an imbalance in the renin-angiotensin system (RAS), we were still far from understanding the complexity of the mechanisms which are controlled by ACE2 in different cell types. To gain insight into the physiopathology of SARS-CoV-2 infection, it is essential to consider the polymorphism and expression levels of the *ACE2* gene (including its alternative isoforms). Over the past 2years, an impressive amount of new results have come to shed light on the role of ACE2 in the pathophysiology of COVID-19, requiring us to update our analysis. Genetic linkage studies have been reported that highlight a relationship between ACE2 genetic variants and the risk of developing hypertension. Currently, many research efforts are being undertaken to understand the links between ACE2 polymorphism and the severity of COVID-19. In this review, we update the state of knowledge on

the polymorphism of ACE2 and its consequences on the susceptibility of individuals to SARS-CoV-2. We also discuss the link between the increase of angiotensin II levels among SARS-CoV-2-infected patients and the development of a cytokine storm associated microvascular injury and obstructive thrombo-inflammatory syndrome, which represent the primary causes of severe forms of COVID-19 and lethality. Finally, we summarize the therapeutic strategies aimed at preventing the severe forms of COVID-19 that target ACE2. Changing paradigms may help improve patients' therapy.

KEYWORDS

ACE2, renin-angiotensin system, hypertension, coagulation, coronavirus—COVID-19, therapy

Introduction

Present in a large number of tissues, including endothelial cells of the arteries, arterioles, and venules of the heart and kidney, angiotensin-converting enzyme 2 (ACE2) is a fascinating molecule which plays a crucial role in maintaining blood pressure homeostasis. ACE2 is only one of the actors in a complex biological network known as the renin-angiotensin system (RAS). ACE2 mainly exerts its functions by regulating the ratio of two major mediators: angiotensin II (Ang II) and angiotensin-[1–7; Ang-(1–7)]. Ang II synthesis is catalyzed by angiotensin-converting enzyme (ACE) while Ang-(1–7) is obtained after hydrolysis of Ang II by ACE2. Ang-(1–7) can also be generated from Ang-(1–9) formed after the action of ACE2 on Ang I by the action of ACE itself. Despite their contrasting physiological functions, the ACE2 is considered to have evolved through ACE gene duplication and exhibits 42% amino acid homology with ACE (Donoghue et al., 2000; Turner and Hooper, 2002; Towler et al., 2004).

Besides being widely studied in cardiology, ACE2 became attractive for other fields of medical sciences and, particularly, virology (Devaux et al., 2020). In 2003 a novel coronavirus infecting humans, the severe acute respiratory syndrome coronavirus (SARS-CoV, provisionally renamed SARS-CoV-1) emerged in Asia, causing an outbreak of severe pneumopathy (Ksiazek et al., 2003; Marra et al., 2003; Rota et al., 2003). ACE2 was demonstrated to be the cellular receptor for SARS-CoV-1, as it had been previously reported for another coronaviruses infecting humans, HCoV-NL63, a coronavirus causing the common winter cold (Hofmann et al., 2005; Li et al., 2007; Ge et al., 2013; Graham et al., 2013). In 2019, new cases of severe pneumopathy were reported in China, with the disease being characterized by a multiple organ dysfunction syndrome (MODS) as well as acute respiratory distress syndrome (ARDS) sometimes requiring the need for ventilation or extracorporeal membrane oxygenation (ECMO). The severe forms of the disease lead to death in ∼ 0.5–2.5% of cases, with a high fatality risk increasing with age and the existence of underlying comorbidities (Huang et al., 2020; Zhou et al., 2020; Zhu et al., 2020). Under chest computerized tomography (CT) scans, the majority of patients show bilateral ground glass-like opacities and subsegmental areas of consolidation indicative of pneumonia. This disease was later defined as COVID-19, the aetiological agent of which was found to be a new human coronavirus named severe acute respiratory syndrome coronavirus (SARS-CoV-2). Although not highly symptomatic for the majority of those infected, the virus has spread worlwide causing more than 6 million deaths for ∼603 million reported cases of infections (World Health Organization COVID-19 Dashboard on 6 September 2022; https://covid19.who.int/). SARS-CoV-2 shares 79.5% nucleotide identity with SARS-CoV-1, and both these Sarbecoviruses isolated from humans are genetically close to coronaviruses circulating in wildlife (Ge et al., 2013; Afelt et al., 2018; Wang et al., 2020; Zhou et al., 2020; Frutos et al., 2021). Once SARS-CoV-2 was characterized, the search for its cellular receptor became a priority. Due to the sequence similarity between SARS-CoV-1 and SARS-CoV-2, studies quickly focused on ACE2 and the role of this molecule as a viral entry receptor was demonstrated (Qiu et al., 2020; Yan et al., 2020).

Due to the central role played by ACE2 in maintaining blood pressure homeostasis, the objective of this work is to review the state of knowledge regarding the possible imbalance of the RAS in the context of a SARS-CoV-2 infection and to highlight the role of ACE2 in SARS-CoV-2 infection and replication, as well as its contribution in the severity of COVID-19.

The renin-angiotensin system: A molecular network which regulates blood pressure homeostasis and ion-fluid balance

In humans and other mammals, intravascular RAS plays a key role in maintaining blood pressure homeostasis as well as fluid and salt balance, while tissue RAS is mainly involved in the pathogenesis of inflammatory diseases (Paul et al., 2006; Greenberg, 2008; de Kloet et al., 2010). The kidneys, as a sensor of

ion fluid balance and producer of renin, play a fundamental role in the long-term control of arterial pressure (Tigerstedt and Bergman, 1898; Phillips and Schmidt-Ott, 1999; Yim and Yoo, 2008; Prieto et al., 2011; Gonzalez et al., 2017). Active renin is secreted into the blood circulation in response to hypotension or hypernatremia. Upon activation of the juxtaglomerular apparatus of the kidneys' afferent arterioles, proteases (proconvertase 1, cathepsin B) catalyze the removal of the 20-amino-acid terminal prosegment of prorenin to produce a polypeptide composed of 297 amino-acids (Davis and Freeman, 1976; Hadman et al., 1984; Cohen-Haguenauer et al., 1989; Sealey and Rubattu, 1989; Neves et al., 1996; Muller et al., 1999). The active form of renin cleaves the alpha-globulin angiotensinogen (formerly angiotonin, a 118-amino-acid-long polypeptide), giving rise to angiotensin I (Ang I), the N-terminal decapeptide of angiotensinogen (Goldblatt et al., 1934; Page and Helmer, 1940; James and Sielecki, 1985). The conversion of Ang I (Asp-Arg-Val-Tyr-Ile-His-Pro-Phe-His-Leu) to the octapeptide Ang II (Asp-Arg-Val-Tyr-Ile-His-Pro-Phe), requires the cleavage of its C-terminal dipeptide catalyzed by ACE (provisionally named ACE1) expressed at the endothelial surface of the blood vessels, epithelium of the lungs and upper respiratory system (Skeggs et al., 1956; Crisan and Carr, 2000; Wakahara et al., 2007). The vasoconstrictor octapeptide Ang II was evidenced to be a substrate for ACE2, which acts as an essential factor in the RAS pathway homeostasis. By removing a single residue phenylalanine (Phe) from Ang II, the membrane form of ACE2 (mACE2) plays a central role in the synthesis of the cardiovascular protective heptapeptide Ang-(1–7) that acts by limiting the adverse vasoconstrictor and profibrotic effects of Ang II and reduces the oxidative stress of Ang II on endothelial arteries (Crackower et al., 2002; Pena Silva et al., 2012). ACE2 can also catalyze the conversion of Ang I to Ang-(1–9) by removing the C-terminal leucine (Leu) residue of Ang I, but with a catalytic efficiency ~ 400-fold lower than the hydrolysis of Ang II to produce Ang-(1–7). Besides Ang II and Ang I, ACE2 can cleave several other substrates including des-Arg9-bradykinin (DABK), apelin-13, and dynorphin A-(1–13; Skidgel and Erdos, 1987; Ferrario et al., 1997; Vickers et al., 2002; Oudit et al., 2003) In addition to its membrane form, ACE2 can be found in a soluble form (sACE2) and increasing sACE2 has been reported in patients with cardiomyopathies and heart failure (Epelman et al., 2008). In patients with aortic stenosis, increasing levels of sACE2 associated with reduced myocardial *ACE2* gene expression and severe myocardial fibrosis is considered as a death risk biomaker (Rajagopal et al., 2010). Thus, increased sACE2 plasma levels have been associated with heart failure, cardiovascular disease, and cardiac remodeling (Epelman et al., 2009; Sama et al., 2020; Garcia-Escobar et al., 2021). Using animal models, it was shown that knocking out (KO) of the *ACE2* gene results in increased levels of Ang II, followed by vasoconstriction reducing coronary blood flow and leading to cardiac dysfunction (Danilczyk et al., 2003). The expression of mACE2 in the kidneys and heart is influenced by salt rich and/or glucose-rich diets, and can be correlated with pathological disorders (Reich et al., 2008; Lavrentyev and Malik, 2009; Bernardi et al., 2012; Wysocki et al., 2013). In the respiratory tract, DABK is a substrate of mACE2 and a decrease in ACE2 could lead to an increase in vascular permeability and fluid extravasation (Chung et al., 2020). Using a mouse animal model, it was found that loss of ACE2 led to activation of the DABK/braddykinin receptor B1 (BKB1R) axis associated with release of proinflammatory chemokines (e.g., CXCL5, MIP2, and TNFα) and increase in neutrophil infiltration (Sodhi et al., 2017).

Resulting from the cleavage of Ang II by the mACE2 protease, Ang-(1–7) exhibits vasodilatory, anti-proliferative, anti-inflammatory, and antifibrotic effects *via* the G protein-coupled receptor (GPGR) known as Mas 1 (Santos et al., 2003, 2018; Simoes e Silva et al., 2013; Patel et al., 2016; Karnik et al., 2017; Bader et al., 2018). However, biochemical studies have failed to demonstrate a direct interaction between Ang-(1–7) and Mas1 (Gaidarov et al., 2018). In addition to mACE2, several peptidases, including vascular endothelium prolyl peptidases, neprilysin (NEP), and smooth muscle thimet oligopeptidase, can produce Ang-(1–7; Chappell, 2019). NEP and thimet oligopeptides produce Ang-(1–7) directly from Ang I. Ang-(1–7) has been shown to potentiate bradykinin (BK 1–9), a potent vasodilator of the kinin system which mediates its effects through the B2 receptor (BKB2R) abundant in vascular tissue (Jackman et al., 2002). ACE2 overexpression and Ang-(1–7) infusion have beneficial effects on atherosclerosis, whereas ACE2 deficiency accentuates vascular atherosclerosis in animal models (Dong et al., 2008; Thomas et al., 2010; Yang et al., 2013). The up-regulation of the ACE2/Ang-(1–7)/MasR axis promotes the expression of E-cadherin (E-cad) adhesion molecules by suppressing the PAK1/NF-κB/Snail1 pathway (Yu et al., 2016). Moreover, Ang-(1–7) can exert cerebroprotective functions in endothelin-1-induced ischaemic stroke (Mecca et al., 2011).

For many years, it has been known that there is cross-talk between insulin and the RAS, providing possible links between hypertension, obesity, and diabetes (Alderman et al., 1991; Frederich et al., 1992; Velloso et al., 1996; Boustany et al., 2004; Schmieder et al., 2007). Moreover, a low expression of ACE2 mRNA or protein is associated with an increase in AngII levels, hypertension, diabetes and heart disease (Crackower et al., 2002; Diez-Freire et al., 2006; Tikellis et al., 2012; Velkoska et al., 2016). Interestingly, these diseases are the major comorbidities in the severe forms of COVID-19 (Bavishi et al., 2020). The occurrence of specific comorbidities associated with an RAS imbalance could be decisive for the clinical outcome of COVID-19 (Devaux et al., 2020; Rysz et al., 2021).

RAS imbalance and overproduction of harmful Ang II

Clinical investigations have provided convincing evidence that RAS imbalance is capable of stimulating atherosclerosis, which ultimately lead to the rupture of atherosclerosis plaques and

thrombosis (Schmidt-Ott et al., 2000; Jacoby and Rader, 2003; Verdecchia et al., 2008). Ang II is the main harmful effector molecule synthesized in excess in situations of RAS imbalance. Ang II, inactivates the vasodilator bradykinin and can control the ion-fluid balance by acting on the adrenal cortex to stimulate the release of aldosterone, leading to sodium and water retention (Jaspard et al., 1993; Brewster and Perazella, 2004; Xue et al., 2012; Aroor et al., 2016; Nishimura, 2017). The action of Ang II (proximal tubule) and aldosterone (collecting duct) are complementary to influence sodium reabsorption across the nephron (Gurley et al., 2011). Thereby, Ang II functions as a powerful regulator of vascular tone and intravascular volume. Increased circulating levels of Ang II is associated with vasoconstriction and hypertension and accelerates thrombosis in arterioles by activating the coagulation cascade and the platelet-derived growth factor (PDGF; Gustafsson and Holstein-Rathlou, 1999; Heeneman et al., 2000; Senchenkova et al., 2010, 2014; Singh and Karnik, 2016; Samavati and Uhal, 2020). It also induces hypertrophy of vascular smooth muscle cells (Berk et al., 1989; Griendling et al., 1997; Funakoshi et al., 2002). Ang II can also exert tissue-specific actions, such as neurotransmission inducing adipocytes growth in adipose tissues (Li and Ferguson, 1993; Massiéra et al., 2001).

These multiple effects of Ang II are obtained through its ability to bind to Ang II type I and type II receptors (AT1R and AT2R, respectively) expressed in arterioles and several organs including the kidney, pancreas, heart, and the brain. The AT1R, a 359-amino-acids protein spanning cell membrane, and AT2R have a 34% nucleic acid sequence homology (Arendse et al., 2019). Ang II can bind to both to AT1R and AT2R, which are receptors with opposite effects (i.e., AT1R mediates vasoconstriction, inflammation and fibrosis while AT2R mediates opposite effects). AT2R is poorly expressed compared to AT1R, which causes the Ang II to primarily exhibit an effect through AT1R (Murphy et al., 1991; de Gasparo et al., 2000; Forrester et al., 2018; Furuhashi et al., 2020). The activation of AT1R by Ang II is transient and associated with the phosphorylation of the receptor by kinases, including PKC and GRKs. The phosphorylated AT1R is internalized through a mechanism that involves β-arrestin 2, the adaptor protein complex 2 (APC2), clathrin, and intersectin 2 (AbdAlla et al., 2000; de Gasparo et al., 2000; Gáborik et al., 2001). These AT1R-mediated signals lead to overexpression of the prorenin receptor (PRR), thereby increasing renin activity and contributing to the local accumulation of Ang II, fibrosis, and hypertension (Nguyen et al., 2002; Advani et al., 2009; Peng et al., 2013; Wang et al., 2014; Xu et al., 2016; Ichihara and Yatabe, 2019). At the opposite, Ang II also exerts a negative feedback signaling on juxtaglomerular cells that reduces the *REN* gene transcription and renal renin secretion (Naftilan and Oparil, 1978).

The interaction of Ang II with AT1R functions as a pluripotent mediator to enhance oxidative injury by reactive oxygen species (ROS), and endothelial injury by inhibiting nitric oxide (NO) synthesis. Ang II is a potent activator of NADPH oxidase and an inducer of ROS (Garrido and Griendling, 2009). Interestingly, CHOP−/− mice are protected from Ang II-induced NADPH oxidase activation, hypertension, and cardiovascular disease (Kassan et al., 2016). This is consistent with the observation that Ang II increases the transcription of the *CHOP* and *ATF4* genes (Kassan et al., 2012; Spitler and Webb, 2014; Takayanagi et al., 2015). Activation of AT1R by Ang II also induces various signaling pathways, including G-protein-coupled receptors, PKC, serine/threonine kinase, serine tyrosine kinases, ERK/JNK activation, leading to proinflammatory responses characterized by the synthesis of IL-6, TNFα, and other cytokines (Sadoshima et al., 1995; Han et al., 1999; Nataraj et al., 1999; Ruiz-Ortega et al., 2001; Watanabe et al., 2005; Luther et al., 2006; Rushworth et al., 2008; Dikalov and Nazarewicz, 2013). Furthermore, Ang II activates the flow of neutrophils and macrophages to the affected tissues and inhibits the production of NO, leading to vascular injury (Nabah et al., 2004).

ACE2 tissue distribution in human

Angiotensin-converting enzyme 2 is expressed in virtually all organs with higher levels in capillary rich organs such as the lungs, heart, or kidneys (Donoghue et al., 2000; Tipnis et al., 2000; Ferrario and Varagic, 2010; Tikellis and Thomas, 2012; Figure 1). A study of ACE2 mRNA and protein in more than 150 cell types concluded that ACE2 is mainly observed in enterocytes, renal tubules, the gallbladder, cardiomyocytes, male reproductive cells, placental trophoblasts, ductal cells, eyes, and the vasculature. In the respiratory system, its expression was limited to a subset of cells (Hikmet et al., 2020).

Remarkably, in the upper airway, goblet and ciliated cells show the highest expression of ACE2 and are thought to play a major role in human infection with SARS-CoV-2. The expression of the mACE2 protein is highest within regions of the sinonasal cavity and pulmonary alveoli and in the lung parenchyma (Descamps et al., 2020; Ortiz et al., 2020). In normal human lungs, the mACE2 protein is found on a very small subset of alveolar type II epithelial lung cells (Ortiz et al., 2020; Delorey et al., 2021). Alveolar epithelial type II cells (which represent ~5% of the alveoli and serves at stem cells to generate type I alveolar epithelial cells), are thought to be a main target for SARS-CoV-2 in the respiratory tract and, consequently, can be destroyed during viral replication (Barkauskas et al., 2013). However, ACE2-positive cells are more abundant in the nasal mucosa than in the bronchus (Hikmet et al., 2020). Moreover, the mACE2 peptidase is also expressed in the arterial and venous endothelial cells present in abundance in the lungs and arterial smooth muscles (Hamming et al., 2004). Expression of ACE2 was found to be drastically increased in airway epithelial cells 24 h after SARS-CoV-1 infection (Li et al., 2020). In COVID-19 related ARDS, ACE2 was found to be upregulated in endothelial cells, but not in type II alveolar epithelial lung cells (Gerard et al., 2021).

The expression of ACE2 in the heart is higher than in the lungs and ACE2 is found in the endothelial cells of coronary

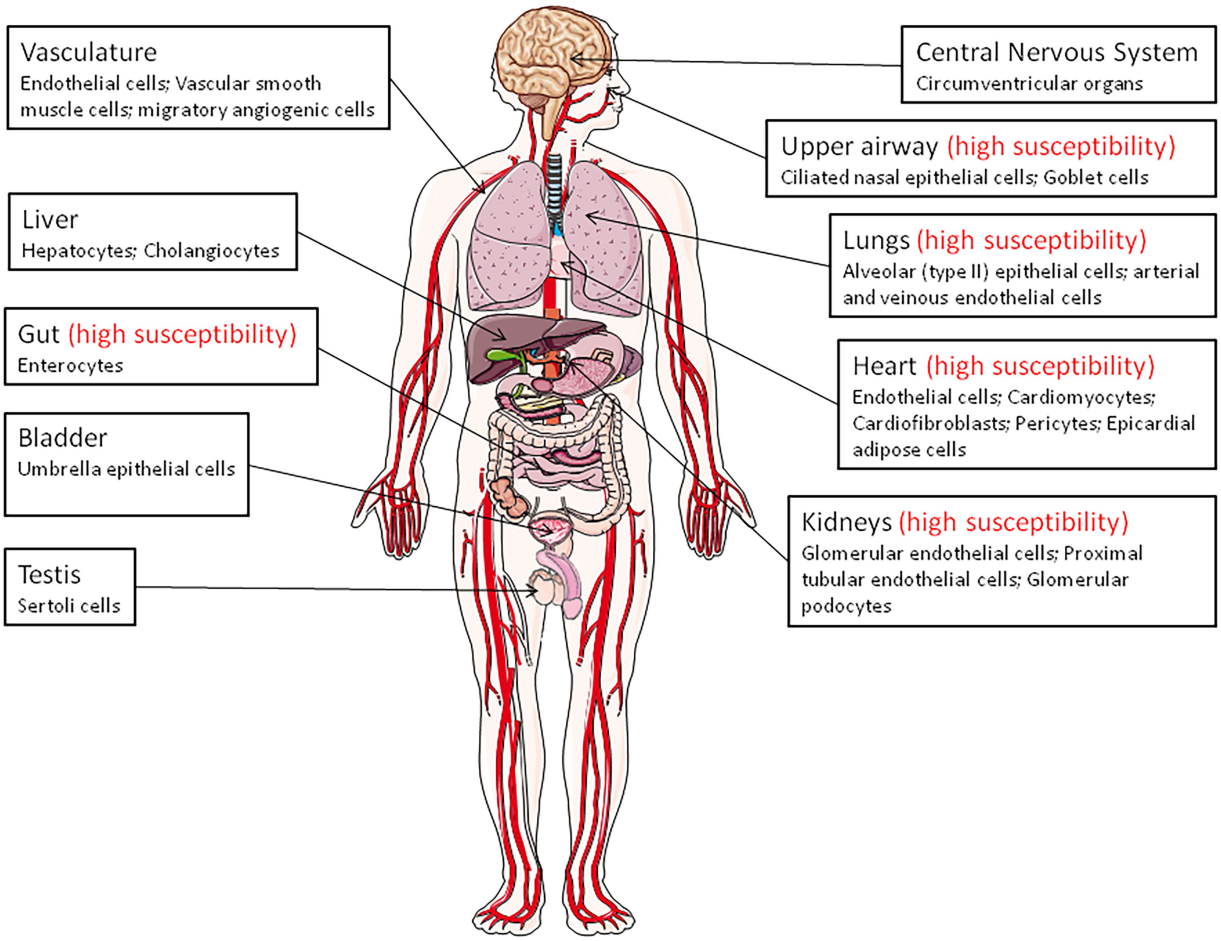

FIGURE 1
Angiotensin-converting enzyme 2 (ACE2) expression throughout the body (the main ACE2$^+$ target cells are indicated). The organs vulnerability to SARS-CoV-2 infection is also indicated (high susceptibility).

arteries, arterioles, venules, and capillaries (Danilczyk et al., 2003; Robinson et al., 2020). The mACE2 is strongly expressed in cardiomyocytes, endothelial cells, cardiac fibroblasts, vascular smooth muscle cells, and was also found in cardiac pericytes, which play crucial role in the microvasculature and may be the target for SARS-CoV-2 (Chen et al., 2020; Hikmet et al., 2020). Patients with heart failure show a significant increase in ACE2 mRNA expression (Goulter et al., 2004), suggesting that *ACE2* gene overexpression may explain why heart dysfunction is found within the list of COVID-19 comorbidities. In a rat model of diabetic cardiomyopathy, the overexpression of ACE2 attenuates cardiac hypertrophy, myocardial fibrosis, and dysfunction induced by diabetes (Dong et al., 2012). Post-mortem examinations of endomyocardial biopsies from COVID-19 patients highlighted the presence of SARS-CoV-2 in the myocardium (Lindner et al., 2020; Marchiano et al., 2021).

In the kidneys, ACE2 is expressed in the proximal tubule cells, epithelial cells of the Bowman's capsule, endothelial cells, mesengial cells (glomerulus central area), glomerular podocytes, proximal cell brush border, and cells from the collecting ducts (Aragao et al., 2011; Hikmet et al., 2020; Martinez-Rojas et al., 2020). Patients with diabetic or hypertensive nephropathy had lower glomerular ACE2 expression compared to healthy controls (Mizuiri et al., 2008; Wysocki et al., 2013). Between 3 and 10% of COVID-19 patients have abnormal renal function (diagnosed with elevated creatinine or urea nitrogen), and 7% experienced acute renal injury (Fan et al., 2021). In the pancreas, ACE2 plays a major glycemia-protective role (Pedersen et al., 2013). In testis, the Sertoli cells, which protect germ cells by forming blood-testis barrier, have a high expression of mACE2, suggesting that SARS-CoV-2 might cause reproductive disorders in infected patients (Shen et al., 2020; Fan et al., 2021).

A high expression of ACE2 was reported in the epithelial cells of the oral mucosa. This is rarely seen in esophageal mucosa (mainly composed of squamous epithelial cells) and is abundantly expressed in the glandular cells of the gastric, duodenal, and rectal epithelia, possibly contributing to the oral transmission of SARS-CoV-2 and then to viral spreading into the gastrointestinal tract,

a major target for the virus (Lamers et al., 2020; Xu et al., 2020; Devaux et al., 2021a; Osman et al., 2022). mACE2 is highly expressed thorough the ileum where it may cleave circulating Ang II in the mesenteric arterial blood into Ang-(1–7), which is destined for portal circulation and the liver. The mACE2 also exerts RAS-independent functions in the gastrointestinal tract through cleaving carboxy-terminal amino acids from nutrient proteins and by acting as a chaperon for the expression of the B^0AT1 amino acid transporter (Crackower et al., 2002; Camargo et al., 2009; Singer and Camargo, 2011; Fairweather et al., 2012; Hashimoto et al., 2012; Vuille-Dit-Bille et al., 2015; Wang et al., 2015). The mACE2 regulates the gut homeostasis, microbiota composition, the expression of antimicrobial peptides (Reg3γ, α-defensin, such as HD5 and HD6, β-defensin, and lysozyme; Singer et al., 2012; Perlot and Penninger, 2013; Ferrand et al., 2019). This probably explains the diarrhea that is sometimes observed in SARSCoV-2 patients, and supports the use of antibiotic treatment in COVID-19 patients. In addition, it was reported that HD5 secreted by intestinal Paneth cells, interacts with ACE2 (Wang et al., 2020), suggesting that the presence of HD5 in abundance in the ileal fluid may compete with SARS-CoV-2 to bind to ACE2. The infection of Caco2 cells by SARS-CoV-2 was found to be significantly reduced when cultured in the presence of HD5 and this effect was confirmed on intestinal and lung epithelial cells and for different SARS-CoV-2 variants (Wang et al., 2020; Xu et al., 2021). Although the ACE2 regulation of gut homeostasis was considered to be RAS-independent, α-defensins expression has also been associated with atherosclerosis, being involved in the lipoprotein metabolism in the vessel wall and inhibiting fibrinolysis (Kougias et al., 2005; Nassar et al., 2007; Abdeen et al., 2021).

Structure of the human ACE2 protein

The *ACE2* gene encodes a type I transmembrane glycoprotein of ~ 100 kDa composed of 805 amino acids(Figure 2; Marian, 2013; Gheblawi et al., 2020), including six amino acids (Asn_{53}, Asn_{90}, Asn_{103}, Asn_{322}, Asn_{432}, and Asn_{546}), which can potentially be N-glycosylated (Lubbe et al., 2020). This metalloprotease resembles a chimera molecule composed of a single ACE-like catalytic ectodomain (41.8% sequence homology with the amino domain of ACE) fused to a collectrin-like domain (48% homology with collectrin; Donoghue et al., 2000; Zhang et al., 2001). The functional domains of ACE2 include: (i) a N-terminal signal peptide region of 17 amino acid residues; (ii) a peptidase domain (PD; amino acids 19–615) with its zinc binding metalloprotease motif (catalytic domain; amino acids 374–378); (iii) a C-terminal collectrin-like domain (CLD; amino acids 616–768 acting as a regulator of renal amino acid transport and insulin exocytosis), containing a ferredoxin-like fold "neck" domain (amino acids 615–726); and (iv) an hydrophobic transmembrane hydrophobic helix region of 22 amino acids followed by an intracellular cytoplasmic tail of 43 amino acids (Donoghue et al., 2000; Zhang et al., 2001; Cerdà-Costa and Gomis-Rüth, 2014). The C-terminal segment of mACE2 contains a PDZ-binding motif (amino acids 803–805) Thr_{803}-Ser_{804}-Phe_{805} (TSF_{COOH}) targeting protein-interacting domains from proteins (SNX27, SHANK3, MAST2, and NHERF2) involved in protein trafficking (Caillet-Saguy and Wolf, 2021; Kliche et al., 2021).

The mACE2 functions predominantly as a monocarboxypeptidase, with a substrate preference for hydrolysis between a proline and a hydrophobic or basic C-terminal residue (Turner and Hooper, 2002). The catalytic domain of mACE2 consists of two subdomains (subdomains 1 and 2) forming the two sides of a long deep cleft bridged together by a hinge region. Upon substrate binding, the two catalytic subdomains undergo a hinge-bending movement and form a binding cavity required to initiate substrate hydrolysis (Towler et al., 2004). The His-Glu-X-X-His motif (or HEXXH motif where X is any amino acid), coordinates a catalytic zinc ion, characteristic of zinc-dependent metalloproteases. The zinc is co-ordinated by His_{374}, His_{378}, Glu_{402}, and one water molecule in the subdomain 1, whereas a chloride ion is co-ordinated by Arg_{169}, Trp_{477}, and Lys_{481} in the subdomain 2. The Arg_{514} of mACE2 is considered as a residue critical for substrate selectivity (Luther et al., 2006).

Both the PD and neck domains of mACE2 contribute to dimerization, whereas each B^0AT1 interacts with the neck and TM helix in the adjacent mACE2 (Yan et al., 2020). Complexes of mACE2/B^0AT1 heterodimers have been evidenced at the intestinal apical membrane but did not occur in lung pneumocytes. Steric hindrance to the B^0AT1 binding site on mACE2 or down-regulation of mACE2 due to the presence of SARS-CoV-2 is likely to display impaired intestinal tryptophan uptake (Devaux et al., 2021a).

Finally, the Arg_{652} of ACE2 is a target for the catalytic site of proteases ADAM17 and TMPRSS2, which leads to the shedding of a soluble form of ACE2 (sACE2; Heurich et al., 2014; Lanjanian et al., 2021).

The human *ACE2* gene variant mRNAs

The prototype human *ACE2* cDNA (or *ACHE* for angiotensin-converting enzyme homolog) was cloned more than 2 decades ago from a human cardiac left ventricle cDNA library and a lymphoma cDNA library (Donoghue et al., 2000; Ferrario and Varagic, 2010). The *ACE2* gene, which contains 20 introns and 19 exons maps to chromosome Xp22 and spans 39.98 kb of genomic DNA (Turner and Hooper, 2002). Two isoforms of ACE2 with 18 or 19 exons (v1 and v2) that encode the same protein (805 amino acids) have been described, as well as three other smaller variants: x1–x3 (Chen et al., 2020; Khayat et al., 2020). ACE2 shows similarities with the ACE gene located at chromosome 17q23 (Hubert et al., 1991). Although *ACE2* is one of the genes escaping X chromosome inactivation, there is evidence of sex bias

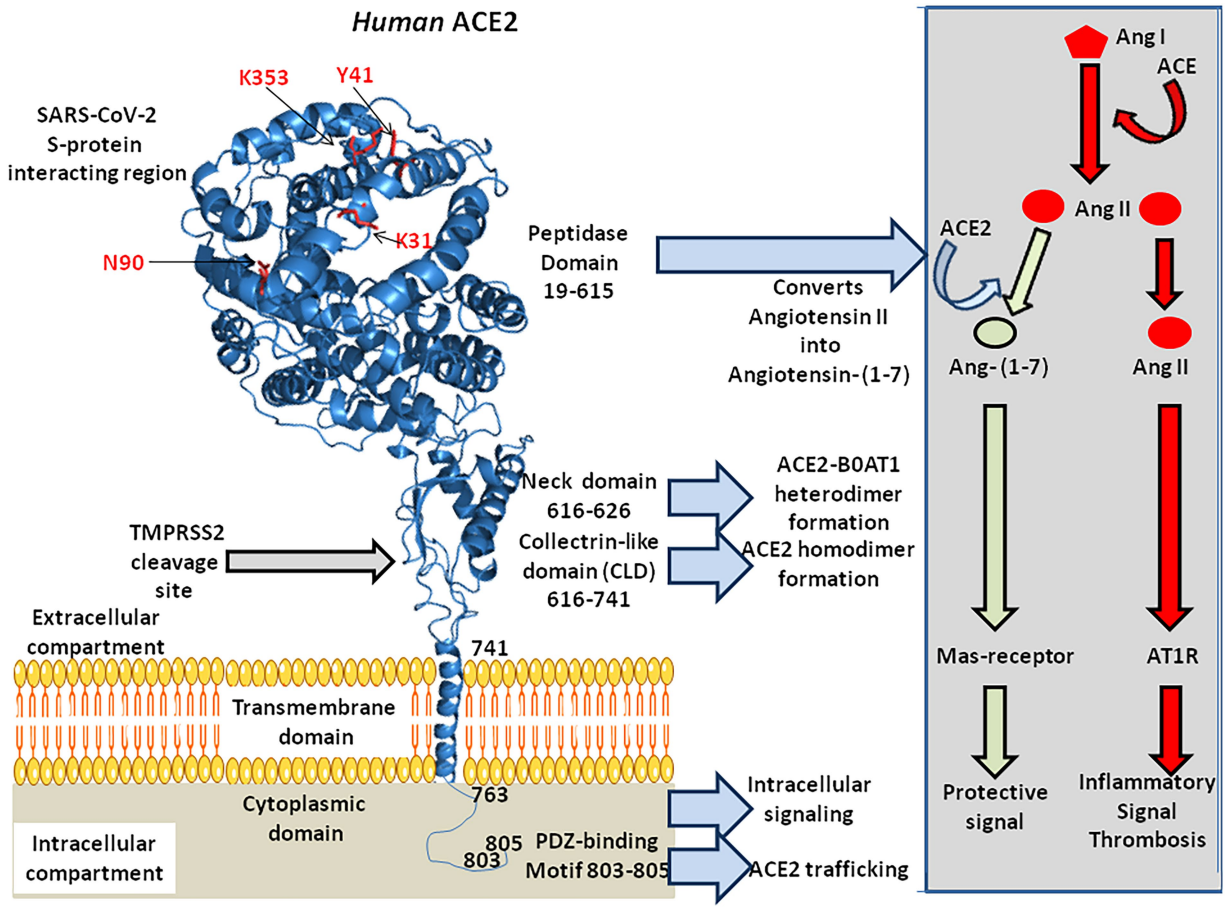

FIGURE 2
3-D model of ACE2 protein structure according to the published data PDB: 6M1D by Yan and colleagues in 2020. ACE2 is composed of 805 amino acids and characterized by an N-terminal signal peptide of 17 amino acid residues, a peptidase domain (PD; residues 19–615) with its HEXXH zinc binding metalloprotease motif, a C-terminal collectrin-like domain (CLD; residues 616–741) that includes a ferredoxin-like fold "neck" domain (616–626), that end with a hydrophobic transmembrane hydrophobic helix region (741–763) followed by an intracellular segment of 43 amino acid residues. No information is available regarding the 3-D structure of the ACE2 cytoplasmic tail (763–805), which was drawn to appear on the diagram. Some of the amino acids which are considered important for SARS-CoV-2 interaction are located in the 3-D model (amino acids in red). Arg_{652}, Arg_{708}, and Arg_{710} (not shown) are the active residues for ACE2-TMPRSS2 docking. The function of each domain is indicated on the middle right side of the figure. The biochemical pathway of the RAS and the beneficial ACE2/Ang-(1–7) arm of RAS are summarized in the right box.

(Tukiainen et al., 2017; Cai, 2020; Gay et al., 2021). Indeed, there is a plausible mechanism of androgen-induced expression of ACE2 that contributes to increased susceptibility or severity of COVID-19 in males (Baratchian et al., 2021). The tissue levels of mACE2 represent equilibrium between transcription/translation of mACE2 and shedding rate of sACE2. It was reported that a positive relationship exists between renin and sACE2 levels in male and female subjects, and between sACE2 levels and body mass index (BMI) in males, with possible implication for COVID-19 (Jehpsson et al., 2021). Variations in mACE2 with age were first demonstrated using animal models (Xie et al., 2006). A negative association between age and sACE2 plasma concentrations in people above the age of 55 year-old, was reported (AlGhatrif et al., 2021). The mACE2 deficiency is considered to be linked to cardiovascular disease and diabetes, suggesting that mACE2 deficiency may increase the risk of developing severe COVID-19 (Oudit and Pfeffer, 2020; Verdecchia et al., 2020; Wang et al., 2020).

The transcription of full-length ACE2 (2,721 bp mRNA) is initiated from either a proximal or a distal promoter with tissue-specific differences in their usage (Itoyama et al., 2005; Fan et al., 2021). The proximal site contains a TATA box motif at position-110/−96 of the transcription start site and a GATA motif and two HNF1 binding sites at position-165/−131. The distal site contains YY1/COUP, C/EBPβ, and STAT/FOXA motifs. Site-directed mutagenesis of the human *ACE2* promoter region from position −2069 to +20, has enabled the identification of an activating domain in the −516 to −481 region (Kuan et al., 2011) and a potential binding site, ATTTGGA, homologous to that of an Ikaros-like binding domain which can be regulated by the levels of Ang II. It has also been reported that the NAD + -dependent deacetylase silent information regulator T1 (SIRT1 known for its

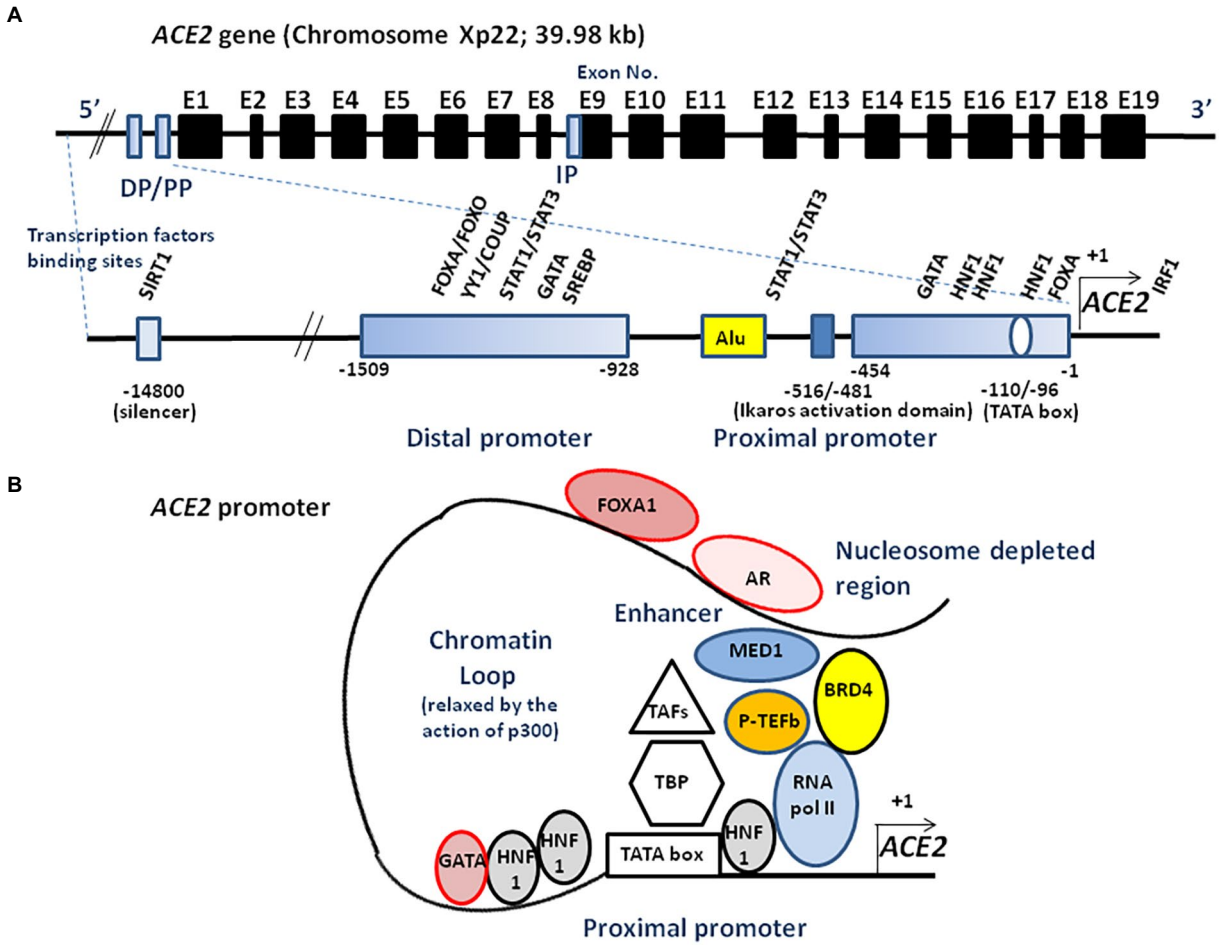

FIGURE 3
Schematic illustration of *ACE2* transcriptional regulation. **(A)** A schematic diagram of the *ACE2* gene structure (upper panel). The known exons (E1–E19) are depicted as black boxes. The location of the distal promotor (DP) and proximal promoter (PP) are depicted as blue boxes. The ACE2 gene can encode several transcript leading to several isoforms. An internal promoter (IP) is thought to activate the transcription of an mRNA encoding a short isoform of ACE2 which lacks the SARS-CoV-2 binding site. The 5′ region upstream of the *ACE2* gene contains two promoters (proximal and distal) separated by a repetitive Alu element (lower panel). The transcription of full-length ACE2 is initiated from either the proximal or distal promoter with tissue-specific differences in their usage. Transcription factors binding to the proximal and the distal upstream promoter regions are indicated. Ang II is likely to regulate the ACE2 expression through the Ikaros activation domain. Truncated ACE2 forms (e.g., *dACE2*) can also be expressed. **(B)** *ACE2* transcriptome. AR binds to the enhancer element of the ACE2 gene, connecting the regulatory circuit between the enhanceosome complex (comprising MED1, BRD4, etc.) and the promoter-bound RNA polymerase machinery to activate gene expression. P-TEFb, positive transcription elongation factor; TBP, TATA-binding protein; TAFs, TBP-associated factors; FOXA1, forkhead box A1; BRD4, bromodomain-containing protein 4; MED1, mediator complex subunit 1; SREBP, sterol regulatory element binding protein; and SIRT1, silent information regulator T1.

ability to deacetylate proteins such as p53 and forkhead box O), binds to the *ACE2* promoter and regulates *ACE2* gene expression under condition of energy stress which increase AMP-activated protein kinase, while IL-1β treatment decreased the binding of SIRT1 to the *ACE2* promoter (Clarke et al., 2014). In addition, there is a cAMP-responsive element (CREB)-binding site within an upstream region of the start site containing both p300 (a CREB co-activator that relaxes the chromatin and recruits RNA polymerase II) and the CREB site (Figure 3).

The *in silico* study of candidate binding sites within the 400 bp upstream of the transcription start site identified putative sites for various DNA-binding molecules, with different tissue expression such as CDX2 in the lungs, colon, and terminal ileum; HNF1A in the colon, kidneys, and terminal ileum; FOXA1 in the cervix, colon and terminal ileum; SOX11 in the kidneys, and TCF7/LEF1 in the lungs (Barker and Parkkila, 2020). The *ACE2* promoter also contains an androgen receptor (AR) binding site, and AR antagonists (e.g., enzalutamide, apalutamide) have been reported as being able to decrease SARS-CoV-2 infection (Qiao et al., 2021). Moreover, forkhead box A1 (FOXA1; also known as HNF3α) involved in AR signaling, and bromodomain-containing protein 4 (BRD4) binding sites, overlap with open chromatin regions. Bromodomain and extra terminal domain (BET) antagonists (e.g., JQ1, OTX015), inhibit BRD4, a factor able to

interact with positive elongation factor (P-TEFb) cyclin-dependent kinase required for transcription elongation through RNA polymerase II (RNA pol II), also decrease SARS-CoV-2 infection through the inhibition of BRD4. The distal-less homeobox 2 (DLX2) and CCAAT/enhancer binding protein epsilon (CEBPE) are more represented in ACE2-expressing cells (Sherman and Emmer, 2021). Evidence for additional transcription factor binding sites (e.g., SP1, CEBP, GATA3, HNF4A, USF1, etc.) has also been reported (Beacon et al., 2021).

Putative binding sites for signal transducer and activator of transcription, STATs (−662 to −647 region and −911 to −897 region), and interferon-regulatory factors, IRFs, have also been demonstrated (Ziegler et al., 2020). Indeed, interferon modulates ACE2 expression and can lead to the transcription of a truncated form of ACE2, designated as deltaACE2 (*dACE2*) which lacks 356 amino-terminal amino acids and fails to bind to SARS-CoV-2 (Onabajo et al., 2020). The transcription of such a truncated form of ACE2 involves the activation of a promoter located downstream of the transcription start site with a splicing event introducing a new ATG start codon. The analysis of this region identified ISGF-3-, AP-1-, and NF-κB-binding sites (Blume et al., 2021). Treating cells with IFNβ significantly induces the dominant expression of *dACE2* over *ACE2* (Onabajo et al., 2020). In addition, the possible role of alternatively spliced isoforms of ACE2 in SARS-CoV-2 homing, infectivity, and influence on COVID-19 evolution, should be investigated (Heyman et al., 2021; Nikiforuk et al., 2021). Polymorphisms in *ACE2* gene 5′ upstream regions might influence ACE2 expression. Differences greater than 1% of minor allele frequency (MAF) in the 10 Kb region upstream to ACE2 analyzed using data from the 1,000 Genomes project, found 57 polymorphisms (Lanjanian et al., 2021). A single nucleotide polymorphism (SNP), rs5934250, with a change from G to T at approximately 5,700 bp upstream of the start codon of the *ACE2* gene, presented a penetration difference among populations. This allele is almost absent in the East Asian population, while it has a MAF in almost half of Europeans (East Asians: 1%; Africans: 10%; South Asians: 22%; Americans: 29%; and Europeans: 47%). Another SNP, rs2097723, also shows a very heterogeneous distribution among populations (Africans: 7%; South Asians: 22%; Europeans: 28%; Americans: 32%; and East Asians: 42%).

Human ACE2 polymorphism

Exploration of the *ACE2* genetic polymorphism was conducted to define SNPs associated with hypertension and heart diseases. Special attention was drawn to 14 SNP (rs2285666, rs1978124, rs2074192, rs2106809, rs4830542, rs4240157, rs879922, rs2158083, rs233574, rs1514282, rs1514283, rs4646155, rs4646176, and rs4646188). The best characterized SNP is a splice region variant (rs2285666, G > A, Intron 3/4), known to be associated with hypertension, coronary heart disease, and diabetes (Yang et al., 2015; Pinheiro et al., 2019; Bosso et al., 2020). A number of SNPs, including genotypes of rs2048683, rs233575, rs2158083, rs2074192, rs2106809, rs4240157, rs4646155, and rs4830542 were linked with moderate risks of hypertension, while rs4646188 and rs879922 were linked to high hypertension risks (Yi et al., 2006; Fan et al., 2009; Patnaik et al., 2014; Dai et al., 2015; Meng et al., 2015; Chen et al., 2016; Liu et al., 2018; Luo et al., 2019), and the rs2074192 and rs2106809 were associated with left ventricular hypertrophy in hypertensive patients (Fan et al., 2019). The *ACE2* $A_{1075}G$ allele found in China was associated with hypertension and the *ACE2* $G_{8790}A$ allele is associated with susceptibility to hypertension, type 2 diabetes, and increased plasma concentration of sACE2 (Niu et al., 2007; Wu et al., 2017; Pinheiro et al., 2019). An allele frequency heterogeneity for the rs2285666 (East Asians: 17%; South Asians: 23%; Americans: 37%; Africans: 48%; Europeans 48%; and with the highest frequency in Indians: 71%) has been reported (Khayat et al., 2020) while the rs4646140 has a MAF ranging from zero in Indians to 13% in Africans. Polymorphisms, including rs233574, rs2074192, and rs4646188 with MAF of 16, 36, and 6%, respectively, were able to induce a significant RNA secondary structure change (Pouladi and Abdolahi, 2021). These alterations may lead to dysregulations in ACE2 transcription/translation or its protein stability. Indeed, in the case of the mutated alleles, the splicing regulatory molecule ETR-3 is unable to bind to the pre-mRNA. Similarly, in the case of the mutated forms of rs2158083 and rs2285666, the binding of YB-1 and hnRNP DL, respectively, are impaired, resulting in exon retention. In the case of the mutated form of rs1514283, the SF2/ASF, and SRp40 proteins bind and lead to the creation of a new intron splicing enhancer and exon inclusion. In the case of the mutated form of rs879922, there is a possibility of interaction with the SC35 and DAZAP1 proteins that leads to exon inclusion. In addition, the binding of proteins of the hnRNP A1, A0, A2/B1, D, and DL family creates a new intronic splice silencer and intron exclusion. In the case of the mutated form of rs4646155, the NOVA-1 protein induces an exon inclusion, while SLM-2 and Sam68 lead to intron exclusion. In the case of the mutated form of rs2106809, the hnRNP H proteins lead to an intron exclusion.

As COVID-19 emerged, it was postulated that SNPs in the *ACE2* gene could affect susceptibility for SARS-CoV-2 infection (Darbani, 2020; Devaux et al., 2020; Hou et al., 2020). Particular attention was paid to the impact of the $G_{8790}A$ mutation on the severity of COVID-19, although its role in this disease remains controversial (Gómez et al., 2020; Möhlendick et al., 2021). About 77% of GG genotype, 13% of GA genotype and 9% of AA genotype were found in Caucasian SARS-CoV-2-positive patients and 70% of GG genotype, 14% of GA genotype and 16% of AA genotype carriers in SARS-CoV-2-negative people, respectively. A meta-analysis concluded that the ACE2 variant rs190509934:C (a rare variant) characterized by a lower ACE2 expression in individuals carrying the C allele, reduces the risk of SARS-CoV-2 infection (Horowitz et al., 2021).

Analysis of inter-individual *ACE2* polymorphism, based on broad genomic databases reveal a link with the susceptibility to SARS-CoV-2 and the severity of COVID-19 (Brest et al., 2020;

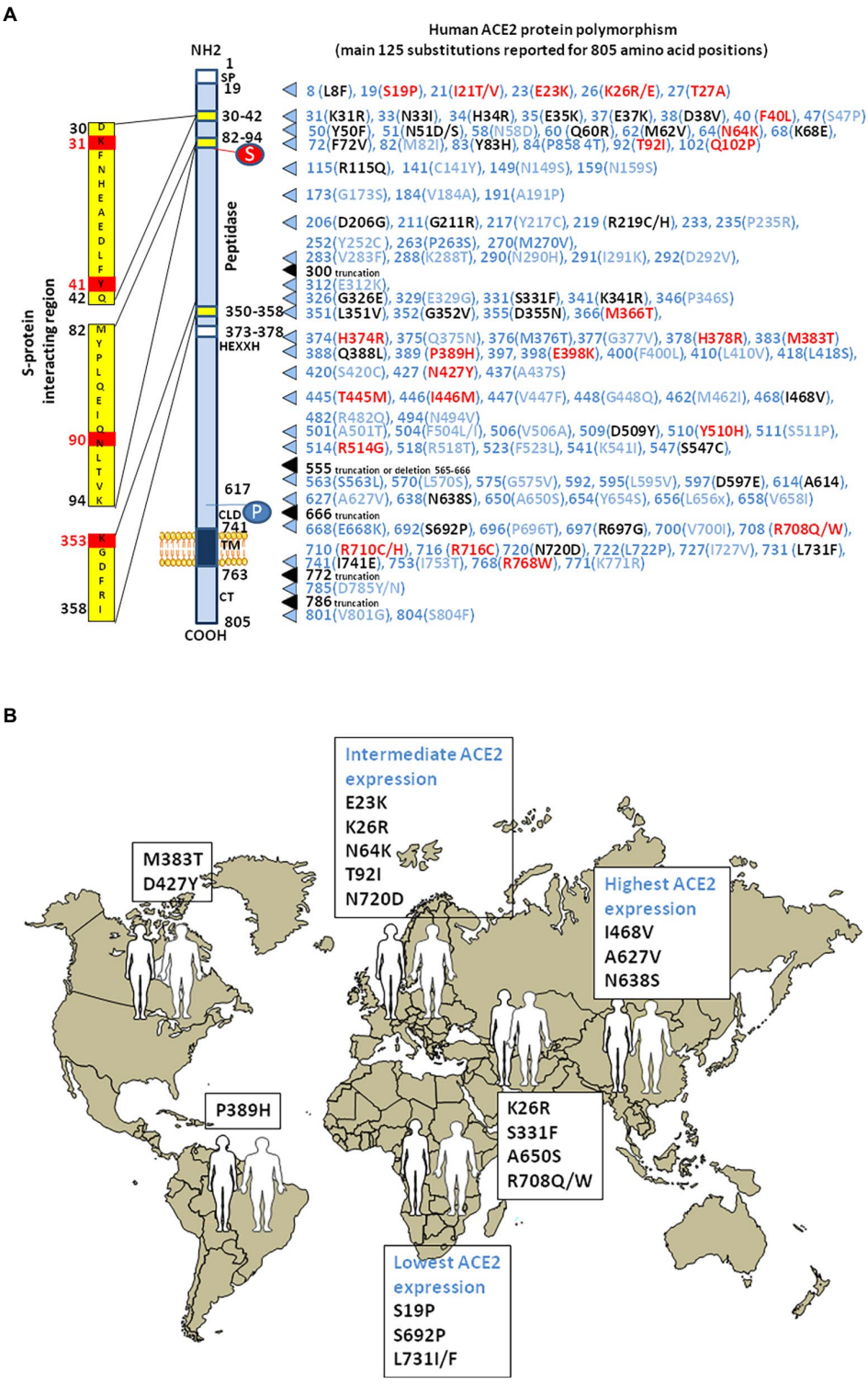

FIGURE 4
Human ACE2 polymorphism. **(A)** Schematic representation of the cell surface of the human ACE2 molecule and its major domains is drawn on left side of the figure. The amino acid positions are in black. Some of the amino acids considered to be important for viral tropism are marked in red. S, sugar; P, phosphorylation. The right part of the figure is a compilation of the main substitutions described in the literature. To simplify the figure, we used the single letter amino acids code instead of multiple letters code. The ACE2 substitutions in blue are considered neutral. The ACE2 substitutions in red are predicted to increase cell susceptibility to SARS-CoV-2. The ACE2 substitutions in black are predicted to decrease cell susceptibility to SARS-CoV-2. Polymorphisms in intronic regions might modify *ACE2* regulation. Polymorphisms were able to induce a significant RNA secondary structure change. These alterations may lead to dysregulations in ACE2 transcription/translation or its protein stability. **(B)** The main geographical distribution of ACE2 protein polymorphisms in human populations. Representative substitutions in the human mACE2 per geographic areas.

Cao et al., 2020). The pioneering work by Cao and colleagues identified 15 unique expression quantitative trait loci variants (14 SNPs and 1 InDel) with a higher frequency of minor alleles in the Asian population than in the European population. For example, the rs143695310 variant among East Asian populations was found to be associated with elevated expression of ACE2. Moreover, it was reported that Asian men have a higher ACE2 mRNA expression in their lungs than women, and that Asian people express higher amount of ACE2 than Caucasian and African American populations according to single-cell RNA-seq analysis (Zhao et al., 2020; Figure 4). Similar data were obtained using expression quantitative trait loci (eQTL), indicating a higher expression of ACE2 in South Asian and East Asian populations compared to Europeans, while the lowest expression levels were observed for Africans (Ortiz-Fernández and Sawalha, 2020). Dozen of human *ACE2* variants were identified, which could impact on protein stability (e.g., $Lys_{26}Arg$, $Gly_{211}Arg$, and $Asn_{720}Asp$ variants) or internalization (e.g., $Leu_{351}Val$ and $Pro_{389}His$ variants; Benetti et al., 2020; Cao et al., 2020; Othman et al., 2020). The rs41303171 C polymorphism, which is practically exclusive to Europeans (MAF 1.8%), is a missense SNP causing an $Asn_{720}Asp$ replacement, which can trigger a conformational disorder in ACE2 changing viral interactions (Khayat et al., 2020). The $Pro_{389}His$ variant occurs in Latino American population with an allele frequency of 0.015%. Only African Americans carry $Met_{383}Thr$ and $Asp_{427}Tyr$ variants with allele frequencies of 0.003 and 0.01%, respectively. The $Arg_{514}Gly$ occurs in African Americans with an allele frequency of 0.003% (Hou et al., 2020). The European population with $Arg_{708}Trp$, $Arg_{710}Cys$, $Arg_{710}His$, or $Arg_{716}Cys$ variants in mACE2 may have mild symptom of COVID-19 as ACE2 lose the cleavage site by TMPRSS2 (Hou et al., 2020; Lanjanian et al., 2021). The $Ser_{19}Pro$ variant (rs73635825 genotype) common in African populations, may protect against COVID-19 while the $Lys_{26}Arg$ variant (rs75548401 genotype) might predispose to severe forms of COVID-19 (Calcagnile et al., 2021). Recently, Suryamohan and colleagues found 298 unique ACE2 variants (Suryamohan et al., 2021). Among these variants they predicted that the $Lys_{31}Arg$ polymorphism breaks an interaction with Gln_{493} in the viral RBD and destabilizes the charge-neutralizing interaction with the virus and that the $Glu_{37}Lys$ polymorphism disrupts the critical interactions with ACE2 Lys_{353} by removing the polar intramolecular interaction that stabilizes contacts with the SARS-CoV-2 RBD. Similarly, the $His_{34}Arg$ was predicted to result in a loss of interface polar contact. Thus, individuals carrying these variants are predicted to be less susceptible to SARS-CoV-2 infection. Fourteen human ACE2 variants ($Ile_{21}Val$, $Glu_{23}Lys$, $Lys_{26}Arg$, $Asn_{64}Lys$, $Thr_{92}Ile$, $Gln_{102}Pro$, $Asp_{206}Gly$, $Gly_{211}Arg$, $Arg_{219}Cys$, $Glu_{329}Gly$, $His_{378}Arg$, $Val_{447}Phe$, $Ala_{501}Thr$, and $Asn_{720}Asp$) which could enhance susceptibility to SARS-CoV-2 were found to have an higher allele frequencies in European populations than East Asian populations, while two additional ACE2 variants ($Glu_{35}Lys$ and $Phe_{72}Val$) possibly conferring resistance to the virus, have higher allele frequencies in East Asian populations, while they are low or not expressed in European populations (Chen et al., 2021). Recently, a total of 570 genetic variations (SNP and InDel) on the *ACE2* gene were reported in the Iranian population (Lanjanian et al., 2021).

ACE2 production and regulation inside human cells

Angiotensin-converting enzyme 2 surface abundance differ among cell types, indicating a complex epigenetic regulation of the *ACE2* gene. The interaction between tissue or cell type specific enhancer/repressor is required for gene expression (Andersson et al., 2014). The *ACE2* gene expression is also increased in individuals with pulmonary arterial hypertension, chronic obstructive pulmonary disease, obesity, diabetes, and older people (Muus et al., 2020; Pinto et al., 2020). In patients with hypertensive cardiopathy a marked ACE upregulation and ACE2 downregulation associated with Ang II/AT1R induced activation of the ERK1/2 and p38 MAP kinase, was reported (Koka et al., 2008). DNA methylation (5mC) was found to be involved in the silencing of *ACE2* gene expression and CpG methylation was greater in patients with hypertension compared to healthy controls (Fan et al., 2017; Chlamydas et al., 2020; Cardenas et al., 2021). In contrast, enhanced ACE2 expression might also be protective in COVID-19 if it increases the peptidase activity of ACE2 thereby reducing Ang II concentration. Hypomethylation of specific sites in the *ACE2* promoter was reported to correlate with increased *ACE2* gene expression (Corley and Ndhlovu, 2020). Three CpGs (cg04013915, cg08559914, and cg03536816) at the *ACE2* gene were reported as having lower methylation in lung epithelial cells compared to the other tissues (Beacon et al., 2021). The search for *ACE2* topologically associating domains (TADs) with active histone markers, including H3 acetylated at K27 (H3K27ac) and H3 trimethylated at K4 (H3K4me3) or repressive histone markers (H3K27me3), revealed the presence of H3K4me3 at the promoter and after the first exon of *ACE2*, and the presence of H3K27ac in human kidneys (Beacon et al., 2021). The association of H3K4me3 correlates with *ACE2* gene expression in the kidneys, heart, and small intestine. In contrast, H3K4me3 peaks are not detected in lung tissues.

MicroRNAs (miRNAs) are non-coding RNAs which can bind the 3′-untranslated regions (3'-UTRs) of target mRNAs, thereby regulating gene expression at a post-transcriptional level. Lysine-specific demethylase 5B, JARID1B, is responsible for the downregulation of several miRNAs that target ACE2 (Henzinger et al., 2020). Putative miRNA-binding sites were identified in the 3′-UTR of the *ACE2* transcript thereby repressing translation. Both the *miR-421,* an miRNA implicated in the development of thrombosis and the miR-*200*c-3p were found to downregulate the ACE2 mRNA expression (Hirano and Murakami, 2020). In contrast the increases ACE2 mRNA expression (Sato et al., 2013; Siddiquee et al., 2013; Zhang et al., 2017). Other miRNAs predicted to bind to ACE2 mRNA 3'-UTR, such as miR-9-5p and

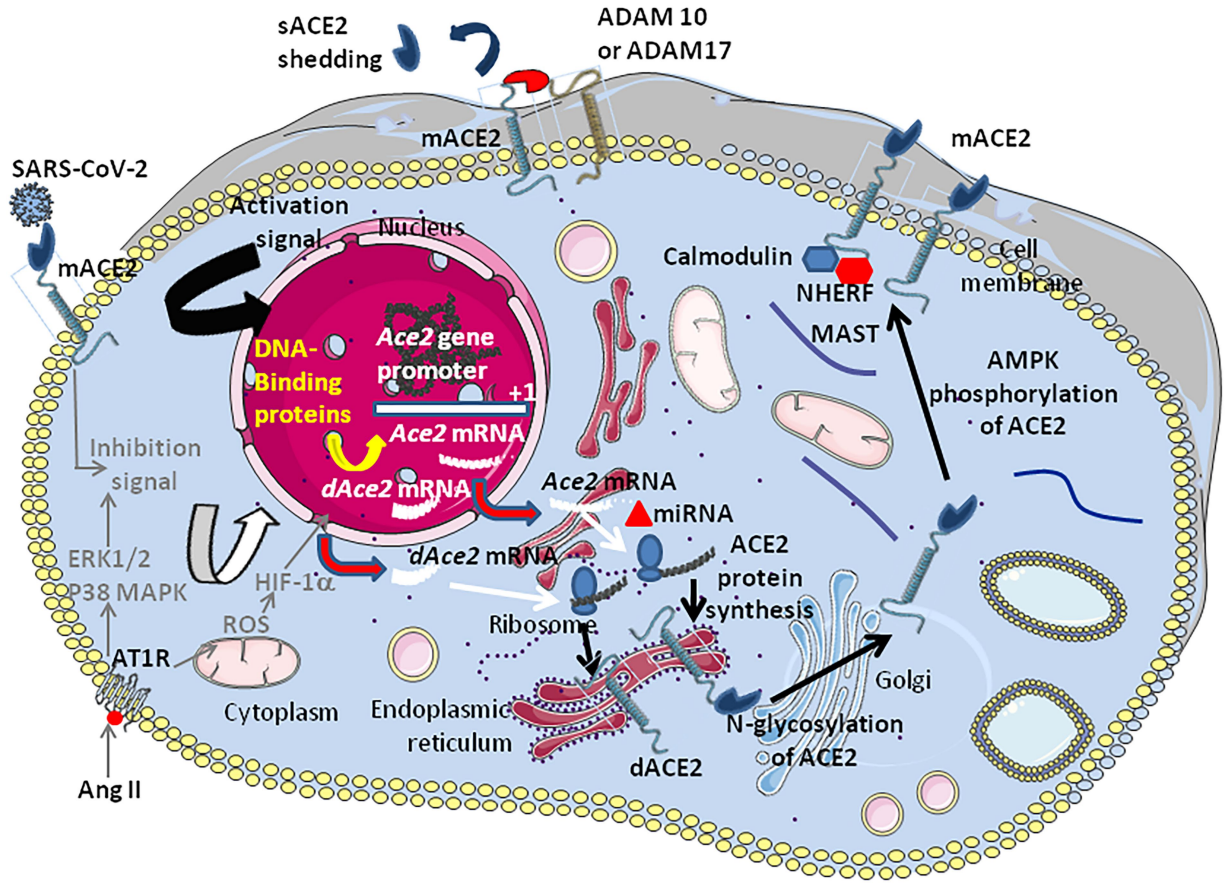

FIGURE 5
Schematic representation of the regulation of ACE2 expression. The transcription of the *Ace2* gene is under control of several DNA-binding proteins that bind the *Ace2* gene promotor (see Figure 3). In patients with hypertension (hypertensive cardiopathy and hypertensive nephropathy) a down-regulation ACE2 is observed. Angiotensin II was shown to down-regulate ACE2. The inhibition of ACE2 expression was shown to be associated with the activation of ERK and p38 MAP kinases (however this signaling pathway also activates NF-κB which is an activator of *ACE2*, suggesting a complex regulation of positive and negative signals which remains to be characterized). The binding of AngII to AT1R induces the hypoxia-inducible factor (HIF)-1α, which regulates several genes involved in the RAS (e.g., ACE1). Post-transcriptional regulation by miRNA (e.g., miRNA143 and miRNA421) could occur. Following translation the newly synthesized ACE2 proteins are target of post-transcriptional modifications such as phosphorylation of Ser680 by AMPK that enhances the stability of ACE2, and N-glycosylations (seven potential N-glycosylation sites). Once expressed at the cell membrane the mACE2 protein can be regulated by sheddases (e.g., ADAM10 and ADAM17) that cleave the ACE2 extracellular domain and release a circulating soluble form, sACE2. IFNβ is likely to induce dominant expression of *dACE2* over *ACE2*.

miR-218-5p, were found to be differentially expressed in different cell types (Pierce et al., 2020). Moreover, the repression of the Xu and Li, 2021; Figure 5).An *in silico* studies aimed at predicting miRNAs that regulate ACE2-related networks with a possible impact on COVID-19 outcome, suggests that the top miRNAs regulating ACE2 networks are miR-27a-3p, miR-26b-5p, miR-10b-5p, miR-302c-5p, hsa-miR-587, hsa-miR-1305, hsa-miR-200b-3p, hsa-miR-124-3p, and hsa-miR-16-5p (Wicik et al., 2020). sACE2 shed into systemic circulation maintains its ability to generate Ang-(1–7). This process is fine-tuned by ADAM17 (also known as TACE), the metalloprotease ADAM10, and the transmembrane protease serine 2 (TMPRSS2), but only TMPRSS2 increases the entry of both SARS-CoV-1 and SARS-CoV-2 into susceptible cells (Lambert et al., 2005; Heurich et al., 2014; Hoffmann et al., 2020; Qiao et al., 2021). The ADAM17 and ADAM10 sheddases can trigger ACE2 ectodomain shedding by cleavage between amino acids 716 and 741 near the predicted transmembrane domain (Xiao et al., 2014), while TMPRSS2 trigger cleavage between amino acids 697 and 716 (Lanjanian et al., 2021). Phorbol ester and ionomycin as well as the proinflammatory cytokines IL-1β and TNF-alpha, can induce cellular proteases to catalyze sACE2 shedding (Jia et al., 2009). A study of plasma samples from 534 subjects indicated that up to 67% of the phenotypic variation in sACE2 shedding could be accounted for by genetic factors (Rice et al., 2006). mACE2 also interacts with several PDZ-binding proteins such as NHERF, involved in the internalization and recycling of mACE2 (Zhang et al., 2021). The *in silico* study of proteins belonging to the ACE2 interactome and which could be affected by SARS-CoV-2 infection, highlighted that the most affected interactions were associated with microtubule-associated serine and threonine kinase 2 (MAST2), and [Calmodulin 1 (CALM1; Wicik et al.,

2020]. It was previously reported that CALM1 inhibitors increase sACE2 shedding by preventing calmodulin binding to the cytoplasmic tail of mACE2 (Lambert et al., 2008).

ACE2 through the ages

Structural comparisons of genes indicated that *ACE2* and *ACE* arose by duplication from a common ancestor (Riordan, 2003). Although the evolutionary tree of *ACE2* genes from 36 representative vertebrates is consistent with the species evolutionary tree, certain differences found in coelacanths and frogs may suggest a very slow evolutionary rate in the initial evolution of *ACE2* in vertebrates (Lv et al., 2018; Damas et al., 2020; Lam et al., 2020; Luan et al., 2020; Lubbe et al., 2020; Liu et al., 2021). Orthologs of *ACE2* and *ACE* also exist in bacteria, chordates and tunicates, suggesting an early origin of the RAS (Fournier et al., 2012). Although intriguing, the observation that the ACE2-like carbopeptidase from *Paenibacillus* sp. B38 catalyzes the conversion of Ang II to Ang-(1–7) and can suppress Ang II-induced hypertension, cardiac hypertrophy, and fibrosis in mice does not necessarily mean that the origin of the RAS goes back to bacteria but that a molecule with an ACE2-like carbopeptidase activity was maintained during speciation (Minato et al., 2020). ACE2-ancestors may then have acquired important new functions in tissues during speciation, as evidenced in humans. Beside the ACE2-like carbopeptidase, bacteria also express the neutral amino acid transporter SLC6A19, the homologous of B^0AT1 in human, suggesting that SLC6A19 and the bacterial ACE2 ortholog may have already been molecular partners in bacteria (Gallucio et al., 2020). It is remarkable to note that an ACE-like bacterial protein named *Xc*ACE from *Xanthomonas axonopodis pv. citri*, hydrolyses Ang I into Ang II (Rivière et al., 2007). Other bacteria belonging to *Lactococcus* (*L. lactis*, *L. helveticus*, *L. acidophilus*, and *L. casei*) and *Bifidobacterium* species, release peptides with *in vitro* ACE-inhibitory activity (Fuglsang et al., 2003; Donkor et al., 2007).

The Ance genes from *Drosophila melanogaster* shares similarities with the human *ACE2* (Burnham et al., 2005). In *Acyrthrosiphon pisum*, expression of the insect *ACE2*-ortholog is inducible upon feeding (Wang et al., 2015). The simultaneous KO of *A. pisum ACE2* and *ACE* resulted in enhanced feeding and increased aphid mortality. It was also reported that the challenging of *Anopheles gambiae* with *Staphylococcus aureus* and *Staphylococcus typhimurium* upregulated the transcription of the Anopheles homolog of *ACE*, named AnoACE (Aguilar et al., 2005). Moreover, it was reported that treatment of *A. gambiae* with an ACE inhibitor resulted in larval death (Abu Hasan et al., 2017).

While searching for the zoonotic origin of SARS-CoV-2, special attention has been drawn to bats, minks and hamsters ACE2 molecules, as they might serve as viral receptors. Using multiple sequence alignments, we found that the bat ACE2 protein polymorphism grouped in the dendrogram according to the 18 subspecies of bats studied (Devaux et al., 2021c). The ACE2 from *Rhinolophus* bats appeared to be an appropriate candidate for interacting with SARS-CoV-2-related viruses, despite species polymorphism (i.e., *R. sinicus* with Lys_{31}, $Tyr_{41}His$, Asn_{82}, Asn_{90}, and Lys_{353}). The $Lys_{31}Asp$ variant found in *R. ferrumequinum* may possibly alter the binding of the SARS-CoV-2 spike to the bat mACE2 receptor. The mACE2 sequences from other bat species showed increasing amino acid substitutions at positions considered to be required for SARS-CoV-2 spike binding (e.g., *D. rotundus* with $Lys_{31}Asn$, Tyr_{41}, $Asn_{82}Thr$, $Asn_{90}Asp.$, and $Lys_{353}Asn$). The mACE2 proteins from *Myotis* bats examined were characterized by $Lys_{31}Asn$, $Tyr_{41}His$, $Asn_{82}Thr$, Asn_{90}, and Lys_{353}, including substitutions incompatible with SARS-CoV-2-like viruses binding. Regarding the ACE2 from minks we found that the mink ACE2 sequences from *Neovison vison* and *Mustela lutreola* displayed 99.51% similarity to one another, but shared only 83.73 and 83.48% amino acid identity with the human ACE2, respectively (Devaux et al., 2021b). The similarity between human ACE2 and mink ACE2 dropped to 63.34% in the region described to be involved in the interaction with the SARS-CoV-2 spike protein (regions 30–41, 82–93, and 353–358). Despite the fact that more than 130 substitutions out of 805 amino acids were observed between the human ACE2 and mink ACE2 (e.g., 131 substitutions and 133 substitutions for *N. vison* ACE2 and *M. lutreola* ACE2, respectively), including an $Asn_{90}Asp$ substitution possibly impacting the affinity of mink ACE2 for the virus, the Lys_{31}, Tyr_{41}, and Lys_{353} amino acids required for human ACE2 interaction with the SARS-CoV-2 spike protein are conserved in minks mACE2. This amino acids triad is also conserved in hamsters. The Figure 6A, illustrates a comparison of ACE2 amino acid sequences from humans, mink, hamsters, mice and bats.

ACE2 as SARS-CoV-2 receptor

Severe acute respiratory syndrome coronavirus is an enveloped single-stranded positive-sense RNA virus (its genome contains ~32 kb). The SARS-CoV-2 viral envelope consists of a lipid bilayer, where the viral membrane (M), envelope (E), and spike (S) structural proteins are anchored. The S proteins surrounding the viral particles consist of two subunits, S1 and S2. This S protein determines the cellular tropism of the virus. In 2020, ACE2 was identified as the main entry receptor for the SARS-CoV-2 virus (Zhao et al., 2020; Zhuang et al., 2020; Baggen et al., 2021). SARS-CoV-2 is the third human coronavirus after SARS-CoV-1 and HCoV-NL63 which use the human mACE2 as a cellular receptor (Li et al., 2003, 2007). A unique feature of SARS-CoV-2 compared with SARS-CoV-1 is the presence of a polybasic motif (RRAR) at the S1/S2 boundary, which can be cleaved by furin (Walls et al., 2020), resulting in a C-terminally exposed RRAR peptide. Two independent studies showed that this peptide directly binds to neuropilin-1 (NRP1) and that NRP1 promotes SARS-CoV-2 infection (Cantuti-Castelvetri et al., 2020; Daly et al., 2020).

A critical step in the SARS-CoV-2 infection cycle is the binding of the homotrimeric viral spike protein through RBD to

the peptidase domain of mACE2 (Lan et al., 2020; Shang et al., 2020; Yan et al., 2020). Despite high similarity between the RBD of SARS-CoV-1 and SARS-CoV-2, several amino acid variations in the binding domain of SARS-CoV-2, increase its affinity for ACE2 (Lan et al., 2020; Yan et al., 2020). The interaction is driven by two domains in the S1 subunit of the molecule, namely the RBD and the N-terminal domain (NTD). The NTD displays a flat electropositive ganglioside binding site enabling the virus to interact with lipid rafts of the cell membrane (Fantini et al., 2021). At the N terminus of the viral spike, Gln_{498}, Thr_{500}, and Asn_{501} of the RBD form a network of H-bonds with Tyr_{41}, Gln_{42}, Lys_{353}, and Arg_{357} of the human mACE2. In addition, in the middle of the bridge, Lys_{417} and Tyr_{453} of the RBD interact with Asp_{30} and His_{34} of ACE2, respectively. Moreover, Gln_{474} of the RBD is H-bonded to Gln_{24} of ACE2, whereas Phe_{486} of the RBD interacts with Met_{82} of ACE2 through van der Waals forces (Yan et al., 2020). Binding of S1 to the mACE2 receptor triggers an ACE2 ectodomain cleavage by ADAM17 (Lambert et al., 2005; Heurich et al., 2014; Oarhe et al., 2015). The ACE2 cleavages by ADAM17 and a serine protease (TMPRSS2 or TMPRSS4) induce the shedding of cellular ACE2 and systemic release of S1/sACE2 complex, and primes for cellular viral entry (Hoffmann et al., 2020). When S1 binds to mACE2, another site on S2 is exposed and cleaved by host proteases. S2 does not interact with mACE2 but harbors the functional elements which guides membrane fusion. So, SARS-CoV-2 can therefore utilize two pathways to infected ACE2 positive cells: the virus can either fuse at the plasma membrane (early pathway) or, it can fuse at the endosomal membrane (late pathway). The privileged pathway is determined by the proteases present at the cell membrane (Wicik et al., 2020; Caillet-Saguy and Wolf, 2021). When the fusion occurs at the cell membrane, this process is followed by the formation of a funnel like structure built by two heptad repeats in the S2 protein in an antiparallel six-helix bundle, facilitating the fusion and release of the viral genome into the cytoplasm. When the protease is absent, SARS-CoV-2 can be endocytosed *via* clathrin-and non-clathrin-mediated internalization and the virion is then activated in endosomal vesicles by the action of low pH-dependant protease Cathepsin L (Tang et al., 2020). Thus, the expression and polymorphism of both ACE2 and TMPRSS2 are likely to dictate SARS-CoV-2 tissue tropism (Hou et al., 2020; Zou et al., 2020). Whether overexpression of mACE2 would facilitate infection (increasing the number of receptors available for the virus) or restrict the risks of developing the most severe forms of the disease, has long been a source of controversy (Vaduganathan et al., 2020). Once bound to mACE2, SARS-CoV-2 down-regulates the cellular expression of the *ACE2* gene and mACE2 protein and the unopposed action of Ang II was deemed responsible for worsening the outcome of COVID-19 (Hendren et al., 2020).

The ACE2 key residues at the ACE2/S-protein-RBD interface include Ser_{19}, Gln_{24}, Thr_{27}, Phe_{28}, Asp_{30}, Lys_{31}, His_{34}, Glu_{35}, Glu_{37}, Asp_{38}, Tyr_{41}, Gln_{42}, Leu_{45}, Leu_{79}, Met_{82}, Tyr_{83}, Thr_{324}, Gln_{325}, Gly_{326}, Glu_{329}, Asn_{330}, Lys_{353}, Gly_{354}, Asp_{355}, Arg_{357}, Pro_{389}, and Arg_{393} (Suryamohan et al., 2021). The Lys_{31} and Lys_{353} residues in human mACE2 form hydrogen bonds with the main chain of Asn_{501} and Gln_{493} in the RBD. ACE2 variants $Ser_{19}Pro$, $Ile_{21}Val$, $Glu_{23}Lys$, and $Lys_{26}Arg$ (which stabilizes core ACE2 α-helical interactions), $Thr_{27}Ala$ (which removes interactions between Thr_{27} and Glu_{30}), $Asn_{64}Lys$, $Thr_{92}Ile$, $Gln_{102}Pro$ and $His_{378}Arg$ were predicted to increase cell susceptibility to SARS-CoV-2. In contrast, ACE2 variants $Lys_{31}Arg$ (which breaks an interaction with Gln_{493} in the SARS-CoV-2 spike RBD), $Asn_{33}Ile$, $His_{34}Arg$ (which results in a loss polar contact at the interface with SARS-CoV-2 spike RBD), $Glu_{35}Lys$ (which affects the critical polar contact with SARS-CoV-2 spike Gln_{493}), $Glu_{37}Lys$, $Asp_{38}Val$ (which compromises the Asp_{38}-Lys_{353} interaction), $Tyr_{50}Phe$, $Asn_{51}Ser$, $Met_{62}Val$, $Lys_{68}Glu$, $Phe_{72}Val$, and $Tyr_{83}His$ (which prevents insertion of SARS-CoV-2 spike residue Phe_{486} into an hydrophobic pocket driven by residue Tyr_{83}), $Gly_{326}Glu$, $Gly_{352}Val$, $Asp_{355}Asn$, $Gln_{388}Leu$, and $Asp_{509}Tyr$ were predicted to be less sensitive to SARS-CoV-2 (Procko, 2020; Suryamohan et al., 2021). When considering ACE2 variants, high mACE2 cell-surface expression can mask the effects of impaired binding while low cell surface expression reveals a range of infection efficiencies across variants, supporting a major role for binding avidity during viral entry (Shukla et al., 2021). Using an *in vitro* model of infection of cells expressing suboptimal surface ACE2, it was found that the mACE2 variants $Asp_{355}Asn$, $Arg_{357}Ala$, and $Arg_{357}Thr$ abrogated entry of SARS-CoV-2 while $Tyr_{41}Ala$ showed only a slight effect on SARS-CoV-2 entry although it inhibited SARS-CoV-1. The NTD and RBD domains in the viral S protein act synergistically to insure virus adhesion (Fantini et al., 2021). Moreover, an inverse correlation was established between ACE2 expression and COVID-19 severity (Chen et al., 2021).

Particular attention was drawn to polymorphism of ACE2 in bat (considered to be a reservoir of SARS-CoV-related virus; Zhou et al., 2020; Wacharapluesadee et al., 2021) this species, and in minks (because they have been shown to be susceptible to infection by SARS-CoV-2 from humans and then to be a source of the virus being able to reinfect humans; Boklund et al., 2021; Oude Munnink et al., 2021; Shuai et al., 2021). It was found that when SARS-CoV-2 of human origin become host-adapted to mink, a $Tyr_{453}Phe$ substitution located in the RBD was selected. This process is driven by the fact that mink mACE2 has a Tyr_{34} instead of the H_{34} found in human mACE2 and that the $Tyr_{453}Phe$ substitution improves the virus binding to the mink mACE2 (Ren et al., 2021). The hamster is another species of interest for ACE2, because hamster-adapted SARS-CoV-2 Delta variants were isolated in Hong Kong, and the virus was transmitted back to human and further human-to-human transmission was then demonstrated (Kok et al., 2022; Yen et al., 2022). We found that once adapted to the hamster ACE2, the variant virus show mutations (e.g., $Asp_{427}Gly$) that could make this virus more efficient at infecting humans (Fantini et al., 2022). Although a large number of animal species were considered to be susceptible to infection by SARS-CoV-2 (Stawiski et al., 2020), SARS-CoV-2 (Wuhan-HU1 strain) cannot use mouse ACE2 (Zhou et al., 2020). The presence of Asn_{30} (instead of Asp_{30}) and Asn_{31} (instead of Lys_{31}) in mouse ACE2 is likely to cause the lack of salt bridges and

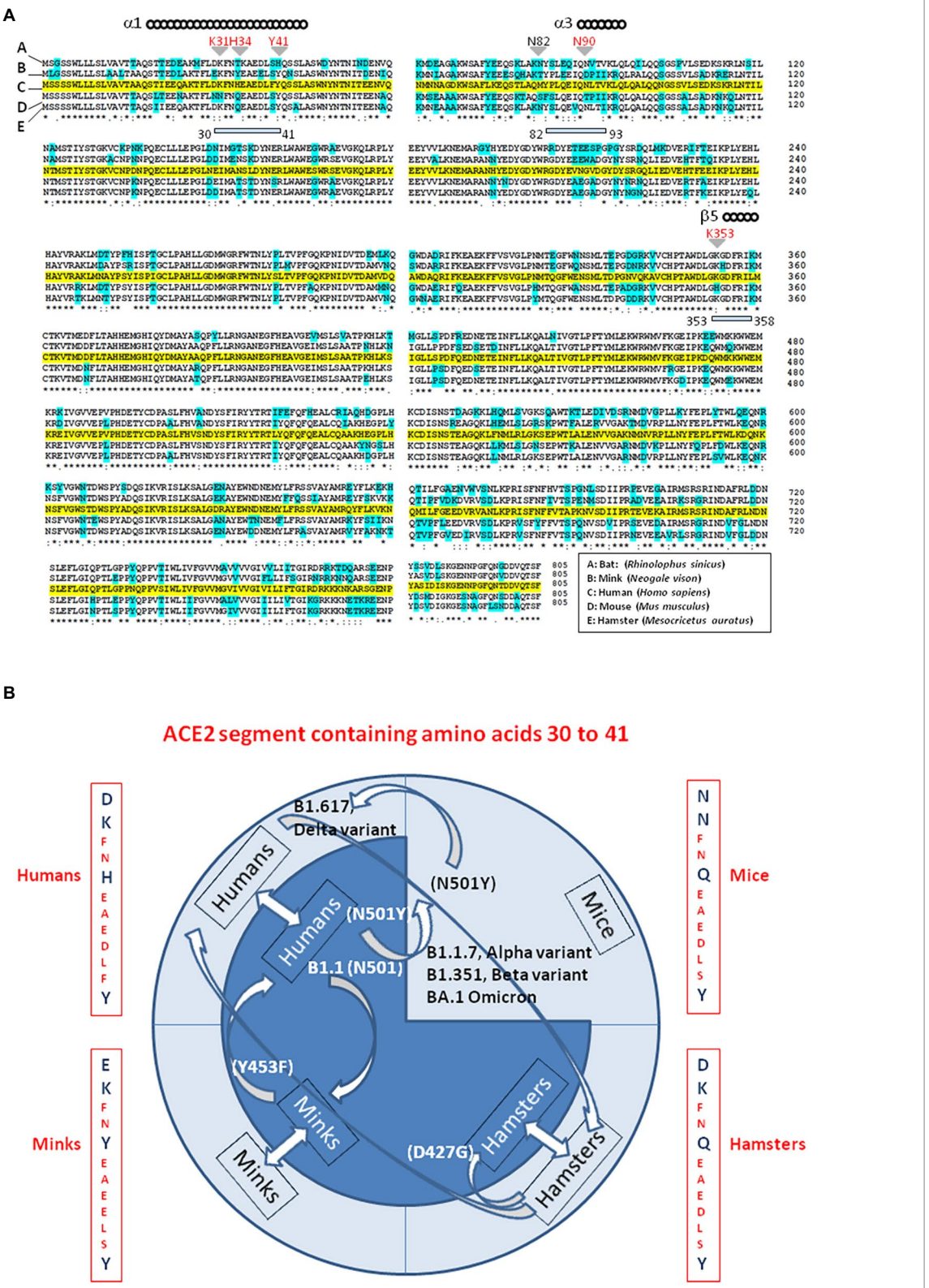

FIGURE 6
Interspecies viral circulation. **(A)** ACE2 multiple sequence alignment. The consensus ACE2 sequence from humans (*Homo sapiens*; GeneBank BAB40370.1) was compared to ACE2 sequences from mink (Neogale vison NCBI ref. sequence XP_044091953.1), hamsters (*Mesocricetus auratus*; NCBI ref. sequence XP_005074266.1), mice (*Mus musculus*; NCBI ref. sequence NP_081562.2), and bats (*Rhinolophus sinicus*; GeneBank: AGZ48803.1), using the Clustal Omega multiple sequence alignment (EMBL-EBI bioinformatic tool; Copyright © EMBL 2020;

(Continued)

FIGURE 6 (Continued)
https://www.ebi.ac.uk/Tools/msa/clustalo/). The human ACE2 sequence is highlighted in yellow. Amino acids that differ from the human ACE2 sequence in ACE2 from other species are highlighted in cyan. The (*) symbol indicates sequence identity between the ACE2 of the five species. Some of the amino acids found to be important for viral tropism in previous studies (in particular amino acid residues 31, 34, 41, 90, and 353 are important for viral spike binding). **(B)** SARS-CoV-2 is spreading on their ability to recognize a receptor and circumvent the host immune defenses. This principle accounts for the circulation of SARS-CoV-2 between species. Species living in various ecosystem show different amino acid substitutions at positions considered to be required for SARS-CoV-2 spike binding to ACE2. The ACE2 from minks shares 83% amino acid identity with the human ACE2 (63% in the region described to be involved in the interaction with the SARS-CoV-2 spike protein). Despite more than 130 substitutions out of 805 amino acids the interspecies transmission of SARS-CoV-2 from humans to minks and back to humans is possible and generates specific amino acid substitutions in each species, which improved the affinity for the ACE2 receptor as observed in Denmark' farms. The same applies in the case of the hamster-adapted Delta variant recently described in Hong Kong. SARS-CoV-2 (Wuhan-HU1 strain) cannot use mouse ACE2. It was reported that the B1.1.7 (20I/501Y.V1; UK variant), **(B)** 1.351 (20H/501Y.V2; South Africa variant) and P1 (20J/501Y.V3, Brazilian variant) SARS-CoV-2 variants and other N501Y-carrying variants exhibit extended host range to mice. Moreover, it has been postulated that the new lineage SARS-CoV-2 Omicron (BA.1, BA.2) could have a murine origin. Omicron variants (e.g., BA.5) are the SARS-CoV-2 lineages that currently cause the most cases of human infections. The amino acid differences in residues 30–41 of the N-terminal region of the ACE2 of humans, minks, hamsters, and mice, are indicated. Arrows indicate interspecies circulation of SARS-CoV-2 strains.

the critical H-bond at the mouseACE2-SARS-COV-2 RBD interface. In addition, the presence of His_{353} (instead of Lys_{353}), leads to unfavorable interactions with the SARS-CoV-2 S protein RBD (Brooke and Prischi, 2020; Gao and Zhang, 2020). However, this does not rule out the possibility of low efficiency mouse infection through an alternative receptor. It was reported that the expression of human basigin/CD147 in mice, enabled SARS-CoV-2 infection with detectable viral loads in the lungs (Wang et al., 2020). However, this model remains controversial (Shilts et al., 2021). It has been reported that the B1.1.7 (20I/501Y.V1; United Kingdom variant), B.1.351 (20H/501Y.V2; South Africa variant), and P1 (20J/501Y.V3; Brazilian variant) SARS-CoV-2 variants and other N501Y-carrying variants exhibit extended host ranges to mice (Montagutelli et al., 2021; Shuai et al., 2021). Moreover, it has been postulated that the new lineage SARS-CoV-2 Omicron variant (BA.1, BA.2), has a murine origin (Wei et al., 2021). Indeed, the interspecies conservation of ACE2 turns out to be sufficient to allow viruses that use this receptor to circulate between animal hosts and humans. Viruses do not spread based on species but based on their ability to recognize a receptor and circumvent the host immune defenses. We have proposed that this general principle accounts for the circulation of SARS-CoV-2 between species (Frutos et al., 2021, 2022; Figure 6B).

Immune response against SARS-CoV-2 and auto-antibodies against ACE2 in COVID-19 patients

Infection with SARS-CoV-2 initiates an antiviral immunoglobulin (Ig)M and IgA response, detectable during the first week of symptoms, whereas IgG are found later. The antibody titres reaches a plateau within 6 days after seroconversion (Guo et al., 2020; Kellam and Barclay, 2020; Long et al., 2020; Zhao et al., 2020). The serum level of SARS-CoV-2 specific IgA is positively correlated with the severity of COVID-19 (Ma et al., 2020; Yu et al., 2020). The state of hyperstimulation of the immune system that occurs in severely ill patients contributes to autoimmune manifestations and is associated with an increased need for oxygen therapy (Gagiannis et al., 2020). Moreover, it was recently reported that Ang II induces ROS release from monocytes able to induce DNA damages and apoptosis in neighboring T-cells leading to lymphopenia in certain patients with severe forms of COVID-19 (Kundura et al., 2022). It is neither the purpose of this paragraph to discuss the complex pattern of immune response in COVID-19 (e.g., a decrease in the total number of CD4+ and CD8+ T cells, B cells, and NK and a recruitment of neutrophils; a massive increase in the release of inflammatory cytokines or 'cytokine storm', and chemokines such as IL-2, IL6, IL-7, IL-8, IL-10, TNF, IFN; Amor et al., 2020; Campbell and Kahwash, 2020; Han et al., 2020; Luo et al., 2020; Mehta et al., 2020; Tay et al., 2020; Vitte et al., 2020; Zheng et al., 2020), nor is it to review the abnormal expression of Ag II in COVID-19 patients that could stimulate proinflammatory processes (Naftilan and Oparil, 1978; Moore et al., 2015; Varanat et al., 2017; Silva et al., 2020; Raghavan et al., 2021; Vandestienne et al., 2021; Yamamoto et al., 2021), but rather to briefly summarize the contribution of anti-ACE2 and anti-AT1R auto-antibodies in COVID-19, since these molecules could play an important role in the immunological puzzle of clinical variability of the disease.

What was intriguing in SARS-CoV-2 infected patients with respect to the RAS, was the report of the development of ACE2 auto-antibodies. Among 53 patients who had detectable anti-SARS-CoV-2 RBD, 40 (75%) had anti-ACE2 antibodies (Arthur et al., 2021). Among them, 26 (81%) belonged to the convalescent group and 14 (15; 93%) were patients hospitalized for symptoms of COVID-19. Healthy controls with no history of SARS-CoV-2 were all negative for anti-ACE2 antibodies. The median activity of sACE2 in patients with ACE2 auto-antibodies was 263 pmol/min/ml compared to 1,056 pmol/min/ml for those who did not develop an anti-ACE2 immune response. The binding of anti-ACE2 antibodies to ACE2 in normal cells could have the potential to mediate profound pathophysiological effects long after the original antigen itself has disappeared, particularly in the long term COVID-19 patients (e.g., possibly inducing myocarditis or neurological illnesses; Figure 7).

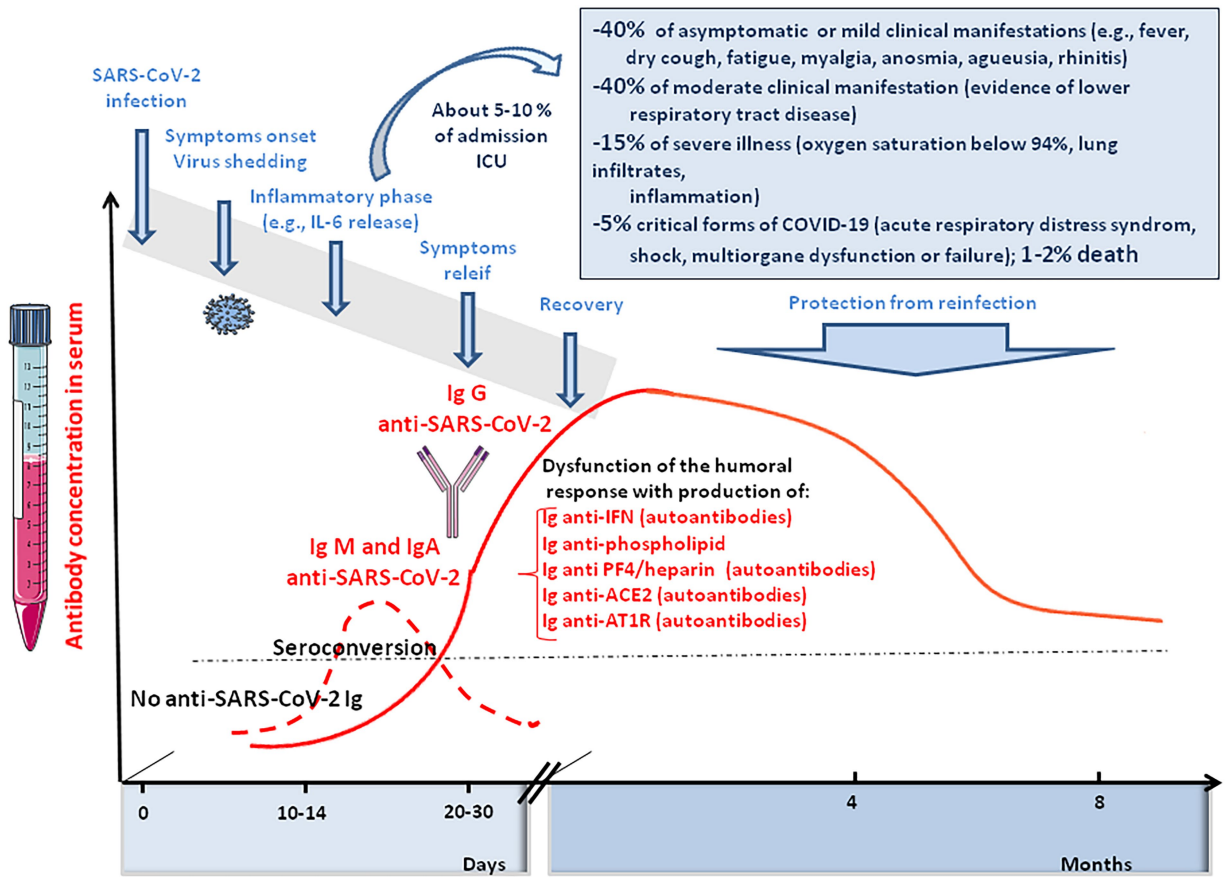

FIGURE 7
Schematic representation of the clinical course of SARS-CoV-2 infection and COVID-19. It illustrates the immune response of SARS-CoV-2 infected people, including anti-SARS-CoV-2 IgM, IgA, and IgG responses and the induction of auto-immune Ig (anti-phospholipid A, anti-PF4/heparin, anti-ACE2, and anti-AT1R).

Considering the similarities between vasculopathy in severe COVID-19 and antibody-mediated rejection after lung transplantation induced by auto-antibodies against AT1R (Cozzi et al., 2017), the presence of AT1R auto-antibodies in COVID-19 patients was investigated and compared to patients with a favorable disease course. A significant increase (42%) of anti-AT1R Ig was found in COVID-19 patients with an unfavorable disease course (Miedema et al., 2021). These AT1R auto-antibodies are expected to mimick the proinflammatory effect of Ang II, as previously reported (Dragun et al., 2005). Tissue transglutaminase (TG2)-mediated modification of AT1R contributes to AT1R auto-antibody production and hypertension associated with preeclampsia; the post-translational modification of Gln_{187} in the second extracellular loop of the AT1R loop creates a neo-epitope that induces the production of an autoantibody that can activate the receptor (Liu et al., 2015). Endothelin receptor type A (ETAR) auto-antibodies were also more frequent in severe COVID-19 patients (Miedema et al., 2021). These antibodies are known to stimulate chemotactic activity and neutrophils trafficking (Cabral-Marques et al., 2018). Both anti-AT1R and anti-ETAR antibodies could be associated with cardiovascular disease and hypertension in severe COVID-19 patients (Philogene et al., 2019).

Among other auto-antibodies found in COVID-19 patients, anti-interferon Ig was found in patients with severe COVID-19 while no such auto-antibodies were found in patients with mild disease (Bastard et al., 2020). Anti-phospholipid antibodies have also been observed as being associated with thrombotic events in COVID-19 cases (Bertin et al., 2020; Daviet et al., 2020; Harzallah et al., 2020; Helms et al., 2020; Manne et al., 2020; Siguret et al., 2020; Tan et al., 2020; Xiao et al., 2020; Zhang Y. et al., 2020; Zuo et al., 2020; Brodard et al., 2021).

SARS-CoV-2 triggers a vascular and coagulation disease

Venous thromboembolism is a relatively common side effect of SARS-CoV-2 infection. It is characterized by an acute pulmonary embolism or intravascular coagulopathy that predisposes the patients to thrombotic events (Faggiano et al., 2020; Leonard-Lorant et al., 2020; Middeldorp et al., 2020). After

the first month of infection, individuals with COVID-19 are at an increased risk of cardiovascular disease, including cerebrovascular disorders, dysrhythmias, ischemic and non-ischemic heart disease, pericarditis, myocarditis, heart failure, and thromboembolic disease (Xie et al., 2022). A nationwide cohort found an increased risk of a deep vein thrombosis up to 3 months after COVID-19, pulmonary embolisms up to 6 months, and bleeding events up to 2 months, with the risk of pulmonary embolism being especially high (Katsoularis et al., 2022). Elevated D-dimers (which reflects the degradation of fibrin and a process of hypercoagulation) upon admission of patients is a marker of hypercoagulation and pulmonary embolism and is associated with increased mortality in severe COVID-19 patients (Lippi and Favaloro, 2020; Sakka et al., 2020; Stefely et al., 2020; Smadja et al., 2021). High levels of D-dimers are found in ~ 20–40% of critically ill COVID-19 patients (Poissy et al., 2020; Zhang Y. et al., 2020; Zhang S. et al., 2020; Xie et al., 2022). Usual thrombosis prophylaxis is often not sufficient to prevent thrombotic coagulopathy in patients with severe forms of COVID-19 (Berthelot et al., 2020). These lesions usually start with intimal proliferation, followed by fragmented and discontinuous internal elastic lamina (Carvelli et al., 2020; Hofman et al., 2021). Perivascular inflammation was reported to be patchy and scattered, composed mainly of lymphocytes, with thrombi in the branches of the pulmonary artery and focal areas of congestion in the alveolar septal capillaries, as well as septal capillary lesions with wall and luminal fibrin deposition (Deshmukh et al., 2020).

The pathological manifestation of COVID-19 has a strong vascular component, with exacerbated effects on the microvasculature comprising the arterioles, capillaries, venules, and microthrombosis events. The increased occurrence of microvascular thrombi provides a good explanation for the sometimes sudden development of hypoxemia in COVID-19 patients, since the thrombi prevent gas exchange in the oxygenated areas of tissues. Beside the formation of fibrin thrombi, ARDS is characterized by increased alveolar capillary permeability and exudation into the alveoli, where inflammatory cells are present in abundance, as well as coagulation factors including fibrinogen. Regarding COVID-19, it was suggested to name severe pulmonary COVID-19 as "MicroCLOTs" for "microvascular COVID-19 lung vessels obstructive thromboinflammatory syndrome" (Ciceri et al., 2020). The analysis of autopsy lung specimens from COVID-19 patients has shown inflammatory perivascular lymphocyte infiltration, the presence of microvascular thrombi containing platelets, fibrin and numerous neutrophil extracellular traps (NETs) releasing (Carsana et al., 2020; Hofman et al., 2021). Deposits of complement components C3, C4d and C5b-9 were found in the microvasculature of the lungs (Magro et al., 2020). Patients diagnosed with elevated D-dimer and thrombosis during severe forms of COVID-19 have higher blood levels of markers of NETs and calprotectin (Zuo et al., 2020). The formation of NETs in turn, perpetuates complement activation. When activated by proinflammatory cytokines, or NETs, the vascular endothelial cells produce von Willebrand factor (vWF) that retains platelets and leucocytes to the vessel wall and activates coagulation leading to the repair of local damage. Finally, microangiopathic vessel occlusions and endothelium damage has been described in the kidneys (Goshua et al., 2020).

Among the mechanisms implicated in this thrombo-inflammation, AngII seems to have pleiotropic effects. Indeed, regarding the central role played by ACE2 as the viral entry receptor, and its role in the regulation of Ang II blood levels, the balance between ACE2 expression and the accumulation of Ang II in the blood stream may contribute to explain the immunothrombosis. The analysis of RAS dysfunction and Ang II side effects is critical for the understanding of the pathophysiological changes due to SARS-CoV-2 infection. Ang II has a significant effect on the platelet and coagulation/fibrinolytic system and causes mild activation of the coagulation cascade with increases in plasma levels of the thrombin–antithrombin complex and prothrombin (Brown and Vaughan, 2000; Larsson et al., 2000; Fletcher-Sandersjöö and Bellander, 2020; Gando and Wada, 2021). The platelet activation described after COVID-19 is thought to be due in part to the binding of AngII to AT1R. Moreover, SARS-CoV-2 can directly activate platelets by binding to platelet ACE2 (Zhang S. et al., 2020). Through binding to AT1R, Ang II stimulates the expression of Tissue Factor (TF), which triggers coagulation cascade (Nemerson, 1988; Nishimura et al., 1997; Muller et al., 2000; Felmeden et al., 2003; He et al., 2006; Brambilla et al., 2018). Ang II also induces expression of plasminogen activator inhibitor-1(PAI-1), the main inhibitor of tissue plasminogen activator and urokinase-type plasminogen activator, in cultured endothelial cells (Fogari et al., 2011). Increased levels of PAI-1 can occur locally upon SARS-CoV-2 infection, leading to the formation of plugs in the body.

The binding of SARS-Cov2 to ACE2 at the surface of endothelial cells (ECs) of blood and lymph vessels, leads to activation of the complement system, promoting a pro-coagulative state, leukocyte infiltration, vascular dysfunction, and thrombosis (Jin et al., 2020). In severe COVID-19 patients, the plasma levels intercellular adhesion molecule 1 (I-CAM-1), vascular cell adhesion molecule-1 (VCAM-1), and vascular adhesion protein-1 (VAP-1), are elevated (Escher et al., 2020; Tong et al., 2020), indicating that the endothelial barrier is damaged consecutive to viral infection. Soluble E-selectin, soluble ICAM-1, and soluble platelet endothelial adhesion molecule 1 (sPECAM-1) correlate with disease severity (Li et al., 2021; Vassiliou et al., 2021). ICAM-1 promotes fibrin adhesion and leukocyte transmigration and increased thrombus formation. Disruption of the vascular barrier is associated with the inhibition of protein C, a major anticoagulant (Dahlbäck and Villoutreix, 2005). The plasma levels of vWF, angiopoietin-2, Fms-related tyrosine kinase 3 ligand (FLT-3L), and PAI-1 are significantly elevated in patients with COVID-19 (Liu and Zhang, 2021; Figure 8). Moreover, a decrease ADAMTS13, which ensure vWF hemostatic function, has been reported in severe forms of COVID-19 (Bazzan et al., 2020; Rodriguez Rodriguez et al., 2021). It was also reported that the

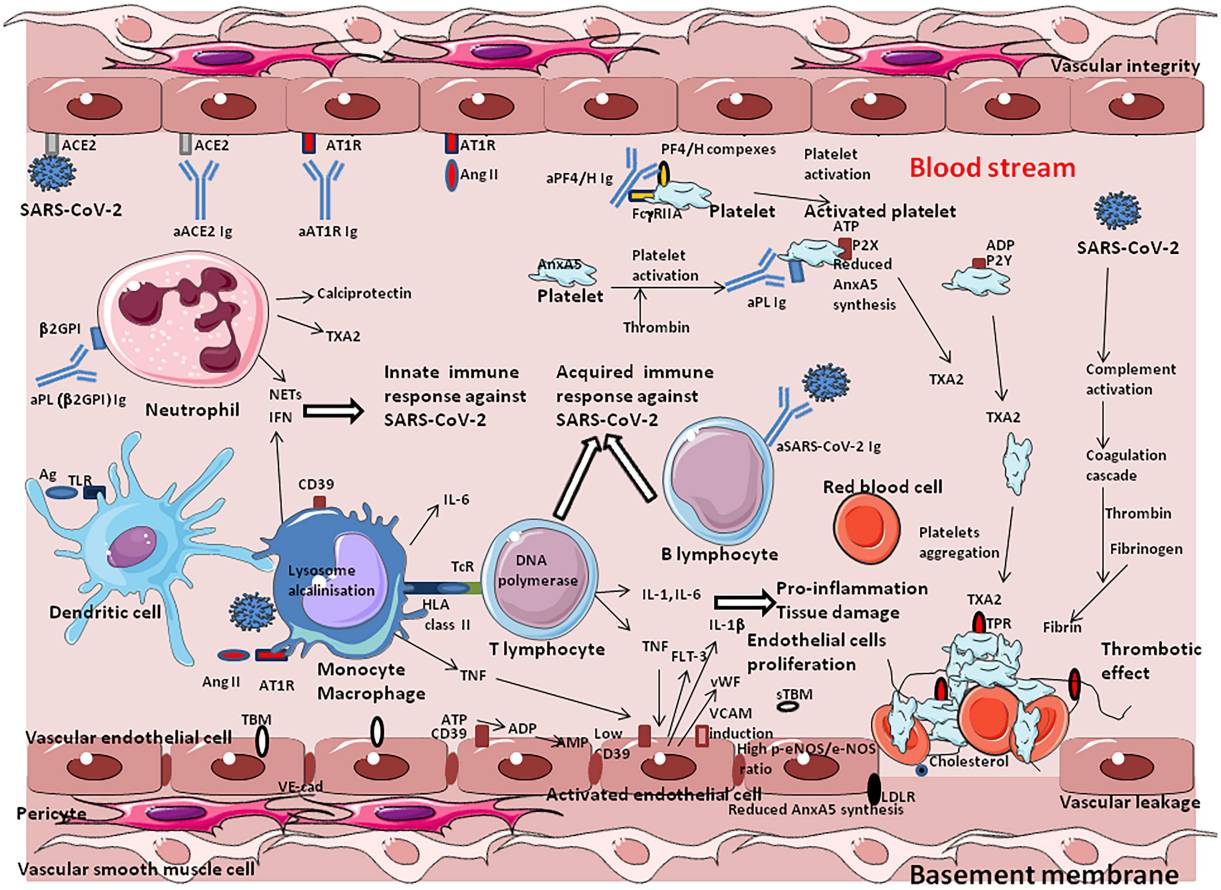

FIGURE 8
Under physiological conditions, the vascular endothelium, composed of vascular endothelial cells (VECs), functions as an integral barrier with intercellular junctions ensured by adhesion molecules such VE-cadherin. It maintains blood fluidity by acting as an anticoagulant through the suppression of platelet activation and the induction of fibrinolysis, a mechanism including heparan sulfate proteoglycans and CD39. During SARS-CoV-2 infection, innate and acquired immune defense mechanisms are activated with the overproduction of cytokines such as IL-1, IL-2, IL-6, IL-8, IL-17, and TNFα (a phenomenon known as the "cytokine storm"), which disrupts blood vessel walls and provokes tissue damage in the lung parenchyma and the immediately adjacent bronchial alveolar lymphoid tissue. The endothelial cells express the ACE2 molecule that acts as a cell-surface-receptor, facilitating SARS-CoV-2 entry into these cells. The SARS-CoV-2 induced increased concentrations of Ang II have mild platelet-activating effects, thereby enhancing coagulation and are also associated with monocyte and macrophage accumulation, which produces proinflammatory cytokines and worsen hypertension. When blood vessels are strained due to high blood pressure, the endothelial cells of the blood vessels are damaged, and the function of the endothelium at preventing arteriosclerosis is lost. When activated by proinflammatory cytokines, or neutrophil extracellular traps, endothelial cells produce von Willebrand factor, which retains platelets and leucocytes to the vessel wall and activates coagulation systems resulting in the rapid activation of mechanisms leading to the repair of local damage, the accumulation of immune cells to prevent infection, and the aggregation of platelets for primary and secondary hemostasis. Anti-PF4/polyanion (heparin) complex immunoglobulins directly activate platelets *via* their Fc gamma type 2 receptor A (FcγRIIA). The hyper-reaction set up in response to vascular damage, can influence a propensity toward local vascular micro-thrombosis. COVID-19 patients suffer from prominent alveolar oedema, intra-alveolar proteinosis, cell infiltration (including lymphocytes), apoptosis of virally-infected pneumocytes, and fibrin deposition. aPL, antiphospholipids immunoglobulins; aACE2 Ig, anti-ACE2 immunoglobulins; aAT1R Ig, anti-AT1R immunoglobulins; aPF4/H Ig, anti-PF4/heparin immunoglobulins; AnxA5, annexinA5 (or annexin V or anchorin CII; anticoagulant, interact with phospholipids); Ag, antigen; Ang II, angiotensin II; AT1R, angiotensin II receptor type 1; IFN, interferon; CD39/ENTPD1, ectonucleoside triphosphate diphosphohydrolase-1 (also known as P2 receptors: P2X receptors are ion channels that open upon binding of ATP; P2Y receptors mediate cellular response to purine and pyrimidine, such as ATP, ADP, and UTP; in physiological conditions CD39 catalyzes the reduction of ATP and ADP pool to AMP and CD73 transform AMP to adenosine whereas nucleotides released during cell activation/injury bind to P2 receptors to activate thrombo-inflammatory programs); IL-6, interleukin-6; LDLR, low density lipoprotein receptor (bind LDL/cholesterol); NETs, neutrophil extracellular traps; TcR, T-cell receptor; TLR, toll like receptor; TNF, tumor necrosis factor; TXA2, Thromboxane A2 (induce platelets aggregation); TPR, thromboxane A2 prostanoid receptor: VE-cad, VE-cadherin; TBM, thrombomodulin prevents thrombosis; upon endothelial cell activation a soluble form of TBM (sTBM) is released in plasma further promoting procoagulant mechanisms. VWF, von Willebrand factor; Fibrin, fibrin is formed from blood plasma fibrinogen (produced in the liver) by the action of thrombin; red thrombus is composed of erythrocytes enmeshed in a fibrin network.

SARS-CoV-2 main protease M^{pro} causes microvascular brain pathology by cleaving NEMO (an essential modulator of NF-κB) in infected brain ECs (Wenzel et al., 2021).

In response to COVID-19, the activation of ECs was also associated with the overexpression of proangiogenic factors, such as vascular endothelial growth factor (VEGF), basic fibroblast

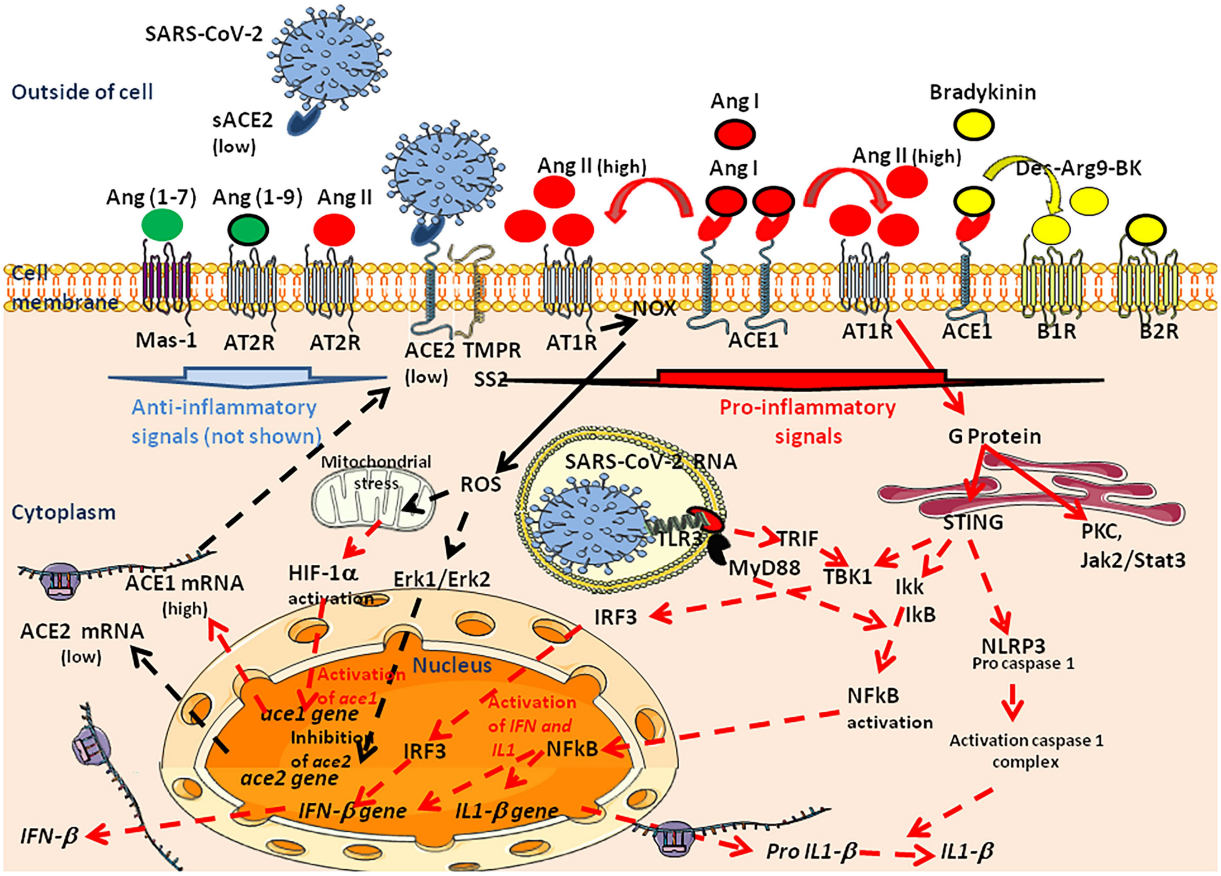

FIGURE 9
Signaling pathways that are activated during SARS-CoV-2 infection and replication. SARS-CoV-2 infects human cells expressing the ACE2 receptor and the serine protease TMPRSS2. This process results in the downregulation of ACE2 mRNA expression, the reduced expression of mACE2, dysfunction of the RAS and increasing levels of AngII in the circulation. High Ang II levels trigger signaling through AT1R. This activates a number of signaling pathways, such as G protein–mediated (Gq and Gi), Janus kinase/signal transducers and activators of transcription, extracellular signal-regulated kinase (ERK), IFN regulatory factor (IRF)3, NF-κB, NLRP3 procaspase 1 pathways leading to induction of IFNs and pro-inflammatory cytokines, and the HIF-1α pathway. In addition, G protein–independent signaling takes place through the adapter proteins β-arrestin 1 and β-arrestin 2 that can have distinct functional and physiological consequences (not shown). Crosstalk between AT1R and AT2R was evidenced and stimulation of one receptor modulates the expression of the other. Ang II can bind both to AT1R and AT2R, which are receptors with opposite effects but the low expression of AT2R compared to AT1R, account for a privilegied effect of Ang II through AT1R when the plasma levels of Ang II increase. The single AT1R gene in humans encodes a 359-amino-acid protein and AT1R is widely expressed and well conserved between species The MAS receptor can interact with AT1R, explaining that it is the physiological antagonist of Ang II signaling. Mas1 activation induces the second-messenger cAMP, phospholipase A2 pathway, and the phosphoinositide 3-kinase/AKT pathway, and mediates antiapoptotic, anti-inflammatory, vasodilatory, and antithrombotic effects. Excess of Ang II results in organ damage, hypertension, thrombotic microangiopathy, progression to fibrosis, and cardiovascular remodeling.

growth factor (FGF-2), and placental growth factors (PlGF; Smadja et al., 2021). Soluble Flt-1 (sFlt-1), a circulating truncated form of the VEGF-A receptor, was markedly increased in severe forms of COVID-19 (Rovas et al., 2020). Damage to ACE2+ pericytes and ECs leads to vascular permeability in severe COVID-19 (Cardot-Leccia et al., 2020; Afzali et al., 2021). The viral Spike induces oxidative stress, ERK1/2 activation through the CD147 receptor and NF-κB nuclear translocation in pericytes, thereby prompting dysfunction of the vascular pericytes (Avolio et al., 2021; Khaddaj-Mallat et al., 2021). CD147, considered to have a potential proatherosclerotic effect (Wang et al., 2015), is upregulated in COVID-19 patients and can act as a receptor for SARS-CoV-2 in cells expressing low ACE2 (Radzikowska et al., 2020). Interestingly, statins, the action of which partly relies on CD147 downregulation, have been recommended in the therapeutic arsenal against COVID-19 (Zhang X.J. et al., 2020).

Modulation of ACE2 and other actors of the RAS in COVID-19 patients

Coronavirus disease 2019 is a systemic disease characterized by a cytokine storm associated with high levels of C reactive protein (CRP), high fibrinogen, high fibrin degradation to D-Dimers, microvascular injury, and obstructive

thrombo-inflammatory syndrome. As knowledge grows, the need for a deeper understanding of the molecular cross-talk leading to thrombosis appears as a research priority in order to gain a better understanding of ARDS and MODS associated with severe COVID-19.

In a pioneer study it was demonstrated that SARS-CoV-1 infection was associated with ACE2 downregulation and impaired degradation of Ang II (Kuba et al., 2005). Since both SARS-CoV-1 and SAR-CoV-2 enter cells through ACE2 and induce simimlar diseases, attention rapidely focused on the consequences of virus-ACE2 interaction on the dysregulation of RAS. This is complexified by the fact that SARS-CoV-2 infection triggers IFN activation, which in turn can upregulate ACE2 (Garvin et al., 2020). Another element of complexity resides in the fact that a greater number of ACE2+ cells seems to circulate in the lungs of patients with severe COVID-19 (Ackermann et al., 2020). Using a swine animal model it was demonstrated that blocking ACE2 (or infusing Ang II) leads to increased pulmonary artery pressure, reduced blood oxygenation, increased coagulation, diffuse alveolar damage, and acute tubular necrosis (Aroor et al., 2016).

Despite efforts that have been made to quantify the compound of the RAS in COVID-19 patients, this exploration remained incomplete and debatable. An early study found no difference in the Ang II/Ang I ratio in the plasma sample of 31 COVID-19 patients, but reported that the plasma sACE2 activity was increased in patients treated with an ACE inhibitor (Kintscher et al., 2020). Another study reported increased plasma levels of Ang II in 12 patients with severe COVID-19 pneumonia (Liu et al., 2020). Furthermore, no alteration of RAS was found in a cohort of nonsevere COVID-19 patients (Rieder et al., 2021). More recently, a sevenfold ACE2 increase was found in patients with COVID-19 and Ang II as well as Ang-(1–7) concentrations was significantly higher in patients with severe COVID-19 (Reindl-Schwaighofer et al., 2021). Another investigation in a cohort of 306 COVID-19 patients revealed that elevated plasma sACE2 from COVID-19 patients was significantly associated with severe forms of disease, particularly in hospitalized patients intubated at the time of sample collection (Kragstrup et al., 2021). ARDS in patients with COVID-19 was found associated with an increase in blood pressure and decrease in serum potassium concentration (Vicenzi et al., 2020). Surprisingly, another recent report suggests a significant reduction of Ang II concentration and increased Ang-(1–7) in COVID-19 patients (Martins et al., 2021). The divergent results reported concerning the variation of RAS molecules in plasma from SARS-CoV-2-positive patients could either be explained by the differing severity of COVID-19 in the groups of patients tested and/or by the method used for quantification of the molecules (Figure 9).

Recently, by exploring different biomarkers in a cohort of COVID-19 patients (30 prolonged viral shedders and 14 short viral shedders) we found that circulating blood cells (in particular monocytes) from COVID-19 patients expressed less ACE2 mRNA than cells from healthy volunteers (Osman et al., 2021). Moreover, although we found the expression of sACE2 to be heterogenous among individuals from each group, the sACE2 plasma concentrations were found to be lower in prolonged viral shedders than in healthy controls, while the concentration of sACE2 returned to normal levels in short viral shedders. In the plasma of prolonged viral shedders, we also found higher concentrations of Ang II and Ang I. However, the plasma levels of Ang-(1–7) were found to be almost stable in prolonged viral shedders, but seemed insufficient to prevent the adverse effects of Ang II accumulation, strongly suggesting that increased levels of Ang II contribute to thrombotic events associated with the severe forms of COVID-19.

Targeting ACE2 for the therapeutic prevention of severe forms of COVID-19

In COVID-19 patients, the downregulation of ACE2 and the reduced capacity to counteract the detrimental effects of Ang II are likely to play a critical role in the development of severe forms of the disease. In experimental animal models, ACE2 KO mice experienced more severe forms of acute lung injury than wild type mice, highlighting the protective role of ACE2 (Imai et al., 2005). The loss of ACE2 resulted in enhanced vascular permeability, neutrophils accumulation and increased lung edema. Both angiotensinogen-specific antisense oligonucleotides and small interfering RNA (siRNA) lowered blood pressure in rat models of hypertension (Mullick et al., 2017; Uijl et al., 2019). In humans with weight excess and hypertension, renin inhibitors (e.g., aliskiren) and ACEi (e.g., ramipril), improve renal and systemic hemodynamics and reduce arterial pressure (Kwakernaak et al., 2017). Thus, therapeutic solutions for reducing COVID-19 severity could be found in the pharmacopeia used by cardiologists to intervene on the RAS.

All FDA approved drugs for treatment of patients with high blood pressure (renin inhibitors, ACEi, and ARBs) are primarily designed to block or reduce the detrimental effects of Ang II (Wright, 2000; Mentz et al., 2013; Arendse et al., 2019; Figure 10A). Reducing the formation of Ang II by ACEi or antagonizing its effect by blocking the AT1R through ARBs may be a suitable strategy for reducing symptoms of COVID-19 patients (Schiffrin et al., 2020). ARBs (e.g., losartan) were found to protect against acute lung injury through the reduction of Ang II/AT1R stimulation (Shen et al., 2009; Meng et al., 2020). Hypertensive patients taking ARBs presented a lower risk of severe COVID-19 (Sarzani et al., 2020). However, the interpretation of the benefits and harmful effects of ACEi and ARBs may be premature due to the multiple effects of such molecules on the RAS (Kai et al., 2021; Tereshchenko et al., 2022). Indeed, it has been reported that ACEi and ARBs increase ACE2 (Ferrario et al., 2005; Furuhashi et al., 2015), which could also increase the binding of SARS-CoV-2. However, it has been reported that ACE2 is not increased by ACEi or ARBS in the respiratory cilia (Lee et al., 2020). We recently reported that *in vitro* treatment of SARS-CoV-2 permissive ACE2+/AT1R+ Vero E6 cells with various ARBs resulted into

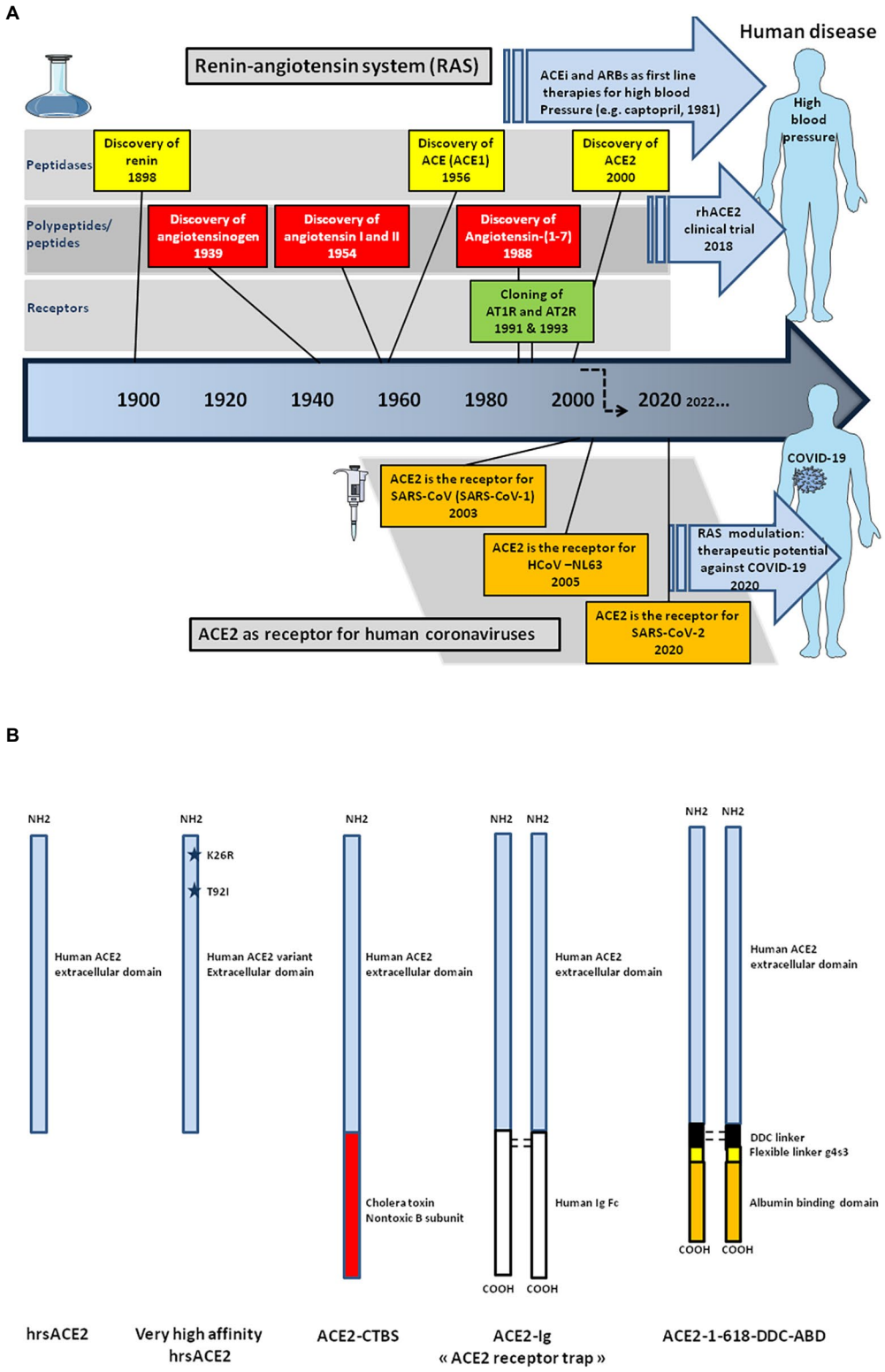

FIGURE 10
Schematic representation of the historical discovery of the main components of the renin-angiotensin system (RAS) and ACE2 candidate therapeutic molecules. **(A)** In 1898, renin was the first component of the RAS to be discovered. Vasoconstriction of the renal artery was then shown to lead to high blood pressure, thus driving the discovery of hypertensin and angiotonin (a compound later termed angiotensin). Angiotensin was subsequently characterized, as well as two downstream conpounds, the Ang I and Ang II, respectively. The ACE peptidase responsible for processing of Ang I into Ang II was subsequently characterized in 1956. The first orally active angiotensin-converting enzyme

(Continued)

FIGURE 10 (Continued)
inhibitor, captopril, was used as antihypertensive therapy in patients with high blood pressure from the early 80s. The AT1R receptor was cloned in 1991, followed by the cloning of AT2R. Then, the counter-regulatory pathway of RAS was described in 2000, with the discovery of ACE2 by two independent research groups and identification of the Ang-(1–7)/Mas receptor interacting partners was achieved two decades later. The cardioprotective effects of ACE2 were discovered as was its ability to process Ang II into Ang-(1–7). Finally, studies have identified the ACE2 protease domain as the receptor for severe acute respiratory syndrome-coronavirus (SARS-CoV-1) in 2003, HCoV-NL63 in 2005, and, more recently (2020), SARS-CoV-2. **(B)** The ACE2 peptidase extracellular domain known to bind the SARS-CoV-2 Spike can be produced as a recombinant soluble molecule able to neutralize SARS-CoV-2. Various amino acid substitutions can be introduced in the sequence of the ACE2 extracellular domain by genetic engeneering to change the affinity of the recombinant molecule for the viral spike. However, hrsACE2 appears to have a short half-life the efficiency of which could be improved by engineering fusion proteins. The fusion of the rhACE2 extracellular domain with the nontoxic subunit B of cholera toxin (ACE2-CTBS) improves transmucosal transport. The recombinant ACE2-Ig fusion protein consists of a homodimer of the ACE2 extracellular domain linked to an Fc domain of human IgG increasing the stability of the molecule but could also act as cargo for the virus through the Fc-Tag to attach cells like macrophages that express high levels of the Fc receptor. The addition of an albumin binding domain in fusion with ACE2 extend the duration of ACE2 action.

~50% increase in SARS-CoV-2 production correlated with the ARBs-induced up-regulation of ACE2 expression (Pires de Souza et al., 2022). However, we also observed a downregulation of AT1R, suggesting that Ang II harmful effects should be strongly reduced (Pires de Souza et al., 2022). The upregulation of ACE2 can have opposed effects on SARS-CoV-2 infection and organ pathophysiology (Devaux, 2020). The study of large cohorts support the beneficial effects of RAS inhibitors in patients with COVID-19 (Bean et al., 2020; Zhang P. et al., 2020). In patients, ARBs is preferred over ACEi for first line hypertension treatment and discontinuing treatment is not required (Abbasi, 2021; Lopez et al., 2021). Since, the activation of AT1R by Ang II induces ROS through the NADPH oxidase pathway and activates the hypoxia-inducible factor (HIF)-1α leading to the synthesis of the transient receptor potential channel ankyrin repeat (TRPA1) which controls intracellular calcium increase and potentially contributes to pulmonary inflammation, it was also suggested to use calcium channel blokers as an alternative to ACEi and ARBS (Fang and Karakiulakis, 2020; Tignarelli et al., 2020; Devaux and Raoult, 2022; Zhang et al., 2022). Moreover, acting on HIF-1α, may improve the outcome of COVID-19 by decreasing hypoxia (Devaux and Raoult, 2022).

In silico methods of molecular docking have been used to develop allosteric activators of ACE2 such as xanthenone (XNT), the antiprotozoal dimiazene aceturate (DIZE) drug, and resorcinolnaphthalein (Hernández Prada et al., 2008; Gjymishka et al., 2010). Activation of ACE2 by XNT, prevented elevated right ventricular systolic pressure, ventricular hypertrophy, and increased pulmonary vessel wall thickness (Ferreira et al., 2009; Fraga-Silva Rodrigo et al., 2013; Cole-Jeffrey et al., 2015). DIZE was found to reduce the severity of hyperoxic lungs injury by inhibiting the inflammatory response and oxidative stress, to attenuate the myocardial infarction, and to prevent atherosclerosis by increasing ACE2 mRNA expression (Kulemina and Ostrov, 2011; Qi et al., 2013; Shenoy et al., 2013; Haber et al., 2014; Qiu et al., 2014; Goru et al., 2017; Fang et al., 2019; Qaradakhi and Gadanec, 2020). Various FDA-approved molecules are under study for evaluating their ability to reduce COVID-19 severity (Albini et al., 2020; Lubbe et al., 2020; Qaradakhi and Gadanec, 2020). For example, the virtual screening of 2,456 approved drugs as inhibitors of SARS-CoV-2 spike-ACE2 interaction highlighted the properties of riboflavin (a vitamin), fenoterol (a bronchodilator), vidaranine (an anti-neoplastic agent), and cangrelor (an anti-platelet agent; Prajapat et al., 2020).

A better understanding of the role of the ACE2, encouraged the use of human recombinant soluble ACE2 (hrsACE2) in medicine (Kuba et al., 2005; Oudit et al., 2010; Johnson et al., 2011). In a tolerability study in healthy volunteers, doses up to 1.2 mg/kg hrsACE2 were administered intraveinously and the plasma half-life of the molecule was in the range of 10 h (Haschke et al., 2013). Despite a fast clearance rate, the administration of hrsACE2 alleviated the severity of influenza A H7N9 and respiratory syncytial virus (RSV)-induced lung injury (Yang et al., 2014; Gu et al., 2016). This hrsACE2 was also found to reduce IL-6 when given to healthy volunteers suffering from ARDS (Khan et al., 2017; Zhang and Baker, 2017). Through its binding to the viral S protein, sACE2 could act as a decoy receptor and could reduce the harmful effect of Ang II by making mACE2 available for the conversion of Ang II (Patel et al., 2014; Devaux et al., 2020; Issa et al., 2021; Krishnamurthy et al., 2021). The infusion of a single dose of hrsACE2 (GSK2586881 at 0.4 mg/kg *i.v.*), was found to be well-tolerated and to have potential haemodynamic benefits in pulmonary arterial hypertension (Hemnes et al., 2018). A hrsACE2 clinical trial is ongoing (NCT00886353) for the treatment of cardiovascular diseases (Ghatage et al., 2021). It has been reported that ACE2 S_{680}D gain-function knock-in mice are protected against hypoxia-induced pulmonary hypertension (Zhang et al., 2018). This has also opened the way to modified *ACE2* for gene transfer (Guignabert et al., 2018). It was recently demonstrated that recombinant ACE2 is effective for treating SARS-CoV-2 RBD protein-aggravated LPS-induced acute lung injury in a mouse experimental model and that the protection occurs by acting on the ACE2-AngII-AT1R-NOX1/2 axis that is otherwise overactivated by the SARS-CoV-2 infection (Zhang et al., 2022).

A proof-of-concept of the efficiency of the hrsACE2 therapeutic approach in COVID-19 was described in a case report of a 45-year-old woman infected by SARS-CoV-2 who was admitted to hospital with a 7-day history of severe symptoms. Two days after hospital admission, she was treated with 0.4 mg/kg of

hrsACE2 intravenous infusion twice daily. Surprisingly after the first injection the patient became afebrile, the biological investigation indicated a marked reduction of Ang II, an increase of sACE2 in plasma, and her clinical condition improved gradually (Zoufaly et al., 2020). A large phase II clinical trial has been initiated by the Austrian pharmaceutical company APEIRON to treat COVID-19 patients with APN01-rhACE2. More recently, hrsACE2, in combination with sub-toxic remdesivir, was found to reduce viral load by 60% in a model of SARS-CoV-2 infected kidney organoids (Monteil et al., 2021).

Given such encouraging results, it seemed important to design molecules with improved activity against SARS-CoV-2 (Maiti, 2021; Figure 10B) A fusion molecule consisting of murine rACE2 with a Fc fragment (rACE2-Fc), demonstrated a long-lasting ability to protect organs in mice models of Ang II-dependent hypertension (Liu et al., 2018). It was also reported that *Lactobacillus paracasi* probiotic expressing a hrACE2 extracellular domain in fusion with the nontoxic subunit B of cholera toxin, resulted in increased ACE2 activities in serum of mice treated with this compound (Verma et al., 2019). Another molecule, rACE2 extracellular domain fused to the FC region of the IgG1, has been shown to neutralize viruses pseudotyped with SARS-CoV-2 spike proteins *in vitro* (Lei et al., 2020). A new set of molecules named "ACE2 receptor trap" that contain the extracellular domain residues 18–614 (including the SARS-CoV-2 RBD), and collectrin domain of ACE2 fused to human IgG1 Fc fragment for increased stabilization and avidity, were designed (Glasgow et al., 2020). *In silico*, ACE2 variants $Lys_{26}Arg$ and $Thr_{92}Ile$ were predicted to have increased affinity for the viral S protein when compared to wildtype ACE2. Consistent with this, soluble ACE2 $Lys_{26}Arg$ and $Thr_{92}Ile$ were more effective in blocking the entry of the SARS-CoV-2 S protein pseudotyped virus (Suryamohan et al., 2021). Another type of therapeutic molecules containging the hrsACE2 fused with a 5 kD albumin binding domain and bridged *via* a dimerization hinge-like peptide motif (termed ACE2 1-618-DDC-ABD) was first tested in an animal model prevented mortality in the treated group while untreated animals became severely hill and were found to have extensive pulmonary hemorrhage and mononuclear infiltrates (Hassler et al., 2021). The very rapid accumulation of three-dimensional structural data is likely to greatly accelerate the development of molecules aimed at treating COVID-19 patients (Sorokina et al., 2020).

Discussion

For virologists, ACE2 is the receptor for Sarbecoviruses. But to see ACE2 as a simple receptor necessary to initiate the replication cycle of the virus would be to ignore the essential role of ACE2 in the pathophysiology of COVID-19. ACE2 was not maintained during species evolution to wait for an unlikely meeting with a spike of Sarbecovirus. The regulatory function of the RAS pathway naturally devolved to ACE2 is the key element to be considered. The imbalance of the RAS pathway followed by the uncontrolled elevation of Ang II levels in SARS-CoV-2 infected patients and signaling through AT1R is the triggering event that can lead to severe forms of COVID-19. Thereby, COVID-19 is primarily a vascular rather than a respiratory disease and Ang II/AT1R blockade might attenuate progression to COVID-19.

The global COVID-19 Host Genetics Initiative (HGI) was set up to bring together international experts in human genetics and epidemiology to explore the genetic determinants of COVID-19 susceptibility, who have shed light on several host factors including ACE2, ACE, TMPRSS2, several chemokine receptors, the IL-6 receptor, IFN, and HLA, which are likely at the forefront of parameters affecting the disease severity (Correale et al., 2020; Ellinghaus et al., 2020; Initiative, 2020; Karaderi et al., 2020; Lorente et al., 2020; Nguyen et al., 2020; Strafella et al., 2020; Zhang Q. et al., 2020; Fricke-Galindo, 2021; Goujon et al., 2021; Martin-Sanchos et al., 2021; Pairo-Castineira et al., 2021). The list of genes possibly involved in the severity of COVID-19 continues to grow and indicates that the predisposition to severe COVID-19 is multifactorial. Understanding these pathways may help identifying targets for COVID-19 therapy and prophylaxis. Although the implication of a multiplicity of genes in the severity of COVID-19 is oubvious when considering the heterogenity in patient's cases, we consider members of RAS as the main actors of the pathophysiological process. Besides ACE2 and Ang II, RAS can also be regulated by insertion/deletion (I/D) polymorphism of the ACE gene increasing the risk of severe forms of COVID-19 (Marshall et al., 2002; Harrap et al., 2003; Sayed-Tabatabaei et al., 2006; Gupta et al., 2009; Yamamoto et al., 2021). Association between the I/D polymorphism and blood pressure status has been reported (Jeunemaitre et al., 1992; Schmidt et al., 1993; Duru et al., 1994; Kario et al., 1999; Giner et al., 2000; Martinez et al., 2000; Agachan et al., 2003). Infusion of Ang I into normosensitive men was followed by higher venous levels of Ang II and increase in blood pressure in D/D carriers compared with I/I carriers (Ueda et al., 1995). Moreover, it has been reported that higher plasma IL-6 levels can be detected in ST segment elevation myocardial infarction patients, when the D allele is present (Dai et al., 2019). The possible association between the ACE genotype and the severity of COVID-19 should be further explored (Celik et al., 2021; Verma et al., 2021). One report indicates that the prevalence of D/D polymorphism is higher in COVID-19 patients with pulmonary embolism (PE) than patients without PE (Calabrese et al., 2021).

Our review highlights that the most important factors associated with severe COVID-19 outcome are related to the RAS and the regulation of blood pressure and coagulation. By focusing our attention to ACE2, we have come to the conclusion that this molecule may potentially play contrasting roles at different stages of the disease, with its ability to enable viral entry into the cell at early stages of infection thereby increasing disease susceptibility

and later by decreasing Ang II/AT1R signaling thereby reducing the severity of the disease. Revisiting the structure and function of this molecule highlights the crucial role of ACE2 in the pathophysiology of sarbecoviruses-induced diseases, particularly in the context of inflammation and thrombosis. A low expression of ACE2 in the respiratory tract (e.g., epithelial cells, arterial and venous endothelial cells present in abundance in the lungs, and arterial smooth muscles) is associated with increased circulating levels of Ang II. The interaction of Ang II with AT1R and activation of various AT1R-dependent signaling pathways induce ROS release from monocytes able to trigger DNA damages and apoptosis in neighboring T-cells leading to lymphopenia, and endothelial injury by inhibiting NO synthesis. It is associated with vasoconstriction, hypertension, vascular permeability, fluid extravasation, and accelerated thrombosis in arterioles by activating hemostasis and the complement system. This process is accompanied by a recruitment of neutrophils and macrophages to the affected tissues leading to the "cytokine storm" (e.g., IL-6, MIP2, TNFα, and IFN responses). Perivascular inflammation is composed mainly of lymphocytes, with thrombi in the branches of the pulmonary artery and focal areas of congestion in the alveolar septal capillaries, as well as septal capillary lesions with wall and luminal fibrin deposition. Taken as a whole, these observations lead us to assume that instead of considering COVID-19 as respiratory tract diseases, we should rather see this disease as a clinical picture of hypercoagulopathy, microvascular immunothrombosis, and hyperinflammation. The loss of ACE2 function after the binding of SARS-CoV-2 is driven by mACE2 receptor endocytosis, activation of proteolytic cleavage of mACE2 and *ACE2* gene transcriptional downregulation. Accurate quantification of RAS biomarkers should be added to the collection of tools aimed at monitoring COVID-19 infection both at pre-clinical and clinical levels.

According to the literature and our own observations, ACE2 and Ang II are the most relevant host factors in later stages of the disease and ACE2 should be seen as an ally in the global fight against COVID-19 and should be considered when designing appropriated drugs for COVID-19 therapy. It now appears that we can see the direction in wich work to deal with this disease should head. It requires treatment consisting in maintaining the homeostasis of the RAS pathway by preventing the elevation of the circulating levels of Ang II through sufficient biodisponibility of ACE2 to hydrolyze Ang II (including the use of human recombinant soluble ACE2), by inhibiting the Ang II/AT1R axis using ARBs which decrease the surface expression of AT1R, and/or by using calcium channel blokers as an alternative to ACEi and ARBS.

Author contributions

CD conceived the manuscript and wrote the first draft. LC-J participated in the correction of the manuscript. Both authors contributed to the article and approved the submitted version.

Funding

This work was supported by the French Government under the "Investissements d'avenir" (Investments for the Future) program managed by the Agence Nationale de la Recherche (French ANR: National Agency for Research; reference: Méditerranée Infection 10-IAHU-03 to Professor Didier Raoult), and annual funds from Aix-Marseille university and IRD to the MEPHI research unit (Director: Professor Jean-Christophe Lagier). Other funding sources were limited to the salaries of the authors (Center National de la Recherche Scientifique for CAD, Assistance Publique Hôpitaux de Marseille for LCJ), with no other role or involvement.

Acknowledgments

We thank JC Lagier and D. Raoult for stimulating discussions and their unwavering support. Figures were designed using the Servier Medical Art supply of images available under a Creative Commons CC BY 3.0 license.

Conflict of interest

CD declares a link of interest with the Sanofi and Merck pharmaceutical companies.

The remaining author declares that the research was conducted in the absence of any commercial or financial relationships that could be construed as a potential conflict of interest.

Publisher's note

References

Abbasi, J. (2021). Choose ARBs over ACE inhibitors for first-line hypertension treatment, large new analysis suggests. *JAMA* 326, 1244–1245. doi: 10.1001/jama.2021.14017

AbdAlla, S., Lother, H., and Quitterer, U. (2000). AT1-receptor heterodimers show enhanced G-protein activation and altered receptor sequestration. *Nature* 407, 94–98. doi: 10.1038/35024095

Abdeen, S., Bdeir, K., Abu-Fanne, R., Maraga, E., Higazi, M., Khurram, N., et al. (2021). Alpha-defensins: risk factor for thrombosis in COVID-19 infection. *Brit. J. Haematol.* 194, 44–52. doi: 10.1111/bjh.17503

Abu Hasan, Z., Williams, H., Ismail, N. M., Othman, H., Cozier, G. E., Acharya, K. R., et al. (2017). The toxicity of angiotensin converting enzyme inhibitors to larvae of the disease vectors Aedes aegypti and Anopheles gambiae. *Sci. Rep.* 7:45409. doi: 10.1038/srep45409

Ackermann, M., Verleden, S. E., Kuehnel, M., Haverich, A., Welte, T., Laenger, F., et al. (2020). Pulmonary vascular endothelialitis, thrombosis, and angiogenesis in Covid-19. *N. Engl. J. Med.* 383, 120–128. doi: 10.1056/NEJMoa2015432

Advani, A., Kelly, D. J., Cox, A. J., White, K. E., Advani, S. L., Thai, K., et al. (2009). The (pro)renin receptor: site-specific and functional linkage to the vacuolar H+-ATPase in the kidney. *Hypertension* 54, 261–269. doi: 10.1161/HYPERTENSIONAHA.109.128645

Afelt, A., Frutos, R., and Devaux, C. (2018). Bats, coronaviruses, and deforestation: toward the emergence of novel infectious diseases? *Front. Microbiol.* 9:702. doi: 10.3389/fmicb.2018.00702

Afzali, B., Noris, M., Lambrecht, B. N., and Kemper, C. (2021). The state of complement in COVID-19. *Nat. Rev. Immunol.* 22, 77–84. doi: 10.1038/s41577-021-00665-1

Agachan, B., Isbir, T., Yilmaz, H., and Akoglu, E. (2003). Angiotensin converting enzyme I/D, angiotensinogen T174M-M235T and angiotensin II type 1 receptor A1166C gene polymorphisms in Turkish hypertensive patients. *Exp. Mol. Med.* 35, 545–549. doi: 10.1038/emm.2003.71

Aguilar, R., Jedlicka, A. E., Mintz, M., Mahairaki, V., Scott, A. L., and Dimopoulos, G. (2005). Global gene expression analysis of Anopheles gambiae responses to microbial challenge. *Insect Biochem. Mol. Biol.* 35, 709–719. doi: 10.1016/j.ibmb.2005.02.019

Albini, A., Di Guardo, G., McClain Noonan, D., and Lombardo, M. (2020). The SARS-CoV-2 receptor, ACE-2, is expressed on many diferent cell types: implications for ACE-inhibitor-and angiotensin II receptor blocker-based cardiovascular therapies. *Intern. Emerg. Med.* 15, 759–766. doi: 10.1007/s11739-020-02364-6

Alderman, M. H., Madhavan, S., Ooi, W. L., Cohen, H., Sealey, J. E., and Laragh, J. H. (1991). Association of the renin sodium profile with the risk of myocardial-infarction in patients with hypertension. *New Engl. J. Med.* 324, 1098–1104. doi: 10.1056/NEJM199104183241605

AlGhatrif, M., Tanaka, T., Moore, A. Z., Bandinelli, S., Lakatta, E. G., and Ferrucci, L. (2021). Age-associated difference in circulating ACE2, the gateway for SARS-COV-2, in humans: results from the InCHIANTI study. *GeroScience* 43, 619–627. doi: 10.1007/s11357-020-00314-w

Amor, S., Fernandez Blanco, L., and Baker, D. (2020). Innate immunity during SARS-CoV-2: evasion strategies and activation trigger hypoxia and vascular damage. *Clin. Exp. Immunol.* 202, 193–209. doi: 10.1111/cei.13523

Andersson, R., Gebhard, C., Miguel-Escalada, I., Hoof, I., Bornholdt, J., Boyd, M., et al. (2014). An atlas of active enhancers across human cell types and tissues. *Nature* 507, 455–461. doi: 10.1038/nature12787

Aragao, D. S., Cunha, T. S., Arita, D. Y., Andrade, M. C. C., Fernandes, A. B., Watanabe, I. K. M., et al. (2011). Purification and characterization of angiotensin converting enzyme 2 (ACE2) from murine model of mesangial cell in culture. *Int. J. Biol. Macromol.* 49, 79–84. doi: 10.1016/j.ijbiomac.2011.03.018

Arendse, L. B., Danser, A. H. J., Poglitsch, M., Touyz, R. M., Burnett, J. C., Llorens-Cortes, C., et al. (2019). Novel therapeutic approaches targeting the renin-angiotensin system and associated peptides in hypertension and heart failure. *Pharmacol. Rev.* 71, 539–570. doi: 10.1124/pr.118.017129

Aroor, A., Zuberek, M., Duta, C., Meuth, A., Sowers, J. R., Whaley-Connell, A., et al. (2016). Angiotensin II stimulation of DPP4 activity regulates megalin in the proximal tubules. *Int. J. Mol. Sci.* 17:780. doi: 10.3390/ijms17050780

Arthur, J. M., Forrest, J. C., Boehme, K. W., Kennedy, J. L., Owens, S., Herzog, C., et al. (2021). Development of ACE2 autoantibodies after SARSCoV-2 infection. *PLoS One* 16:e0257016. doi: 10.1371/journal.pone.025701

Avolio, E., Carrabba, M., Milligan, R., Kavanagh Williamson, M., Beltrami, A. P., Gupta, K., et al. (2021). The SARS-CoV-2 spike protein disrupts human cardiac pericytes function through CD147-receptor-mediated signalling: a potential non-infective mechanism of COVID-19 microvascular disease. *Clin. Sci.* 135, 2667–2689. doi: 10.1042/CS20210735

Bader, M., Alenina, N., Young, D., Santos, R. A. S., and Touyz, R. M. (2018). The meaning of Mas. *Hypertension* 72, 1072–1075. doi: 10.1161/HYPERTENSIONAHA.118.10918

Baggen, J., Vanstreels, E., Jansen, S., and Daelemans, D. (2021). Cellular host factors for SARS-CoV-2 infection. *Nat. Microbiol.* 6, 1219–1232. doi: 10.1038/s41564-021-00958-0

Baratchian, M., McManus, J. M., Berk, M. P., Nakamura, F., Mukhopadhyay, S., Xu, W., et al. (2021). Androgen regulation of pulmonary AR, TMPRSS2 and ACE2 with implications for sex-discordant COVID-19 outcomes. *Sci. Rep.* 11:11130. doi: 10.1038/s41598-021-90491-1

Barkauskas, C. E., Cronce, M. J., Rackley, C. R., Bowie, E. J., Keene, D. R., Stripp, B. R., et al. (2013). Type 2 alveolar cells are stem cells in adult lung. *J. Clin. Invest.* 123, 3025–3036. doi: 10.1172/JCI68782

Barker, H., and Parkkila, S. (2020). Bioinformatic characterization of angiotensin-converting enzyme 2, the entry receptor for SARS-CoV-2. *PLoS One* 15:e0240647. doi: 10.1371/journal.pone.0240647

Bastard, P., Rosen, L. B., Zhang, Q., Michailidis, E., Hoffmann, H. H., Zhang, Y., et al. (2020). Autoantibodies against type I IFNs in patients with life-threatening COVID-19. *Science* 370:eabd4585. doi: 10.1126/science.abd4585

Bavishi, C., Maddox, T. M., and Messerli, F. H. (2020). Coronavirus disease 2019 (COVID-19) infection and renin angiotensin system blockers. *JAMA Cardiol.* 5, 745–747. doi: 10.1001/jamacardio.2020.1282

Bazzan, M., Montaruli, B., Sciascia, S., Cosseddu, D., Norbiato, C., and Roccatello, D. (2020). Low ADAMTS 13 plasma levels are predictors of mortality in COVID-19 patients. *Intern. Emerg. Med.* 15, 861–863. doi: 10.1007/s11739-020-02394-0

Beacon, T. H., Delcuve, G. P., and Davie, J. R. (2021). Epigenetic regulation of ACE2, the receptor of the SARS-CoV-2 virus. *Genome* 64, 386–399. doi: 10.1139/gen-2020-0124

Bean, D. M., Kraljevic, Z., Searle, T., Bendayan, R., Kevin, O., Pickles, A., et al. (2020). Angiotensin-converting enzyme inhibitors and angiotensin II receptor blockers are not associated with severe COVID-19 infection in a multi-site UK acute hospital trust. *Eur. J. Heart Fail.* 22, 967–974. doi: 10.1002/ejhf.1924

Benetti, E., Tita, R., Spiga, O., Ciolfi, A., Birolo, G., Bruselles, A., et al. (2020). ACE2 gene variants may underlie interindividual variability and susceptibility to COVID-19 in the Italian population. *Eur. J. Hum. Genet.* 28, 1602–1614. doi: 10.1038/s41431-020-0691-z

Berk, B. C., Vekshtein, V., Gordon, H. M., and Tsuda, T. (1989). Angiotensin II-stimulated protein synthesis in cultured vascular smooth muscle cells. *Hypertension* 13, 305–314. doi: 10.1161/01.HYP.13.4.305

Bernardi, S., Toffoli, B., Zennaro, C., Tikellis, C., Monticone, S., Losurdo, P., et al. (2012). High-salt diet increases glomerular ACE/ACE2 ratio leading to oxidative stress and kidney damage. *Nephrol. Dial. Transplant.* 27, 1793–1800. doi: 10.1093/ndt/gfr600

Berthelot, J. M., Drouet, L., and Lioté, F. (2020). Kawasaki-like diseases and thrombotic coagulopathy in COVID-19: delayed over-activation of the STING pathway? *Emerg. Microb. Infect.* 9, 1514–1522. doi: 10.1080/22221751.2020.1785336

Bertin, D., Brodovitch, A., Beziane, A., Hug, S., Bouamri, A., Mege, J. L., et al. (2020). Anticardiolipin IgG autoantibody level is an independent risk factor for COVID-19 severity. *Arthritis Rheum.* 72, 1953–1955. doi: 10.1002/art.41409

Blume, C., Jackson, C. L., Spalluto, C. M., Legebeke, J., Nazlamova, L., Conforti, F., et al. (2021). A novel ACE2 isoform is expressed in human respiratory epithelia and is upregulated in response to interferons and RNA respiratory virus infection. *Nat. Genet.* 53, 205–214. doi: 10.1038/s41588-020-00759

Boklund, A., Hammer, A. S., Quaade, M. L., Rasmussen, T. B., Lohse, L., Strandbygaard, B., et al. (2021). SARS-CoV-2 in danish mink farms: course of the epidemic and a descriptive analysis of the outbreaks in 2020. *Animals* 11:164. doi: 10.3390/ani11010164

Bosso, M., Thanaraj, T. A., Abu-Farha, M., Alanbaei, M., Abubaker, J., and Fahd, A.-M. (2020). The two faces of ACE2: the role of ACE2 receptor and its polymorphisms in hypertension and COVID-19. *Mol. Ther. Meth. Clin. Dev.* 18, 321–327. doi: 10.1016/j.omtm.2020.06.017

Boustany, C. M., Bharadwaj, K., Daugherty, A., Brown, D. R., Randall, D. C., and Cassis, L. A. (2004). Activation of the systemic and adipose renin-angiotensin system in rats with diet-induced obesity and hypertension. *Am. J. Physiol. Regul. Integrat. Comparat. Physiol.* 287, R943–R949. doi: 10.1152/ajpregu.00265.2004

Brambilla, M., Gelosa, P., Rossetti, L., Castiglioni, L., Zara, C., Canzano, P., et al. (2018). Impact of angiotensin-converting enzyme inhibition on platelet tissue factor expression in stroke-prone rats. *J. Hypertens.* 36, 1360–1371. doi: 10.1097/HJH.0000000000001702

Brest, P., Refae, S., Mograbi, B., Hofman, P., and Milano, G. (2020). Host polymorphisms may impact SARS-CoV-2 infectivity. *Trends Genet.* 36, 813–815. doi: 10.1016/j.tig.2020.08.003

Brewster, U. C., and Perazella, M. A. (2004). The renin-angiotensinaldosterone system and the kidney disease. *Am. J. Med.* 116, 263–272. doi: 10.1016/j.amjmed.2003.09.034

Brodard, J., Kremer Hovinga, J. A., Fontana, P., Studt, J. D., Gruel, Y., and Greinacher, A. (2021). COVID-19 patients often show high-titer non-platelet-activating anti-PF4/heparin IgG antibodies. *J. Thromb. Haemost.* 19, 1294–1298. doi: 10.1111/jth.15262

Brooke, G. N., and Prischi, F. (2020). Structural and functional modelling of SARS-CoV-2 entry in animal models. *Sci. Rep.* 10:15917. doi: 10.1038/s41598-020-72528-z

Brown, N. J., and Vaughan, D. E. (2000). Prothrombotic effects of angiotensin. *Adv. Intern. Med.* 45, 419–429.

Burnham, S., Smith, J. A., Lee, A. J., Isaac, R. E., and Shirras, A. D. (2005). The angiotensin-converting enzyme (ACE) gene family of Anopheles gambiae. *BMC Genomics* 6:172. doi: 10.1186/1471-2164-6-172

Cabral-Marques, O., Marques, A., Giil, L. M., De Vito, R., Rademacher, J., Gunther, J., et al. (2018). GPCR-specific autoantibody signatures are associated with physiological and pathological immune homeostasis. *Nat. Commun.* 9:5224. doi: 10.1038/s41467-018-07598-9

Cai, H. (2020). Sex difference and smoking predisposition in patients with COVID-19. *Lancet Respir. Med.* 8:e20. doi: 10.1016/S2213-2600(20)30117-X.P

Caillet-Saguy, C., and Wolf, N. (2021). PDZ-containing proteins targeted by the ACE2 receptor. *Viruses* 13:2281. doi: 10.3390/v13112281

Calabrese, C., Annunziata, A., Coppola, A., Pafundi, P. C., Guarino, S., Di Spirito, V., et al. (2021). ACE gene I/D polymorphism and acute pulmonary embolism in COVID19 pneumonia: a potential predisposing role. *Front. Med.* 7:631148. doi: 10.3389/fmed.2020.631148

Calcagnile, M., Forgez, P., Iannelli, A., Bucci, C., Alifano, M., and Alifano, P. (2021). Molecular docking simulation reveals ACE2 polymorphisms that may increase the affinity of ACE2 with the SARS-CoV-2 spike protein. *Biochimie* 180, 143–148. doi: 10.1016/j.biochi.2020.11.004

Camargo, S. M., Singer, D., Makrides, V., Huggel, K., Pos, K. M., Wagner, C. A., et al. (2009). Tissue-specific amino acid transporter partners ACE2 and collectrin differentially interact with hartnup mutations. *Gastroenterology* 136, 872–882.e3. doi: 10.1053/j.gastro.2008.10.055

Campbell, C. M., and Kahwash, R. (2020). Will complement inhibition be the new target in treating COVID-19 related systemic thrombosis? *Circulation* 141, 1739–1741. doi: 10.1161/CIRCULATIONAHA.120.047419

Cantuti-Castelvetri, L., Ojha, R., Pedro, L. D., Djannatian, M., Franz, J., Kuivanen, S., et al. (2020). Neuropilin-1 facilitates SARS-CoV-2 cell entry and infectivity. *Science* 370, 856–860. doi: 10.1126/science.abd2985

Cao, Y., Li, L., Feng, Z., Wan, S., Huang, P., Sun, X., et al. (2020). Comparative genetic analysis of the novel coronavirus (2019-nCoV/SARS-CoV-2) receptor ACE2 in different populations. *Cell Discov.* 6, 4–7. doi: 10.1038/s41421-020-0147-1

Cardenas, A., Rifas-Shiman, S. L., Sordillo, J. E., DeMeo, D. L., and Baccarelli, A. A. (2021). DNA methylation architecture of the ACE2 gene in nasal cells of children. *Sci. Rep.* 11:7107. doi: 10.1038/s41598-021-86494-7

Cardot-Leccia, N., Hubiche, T., Dellamonica, J., and Burel-Vandenbos, F. (2020). Pericyte alteration shed light on micro-vasculopathy in COVID-19 infection. *Intensive Care Med.* 46, 1777–1778. doi: 10.1007/s00134-020-06147-7

Carsana, L., Sanzagni, A., Nasr, A., Rossi, R. S., Pellegrinelli, A., Zerbi, P., et al. (2020). Pulmonary post-mortem findings in a series of COVID-19 cases from northern Italy: a two-Centre descriptive study. *Lancet* 20, 1135–1140. doi: 10.1016/S1473-3099(20)30434-5

Carvelli, J., Demaria, O., Vély, F., Batista, L., Chouaki Benmansour, N., Fares, J., et al. (2020). Association of COVID-19 inflammation with activation of the C5a–C5aR1 axis. *Nature* 588, 146–150. doi: 10.1038/s41586-020-2600-6

Celik, S. K., Genç, G. C., Piskin, N., Açikgöz, B., Altinsoy, B., Issiz, B. K., et al. (2021). Polymorphisms of ACE (I/D) and ACE2 receptor gene (Rs2106809, Rs2285666) are not related to the clinical course of COVID-19: a case study. *J. Med. Virol.* 93, 5947–5952. doi: 10.1002/jmv.27160

Cerdà-Costa, N., and Gomis-Rüth, F. X. (2014). Architecture and function of metallopeptidase catalytic domains. *Protein Sci.* 23, 123–144. doi: 10.1002/pro.2400

Chappell, M. C. (2019). The angiotensin-(1-7) Axis: formation and metabolism pathways. Springer nature Switzerland. *Angiotensin* 22, 1–26. doi: 10.1007/978-3-030-22696-1_1

Chen, J., Jiang, Q., Xia, X., Liu, K., Yu, Z., Tao, W., et al. (2020). Individual variation of the SARS-CoV-2 receptor ACE2 gene expression and regulation. *Aging Cell* 19:e13168. doi: 10.1111/acel.13168

Chen, L., Li, X., Chen, M., Feng, Y., and Xiong, C. (2020). The ACE2 expression in human heart indicates new potential mechanism of heart injury among patients infected with SARS-CoV-2. *Cardiovasc. Res.* 116, 1097–1100. doi: 10.1093/cvr/cvaa078

Chen, Y. Y., Liu, D., Zhang, P., and Zhong, J. C. (2016). Impact of ACE2 gene polymorphism on antihypertensive efficacy of ACE inhibitors. *J. Hum. Hypertens.* 30, 766–771. doi: 10.1038/jhh.2016.24

Chen, F., Zhang, Y., Li, X., Li, W., Liu, X., and Xue, X. (2021). The impact of ACE2 polymorphisms on COVID-19 disease: susceptibility, severity, and therapy. *Front. Cell. Infect. Microbiol.* 11:753721. doi: 10.3389/fcimb.2021.753721

Chlamydas, S., Papavassiliou, A. G., and Piperi, C. (2020). Epigenetic mechanisms regulating COVID-19 infection. *Epigenetics* 16, 263–270. doi: 10.1080/15592294.2020.1796896

Chung, M. K., Karnik, S., Saef, J., Bergmann, C., Barnard, J., Lederman, M. M., et al. (2020). SARS-CoV-2 and ACE2: the biology and clinical data settling the ARB and ACEI controversy. *EBioMed.* 58:102907. doi: 10.1016/j.ebiom.2020.102907

Ciceri, F., Beretta, L., Mara Scandroglio, A., Colombo, S., Landoni, G., Ruggeri, A., et al. (2020). Microvascular COVID-19 lung vessels obstructive thromboinflammatory syndrome (MicroCLOTS): an atypical acute respiratory distress syndrome working hypothesis. *Crit. Care Resusc.* 22, 95–97. doi: 10.51893/2020.2.pov2

Clarke, N. E., Belyaev, N. D., Lambert, D. W., and Turner, A. J. (2014). Epigenetic regulation of angiotensin-converting enzyme 2 (ACE2) by SIRT1 under conditions of cell energy stress. *Clin. Sci.* 126, 507–516. doi: 10.1042/CS20130291

Cohen-Haguenauer, O., Soubrier, F., Van Cong, N., Serero, S., Turleau, C., Jegou, C., et al. (1989). Regional mapping of the human renin gene to 1q32 by in situ hybridisation. *Ann. Genet.* 32, 16–20.

Cole-Jeffrey, C. T., Liu, M., Katovich, M. J., Raizada, M. K., and Shenoy, V. (2015). ACE2 and microbiota: emerging targets for cardiopulmonary disease therapy. *J. Cardiovasc. Pharmacol.* 66, 540–550. doi: 10.1097/FJC.0000000000000307

Corley, MJ, and Ndhlovu, LC. DNA methylation analysis of the COVID-19 host cell receptor, angiotensin I converting enzyme 2 gene (ACE2) in the respiratory system reveal age and gender differences. (2020). Preprints [Preprint]. doi: 10.20944/preprints 202003.0295.v1

Correale, P., Mutti, L., Pentimalli, F., Baglio, G., Saladino, R. E., Sileri, P., et al. (2020). HLAB * 44 and C * 01 prevalence correlates with Covid19 spreading across Italy. *Int. J. Mol. Sci.* 21:5205. doi: 10.3390/ijms21155205

Cozzi, E., Calabrese, F., Schiavon, M., Feltracco, P., Seveso, M., Carollo, C., et al. (2017). Immediate and catastrophic antibody-mediated rejection in a lung transplant recipient with anti-angiotensin ii receptor type 1 and AntiEndothelin-1 receptor type a antibodies. *Am. J. Transplant.* 17, 557–564. doi: 10.1111/ajt.14053

Crackower, M. A., Sarao, R., Oudit, G. Y., Yagil, C., Kozieradzki, I., Scanga, S. E., et al. (2002). Angiotensinconverting enzyme 2 is an essential regulator of heart function. *Nature* 417, 822–828. doi: 10.1038/nature00786

Crisan, D., and Carr, J. (2000). Angiotensin I-converting enzyme. *J. Mol. Diagn.* 2, 105–115. doi: 10.1016/S1525-1578(10)60624-1

Dahlbäck, B., and Villoutreix, B. O. (2005). Regulation of blood coagulation by the protein C anticoagulant pathway: novel insights into structure-function relationships and molecular recognition Arterioscler. *Thromb. Vasc. Biol.* 25, 1311–1320. doi: 10.1161/01.ATV.0000168421.13467.82

Dai, S., Ding, M., Liang, N., Li, Z., Guan, L., and Liu, H. (2019). Associations of ACE I/D polymorphism with the levels of ACE, kallikrein, angiotensin II and interleukin-6 in STEMI patients. *Sci. Rep.* 9:19719. doi: 10.1038/s41598-019-56263-8

Dai, C. F., Xie, X., Ma, Y. T., Yang, Y. N., Li, X. M., Fu, Z. Y., et al. (2015). Relationship between CYP17A1 genetic polymorphism and essential hypertension in a Chinese population. *Aging Dis.* 6, 486–498. doi: 10.14336/AD.2015.0505

Daly, J. L., Simonetti, B., Klein, K., Chen, K. E., Williamson, M. K., Anton-Plagaro, C., et al. (2020). Neuropilin-1 is a host factor for SARS-CoV-2 infection. *Science* 370, 861–865. doi: 10.1126/science.abd3072

Damas, J., Hughes, G. M., Keough, K. C., Painter, C. A., Persky, N. S., Corbo, M., et al. (2020). Broad host range of SARS-CoV-2 predicted by comparative and structural analysis of ACE2 in vertebrates. *Proc. Natl. Acad. Sci. U. S. A.* 117, 22311–22322. doi: 10.1073/pnas.2010146117

Danilczyk, U., Eriksson, U., Crackower, M. A., and Penninger, J. M. (2003). A story of two ACEs. *J. Mol. Med.* 81, 227–234. doi: 10.1007/s00109-003-0419-x

Darbani, B. (2020). The expression and polymorphism of entry machinery for COVID-19 in human: juxtaposing population groups, gender, and different tissues. *Int. J. Environ. Res. Public Health* 17:3433. doi: 10.3390/ijerph17103433

Daviet, F., Guervilly, C., Baldesi, O., Bernard-Guervilly, F., Pilarczyk, E., Genin, A., et al. (2020). Heparin-induced thromcytopenia in severe COVID-19. *Circulation* 142, 1875–1877. doi: 10.1161/CIRCULATIONAHA.120.049015

Davis, J. O., and Freeman, R. H. (1976). Mechanisms regulating renin release. *Physiol. Rev.* 56, 1–56. doi: 10.1152/physrev.1976.56.1.1

de Gasparo, M., Catt, K. J., Inagami, T., Wright, J. W., and Unger, T.International Union of Pharmacology. XXIII (2000). The angiotensin II receptors. *Pharmacol. Rev.* 52, 415–472.

de Kloet, A. D., Krause, E. G., and Woods, S. C. (2010). The renin angiotensin system and the metabolic syndrome. *Physiol. Behav.* 100, 525–534. doi: 10.1016/j.physbeh.2010.03.018

Delorey, T. M., Ziegler, C. G. K., Heimberg, G., Normand, R., Yang, Y., Segerstolpe, A., et al. (2021). COVID-19 tissue atlases reveal SARS-CoV-2 pathology and cellular targets. *Nature* 595, 107–113. doi: 10.1038/s41586-021-03570-8

Descamps, G., Verset, L., Trelcat, A., Hopkins, C., Lechien, J. R., Journe, F., et al. (2020). ACE2 protein landscape in the head and neck region: the conundrum of SARS-CoV-2 infection. *Biology* 9:235. doi: 10.3390/biology9080235

Deshmukh, V., Motwani, R., Kumar, A., Kurnari, C., and Raza, K. (2020). Histopathological observations in COVID-19: a systematic review. *J. Clin. Pathol.* 74, 76–83. doi: 10.1136/jclinpath-2020-206995

Devaux, C. A. (2020). Are ACE inhibitors and ARBs more beneficials than harmful in the treatment of severe COVID-19 disease? *Cardiovasc. Med. Cardiol.* 7, 101–103. doi: 10.17352/2455-2976.000122

Devaux, C. A., Lagier, J.-C., and Raoult, D. (2021a). New insights into the physiopathology of COVID-19: SARS-CoV-2-associated gastrointestinal illness. *Front. Med.* 8:640073. doi: 10.3389/fmed.2021.640073

Devaux, C. A., Pinault, L., Delerce, J., Raoult, D., Levasseur, A., and Frutos, R. (2021b). Spread of mink SARS-CoV-2 variants in humans: a model of Sarbecovirus interspecies evolution. *Front. Microbiol.* 12:675528. doi: 10.3389/fmicb.2021.675528

Devaux, C. A., Pinault, L., Osman, I. O., and Raoult, D. (2021c). Can ACE2 receptor polymorphism predict species susceptibility to SARS-CoV-2? *Front. Public Health* 8:608765. doi: 10.3389/fpubh.2020.608765

Devaux, C. A., and Raoult, D. (2022). The impact of COVID-19 on populations living at high altitude: role of hypoxia-inducible factors (HIFs) signaling pathway in SARS-CoV-2 infection and replication. *Front. Physiol.* 13:960308. doi: 10.3389/fphys.2022.960308

Devaux, C. A., Rolain, J. M., and Raoult, D. (2020). ACE2 receptor polymorphism: susceptibility to SARS-CoV-2, hypertension, multi-organ failure, and COVID-19 disease outcome. *J. Microbiol. Immnol. Inf.* 53, 425–435. doi: 10.1016/j.jmii.2020.04.015

Diez-Freire, C., Vazquez, J., Correa de Adjounian, M. F., Ferrari, M. F. R., Yuan, L., Silver, X., et al. (2006). ACE2 gene transfer attenuates hypertension-linked pathophysiological changes in the SHR. *Physiol. Genomics* 27, 12–19. doi: 10.1152/physiolgenomics.00312.2005

Dikalov, S. I., and Nazarewicz, R. R. (2013). Angiotensin II-induced production of mitochondrial reactive oxygen species: potential mechanisms and relevance for cardiovascular disease. *Antioxid. Redox Signal.* 19, 1085–1094. doi: 10.1089/ars.2012.4604

Dong, B., Yu, Q. T., Dai, H. Y., Gao, Y. Y., Zhou, Z. L., Zhang, L., et al. (2012). Angiotensin-converting enzyme-2 overexpression improves left ventricular remodeling and function in a rat model of diabetic cardiomyopathy. *J. Am. Coll. Cardiol.* 59, 739–747. doi: 10.1016/j.jacc.2011.09.071

Dong, B., Zhang, C., Feng, J. B., Zhao, Y. X., Li, S. Y., Yang, Y. P., et al. (2008). Overexpression of ACE2 enhances plaque stability in a rabbit model of atherosclerosis. *Arteriosc. Thromb. Vascular Biol.* 28, 1270–1276. doi: 10.1161/ATVBAHA.108.164715

Donkor, O. N., Henriksson, A., Vasiljevic, T., and Shah, N. P. (2007). Proteolytic activity of dairy lactic acid bacteria and probiotics as determinant of growth and in vitro angiotensin-converting enzyme inhibitory activity in fermented milk. *Lait* 86, 21–38. doi: 10.1051/lait:2006023

Donoghue, M., Hsieh, F., and Baronas, E. (2000). A novel angiotensin-converting enzyme-related carboxypeptidase (ACE2) converts angiotensin I to angiotensin 1-9. *Circ. Res.* 87, E1–E9. doi: 10.1161/01.RES.87.5.e1

Dragun, D., Muller, D. N., Brasen, J. H., Fritsche, L., Nieminen-Kelha, M., Dechend, R., et al. (2005). Angiotensin II type 1-receptor activating antibodies in renal allograft rejection. *N. Engl. J. Med.* 352, 558–569. doi: 10.1056/NEJMoa035717

Duru, K., Farrow, S., Wang, J. M., Lockette, W., and Kurtz, T. (1994). Frequency of a deletion polymorphism in the gene for angiotensin converting enzyme is increased in african-Americans with hypertension. *Am. J. Hypertens.* 7, 759–762. doi: 10.1093/ajh/7.8.759

Ellinghaus, D., Degenhardt, F., Bujanda, L., Buti, M., Albillos, A., Invernizzi, P., et al. (2020). Genomewide association study of severe Covid-19 with respiratory failure. *N. Engl. J. Med.* 383, 1522–1534. doi: 10.1056/NEJMoa2020283

Epelman, S., Shrestha, K., Troughton, R. W., Francis, G. S., Sen, S., Klein, A. L., et al. (2009). Soluble angiotensin-converting enzyme 2 in human heart failure: relation with myocardial function and clinical outcomes. *J. Card. Fail.* 15, 565–571. doi: 10.1016/j.cardfail.2009.01.014

Epelman, S., Tang, W. H., Chen, S. Y., Lente, F. V., Francis, G. S., Sen, S., et al. (2008). Detection of soluble angiotensin-converting enzyme 2 in heart failure: insights into the endogenous counter-regulatory pathway of the renin-angiotensin-aldosterone system. *J. Am. Coll. Cardiol.* 52, 750–754. doi: 10.1016/j.jacc.2008.02.088

Escher, R., Breakey, N., and Lammle, B. (2020). Severe COVID-19 infection associated with endothelial activation. *Thromb. Res.* 190:62. doi: 10.1016/j.thromres.2020.04.014

Faggiano, P., Bonelli, A., Paris, S., Milesi, G., Bisegna, S., Bernardi, N., et al. (2020). Acute pulmonary embolism in COVID-19 disease: preliminary report on seven patients. *Int. J. Cardiol.* 313, 129–131. doi: 10.1016/j.ijcard.2020.04.028

Fairweather, S. J., Broer, A., O'Mara, M. L., and Broer, S. (2012). Intestinal peptidases from functional complexes with neutral amino acid transporter B0AT1. *Biochem. J.* 446, 135–148. doi: 10.1042/BJ20120307

Fan, C., Lu, W., Li, K., Ding, Y., and Wang, J. (2021). ACE2 expression in kidney and testis may cause kidney and testis infection in COVID-19 patients. *Front. Med.* 7:563893. doi: 10.3389/fmed.2020.563893

Fan, R., Mao, S. Q., Gu, T. L., Zhong, F. D., Gong, M. L., Hao, L. M., et al. (2017). Preliminary analysis of the association between methylation of the ACE2 promoter and essential hypertension. *Mol. Med. Rep.* 15, 3905–3911. doi: 10.3892/mmr.2017.6460

Fan, Z., Wu, G., Yue, M., Ye, J., Chen, Y., Xu, B., et al. (2019). Hypertension and hypertensive left ventricular hypertrophy are associated with ACE2 genetic polymorphism. *Life Sci.* 225, 39–45. doi: 10.1016/j.lfs.2019.03.059

Fan, X., Yb, W., Wang, H., Sun, K., Zhang, W.-l., Song, X., et al. (2009). Polymorphisms of angiotensinconverting enzyme (ACE) and ACE2 are not associated with orthostatic blood pressure dysregulation in hypertensive patients. *Acta Pharmacol. Sin.* 30, 1237–1244. doi: 10.1038/aps.2009.110

Fang, Y., Gao, F., and Liu, Z. (2019). Angiotensin-converting enzyme 2 attenuates inflammatory response and oxidative stress in hyperoxic lung injury by regulating NF-κB and Nrf2 pathways. *QJM* 112, 914–924. doi: 10.1093/qjmed/hcz206

Fang, L., and Karakiulakis, R. M. (2020). Are patients with hypertension and diabetes mellitus at increased risk for COVID-19 infection? *Lancet Respir. Med.* 8:e21. doi: 10.1016/S2213-2600(20)30116-8

Fantini, J., Chahinian, H., and Yahi, N. (2021). Leveraging coronavirus binding to gangliosides for innovative vaccine and therapeutic strategies against COVID-19. *Biochem. Biophys. Res. Commun.* 538, 132–136. doi: 10.1016/j.bbrc.2020.10.015

Fantini, J., Devaux, C. A., Yahi, N., and Frutos, R. (2022). The novel hamster-adapted SARS-CoV-2 Delta variant may be selectively advantaged in humans. *J. Inf. Secur.* 84, e53–e54. doi: 10.1016/j.jinf.2022.03.001

Felmeden, D. C., Spencer, C. G. C., Chung, N. A. Y., Belgore, F. M., Blann, A. D., Beevers, D. G., et al. (2003). Relation of thrombogenesis in systemic hypertension to angiogenesis and endothelial damage/dysfunction (a substudy of the Anglo-Scandinavian cardiac outcomes trial [ASCOT]). *Am. J. Cardiol.* 92, 400–405. doi: 10.1016/s0002-9149(03)00657-x

Ferrand, A., Nabhani, Z. A., Tapias, N. S., Mas, E., Hugoy, J. P., and Barreau, F. (2019). NOD2 expression in intestinal epithelial cells protects toward the development of inflammation and associated carcinogenesis. *Cell. Mol. Gastroenterol. Hepatol.* 7, 357–369. doi: 10.1016/j.jcmgh.2018.10.009

Ferrario, C. M., Chappell, M. C., Tallant, E. A., Brosnihan, K. B., and Diz, D. I. (1997). Counterregulatory actions of angiotensin-(1-7). *Hypertension* 30, 535–541. doi: 10.1161/01.hyp.30.3.535

Ferrario, C. M., Jessup, J., Chappell, M. C., Averill, D. B., Brosnihan, K. B., Tallant, E. A., et al. (2005). Effect of angiotensin-converting enzyme inhibition and angiotensin II receptor blockers on cardiac angiotensin-converting enzyme 2. *Circulation* 111, 2605–2610. doi: 10.1161/CIRCULATIONAHA.104.510461

Ferrario, C. M., and Varagic, J. (2010). The ANG-(1-7)/ACE2/mas axis in the regulation of nephron function. *Am. J. Physiol. Ren. Physiol.* 298, F1297–F1305. doi: 10.1152/ajprenal.00110.2010

Ferreira, A. J., Shenoy, V., Yamazato, Y., Sriramula, S., Francis, J., Yuan, L., et al. (2009). Evidence for angiotensin-converting enzyme 2 as a therapeutic target for the prevention of pulmonary hypertension. *Am. J. Respir. Crit. Care Med.* 179, 1048–1054. doi: 10.1164/rccm.200811-1678OC

Fletcher-Sandersjöö, A., and Bellander, B. M. (2020). Is COVID-19 associated thrombosis caused by overactivation of the complement cascade? *Thromb. Res.* 194, 36–41. doi: 10.1016/j.thromres.2020.06.027

Fogari, R., Zoppi, A., Mugellini, A., Maffioli, P., Lazzari, P., and Derosa, G. (2011). Role of angiotensin II in plasma PAI-1 changes induced by imidapril or candesartan in hypertensive patients with metabolic syndrome. *Hypertens. Res.* 34, 1321–1326. doi: 10.1038/hr.2011.137

Forrester, S. J., Booz, G. W., Sigmund, C. D., Coffman, T. M., Kawai, T., Rizzo, V., et al. (2018). Angiotensin II signal transduction: an update on mechanisms of physiology and pathophysiology. *Physiol. Rev.* 98, 1627–1738. doi: 10.1152/physrev.00038.2017

Fournier, D., Luft, F. C., Bader, M., Ganten, D., and Andrade-Navarro, M. A. (2012). Emergence and evolution of the renin–angiotensin–aldosterone system. *J. Mol. Med.* 90, 495–508. doi: 10.1007/s00109-012-0894-z

Fraga-Silva Rodrigo, A., Costa-Fraga Fabiana, P., Murca Tatiane, M., Moraes Patrıcia, L., Martins Lima, A., Lautner Roberto, Q., et al. (2013). Angiotensin-converting enzyme 2 activation improves endothelial function. *Hypertension* 61, 1233–1238. doi: 10.1161/HYPERTENSIONAHA.111.00627

Frederich, R. C. Jr., Kahn, B. B., Peach, M. J., and Flier, J. S. (1992). Tissue-specific nutritional regulation of angiotensinogen in adipose tissue. *Hypertension* 19, 339–344. doi: 10.1161/01.hyp.19.4.339

Fricke-Galindo, I. (2021). Falfa´ n-Valencia R genetics insight for COVID-19 susceptibility and severity: a review. *Front. Immunol.* 12:622176. doi: 10.3389/fimmu.2021.622176

Frutos, R., Gavotte, L., and Devaux, C. A. (2021). Understanding the origin of COVID-19 requires to change the paradigm on zoonotic emergence from the spillover to the circulation model. *Infect. Genet. Evol.* 95:104812. doi: 10.1016/j.meegid.2021.104812

Frutos, R., Serra-Cobo, J., Pinault, L., Lopez Roig, M., and Devaux, C. A. (2021). Emergence of bat-related Betacoronaviruses: Hazard and risks. *Front. Microbiol.* 12:591535. doi: 10.3389/fmicb.2021.591535

Frutos, R., Yahi, N., Gavotte, L., Fantini, J., and Devaux, C. A. (2022). Role of spike compensatory mutations in the interspecies transmission of SARS-CoV-2. *One Health* 15:100429. doi: 10.1016/j.onehlt.2022.100429

Fuglsang, A., Rattray, F. P., Nilsson, D., and Nyborg, N. C. B. (2003). Lactic acid bacteria: inhibition of angiotensin converting enzyme in vitro and in vivo. *Antonie Van Leeuwenhoek* 83, 27–34. doi: 10.1023/A:1022993905778

Funakoshi, Y., Ichiki, T., Takeda, K., Tokuno, T., Lino, N., and Takeshita, A. (2002). Critical role of cAMP-response element-binding protein for angiotensin II-induced hypertrophy of vascular smooth muscle cells. *J. Biol. Chem.* 277, 18710–18717. doi: 10.1074/jbc.M110430200

Furuhashi, M., Moniwa, N., Mita, T., Fuseya, T., Ishimura, S., Ohno, K., et al. (2015). Urinary angiotensin-converting enzyme 2 in hypertensive patients may be increased by olmesartan, an angiotensin II receptor blocker. *Am. J. Hypertens.* 28, 15–21. doi: 10.1093/ajh/hpu086

Furuhashi, M., Moniwa, N., Takizawa, H., Ura, N., and Shimamoto, K. (2020). Potential differential effects of renin-angiotensin system inhibitors on SARS-CoV-2 infection and lung injury in COVID-19. *Hypertens. Res.* 43, 837–840. doi: 10.1038/s41440-020-0478-1

Gáborik, Z., Szaszák, M., Szidonya, L., Balla, B., Paku, S., Catt, K. J., et al. (2001). Beta-arrestin-and dynamin-dependent endocytosis of the AT1 angiotensin receptor. *Mol. Pharmacol.* 59, 239–247. doi: 10.1124/mol.59.2.239

Gagiannis, D., Steinestel, J., Hackenbroch, C., Schreiner, B., Hannemann, M., Bloch, W., et al. (2020). Clinical, serological, and histopathological similarities between severe COVID-19 and acute exacerbation of connective tissue disease-associated interstitial lung disease (CTD-ILD). *Front. Immunol.* 11:587517. doi: 10.3389/fimmu.2020.587517

Gaidarov, I., Adams, J., Frazer, J., Anthony, T., Chen, X., Gatlin, J., et al. (2018). Angiotensin (1-7) does not interact directly with MAS1, but can potently antagonize signaling from the AT1 receptor. *Cell. Signal.* 50, 9–24. doi: 10.1016/j.cellsig.2018.06.007

Gallucio, M., Pantanella, M., Gludice, D., Brescia, S., and Indiveri, C. (2020). Low temperature bacterial expression of the neutral amino acid transporters SLC1A5 (ASCT2), and SLC6A19 (B0AT1). *Mol. Biol. Rep.* 47, 7283–7289. doi: 10.1007/s11033-020-05717-8

Gando, S., and Wada, T. (2021). Thromboplasminflammation in COVID-19 coagulopathy: three viewpoints for diagnostic and therapeutic strategies. *Front. Immunol.* 12:649122. doi: 10.3389/fimmu.2021.649122

Gao, S., and Zhang, L. (2020). ACE2 partially dictates the host range and tropism of SARS-CoV-2. *Comput. Struct. Biotechnol. J.* 18, 4040–4047. doi: 10.1016/j.csbj.2020.11.032

Garcia-Escobar, A., Jimenez-Valero, S., Galeote, G., Jurado-Roman, A., Garcia-Rodriguez, J., and Moreno, R. (2021). The soluble catalytic ectodomain of ACE2 a biomarker of cardiac remodelling: new insights for heart failure and COVID19. *Heart Fail. Rev.* 26, 961–971. doi: 10.1007/s10741-020-10066-6

Garrido, A. M., and Griendling, K. K. (2009). NADPH oxidases and angiotensin II receptor signaling. *Mol. Cell. Endocrinol.* 302, 148–158. doi: 10.1016/j.mce.2008.11.003

Garvin, M. R., Alvarez, C., Miller, J. I., Prates, E. T., Walker, A. M., Amos, B. K., et al. (2020). A mechanistic model and therapeutic interventions for COVID-19 involving a RAS-mediated bradykinin storm. *elife* 9:e59177. doi: 10.7554/eLife.59177

Gay, L., Melenotte, C., Lakbar, I., Mezouar, S., Devaux, C., Raoult, D., et al. (2021). Sexual dimorphism and gender in infectious diseases. *Front. Immunol.* 12:698121. doi: 10.3389/fimmu.2021.698121

Ge, X. Y., Li, J. L., Yang, X. L., Chmura, A. A., Zhu, G., Epstein, J. H., et al. (2013). Isolation and characterization of a bat SARS-like coronavirus that uses the ACE2 receptor. *Nature* 503, 535–538. doi: 10.1038/nature12711

Gerard, L., Lecocq, M., Bouzin, C., Hoton, D., Schmit, G., Pereira, J. P., et al. (2021). Increased angiotensin-converting enzyme 2 and loss of alveolar type II cells in COVID-19 related ARDS. *Am. J. Respir. Crit. Care Med.* 204, 1024–1034. doi: 10.1164/rccm.202012-4461OC

Ghatage, T., Gopal Goyal, S., Dhar, A., and Bhat, A. (2021). Novel therapeutics for the treatment of hypertension and its associated complications: peptide-and nonpeptide-based strategies. *Hypertens. Res.* 44, 740–755. doi: 10.1038/s41440-021-00643-z

Gheblawi, M., Wang, K., Viveiros, A., Nguyen, Q., Zhong, J. C., Turner, A. J., et al. (2020). Angiotensin-converting enzyme 2: SARS-CoV-2 receptor and regulator of the renin-angiotensin system: celebrating the 20th anniversary of the discovery of ACE2. *Circ. Res.* 126, 1456–1474. doi: 10.1161/CIRCRESAHA.120.317015

Giner, V., Poch, E., Bragulat, E., Oriola, J., Gonzalez, D., Coca, A., et al. (2000). Renin-angiotensin system genetic polymorphisms and salt sensitivity in essential hypertension. *Hypertension* 35, 512–517. doi: 10.1161/01.hyp.35.1.512

Gjymishka, A., Kulemina, L. V., Shenoy, V., Katovich, M. J., Ostrov, D. A., and Raizada, M. K. (2010). Diminazene aceturate is an ACE2 activator and a novel antihypertensive drug. *FASEB J.* 24:1032. doi: 10.1096/fasebj.24.1_supplement.1032.3

Glasgow, A., Glasgow, J., Limonta, D., Solomon, P., Lui, I., Zhang, Y., et al. (2020). Engineered ACE2 receptor traps potently neutralize SARS-CoV-2. *Proc. Natl. Acad. Sci. U. S. A.* 117, 28046–28055. doi: 10.1073/pnas.2016093117

Goldblatt, H., Lynch, J., Hanzal, R. F., and Summerville, W. W. (1934). Studies on experimental hypertension: I. the production of persistent elevation of systolic blood pressure by means of renal ischemia. *J. Exp. Med.* 59, 347–379. doi: 10.1084/jem.59.3.347

Gómez, J., Albaiceta, G. M., García-Clemente, M., López-Larrea, C., Amado Rodríguez, L., Lopez-Alonso, I., et al. (2020). Angiotensin-converting enzymes (ACE, ACE2) gene variants and COVID-19 outcome. *Gene* 762:145102. doi: 10.1016/j.gene.2020.145102

Gonzalez, A. A., Lara, L. S., and Prieto, M. C. (2017). Role of collecting duct renin in the pathogenesis of hypertension. *Curr. Hypertens. Rep.* 19:62. doi: 10.1007/s11906-017-0763-9

Goru, S. K., Kadakol, A., Malek, V., Pandey, A., and Gaikwad, S. N. A. B. (2017). Diminazene aceturate prevents nephropathy by increasing glomerular ACE2 and AT(2) receptor expression in a rat model of type1 diabetes. *Br. J. Pharmacol.* 174, 3118–3130. doi: 10.1111/bph.13946

Goshua, G., Pine, A. B., Meizlish, M. L., Chang, C. H., Zhang, H., Bahel, P., et al. (2020). Endotheliopathy in COVID-19-associated coagulopathy: evidence from a single-Centre, cross-sectional study. *Lancet Heamatol.* 7, e575–e582. doi: 10.1016/S2352-3026(20)30216-7

Goujon, C, Rebendenne, A, Roy, P, Bonaventure, B, Valadao, AC, Desmarets, L, et al. (2021). Bidirectional genome-wide CRISPR screens reveal host factors regulating SARS-CoV-2, MERS-CoV and seasonal HCoVs. Research Square [Preprint]. doi: 10.21203/rs.3.rs-555275/v1

Goulter, A. B., Goddard, M. J., Allen, J. C., and Clark, K. L. (2004). ACE2 gene expression is up-regulated in the human failing heart. *BMC Med.* 2:19. doi: 10.1186/1741-7015-2-19

Graham, R. L., Donaldson, E. F., and Baric, R. S. (2013). A decade after SARS: strategies to control emerging coronaviruses. *Nat. Rev. Microbiol.* 11, 836–848. doi: 10.1038/nrmicro3143

Greenberg, B. (2008). An ACE in the hole alternative pathways of the renin angiotensin system and their potential role in cardiac remodeling. *J. Am. Coll. Cardiol.* 52, 755–757. doi: 10.1016/j.jacc.2008.04.059

Griendling, K. K., Ushio-Fukai, M., Lassègue, B., and Alexander, R. W. (1997). Angiotensin II signaling in vascular smooth muscle. *Hypertension* 29, 366–370. doi: 10.1161/01.HYP.29.1.366

Gu, H., Xie, Z., Li, T., Zhang, S., Lai, C., Zhu, P., et al. (2016). Angiotensin-converting enzyme 2 inhibits lung injury induced by respiratory syncytial virus. *Sci. Rep.* 6:19840. doi: 10.1038/srep19840

Guignabert, C., de Man, F., and Lombes, M. (2018). ACE2 as therapy for pulmonary arterial hypertension: the good outweighs the bad. *Eur. Respir. J.* 51:1800848. doi: 10.1183/13993003.00848-2018

Guo, L., Ren, L., Yang, S., Xiao, M., Chang, D., Yang, F., et al. (2020). Profiling early humoral response to diagnose novel coronavirus disease (COVID-19). *Clin. Infect. Dis.* 71, 778–785. doi: 10.1093/cid/ciaa310

Gupta, S., Aqrawal, B. K., Goel, R. K., and Sehajpal, P. K. (2009). Angiotensin-converting enzyme gene polymorphism in hypertensive rural population of Haryana, India. *J. Emerg. Trauma Shock.* 2, 150–154. doi: 10.4103/0974-2700.55323

Gurley, S. B., Riquier-Brison, A. D. M., Schnermann, J., Sparks, M. A., Allen, A. M., Haase, V. H., et al. (2011). AT1A angiotensin receptors in the renal proximal tubule regulate blood pressure. *Cell Metab.* 13, 469–475. doi: 10.1016/j.cmet.2011.03.001

Gustafsson, F., and Holstein-Rathlou, N. H. (1999). Angiotensin II modulates conducted vasoconstriction to norepinephrine and local electrical stimulation in rat mesenteric arterioles. *Cardiovasc. Res.* 44, 176–184. doi: 10.1016/S0008-6363(99)00174-1

Haber, P. K., Ye, M., Wysocki, J., Maier, C., Haque, S. K., and Battle, D. (2014). Angiotensin-converting enzyme 2–independent action of presumed angiotensin-converting enzyme 2 activators. *Hypertension* 63, 774–782. doi: 10.1161/HYPERTENSIONAHA.113.02856

Hadman, J. A., Mort, Y. J., Catanzaro, D. F., Tallam, J. T., Baxter, J. D., Morris, B. J., et al. (1984). Primary structure of human renin gene. *DNA* 3, 457–468. doi: 10.1089/dna.1.1984.3.457

Hamming, I., Timens, W., Bulthuis, M., Lely, T., Navis, G., and van Goor, H. (2004). Tissue distribution of ACE2 protein, the functional receptor for SARS coronavirus. *J. Pathol.* 203, 631–637. doi: 10.1002/path.1570

Han, H., Ma, Q., Li, C., Liu, R., Zhao, L., Wang, W., et al. (2020). Profiling serum cytokines in COVID-19 patients reveals IL-6 and IL-10 are disease severity predictors. *Emerg. Microb. Infect.* 9, 1123–1130. doi: 10.1080/22221751.2020.1770129

Han, Y., Runge, M. S., and Brasier, A. R. (1999). Angiotensin II induces Interleukin-6 transcription in vascular smooth muscle cells through pleiotropic activation of nuclear factor-kB transcription factors. *Circ. Res.* 84, 695–703. doi: 10.1161/01.RES.84.6.695

Harrap, S. B., Tzourio, C., Cambien, F., Poirier, O., Raoux, S., Chalmers, J., et al. (2003). The ACE gene I/D polymorphism is not associated with the blood pressure and cardiovascular benefits of ACE inhibition. *Hypertension* 42, 297–303. doi: 10.1161/01.HYP.0000088322.85804.96

Harzallah, I., Debliquis, A., and Drenou, B. (2020). Lupus anticoagulant is frequent in patients with Covid-19. *J. Thromb. Haemost.* 18, 2064–2065. doi: 10.1111/jth.14867

Haschke, M., Schuster, M., Poglitsch, M., Loiner, H., Salzberg, M., Bruggisser, M., et al. (2013). Pharmacokinetics and pharmacodynamics of recombinant human angiotensin-converting enzyme 2 in healthy human subjects. *Clin. Pharmacokinet.* 52, 783–792. doi: 10.1007/s40262-013-0072-7

Hashimoto, T., Perlot, T., Rehman, A., Trichereau, J., Ishiguro, H., Paolino, M., et al. (2012). ACE2 links amino acid malnutrition to microbial ecology and intestinal inflammation. *Nature* 487, 477–481. doi: 10.1038/nature11228

Hassler, L, Wysocki, J, Gelarden, I, Tomatsidou, A, Gula, H, Nicoleascu, V, et al. (2021). A novel soluble ACE2 protein totally protects from lethal disease caused by SARS-CoV-2 infection. bioRxiv [Preprint] doi: 10.1101/2021.03.12.435191

He, M., He, X., Xie, Q., Chen, F., and He, S. (2006). Angiotensin II induces the expression of tissue factor and its mechanism in human monocytes. *Thromb. Res.* 117, 579–590. doi: 10.1016/j.thromres.2005.04.033

Heeneman, S., Haendeler, J., Saito, Y., Ishida, M., and Berk, B. C. (2000). Angiotensin II induces transactivation of two different populations of the platelet-derived growth factor beta receptor. Key role for the p66 adaptor protein Shc. *J. Biol. Chem.* 275, 15926–15932. doi: 10.1074/jbc.M909616199

Helms, J., Tacquard, C., Severac, F., Leonard-Lorant, I., Ohana, M., Delabranche, X., et al. (2020). High risk of thrombosis in patients with severe SARS-CoV-2 infection: a multicenter prospective cohort study. *Intensive Care Med.* 46, 1089–1098. doi: 10.1007/s00134-020-06062-x

Hemnes, A. R., Rathinasabapathy, A., Austin, E. A., Brittain, E. L., Carrier, E. J., Chen, X., et al. (2018). A potential therapeutic role for angiotensin-converting enzyme 2 in human pulmonary arterial hypertension. *Eur. Respir. J.* 51:1702638. doi: 10.1183/13993003.02638-2017

Hendren, N. S., Drazner, M. H., Bozkurt, B., and Cooper, L. T. (2020). Description and proposed management of the acute COVID-19 cardiovascular syndrome. *Circulation* 141, 1903–1914. doi: 10.1161/CIRCULATIONAHA.120.047349

Henzinger, H., Barth, D. A., Klec, C., and Pichler, M. (2020). Non-Coding RNAs and SARS-related coronaviruses. *Viruses* 12:1374. doi: 10.3390/v12121374

Hernández Prada, J. A., Ferreira, A. J., Katovich, M. J., Shenoy, V., Qi, Y., Santos, R. A., et al. (2008). Structure-based identification of small-molecule angiotensin-converting enzyme 2 activators as novel antihypertensive agents. *Hypertension* 51, 1312–1317. doi: 10.1161/HYPERTENSIONAHA.107.108944

Heurich, A., Hofmann-Winkler, H., Gierer, S., Liepold, T., Jahn, O., and Pöhlmann, S. (2014). TMPRSS2 and ADAM17 cleave ACE2 differentially and only proteolysis by TMPRSS2 augments entry driven by the severe acute respiratory syndrome coronavirus spike protein. *J. Virol.* 88, 1293–1307. doi: 10.1128/JVI.02202-13

Heyman, S. N., Kinaneh, S., and Abassi, Z. (2021). The duplicitous nature of ACE2 in COVID-19 disease. *EBioMed.* 67:103356. doi: 10.1016/j.ebiom.2021.103356

Hikmet, F., Méar, L., Edvinsson, A., Micke, P., Uhlén, M., and Lindskog, C. (2020). The protein expression profile of ACE2 in human tissues. *Mol. Syst. Biol.* 16:e9610. doi: 10.15252/msb.20209610

Hirano, T., and Murakami, M. (2020). COVID-19: a new virus, but a familiar receptor and cytokine release syndrome. *Immunity* 52, 731–733. doi: 10.1016/j.immuni.2020.04.003

Hoffmann, M., Kleine-Weber, H., Schroeder, S., Kruger, N., Herrler, T., Erichsen, S., et al. (2020). SARS-CoV-2 cell entry depends on ACE2 and TMPRSS2 and is blocked by a clinically proven protease inhibitor. *Cells* 181, 271–280.e8. doi: 10.1016/j.cell.2020.02.052

Hofman, P., Copin, M. C., Tauziede-Espariat, A., Adle-Biassette, H., Fortarezza, F., Passeron, T., et al. (2021). Histopathological features due to the SARS-CoV-2 [in French]. *Ann. Pathol.* 41, 9–22. doi: 10.1016/j.annpat.2020.1 2.009

Hofmann, H., Pyrc, K., van der Hoek, L., Geier, M., Berkhout, B., and Pöhlmann, S. (2005). Human coronavirus NL63 employs the severe acute respiratory syndrome coronavirus receptor for cellular entry. *Proc. Natl. Acad. Sci. U. S. A.* 102, 7988–7993. doi: 10.1073/pnas.0409465102

Horowitz, JE, Kosmicki, JA, Damask, A, Sharma, D, Roberts, GHL, Justice, AE, et al. Genome-wide analysis in 756, 646 individuals provides first genetic evidence that ACE2 expression influences COVID-19 risk and yields genetic risk scores predictive of severe disease [Internet]. medRxiv [Preprint]. (2021). doi: 10.1101/2020.12.14.20248176

Hou, Y., Zhao, J., Martin, W., Kallianpur, A., Chung, M. K., Jehi, L., et al. (2020). New insights into genetic susceptibility of COVID-19: an ACE2 and TMPRSS2 polymorphism analysis. *BMC Med.* 18:216. doi: 10.1186/s12916-020-01673-z

Huang, C., Wang, Y., Li, X., Ren, L., Zhao, J., Hu, Y., et al. (2020). Clinical features of patients infected with 2019 novel coronavirus in Wuhan, China. *Lancet* 395, 497–506. doi: 10.1016/S0140-6736(20)30183-5

Hubert, C., Houot, A. M., Corvol, P., and Soubrier, F. (1991). Structure of the angiotensin I-converting enzyme gene. Two alternate promoters correspond to evolutionary steps of a duplicated gene. *J. Biol. Chem.* 266, 15377–15383. doi: 10.1016/S0021-9258(18)98626-6

Ichihara, A., and Yatabe, M. S. (2019). The (pro)renin receptor in health and disease. *Nat. Rev. Nephrol.* 15, 693–712. doi: 10.1038/s41581-019-0160-5

Imai, Y., Kub, K., Rao, S., Huan, Y., Guo, F., Guan, B., et al. (2005). Angiotensin-converting enzyme 2 protects from severe acute lung failure. *Nature* 436, 112–116. doi: 10.1038/nature03712

Initiative, C.-H. G. (2020). The COVID-19 host genetics Initiative, a global initiative to elucidate the role of host genetic factors in susceptibility and severity of the SARSCoV-2 virus pandemic. *Eur. J. Hum. Genet.* 28, 715–718. doi: 10.1038/s41431-020-0636-6

Issa, H., Eid, A. H., Berry, B., Takhviji, V., Khosravi, A., Mantash, S., et al. (2021). Combination of angiotensin (1-7) agonists and convalescent plasma as a new strategy to overcome angiotensin converting enzyme 2 (ACE2) inhibition for the treatment of COVID-19. *Front. Med.* 8:620990. doi: 10.3389/fmed.2021.620990

Itoyama, S., Keicho, N., Hijikata, M., Quy, T., Chi Phi, N., Long, H. T., et al. (2005). Identifcation of an alternative 5'-untranslated exon and new polymorphisms of angiotensin-converting enzyme 2 gene: lack of association with SARS in the Vietnamese population. *Am. J. Med. Genet.* 136, 52–57. doi: 10.1002/ajmg.a.30779

Jackman, H. L., Massad, M. G., Sekosan, M., Tan, F., Brovkovych, V., Marcic, B. M., et al. (2002). Angiotensin 1-9 and 1-7 release in human heart: role of cathepsin a. *Hypertension* 39, 976–981. doi: 10.1161/01.HYP.0000017283.67962.02

Jacoby, D. S., and Rader, D. J. (2003). Renin-angiotensin system and atherothrombotic disease: from genes to treatment. *Arch. Intern. Med.* 163, 1155–1164. doi: 10.1001/archinte.163.10.1155

James, M. N., and Sielecki, A. R. (1985). Stereochemical analysis of peptide bond hydrolysis catalyzed by the aspartic proteinase penicillopepsin. *Biochemistry* 24, 3701–3713. doi: 10.1021/bi00335a045

Jaspard, E., Wei, I., and Alhenc-Gelas, F. (1993). Differences in the properties and enzymatic specifities of the two active sites of angiotensin I-converting enzyme (kininase II). Studies with bradykinin and other natural peptides. *J. Biol. Chem.* 268, 9496–9503. doi: 10.1016/S0021-9258(18)98378-X

Jehpsson, L., Sun, J., Nilsson, P. M., Edsfeldt, A., and Swärd, P. (2021). Serum renin levels increase with age in boys resulting in higher renin levels in Young men compared to Young women, and soluble angiotensin-converting enzyme 2 correlates with renin and body mass index. *Front. Physiol.* 11:622179. doi: 10.3389/fphys.2020.622179

Jeunemaitre, X., Lifton, R. P., Hunt, S. C., Williams, R. R., and Lalouel, J. M. (1992). Absence of linkage between the angiotensin converting enzyme locus and human essential hypertension. *Nat. Genet.* 1, 72–75. doi: 10.1038/ng0492-72

Jia, H. P., Look, D. C., and Tan, P. (2009). Ectodomain shedding of angiotensin converting enzyme 2 in human airway epithelia. *Am. J. Phys. Lung Cell. Mol. Phys.* 297, L84–L96. doi: 10.1152/ajplung.00071.2009

Jin, Y., Ji, W., Yang, H., Chen, S., Zhang, W., and Duan, G. (2020). Endothelial activation and dysfunction in COVID-19: from basic mechanisms to potential therapeutic approaches. *Signal Transduct. Target. Ther.* 5:293. doi: 10.1038/s41392-020-00454-7

Johnson, J. A., West, J., Maynard, K. B., and Hemnes, A. R. (2011). ACE2 improves right ventricular function in a pressure overload model. *PLoS One* 6:e20828. doi: 10.1371/journal.pone.0020828

Kai, H., Kai, M., Niiyama, H., Okina, N., Sasaki, M., Maeda, T., et al. (2021). Overexpression of angiotensin-converting enzyme 2 by renin-angiotensin system inhibitors. Truth or myth? A systematic review of animal studies. *Hypertens. Res.* 44, 955–968. doi: 10.1038/s41440-021-00641-1

Karaderi, T., Bareke, H., Kunter, I., Seytanoglu, A., Cagnan, I., Balci, D., et al. (2020). Host genetics at the intersection of autoimmunity and COVID-19: a

potential key for heterogeneous COVID-19 severity. *Front. Immunol.* 11:586111. doi: 10.3389/fimmu.2020.586111

Kario, K., Hoshide, S., Umeda, Y., Sato, Y., Ikeda, U., Nishiuma, S., et al. (1999). Angiotensinogen and angiotensin-converting enzyme genotypes, and day and night blood pressures in elderly Japanese hypertensives. *Hypertens. Res.* 22, 95–103. doi: 10.1291/hypres.22.95

Karnik, S. S., Singh, K. D., Tirupula, K., and Unal, H. (2017). Significance of angiotensin 1-7 coupling with MAS1 receptor and other GPGRs to the renin-angiotensin system: IUPHAR review 22. *Br. J. Pharmacol.* 174, 737–753. doi: 10.1111/bph.13742

Kassan, M., Ait-Aissa, K., Radwan, E., Mali, V., Haddox, S., Gabani, M., et al. (2016). Essential role of smooth muscle STIM1 in hypertension and cardiovascular dysfunction. *Arterioscler. Thromb. Vasc. Biol.* 36, 1900–1909. doi: 10.1161/ATVBAHA.116.307869

Kassan, M., Galán, M., Partyka, M., Saifudeen, Z., Henrion, D., Trebak, M., et al. (2012). Endoplasmic reticulum stress is involved in cardiac damage and vascular endothelial dysfunction in hypertensive mice. *Arterioscler. Thromb. Vasc. Biol.* 32, 1652–1661. doi: 10.1161/ATVBAHA.112.249318

Katsoularis, I., Fonseca-Rodriguez, O., Farrington, P., Jerndal, H., Häggström Lundevaller, E., Sund, M., et al. (2022). Risks of deep vein thrombosis, pulmonary embolism, and bleeding after covid-19: nationwide self-controlled cases series and matched cohort study. *BMJ* 377:e069590. doi: 10.1136/bmj-2021-069590

Kellam, P., and Barclay, W. (2020). The dynamics of humoral immune responses following SARS-CoV-2 infection and the potential for reinfection. *J. Gen. Virol.* 101, 791–797. doi: 10.1099/jgv.0.001439

Khaddaj-Mallat, R., Aldib, N., Bernard, M., Paquette, A. S., Ferreira, A., Lecordier, S., et al. (2021). SARS-CoV-2 deregulates the vascular and immune functions of brain pericytes via spike protein. *Neurobiol. Dis.* 161:105561. doi: 10.1016/j.nbd.2021.105561

Khan, A., Benthin, C., Zeno, B., Albertson, T. E., Boyd, J., Christie, J. D., et al. (2017). A pilot clinical trial of recombinant human angiotensin-converting enzyme 2 in acute respiratory distress syndrome. *Crit. Care* 21:234. doi: 10.1186/s13054-017-1823-x

Khayat, AS, de Assumpc, PP, Meireles Khayat, BC, Thomaz Arau Jo, TM, Batista-Gomes, JA, Imbiriba, L.C., et al. (2020). ACE2 polymorphisms as potential players in COVID-19 outcome. *PLoS One* 15:e0243887. doi: 10.1371/journal.pone.024388

Kintscher, U., Slagman, A., Domenig, O., Röhle, R., Konietschke, F., Poglitsch, M., et al. (2020). Plasma angiotensin peptide profiling and ACE (angiotensin-converting enzyme)-2 activity in COVID-19 patients treated with pharmacological blockers of the renin-angiotensin system. *Hypertension* 76, e34–e36. doi: 10.1161/HYPERTENSIONAHA.120.15841

Kliche, J., Kuss, H., Ali, M., and Ivarsson, Y. (2021). Cytoplasmic short linear motifs in ACE2 and integrin B3 link SARS-CoV-2 host cell receptors to mediators of endocytosis and autophagy. *Sci. Signal.* 14:ebaf1117. doi: 10.1126/scisignal.abf1117

Kok, K. H., Wong, S. C., Chan, W. M., Lei, W., Chu, A. W. H., Ip, J. D., et al. (2022). Cocirculation of two SARSCoV-2 variant strains within imported pet hamsters in Hong Kong. *Emerg. Microb. Infect.* 11, 689–698. doi: 10.1080/22221751.2022.2040922

Koka, V., Huang, X. R., Chung, A. C. K., Wang, W., Truong, L. D., and Lan, H. Y. (2008). Angiotensin II up-regulates angiotensin I converting enzyme (ACE), but Down-regulates ACE2 via the AT1-ERK/p38 MAP kinase pathway. *Am. J. Pathol.* 172, 1174–1183. doi: 10.2353/ajpath.2008.070762

Kougias, P., Chai, H., Lin, P. H., Yao, Q., Lumsden, A. B., and Chen, C. (2005). Defensins and cathelicidins: neutrophil peptides with roles in inflammation, hyperlipidemia and atherosclerosis. *J. Cell. Mol. Med.* 9, 3–10. doi: 10.1111/j.1582-4934.2005.tb00332.x

Kragstrup, T. W., Sogaard Singh, H., Grundberg, I., Langkilde-Lauesen Nielsen, A., Rivellese, F., Mehta, A., et al. (2021). Plasma ACE2 predicts outcome of COVID-19 in hospitalized patients. *PLoS One* 16:e0252799. doi: 10.1371/journal.pone.0252799

Krishnamurthy, S., Lockey, R. F., and Kolliputi, N. (2021). Soluble ACE2 as a potential therapy for COVID-19. *Am. J. Phys. Cell Physiol.* 320, C279–C281. doi: 10.1152/ajpcell.00478.2020

Ksiazek, T. G., Erdman, D., Goldsmith, C. S., Zaki, S. R., Peret, T., Emery, S., et al. (2003). A novel coronavirus associated with severe acute respiratory syndrome. *N. Engl. J. Med.* 348, 1953–1966. doi: 10.1056/NEJMoa030781

Kuan, T. C., Yang, T. H., Wen, C. H., Chen, M. Y., Lee, I. L., and Lin, C. S. (2011). Identifying the regulatory element for human angiotensin-converting enzyme 2 (ACE2) expression in human cardiofibroblasts. *Peptides* 32, 1832–1839. doi: 10.1016/j.peptides.2011.08.009

Kuba, K., Imai, Y., Rao, S., Gao, H., Guo, F., Guan, B., et al. (2005). A crucial role of angiotensin converting enzyme 2 (ACE2) in SARS coronavirus-induced lung injury. *Nat. Med.* 11, 875–879. doi: 10.1038/nm1267

Kulemina, L. V., and Ostrov, D. A. (2011). Prediction of off-target effects on angiotensin-converting enzyme 2. *J. Biomol. Screen.* 16, 878–885. doi: 10.1177/1087057111413919

Kundura, L., Gimenez, S., Cezar, R., André, S., Younas, M., Lin, Y. L., et al. (2022). Angiotensin II induces reactive oxygen species, DNA damage, and T-cell apoptosis in severe COVID-19. *J. Allergy Clin. Immunol.* 150, 594–603.e2. doi: 10.1016/j.jaci.2022.06.020

Kwakernaak, A. J., Roksnoer, L. C., Lambers Heerspink, H. J., Ven den Berg-Garrelds, I., Lochorn, G. A., Embden, J. H., et al. (2017). Effects of direct renin blockade on renal & systemic hemodynamics and on RAAS activity, in weight excess and hypertension: a randomized clinical trial. *PLoS One* 12:e0169258. doi: 10.1371/journal.pone.0169258

Lam, S. D., Bordin, N., Waman, V. P., Scholes, H. M., Ashford, P., Sen, N., et al. (2020). SARS-CoV-2 spike protein predicted to form complexes with host receptor protein orthologues from a broad range of mammals. *Sci. Rep.* 10:16471. doi: 10.1038/s41598-020-71936-5

Lambert, D. W., Clarke, N. E., Hooper, N. M., and Turner, A. J. (2008). Calmodulin interacts with angiotensin-converting enzyme-2 (ACE2) and inhibits shedding of its ectodomain. *FEBS Lett.* 582, 385–390. doi: 10.1016/j.febslet.2007.11.085

Lambert, D. W., Yarski, M., and Warner, F. J. (2005). Tumor necrosis factor-alpha convertase (ADAM17) mediates regulated ectodomain shedding of the severe-acute respiratory syndrome-coronavirus (SARS-CoV) receptor, angiotensin-converting enzyme-2 (ACE2). *J. Biol. Chem.* 280, 30113–33019. doi: 10.1074/jbc.M505111200

Lamers, M. M., Beumer, J., van der Vaart, J., Knoops, K., Puschhof, J., Breugem, T. I., et al. (2020). SARS-CoV-2 productively infects human gut enterocytes. *Science* 369, 50–54. doi: 10.1126/science.abc1669

Lan, J., Ge, J., Yu, J., Shan, S., Zhou, H., Fan, S., et al. (2020). Structure of the SARS-CoV-2 spike receptor-binding domain bound to the ACE2 receptor. *Nature* 581, 215–220. doi: 10.1038/s41586-020-2180-5

Lanjanian, H., Moazzam-Jazi, M., Hedayati, M., Akbarzadeh, M., Guity, K., Sedaghati-Khayat, B., et al. (2021). SARS-CoV-2 infection susceptibility infuenced by ACE2 genetic polymorphisms: insights from Tehran cardio-metabolic genetic study. *Sci. Rep.* 11:1529. doi: 10.1038/s41598-020-80325-x

Larsson, P. T., Schwieler, J. H., and Wallen, N. H. (2000). Platelet activation during angiotensin II infusion in healthy volunteers. Blood Coag. *Fibrinolysis* 11, 61–69. doi: 10.1097/00001721-200011010-00007

Lavrentyev, E. N., and Malik, K. U. (2009). High glucose-induced Nox1-derived superoxides downregulate PKC-βII, which subsequently decreases ACE2 expression and ANG(1-7) formation in rat VSMCs. *Am. J. Physiol. Circ. Physiol.* 296, H106–H118. doi: 10.1152/ajpheart.00239.2008

Lee, I. I., Nakayama, T., Wu, C. T., Goltsey, Y., Jiang, S., Gall, P. A., et al. (2020). ACE2 localizes to the respiratory cilia and is not increased by ACE inhibitors or ARBs. *Nat. Commun.* 11:5453. doi: 10.1038/s41467-020-19145-6

Lei, C., Qian, K., Li, T., Zhang, S., Fu, W., Ding, M., et al. (2020). Neutralization of SARS-CoV-2 spike pseudotyped virus by recombinant ACE2-Ig. *Nat. Commun.* 11:2070. doi: 10.1038/s41467-020-16048-4

Leonard-Lorant, I., Delabranche, X., Severac, F., Helms, J., Pauzet, C., Collange, O., et al. (2020). Acute pulmonary embolism in COVID-19 patients on CT angiography and relationship to D-dimer levels. *Radiology* 296, E189–E191. doi: 10.1148/radiol.2020201561

Li, Z., and Ferguson, A. V. (1993). Subfornical organ efferents to paraventricular nucleus utilize angiotensin as a neurotransmitter. *Am. J. Phys. Regul. Integr. Comp. Phys.* 265, R302–R309. doi: 10.1152/ajpregu.1993.265.2.R302

Li, G., He, X., Zhang, L., Ran, Q., Wang, J., Xiong, A., et al. (2020). Assessing ACE2 expression patterns in lung tissues in the pathogenesis of COVID-19. *J. Autoimmun.* 112:102463. doi: 10.1016/j.jaut.2020.102463

Li, L., Huang, M., Shen, J., Wang, Y., Wang, R., Yuan, C., et al. (2021). Serum levels of soluble platelet endothelial cell adhesion molecule 1 in COVID-19 patients are associated with disease severity. *J. Infect. Dis.* 223, 178–179. doi: 10.1093/infdis/jiaa642

Li, W., Moore, M. J., Vasilieva, N., Sui, J., Wong, S. K., Berne, M. A., et al. (2003). Angiotensin-converting enzyme 2 is a functional receptor for the SARS coronavirus. *Nature* 426, 450–454. doi: 10.1038/nature02145

Li, W., Sui, J., Huang, I. C., Kuhn, J. H., Radoshitzky, S. R., Marasco, W. A., et al. (2007). The S proteins of human coronavirus NL63 and severe acute respiratory syndrome coronavirus bind overlapping regions of ace2. *Virology* 367, 367–374. doi: 10.1016/j.virol.2007.04.035

Lindner, D., Fitzek, A., Bräuninger, H., Aleshcheva, G., Edler, C., Meissner, K., et al. (2020). Association of cardiac infection with SARS-CoV-2 in confirmed COVID-19 autopsy cases. *JAMA Cardiol.* 5, 1281–1285. doi: 10.1001/jamacardio.2020.3551

Lippi, G., and Favaloro, E. J. (2020). D-dimer is associated with severity of coronavirus disease 2019: a pooled analysis. *Thromb. Haemost.* 120, 876–878. doi: 10.1055/s-0040-1709650

Liu, Y., Hu, G., Wang, Y., Ren, W., Zhao, X., Ji, F., et al. (2021). Functional and genetic analysis of viral receptor ACE2 orthologs reveals a broad potential host range of SARS-CoV-2. *Proc. Natl. Acad. Sci. U. S. A.* 118:e2025373118. doi: 10.1073/pnas.2025373118

Liu, C., Li, Y., Guan, T., Lai, Y., Shen, Y., Zeyaweiding, A., et al. (2018). ACE2 polymorphisms associated with cardiovascular risk in Uygurs with type 2 diabetes mellitus. *Cardiovasc. Diabetol.* 17:127. doi: 10.1186/s12933-018-0771-3

Liu, C., Luo, R., Elliott, S. E., Wang, W., Parchim, N. F., Iriyama, T., et al. (2015). Elevated transglutaminase activity triggers angiotensin receptor activating autoantibody production and pathophysiology of preeclampsia. *J. Am. Heart Assoc.* 4:e002323. doi: 10.1161/JAHA.115.002323

Liu, P., Wysocki, J., Souma, T., Ye, M., Ramirez, V., Zhou, B., et al. (2018). Novel ACE2-fc chimeric fusion provides long-lasting hypertension control and organ protection in mouse models of systemic renin angiotensin system activation. *Kidney Int.* 94, 114–125. doi: 10.1016/j.kint.2018.01.029

Liu, Y., Yang, Y., Zhang, C., Huang, F., Wang, F., Yuan, J., et al. (2020). Clinical and biochemical indexes from 2019-nCoV infected patients linked to viral loads and lung injury. *Sci. China Life Sci.* 63, 364–374. doi: 10.1007/s11427-020-1643-8

Liu, Y., and Zhang, H. G. (2021). Vigilance on new-onset atherosclerosis following SARS-CoV-2 infection. *Front. Med.* 7:629413. doi: 10.3389/fmed.2020.629413

Long, Q. X., Liu, B. Z., Deng, H. J., Wu, G. C., Deng, K., Chen, Y. K., et al. (2020). Antibody responses to SARS-CoV-2 in patients with COVID-19. *Nat. Med.* 26, 845–848. doi: 10.1038/s41591-020-0897-1

Lopez, R. D., Macedo, A. V. S., de Baros, E., Silva, P. G. M., Moll-Bernardes, J., dos Santos, T., et al. (2021). Continuing angiotensin-converting enzyme inhibitors and angiotensin II receptor blockers on days alive and out of the hospital in patients admitted with COVID-19. A randomized clinical trial. *JAMA* 325, 254–264. doi: 10.1001/jama.2020.25864

Lorente, L., Martın, M. M., Franco, A., Barrios, Y., Caceres, J. J., Solé-Violán, J., et al. (2020). HLA genetic polymorphisms and prognosis of patients with COVID-19. *Med. Int.* 45, 96–103. doi: 10.1016/j.medin.2020.08.004

Luan, J., Lu, Y., Jin, X., and Zhang, L. (2020). Spike protein recognition of mammalian ACE2 predicts the host range and an optimized ACE2 for SARSCoV-2 infection. *Biochem. Biophys. Res. Commun.* 526, 165–169. doi: 10.1016/j.bbrc.2020.03.047

Lubbe, L., Cozier, G. E., Dosthuizen, D., Acharya, K. R., and Sturrock, E. D. (2020). ACE2 and ACE: structure-based insights into mechanism, regulation and receptor recognition by SARS-CoV. *Clin. Sci.* 134, 2851–2871. doi: 10.1042/CS20200899

Luo, Y., Liu, C., Guan, T., Li, Y., Lai, Y., Li, F., et al. (2019). Association of ACE2 genetic polymorphisms with hypertension-related target organ damages in South Xinjiang. *Hypertens. Res.* 42, 681–689. doi: 10.1038/s41440-018-0166-6

Luo, Y., Mao, L., Yan, X., Xue, Y., Lin, Q., Tang, G., et al. (2020). Predicted model based on the combination of cytokines and lymphocytes subsets for prognosis of SARS-CoV-2 infection. *J. Clin. Immunol.* 40, 960–969. doi: 10.1007/s10875-020-00821-7

Luther, J. M., Gainer, J. V., Murphey, L. J., Yu, C., Vaughan, D. E., Morrow, J. D., et al. (2006). *Hypertension* 48, 1050–1057. doi: 10.1161/01.HYP.0000248135.97380.76

Lv, Y., Li, Y., Yi, Y., Zhang, L., Shi, Q., and Yang, J. (2018). A genomic survey of angiotensin-converting enzymes provides novel insights into their molecular evolution in vertebrates. *Moelcules* 23:2923. doi: 10.3390/molecules23112923

Ma, H., Zeng, W., He, H., Zhao, D., Jiang, D., Zhou, P., et al. (2020). Serum IgA, IgM, and IgG responses in COVID-19. *Cell. Mol. Immunol.* 17, 773–775. doi: 10.1038/s41423-020-0474-z

Magro, C., Mulvey, J. J., Berlin, D., Nuovo, G., Salvatore, S., Harp, J., et al. (2020). Complement associated microvascular injury and thrombosis in the pathogenesis of severe COVID-19 infection: a report of five cases. *Transl. Res.* 220, 1–13. doi: 10.1016/j.trsl.2020.04.007

Maiti, B. K. (2021). Bioengineered angiotensin-converting-enzyme-2: a potential therapeutic option against SARS-CoV-2 infection. *J. Hum. Hypertens.* 36, 488–492. doi: 10.1038/s41371-021-00636-y

Manne, B. K., Denorme, F., Middleton, E. A., Portier, I., Rowley, J. W., Stubben, C. J., et al. (2020). Platelet gene expression and function in COVID-19 patients. *Blood* 136, 1317–1329. doi: 10.1182/- blood.2020007214

Marchiano, S., Hsiang, T. Y., Khanna, A., Higashi, T., Whitmore, L. S., Bargehr, J., et al. (2021). SARS-CoV-2 infects human pluripotent stem cell-derived cardiomyocytes, impairing electrical and mechanical function. *Stem Cell Rep.* 16, 478–492. doi: 10.1016/j.stemcr.2021.02.008

Marian, A. J. (2013). The discovery of the ACE2 gene. *Circ. Res.* 112, 1307–1309. doi: 10.1161/CIRCRESAHA.113.301271

Marra, M. A., Jones, S. J., Astell, C. R., Holt, R. A., Brooks-Wilson, A., Butterfield, Y. S., et al. (2003). The genome sequence of the SARS-associated coronavirus. *Science* 300, 1399–1404. doi: 10.1126/science.1085953

Marshall, R. P., Webb, S., Bellingan, G. J., Montgomery, H. E., Chaudhari, B., Mc Arthur, R. J., et al. (2002). Angiotensin converting enzyme insertion/deletion polymorphism is associated with susceptibility and outcome in acute respiratory distress syndrome. *Am. J. Respir. Crit. Care Med.* 166, 646–650. doi: 10.1164/rccm.2108086

Martinez, E., Pura, A., Escribano, J., Sanchis, C., Carrion, L., Artigao, M., et al. (2000). Angiotensin-converting enzyme (ACE) gene polymorphisms, serum ACE activity and blood pressure in a Spanish-Mediterranean population. *J. Hum. Hypertens.* 14, 131–135. doi: 10.1038/sj.jhh.1000958

Martinez-Rojas, M. A., Vega-Vega, O., and Bobadilla, X. N. A. (2020). Is the kidney a target of SARS-CoV-2? *Am. J. Physiol. Ren. Physiol.* 318, F1454–F1462. doi: 10.1152/AJPRENAL.00160.2

Martins, A. L. V., da Silva, F. A., Bolais-Ramos, L., Capanema de Oliveira, G., Cunha Ribeiro, R., Alves Pereira, D. A., et al. (2021). Increased circulating levels of angiotensin-(1–7) in severely ill COVID-19 patients. *ERJ Open Res.* 7, 00114–02021. doi: 10.1183/23120541.00114-2021

Martin-Sanchos, L., Lewinski, M. K., Pache, L., Stoneham, C. A., Yin, X., Becker, M., et al. (2021). Functional landscape of SARS-CoV-2 cellular restriction. *Mol. Cell* 81, 2656–2668.e8. doi: 10.1016/j.molcel.2021.04.008

Massiéra, F., Bloch-Faure, M., Ceiler, D., Murakami, K., Fukamizu, A., Gasc, J.-M., et al. (2001). Adipose angiotensinogen is involved in adipose tissue growth and blood pressure regulation. *FASEB J.* 15, 2727–2729. doi: 10.1096/fj.01-0457fje

Mecca, A. P., Regenhardt, R. W., O'Connor, T. E., Jospeh, J. P., Raizada, M. K., Katovich, M. J., et al. (2011). Cerebroprotection by angiotensin-(1-7) in endothelin-1-induced ischaemic stroke. *Exp. Physiol.* 96, 1084–1096. doi: 10.1113/expphysiol.2011.058578

Mehta, P., Mc Autley, D. F., Brown, M., Sanchez, E., Tattersall, R. S., Manson, J. J., et al. (2020). COVID-19: consider cytokine storm syndromes and immunosuppression. *Lancet* 395, 1033–1034. doi: 10.1016/S0140-6736(20)30628-0

Meng, J., Xiao, G., Zhang, J., He, X., Ou, M., Bi, J., et al. (2020). Renin-angiotensin system inhibitors improve the clinical outcomes of COVID-19 patients with hypertension. *Emerg. Microb. Infect.* 9, 757–760. doi: 10.1080/22221751.2020.1746200

Meng, N., Zhang, Y., Ma, J., Li, H., Zhou, F., and Qu, Y. (2015). Association of polymorphisms of angiotensin I converting enzyme 2 with retinopathy in type 2 diabetes mellitus among Chinese individuals. *Eye* 29, 266–271. doi: 10.1038/eye.2014.254

Mentz, R. J., Bakris, G. L., Waeber, B., McMurray, J. J., Gheorghiade, M., Ruilope, L. M., et al. (2013). The past, present and future of renin-angiotensin aldosterone system inhibition. *Int. J. Cardiol.* 167, 1677–1687. doi: 10.1016/j.ijcard.2012.10.007

Middeldorp, S., Coppens, M., van Haaps, T. F., Foppen, M., Vlaar, A. P., Miller, M. C. A., et al. (2020). Incidence of venous thromboembolism in hospitalized patients with COVID-19. *J. Thromb. Haemost.* 18, 1995–2002. doi: 10.1111/jth.14888

Miedema, J., Schreurs, M., van der Sarvan der Brugge, S., Paats, M., Baart, S., Bakker, M., et al. (2021). Antibodies against angiotensin II receptor type 1 and endothelin a receptor are associated with an unfavorable COVID19 disease course. *Front. Immunol.* 12:684142. doi: 10.3389/fimmu.2021.684142

Minato, T., Nirasawa, S., Sato, T., Yamaguchi, T., Hoshizaki, M., Inagaki, T., et al. (2020). B38-CAP is a bacteria-derived ACE2-like enzyme that suppresses hypertension and cardiac dysfunction. *Nat. Commun.* 11:1058. doi: 10.1038/s41467-020-14867-z

Mizuiri, S., Hemmi, H., Arita, M., Ohashi, Y., Tanaka, Y., Miyagi, M., et al. (2008). Expression of ACE and ACE2 in individuals with diabetic kidney disease and healthy controls. *Am. J. Kidney Dis.* 51, 613–623. doi: 10.1053/j.ajkd.2007.11.022

Möhlendick, B., Schönfelder, K., Breuckmann, K., Elsner, C., Babel, N., Balfanz, P., et al. (2021). ACE2 polymorphism and susceptibility for SARS-CoV-2 infection and severity of COVID-19. *Pharmacogenet. Genomics* 31, 165–171. doi: 10.1097/FPC.0000000000000436

Montagutelli, X, Prot, M, Levillayer, L, Baquero SAlazar, E, Jouvion, G, Conquet, L., et al. The B1.351 and P. 1 variants extend SARS-CoV-2 host range to mice. bioRxiv [Preprint]. (2021). doi: 10.1101/2021.03.18.436013

Monteil, V., Dyczynski, M., Lauschke, V. M., Kwon, H., Wirnsberger, G., Youhanna, S., et al. (2021). Human soluble ACE2 improves the effect of remdesivir in SARS-CoV-2 infection. *EMBO Mol. Med.* 13:e13426. doi: 10.15252/emmm.202013426

Moore, J. P., Vinh, A., Tuck, K., Sakkal, S., Krishnan, S. M., Chan, C. T., et al. (2015). M2 macrophage accumulation in the aortic wall during angiotensin II infusion in mice is associated with fibrosis, elastin loss, and elevated blood pressure. *Am. J. Physiol. Circ. Physiol.* 309, H906–H917. doi: 10.1152/ajpheart.00821.2014

Muller, D. N., Hilgers, K. F., Mathews, S., Breu, V., Fischli, W., Uhlmann, R., et al. (1999). Effects of human prorenin in rats transgenic for human angiotensinogen. *Hypertension* 33, 312–317. doi: 10.1161/01.HYP.33.1.312

Muller, D. N., Mervaala, E. M. A., Dechend, R., Fiebeler, A., Park, J. K., Schmidt, F., et al. (2000). Angiotensin II (AT_1) receptor blockade reduces vascular tissue factor

in angiotensin II-induced cardiac vasculopathy. *Am. J. Pathol.* 157, 111–122. doi: 10.1016/S0002-9440(10)64523-3

Mullick, A. E., Yeh, S. T., Graham, M. J., Engelhardt, J. A., Prakash, T. P., and Crooke, R. M. (2017). Blood pressure lowering and safety improvements with liver angiotensinogen inhibition in models of hypertension and kidney injury. *Hypertension* 70, 566–576. doi: 10.1161/HYPERTENSIONAHA.117.09755

Murphy, T. J., Alexander, R. W., Griendling, K. K., Runge, M. S., and Bernstein, K. E. (1991). Isolation of a cDNA encoding the vascular type-1 angiotensin II receptor. *Nature* 351, 233–236. doi: 10.1038/351233a0

Muus, C, Luecken, M, Eraslan, G, Waghray, A, Heimberg, G, Sikkema, L, et al. (2020). Integrated analyses of single-cell atlases reveal age, gender, and smoking status associations with cell type-specific expression of mediators of SARS-CoV-2 viral entry and highlights inflammatory programs in putative target cells. bioRxiv [Preprint]. doi: 10.1101/2020.04.19.049254

Nabah, Y. N. A., Mateo, T., Estellés, R., Mata, M., Zagorski, J., Sarau, H., et al. (2004). Angiotensin II induces neutrophil accumulation in vivo through generation and release of CXC chemokines. *Circulation* 110, 3581–3586. doi: 10.1161/01.CIR.0000148824.93600.F3

Naftilan, A. J., and Oparil, S. (1978). Inhibition of renin release from rat kidney slices by the angiotensins. *Am. J. Phys.* 235, F62–F68. doi: 10.1152/ajprenal.1978.235.1.F62

Nassar, H., Lavi, E., Akkawi, S., Bdeir, K., Heyman, S. M., Raghunath, P. N., et al. (2007). Alpha-Defensin: link between inflammation and atherosclerosis. *Atherosclerosis* 194, 452–457. doi: 10.1016/j.atherosclerosis.2006.08.046

Nataraj, C., Oliverio, M. I., Mannon, R. B., Mannon, P. J., Audoly, L. P., Amuchastegui, C. S., et al. (1999). Angiotensin II regulates cellular immune responses through a calcineurin-dependent pathway. *J. Clin. Invest.* 104, 1693–1701. doi: 10.1172/JCI7451

Nemerson, Y. (1988). Tissue factor and hemostasis. *Blood* 71, 1–8. doi: 10.1182/blood.V71.1.1.1

Neves, F. A., Duncan, K. G., and Baxter, J. D. (1996). Cathepsin B is a prorenin processing enzyme. *Hypertension* 27, 514–517. doi: 10.1161/01.hyp.27.3.514

Nguyen, A., David, J. K., Maden, S. K., Wood, M. A., Weeder, B. R., Nellore, A., et al. (2020). Human leukocyte antigen susceptibility map for severe acute respiratory syndrome coronavirus 2. *J. Virol.* 94, e00510–e00520. doi: 10.1128/JVI.00510-20

Nguyen, G., Delarue, F., Burcklé, C., Bouzhir, L., Giller, T., and Sraer, J. D. (2002). Pivotal role of the renin/prorenin receptor in angiotensin II production and cellular responses to renin. *J. Clin. Invest.* 109, 1417–1427. doi: 10.1172/JCI14276

Nikiforuk, A. M., Kuchinski, K. S., Twa, D. D. W., Lukac, C. D., Sbihi, H., Basham, C. A., et al. (2021). The contrasting role of nasopharyngeal angiotensin converting enzyme 2 (ACE2) expression in SARS-CoV-2 infection: a cross-sectional study of people tested for COVID-19 in British Columbia. *EBio Med.* 66:103316. doi: 10.1016/j.ebiom.2021.103316

Nishimura, H. (2017). Renin-angiotensin system in vertebrates: phylogenetic view of structure and function. *Anat. Sci. Int.* 92, 215–247. doi: 10.1007/s12565-016-0372-8

Nishimura, H., Tsuji, H., Masuada, H., Nakagawa, K., Nakahara, Y., Kitamura, H., et al. (1997). Angiotensin II increases plasminogen activator Inhibitor-1 and tissue factor mRNA expression without changing that of tissue type plasminogen activator or tissue factor pathway inhibitor in cultured rat aortic endothelial cells. *Thromb. Haemost.* 77, 1189–1195. doi: 10.1055/s-0038-1656136

Niu, W., Qi, Y., Hou, S., Zhou, W., and Qiu, C. (2007). Correlation of angiotensin-converting enzyme 2 gene polymorphisms with stage 2 hypertension in Han Chinese. *Transl. Res.* 150, 374–380. doi: 10.1016/j.trsl.2007.06.002

Oarhe, C. I., Dang, V., Dang, M. T., Nguyen, H., Gopallawa, I., Gewolb, I. H., et al. (2015). Hyperoxia downregulates angiotensin-converting enzyme-2 in human fetal lung fibroblasts. *Pediatr. Res.* 77, 656–662. doi: 10.1038/pr.2015.27

Onabajo, O. O., Banday, A. R., Stanifer, M. L., Yan, W., Obajemu, A., Santer, D. M., et al. (2020). Interferons and viruses induce a novel truncated ACE2 isoform and not the full-length SARS-CoV-2 receptor. *Nat. Genet.* 52, 1283–1293. doi: 10.1038/s41588-020-00731-9

Ortiz, M. E., Thurman, A., Pezzulo, A. A., Leidinger, M. R., Klesney-Tait, J. A., Karp, P. H., et al. (2020). Heterogeneous expression of the SARS Coronavirus-2 receptor ACE2 in the human respiratory tract. *EBioMed.* 60:102976. doi: 10.1016/j.ebiom.2020.102976

Ortiz-Fernández, L., and Sawalha, A. H. (2020). Genetic variability in the expression of the SARS-CoV-2 host cell entry factors across populations. *Genes Immun.* 21, 269–272. doi: 10.1038/s41435-020-0107-7

Osman, I. O., Garrec, C., de Souza, G. A. P., Zarubica, A., Belhaouari, D. B., Baudoin, J.-P., et al. (2022). Control of CDH1/E-cadherin gene expression and release of a soluble form of E-cadherin in SARS-CoV-2 infected Caco-2 intestinal cells: Physiopathological consequences for the intestinal forms of COVID-19. *Front. Cell. Infect. Microbiol.* 12:798767. doi: 10.3389/fcimb.2022.798767

Osman, I. O., Melenotte, C., Brouqui, P., Million, M., Lagier, J.-C., Parola, P., et al. (2021). Expression of ACE2, soluble ACE2, angiotensin I, angiotensin II and angiotensin-(1-7) is modulated in COVID-19 patients. *Front. Immunol.* 12:625732. doi: 10.3389/fimmu.2021.625732

Othman, H., Bouslama, Z., Brandenburg, J. T., da Rocha, J., Hamdi, Y., Ghedira, K., et al. (2020). Interaction of the spike protein RBD from SARS-CoV-2 with ACE2: similarity with SARS-CoV, hot-spot analysis and effect of the receptor polymorphism. *Biochem. Biophys. Res. Commun.* 527, 702–708. doi: 10.1016/j.bbrc.2020.05.028

Oude Munnink, B. B., Sikkema, R. S., Nieuwenhuijse, D. F., Molenaar, R. J., Munger, E., Molenkamp, R., et al. (2021). Transmission of SARS-CoV-2 on mink farms between humans and mink and back to humans. *Science* 371, 172–177. doi: 10.1126/science.abe5901

Oudit, G. Y., Crackower, M. A., Backx, P. H., and Penninger, J. M. (2003). The role of ACE2 in cardiovascular physiology. *Trends Cardiovasc. Med.* 13, 93–101. doi: 10.1016/s1050-1738(02)00233-5

Oudit, G. Y., Liu, G. C., Zhong, J., Basu, R., Chow, F. L., Zhou, J., et al. (2010). Human recombinant ACE2 reduces the progression of diabetic nephropathy. *Diabetes* 59, 529–538. doi: 10.2337/db09-1218

Oudit, G. Y., and Pfeffer, M. A. (2020). Plasma angiotensin-converting enzyme 2: novel biomarker in heart failure with implications for COVID-19. *Eur. Heart J.* 41, 1818–1820. doi: 10.1093/eurheartj/ehaa414

Page, I. H., and Helmer, O. M. (1940). Angiotonin-activator, renin-and angiotonin-inhibitor, and the mechanism of angiotonin tachyphylaxis in normal, hypertensive, and nephrectomized animals. *J. Exp. Med.* 71, 495–519. doi: 10.1084/jem.71.4.495

Pairo-Castineira, E., Clohisey, S., Klaric, L., Bretherick, A., Rawlik, K., Parkinson, N., et al. (2021). Genetic mechanisms of critical illness in Covid-19. *Nature* 591, 92–98. doi: 10.1038/s41586-020-03065-y

Patel, S. K., Velkoska, E., Freeman, M., Wai, B., Lancefield, T. F., and Burrell, L. M. (2014). From gene to protein - experimental and clinical studies of ACE2 in blood pressure control and arterial hypertension. *Front. Physiol.* 5:227. doi: 10.3389/fphys.2014.00227

Patel, V. B., Zhong, J. C., Grant, M. B., and Oudit, G. Y. (2016). Role of the ACE2/angiotensin 1-7 axis of the renin-angiotensin system in heart failure. *Circ. Res.* 118, 1313–1326. doi: 10.1161/CIRCRESAHA.116.307708

Patnaik, M., Pati, P., Swain, S. N., Mohapatra, M. K., Dwibedi, B., Kar, S. K., et al. (2014). Association of angiotensinconverting enzyme and angiotensin-converting enzyme-2 gene polymorphisms with essential hypertension in the population of Odisha, India. *Ann. Hum. Biol.* 41, 145–152. doi: 10.3109/03014460.2013.837195

Paul, M., Poyan Mehr, A., and Kreutz, R. (2006). Physiology of local renin-angiotensin systems. *Physiol. Rev.* 86, 747–803. doi: 10.1152/physrev.00036.2005

Pedersen, K. B., Chhabra, K. H., Nguyen, V. K., Xia, H., and Lazartigues, E. (2013). The transcription factor HNF1alpha induces expression of angiotensin-converting enzyme 2 (ACE2) in pancreatic islets from evolutionarily conserved promoter motifs. *Biochim. Biophys. Acta* 1829, 1225–1235. doi: 10.1016/j.bbagrm.2013.09.007

Pena Silva, R. A., Chu, Y., Miller, J. D., Mitchell, I. J., Penninger, J. M., Faraci, F. M., et al. (2012). Impact of ACE2 deficiency and oxidative stress on cerebrovascular function with aging. *Stroke* 43, 3358–3363. doi: 10.1161/STROKEAHA.112.667063

Peng, H., Li, W., Seth, D. M., Nair, A. R., Francis, J., and Feng, Y. (2013). (pro)renin receptor mediates both angiotensin II-dependent and-independent oxidative stress in neuronal cells. *PLoS One* 8:e58339. doi: 10.1371/journal.pone.0058339

Perlot, T., and Penninger, J. M. (2013). ACE2-from the renin-angiotensin system to gut microbiota and malnutrition. *Microbes Infect.* 15, 866–873. doi: 10.1016/j.micinf.2013.08.003

Phillips, M. I., and Schmidt-Ott, K. M. (1999). The discovery of renin 100 years ago. *News Physiol. Sci.* 14, 271–274. doi: 10.1152/physiologyonline.1999.14.6.271

Philogene, M. C., Johnson, T., Vaught, A. J., Zakaria, S., and Fedarko, N. (2019). Antibodies against angiotensin II type 1 and endothelin a receptors: relevance and pathogenicity. *Hum. Immunol.* 80, 561–567. doi: 10.1016/j.humimm.2019.04.012

Pierce, J. B., Simion, V., Icli, B., Perez-Cremades, D., Cheng, H. S., and Feinberg, M. W. (2020). Computational analysis of targeting SARS-CoV-2, viral entry proteins ACE2 and TMPRSS2, and interferon genes by host MicroRNAs. *Genes (Basel)* 11:1354. doi: 10.3390/genes11111354

Pinheiro, D. S., Santos, R. S., Jardim, P. C. B. V., Silva, E. G., Reis, A. A. S., Pedrino, G. R., et al. (2019). The combination of ACE I/D and ACE2 G8790A polymorphisms reveals susceptibility to hypertension: a genetic association study in Brazilian patients. *PLoS One* 14:e0221248. doi: 10.1371/journal.pone.0221248

Pinto, B. G. G., Oliveira, A. E. R., Singh, Y., Jimenez, L., Gonçalves, A. N. A., Ogava, R. L. T., et al. (2020). ACE2 expression is increased in the lungs of patients with comorbidities associated with severe COVID-19. *J. Infect. Dis.* 222, 556–563. doi: 10.1093/infdis/jiaa332

Pires de Souza, G. A., Osman, I. O., Le Bideau, M., Baudoin, J.-P., Jaafar, R., Devaux, C., et al. (2022). Angiotensin II receptor blockers (ARBs antihypertensive

agents) increase replication of SARS-CoV-2 in Vero E6 cells. *Front. Cell. Infect. Microbiol.* 11:639177. doi: 10.3389/fcimb.2021.639177

Poissy, J., Goutay, J., Caplan, M., Parmentier, E., Duburcq, T., Lassale, F., et al. (2020). Pulmonary embolism in patients with COVID19. *Circulation* 142, 184–186. doi: 10.1161/CIRCULATIONAHA.120.047430

Pouladi, N., and Abdolahi, S. (2021). Investigating the ACE2 polymorphisms in COVID-19 susceptibility: An in silico analysis. *Mol. Genet. Genom. Med.* 9:e1672. doi: 10.1002/mgg3.1672

Prajapat, M., Shekhar, N., Sarma, P., Avti, P., Singh, S., Kaur, H., et al. (2020). Virtual screening and molecular dynamics study of approved drugs as inhibitors of spike protein S1 domain and ACE2 interaction in SARS-CoV-2. *J. Mol. Graph. Model.* 101:107716. doi: 10.1016/j.jmgm.2020.107716

Prieto, M. C., Gonzalez-Villalobos, R. A., Botros, F. T., Martin, V. L., Pagan, J., Satou, R., et al. (2011). Reciprocal changes in renal ACE/ANG II and ACE2/ANG 1-7 are associated with enhanced collecting duct renin in Goldblatt hypertensive rats. *Am. J. Physiol. Ren. Physiol.* 300, F749–F755. doi: 10.1152/ajprenal.00383.2009

Procko, E. The sequence of human ACE2 is suboptimal for binding the S spike protein of SARS coronavirus 2. bioRxiv [Preprint]. (2020). doi: 10.1101/2020.1103.1116.994236

Qaradakhi, T., and Gadanec, L. (2020). Could DIZE be the answer to COVID-19? *Maturitas* 140, 83–84. doi: 10.1016/j.maturitas.2020.07.002

Qi, Y. F., Zhang, J., Cole-Jeffrey, C. T., Shenoy, V., Espejo, A., Hanna, M., et al. (2013). Diminazene Aceturate enhances angiotensin-converting enzyme 2 activity and attenuates ischemia-induced cardiac pathophysiology. *Hypertension* 62, 746–752. doi: 10.1161/HYPERTENSIONAHA.113.01337

Qiao, Y., Wang, X. M., Mannan, R., Pitchiaya, S., Zhang, Y., Wotring, J. W., et al. (2021). Targeting transcriptional regulation of SARS-CoV-2 entry factors ACE2 and TMPRSS2. *Proc. Natl. Acad. Sci. U. S. A.* 118:e2021450118. doi: 10.1073/pnas.2021450118

Qiu, Y., Shil, P. K., Zhu, P., Yang, H., Verma, A., Lei, B., et al. (2014). Angiotensin-converting enzyme 2 (ACE2) activator Diminazene Aceturate ameliorates endotoxin-induced uveitis in mice. *Invest. Ophthalmol. Vis. Sci.* 55, 3809–3818. doi: 10.1167/iovs.14-13883

Qiu, Y., Zhao, Y. B., Wang, Q., Li, J. Y., Zhou, Z. J., Liao, C. H., et al. (2020). Predicting the angiotensin converting enzyme 2 (ACE2) utilizing capability as the receptor of SARS-CoV-2. *Microbes Infect.* 22, 221–225. doi: 10.1016/j.micinf.2020.03.003

Radzikowska, U., Ding, M., Tan, G., Zhakparov, D., Peng, Y., Wawrzyniak, P., et al. (2020). Distribution of ACE2, CD147, CD26, and other SARS-CoV-2 associated molecules in tissues and immune cells in health and in asthma, COPD, obesity, hypertension, and COVID-19 risk factors. *Allergy* 75, 2829–2845. doi: 10.1111/all.14429

Raghavan, S., Kenchappa, D. B., and Leo, M. D. (2021). SARS-CoV-2 spike protein induces degradation of junctional proteins that maintain endothelial barrier integrity. *Front. Cardiovasc. Med.* 8:687783. doi: 10.3389/fcvm.2021.687783

Rajagopal, S., Rajagopal, K., and Lefkowitz, R. J. (2010). Teaching old receptors new tricks: biasing seven-transmembrane receptors. *Nat. Rev. Drug Discov.* 9, 373–386. doi: 10.1038/nrd3024

Reich, H. N., Oudit, G. Y., Penninger, J. M., Scholey, J. W., and Herzenberg, A. M. (2008). Decreased glomerular and tubular expression of ACE2 in patients with type 2 diabetes and kidney disease. *Kidney Int.* 74, 1610–1616. doi: 10.1038/ki.2008.497

Reindl-Schwaighofer, R., Hödlmoser, S., Eskandary, F., Poglitsch, M., Bonderman, D., Strassl, R., et al. (2021). ACE2 elevation in severe COVID-19. *Am. J. Resp. Critic. Care Med.* 203, 1191–1196. doi: 10.1164/rccm.202101-0142LE

Ren, W., Lan, J., Ju, X., Gong, M., Long, Q., Zhu, Z., et al. (2021). Mutation Y453F in the spike protein of SARS-CoV-2 enhances interaction with the mink ACE2 receptor for host adaption. *PLoS Pathog.* 17:e1010053. doi: 10.1371/journal.ppat.1010053

Rice, G. I., Jones, A. L., Grant, P. J., Carter, A. M., Turner, A. J., and Hooper, N. M. (2006). Circulating activities of angiotensin-converting enzyme, its homolog, angiotensin-converting enzyme 2, and neprilysin in a family study. *Hypertension* 48, 914–920. doi: 10.1161/01.HYP.0000244543.91937.79

Rieder, M., Wirth, L., Pollmeier, L., Jeserich, M., Goller, I., Baldus, N., et al. (2021). Serum ACE2, angiotensin II, and aldosterone levels are unchanged in patients with COVID-19. *Am. J. Hypertens.* 34, 278–281. doi: 10.1093/ajh/hpaa169

Riordan, J. F. (2003). Angiotensin-I-converting enzyme and its relatives. *Genome Biol.* 4:225. doi: 10.1186/gb-2003-4-8-225

Rivière, G., Michaud, A., Corradi, H. R., Sturrock, E. D., Acharya, K. R., Coqez, V., et al. (2007). Characterization of the first angiotensin-converting like enzyme in bacteria: ancestor ACE is already active. *Gene* 399, 81–91. doi: 10.1016/j.gene.2007.05.010

Robinson, F. A., Mihealsick, R. P., Wagener, B. M., Hanna, P., Poston, M. D., Efimov, I. R., et al. (2020). Role of angiotensin-converting enzyme 2 and pericytes in cardiac complications of COVID-19 infection. *Am. J. Physiol. Heart Circ. Physiol.* 319, H1059–H1068. doi: 10.1152/ajpheart.00681.2020

Rodriguez Rodriguez, M., Castro Quismondo, N., Zafra Torres, D., Gil Alos, D., Ayala, R., and Martinez-Lopez, J. (2021). Increased von Willebrand factor antigen and low ADAMTS13 activity are related to poor prognosis in covid-19 patients. *Int. J. Lab. Hematol.* 43, O152–O155. doi: 10.1111/ijlh.13476

Rota, P. A., Oberste, M. S., Monroe, S. S., Nix, W. A., Campagnoli, R., Icenogle, J. P., et al. (2003). Characterization of a novel coronavirus associated with severe acute respiratory syndrome. *Science* 300, 1394–1399. doi: 10.1126/science.1085952

Rovas, A., Osiaevi, I., Buscher, K., Sackarnd, J., Tepasse, P. R., Fobker, M., et al. (2020). Microvascular dysfunction in COVID-19: the MYSTIC study. *Angiogenesis* 24, 145–157. doi: 10.1007/s10456-020-09753-7

Ruiz-Ortega, M., Lorenzo, O., Suzuki, Y., Rupe'rez, M., and Egido, J. (2001). Proinflammatory actions of angiotensins. *Curr. Opin. Nephrol. Hypertens.* 10, 321–329. doi: 10.1097/00041552-200105000-00005

Rushworth, C. A., Guy, J. L., and Turner, A. J. (2008). Residues affecting the chloride regulation and substrate selectivity of the angiotensin-converting enzymes (ACE and ACE2) identified by site-directed mutagenesis. *FEBS J.* 275, 6033–6042. doi: 10.1111/j.1742-4658.2008.06733.x

Rysz, S., Al-Saadi, J., Sjöström, A., Farm, M., Campoccia Jalde, F., Plattén, M., et al. (2021). COVID-19 pathophysiology may be driven by an imbalance in the renin-angiotensin-aldosterone system. *Nat. Commun.* 12:2417. doi: 10.1038/s41467-021-22713-z|

Sadoshima, J., Qiu, Z. H., Morgan, J. P., and Izumo, S. (1995). Angiotensin-II and other hypertrophic stimuli mediated by G-protein-coupled receptors activate tyrosine kinase, mitogen-activated protein-kinase, and 90-Kd S6 kinase in cardiac myocytes - the critical role of Ca2+−dependent signaling. *Circ. Res.* 76, 1–15. doi: 10.1161/01.res.76.1.1

Sakka, M., Connors, J. M., He Kimian, G., Martin-Toutain, I., Crichi, B., Colmegna, I., et al. (2020). Association between D-dimer levels and mortality in patients with coronavirus disease 2019 COVID19: a systematic review and pooled analysis. *J. Med. Vasc.* 45, 268–274. doi: 10.1016/j.jdmv.2020.05.003

Sama, I. E., Ravera, A., Santema, B. T., van Goor, H., ter Maaten, J. M., Cleland, J. G. F., et al. (2020). Circulating plasma concentrations of angiotensin-converting enzyme 2 in men and women with heart failure and effects of renin–angiotensin–aldosterone inhibitors. *Eur. Heart J.* 41, 1810–1817. doi: 10.1093/eurheartj/ehaa373

Samavati, L., and Uhal, B. D. (2020). ACE2, much more than just a receptor for SARS-COV-2. *Front. Cell. Infect. Microbiol.* 10:317. doi: 10.3389/fcimb.2020.00317

Santos, R. A. S., Sampaio, W. O., Alzamora, A. C., Motta-Santos, D., Alenina, N., Bader, M., et al. (2018). The ACE2/angiotensin-(1–7)/MAS axis of the renin-angiotensin system: focus on angiotensin-(1–7). *Physiol. Rev.* 98, 505–553. doi: 10.1152/physrev.00023.2016

Santos, R. A., Silva AC, S. E., Maric, C., DMR, S., Machado, R. P., de Buhr, I., et al. (2003). Angiotensin-(1-7) is an endogenous ligand for the G protein-coupled receptor Mas. *Proc. Natl. Acad. Sci. U. S. A.* 100, 8258–8263. doi: 10.1073/pnas.1432869100

Sarzani, R., Giulietti, F., Di Pentima, C., Filipponi, A., and Spannella, F. (2020). Antagonizing the renin-angiotensin-aldosterone system in the era of COVID-19. *Intern. Emerg. Med.*, 15, 885–887. doi: 10.1007/s11739-020-02365-5

Sato, T., Suzuki, T., Watanabe, H., Kadowaki, A., Fukamizu, A., Liu, P. P., et al. (2013). Apelin is a positive regulator of ACE2 in failing hearts. *J. Clin. Invest.* 123, 5203–5211. doi: 10.1172/JCI69608

Sayed-Tabatabaei, F. A., Oostra, B. A., Isaacs, A., van Duijn, C. M., and Witteman, J. C. M. (2006). ACE polymorphism. *Circ. Res.* 98, 1123–1133. doi: 10.1161/01.RES.0000223145.74217.e7

Schiffrin, E. L., Flack, J. M., Ito, S., Muntner, P., and Webb, R. C. (2020). Hypertension and COVID-19. *Am. J. Hypertens.* 33, 373–374. doi: 10.1093/ajh/hpaa057

Schmidt, S., van Hooft, I. M., Grobbee, D. E., Ganten, D., and Ritz, E. (1993). Polymorphism of the angiotensin I converting enzyme gene is apparently not related to high blood pressure: Dutch hypertension and offspring study. *J. Hypertens.* 11, 345–348. doi: 10.1097/00004872-199304000-00003

Schmidt-Ott, K. M., Kagiyama, S., and Philips, M. I. (2000). The multiple actions of angiotensin II in atherosclerosis. *Regul. Pept.* 93, 65–77. doi: 10.1016/s0167-0115(00)00178-6

Schmieder, R. E., Hilgers, K. F., Schlaich, M. P., and Schmidt, B. M. W. (2007). Renin-angiotensin system and cardiovascular risk. *Lancet* 369, 1208–1219. doi: 10.1016/S0140-6736(07)60242-6

Sealey, J. E., and Rubattu, S. (1989). Prorenin and renin as separate mediators of tissue and circulating systems am. *J. Hypertens.* 2, 358–366. doi: 10.1093/ajh/2.5.358

Senchenkova, E. Y., Russell, J., Almeida-Paula, L. D., Harding, J. W., and Granger, D. N. (2010). Angiotensin II-mediated microvascular thrombosis. *Hypertension* 56, 1089–1095. doi: 10.1161/HYPERTENSIONAHA.110.158220

Senchenkova, E. Y., Russell, J., Esmon, C. T., and Granger, D. N. (2014). Roles of coagulation and fibrinolysis in angiotensin II enhanced microvascular thrombosis. *Microcirculation* 21, 401–407. doi: 10.1111/micc.12120

Shang, J., Ye, G., Shi, K., Wan, Y., Luo, C., Aihara, H., et al. (2020). Structural basis of receptor recognition by SARS-CoV-2. *Nature* 581, 221–224. doi: 10.1038/s41586-020-2179-y

Shen, L., Mo, H., Cai, L., Kong, T., Zheng, W., Ye, J., et al. (2009). Losartan prevents sepsis-induced acute lung injury and decreases activation of nuclear factor kappaB and mitogen-activated protein kinases. *Shock* 31, 500–506. doi: 10.1097/SHK.0b013e318189017a

Shen, Q., Xiao, X., Aierken, A., Yue, W., Wu, X., Liao, M., et al. (2020). The ACE2 expression in Sertoli cells and germ cells may cause male reproductive disorder after SARS-CoV-2 infection. *J. Cell. Mol. Med.* 24, 9472–9477. doi: 10.1111/jcmm.15541

Shenoy, V., Gjymishka, A., Jarajapu, Y. P., Qi, Y., Afzal, A., Rigatto, K., et al. (2013). Diminazene attenuates pulmonary hypertension and improves angiogenic progenitor cell functions in experimental models. *Am. J. Respir. Crit. Care Med.* 187, 648–657. doi: 10.1164/rccm.201205-0880OC

Sherman, E. J., and Emmer, B. T. (2021). ACE2 protein expression within isogenic cell lines is heterogeneous and associated with distinct transcriptomes. *Sci. Rep.* 11:15900. doi: 10.1038/s41598-021-95308-9

Shilts, J., Crozier, T. W. M., Greenwood, E. J. D., Lehner, P. J., and Wright, G. J. (2021). No evidence for basigin/CD147 as a direct SARS-CoV-2 spike binding receptor. *Sci. Rep.* 11:413. doi: 10.1038/s41598-020-80464-1

Shuai, H., Chan, J. F. W., Yuen, T. T. T., Yoon, C., Hu, J. C., Wen, L., et al. (2021). Emerging SARS-CoV-2 variants expand species tropism to murines. *eBioMed.* 73:103643. doi: 10.1016/j.ebiom.2021.103643

Shukla, N., Roelle, S. M., Suzart, V. G., Bruchez, A. M., and Matreyek, K. A. (2021). Mutants of human ACE2 differentially promote SARS-CoV and SARS-CoV-2 spike mediated infection. *PLoS Pathog.* 17:e1009715. doi: 10.1371/journal.ppat.1009715

Siddiquee, K., Hampton, J., McAnally, D., May, L., and Smith, L. (2013). The apelin receptor inhibits the angiotensin II type 1 receptor via allosteric trans-inhibition. *Br. J. Pharmacol.* 168, 1104–1117. doi: 10.1111/j.1476-5381.2012.02192.x

Siguret, V., Voicu, S., Neuwirth, M., Delrue, M., Gayat, E., Stépanian, A., et al. (2020). Are antiphospholipid antibodies associated with thrombotic complications in critically ill COVID-19 patients? *Thromb. Res.* 195, 74–76. doi: 10.1016/j.thromres.2020.07.016

Silva, G. M., França-Falcão, M. S., Calzerra, N. T. M., Luz, M. S., Gadelha, D. D. A., Balarini, C. M., et al. (2020). Role of renin angiotensin system components in atherosclerosis: focus on Ang-II, ACE2, and Ang-1–7. *Front. Physiol.* 11:1067. doi: 10.3389/fphys.2020.01067

Simoes e Silva, A. C., Silveira, K. D., Ferreira, A. J., and Teixeira, M. M. (2013). ACE2, angiotensin-(1-7) and Mas receptor axis in inflammation and fibrosis. *Br. J. Pharmacol.* 169, 477–492. doi: 10.1111/bph.12159

Singer, D., and Camargo, S. M. R. (2011). Collectrin and ACE2 in renal and intestinal amino acid transport. *Channels* 5, 410–423. doi: 10.4161/chan.5.5.16470

Singer, D., Camargo, S. M. R., Ramadam, T., Schäfer, M., Mariotta, L., Herzog, B., et al. (2012). Defective intestinal amino acidabsorption in ACE2 null mice. *Am. J. Physiol. Gastrointest. Liver Physiol.* 303, G686–G695. doi: 10.1152/ajpgi.00140.2012

Singh, K. D., and Karnik, S. S. (2016). Angiotensin receptors: structure, function, signaling and clinical applications. *J. Cell Signal.* 1:111. doi: 10.4172/jcs.1000111

Skeggs, L. T. Jr., Kahn, J. R., and Shumway, N. P. (1956). The preparation and function of the hypertensin-converting enzyme. *J. Exp. Med.* 103, 295–299. doi: 10.1084/jem.103.3.295

Skidgel, R. A., and Erdos, E. G. (1987). The broad substrate specificity of human angiotensin I converting enzyme. *Clin. Exp. Hypertens. A* 9, 243–259. doi: 10.3109/10641968709164184

Smadja, D. M., Mentzer, S., Fontenay, M., Laffan, M. A., Ackermann, M., Helms, J., et al. (2021). COVID-19 is a systemic vascular hemopathy: insight for mechanistic and clinical aspects. *Angiogenesis* 24, 755–788. doi: 10.1007/s10456-021-09805-6

Sodhi, C. P., Wohlford-Lenane, C., Yamaguchi, Y., Prindle, T., Fulton, W. B., Wang, S., et al. (2017). Attenuation of pulmonary ACE2 activity impairs inactivation of des-Arg9 bradykinin/BKB1R axis and facilitates LPS-induced neutrophil infiltration. *AJP Lung Cell. Mol. Physiol.* 314, L17–L31. doi: 10.1152/ajplung.00498.2016

Sorokina, M., Teixeira, J. M. C., Barrera-Vilarmau, S., Paschkle, R., Papasotiriou, I., Rodrigues, J. P. L. M., et al. (2020). Structural models of human ACE2 variants with SARS-CoV-2 spike protein for structure-based drug design. *Sci. Data* 7:309. doi: 10.1038/s41597-020-00652-6

Spitler, K. M., and Webb, R. C. (2014). Endoplasmic reticulum stress contributes to aortic stiffening via proapoptotic and fibrotic signaling mechanisms. *Hypertension* 63, e40–e45. doi: 10.1161/HYPERTENSIONAHA.113.02558

Stawiski, EW, Diwanji, D, Suryamohan, K, Gupta, R., Fellouse, FA, Sathirapongsasuti, JF, et al. Human ACE2 receptor polymorphisms predict SARS-CoV-2 susceptibility. bioRxiv [Preprint] (2020). doi: 10.1101/2020.04.07.024752

Stefely, J. A., Christensen, B. B., Gogakos, T., Conne Sullivan, J. K., Montgomery, G. G., Barranco, J. P., et al. (2020). Marked factor V activity elevation in severe COVID-19 is associated with venous thromboembolism. *Am. J. Hematol.* 95, 1522–1530. doi: 10.1002/ajh.25979

Strafella, C., Caputo, V., Termine, A., Barati, S., Caltagirone, C., Giardina, E., et al. (2020). Investigation of genetic variations of IL6 and IL6r as potential prognostic and pharmacogenetics biomarkers: implications for covid-19 and neuroinflammatory disorders. *Lifestyles* 10, 1–10. doi: 10.3390/life10120351

Suryamohan, K., Diwanji, D., Stawiski, E. W., Gupta, R., Miersch, S., Liu, J., et al. (2021). Human ACE2 receptor polymorphisms and altered susceptibility to SARS-CoV-2. *Comm. Biol.* 4:475. doi: 10.1038/s42003-021-02030-3

Takayanagi, T., Kawai, T., Forrester, S. J., Obama, T., Tsuji, T., Fukuda, Y., et al. (2015). Role of epidermal growth factor receptor and endoplasmic reticulum stress in vascular remodeling induced by angiotensin II. *Hypertension* 65, 1349–1355. doi: 10.1161/HYPERTENSIONAHA.115.05344

Tan, Y. K., Goh, C., Leow, A. S. T., Tambyah, P. A., Ang, A., Yap, E. S., et al. (2020). COVID-19 and ischemic stroke: a systematic review and meta-summary of the literature. *J. Thromb. Thrombolysis* 50, 587–595. doi: 10.1007/s11239-020-02228-y

Tang, T., Bidon, M., Jaimes, J. A., Whittaker, G. R., and Daniel, S. (2020). Coronavirus membrane fusion mechanism offers a potential target for antiviral development. *Antivir. Res.* 178:104792. doi: 10.1016/j.antiviral.2020.104792

Tay, M. Z., Poh, C. M., Renia, L., MacAry, P. A., and Ng, L. F. P. (2020). The trinity of COVID19: immunity, inflammation and intervention. *Nat. Rev. Immunol.* 20, 363–374. doi: 10.1038/s41577-020-0311-8

Tereshchenko, L. G., Johnson, K., Khayyat-Kholghi, M., and Johnson, B. (2022). Rate of angiotensin-converting enzyme inhibitors and angiotensin receptor blockers use and the number of COVID-19–confirmed cases and deaths. *Am. J. Cardiol.* 165, 101–108. doi: 10.1016/j.amjcard.2021.10.050

Thomas, M. C., Pickering, R. J., Tsorotes, D., Koitka, A., Sheehy, K., Bernardi, S., et al. (2010). Genetic Ace2 deficiency accentuates vascular inflammation and atherosclerosis in the ApoE knockout mouse. *Circ. Res.* 107, 888–897. doi: 10.1161/CIRCRESAHA.110.219279

Tigerstedt, R., and Bergman, P. G. (1898). Niere und kreislauf. *Skand. Arch. Physiol.* 8, 223–271. doi: 10.1111/j.1748-1716.1898.tb00272.x

Tignarelli, C. J., Ingraham, N. E., Sparks, M. A., Reilkoff, R., Bezdicek, T., Benson, B., et al. (2020). Antihypertensive drugs and risk of COVID-19? *Lancet Respir. Med.* 8, e30–e31. doi: 10.1016/S2213-2600(20)30153-3

Tikellis, C., Pickering, R., Tsorotes, D., Du, X. J., Kiriazis, H., Nguyen-Huu, T. P., et al. (2012). Interaction of diabetes and ACE2 in the pathogenesis of cardiovascular disease in experimental diabetes. *Clin. Sci. (Lond.)* 123, 519–529. doi: 10.1042/CS20110668

Tikellis, C., and Thomas, M. C. (2012). Angiotensin-converting enzyme 2 (ACE2) is a key modulator of the renin angiotensin system in health and disease. *Int. J. Pept. Actions* 2012:256294. doi: 10.1155/2012/256294

Tipnis, S. R., Hooper, N. M., and Hyde, R. (2000). A human homolog of angiotensin-converting enzyme. Cloning and functional expression as a captopril-insensitive carboxypeptidase. *J. Biol. Chem.* 275, 33238–33243. doi: 10.1074/jbc.M002615200

Tong, M., Jiang, Y., Xia, D., Xiong, Y., Zheng, Q., Chen, F., et al. (2020). Elevated serum endothelial cell adhesion molecules expression in COVID-19 patients. *J. Infect. Dis.* 222, 894–898. doi: 10.1093/infdis/jiaa349

Towler, P., Staker, B., Prasad, S. G., Menon, S., Tang, J., Parsons, T., et al. (2004). ACE2 X-ray structures reveal a large hinge-bending motion important for inhibitor binding and catalysis. *J. Biol. Chem.* 279, 17996–18007. doi: 10.1074/jbc.M311191200

Tukiainen, T., Villani, A. C., Yen, A., Rivas, M. A., Marshall, J. L., Satija, R., et al. (2017). Landscape of X chromosome inactivation across human tissues. *Nature* 550, 244–248. doi: 10.1038/nature24265

Turner, A. J., and Hooper, N. M. (2002). The angiotensin-converting enzyme gene family: genomics and pharmacology. *Trends Pharmacol. Sci.* 23, 177–183. doi: 10.1016/s0165-6147(00)01994-5

Ueda, S., Elliott, H. L., Morton, J. J., and Connell, J. M. (1995). Enhanced pressor response to angiotensin I in normotensive men with the deletion genotype (DD) for angiotensin-converting enzyme. *Hypertension* 25, 1266–1269. doi: 10.1161/01.hyp.25.6.1266

Uijl, E., Mirabito Colafella, K. M., Sun, Y., Ren, L., van Veghel, R., Garrelds, I. M., et al. (2019). Strong and sustained antihypertensive effect of small interfering RNA targeting liver angiotensinogen. *Hypertension* 73, 1249–1257. doi: 10.1161/HYPERTENSIONAHA.119.12703

Vaduganathan, M., Varden, O., Michel, T., McMurray, J. J. V., Pfeffer, M. A., and Solomon, S. D. (2020). Renin–angiotensin–aldosterone system inhibitors in patients with Covid-19. *N. Engl. J. Med.* 382, 1653–1659. doi: 10.1056/NEJMsr2005760

Vandestienne, M., Zhang, Y., Santos-Zas, I., Al-Rifai, R., Joffre, J., Giraud, A., et al. (2021). TREM-1 orchestrates angiotensin II-induced monocyte trafficking and promotes experimental abdominal aortic aneurysm. *J. Clin. Invest.* 131:e142468. doi: 10.1172/JCI142468

Varanat, M., Haase, E. M., Kay, J. G., and Scannapieco, F. A. (2017). Activation of the TREM-1 pathway in human monocytes by periodontal pathogens and oral commensal bacteria. *Mol Oral Microbiol* 32, 257–287. doi: 10.1111/omi.12169

Vassiliou, A. G., Keskinidou, C., Jahaj, E., Gallos, P., Dimopoulou, I., Kotanidou, A., et al. (2021). ICU admission levels of endothelial biomarkers as predictors of mortality in critically ill COVID-19 patients. *Cells* 10:186. doi: 10.3390/cells10010186

Velkoska, E., Patel, S. K., and Burrell, L. M. (2016). Angiotensin converting enzyme 2 and diminazene: role in cardiovascular and blood pressure regulation. *Curr. Opin. Nephrol. Hypertens.* 25, 384–395. doi: 10.1097/MNH.0000000000000254

Velloso, L. A., Folli, F., Sun, X. J., White, M. F., Saad, M. J. A., and Kahn, C. R. (1996). Cross-talk between the insulin and angiotensin signaling systems. *Proc. Natl. Acad. Sci. U. S. A.* 93, 12490–12495. doi: 10.1073/pnas.93.22.12490

Verdecchia, P., Angeli, F., Mazzotta, G., Gentile, G., and Reboldi, G. (2008). The renin angiotensin system in the development of cardiovascular disease: role of aliskiren in risk reduction. *Vasc. Health Risk Manag.* 4, 971–981. doi: 10.2147/vhrm.s3215

Verdecchia, P., Cavallini, C., Spanevello, A., and Angeli, F. (2020). The pivotal link between ACE2 deficiency and SARS-CoV-2 infection. *Eur. J. Intern. Med.* 76, 14–20. doi: 10.1016/j.ejim.2020.04.037

Verma, S., Abbas, M., Verma, S., Khan, F. H., Raza, S. T., Siddigi, Z., et al. (2021). Impact of I/D polymorphism of angiotensin-converting enzyme 1 (ACE1) gene on the severity of COVID-19 patients. *Infect. Genet. Evol.* 91:104801. doi: 10.1016/j.meegid.2021.104801

Verma, A., Xu, K., Du, T., Zhu, P., Liang, Z., Liao, S., et al. (2019). Expression of human ACE2 in lactobacillus and beneficial effects in diabetic retinopathy in mice. *Mol. Ther. Methods Clin. Dev.* 14, 161–170. doi: 10.1016/j.omtm.2019.06.007

Vicenzi, M., Di Cosola, R., Ruscica, M., Ratti, A., Rota, I., Rota, F., et al. (2020). The liaison between respiratory failure and high blood pressure: evidence from COVID-19 patients. *Eur. Respir. J.* 56:2001157. doi: 10.1183/13993003.01157-2020

Vickers, C., Hales, P., Kaushik, V., Dick, L., Gavin, J., Tang, J., et al. (2002). Hydrolysis of biological peptides by human angiotensin-converting enzyme-related carboxypeptidase. *J. Biol. Chem.* 277, 14838–14843. doi: 10.1074/jbc.M200581200

Vitte, J., Diallo, A. B., Boumaza, A., Lopez, A., Michel, M., Allardet-Servent, J., et al. (2020). A granulocytic signature identifies COVID-19 and its severity. *J. Infect. Dis.* 222, 1985–1996. doi: 10.1093/infdis/jiaa591

Vuille-Dit-Bille, R. N., Camargo, S. M., Emmenegger, L., Sasse, T., Kummer, E., Jando, J., et al. (2015). Human intestine luminal ACE2 and amino acid transporter expression increased by ACE-inhibitors. *Amino Acids* 47, 693–705. doi: 10.1007/s00726-014-1889-6

Wacharapluesadee, S., Tan, C. W., Maneeorn, P., Duengkae, P., Zhu, F., Joyjinda, Y., et al. (2021). Evidence for SARS-CoV-2 related coronaviruses circulating in bats and pangolins in Southeast Asia. *Nat. Commun.* 12:972. doi: 10.1038/s41467-021-21240-1

Wakahara, S., Konoshita, T., Mizuno, S., Motomura, M., Aoyama, C., Makino, Y., et al. (2007). Synergistic expression of angiotensin-converting enzyme (ACE) and ACE2 in human renal tissue and confounding effects of hypertension on the ACE to ACE2 ratio. *Endocrinology* 148, 2453–2457. doi: 10.1210/en.2006-1287

Walls, A. C., Park, Y. J., Tortorici, M. A., Wall, A., McGuire, A. T., and Veesler, D. (2020). Structure, function, and antigenicity of the SARS-CoV-2 spike glycoprotein. *Cells* 181, 281–292. doi: 10.1016/j.cell.2020.02.058

Wang, K., Chen, W., Zhang, Z., Deng, Y., Lian, J. Q., Peng, D., et al. (2020). CD147-spike protein is a novel route for SARS-CoV-2 infection to host cells. *Signal Transduct. Target. Ther.* 5:283. doi: 10.1038/s41392-020-00426-x

Wang, H., Ji, Y., Wu, G., Sun, K., Sun, Y., Li, W., et al. (2015). L-tryptophan activates mammalian target of rapamycin and enhances expression of tight junction proteins in intestinal porcine epithelial cells. *J. Nutr.* 145, 1156–1162. doi: 10.3945/jn.114.209817

Wang, C., Jin, R., Zhu, X., Yan, J., and Li, G. (2015). Function of CD147 in atherosclerosis and atherothrombosis. *J. Cardiovasc. Transl. Res.* 8, 59–66. doi: 10.1007/s12265-015-9608-6

Wang, F., Lu, X., Peng, K., Zhou, L., Li, C., Wang, W., et al. (2014). COX-2 mediates angiotensin II-induced (pro)renin receptor expression in the rat renal medulla. *Am. J. Physiol. Ren. Physiol.* 307, F25–F32. doi: 10.1152/ajprenal.00548.2013

Wang, W., Luo, L., Lu, H., Chen, S., Kang, L., and Cui, F. (2015). Angiotensin-converting enzymes modulate aphid–plant interactions. *Sci. Rep.* 5:8885. doi: 10.1038/srep08885

Wang, C., Wang, S., Li, D., Wei, D. Q., Zhao, J., and Wang, J. (2020). Human intestinal defensin 5 inhibits SARS-CoV-2 invasion by cloaking ACE2. *Gastroenterology* 159, 1145–1147.e4. doi: 10.1053/j.gastro.2020.05.015

Wang, Q., Zhang, Y., Wu, L., Niu, S., Song, C., Zhang, Z., et al. (2020). Structural and functional basis of SARS-CoV-2 entry by using human ACE2. *Cells* 181, 894–904.e9. doi: 10.1016/j.cell.2020.03.045

Wang, M. Y., Zhao, R., Gao, L. J., Gao, X. F., Wang, D. P., and Cao, J. M. (2020). SARS-CoV-2: structure, biology, and structure-based therapeutics development. *Front. Cell. Infect. Microbiol.* 10:587269. doi: 10.3389/fcimb.2020.587269

Watanabe, T., Barker, T. A., and Berk, B. C. (2005). Angiotensin II and the endothelium: diverse signals and effects. *Hypertension* 45, 163–169. doi: 10.1161/01.HYP.0000153321.13792.b9

Wei, C., Shan, K. J., Wang, W., Zhang, S., Huan, Q., and Qian, W. (2021). Evidence for a mouse origin of the SARS-CoV-2 omicron variant. *J. Genet. Genom.* 48, 1111–1121. doi: 10.1016/j.jgg.2021.12.003

Wenzel, J., Lampe, J., Müller-Fielitz, H., Schuster, R., Zille, M., Müller, K., et al. (2021). The SARS-CoV-2 main protease Mpro causes microvascular brain pathology by cleaving NEMO in brain endothelial cells. *Nat. Neurosci.* 24, 1522–1533. doi: 10.1038/s41593-021-00926-1

Wicik, Z., Eyileten, C., Jakubik, D., Simoes, S. N., Martins, D. C. Jr., Pavao, R., et al. (2020). ACE2 interaction networks in COVID-19: a physiological framework for prediction of outcome in patients with cardiovascular risk factors. *J. Clin. Med.* 9:3743. doi: 10.3390/jcm9113743

Wright, J. M. (2000). Choosing a first-line drug in the management of elevated blood pressure: what is the evidence? 3: angiotensin-converting-enzyme inhibitors. *CMAJ* 163, 293–296.

Wu, Y.-H., Li, J.-Y., Wang, C., Zhang, L.-M., and Qiao, H. (2017). The ACE2 G8790A polymorphism: involvement in type 2 diabetes mellitus combined with cerebral stroke. *J. Clin. Lab. Anal.* 31:e22033. doi: 10.1002/jcla.22033

Wysocki, J., Garcia-Halpin, L., Ye, M., Maier, C., Sowers, K., Burns, K. D., et al. (2013). Regulation of urinary ACE2 in diabetic mice. *Am. J. Physiol. Physiol.* 305, F600–F611. doi: 10.1152/ajprenal.00600.2012

Xiao, M., Zhang, Y., Zhang, S., Qin, X., Xia, P., Cao, W., et al. (2020). Anti-phospholipid antibodies in critically ill patients with coronavirus disease 2019 (COVID-19). *Arthritis Rheum.* 72, 1998–2004. doi: 10.1002/art.41425

Xiao, F., Zimpelmann, J., Agaybi, S., Gurley, S. B., Puente, L., and Burns, K. D. (2014). Characterization of angiotensin-converting enzyme 2 ectodomain shedding from mouse proximal tubular cells. *PLoS One* 9:e85958. doi: 10.1371/journal.pone.0085958

Xie, X., Chen, J., Wang, X., Zhang, F., and Liu, Y. (2006). Age-and genderrelated difference of ACE2 expression in rat lung. *Life Sci.* 78, 2166–2171. doi: 10.1016/j.lfs.2005.09.038

Xie, Y., Xu, E., Bowe, B., and Al-Aly, Z. (2022). Long-term cardiovascular outcomes of COVID-19. *Nat. Med.* 28, 583–590. doi: 10.1038/s41591-022-01689-3

Xu, Q., Jensen, D. D., Peng, H., and Feng, Y. (2016). The critical role of the central nervous system (pro)renin receptor in regulating systemic blood pressure. *Pharmacol. Ther.* 164, 126–134. doi: 10.1016/j.pharmthera.2016.04.006

Xu, Y., and Li, Y. (2021). MicroRNA-28-3p inhibits angiotensin-converting enzyme 2 ectodomain shedding in 293T cells treated with the spike protein of severe acute respiratory syndrome coronavirus 2 by targeting a disintegrin and metalloproteinase 17. *Int. J. Mol. Med.* 48:189. doi: 10.3892/ijmm.2021.5022

Xu, C., Wang, A., Marin, M., Honnen, W., Ramasamy, S., Porter, E., et al. (2021). Human Defensins inhibit SARS-CoV-2 infection by blocking viral entry. *Viruses* 13:1246. doi: 10.3390/v13071246

Xu, H., Zhong, L., Deng, J., Peng, J., Dan, H., Zeng, X., et al. (2020). High expression of ACE2 receptor of 2019-nCoV on the epithelial cells of oral mucosa. *Int. J. Oral Sci.* 12:8. doi: 10.1038/s41368-020-0074-x

Xue, B., Zhang, Z., Roncari, C. F., Guo, F., and Johnson, A. K. (2012). Aldosterone acting through the central nervous system sensitizes angiotensin II-induced hypertension. *Hypertension* 60, 1023–1030. doi: 10.1161/HYPERTENSIONAHA.112.196576

Yamamoto, N., Nishida, N., Yamamoto, R., Gojobori, T., Shimotohno, K., Mizokami, M., et al. (2021). Angiotensin–converting enzyme (ACE) 1 gene polymorphism and phenotypic expression of COVID-19 symptoms. *Gene* 12:1572. doi: 10.3390/genes12101572

Yan, R., Zhang, Y., Li, Y., Xia, L., Guo, Y., Zhou, Q., et al. (2020). Structural basis for the recognition of the SARS-CoV-2 by full-length human ACE2. *Science* 367, 1444–1448. doi: 10.1126/science.abb2762

Yang, J. M., Dong, M., Meng, X., Zhao, Y. X., Yang, X. Y., Liu, X. L., et al. (2013). Angiotensin-(1-7) dose-dependently inhibits atherosclerotic lesion formation and enhances plaque stability by targeting vascular cells. *Arteriosc. Thromb. Vascular Biol.* 33, 1978–1985. doi: 10.1161/ATVBAHA.113.301320

Yang, P., Gu, H., Zhao, Z., Wang, W., Cao, B., Lai, C., et al. (2014). Angiotensin-converting enzyme 2 (ACE2) mediates influenza H7N9 virus-induced acute lung injury. *Sci. Rep.* 4:7027. doi: 10.1038/srep07027

Yang, M., Zhao, J., Xing, L., and Shi, L. (2015). The association between angiotensinconverting enzyme 2 polymorphisms and essential hypertension risk: a meta-analysis involving 14, 122 patients. *J. Renin-Angiotensin-Aldosterone Syst.* 16, 1240–1244. doi: 10.1177/1470320314549221

Yen, H. L., Sit, T. H. C., Brackman, C. J., Chuk, S. S. Y., Gu, H., Tam, K. W. S., et al. (2022). Transmission of SARS-CoV-2 delta variant (AY.127) from pet hamsters to humans leading to onward human-to-human transmission: a case study. *Lancet* 399, 1070–1078. doi: 10.1016/S0140-6736(22)00326-9

Yi, L., Gu, Y. H., Wang, X. L., An, L. Z., Xie, X. D., Shao, W., et al. (2006). Association of ACE, ACE2 and UTS2 polymorphisms with essential hypertension in Han and Dongxiang populations from North-Western China. *J. Int. Med. Res.* 34, 272–283. doi: 10.1177/147323000603400306

Yim, H. E., and Yoo, K. H. (2008). Renin-angiotensin system-considerations for hypertension and kidney. *Electrol. Blood Press.* 6, 42–50. doi: 10.5049/EBP.2008.6.1.42

Yu, H. Q., Sun, B. Q., Fanf, Z. F., Zhao, J. C., Liu, X. Y., Li, Y. M., et al. (2020). Distinct features of SARS-CoV-2-specific IgA response in COVID-19 patients. *Eur. Respir. J.* 56:2001526. doi: 10.1183/13993003.01526-2020

Yu, C., Tang, W., Wang, Y., Shen, Q., Wang, B., Cai, C., et al. (2016). Downregulation of ACE2/Ang-(1-7)/Mas axis promotes breast cancer metastasis by enhancing store-operated calcium entry. *Cancer Lett.* 376, 268–277. doi: 10.1016/j.canlet.2016.04.006

Zhang, H., and Baker, A. (2017). Recombinant human ACE2: acing out angiotensin II in ARDS therapy. *Crit. Care* 21:305. doi: 10.1186/s13054-017-1882-z

Zhang, Q., Bastard, P., Liu, Z., Le Pen, J., Moncada-Velez, M., Chen, J., et al. (2020). Inborn errors of type I IFN immunity in patients with life-threatening COVID-19. *Science* 370:eabd4570. doi: 10.1126/science.abd4570

Zhang, J., Dong, J., Martin, M., He, M., Gongol, B., Marin, T. L., et al. (2018). AMP-activated protein kinase phosphorylation of ACE2 in endothelium mitigates pulmonary hypertension. *Am. J. Respir. Crit. Care Med.* 198, 509–520. doi: 10.1164/rccm.201712-2570OC

Zhang, Q., Gefter, J., Sneddon, W. B., Mamonava, T., and Friedman, P. A. (2021). ACE2 interaction with cytoplasmic PDZ protein enhances SARS-CoV-2 invasion. *iScience* 24:102770. doi: 10.1016/j.isci.2021.102770

Zhang, S., Liu, Y., Wang, X., Yang, L., Li, H., Wang, Y., et al. (2020). SARS-CoV-2 binds platelet ACE2 to enhance thrombosis in COVID-19. *J. Hematol. Oncol.* 13:120. doi: 10.1186/s13045-020-00954-7

Zhang, X. J., Qin, J. J., Cheng, X., Shen, L., Zhao, Y. C., Yuan, Y., et al. (2020). In-hospital use of statins is associated with a reduced risk of mortality among individuals with COVID-19. *Cell Metab.* 32, 176–187. doi: 10.1016/j.cmet.2020.06.015.e4

Zhang, C., Shen, L., Le, K. J., Pan, M. M., Kong, L. C., Gu, Z. C., et al. (2020). Incidence of venous thromboembolism in hospitalized coronavirus disease 2019 patients: a systematic review and meta-analysis. *Front. Cardiovasc. Med.* 7:151. doi: 10.3389/fcvm.2020.00151

Zhang, H., Wada, J., Hida, K., Tsuchiyama, Y., Hiragushi, K., Shikata, K., et al. (2001). Collectrin, a collecting duct-specific transmembrane glycoprotein, is a novel homolog of ACE2 and is developmentally regulated in embryonic kidneys. *J. Biol. Chem.* 276, 17132–17139. doi: 10.1074/jbc.M006723200

Zhang, Z. Z., Wang, W., Jin, H. Y., Chen, X., Cheng, Y. W., Xu, Y. L., et al. (2017). Apelin is a negative regulator of angiotensin II-mediated adverse myocardial remodeling and dysfunction. *Hypertension* 70, 1165–1175. doi: 10.1161/HYPERTENSIONAHA.117.10156

Zhang, Y., Xiao, M., Zhang, S., Xia, P., Cao, W., Jiang, W., et al. (2020). Coagulopathy and antiphospholipid antibodies in patients with Covid-19. *N. Engl. J. Med.* 382:e38. doi: 10.1056/NEJMc2007575

Zhang, L., Zhang, Y., Qin, X., Jiang, X., Zhang, J., Mao, L., et al. (2022). Recombinant ACE2 protein protects against acute lung injury induced by SARS-CoV-2 spike RBD protein. *Crit. Care* 26:171. doi: 10.1186/s13054-022-04034-9

Zhang, P., Zhu, L., Cai, J., Lei, F., Qin, J. J., Xie, J., et al. (2020). Association of inpatient use of angiotensin-converting enzyme inhibitors and angiotensin II receptor blockers with mortality among patients with hypertension hospitalized with COVID-19. *Circ. Res.* 126, 1671–1681. doi: 10.1161/CIRCRESAHA.120.317242

Zhao, J., Yuan, Q., Wang, H., Liu, W., Liao, X., Su, Y., et al. (2020). Antibody responses to SARS-CoV-2 in patients of novel coronavirus disease 2019. *Clin. Infect. Dis.* 71, 2027–2034. doi: 10.1093/cid/ciaa344

Zhao, Y., Zhao, Z., Wang, Y., Zhou, Y., Ma, Y., and Zuo, W. (2020). Single-cell RNA expression profiling of ACE2, the receptor of SARS-CoV-2. *Am. J. Respir. Crit. Care Med.* 202, 756–759. doi: 10.1164/rccm.202001-0179LE

Zheng, M., Gao, Y., Wang, G., Song, G., Liu, S., Sun, D., et al. (2020). Functional exhaustion of antiviral lymphocytes in COVID-19 patients. *Cell. Mol. Immunol.* 17, 533–535. doi: 10.1038/s41423-020-0402-2

Zhou, P., Yang, X. L., Wang, X. G., Hu, B., Zhang, L., Zhang, W., et al. (2020). A pneumonia outbreak associated with a new coronavirus of probable bat origin. *Nature* 579, 270–273. doi: 10.1038/s41586-020-2012-7

Zhou, F., Yu, T., Du, R., Fan, G., Liu, Y., Liu, Z., et al. (2020). Clinical course and risk factors for mortality of adult inpatients with COVID-19 in Wuhan, China: a retrospective cohort study. *Lancet* 395, 1054–1062. doi: 10.1016/S0140-6736(20)30566-3

Zhu, N., Zhang, D., Wang, W., Li, X., Yang, B., Song, J., et al. (2020). A novel coronavirus from patients with pneumonia in China, 2019. *N. Engl. J. Med.* 382, 727–733. doi: 10.1056/NEJMoa2001017

Zhuang, M. W., Cheng, Y., Zhang, J., Jiang, X. M., Wang, L., Deng, J., et al. (2020). Increasing host cellular receptor-angiotensin-converting enzyme 2 (ACE2) expression by coronavirus may facilitate 2019-nCoV (or SARS-CoV2) infection. *J. Med. Virol.* 92, 2693–2701. doi: 10.1002/jmv.26139

Ziegler, C. G. K., Allon, S. J., Nyquist, S. K., Mbano, I. M., Miao, V. N., Tzouanas, C. N., et al. (2020). SARS-CoV-2 receptor ACE2 is an interferon-stimulated gene in human airway epithelial cells and is detected in specific cell subsets across tissues. *Cells* 181, 1016–1035.e19. doi: 10.1016/j.cell.2020.04.035

Zou, X., Chen, K., Zou, J., Han, P., Hao, J., and Han, Z. (2020). Single-cell RNA-seq data analysis on the receptor ACE2 expression reveals the potential risk of different human organs vulnerable to 2019-nCoV infection. *Front. Med.* 14, 185–192. doi: 10.1007/s11684-020-0754-0

Zoufaly, A., Poglitsch, M., Aberle, J. H., Hoepler, W., Seitz, T., Traugott, M., et al. (2020). Human recombinant soluble ACE2 in severe COVID-19. *Lancet Respir. Med.* 8, 115–120. doi: 10.1016/S2213-2600(20)30418-5

Zuo, Y., Yalavarthi, S., Shi, H., Gockman, K., Zuo, M., Madison, J. A., et al. (2020). Neutrophil extracellular traps in COVID-19. *JCI Insight* 5:e138999. doi: 10.1172/jci.insight.138999

frontiers | Frontiers in Microbiology

TYPE Original Research
PUBLISHED 01 December 2022
DOI 10.3389/fmicb.2022.1071394

OPEN ACCESS

EDITED BY
Jian Shang,
Zhengzhou University,
China

REVIEWED BY
Xin Yin,
Harbin Veterinary Research Institute (CAAS),
China
Benjie Chai,
Tsinghua University,
China
Weili Kong,
Gladstone Institutes,
United States

*CORRESPONDENCE
He Huang
huanghe@hemubiotech.com
Yan-ming Zhang
zhangym@nwafu.edu.cn

†These authors have contributed equally to this work

SPECIALTY SECTION
This article was submitted to Virology, a section of the journal Frontiers in Microbiology

RECEIVED 16 October 2022
ACCEPTED 10 November 2022
PUBLISHED 01 December 2022

CITATION
Zheng H-q, Li C, Zhu X-f, Wang W-X, Yin B-y, Zhang W-j, Feng S-l, Yin X-h, Huang H and Zhang Y-m (2022) miR-615 facilitates porcine epidemic diarrhea virus replication by targeting *IRAK1* to inhibit type III interferon expression. *Front. Microbiol.* 13:1071394. doi: 10.3389/fmicb.2022.1071394

miR-615 facilitates porcine epidemic diarrhea virus replication by targeting *IRAK1* to inhibit type III interferon expression

Hong-qing Zheng[1,3†], Cheng Li[2,3†], Xiao-fu Zhu[1†], Wei-Xiao Wang[4†], Bao-ying Yin[1], Wen-juan Zhang[1], Shu-lin Feng[1], Xun-hui Yin[5], He Huang[4*] and Yan-ming Zhang[3*]

[1]Key Laboratory of Animal Epidemic Disease Diagnostic Laboratory of Molecular Biology in Xianyang City, Institute of Animal Husbandry and Veterinary Medicine, Xianyang Vocational Technical College, Xianyang, Shaanxi, China, [2]Tianjin Institute of Animal Husbandry and Veterinary Medicine, Tianjin Academy of Agricultural Sciences, Tianjin, China, [3]College of Veterinary Medicine, Northwest A&F University, Yangling, Shaanxi, China, [4]Institute of Hemu Biotechnology, Beijing Hemu Biotechnology Co. Ltd., Beijing, China, [5]Liangshan County Animal Husbandry and Veterinary Development Center, Liangshan County Animal Husbandry Bureau, Jining, China

Porcine epidemic diarrhea virus (PEDV) in the Coronavirus family is a highly contagious enteric pathogen in the swine industry, which has evolved mechanisms to evade host innate immune responses. The PEDV-mediated inhibition of interferons (IFNs) has been linked to the nuclear factor-kappa B (NF-κB) pathway. MicroRNAs (miRNAs) are involved in virus–host interactions and IFN-I regulation. However, the mechanism by which the PEDV regulates IFN during PEDV infection has not yet been investigated in its natural target cells. We here report a novel mechanism of viral immune escape involving miR-615, which was screened from a high-throughput sequencing library of porcine intestinal epithelial cells (IECs) infected with PEDV. PEDV infection altered the profiles of miRNAs and the activities of several pathways involved in innate immunity. Overexpression of miR-615 increased PEDV replication, inhibited IFN expression, downregulated the NF-κB pathway, and blocked p65 nuclear translocation. In contrast, knockdown of miR-615 enhanced IFN expression, suppressed PEDV replication, and activated the NF-κB pathway. We further determined that *IRAK1* is the target gene of miR-615 in IECs. Our findings show that miR-615 suppresses activation of the NF-κB pathway by suppressing the IRAK1 protein and reducing the generation of IFN-IIIs, which in turn facilitates PEDV infection in IECs. Moreover, miR-615 inhibited PEDV replication and NF-κB pathway activation in both IECs and MARC-145 cells. These findings support an important role for miR-615 in the innate immune regulation of PEDV infections and provide a novel perspective for developing new treatments.

KEYWORDS

miR-615, IFN, innate immunity, porcine epidemic diarrhea virus, intestinal epithelial cells, miRNA high-throughput, NF-kappa B, *IRAK1*

Introduction

The emerging and re-emerging Coronavirus family member porcine epidemic diarrhea virus (PEDV) attacks neonatal piglets and causedto cause acute watery diarrhea, with a substantial mortality rate. The global swine industry has sustained tremendous financial losses as a result of PEDV infections (Akira et al., 2006; Li et al., 2012; Dong and Soong, 2021). The target cells for PEDV are porcine intestinal epithelial cells (IECs), and PEDV strain CV777 could successfully infect an immortalized IEC line (Cao et al., 2015b; Lin et al., 2015; Wang et al., 2016). Previous studies have shown that type-I interferons (IFN-Is), which are produced by the host innate immune response, are crucial in limiting PEDV replication by eliciting an innate antiviral response (Zhang et al., 2016; Jegaskanda et al., 2018). IFN-Is also promote adaptive immunity during influenza virus infections by enhancing natural killer cell function (Hoffmann et al., 2015).

Type-III interferons (IFN-IIIs) are believed to employ the same antiviral mechanism as IFN-Is and induce IFN-stimulated gene expression, with IFN-III receptors being distributed primarily in gastrointestinal and respiratory epithelial cells (Li et al., 2016). Studies on PEDV-infected IECs (IPEC-J2), as well as several other reports, have shown that IFN-IIIs play an important role in inhibiting PEDV infection in IECs (Li et al., 2016; Lui et al., 2016). IFN-IIIs also exhibit strong antiviral activity in Vero cells (Ma et al., 2018; Xue et al., 2018). Therefore, IFN-IIIs may be key factors regulating PEDV infection.

Viruses generally develop diverse mechanisms to evade the host innate immune response, such as by antagonizing IFN production (Li et al., 2017a; Zhang et al., 2018b). IFN antagonism and production have also been implicated in PEDV mechanisms for evading innate immunity (Annamalai et al., 2015; Li et al., 2017b). Therefore, identification of the antiviral factors of the innate immune system is crucial for the control of PEDV infection. IRF3, nuclear factor kappa B (NF-κB), and IRF7 activation are crucial for the release of IFN-IIIs. IFN-λ1, −λ4, and -λ3 have been identified in IPEC-J2 cells (Li et al., 2017b; Zhang et al., 2018b). In small intestinal epithelial cells (IPEC-J2), PEDV inhibited IFN-III secretion through interfering with IRF and NF-κB (Zhang et al., 2018b). However, PEDV regulates small intestinal epithelial cells of different origins in different ways. In IECs, PEDV could induce NF-κB activation through the Toll-like receptor (TLR)2, TLR3, and TLR9 pathways in porcine intestinal epithelial cells at 24 h.

The NF-κB pathway has been reported to affect the secretion of IFN-IIIs more potently than IFN-I pathways (Pu et al., 2017). Additionally, the majority of TLRs use myeloid differentiation primary response 88 (MyD88), which participates in the recruitment of interleukin-1 receptor-associated kinase (IRAK)1 and 4 (Fisher et al., 2021). Tumor necrosis factor (TNF) receptor-associated factor 6 (TRAF-6) is triggered by IRAK1 phosphorylation, which activates NF-κB and mitogen-activated protein kinase (MAPK; Akira et al., 2006). Furthermore, PEDV-infected cells were found to alter the activity of the NF-κB pathway (Wang et al., 2016).

MicroRNAs (miRNAs) are small RNAs that are 18–23-nucleotides in length and exhibit various effects on cell proliferation, differentiation, and apoptosis, and in viral infections (Huang et al., 2018). Viral infections result in the dysregulated expression of miRNAs, and these changes in miRNA abundance can in turn affect viral infection and cellular physiological processes by regulating innate immunity. Several reports have shown that miRNAs inhibit PEDV infection by downregulating different target genes that are required for innate immunity (Wu et al., 2013; Zheng et al., 2018; Qi et al., 2021). In particular, miR-221-5p was found to decrease the rate of PEDV replication in MARC-145 cells by boosting activation of the NF-κB pathway (Zheng et al., 2018). In addition, miR-129-3p, which was identified in the process of studying porcine circovirus 2-infected cells, inhibited PEDV replication by targeting the NF-κB pathway in IPEC-J2 cells (Annamalai et al., 2015). By suppressing the expression of the proteins acting downstream of the NF-κB pathway in porcine kidney (PK) cells, miR-30c-5p reduces the expression of IFN-IIIs (Zhao et al., 2012; Buggele and Horvath, 2013; Song et al., 2015). However, the role and underlying mechanism of the miRNA-mediated regulation of the NF-κB pathway in PEDV infection in IECs have not yet been elucidated.

In this study, to ascertain the function of miRNAs in the innate immune response to PEDV infection, we performed high-throughput sequencing on PEDV-infected IECs, revealing a change in miRNA expression and innate immunity pathways under infectious conditions. Among the screened miRNAs, miR-615 was predicted to function in the NF-κB pathway and facilitate PEDV replication. We further found that miR-615 inhibits IFN-III expression and NF-κB pathway activation by targeting IRAK1. Conversely, miR-615 induced PEDV replication and inhibited the NF-κB pathway in two different types of cells (IECs and MARC-145). These data imply that miR-615 is a crucial PEDV target, and thus may be a potential target for PEDV treatment and prevention strategies.

Materials and methods

Cells and viruses

MARC-145 cells, which are kidney cells from an African green monkey, were grown in Dulbecco's modified Eagle medium (DMEM; Hyclone, Logan, UT, USA) with 10% heat-inactivated fetal bovine serum (FBS; PAN-Biotech), and 100-times diluted penicillin and streptomycin (Hyclone). MARC-145 cells were used to validate the effect of miR-615 during PEDV infection. The IECs were cultivated in DMEM-F12 (Hyclone) supplemented with 10% FBS, penicillin, and streptomycin at the same concentrations as indicated above. All

cells were kept in an incubator with 5% CO_2 at 37°C as previously described (Wang et al., 2014). PEDV strains CV777 (GenBank accession number KT323979.1) and NW-17 (GenBank accession number MF782686.1) were provided by Nuoweilihua Biotechnology Co., which have an *S* gene from the epidemic strain group II. Strain NW-17 could infect IECs without trypsin and was therefore selected as an optimal strain for IEC infection. Vero cells were used to prepared the PEDV stock by three cycles of freezing and thawing, and were stored at −80°C.

Immunofluorescence assays (IFAs)

After 20 min of fixation at a 4:1 ratio of cold acetone and methanol, the cell samples were washed three times in phosphate-buffered saline (PBS). The cells were incubated with a monoclonal antibody (mAb) against the PEDV N or NF-κB p65 protein for 2 h. The cells were then rinsed three times with PBS and incubated for 1 h with a fluorescein isothiocyanate-conjugated AffiniPure Goat Anti-rabbit/Mouse secondary antibody (Sungene Biotech, Tianjin, China). Hoechst 33258 was utilized to stain the nucleus, and the cell samples were analyzed with a laser-scanning confocal microscope after three PBS rinses (Olympus). The experiment was performed at room temperature.

Mirna microarray and predicting the mRNA targets of differentially expressed miRNAs (DEMiRs)

Deep sequencing was carried out at Novogene (Beijing, China). IECs were infected in triplicates for 24 h with CV777, NW-17, or a mock infection at a multiplicity of infection (MOI) of 1. The mock group was treated with PBS. Total RNA was isolated using Trizol reagent (Invitrogen). Nine small RNA libraries (triplicate samples of the control mock-, CV777-, and NW-17-infected groups) were generated for Illumina sequencing. The microarray assay was conducted as previously described (Hallman et al., 2013). The prediction of target genes of DEMiRs was performed using miRanda (John et al., 2004; version 3.3a), PITA[1], and RNAhybrid.[2] Gene Ontology enrichment analysis was performed to screen the potential functions of the significantly enriched target genes. Kyoto Encyclopedia of Genes and Genomes (KEGG) pathway analysis was applied to identify the potential pathways associated with the target genes of the DEMiRs (Kanehisa et al., 2008). *p*-values were corrected using the Benjamini–Hochberg strategy (Benjamini and Hochberg, 1995). Statistical significance was defined as a corrected *p*-value <0.05.

1 http://www.pita.org.fj/

2 https://bibiserv.cebitec.unibielefeld.de/rnahybrid/

Validation of DEMiRs using reverse transcriptase-quantitative polymerase chain reaction (RT-qPCR)

Total RNA was extracted from IECs 24 h after infection at an MOI of 1. The Real-time Quantitative PCR Detection System and SYBR PrimeScript™ miRNA RT-PCR Kit were used to perform RT-qPCR. One microliter of each primer, 2.0 μl of diluted cDNA, and 12.5 μl of SYBR Green Premix Ex Taq II were included in each 25 μl reaction mixture. The thermocycling conditions comprised 95°C for 30 s, followed by 40 cycles of 95°C for 5 s and 60°C for 20 s. Each sample was processed in triplicates. Fifteen miRNAs were selected for testing. The expression of the U6 small RNA was used as the reference for data normalization. Table 1 contains the primer sequences for each miRNA and gene.

Transfection of miRNA mimics, miRNA inhibitors, and siRNAs

A miRNA mimics is a chemically synthesized double-stranded RNA identical to a mature miRNA sequence. A miRNA inhibitor is a chemically modified single-stranded RNA that is complementary to the mature miRNA sequenc. After 12 h of culture, MARC-145 cells and IECs were transfected for 24 h using Lipofectamine 3000 (Invitrogen) with mimic control (MC), miR-615 mimics, miR-615 inhibitor (miR-615 inhi; 100 nM), inhibitor control (IC; 100 nM), small interfering RNA (siRNAs; si-IRAK1), or siRNA control (SC; 50 nM), which were synthesized at RiboBio (Guangzhou, China). Subsequently, the cells were infected with PEDV at an MOI of 1.0. After 24 h of infection, the cells were examined for indirect immunofluorescent labeling, or collected for RNA quantification or western blotting.

Plasmids

pCDNA3.1+ plasmid was used to clone the Flag-IRAK1 plasmid at Genecreate using the BamHI and EcoRI restriction sites (Wuhan, China). The miRNA reporter plasmids, WT-pmirGLO-IRAK1 (wild-type, WT), and MuTpmirGLO-IRAK1 (mutant type; MuT) were subcloned into pmirGLO using the Nhel and SalI sites at Genecreate. pNiFty-luc plasmids is composed of a minimal Promoter, five NF-κB repeated transcription factor binding sites and a Luc (Luciferase) reporter gene of mammal.

Dual-luciferase reporter assays

The potential miR-615 target genes in the 3′-untranslated region (3′-UTR) of IRAK1 were identified using the luciferase vector pmirGLO (Promega, Madison, WI, USA). The wild-type (WT-pmirGLO-IRAK1) or mutant (MuTpmirGLO-IRAK1)

TABLE 1 Sequences of the miRNA mimic and inhibitor primers used in this study.

Genes	Forward primer (5′–3′)	Reverse primer (5′–3′)	Use
susIFN-β	AGTGCATCCTCCAAATCGCT	GCTCATGGAAAGAGCTGTGGT	RT-qPCR
g*PEDV*	AGTACGGGGCTCTAGTGCFigAG	GCTTATCCAAATTCTTCAGGCG	RT-qPCR
m*β-actin*	ATCGTGCGTGACATTAAG	ATTGCCAATGGTGATGAC	RT-qPCR
miR-615 mimics	UCCGAGCCUGGGUCUCCCUCU	AGAGGGAGACCCAGGCTCGGA	Overexpression of miR-615
miR-615 inhibitors	AGAGGGAGACCCAGGCTCGGA		Silencing of miR-615
U6	CTCGCTTCGGCAGCACA	AACGCTTCACGAATTTGCGT	RT-qPCR
IFN-λ1	GGTGCTGGCGACTGTGATG	GATTGGAACTGGCCCATGTG	RT-qPCR
IFN-λ3	ACTTGGCCCAGTTCAAGTCT	CATCCTTGGCCCTCTTGA	RT-qPCR
susβ-actin	AGGGTGTAATGGTGGGAATG	GCCGTGTTCAATGGGGTAT	RT-qPCR
miR-615	AGCCTGGGTCTCCCTCTAAA		RT-qPCR
miR-708-5p	AAGGAGCTTACAATCTAGCTGGG		RT-qPCR
miR-30e-5p	GGTGTAAACATCCTTGACTGGAAGCT		RT-qPCR
miR-148a-3p	TCAGTGCACTACAGAACTTTGT		RT-qPCR
miR-129a-5p	CTTTTTGCGGTCTGGGCTTG		RT-qPCR
miR-486	TTCCTGTACTGAGCTGCCC		RT-qPCR
miR-532-5p	CATGCCTTGAGTGTAGGACC		RT-qPCR
miR-542-3p	GGTGTGACAGATTGATAACTGAAA		RT-qPCR
miR-133a-5p	GAGCTGGTAAAATGGAACCAAAT		RT-qPCR
miR-206	TGGAATGTAAG GAAGTGTGTGA		RT-qPCR
miR-20a	ACTGCATTATGAGCACTTAAAG		RT-qPCR
miR-671-5p	AGGAAGCCCTGGAGGGGCTG		RT-qPCR

3′-UTR sections of IRAK1 were subcloned into the pmirGLO vector and co-transfected into 293 T cells with miR-615. NF-κB activity was detected using pNiFty-luc and pRL-TK plasmids with the Dual-Luciferase Reporter Assay System (Promega, Madison, WI, USA) according to the manufacturer instructions.

Western blotting

The cells were lysed using radioimmunoprecipitation assay buffer (Beyotime, Shanghai, China) and centrifuged at 4°C for 12,000 rpm. The concentration of the lysate was evaluated using a bicinchoninic acid (Thermo Scientific) protein assay kit. Each sample was diluted with 5Xloading buffer, boiled for 10 min, resolved on a sodium dodecyl sulfate-polyacrylamide gel electrophoresis gel, and then deposited onto polyvinylidene fluoride membranes at equal amounts. The membranes were blocked with 5% skim milk for 1 h and incubated overnight at 4°C with the primary antibodies against β-actin (1:1,000; 5,057; Cell Signaling Technology, Danvers, MA, USA), phospho-NF-κB p65 antibody (1:1,000; 3,033; Cell Signaling Technology), NF-κB p65 (1:1,000; 6,956; Cell Signaling Technology), and MyD88 (1:1,000; NB100-5698SS; RDSC). Proteins were detected using enhanced chemiluminescence detection reagents after being treated with secondary antibodies, HRP-conjugated goat anti-mouse IgG or goat anti-rabbit IgG (Beyotime). All samples were incubated along with β-actin as an internal standard. PEDV anti-nucleocapsid (N) protein antibody (1:1,000) was gifted by Prof. Tong Guangzhi, Shanghai Veterinary Research Institute.

Statistical analyses

All data were statistically analyzed using Student's t-test in Graphpad Prism 9.3.1 for analysis of variance (ANOVA).

Results

Dysregulated expression of miRNAs in circulating and vaccine strain-infected IECs

Villous epithelial cells are the primary target cells of PEDV infection; therefore, IECs are a suitable model for studying virus–cell interactions in the intestinal epithelia (Wang et al., 2014). IECs have been found to be susceptible to certain PEDV strains such as CV777, independent of high concentrations of trypsin (Cao et al., 2015b).

The IFA results of the IECs at 24 h post-inoculation (hpi) with CV777 and NW-17 (MOI = 1) suggested significantly higher fluorescence in the CV777- and NW-17-infected groups than that in the mock-infected group (Figure 1A). This observation confirmed that CV777 and NW-17 could infect IECs effectively.

To identify whether miRNAs play a role in virus–cell interactions, we performed high-throughput sequencing to obtain

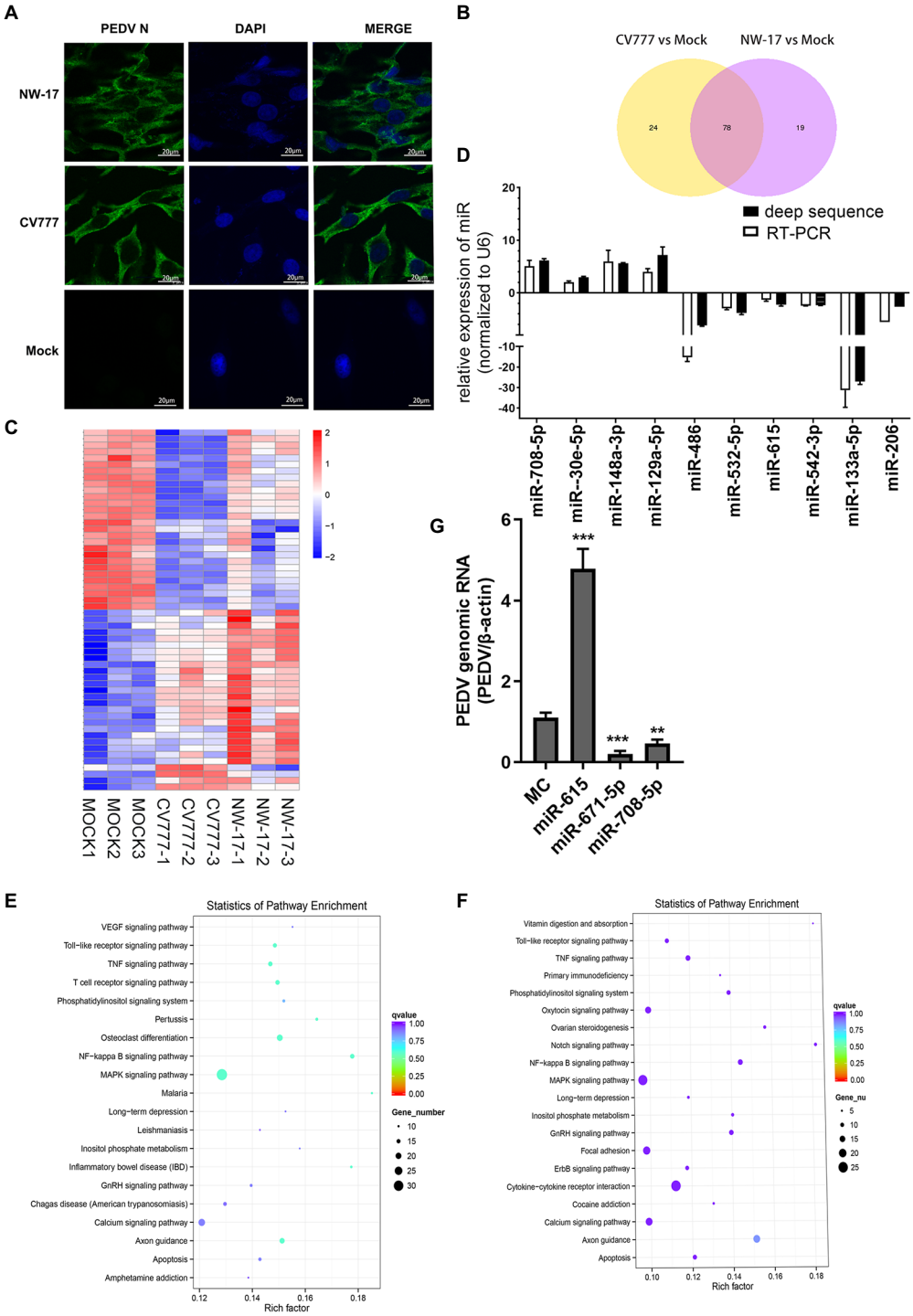

FIGURE 1
PEDV infection changes cellular microRNA profiles. **(A)** Immunofluorescence showing PEDV N protein expression in IECs (green). IECs were infected with the CV777 and NW-17 strains at a multiplicity of infection (MOI) of 1. Cells were fixed and stained with a mouse anti-N monoclonal antibody (mAb). Scale bar=20μm. **(B)** Venn diagrams showing the differentially expressed microRNAs (DEMiRs) among CV777-infected vs. mock-infected cells and NW-17-infected vs. mock-infected cells. **(C)** Heatmap showing the high abundance of DEMiRs. **(D)** Verification of the miRNA microarray assay using RT-qPCR. Data from RT-qPCR are shown as the mean±SD of three independent experiments. U6 mRNA was detected as a control. (E and F) KEGG pathway enrichment analysis of the main DEMiRs for the CV777- and NW-17-infected groups, respectively. (G) Transfection of miRNAs inhibited or enhanced viral replication. IECs were transfected with the miR-671-5p, miR-708-5p, miR-615, or MC mimics at 50nmol, followed by infection with PEDV (MOI=1). Cells were collected for RT-qPCR at 24h post-infection (hpi). PEDV genomic RNA was determined by RT-qPCR. Asterisks indicate statistical significance. *p<0.05; **p<0.01; ***p<0.001.

the miRNA profiles of mock-infected or PEDV (CV777 and NW-17)-infected IECs at an MOI of 1 at 24 hpi. In comparison to the mock-infected group, 102 known miRNAs were found to be differentially expressed in the CV777-infected group and 98 known miRNAs were differentially expressed in the NW-17-infected group. Among them, 78 miRNAs were commonly differentially expressed in both infection groups (Figure 1B).

A total of 55 high-abundance miRNAs were selected by setting the read count to >250 ($p < 0.05$; Figure 1C). Of these miRNAs, 28 were upregulated and 27 were downregulated. To validate the high-throughput results of the DEMiRs, RT-qPCR was used to analyze the expression of 13 DEMiRs that were common to both groups (Figure 1D).

Using the KEGG pathway database, the roles of the DEMiRs in response to the PEDV strains were predicted, showing enrichment in several pathways, including the NF-κB, apoptosis, MAPK, TNF, and TLR signaling pathways, which participate in antiviral activities (Figures 1E,F). The high enrichment scores for the NF-κB and TLR signaling pathways indicated that innate immunity plays an important role in PEDV infection.

The DEMiRs enriched in the NF-κB pathway, miR-615, miR-708, miR-221-5p, and miR-671-5p, were selected for further investigation. Three miRNAs (miR-708, miR-671-5p, and miR-221-5p) were found to exert inhibition on PEDV replication by RT-qPCR. In particular, miR-615 overexpression significantly boosted viral replication compared to that in the MC group ($p < 0.01$; Figure 1G).

Mir-615 promoted PEDV infection and replication in IECs and MARC-145 cells

To further evaluate the interaction between miR-615 and PEDV in IECs and MARC-145 cells during PEDV infection, PEDV genomic and miR-615 RNA were detected using RT-qPCR. In IECs, the expression of miR-615 showed a downward trend ($p < 0.01$; Figure 2A). In MARC-145 cells, miR-615 expression was up-regulated at 12 h and was down-regulated at 24 h ($p < 0.001$; Figure 2B). The overexpression of miR-615 promoted viral replication in IECs ($p < 0.01$; Figure 2C) and MARC-145 cells ($p < 0.001$; Figure 2E). Conversely, the downregulation of miR-615 expression inhibited viral replication compared to that in the IC group in the IECs ($p < 0.001$; Figure 2D) and MARC-145 cells ($p < 0.001$; Figure 2F).

Western blotting showed that the level of PEDV N protein expression increased in IECs (Figure 2G) and MARC-145 cells (Figure 2H) after transfection with the miR-615 mimic for 6 and 12 h.

Mir-615 inhibited the expression of IFN-IIIs in IECs and IFN-Is in MARC-145 cells

Recent studies suggested that IFN-III has an important effect on the antiviral activity of small IECs (Zhang et al., 2018b). Consistently, we found that PEDV replication could be inhibited by IFN-λ3 (Figure 3A). Therefore, we hypothesized that miR-615 affects the expression of IFN-IIIs or IFN-Is, which in turn enhances viral replication. To test this hypothesis, we assessed the expression of IFN-IIIs in PEDV-infected IECs and of IFN-I in MARC-145 cells.

miR-615 mimics were transfected into the cells and/or poly (I:C) was used to stimulate the cells for 24 h. RT-qPCR was used to examine the expression of the two IFN-III subtypes, IFN-λ1 and-λ3. IFN-λ1 and λ3 expression was upregulated after stimulation with poly (I:C), which served as a positive control; however, the expression levels of IFN-λ1 and -λ3 significantly decreased following miR-615 transfection in IECs ($p < 0.01$; Figures 3B,C).

We also evaluated IFN-β and -α levels in miR-615-transfected MARC-145 cells. Poly (I:C) stimulation upregulated IFN-β and -α expression, whereas miR-615 transfection significantly downregulated their expression ($p < 0.01$; Figures 3D,E). The downregulation of IFN-Is and -III expression suggests that miR-615 may affect the IFN pathway in these two types of cells when infected with PEDV.

Mir-615 inhibits NF-κB pathway activation in IECs and MARC-145 cells

Based on our preliminary findings, we hypothesized that miR-615 restricts the NF-κB pathway from being activated. The expression of IFNs is induced when NF-κB binds to the positive regulatory domain (PRD) II in the nucleus after translocation. Thus, we further examined NF-κB activity to explore whether the pathway was inhibited by miR-615 or miR-615 inhibitors. The NF-κB reporter luciferase plasmid (pNiFty-luc; containing five PRDII sites), thymidine kinase promoter-*Renilla* luciferase reporter plasmid (pRL-TK; an internal control plasmid), and miR-615 mimics or inhibitors were co-transfected into IECs, followed by poly (I:C) stimulation; thereafter, cell lysates were collected to detect luciferase activity at 24 hpi. The luciferase reporter assays showed that miR-615 markedly inhibited poly (I:C)-induced PRDII activity in IECs ($p < 0.01$; Figure 4A). Conversely, miR-615 inhibitors increased PRDII activity ($p < 0.01$; Figure 4B). Comparable results were observed in MARC-145 cells (Figures 4C,D). These results verified our hypothesis that miR-615 inhibits NF-κB pathway activity in both IECs and MARC-145 cells.

Mir-615 inhibits NF-κB activation by suppressing p65 nuclear translocation

Next, we explored the mechanism of NF-κB inhibition. The IFA results revealed a significant reduction in the nuclear abundance of p65 protein in the miR-615 transfection group as compared to that in the MC-transfected group in both IECs (Figure 5A) and MARC-145 cells (Figure 5C). The abundance of

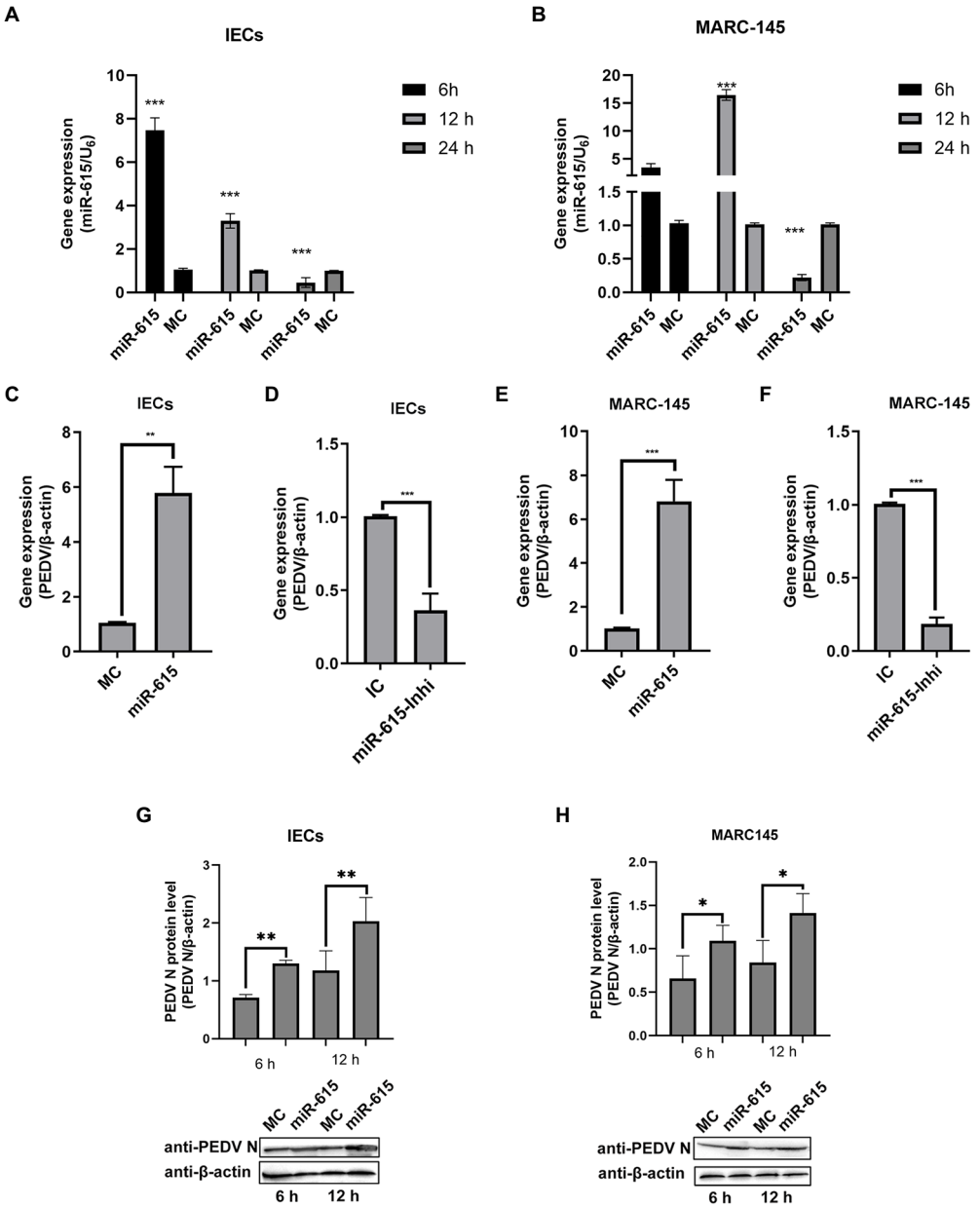

FIGURE 2
miR-615 facilitates PEDV infection in MARC-145 cells and IECs. (A and B) PEDV regulated miR-615 expression in IECs and MARC-145 cells. IECs **(A)** and MARC-145 cells **(B)** were infected with PEDV at a multiplicity of infection (MOI) of 1 and samples were collected at 6, 12, and 24h post-infection. RT-qPCR was used to assess miR-615 expression. **(C–F)** IECs and MARC-145 cells were transfected with the MC, miR-615 mimic, IC, or miR-615 inhibitor (100nmol). After 24h, the cells were infected with PEDV at an MOI of 1. After 18h, the PEDV genomic RNA of the MC, miR-615 mimic, IC, and miR-615 inhibitor in the IECs **(A,B)** and transfected MARC-145 cells **(C,D)** were assessed using RT-qPCR. PEDV N protein level was measured using western blotting following transfection with the MC or miR-615 mimic for 6 and 12h in the IECs **(G)** and MARC-145 cells **(H)**. The intensity represents PEDV N protein levels normalized against that of β-actin across three independent experiments in IECs and MARC-145 cells, respectively. The data are presented as the mean±SD of three independent experiments, performed with technical duplicates. *p<0.05, **p<0.01, ***p<0.001.

p-p65 was found to decrease following transfection with miR-615 mimics in both the poly (I:C)-induced and non-poly (I:C)-induced groups (Figure 5B). We further examined p-p65 proteins upstream of MyD88 to investigate the mechanism underlying NF-κB downregulation. The results showed that p-p65 expression was downregulated, whereas MyD88 expression was not changed with the transfection of miR-615 in IECs (Figure 5B) and MARC-145 cells (Figure 5D). These results suggested that miR-615 inhibits the NF-κB pathway by repressing p65 nuclear translocation.

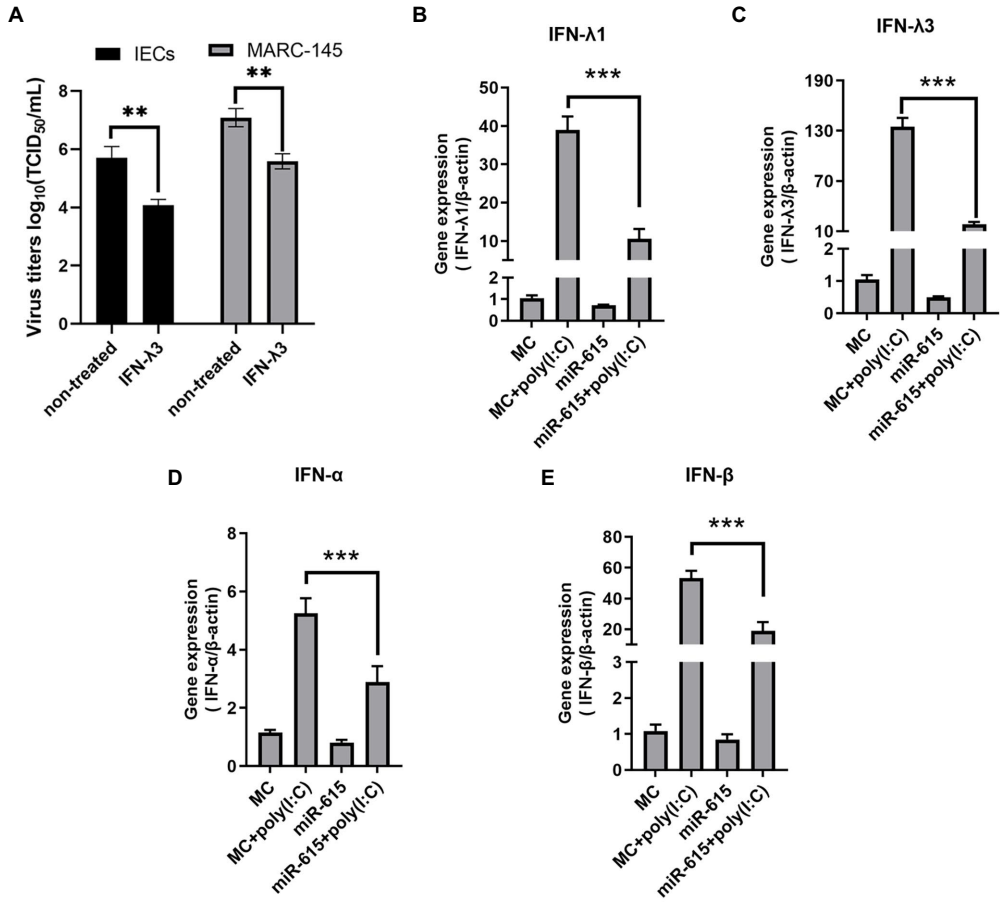

FIGURE 3
miR-615 downregulated the levels of IFN-Is in MARC-145 cells and of IFN-IIIs in IECs. **(A)** IFN-λ3 inhibited PEDV replication in IECs and MARC-145 cells. IECs and MARC-145 cells were seeded and treated with 100ng/ml IFN-λ3 for 12h, followed by infection with PEDV at a multiplicity of infection (MOI) of 1 with incubation for 2h and replenished with fresh infection medium containing the IFN-λ3. Cell culture supernatants were collected at 12 and 24h post-infection and titrated to determine the $TCID_{50}$. MARC-145 and IECs were transfected with miR-615 for 24h and then stimulated with poly (I:C; 10μg/ml) for 24h during PEDV infection. The cells were then harvested for RT-qPCR to determine the levels of **(B)** IFN-λ1 and **(C)** IFN-λ3 in the IECs, and of **(D)** IFN-α and **(E)** IFN-β in MARC-145 cells. The data are representative of three independent experiments (mean±SD). ***$p<0.001$, **$p<0.01$.

Identification of *IRAK1* As a target gene of miR-615 in IECs

To explore the mechanism whereby miR-615 inhibits NF-κB activation, target gene prediction was conducted using miRanda[3], PITA[4], and RNAhybrid[5], which identified 167 target genes (Supplementary Table S1). The most interesting candidate target gene was *IRAK1* as it had the highest prediction score (174) and was enriched in the NF-κB pathway. Therefore, we hypothesized that *IRAK1* is a target gene of miR-615.

Two reporter gene plasmids were constructed containing WT and seed region-Mut target sites (MuT) with matching or mutated target gene seed sites of miR-615 in the 3′-UTR of *IRAK1* (Figure 6A). miR-615 inhibited the luciferase activity of the WT reporter plasmid when compared with that in the MC-transfected group; however, miR-615 did not repress the activity of the mutated dual-luciferase reporter gene plasmid (Figure 6B). Moreover, transfection with miR-615 mimics downregulated IRAK1 protein expression, whereas transfection with miR-615 inhibitors upregulated its expression (Figure 6C).

Mir-615 inhibits activation of the NF-κB pathway and promotes viral replication by targeting *IRAK1*

To determine whether repression of the NF-κB pathway by miR-615 is dependent on the regulation of *IRAK1* expression, we first examined the effect of IRAK1 on the NF-κB pathway

3 http://www.microrna.org/microrna/hom.do
4 http://genie.weizmann.ac.il/pubs/mir07/mir07_dyn_data.html
5 https://bibiserv.cebitec.unibielefeld.de/rnahybrid/

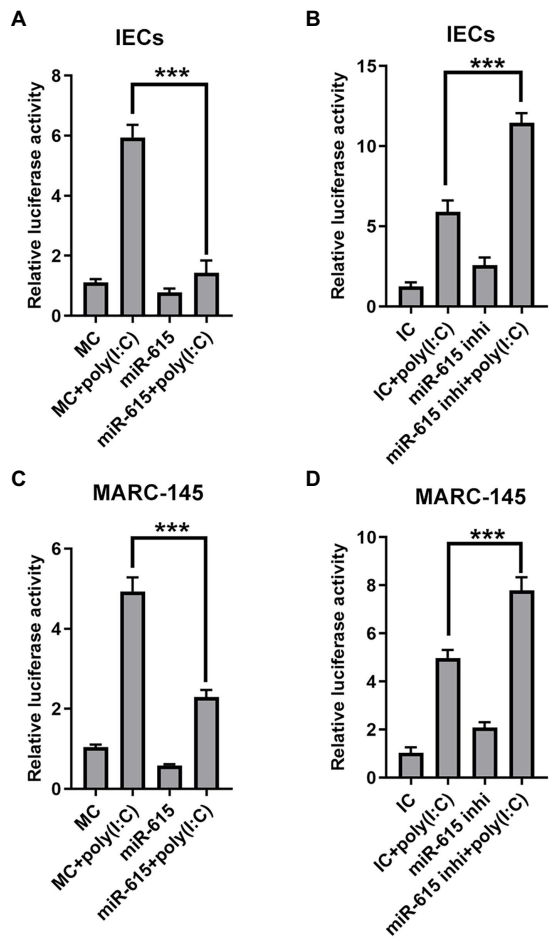

FIGURE 4
miR-615 inhibits NF-κB activation. Luciferase activity in IECs and MARC-145 cells. Cells were co-transfected using a dual-luciferase reporter system (pNiFty-luc and pRL-TK vectors, the activities of which indicate NF-κB-promoter activation) and miR-615 mimics or inhibitors for 24h, and stimulated with poly (I:C) for 24h during PEDV infection at a multiplicity of infection (MOI) of 1. Luciferase reporter activity of the miR-615 mimics in IECs **(A)** and MARC-145 cells **(C)**. Luciferase reporter activity of the miR-615 inhibitors in IECs **(B)** and MARC-145 cells **(D)**. The data are representative of three independent experiments (mean±SD). ***$p<0.001$.

using a dual-luciferase reporter assay with overexpression and knockdown of *IRAK1* in PEDV-infected IECs stimulated with poly (I:C). The NF-κB pathway was activated by *IRAK1* overexpression (Figure 7A) and was downregulated by knockdown of *IRAK1* (Figure 7B). In addition, *IRAK1* overexpression upregulated IFN-λ1 and -λ3 expression during viral infection (Figures 7C,D).

To further examine whether the effect of miR-615 on the NF-κB pathway was dependent on its regulation of *IRAK1* expression, miR-615 and *IRAK1* were overexpressed and the effects on the NF-κB pathway activity were examined. Porcine IECs were co-transfected with pNif-TK, pRL-TK, miR-615 mimics, or Flag-IRAK1, and poly (I:C) was used to induce NF-κB pathway activation. The rescue experiment showed that IRAK1 overexpression promoted NF-κB pathway activation and reversed the miR-615-dependent repression of the NF-κB pathway (Figure 7E). Collectively, these data indicate that miR-615 inhibits the NF-κB pathway by targeting *IRAK1*. The knockdown and overexpression of IRAK1 protein were further confirmed using western blotting (Figure 7F).

Discussion

PEDV infection has been reported to antagonize innate immunity (Annamalai et al., 2015; Cao et al., 2015a). The main factors involved in antiviral innate immunity are IFN-Is and -IIIs. Notably, IFN-IIIs are involved in innate immunity in IECs. Multiple PEDV-encoded proteins inhibit the production of IFNs (Ding et al., 2014; Zhang et al., 2017). miRNAs have been reported to play a pivotal role in the regulation of viral infections by targeting the viral genome or regulating host cytokines to modulate the cellular environment (Bartel, 2009). To further examine the mechanisms and interactions between miRNAs and PEDV in porcine IECs, deep-sequencing techniques were used to analyze miRNA expression profiles. We found that PEDV infection altered cellular miRNA expression profiles in IECs. Furthermore, the innate immunity pathway was confirmed to be involved in PEDV infection. miR-615 was enriched in this pathway, and its overexpression promoted viral replication by inhibiting IFN-III expression and targeting IRAK1 in the NF-κB pathway. To the best of our knowledge, this is the first report of an miRNA targeting *IRAK1* during PEDV infection in IECs to function as a negative regulator of IFN-IIIs production.

PEDV infection has previously been shown to affect miRNA profiles and innate immunity (Huang et al., 2016; Zhang et al., 2018a; Qi et al., 2021). High-throughput sequencing of miRNAs in PEDV-infected IPEC-J2 cells revealed few identical differential miRNAs were expressed compared to our study. However, the KEGG pathway analysis showed that TLRs, Janus kinase-signal transducer and activator of transcription (JAK–STAT), retinoic acid-inducible gene I (RIG-I), and autophagy were involved in the response to PEDV infection. Our deep-sequencing KEGG analysis showed enrichment in the primary pathways involved in innate immunity (NF-κB and TLR signaling pathways; Zhang et al., 2018a). Another study using miRNA-mRNA high-throughput sequencing in PEDV-infected ST cells showed that innate immunity pathways were enriched following PEDV infection. Moreover, infection with different strains can induce the activation of different signaling pathways (Zhang et al., 2021). In PEDV-infected PK cells, high-throughput sequencing revealed few similar DEmiRNAs compared to those identified in other studies (Huang et al., 2016). However, PEDV-infected IECs (Cao et al., 2015b) showed activation of the NF-κB pathway. This may suggest that cells from the same source will have similar immune regulatory mechanisms after being infected by different PEDV

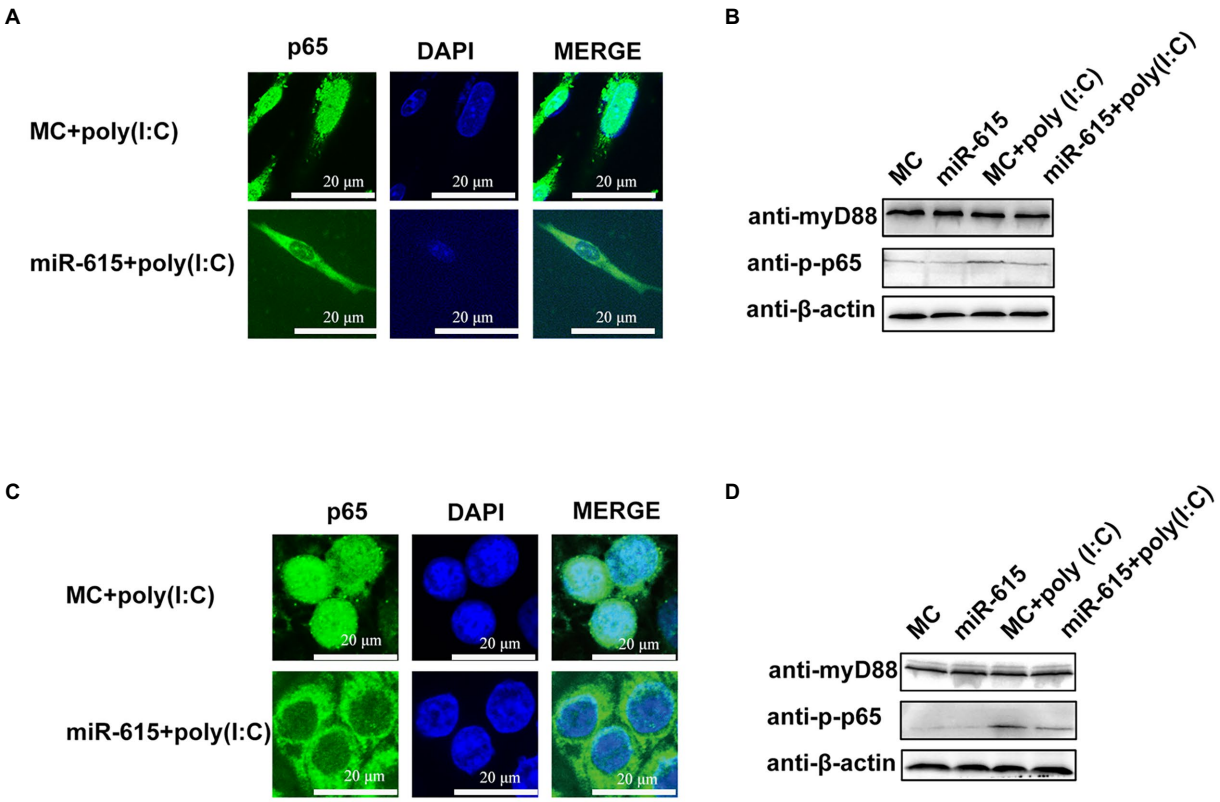

FIGURE 5
miR-615 inhibits the nuclear translocation and downregulates the phosphorylation of p65. **(A,C)** Immunofluorescence analysis of the nuclear translocation of p65 protein after transfection of miR-615 mimics during PEDV infection in IECs and MARC-145 cells. IECs and MARC-145 cells were transfected with miR-615. Poly (I:C) stimulation was added for 24h during PEDV infection. Cells were fixed and stained with a rabbit anti-phosphorylated (p)-p65 and MyD88 monoclonal antibodies. Scale bar=15μm. **(B,D)** Western blot analysis for detection of the (p)-p65 and MyD88 proteins.

strains. Our results thus provide insight into the mechanism of NF-κB pathway activation after PEDV infection of IECs. The inconsistency between our results and those of other studies may be attributed to different mechanisms of PEDV infection regulation in cells of different origins and the effects of different PEDV strains. Thus, our sequencing results provide insight on PEDV infection at the RNA level.

IFN-IIIs play a key role in antiviral innate immunity in the gut and at the mucosal surface. Compared with IFN-Is, IFN-IIIs preferentially inhibit PEDV infection in IECs (Li et al., 2017b). The robust activation of JAK–STAT signaling is induced to a greater degree by IFN-λ3 than by IFN-α. IFN-λ3 further plays a critical role in PEDV infection (Li et al., 2019). Similarly, IFN-λ1 exhibited strong anti-PEDV effects on IECs by activating the JAK–STAT signaling pathway. Furthermore, both IRF1 and NF-κB are related to PEDV-mediated IFN-IIIs suppression (Xue et al., 2018). In this study, we found that miR-615 downregulated IFN-λ1 and -λ3 expression by repressing the NF-κB pathway to facilitate PEDV replication. These results provide new insight into the mechanism by which IECs and PEDV interact through the NF-κB pathway. In addition, the transcription of IFN-III genes is more dependent on the NF-κB pathway than on the IRF system (Zhang et al., 2018b). This suggests that miR-615 is an important factor in cellular antiviral responses and an important anti-PEDV target. Notably, we did not identify changes in IFN-λ4 in IECs, which may be attributable to the low expression of IFN-λ4.

The inhibitory effect of miR-615 on the NF-κB pathway has been suggested in many other studies. In non-small cell lung cancer cells, miR-615-3p has been shown to be crucial in preventing cancer cell proliferation and metastasis by targeting insulin-like growth factor 2 (Liu et al., 2018). In breast cancer research, miR-615 was reported as a potential anti-onco-miR by targeting AKT serine/threonine kinase 2 expression (Bai et al., 2015). However, both the insulin-like growth factor 2 and AKT serine pathways could have an effect on the activity of the NF-κB pathway. In our study, miR-615 inhibited activation of the NF-κB pathway. This further suggests that miR-615 could exert its biological function by affecting the NF-κB pathway. It is worth noting that the NF-κB pathway is often activated in certain tumor cells, which further supports the role of miR-615 in affecting the NF-κB pathway. Finally, miR-615 promoted viral replication and

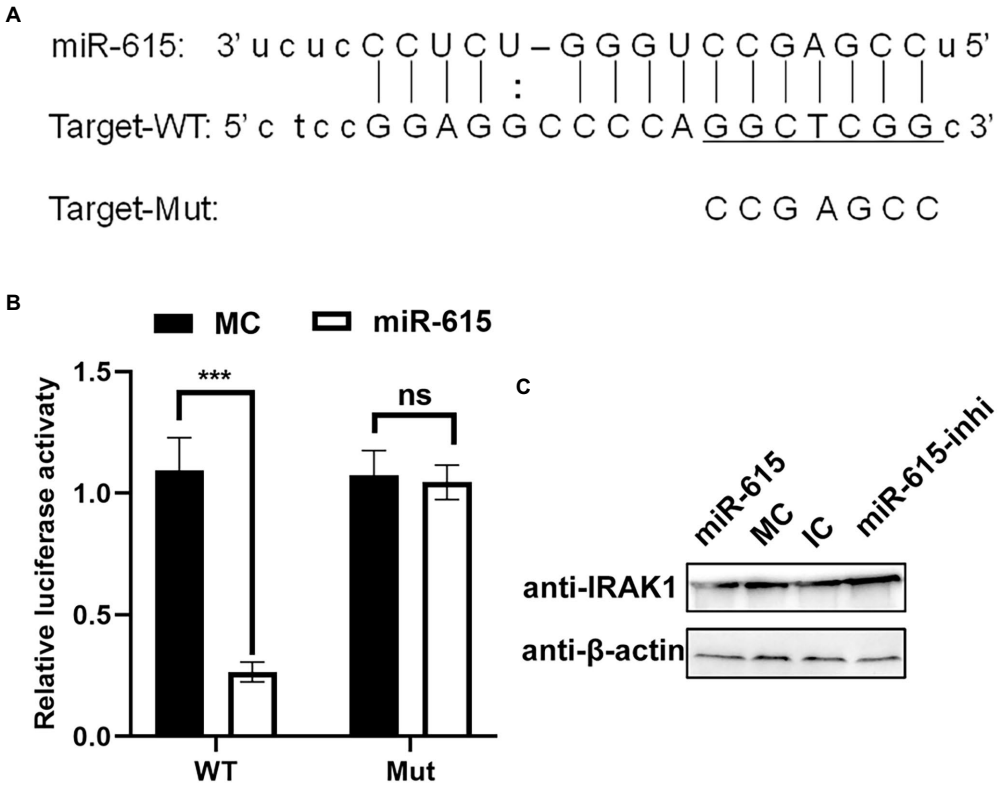

FIGURE 6
miR-615 targets *IRAK1*. **(A)** Bioinformatic prediction of the interactions between miR-615 and the 3′-UTR of swine *IRAK1*. For each schematic, the upper sequence is the sequence of mature miR-615, the middle sequence is the sequence in the binding site of miR-615 in the 3′-UTR of swine *IRAK1*, and the lower sequence is the mutated sequence of the *IRAK1* 3′-UTR. The seed sequence is underlined. **(B)** Luciferase activity in 293T cells co-transfected with miR-615 mimics (or MC) and luciferase reporter gene plasmids containing the WT and Mut 3′-UTRs of *IRAK1* for 48h. Data are normalized against firefly luciferase activity. Comparisons between groups were determined using Student's t-tests. ***$p<0.001$, **$p<0.01$. **(C)** The level of the IRAK1 protein during transfection with miR-615 mimics or inhibitors in IECs detected using western blotting during PEDV infection. Western blotting was conducted using anti-IRAK1 antibody at 24h post-infection (hpi).

inhibited the activation of the NF-κB pathway in both IECs and MARC-145 cells, suggesting the conserved role of miRNAs in different cells.

IRAK1 plays a critical role in TNF-α-induced NF-κB activation (Kim et al., 2012). The miRNAs miR-21, miR-146, miR-223, and miR-142a-3p have been reported to repress the NF-κB pathway by targeting *IRAK1* (Chen et al., 2013; Hung et al., 2013; Xu et al., 2013). In this study, we strongly suggest that miR-615 inhibited activation of the NF-κB pathway by targeting *IRAK1*. This further demonstrated the key role of IRAK1 in NF-κB pathway activation and also supports that the same target gene can be regulated by multiple miRNAs.

Collectively, our study showed that PEDV infection affects the NF-κB pathway and other innate immune-related pathways by changing the miRNA profiles. Our data further revealed the mechanism by which PEDV infection inhibits the secretion of IFN-IIIs in IECs and provides a new perspective for understanding the function of miR-615. Furthermore, we provide novel information regarding the intricate interplay between PEDV and cellular innate immunity in IECs during PEDV infection, which may offer new targets for the development of effective therapies to control PEDV and other coronaviruses.

Data availability statement

The datasets presented in this study can be found in online repositories. The names of the repository/repositories and accession number(s) can be found in the article/Supplementary material.

Author contributions

Y-MZ and HH designed the study. H-QZ, X-FZ, W-XW, and CL performed the experiments and collected the data. B-YY, W-JZ, S-LF, and X-HY analyzed and interpreted the data. H-QZ and X-FZ wrote the draft of the manuscript. W-XW, S-LF, B-YY, and CL edited and revised the manuscript. Y-MZ and HH coordinated the whole project. All authors contributed to the article and approved the submitted version.

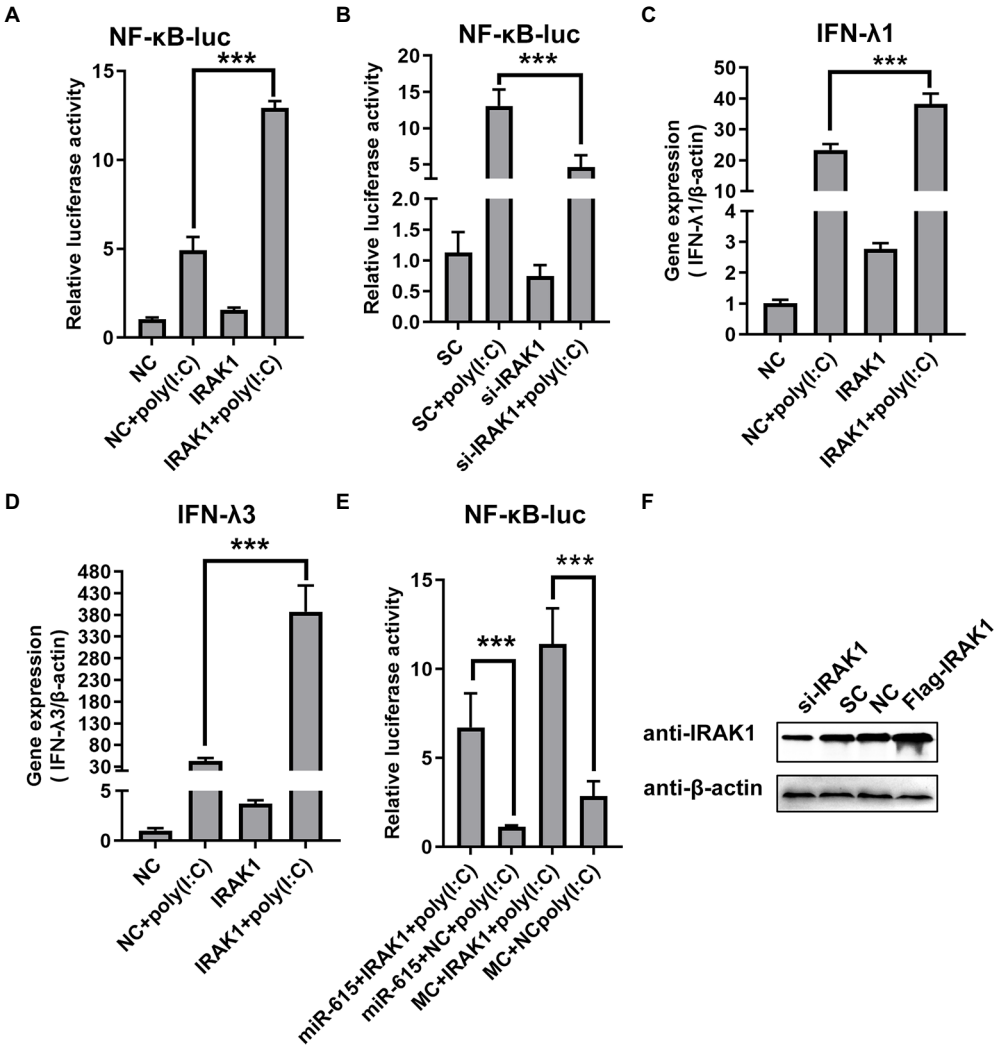

FIGURE 7
miR-615 inhibits NF-κB pathway activation by regulating *IRAK1*. **(A)** IRAK1-flag or negative control (NC) and **(B)** si-*IRAK1* or siRNA control (SC) were co-transfected with pNiFty-luc and pRL-TK into IECs. Cells were then stimulated with poly (I:C) and infected with PEDV (MOI=1) at 24h post-infection (hpi) or left untreated (unstimulated). Cells were then collected for the dual-luciferase reporter assay. **(C,D)** IECs were transfected with *IRAK1*-flag (or NC) or si-IRAK1 (or SC) for 24h. Poly (I:C) stimulation and viral infection were then induced. After 24h, IECs were collected for RT-qPCR to determine **(C)** IFN-λ1 and **(D)** IFN-λ3 expression. **(E)** Rescue experiment. Luciferase activity was rescued by *IRAK1* overexpression. IECs were co-transfected with miR-615 (or MC) and *IRAK1*-flag (or NC). At 24hpi, poly (I:C) stimulation and viral infection were induced. After 24h of stimulation, cells were collected and the luminescence activity was determined. **(F)** IRAK1 knockdown and overexpression were confirmed using western blotting. The data are representative of three independent experiments (mean±SD). ***$p<0.001$.

Funding

This research was funded in part by the Natural Science Basic Research Program of Shaanxi Province (grant number 2021JQ-900), Shaanxi Province Key Research and Development Project (grant number 2021NY-037), Research Fund Project of Xianyang Vocational and Technical College (2020KJA01 and 2018KYB01), Doctoral Research Foundation Project of Xianyang Vocational and Technical College (2021BK04 and 2019BK03), Key Research Projects of Xianyang Science, Technology Research and Development Program (grant number 2020k02-63), and Innovative Research and Experimental Project of Young Scientific Researchers (grant number 2022012).

Acknowledgments

We would like to thank Editage (www.editage.cn) for English language editing.

Conflict of interest

Authors W-XW and HH were employed by Beijing Hemu Biotechnology Co., Ltd.

The remaining authors declare that the research was conducted in the absence of any commercial or financial

relationships that could be construed as a potential conflict of interest.

Publisher's note

All claims expressed in this article are solely those of the authors and do not necessarily represent those of their affiliated organizations, or those of the publisher, the editors and the reviewers. Any product that may be evaluated in this article, or claim that may be made by its manufacturer, is not guaranteed or endorsed by the publisher.

Supplementary material

The Supplementary material for this article can be found online at: https://www.frontiersin.org/articles/10.3389/fmicb.2022.1071394/full#supplementary-material

References

Akira, S., Uematsu, S., and Takeuchi, O. (2006). Pathogen recognition and innate immunity. *Cells* 124, 783–801. doi: 10.1016/j.cell.2006.02.015

Annamalai, T., Saif, L. J., Lu, Z., and Jung, K. (2015). Age-dependent variation in innate immune responses to porcine epidemic diarrhea virus infection in suckling versus weaned pigs. *Vet. Immunol. Immunopathol.* 168, 193–202. doi: 10.1016/j.vetimm.2015.09.006

Bai, Y., Li, J., Li, J., Liu, Y., and Zhang, B. (2015). MiR-615 inhibited cell proliferation and cell cycle of human breast cancer cells by suppressing of AKT2 expression. *Int. J. Clin. Exp. Med.* 8, 3801–3808.

Bartel, D. P. (2009). MicroRNAs: target recognition and regulatory functions. *Cells* 136, 215–233. doi: 10.1016/j.cell.2009.01.002

Benjamini, Y., and Hochberg, Y. (1995). Controlling the false discovery rate: a practical and powerful approach to multiple testing. *J. R. Stat. Soc.* 57, 289–300. doi: 10.1111/j.2517-6161.1995.tb02031.x

Buggele, W. A., and Horvath, C. M. (2013). MicroRNA profiling of Sendai virus-infected A549 cells identifies miR-203 as an interferon-inducible regulator of IFIT1/ISG56. *J. Virol.* 87, 9260–9270. doi: 10.1128/jvi.01064-13

Cao, L., Ge, X., Gao, Y., Herrler, G., Ren, Y., Ren, X., et al. (2015a). Porcine epidemic diarrhea virus inhibits dsRNA-induced interferon-beta production in porcine intestinal epithelial cells by blockade of the RIG-I-mediated pathway. *Virol. J.* 12:127. doi: 10.1186/s12985-015-0345-x

Cao, L., Ge, X., Gao, Y., Ren, Y., Ren, X., and Li, G. (2015b). Porcine epidemic diarrhea virus infection induces NF-kappaB activation through the TLR2, TLR3 and TLR9 pathways in porcine intestinal epithelial cells. *J. Gen. Virol.* 96, 1757–1767. doi: 10.1099/vir.0.000133

Chen, Y., Chen, J., Wang, H., Shi, J., Wu, K., Liu, S., et al. (2013). HCV-induced miR-21 contributes to evasion of host immune system by targeting MyD88 and IRAK1. *PLoS Pathog.* 9:e1003248. doi: 10.1371/journal.ppat.1003248

Ding, Z., Fang, L., Jing, H., Zeng, S., Wang, D., Liu, L., et al. (2014). Porcine epidemic diarrhea virus nucleocapsid protein antagonizes beta interferon production by sequestering the interaction between IRF3 and TBK1. *J. Virol.* 88, 8936–8945. doi: 10.1128/jvi.00700-14

Dong, X., and Soong, L. (2021). Emerging and re-emerging zoonoses are major and global challenges for public health. *Zoonoses* 1:1. doi: 10.15212/ZOONOSES-2021-0001

Fisher, J. R., Chroust, Z. D., Onyoni, F., and Soong, L. (2021). Pattern recognition receptors in innate immunity to obligate intracellular bacteria. *Zoonoses* 1:10. doi: 10.15212/zoonoses-2021-0011

Hallman, J., Avesson, L., Reimegard, J., Kaller, M., and Soderbom, F. (2013). Identification and verification of microRNAs by high-throughput sequencing. *Methods Mol. Biol.* 983, 125–138. doi: 10.1007/978-1-62703-302-2_7

Hoffmann, H. H., Schneider, W. M., and Rice, C. M. (2015). Interferons and viruses: an evolutionary arms race of molecular interactions. *Trends Immunol.* 36, 124–138. doi: 10.1016/j.it.2015.01.004

Huang, J., Lang, Q., Li, X., Xu, Z., Zhu, L., and Zhou, Y. (2016). MicroRNA expression profiles of porcine kidney 15 cell line infected with porcine epidemic diahorrea virus. *Bing Du Xue Bao* 32, 465–471.

Huang, Y., Wang, W., Xu, Z., Pan, J., Zhao, Z., and Ren, Q. (2018). Eriocheir sinensis microRNA-7 targets crab Myd88 to enhance white spot syndrome virus replication. *Fish Shellfish Immunol.* 79, 274–283. doi: 10.1016/j.fsi.2018.05.028

Hung, P. S., Liu, C. J., Chou, C. S., Kao, S. Y., Yang, C. C., Chang, K. W., et al. (2013). miR-146a enhances the oncogenicity of oral carcinoma by concomitant targeting of the IRAK1, TRAF6 and NUMB genes. *PLoS One* 8:e79926. doi: 10.1371/journal.pone.0079926

Jegaskanda, S., Vanderven, H. A., Tan, H. X., Alcantara, S., Wragg, K., Parsons, M. S., et al. (2018). Influenza infection enhances antibody-mediated NK cell functions via type I interferon dependent pathways. *J. Virol.* 93, e02090–e02018. doi: 10.1128/jvi.02090-18

John, B., Enright, A. J., Aravin, A., Tuschl, T., Sander, C., and Marks, D. S. (2004). Human MicroRNA targets. *PLoS Biol.* 2, e363–e1879. doi: 10.1371/journal.pbio.0020363

Kanehisa, M., Araki, M., Goto, S., Hattori, M., Hirakawa, M., Itoh, M., et al. (2008). KEGG for linking genomes to life and the environment. *Nucleic Acids Res.* 36, D480–D484. doi: 10.1093/nar/gkm882

Kim, J. M., Cho, H. H., Lee, S. Y., Hong, C. P., Yang, J., Kim, Y. S., et al. (2012). Role of IRAK1 on TNF-induced proliferation and NF-kB activation in human bone marrow mesenchymal stem cells. *Cell. Physiol. Biochem.* 30, 49–60. doi: 10.1159/000339045

Li, L., Fu, F., Xue, M., Chen, W., Liu, J., Shi, H., et al. (2017b). IFN-lambda preferably inhibits PEDV infection of porcine intestinal epithelial cells compared with IFN-alpha. *Antivir. Res.* 140, 76–82. doi: 10.1016/j.antiviral.2017.01.012

Li, W., Li, H., Liu, Y., Pan, Y., Deng, F., Song, Y., et al. (2012). New variants of porcine epidemic diarrhea virus, China, 2011. *Emerg. Infect. Dis.* 18, 1350–1353. doi: 10.3201/eid1808.120002

Li, S. W., Wang, C. Y., Jou, Y. J., Huang, S. H., Hsiao, L. H., Wan, L., et al. (2016). SARS coronavirus papain-like protease inhibits the TLR7 signaling pathway through removing Lys63-linked polyubiquitination of TRAF3 and TRAF6. *Int. J. Mol. Sci.* 17:678. doi: 10.3390/ijms17050678

Li, L., Xue, M., Fu, F., Yin, L., Feng, L., and Liu, P. (2019). IFN-lambda 3 mediates antiviral protection against porcine epidemic diarrhea virus by inducing a distinct antiviral transcript profile in porcine intestinal epithelia. *Front. Immunol.* 10:2394. doi: 10.3389/fimmu.2019.02394

Li, G., Zhang, W., Gong, L., and Huang, X. (2017a). MicroRNA-125a-5p inhibits cell proliferation and induces apoptosis in hepatitis B virus-related hepatocellular carcinoma by downregulation of ErbB3. *Oncol. Res.* 27, 449–458. doi: 10.3727/096504017x15016337254623

Lin, C. M., Annamalai, T., Liu, X., Gao, X., Lu, Z., El-Tholoth, M., et al. (2015). Experimental infection of a US spike-insertion deletion porcine epidemic diarrhea virus in conventional nursing piglets and cross-protection to the original US PEDV infection. *Vet. Res.* 46:134. doi: 10.1186/s13567-015-0278-9

Liu, J., Jia, Y., Jia, L., Li, T., Yang, L., and Zhang, G. (2018). MicroRNA-615-3p inhibits the tumor growth and metastasis of NSCLC via inhibiting IGF2. *Oncol. Res.* 27, 269–279. doi: 10.3727/096504018x15215019227688

Lui, P. Y., Wong, L. Y., Fung, C. L., Siu, K. L., Yeung, M. L., Yuen, K. S., et al. (2016). Middle East respiratory syndrome coronavirus M protein suppresses type I interferon expression through the inhibition of TBK1-dependent phosphorylation of IRF3. *Emerg. Microbes Infect.* 5:e39, 1–9. doi: 10.1038/emi.2016.33

Ma, Y., Wang, C., Xue, M., Fu, F., Zhang, X., Li, L., et al. (2018). The coronavirus transmissible gastroenteritis virus evades the type I interferon response through IRE1alpha-mediated manipulation of the microRNA miR-30a-5p/SOCS1/3 axis. *J. Virol.* 92:e00728-18. doi: 10.1128/jvi.00728-18

Pu, J., Wu, S., Xie, H., Li, Y., Yang, Z., Wu, X., et al. (2017). miR-146a inhibits dengue-virus-induced autophagy by targeting TRAF6. *Arch. Virol.* 162, 3645–3659. doi: 10.1007/s00705-017-3516-9

Qi, X., Cao, Y., Wu, S., Wu, Z., and Bao, W. (2021). miR-129a-3p inhibits PEDV replication by targeting the EDA-mediated NF-κB pathway in IPEC-J2 cells. *Int. J. Mol. Sci.* 22:8133. doi: 10.3390/ijms22158133

Song, X., Zhao, X., Huang, Y., Xiang, H., Zhang, W., and Tong, D. (2015). Transmissible gastroenteritis virus (TGEV) infection alters the expression of cellular microRNA species that affect transcription of TGEV gene 7. *Int. J. Biol. Sci.* 11, 913–922. doi: 10.7150/ijbs.11585

Wang, D., Fang, L., Shi, Y., Zhang, H., Gao, L., Peng, G., et al. (2016). Porcine epidemic diarrhea virus 3C-like protease regulates its interferon antagonism by cleaving NEMO. *J. Virol.* 90, 2090–2101. doi: 10.1128/jvi.02514-15

Wang, J., Hu, G., Gao, W., Xu, L., Ning, P., and Zhang, Y. (2014). Immortalized porcine intestinal epithelial cell cultures susceptible to porcine rotavirus infection. *J. Virol. Methods* 202, 87–94. doi: 10.1016/j.jviromet.2014.03.007

Wu, S., He, L., Li, Y., Wang, T., Feng, L., Jiang, L., et al. (2013). miR-146a facilitates replication of dengue virus by dampening interferon induction by targeting TRAF6. *J. Infect.* 67, 329–341. doi: 10.1016/j.jinf.2013.05.003

Xu, G., Zhang, Z., Wei, J., Zhang, Y., Zhang, Y., Guo, L., et al. (2013). microR-142-3p down-regulates IRAK-1 in response to Mycobacterium bovis BCG infection in macrophages. *Tuberculosis* 93, 606–611. doi: 10.1016/j.tube.2013.08.006

Xue, M., Fu, F., Ma, Y., Zhang, X., Li, L., Feng, L., et al. (2018). The PERK arm of the unfolded protein response negatively regulates transmissible gastroenteritis virus replication by suppressing protein translation and promoting type I interferon production. *J. Virol.* 92, e00431–e00418. doi: 10.1128/jvi.00431-18

Zhang, C., Chen, J., Wen, J., and Liu, G. (2018a). Analysis and verification of miRNA expression profiles of PEDV infected IPEC-J2 and effect of novel-miR-877 and ssc-miR-219a on PEDV replication. *Chin. J. Prevent Vet. Med.* 40, 1095–1099.

Zhang, Q., Ke, H., Blikslager, A., Fujita, T., and Yoo, D. (2018b). Type III interferon restriction by porcine epidemic diarrhea virus and the role of viral protein nsp1 in IRF1 signaling. *J. Virol.* 92, e01677–e01617. doi: 10.1128/jvi.01677-17

Zhang, X., Li, C., Zhang, B., Li, Z., Zeng, W., Luo, R., et al. (2021). Differential expression and correlation analysis of miRNA-mRNA profiles in swine testicular cells infected with porcine epidemic diarrhea virus. *Sci. Rep.* 11:1868. doi: 10.1038/s41598-021-81189-5

Zhang, Q., Ma, J., and Yoo, D. (2017). Inhibition of NF-kappaB activity by the porcine epidemic diarrhea virus nonstructural protein 1 for innate immune evasion. *Virology* 510, 111–126. doi: 10.1016/j.virol.2017.07.009

Zhang, Q., Shi, K., and Yoo, D. (2016). Suppression of type I interferon production by porcine epidemic diarrhea virus and degradation of CREB-binding protein by nsp1. *Virology* 489, 252–268. doi: 10.1016/j.virol.2015.12.010

Zhao, P., Zhao, L., Zhang, K., Feng, H., Wang, H., Wang, T., et al. (2012). Infection with street strain rabies virus induces modulation of the microRNA profile of the mouse brain. *Virol. J.* 9:159. doi: 10.1186/1743-422x-9-159

Zheng, H., Xu, L., Liu, Y., Li, C., Zhang, L., Wang, T., et al. (2018). MicroRNA-221-5p inhibits porcine epidemic diarrhea virus replication by targeting genomic viral RNA and activating the NF-kappaB pathway. *Int. J. Mol. Sci.* 19:3381. doi: 10.3390/ijms19113381

frontiers | Frontiers in Microbiology

TYPE Mini Review
PUBLISHED 19 January 2023
DOI 10.3389/fmicb.2022.1093646

OPEN ACCESS

EDITED BY
Jian Shang,
Zhengzhou University,
China

REVIEWED BY
Jun Wang,
Rutgers, The State University of New Jersey, United States

*CORRESPONDENCE
Shuiqing Gui
✉ guishuiqing@163.com
Liang Li
✉ lil@sustech.edu.cn
Shuo Li
✉ Shuoli@email.szu.edu.cn

†These authors share first authorship

SPECIALTY SECTION
This article was submitted to Virology, a section of the journal Frontiers in Microbiology

RECEIVED 09 November 2022
ACCEPTED 08 December 2022
PUBLISHED 19 January 2023

CITATION
Tang M, Zhang X, Huang Y, Cheng W, Qu J, Gui S, Li L and Li S (2023) Peptide-based inhibitors hold great promise as the broad-spectrum agents against coronavirus. *Front. Microbiol.* 13:1093646. doi: 10.3389/fmicb.2022.1093646

Peptide-based inhibitors hold great promise as the broad-spectrum agents against coronavirus

Mingxing Tang[1,2,3†], Xin Zhang[3†], Yanhong Huang[1,3†], Wenxiang Cheng[4], Jing Qu[5], Shuiqing Gui[6*], Liang Li[3*] and Shuo Li[2*]

[1]Shenzhen Institutes of Advanced Technology, Chinese Academy of Sciences, Shenzhen, China, [2]Department of Otolaryngology, Huazhong University of Science and Technology Union Shenzhen Hospital, Shenzhen, China, [3]School of Medicine, Southern University of Science and Technology, Shenzhen, China, [4]Center for Translational Medicine Research and Development, Shenzhen Institutes of Advanced Technology, Chinese Academy of Sciences, Shenzhen, China, [5]Department of Pathogen Biology, Shenzhen Center for Disease Control and Prevention, Shenzhen, China, [6]Department of Critical Care Medicine, Shenzhen Second People's Hospital, The First Affiliated Hospital of Shenzhen University, Shenzhen, China

Severe Acute Respiratory Syndrome Coronavirus (SARS-CoV), Middle East Respiratory Syndrome (MERS), and the recent SARS-CoV-2 are lethal coronaviruses (CoVs) that have caused dreadful epidemic or pandemic in a large region or globally. Infections of human respiratory systems and other important organs by these pathogenic viruses often results in high rates of morbidity and mortality. Efficient anti-viral drugs are needed. Herein, we firstly take SARS-CoV-2 as an example to present the molecular mechanism of CoV infection cycle, including the receptor binding, viral entry, intracellular replication, virion assembly, and release. Then according to their mode of action, we provide a summary of anti-viral peptides that have been reported in peer-reviewed publications. Even though CoVs can rapidly evolve to gain resistance to the conventional small molecule drugs, peptide-based inhibitors targeting various steps of CoV lifecycle remain a promising approach. Peptides can be continuously modified to improve their antiviral efficacy and spectrum along with the emergence of new viral variants.

KEYWORDS

SARS-CoV-2, viral infection, spike protein, anti-viral peptides, host protease, host receptors

Introduction

Coronaviruses are membrane enveloped virus particles, which contain a single-stranded positive-sense ribonucleic acid (RNA) genome and a matrix of RNA-associated capsid proteins (Zhou et al., 2020; Li et al., 2022). Taxonomically, four genera are classified within the *coronaviridae* family, including alpha-, beta-, gamma-, and delta-coronaviruses. Among them, seven alpha-and beta-CoV species have been identified as zoonotic

coronaviruses (HCoVs). The highly pathogenic members are Severe Acute Respiratory Syndrome Coronavirus (SARS-CoV), Middle East Respiratory Syndrome Coronavirus (MERS-CoV), and the recently emerged SARS-CoV-2, all of which are capable of causing severe respiratory tract infections and acute respiratory distress syndrome (ARDS). Infections by the intensively pathogenic HCoVs, especially SARS-CoV-2, have been the top concern of public health in recent years. The other HCoVs, HCoV-229E, HCoV-NL63, HCoV-OC43, and HCoV-HKU1 that normally cause mild respiratory illness have circulated within human populations for centuries. Although numerous drugs and vaccines have been developed and applied to combating SARS-CoV-2 or subsequent variants, drug resistance raises great concern (Rawson et al., 2020; Tannock et al., 2020; Kasuga et al., 2021; Şimşek-Yavuz and Komsuoğlu elikyurt, 2021). For example, the SARS-CoV-2 B.1.617.2 (delta) variant can rapidly gain resistance to monoclonal antibody after treatment (Rockett et al., 2022). The more recent B.1.1.529 (Omicron) variant is highly resistant to the majority of existing SARS-CoV-2 neutralizing antibodies (Cao et al., 2022; Hoffmann et al., 2022) as well as mRNA vaccines (Cele et al., 2022; Edara et al., 2022). Therefore, effective broad-spectrum antiviral therapeutics are still needed.

Recent observations indicated that peptides of diverse sources (either natural or synthetic) represent a class of promising antivirals. Peptides are small fragments of proteins typically comprising of 2–50 amino acid residues. These peptides achieve viral inhibition through various modes of actions, including direct binding to virions or host cell-surface receptors, blocking viral entry, interfering enzymatic activity to inhibit intracellular replication, and indirectly modulating immune responses(Schütz et al., 2020; Ghosh and Weinberg, 2021; Heydari et al., 2021). Compared to the conventional small molecule drugs, peptide synthesis can be quickly launched and modified (Vagner et al., 2008; Gao et al., 2018). More importantly, the chemical composition makes peptides highly specific and effective to their targets, even at nanomolar or picomolar concentrations (Cao et al., 2020; Schütz et al., 2020; Heydari et al., 2021; Shah et al., 2022; Yang et al., 2022).

Herein, we take SARS-CoV-2 as an instance to introduce the structural and functional properties of coronaviruses, and the viral infection process. Then, a state-of-the-art overview is provided to summarize recent researches that report the anti-CoV efficacy of peptides and their potentials in clinical use.

CoV genome structure and viral infection mechanism

Structural and functional dissection of SARS-CoV-2 genome encoded proteins

The full-length genome of SARS-CoV-2 consists of 29,870 bases with a 5′-cap and a 3′- poly(A) tail of variable length (Wu et al., 2020; Zhu N. et al., 2020; Figure 1A). Three functional types of proteins are encoded by the viral genome (Bai et al., 2022), including (1) structural proteins spike (S), membrane (M), envelop (E), and nucleocapsid (N) that constitute virions; (2) non-structural proteins that are mainly responsible for proteolysis and RNA synthesis; and (3) accessory proteins that are mainly involved in immune evasion (Figure 1B).

The 5′-proximal three quarters of the genome encode the replicases pp1a and pp1ab (Figure 1A), which can be further cleaved by the virus-encoded proteases papain-like protease (PL^{pro}) and chymotrypsin-like or main protease (M^{pro}), to generate 16 nonstructural proteins (NSP 1–16). The yield balance between pp1a and pp1ab is controlled through a fine-tuning regulatory mechanism named programmed ribosomal frameshifting, which has been nicely summarized elsewhere (Malone et al., 2022). Nonstructural proteins have multiple roles in genome replication, transcription, viral morphogenesis, and dysregulation of host immune responses (Malone et al., 2022; Yan et al., 2022). For example, when mature NSP1 is released from the replicase polyproteins following proteolytic cleavage, it rapidly induces host mRNA degradation and shuts down translation of host proteins (Huang et al., 2011; Thoms et al., 2020), while the other NSPs come to form the replication-transcription complex (RTC). NSP12, in synergy with its auxiliary co-factors NSP7 and NSP8, constitutes the RNA-dependent RNA polymerase complex (RdRp) and serves as the replication/transcription machinery to replicate viral genome, rather than host polymerase (Kirchdoerfer and Ward, 2019; Yan et al., 2021).

The 3′-proximal one quarter of the viral genome is transcribed into a nested set of sub-genomic RNAs that are in turn translated to structural proteins and accessory proteins. As with all CoVs, SARS-CoV-2 structure proteins include S, M, E, and N proteins. The S protein, protruding from the viral surface, binds to the angiotensin-converting enzyme 2 (ACE2) to initiate viral entry into host cells, a vital process for CoV infection (Huang et al., 2020; Walls et al., 2020). Thus, as the most easily accessible but also an indispensable viral component, the S protein has become an attractive target of anti-coronavirus peptides in a vast number of researches (Huang et al., 2020; Schütz et al., 2020). Structurally, S protein possesses two subunits, S1 and S2. The S1 subunit consists of N-and C-terminal domains and an important receptor-binding domain (RBD), while the S2, involved in membrane fusion and viral entry, contains a fusion peptide (FP), two heptapeptide repeat (HR1 and HR2), a transmembrane (TM), and cytoplasmic (CT) domains (Huang et al., 2020; Figure 1C). The E protein is a transmembrane protein responsible for viral assembly, budding, morphogenesis, and trafficking (Schoeman and Fielding, 2019). E protein directly contributes to the viral pathogenesis since it not only activates the host NACHT, LRR, and PYD domain-containing protein 3 (NLRP3) inflammasome (Nieto-Torres et al., 2015), but also undermines the tight junction protein complex of the lung epithelium (Chai et al., 2021; Javorsky et al., 2021). The M protein is the major component of the viral envelop, conferring the virion size and spherical structure. M protein is involved in interaction and trafficking of multiple viral proteins,

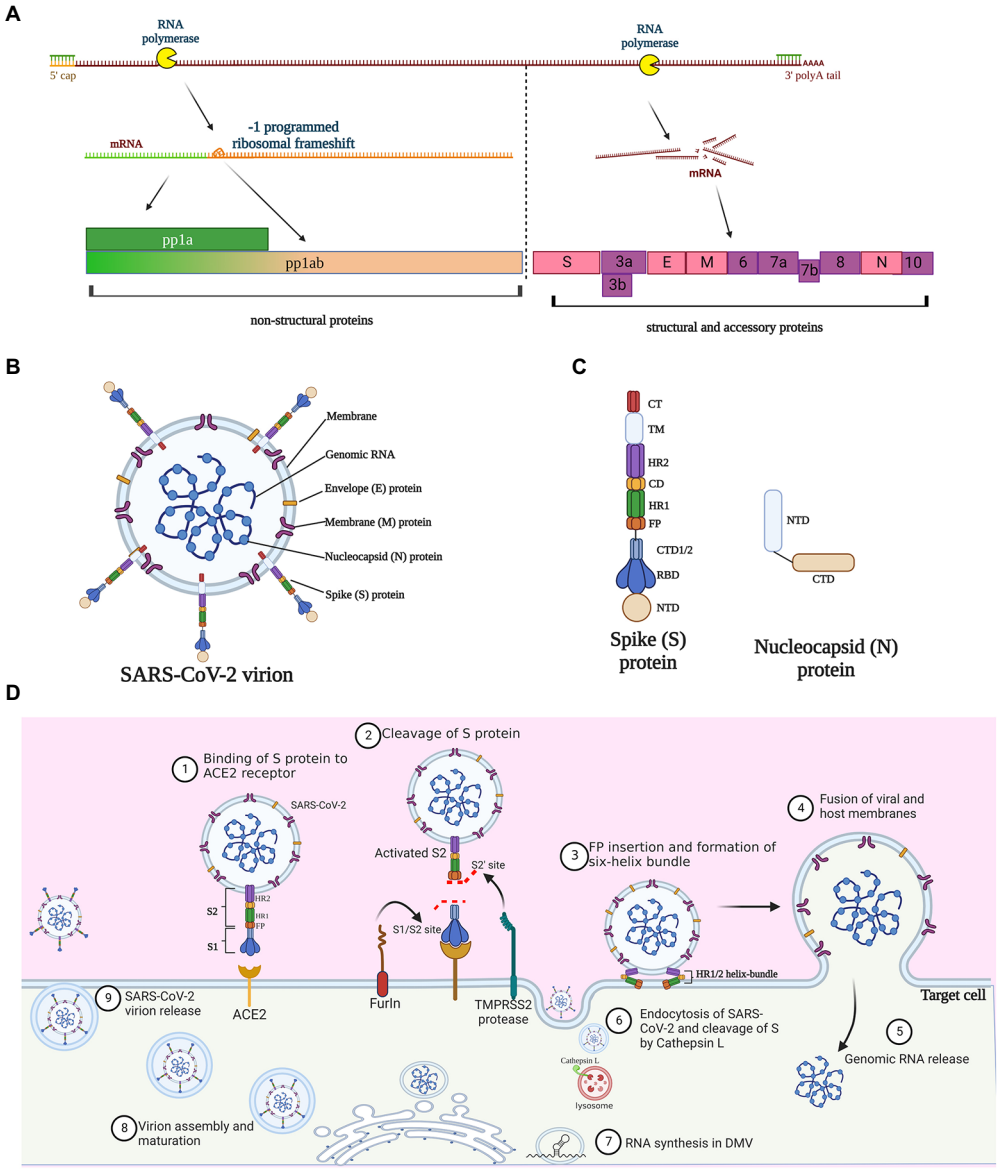

FIGURE 1
Molecular and structural bases of SARS-CoV-2 infection. **(A)** Proteins encoded by SARS-CoV-2 genome. Three quarters of the genome at the 5′-terminus encode the replicase polyproteins pp1a and pp1ab, which can be cleaved to generate 16 nonstructural proteins; pp1ab is derived from minus 1 site programmed ribosomal frameshift at the stop codon during the synthesis of pp1a. The 3′-terminus one quarter of the viral genome encode four structural proteins and accessory proteins. S, spike; E, envelope; M, membrane; and N, nucleocapsid. **(B)** Schematic diagram of SARS-CoV-2 virion structure. **(C)** Protein structure of spike protein and nucleocapsid protein. NTD, N-terminal domain; RBD, receptor-binding domain; CTD, C-terminal domain; FP, fusion peptide; HR, heptad repeat; CD, connector domain; TM, transmembrane domain; and CT, cytoplasmic tail. **(D)** The infection lifecycle of SARS-CoV-2. TMPRSS2, Type II transmembrane serine protease; ACE2, angiotensin-converting enzyme 2.

as well as assembly and release of virion particles (Yan et al., 2022). The SARS-CoV M protein can stimulate the host to produce a specific $CD8^+$ T cell immune response (Li et al., 2021). Owning to the high sequence identity (90.5%) of the M protein gene between SARS-CoV-2 and SARS-CoV (Mahtarin et al., 2022), the SARS-CoV-2 M protein is likely to have similar immunogenic effects (Su et al., 2021). The main role of the N protein is binding to genomic RNA to form a ribonucleoprotein complex, which is related to viral replication and assembly (Mcbride et al., 2014; Guo et al., 2016). Compared to the other structure proteins, the gene encoding N protein is highly conserved and stable with few mutations over time (Hodge et al., 2021; Figure 1C). The C-terminal region of N protein favors viral immune evasion by antagonizing the host interferon-beta (IFN-β) pathway (Lu et al., 2011). Given these basic findings, the N protein is a great potential target for diagnosis and therapy against CoV infection.

Eleven genes encoding accessory proteins also locate within the 3′- proximal part of SARS-CoV-2 genome and they are

interlaced with structural protein genes. Although the characterization of these accessory proteins is relatively limited, they appear to have important roles in pathogenesis and immune evasion, rather than virus replication (Redondo et al., 2021). Mutations are frequently detected in accessory proteins among variants of concern, indicative of increasing transmissibility and immune evasion (Shang et al., 2020). In light of their frequent mutations, accessory proteins might not be favorable targets of the broad-spectrum anti-coronavirus peptides. Functional analysis of those proteins substantiates the bioinformatic indication. Through diverse strategies, the accessory proteins, ORF3b (Konno et al., 2020), ORF6 (Miorin et al., 2020), ORF7a (Cao et al., 2021), and ORF8 (Lei et al., 2020), can antagonize the type I IFN response, an important host defense reaction against viral infection.

Infection mechanism of SARS-CoV-2—binding, entry, intracellular replication, virion assembly, and release

The SARS-CoV-2 infection involves multiple steps (Figure 1D). Initially, the S protein is cleaved and activated by the host proprotein convertase furin, leaving the protruding extracellular S1 subunit and the transmembrane S2 subunit non-covalently bounded (Peacock et al., 2021). The cleavage exposes the RBD in S1, which directly interacts with the peptidase domain of ACE2 and induces drastic transformational alteration of S2 (Cai et al., 2020; Liu et al., 2020). The cleavage of S2 by Type II transmembrane serine protease (TMPRSS2) further exposes the fusion peptide, thus facilitating its insertion into cellular membrane (Fraser et al., 2022; Iwata-Yoshikawa et al., 2022). Simultaneously, the HR1 and HR2 in S2 form a six-helix bundle fusion core, which acts as a hinge to bring the viral and host cell membrane in close proximity (Yao H. et al., 2020; Xia et al., 2020b). Alternatively, the pH-dependent enzyme cathepsin L can also implement the cleavage of S2 when viral entry is dependent on endocytosis (Matsuyama et al., 2020; Hoffmann et al., 2020b). After the membrane fusion or endocytosis, the SARS-CoV-2 gRNAs are released into cytosol, and soon translated into two replicase polyproteins pp1a and pp1ab, by hijacking the host cell ribosomes. pp1a and pp1ab are digested by the viral proteases, M^{pro} and PL^{pro}, into 16 non-structural proteins, which further form the RTCs for RNA synthesis (Malone et al., 2022). NSP3 and NSP4 drive the rearrangement of the endoplasmic reticulum (ER) into double membrane vesicles (DMVs; Snijder and Limpens, 2020), where the RTCs produce new gRNA and a set of sub-genomic mRNAs that are finally translated into four structural proteins and a few accessory proteins. SARS-CoV-2 assembly commences as the gRNAs are coated with nucleocapsid proteins, resulting in RNA-nucleocapsid complexes that bud into the endoplasmic reticulum-Golgi intermediate compartment (ERGIC) to form mature virions (Boson et al., 2021). Finally, the virus particles are released *via* the budding of the Golgi apparatus and exocytosis of the cell membrane for a new round of infections.

Peptides working at different infection stages are potent anti-CoV agents

Peptides targeting initial binding of S protein to the ACE2 receptor

Targeting the RBD domain in S protein to inhibit its binding to ACE2 has been so far an intensively popular strategy against CoVs (Figure 2A). The charged amino acids between residues 22 and 57 of ACE2 are predicted to be the critical interaction site (Han et al., 2006). In an early work, two peptides P4 and P5 that mimicked this region can bind to SARS-CoV S1 RBD and inhibit pseudo-virion infection with a high half-maximal-inhibitory concentration (IC_{50}) of 50 and 6 μM, respectively. Interestingly, another peptide comprised of two discontinuous segments of ACE2 (a.a. 22–44 and 351–357) showed higher antiviral efficacy (IC_{50}: 0.1 μM) in a HeLa cell model (Han et al., 2006). The S proteins of SARS-CoV and SARS-CoV-2 share 76% sequence homology while their RBDs share 75% similarity (Jaimes et al., 2020). Although SARS-CoV-2 has greater ACE2 binding affinity (Wrapp et al., 2020) and higher transmissibility (Zhou et al., 2020), the high sequence similarity indicates that peptides effectively blocking the S1 RBD of SARS-CoV might also inhibit SARS-CoV-2 infection. To address the SARS-CoV-2 infection, a series of RBD-targeting peptides have been synthesized or discovered (Cao et al., 2020; Jaiswal and Kumar, 2020; Tavassoly et al., 2020; Wang et al., 2021). Using ACE2 as the scaffold, researchers synthesized two peptides AHB1 and AHB2, which neutralized SARS-CoV-2 with IC_{50} values of 35 and 16 nM, respectively (Cao et al., 2020). Surprisingly, another two peptides (LCB1 and LCB3) based on *de-novo* sequencing of the RBD-binding motifs showed a much higher potency in preventing SARS-CoV-2 infection of mammalian Vero-E6 cells, with IC_{50} values of 23.54 and 48.1 pM, respectively (Cao et al., 2020). Except the abovementioned synthetic peptides, a natural peptide produced by airway epithelium, human cathelicidin LL37, can bind to the S1 RBD and inhibit SARS-CoV-2 S pseudo-virion infection with a IC_{50} value of 4.74 μg/ml (Wang et al., 2021). Notably, the RBD is not the exclusive ACE2-interaction site, since peptides targeting other regions in S1 were also able to neutralize SARS-CoV (Zheng et al., 2005) and, thus potentially SARS-CoV-2.

HCoV-NL63, SARS-CoV, and SARS-CoV-2 employ ACE2 as the entry receptor, thus peptides targeting ACE2 can shield the binding of S proteins (Figure 2A). Based on this, different inhibitors cloaking the ACE2 have been therefore synthesized, but their antiviral efficacy varies considerably, with IC_{50} values ranging from nanomolar to millimolar concentrations (Huang et al., 2003; Hu et al., 2005; Ho et al., 2006; Struck

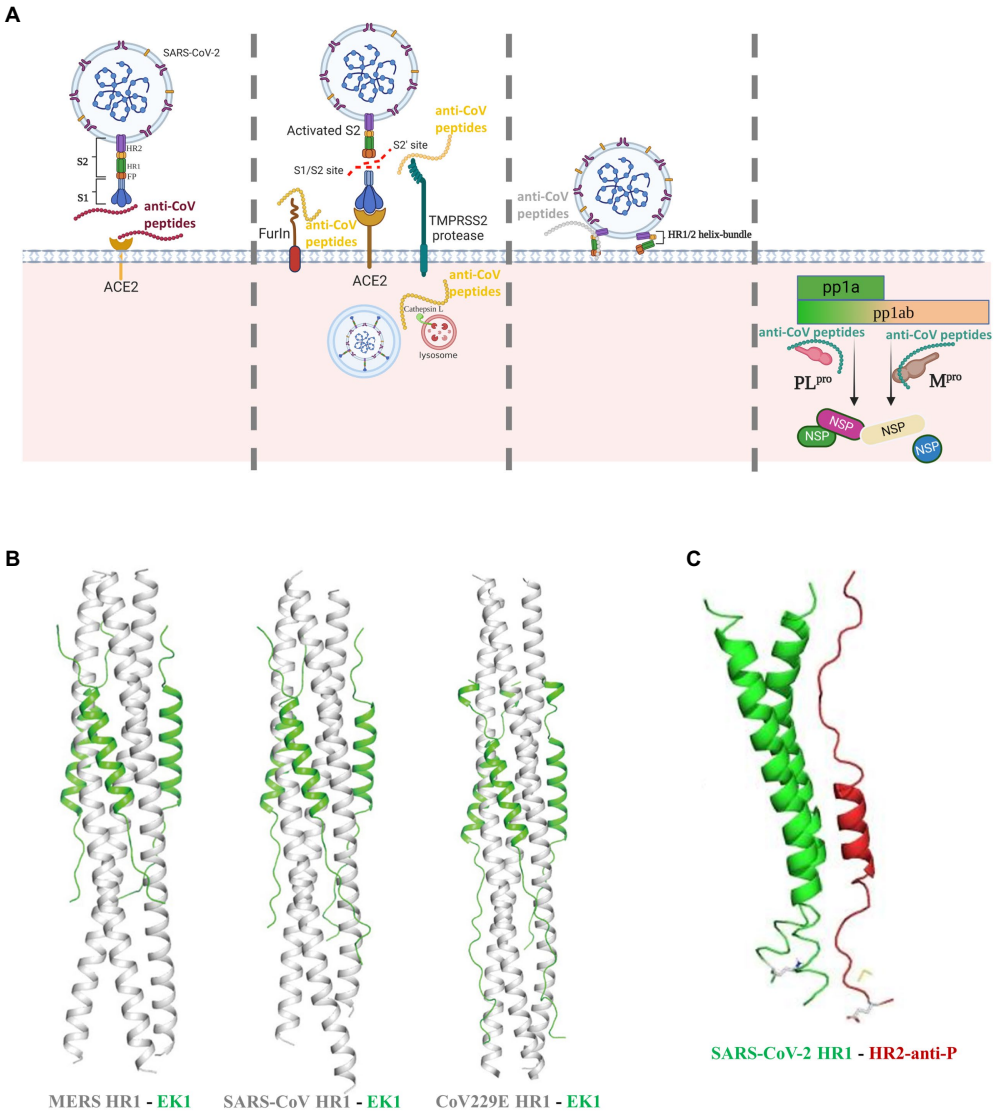

FIGURE 2
Peptides as potent inhibitors against coronavirus. **(A)** Anti-CoV peptides can work with diverse modes of actions by targeting the binding of S protein to host receptor, or the proteolytic processing of S proteins by host proteases, or the host-viral membrane fusion, or the viral proteases that are responsible for cleavage of replicase polyproteins into non-structural proteins. **(B)** The X-ray crystal structures of membrane-fusion inhibitory peptide EK1 shown as green in complex with the S protein HR1 regions of various CoVs shown as white (Xia et al., 2019b). **(C)** The X-ray crystal structures of membrane-fusion inhibitory peptide HR2-anti-P shown as red binding to the SARS-CoV-2 HR1 region shown as green (Ling et al., 2020).

et al., 2012). Of note, recent studies discovered that some natural peptides can also target ACE2 to inhibit SARS-CoV-2 infection (Wang et al., 2020; Beddingfield et al., 2021). Human defensin 5 (HD5), a natural lectin-like α-defensin produced by the Paneth cells, can stably bind to ACE2 and prevent infection of S protein-expressing pseudo-virions at concentrations as low as 10 μg/ml (Wang et al., 2020). ATN-161, a fibronectin derivative, might also bind to ACE2 to significantly reduce SARS-CoV-2 infection (IC_{50}: 3 μM; Beddingfield et al., 2021). However, clinical use of such ACE2-blocking peptides or drugs warrants serious attention, as ACE2 belongs to the renin-angiotensiongen system where it promotes vasodilation, while interference might have life-threatening side effects.

Peptides targeting proteolytic activation of S protein

As mentioned above, cleavage and activation of S proteins by host proteases are crucial to establish CoV infection, while peptides targeting them can efficiently inhibit viral infection (Figure 2A). Although proteins of multiple viruses can be activated by the proprotein convertase furin (Volchkov et al., 1998; Sugrue

et al., 2001; Braun and Sauter, 2019), this feature distinguishes SARS-CoV-2 from SARS-CoV (Matsuyama et al., 2018; Schütz et al., 2020). Two recent studies showed that treatment by the furin inhibitors decanoyl-RVKR-chloromethylketone and MI-1851 can abolish furin cleavage and inhibit SARS-CoV-2 infection of mammalian cells (Bestle et al., 2020; Cheng et al., 2020). Different from furin, TMPRSS2 is involved in proteolytic activation of more CoV species (Shen et al., 2017; Böttcher-Friebertshäuser, 2018), while inhibitors blocking its enzymatic activity could be promising broad-spectrum antivirals. A previous work demonstrated that three different TMPRSS2 inhibitors strongly prevented SARS-CoV-2 and SARS-CoV multiplication in Calu-3 cells in a dose-dependent manner (Bestle et al., 2020). More excitingly, Shapira and coworkers recently synthesized a more potent TMPRSS2 inhibitor N-0385, which can act as a pan-SARS-CoV-2 prophylactic and therapeutic agent and inhibit the cellular entry of multiple SARS-CoV-2 variants of concern at nanomolar concentrations (Shapira et al., 2022). Cellular entry of CoVs might occur through either membrane fusion or endocytosis. In the latter case, the S protein should be activated by proteolysis of cathepsin L, a lysosome-associated protease (Gomes et al., 2020; Zhao M. M. et al., 2021). Blocking the cathepsin L to inhibit SARS-CoV-2 has been tested. P9, a derivate peptide of mouse β-defensin-4, exhibited broad antiviral activities against SARS-CoV, SARS-CoV-2, MERS-CoV and influenza virus, *via* interfering cathepsin L and preventing endosomal acidification (Zhao et al., 2016, 2020). In the follow-up works, this peptide was further optimized into P9R and 8P9R, which showed higher level of anti-SARS-CoV-2 potency, with IC_{50} values of 0.9 and 0.3 μg/ml, respectively (Zhao et al., 2020; Zhao H. et al., 2021). In sum, inhibition of host proteases seems a promising antiviral strategy. However, as with the case of ACE2, interference of the physiologically relevant proteases may induce unwanted adverse effect. This calls for sufficient trials in the future to test the potential cytotoxicity and global impact if the protease inhibitors are to be applied to clinical use.

Peptides targeting membrane fusion process

In the past 2 decades, a vast number of studies have synthesized diverse anti-viral peptides that target the membrane fusion step (Schütz et al., 2020; Heydari et al., 2021). These fusion inhibitors have been so far the most extensively studied and the most promising ones to be translated into therapeutic peptides. Mechanistically, they were designed to mimic one of the HR regions in the S2 subunit, interact with the complementary HR, block formation of the HR1-HR2 helix bundle, and thus interfere with virus-host membrane fusion (Figure 2A). Comparatively, peptides derived from HR1 (that target HR2) appear often poorly active (Bosch et al., 2004; Liu et al., 2004; Xia et al., 2020b), likely owing to their propensity to self-aggregation. A large number of peptides have been synthesized to address the previous SARS-CoV and MERS-CoV pandemics, mostly showing strong anti-CoV activity with IC_{50} values ranging in micromolar concentrations (Barnard et al., 2004; Liu et al., 2004; Yuan et al., 2004; Zheng et al., 2005; Chu et al., 2008; Ujike et al., 2008; O'keefe et al., 2010; Lu et al., 2014; Channappanavar et al., 2015; Zhao et al., 2016; Sun et al., 2017; Wang et al., 2018; Huang et al., 2019; Xia et al., 2019a). Since the HR1 amino acid sequences of SARS-CoV and SARS-CoV-2 share 92.6% similarity and their HR2 is almost identical (Xia et al., 2020b), peptides derived from SARS-CoV HR2 are very likely to inhibit SARS-CoV-2 infection. In agreement with this suggestion, a pan-coronavirus fusion inhibitor EK1, which was previously identified as a potent antiviral agent against SARS-CoV and MERS-CoV (Figure 2B), also reduced SARS-CoV-2 infection of TMPRSS2-negative Vero-E6 cells with an IC_{50} value of 2.5 μM (Xia et al., 2019b, 2020a). Of interest, the IC_{50} value was 10-fold lower in TMPRSS2-positive Caco-2 cells (Conzelmann et al., 2020; Xia et al., 2020a), reinforcing again the importance of S protein processing in CoV infection. Computational analysis is a powerful tool in designing the potent SARS-CoV-2 inhibitors. For instance, at the onset of the COVID-19 pandemic, researchers used the *in silico* approaches to design a potent HR1-targeting peptide to prevent membrane fusion (Figure 2C; Ling et al., 2020). In another work, two potent peptides Fp13-HR1 and Fp14-HR1, that were screened from 17 SARS-CoV HR2-derived fusion inhibitors, were predicted to have a high binding affinity to SARS-CoV-2 HR1, thus they might be effective fusion inhibitors of SARS-CoV-2 (Efaz et al., 2021). To improve antiviral efficacy and stability, rational modifications of the existing inhibitory peptides are also of great importance. This has been nicely exemplified by the modification of the abovementioned EK1 into EK1C4 by linking a cholesterol group to the C-terminus. The optimized peptide displayed more than 19–190-fold potency in preventing the infection of several CoVs, including SARS-CoV-2 (Xia et al., 2020a). Another representative is IPB-02, which was modified from the HR1-targeting peptide IPB-01 by conjugation of a cholesterol group. The refined peptide showed stronger antiviral effect against SARS-CoV-2 with the IC_{50} value decreasing from 22 to 0.08 μM (Zhu Y. et al., 2020). Optimization of fusion inhibitors is not limited to linkage of current peptides to functional groups. Although previously reported HR1-derived peptide inhibitors exhibit poor inhibitory activities, foldon-mediated trimerization of the C-terminus conferred a HR1-derived peptide with higher inhibitory activity against SARS-CoV-2, SARS-CoV-2 variants of concern (VOCs), SARS-CoV, and MERS-CoV (Bi et al., 2022). Moreover, an inspirational work identified that the extended N-terminus of HR2 also involves in interacting with HR1, and a synthetic peptide including this region achieved single-digit nanomolar inhibition of several SARS-CoV-2 variants (Yang et al., 2022).

Peptides targeting intracellular replication and assembly of coronavirus

Coronavirus infection can also be impeded intracellularly. For example, several chemical compounds Boceprevir, GC-376, calpain inhibitors II and XII had a wide range antiviral activity, *via* a dual

mechanism of action by targeting both viral M^{pro} and host cell cathepsin L (Fu et al., 2020; Hu et al., 2020; Ma et al., 2020). These findings indicated that the viral components necessary for RNA replication and assembly are also favorable targets for the anti-CoV peptide design (Figure 2A). Indeed, an early study showed that a M^{pro}-targeting octapeptide impeded replication of the SARS-CoV at the concentration of 1 mg·L^{-1} (Gan et al., 2006). Another research reported that Cbz-AVLQ-CN, a broad-spectrum peptide, effectively inhibited six different CoV species with IC_{50} values of 1.3–4.6 μM (Chuck et al., 2014). Interestingly, several active peptides that can bind to both M^{pro} and monoamine oxidase A of SARS-CoV-2 can be generated from hydrolysis of fish proteins, representing potential inhibitors from food source against CoV (Yao Y. et al., 2020). Blocking other enzymes of CoVs is an alternative strategy. Two synthetic peptides K29 and K12 could markedly inhibit the activity of SARS-CoV nsp16 (methytransferase) in a dose-dependent manner, thus disrupting its role in viral RNA synthesis, but viral inhibition assays are still needed (Ke et al., 2012).

In addition to S protein, the N protein might also be a rational target for the anti-CoV peptide design. The C-terminal domains (CTDs) of the N proteins mediate the self-association of the protein to form high-order oligomers, and deletion of 13 amino acids in the HCoV-229E N protein CTD appeared incapable of forming a high degree of oligomerization (Chang et al., 2005). In line with this notion, a C-terminal tail peptide N377–389 interfered with the oligomerization of the CTD of HCoV-229E N protein and inhibited viral replication at 300 μM (Lo et al., 2013). This finding provides insights that blocking the formation of the N protein-RNA higher-order oligomers and in turn the virion assembly can contribute to viral inhibition.

Perspectives and conclusion

To conclude, peptides that can target various steps in CoV lifecycle have shown great potential in combating CoV infection. In some cases, the peptide-based inhibitors seem to have lower possibility to cause drug resistance (Zhao et al., 2020), and they rarely induce detectable cytotoxicity (Gan et al., 2006). Some peptides exhibit significantly strong and broad-spectrum effect against multiple CoV species. More importantly, combination of peptides with different antiviral mechanisms could generate synergistic impact (Bestle et al., 2020; Hoffmann et al., 2020a). However, to translate the peptides into clinical therapeutics, they should be safe and stable *in vivo*, while many works need more effort on this aspect. Therefore, a future perspective is to refine current peptides to be more effective and long-lasting, as with the case of EK14C, which was subject to two rounds of optimization from OC43-HR2P. To this end, a database containing comprehensive and precise information of 214 unique anti-CoV peptides would contribute to more rational design or modification (Zhang et al., 2022).

Author contributions

MT, XZ, YH, and LL devised the framework, wrote and revised the manuscript. WC, JQ, SG, SL, LL, and MT contributed to literature search and gave insightful suggestions in revising this work. All authors contributed to the article and approved the submitted version.

Funding

This work was supported by the National Natural Science Foundation of China (81900071), the Fellowship of China Postdoctoral Science Foundation (2022M713287), the Medical Research Foundation of Guangdong Province (A2022046), and the Shenzhen Science and Technology Innovation Commission for Research and Development Projects (JSGG20200807171603039, JSGG20191118161401741, CYJ20210324112607020 and zJCYJ20220530141616037).

Acknowledgments

BioRender was used to create schematic representations.

Conflict of interest

The authors declare that the research was conducted in the absence of any commercial or financial relationships that could be construed as a potential conflict of interest.

Publisher's note

References

Bai, C., Zhong, Q., and Gao, G. F. (2022). Overview of SARS-CoV-2 genome-encoded proteins. *Sci. China Life Sci.* 65, 280–294. doi: 10.1007/s11427-021-1964-4

Barnard, D. L., Hubbard, V. D., Burton, J., Smee, D. F., Morrey, J. D., Otto, M. J., et al. (2004). Inhibition of severe acute respiratory syndrome-associated coronavirus (SARSCoV) by calpain inhibitors and β-D-N4-Hydroxycytidine. *Antivir. Chem. Chemother.* 15, 15–22. doi: 10.1177/095632020401500102

Beddingfield, B. J., Iwanaga, N., Chapagain, P. P., Zheng, W., Roy, C. J., Hu, T. Y., et al. (2021). The integrin binding peptide, ATN-161, as a novel

therapy for SARS-CoV-2 infection. *JACC. Basic Transl. Sci.* 6, 1–8. doi: 10.1016/j.jacbts.2020.10.003

Bestle, D., Heindl, M. R., Limburg, H., Van Lam, T., Pilgram, O., Moulton, H., et al. (2020). TMPRSS2 and furin are both essential for proteolytic activation of SARS-CoV-2 in human airway cells. *Life Sci. Alliance* 3:e202000786. doi: 10.26508/lsa.202000786

Bi, W., Chen, G., and Dang, B. (2022). Novel engineered SARS-CoV-2 HR1 Trimer exhibits improved potency and broad-Spectrum activity against SARS-CoV-2 and its variants. *J. Virol.* 96, e00681–e00622. doi: 10.1128/jvi.00681-22

Bosch, B. J., Martina, B. E. E., Van Der Zee, R., Lepault, J., Haijema, B. J., Versluis, C., et al. (2004). Severe acute respiratory syndrome coronavirus (SARS-CoV) infection inhibition using spike protein heptad repeat-derived peptides. *Proc. Natl. Acad. Sci. U. S. A.* 101, 8455–8460. doi: 10.1073/pnas.0400576101

Boson, B., Legros, V., Zhou, B., Siret, E., Mathieu, C., Cosset, F.-L., et al. (2021). The SARS-CoV-2 envelope and membrane proteins modulate maturation and retention of the spike protein, allowing assembly of virus-like particles. *J. Biol. Chem.* 296:100111. doi: 10.1073/pnas.0400576101

Böttcher-Friebertshäuser, E. (2018). "Membrane-anchored serine proteases: host cell factors in proteolytic activation of viral glycoproteins" in *Activation of Viruses by Host Proteases*, ed. Böttcher-Friebertshäuser, E., Garten, W. and Klenk, H. (Cham, FL: Springer). 153–203.

Braun, E., and Sauter, D. (2019). Furin-mediated protein processing in infectious diseases and cancer. *Clin. Transl. Immunol.* 8:e1073. doi: 10.1002/cti2.1073

Cai, Y., Zhang, J., Xiao, T., Peng, H., Sterling, S. M., Walsh, R. M., et al. (2020). Distinct conformational states of SARS-CoV-2 spike protein. *Science* 369, 1586–1592. doi: 10.1126/science.abd4251

Cao, L., Goreshnik, I., Coventry, B., Case, J. B., Miller, L., Kozodoy, L., et al. (2020). De novo design of picomolar SARS-CoV-2 miniprotein inhibitors. *Science* 370, 426–431. doi: 10.1126/science.abd9909

Cao, Z., Xia, H., Rajsbaum, R., Xia, X., Wang, H., and Shi, P.-Y. (2021). Ubiquitination of SARS-CoV-2 ORF7a promotes antagonism of interferon response. *Cell. Mol. Immunol.* 18, 746–748. doi: 10.1038/s41423-020-00603-6

Cao, Y., Wang, J., Jian, F., Xiao, T., Song, W., Yisimayi, A., et al. (2022). Omicron escapes the majority of existing SARS-CoV-2 neutralizing antibodies. *Nature* 602, 657–663. doi: 10.1038/s41586-021-04385-3

Cele, S., Jackson, L., Khoury, D. S., Khan, K., Moyo-Gwete, T., Tegally, H., et al. (2022). Omicron extensively but incompletely escapes Pfizer BNT162b2 neutralization. *Nature* 602, 654–656. doi: 10.1038/s41586-021-04387-1

Chai, J., Cai, Y., Pang, C., Wang, L., Mcsweeney, S., Shanklin, J., et al. (2021). Structural basis for SARS-CoV-2 envelope protein recognition of human cell junction protein PALS1. *Nat. Commun.* 12:3433. doi: 10.1038/s41467-021-23533-x

Chang, C.-K., Sue, S.-C., Yu, T.-H., Hsieh, C.-M., Tsai, C.-K., Chiang, Y.-C., et al. (2005). The dimer interface of the SARS coronavirus nucleocapsid protein adapts a porcine respiratory and reproductive syndrome virus-like structure. *FEBS Lett.* 579, 5663–5668. doi: 10.1016/j.febslet.2005.09.038

Channappanavar, R., Lu, L., Xia, S., Du, L., Meyerholz, D. K., Perlman, S., et al. (2015). Protective effect of intranasal regimens containing peptidic middle east respiratory syndrome coronavirus fusion inhibitor against MERS-CoV infection. *J. Infect. Dis.* 212, 1894–1903. doi: 10.1093/infdis/jiv325

Cheng, Y. W., Chao, T. L., Li, C. L., Chiu, M. F., Kao, H. C., Wang, S. H., et al. (2020). Furin inhibitors block SARS-CoV-2 spike protein cleavage to suppress virus production and cytopathic effects. *Cell Rep.* 33:108254. doi: 10.1016/j.celrep.2020.108254

Chu, L. H., Chan, S. H., Tsai, S. N., Wang, Y., Cheng, C. H., Wong, K. B., et al. (2008). Fusion core structure of the severe acute respiratory syndrome coronavirus (SARS-CoV): in search of potent SARS-CoV entry inhibitors. *J. Cell. Biochem.* 104, 2335–2347. doi: 10.1002/jcb.21790

Chuck, C. P., Ke, Z. H., Chen, C., Wan, D. C. C., Chow, H. F., and Wong, K. B. (2014). Profiling of substrate-specificity and rational design of broad-spectrum peptidomimetic inhibitors for main proteases of coronaviruses. *Hong Kong Med. J.* 20, 22–25.

Conzelmann, C., Gilg, A., Groß, R., Schütz, D., Preising, N., Ständker, L., et al. (2020). An enzyme-based immunodetection assay to quantify SARS-CoV-2 infection. *Antivir. Res.* 181:104882. doi: 10.1016/j.antiviral.2020.104882

Edara, V.-V., Manning, K. E., Ellis, M., Lai, L., Moore, K. M., Foster, S. L., et al. (2022). mRNA-1273 and BNT162b2 mRNA vaccines have reduced neutralizing activity against the SARS-CoV-2 omicron variant. *Cell Rep. Med.* 3:100529. doi: 10.1016/j.xcrm.2022.100529

Efaz, F. M., Islam, S., Talukder, S. A., Akter, S., Tashrif, M. Z., Ali, M. A., et al. (2021). Repurposing fusion inhibitor peptide against SARS-CoV-2. *J. Comput. Chem.* 42, 2283–2293. doi: 10.1002/jcc.26758

Fraser, B. J., Beldar, S., Seitova, A., Hutchinson, A., Mannar, D., Li, Y., et al. (2022). Structure and activity of human TMPRSS2 protease implicated in SARS-CoV-2 activation. *Nat. Chem. Biol.* 18, 963–971. doi: 10.1038/s41589-022-01059-7

Fu, L., Ye, F., Feng, Y., Yu, F., Wang, Q., Wu, Y., et al. (2020). Both Boceprevir and GC376 efficaciously inhibit SARS-CoV-2 by targeting its main protease. *Nat. Commun.* 11:4417. doi: 10.1038/s41467-020-18233-x

Gan, Y.-R., Huang, H., Huang, Y.-D., Rao, C.-M., Zhao, Y., Liu, J.-S., et al. (2006). Synthesis and activity of an octapeptide inhibitor designed for SARS coronavirus main proteinase. *Peptides* 27, 622–625. doi: 10.1016/j.peptides.2005.09.006

Gao, Y., Fang, H., Fang, L., Liu, D., Liu, J., Su, M., et al. (2018). The modification and design of antimicrobial peptide. *Curr. Pharm. Des.* 24, 904–910. doi: 10.2174/1381612824666180213130318

Ghosh, S. K., and Weinberg, A. (2021). Ramping up antimicrobial peptides against severe acute respiratory syndrome coronavirus-2. *Front. Mol. Biosci.* 8:620826. doi: 10.3389/fmolb.2021.620806

Gomes, C. P., Fernandes, D. E., Casimiro, F., Da Mata, G. F., Passos, M. T., Varela, P., et al. (2020). Cathepsin L in COVID-19: from pharmacological evidences to genetics. *Front. Cell. Infect. Microbiol.* 10:589505. doi: 10.3389/fcimb.2020.589505

Guo, Y., Wang, W., Sun, Y., Ma, C., Wang, X., Wang, X., et al. (2016). Crystal structure of the core region of hantavirus nucleocapsid protein reveals the mechanism for ribonucleoprotein complex formation. *J. Virol.* 90, 1048–1061. doi: 10.1128/JVI.02523-15

Han, D. P., Penn-Nicholson, A., and Cho, M. W. (2006). Identification of critical determinants on ACE2 for SARS-CoV entry and development of a potent entry inhibitor. *Virology* 350, 15–25. doi: 10.1016/j.virol.2006.01.029

Heydari, H., Golmohammadi, R., Mirnejad, R., Tebyanian, H., Fasihi-Ramandi, M., and Moosazadeh Moghaddam, M. (2021). Antiviral peptides against Coronaviridae family: a review. *Peptides* 139:170526. doi: 10.1016/j.peptides.2021.170526

Ho, T.-Y., Wu, S.-L., Chen, J.-C., Wei, Y.-C., Cheng, S.-E., Chang, Y.-H., et al. (2006). Design and biological activities of novel inhibitory peptides for SARS-CoV spike protein and angiotensin-converting enzyme 2 interaction. *Antivir. Res.* 69, 70–76. doi: 10.1016/j.antiviral.2005.10.005

Hodge, C. D., Rosenberg, D. J., Grob, P., Wilamowski, M., Joachimiak, A., Hura, G. L., et al. (2021). Rigid monoclonal antibodies improve detection of SARS-CoV-2 nucleocapsid protein. *MAbs* 13:1905978. doi: 10.1080/19420862.2021.1905978

Hoffmann, M., Kleine-Weber, H., and Pöhlmann, S. (2020a). A multibasic cleavage site in the spike protein of SARS-CoV-2 is essential for infection of human lung cells. *Mol. Cell* 78, 779–784.e5. doi: 10.1016/j.molcel.2020.04.022

Hoffmann, M., Kleine-Weber, H., Schroeder, S., Krüger, N., Herrler, T., Erichsen, S., et al. (2020b). SARS-CoV-2 cell entry depends on ACE2 and TMPRSS2 and is blocked by a clinically proven protease inhibitor. *Cells* 181, 271–280.e8. doi: 10.1016/j.cell.2020.02.052

Hoffmann, M., Krüger, N., Schulz, S., Cossmann, A., Rocha, C., Kempf, A., et al. (2022). The Omicron variant is highly resistant against antibody-mediated neutralization: Implications for control of the COVID-19 pandemic. *Cells* 185, 447–456.e411. doi: 10.1016/j.cell.2021.12.032

Hu, H., Li, L., Kao, R. Y., Kou, B., Wang, Z., Zhang, L., et al. (2005). Screening and identification of linear B-cell epitopes and entry-blocking peptide of severe acute respiratory syndrome (SARS)-associated coronavirus using synthetic overlapping peptide library. *J. Comb. Chem.* 7, 648–656. doi: 10.1021/cc0500607

Hu, Y., Ma, C., Szeto, T., Hurst, B., Tarbet, B., and Wang, J. (2020). Boceprevir, calpain inhibitors II and XII, and GC-376 have broad-spectrum antiviral activity against coronaviruses. *ACS Infect. Dis.* 7, 586–597. doi: 10.1021/acsinfecdis.0c00761

Huang, X., Li, M., Xu, Y., Zhang, J., Meng, X., An, X., et al. (2019). Novel gold nanorod-based HR1 peptide inhibitor for middle east respiratory syndrome coronavirus. *ACS Appl. Mater. Interfaces* 11, 19799–19807. doi: 10.1021/acsami.9b04240

Huang, C., Lokugamage, K. G., Rozovics, J. M., Narayanan, K., Semler, B. L., and Makino, S. (2011). SARS coronavirus nsp1 protein induces template-dependent endonucleolytic cleavage of mRNAs: viral mRNAs are resistant to nsp1-induced RNA cleavage. *PLoS Pathog.* 7:e1002433. doi: 10.1371/journal.ppat.1002433

Huang, L., Sexton, D. J., Skogerson, K., Devlin, M., Smith, R., Sanyal, I., et al. (2003). Novel peptide inhibitors of angiotensin-converting enzyme 2*. *J. Biol. Chem.* 278, 15532–15540. doi: 10.1074/jbc.M212934200

Huang, Y., Yang, C., Xu, X.-F., Xu, W., and Liu, S.-W. (2020). Structural and functional properties of SARS-CoV-2 spike protein: potential antivirus drug development for COVID-19. *Acta Pharmacol. Sin.* 41, 1141–1149. doi: 10.1038/s41401-020-0485-4

Iwata-Yoshikawa, N., Kakizaki, M., Shiwa-Sudo, N., Okura, T., Tahara, M., Fukushi, S., et al. (2022). Essential role of TMPRSS2 in SARS-CoV-2 infection in murine airways. *Nat. Commun.* 13:6100. doi: 10.1038/s41467-022-33911-8

Jaimes, J. A., André, N. M., Chappie, J. S., Millet, J. K., and Whittaker, G. R. (2020). Phylogenetic analysis and structural modeling of SARS-CoV-2 spike protein reveals an evolutionary distinct and proteolytically sensitive activation loop. *J. Mol. Biol.* 432, 3309–3325. doi: 10.1016/j.jmb.2020.04.009

Jaiswal, G., and Kumar, V. (2020). In-silico design of a potential inhibitor of SARS-CoV-2 S protein. *PLoS One* 15:e0240004. doi: 10.1371/journal.pone.0240004

Javorsky, A., Humbert, P. O., and Kvansakul, M. (2021). Structural basis of coronavirus E protein interactions with human PALS1 PDZ domain. *Commun. Biol.* 4:724. doi: 10.1038/s42003-021-02250-7

Kasuga, Y., Zhu, B., Jang, K.-J., and Yoo, J.-S. (2021). Innate immune sensing of coronavirus and viral evasion strategies. *Exp. Mol. Med.* 53, 723–736. doi: 10.1038/s12276-021-00602-1

Ke, M., Chen, Y., Wu, A., Sun, Y., Su, C., Wu, H., et al. (2012). Short peptides derived from the interaction domain of SARS coronavirus nonstructural protein nsp10 can suppress the 2′-O-methyltransferase activity of nsp10/nsp16 complex. *Virus Res.* 167, 322–328. doi: 10.1016/j.virusres.2012.05.017

Kirchdoerfer, R. N., and Ward, A. B. (2019). Structure of the SARS-CoV nsp12 polymerase bound to nsp7 and nsp8 co-factors. *Nat. Commun.* 10:2342. doi: 10.1038/s41467-019-10280-3

Konno, Y., Kimura, I., Uriu, K., Fukushi, M., Irie, T., Koyanagi, Y., et al. (2020). SARS-CoV-2 ORF3b is a potent interferon antagonist whose activity is increased by a naturally occurring elongation variant. *Cell Rep.* 32:108185. doi: 10.1016/j.celrep.2020.108185

Lei, X., Dong, X., Ma, R., Wang, W., Xiao, X., Tian, Z., et al. (2020). Activation and evasion of type I interferon responses by SARS-CoV-2. *Nat. Commun.* 11:3810. doi: 10.1038/s41467-020-17665-9

Li, J., Guo, M., Tian, X., Wang, X., Yang, X., Wu, P., et al. (2021). Virus-host Interactome and proteomic survey reveal potential virulence factors influencing SARS-CoV-2 pathogenesis. *Medicine* 2, 99–112.e7. doi: 10.1016/j.medj.2020.07.002

Li, J., Jia, H., Tian, M., Wu, N., Yang, X., Qi, J., et al. (2022). SARS-CoV-2 and emerging variants: unmasking structure, function, infection, and immune escape mechanisms. *Front. Cell. Infect. Microbiol.* 12:869832. doi: 10.3389/fcimb.2022.869832

Ling, R., Dai, Y., Huang, B., Huang, W., Yu, J., Lu, X., et al. (2020). In silico design of antiviral peptides targeting the spike protein of SARS-CoV-2. *Peptides* 130:170328. doi: 10.1016/j.peptides.2020.170328

Liu, C., Mendonça, L., Yang, Y., Gao, Y., Shen, C., Liu, J., et al. (2020). The architecture of inactivated SARS-CoV-2 with postfusion spikes revealed by Cryo-EM and Cryo-ET. *Structure* 28, 1218–1224.e4. doi: 10.1016/j.str.2020.10.001

Liu, S., Xiao, G., Chen, Y., He, Y., Niu, J., Escalante, C. R., et al. (2004). Interaction between heptad repeat 1 and 2 regions in spike protein of SARS-associated coronavirus: implications for virus fusogenic mechanism and identification of fusion inhibitors. *Lancet* 363, 938–947. doi: 10.1016/S0140-6736(04)15788-7

Lo, Y.-S., Lin, S.-Y., Wang, S.-M., Wang, C.-T., Chiu, Y.-L., Huang, T.-H., et al. (2013). Oligomerization of the carboxyl terminal domain of the human coronavirus 229E nucleocapsid protein. *FEBS Lett.* 587, 120–127. doi: 10.1016/j.febslet.2012.11.016

Lu, L., Liu, Q., Zhu, Y., Chan, K.-H., Qin, L., Li, Y., et al. (2014). Structure-based discovery of middle east respiratory syndrome coronavirus fusion inhibitor. *Nat. Commun.* 5:3067. doi: 10.1038/ncomms4067

Lu, X., Pan, J., Tao, J., and Guo, D. (2011). SARS-CoV nucleocapsid protein antagonizes IFN-β response by targeting initial step of IFN-β induction pathway, and its C-terminal region is critical for the antagonism. *Virus Genes* 42, 37–45. doi: 10.1007/s11262-010-0544-x

Ma, C., Sacco, M. D., Hurst, B., Townsend, J. A., Hu, Y., Szeto, T., et al. (2020). Boceprevir, GC-376, and calpain inhibitors II, XII inhibit SARS-CoV-2 viral replication by targeting the viral main protease. *Cell Res.* 30:678. doi: 10.1038/s41422-020-0356-z

Mahtarin, R., Islam, S., Islam, M. J., Ullah, M. O., Ali, M. A., and Halim, M. A. (2022). Structure and dynamics of membrane protein in SARS-CoV-2. *J. Biomol. Struct. Dyn.* 40, 4725–4738. doi: 10.1080/07391102.2020.1861983

Malone, B., Urakova, N., Snijder, E. J., and Campbell, E. A. (2022). Structures and functions of coronavirus replication–transcription complexes and their relevance for SARS-CoV-2 drug design. *Nat. Rev. Mol. Cell Biol.* 23, 21–39. doi: 10.1080/07391102.2020.1861983

Matsuyama, S., Nao, N., Shirato, K., Kawase, M., Saito, S., Takayama, I., et al. (2020). Enhanced isolation of SARS-CoV-2 by TMPRSS2-expressing cells. *Proc. Natl. Acad. Sci. U. S. A.* 117, 7001–7003. doi: 10.1073/pnas.2002589117

Matsuyama, S., Shirato, K., Kawase, M., Terada, Y., Kawachi, K., Fukushi, S., et al. (2018). Middle east respiratory syndrome coronavirus spike protein is not activated directly by cellular furin during viral entry into target cells. *J. Virol.* 92, e00683–e00718. doi: 10.1128/JVI.00683-18

Mcbride, R., Van Zyl, M., and Fielding, B. C. (2014). The coronavirus nucleocapsid is a multifunctional protein. *Viruses* 6, 2991–3018. doi: 10.3390/v6082991

Miorin, L., Kehrer, T., Sanchez-Aparicio, M. T., Zhang, K., Cohen, P., Patel, R. S., et al. (2020). SARS-CoV-2 Orf6 hijacks Nup98 to block STAT nuclear import and antagonize interferon signaling. *Proc. Natl. Acad. Sci. U. S. A.* 117, 28344–28354. doi: 10.1073/pnas.2016650117

Nieto-Torres, J. L., Verdiá-Báguena, C., Jimenez-Guardeño, J. M., Regla-Nava, J. A., Castaño-Rodriguez, C., Fernandez-Delgado, R., et al. (2015). Severe acute respiratory syndrome coronavirus E protein transports calcium ions and activates the NLRP3 inflammasome. *Virology* 485, 330–339. doi: 10.1016/j.virol.2015.08.010

O'keefe, B. R., Giomarelli, B., Barnard, D. L., Shenoy, S. R., Chan, P. K., Mcmahon, J. B., et al. (2010). Broad-spectrum in vitro activity and in vivo efficacy of the antiviral protein griffithsin against emerging viruses of the family Coronaviridae. *J. Virol.* 84, 2511–2521. doi: 10.1128/JVI.02322-09

Peacock, T. P., Goldhill, D. H., Zhou, J., Baillon, L., Frise, R., Swann, O. C., et al. (2021). The furin cleavage site in the SARS-CoV-2 spike protein is required for transmission in ferrets. *Nat. Microbiol.* 6, 899–909. doi: 10.1038/s41564-021-00908-w

Rawson, T. M., Ming, D., Ahmad, R., Moore, L. S. P., and Holmes, A. H. (2020). Antimicrobial use, drug-resistant infections and COVID-19. *Nat. Rev. Microbiol.* 18, 409–410. doi: 10.1038/s41579-020-0395-y

Redondo, N., Zaldívar-López, S., Garrido, J. J., and Montoya, M. (2021). SARS-CoV-2 accessory proteins in viral pathogenesis: knowns and unknowns. *Front. Immunol.* 12:708264. doi: 10.3389/fimmu.2021.708264

Rockett, R., Basile, K., Maddocks, S., Fong, W., Agius, J. E., Johnson-Mackinnon, J., et al. (2022). Resistance mutations in SARS-CoV-2 Delta variant after Sotrovimab use. *N. Engl. J. Med.* 386, 1477–1479. doi: 10.1056/NEJMc2120219

Schoeman, D., and Fielding, B. C. (2019). Coronavirus envelope protein: current knowledge. *Virol. J.* 16:69. doi: 10.1186/s12985-019-1182-0

Schütz, D., Ruiz-Blanco, Y. B., Münch, J., Kirchhoff, F., Sanchez-Garcia, E., and Müller, J. A. (2020). Peptide and peptide-based inhibitors of SARS-CoV-2 entry. *Adv. Drug Deliv. Rev.* 167, 47–65. doi: 10.1016/j.addr.2020.11.007

Shah, J. N., Guo, G.-Q., Krishnan, A., Ramesh, M., Katari, N. K., Shahbaaz, M., et al. (2022). Peptides-based therapeutics: emerging potential therapeutic agents for COVID-19. *Therapie* 77, 319–328. doi: 10.1016/j.therap.2021.09.007

Shang, J., Han, N., Chen, Z., Peng, Y., Li, L., Zhou, H., et al. (2020). Compositional diversity and evolutionary pattern of coronavirus accessory proteins. *Brief. Bioinform.* 22, 1267–1278. doi: 10.1093/bib/bbaa262

Shapira, T., Monreal, I. A., Dion, S. P., Buchholz, D. W., Imbiakha, B., Olmstead, A. D., et al. (2022). A TMPRSS2 inhibitor acts as a pan-SARS-CoV-2 prophylactic and therapeutic. *Nature* 605, 340–348. doi: 10.1038/s41586-022-04661-w

Shen, L. W., Mao, H. J., Wu, Y. L., Tanaka, Y., and Zhang, W. (2017). TMPRSS2: a potential target for treatment of influenza virus and coronavirus infections. *Biochimie* 142, 1–10. doi: 10.1016/j.biochi.2017.07.016

Şimşek-Yavuz, S., and Komsuoğlu elikyurt, F. I. (2021). An update of anti-viral treatment of COVID-19. *Turk. J. Med. Sci.* 51, 3372–3390. doi: 10.3906/sag-2106-250

Snijder, E. J., and Limpens, R. (2020). A unifying structural and functional model of the coronavirus replication organelle: tracking down RNA synthesis. *PLoS Biol.* 18:e3000715. doi: 10.1371/journal.pbio.3000715

Struck, A.-W., Axmann, M., Pfefferle, S., Drosten, C., and Meyer, B. (2012). A hexapeptide of the receptor-binding domain of SARS corona virus spike protein blocks viral entry into host cells via the human receptor ACE2. *Antivir. Res.* 94, 288–296. doi: 10.1016/j.antiviral.2011.12.012

Su, C.-M., Wang, L., and Yoo, D. (2021). Activation of NF-κB and induction of proinflammatory cytokine expressions mediated by ORF7a protein of SARS-CoV-2. *Sci. Rep.* 11:13464. doi: 10.1038/s41598-021-92941-2

Sugrue, R. J., Brown, C., Brown, G., Aitken, J., and Mcl Rixon, H. W. (2001). Furin cleavage of the respiratory syncytial virus fusion protein is not a requirement for its transport to the surface of virus-infected cells. *J. Gen. Virol.* 82, 1375–1386. doi: 10.1099/0022-1317-82-6-1375

Sun, Y., Zhang, H., Shi, J., Zhang, Z., and Gong, R. (2017). Identification of a novel inhibitor against middle east respiratory syndrome coronavirus. *Viruses* 9:255. doi: 10.3390/v9090255

Tannock, G. A., Kim, H., and Xue, L. (2020). Why are vaccines against many human viral diseases still unavailable; an historic perspective? *J. Med. Virol.* 92, 129–138. doi: 10.1002/jmv.25593

Tavassoly, O., Safavi, F., and Tavassoly, I. (2020). Heparin-binding peptides as novel therapies to stop SARS-CoV-2 cellular entry and infection. *Mol. Pharmacol.* 98, 612–619. doi: 10.1124/molpharm.120.000098

Thoms, M., Buschauer, R., Ameismeier, M., Koepke, L., Denk, T., Hirschenberger, M., et al. (2020). Structural basis for translational shutdown and immune evasion by the Nsp1 protein of SARS-CoV-2. *Science* 369, 1249–1255. doi: 10.1126/science.abc8665

Ujike, M., Nishikawa, H., Otaka, A., Yamamoto, N., Yamamoto, N., Matsuoka, M., et al. (2008). Heptad repeat-derived peptides block protease-mediated direct entry from the cell surface of severe acute respiratory syndrome coronavirus but not entry via the endosomal pathway. *J. Virol.* 82, 588–592. doi: 10.1128/JVI.01697-07

Vagner, J., Qu, H., and Hruby, V. J. (2008). Peptidomimetics, a synthetic tool of drug discovery. *Curr. Opin. Chem. Biol.* 12, 292–296. doi: 10.1016/j.cbpa.2008.03.009

Volchkov, V. E., Feldmann, H., Volchkova, V. A., and Klenk, H.-D. (1998). Processing of the Ebola virus glycoprotein by the proprotein convertase furin. *Proc. Natl. Acad. Sci. U. S. A.* 95, 5762–5767. doi: 10.1073/pnas.95.10.5762

Walls, A. C., Park, Y.-J., Tortorici, M. A., Wall, A., Mcguire, A. T., and Veesler, D. (2020). Structure, function, and antigenicity of the SARS-CoV-2 spike glycoprotein. *Cells* 181, 281–292.e6. doi: 10.1016/j.cell.2020.02.058

Wang, C., Wang, S., Li, D., Chen, P., Han, S., Zhao, G., et al. (2021). Human cathelicidin inhibits SARS-CoV-2 infection: killing two birds with one stone. *ACS Infect. Dis.* 7, 1545–1554. doi: 10.1021/acsinfecdis.1c00096

Wang, C., Wang, S., Li, D., Wei, D. Q., Zhao, J., and Wang, J. (2020). Human intestinal defensin 5 inhibits SARS-CoV-2 invasion by cloaking ACE2. *Gastroenterology* 159, 1145–1147.e4. doi: 10.1053/j.gastro.2020.05.015

Wang, C., Xia, S., Zhang, P., Zhang, T., Wang, W., Tian, Y., et al. (2018). Discovery of hydrocarbon-stapled short α-helical peptides as promising middle east respiratory syndrome coronavirus (MERS-CoV) fusion inhibitors. *J. Med. Chem.* 61, 2018–2026. doi: 10.1021/acs.jmedchem.7b01732

Wrapp, D., Wang, N., Corbett, K. S., Goldsmith, J. A., Hsieh, C.-L., Abiona, O., et al. (2020). Cryo-EM structure of the 2019-nCoV spike in the prefusion conformation. *Science* 367, 1260–1263. doi: 10.1126/science.abb2507

Wu, F., Zhao, S., Yu, B., Chen, Y.-M., Wang, W., Song, Z.-G., et al. (2020). A new coronavirus associated with human respiratory disease in China. *Nature* 579, 265–269. doi: 10.1038/s41586-020-2008-3

Xia, S., Lan, Q., Pu, J., Wang, C., Liu, Z., Xu, W., et al. (2019a). Potent MERS-CoV fusion inhibitory peptides identified from HR2 domain in spike protein of bat coronavirus HKU4. *Viruses* 11:56. doi: 10.3390/v11010056

Xia, S., Liu, M., Wang, C., Xu, W., Lan, Q., Feng, S., et al. (2020a). Inhibition of SARS-CoV-2 (previously 2019-nCoV) infection by a highly potent pan-coronavirus fusion inhibitor targeting its spike protein that harbors a high capacity to mediate membrane fusion. *Cell Res.* 30, 343–355. doi: 10.1038/s41422-020-0305-x

Xia, S., Yan, L., Xu, W., Agrawal, A. S., Algaissi, A., Tseng, C.-T. K., et al. (2019b). A pan-coronavirus fusion inhibitor targeting the HR1 domain of human coronavirus spike. *Sci. Adv.* 5:eaav4580. doi: 10.1126/sciadv.aav4580

Xia, S., Zhu, Y., Liu, M., Lan, Q., Xu, W., Wu, Y., et al. (2020b). Fusion mechanism of 2019-nCoV and fusion inhibitors targeting HR1 domain in spike protein. *Cell. Mol. Immunol.* 17, 765–767. doi: 10.1038/s41423-020-0374-2

Yan, L., Ge, J., Zheng, L., Zhang, Y., Gao, Y., Wang, T., et al. (2021). Cryo-EM structure of an extended SARS-CoV-2 replication and transcription complex reveals an intermediate state in cap synthesis. *Cells* 184, 184–193.e10. doi: 10.1016/j.cell.2020.11.016

Yan, W., Zheng, Y., Zeng, X., He, B., and Cheng, W. (2022). Structural biology of SARS-CoV-2: open the door for novel therapies. *Signal Transduct. Target. Ther.* 7:26. doi: 10.1038/s41392-022-00884-5

Yang, K., Wang, C., Kreutzberger, A. J. B., Ojha, R., Kuivanen, S., Couoh-Cardel, S., et al. (2022). Nanomolar inhibition of SARS-CoV-2 infection by an unmodified peptide targeting the prehairpin intermediate of the spike protein. *Proc. Natl. Acad. Sci. U. S. A.* 119:e2210990119. doi: 10.1073/pnas.2210990119

Yao, Y., Luo, Z., and Zhang, X. (2020). In silico evaluation of marine fish proteins as nutritional supplements for COVID-19 patients. *Food Funct.* 11, 5565–5572. doi: 10.1039/d0fo00530d

Yao, H., Song, Y., Chen, Y., Wu, N., Xu, J., Sun, C., et al. (2020). Molecular architecture of the SARS-CoV-2 virus. *Cells* 183, 730–738.e13. doi: 10.1016/j.cell.2020.09.018

Yuan, K., Yi, L., Chen, J., Qu, X., Qing, T., Rao, X., et al. (2004). Suppression of SARS-CoV entry by peptides corresponding to heptad regions on spike glycoprotein. *Biochem. Biophys. Res. Commun.* 319, 746–752. doi: 10.1016/j.bbrc.2004.05.046

Zhang, Q., Chen, X., Li, B., Lu, C., Yang, S., Long, J., et al. (2022). A database of anti-coronavirus peptides. *Sci. Data* 9:294. doi: 10.1038/s41597-022-01394-3

Zhao, H., To, K. K. W., Lam, H., Zhou, X., Chan, J. F.-W., Peng, Z., et al. (2021). Cross-linking peptide and repurposed drugs inhibit both entry pathways of SARS-CoV-2. *Nat. Commun.* 12:1517. doi: 10.1038/s41467-021-21825-w

Zhao, H., To, K. K. W., Sze, K.-H., Yung, T. T.-M., Bian, M., Lam, H., et al. (2020). A broad-spectrum virus-and host-targeting peptide against respiratory viruses including influenza virus and SARS-CoV-2. *Nat. Commun.* 11:4252. doi: 10.1038/s41467-020-17986-9

Zhao, M. M., Yang, W.-L., Yang, F.-Y., Zhang, L., Huang, W.-J., Hou, W., et al. (2021). Cathepsin L plays a key role in SARS-CoV-2 infection in humans and humanized mice and is a promising target for new drug development. *Signal Transduct. Target. Ther.* 6:134. doi: 10.1038/s41392-021-00558-8

Zhao, H., Zhou, J., Zhang, K., Chu, H., Liu, D., Poon, V. K.-M., et al. (2016). A novel peptide with potent and broad-spectrum antiviral activities against multiple respiratory viruses. *Sci. Rep.* 6:22008. doi: 10.1038/srep22008

Zheng, B.-J., Guan, Y., He, M.-L., Sun, H., Du, L., Zheng, Y., et al. (2005). Synthetic peptides outside the spike protein heptad repeat regions as potent inhibitors of sars-associated coronavirus. *Antivir. Ther.* 10, 393–403. doi: 10.1177/135965350501000301

Zhou, P., Yang, X.-L., Wang, X.-G., Hu, B., Zhang, L., Zhang, W., et al. (2020). A pneumonia outbreak associated with a new coronavirus of probable bat origin. *Nature* 579, 270–273. doi: 10.1038/s41586-020-2012-7

Zhu, Y., Yu, D., Yan, H., Chong, H., and He, Y. (2020). Design of potent membrane fusion inhibitors against SARS-CoV-2, an emerging coronavirus with high fusogenic activity. *J. Virol.* 94, e00635–e00640. doi: 10.1128/jvi.00635-20

Zhu, N., Zhang, D., Wang, W., Li, X., Yang, B., Song, J., et al. (2020). A novel coronavirus from patients with pneumonia in China, 2019. *N. Engl. J. Med.* 382, 727–733. doi: 10.1056/NEJMoa2001017

frontiers | Frontiers in Microbiology

TYPE Original Research
PUBLISHED 16 February 2023
DOI 10.3389/fmicb.2023.1066493

OPEN ACCESS

EDITED BY
Yang Yang,
Iowa State University,
United States

REVIEWED BY
Christian Albert Devaux,
Centre National de la Recherche Scientifique (CNRS), France
Zhen Luo,
Jinan University,
China

*CORRESPONDENCE
Salvador Meseguer
✉ smeseguer@cipf.es
Fernando Almazan
✉ falmazan@cnb.csic.es
Enric Esplugues
✉ enric.esplugues@yale.edu

†These authors have contributed equally to this work and share senior authorship

SPECIALTY SECTION
This article was submitted to Virology, a section of the journal Frontiers in Microbiology

RECEIVED 10 October 2022
ACCEPTED 26 January 2023
PUBLISHED 16 February 2023

CITATION
Meseguer S, Rubio M-P, Lainez B, Pérez-Benavente B, Pérez-Moraga R, Romera-Giner S, García-García F, Martinez-Macias O, Cremades A, Iborra FJ, Candelas-Rivera O, Almazan F and Esplugues E (2023) SARS-CoV-2-encoded small RNAs are able to repress the host expression of SERINC5 to facilitate viral replication.
Front. Microbiol. 14:1066493.
doi: 10.3389/fmicb.2023.1066493

SARS-CoV-2-encoded small RNAs are able to repress the host expression of SERINC5 to facilitate viral replication

Salvador Meseguer[1]*, Mari-Paz Rubio[1], Begoña Lainez[1], Beatriz Pérez-Benavente[1], Raúl Pérez-Moraga[2], Sergio Romera-Giner[2], Francisco García-García[2], Olalla Martinez-Macias[3], Antonio Cremades[3], Francisco J. Iborra[4], Oscar Candelas-Rivera[5], Fernando Almazan[5]*† and Enric Esplugues[1,6]*†

[1]Molecular and Cellular Immunology Laboratory, Centro de Investigación Príncipe Felipe (CIPF), Valencia, Spain, [2]Bioinformatics and Biostatistics Unit, Centro de Investigación Príncipe Felipe (CIPF), Valencia, Spain, [3]Hospital Universitario de la Ribera, Valencia, Spain, [4]Biological Noise and Cell Plasticity Laboratory, Centro de Investigación Príncipe Felipe (CIPF), Associated Unit to Instituto de Biomedicina de Valencia-CSIC, Valencia, Spain, [5]Molecular and Cellular Biology Department, Centro Nacional de Biotecnología (CNB), CSIC, Madrid, Spain, [6]Department of Comparative Medicine, Yale School of Medicine, New Haven, CT, United States

Serine incorporator protein 5 (SERINC5) is a key innate immunity factor that operates in the cell to restrict the infectivity of certain viruses. Different viruses have developed strategies to antagonize SERINC5 function but, how SERINC5 is controlled during viral infection is poorly understood. Here, we report that SERINC5 levels are reduced in COVID-19 patients during the infection by SARS-CoV-2 and, since no viral protein capable of repressing the expression of SERINC5 has been identified, we hypothesized that SARS-CoV-2 non-coding small viral RNAs (svRNAs) could be responsible for this repression. Two newly identified svRNAs with predicted binding sites in the 3′-untranslated region (3′-UTR) of the SERINC5 gene were characterized and we found that the expression of both svRNAs during the infection was not dependent on the miRNA pathway proteins Dicer and Argonaute-2. By using svRNAs mimic oligonucleotides, we demonstrated that both viral svRNAs can bind the 3′UTR of SERINC5 mRNA, reducing SERINC5 expression *in vitro*. Moreover, we found that an anti-svRNA treatment to Vero E6 cells before SARS-CoV-2 infection recovered the levels of SERINC5 and reduced the levels of N and S viral proteins. Finally, we showed that SERINC5 positively controls the levels of Mitochondrial Antiviral Signalling (MAVS) protein in Vero E6. These results highlight the therapeutic potential of targeting svRNAs based on their action on key proteins of the innate immune response during SARS-CoV-2 viral infection.

KEYWORDS

SARS-CoV-2, viral miRNAs, SERINC5, MAVS, innate immune response

1. Introduction

Host restriction factors are a set of cell proteins that limit the replication of viruses at various stages through different mechanisms (Colomer-Lluch et al., 2018). Many host restriction factors are induced in response to type I interferon (IFN-I), whose expression is stimulated in the detection of viral pathogens by the activation of pattern recognition receptors (PRRs), such as retinoic

acid-induced gene I (RIG-I) and melanoma differentiation-associated protein 5 (MDA5). Serine incorporator protein 5 (SERINC5) is a member of a protein family that participates in lipid biosynthesis and/or transport in mammalian cells (Inuzuka et al., 2005). Although it is not induced by IFN-I, SERINC5 has also been considered a restriction factor since it impairs the infectivity of several retroviruses, such as murine leukemia virus (MLV), human immune deficiency virus (HIV), equine infectious anemia virus (EIAV) (Ahi et al., 2016; Chande et al., 2016; Trautz et al., 2017), and other viruses (Ahi et al., 2016; Firrito et al., 2018). To date, there is limited knowledge of the mechanism of action of the SERINC5 protein (Matheson et al., 2015). Incorporation of this protein into HIV-1 virions has been shown to block the formation of the virus-cell fusion pore, preventing virus entry into new target cells (Matheson et al., 2015; Rosa et al., 2015; Usami et al., 2015). On the other hand, two recent studies have shown two additional antiviral activities for SERINC5. One describes that SERINC5 inhibits Hepatitis B virion (HBV) secretion by interfering with the glycosylation of HBV envelope proteins (Liu et al., 2020), and the other demonstrates that SERINC5 can interact with the outer mitochondrial antiviral signaling protein (MAVS) and the E3 ubiquitin ligase/adaptor protein TRAF6, resulting in MAVS aggregation and polyubiquitination of TRAF6. These events are critical for IFN-I signaling and nuclear factor kappa B (NFkB) activation (Zeng et al., 2021).

Conversely, viruses have developed different strategies to antagonize most of the host restriction factors (Goujon et al., 2013; Kane et al., 2013; Simon et al., 2015; Colomer-Lluch et al., 2018; Ghimire et al., 2018). In the case of SERINC5, its antiviral functions are counteracted by several virus-encoded proteins including, HIV-1 Nef, the glycogag protein of MLV, and the EIAV S2 protein. These viral proteins alter the subcellular localization of SERINC5 and prevent its insertion into viral particles (Chande et al., 2016). For instance, HIV-1 Nef decreases levels of SERINC5 at the plasma membrane and relocates it into the lysosomal compartments to avoid its incorporation in the HIV-1 virions, thus, facilitating the HIV-1 infectivity (Chande et al., 2016). Moreover, mutations in the HIV-1 envelope glycoprotein present in some strains were shown to alter the sensitivity of the virus to SERINC5 (Usami et al., 2015; Ahi et al., 2016; Chande et al., 2016; Beitari et al., 2017). Although the main reported viral mechanism to antagonize the antiviral activity of SERINC5 is to relocate SERINC5 within the cell, it has been shown that expression of SERINC5 can also be down-regulated upon the infection both *in vitro* and *in vivo* (Li et al., 2020). For instance, the infection by the classical swine fever virus (CSFV), which causes a highly contagious viral disease in pigs (Becher et al., 2003), reduces SERINC5 expression by an unknown mechanism (Li et al., 2020). This fact again supports the key role of SERINC5 in the host defense against viral infection.

It has been proved that both DNA and RNA viral genomes can encode non-coding small viral RNAs (svRNAs) like miRNAs (Skalsky and Cullen, 2010; Nanbo et al., 2021). miRNAs are small (19–28 nucleotides) non-coding single-stranded RNAs that bind to the 3′ untranslated regions (3′ UTR) of target mRNA/s, regulating their stability and translation. These elements can be considered more strategic than viral proteins in terms of regulation of gene expression due to their small size, their absence of immunogenicity and their multi-target hit with rapid evolution capacity. When viral miRNAs are expressed in host cells, they can optimize the cellular environment and promote viral replication and survival by targeting host genes involved in proliferation, apoptosis and immune defense (Skalsky and Cullen, 2010; Kincaid and Sullivan, 2012). It was generally believed that RNA viruses would not encode miRNAs to avoid excision of their genomes or transcriptome by the miRNA processing machinery. However, there are RNA viruses that express small regulatory RNAs such as miRNAs. For example hav-miR-1-5p and hav-miR-2-5p are expressed during Hepatitis A virus (HAV) infection (Shi et al., 2014). Moreover, the deep sequencing analysis of small RNAs from lungs of mice infected with severe acute respiratory syndrome coronavirus (SARS-CoV) revealed three 18-22 nt svRNAs originated from the nsp3 and N genomic regions of SARS-CoV. Authors found that one of them, svRNA-N, contributes to SARS-CoV pathogenesis by regulating the production of proinflammatory cytokines (Morales et al., 2017). Despite these examples in RNA viruses, these small RNAs do not seem to possess the canonical stem-loop structure of miRNAs, and their biogenesis and mechanism of action are not completely clear (Varble and ten Oever, 2011; Mishra et al., 2019).

SARS-CoV-2 is an enveloped positive-sense, single-stranded RNA virus, that belongs to the *Sabecovirus* subgenus (Coronaviridae Study Group of the International Committee on Taxonomy of Viruses, 2020) and is behind the current pandemic of Coronavirus disease 2019 (COVID-19). This virus causes symptoms of the common cold (fever, coughing, etc.), unusual symptoms (loss of smell or taste), breathing problems, and gastrointestinal symptoms (nausea, vomiting, etc.). The condition can change into a serious respiratory illness such as severe pneumonia and acute respiratory distress syndrome (ARDS), finally causing death (Redd et al., 2020; Yang et al., 2020). The RNA viral genome (about 30,000 nt) carries two overlapping open reading frames (ORF 1a and 1b) that encode for the main components of the transcription-replication complex and genes encoding for the structural and genus-specific proteins (S, 3a, 3b, E, M, 6, 7a, 7b, 8, N, and 10) (Hartenian et al., 2020; Mittal et al., 2020; Wu et al., 2020; Zhu et al., 2020). Recently, several studies also demonstrated the existence of miRNAs encoded in the SARS-CoV-2 genome and their biological relevance (Grehl et al., 2021; Pawlica et al., 2021; Singh et al., 2022). Also, by using computational approaches, several studies have predicted the possible existence of viral miRNAs with diverse roles in the pathogenicity of this virus (Abedi et al., 2021).

Based on the key role of SERINC5 in virus infection, we have analyzed the expression of SERINC5 during SARS-CoV-2 infection in two distinct cell lines from a GEO dataset. The *in silico* study revealed a decrease of SERINC5 mRNA during the infection course, suggesting that SARS-CoV-2 antagonizes SERINC5 activity by downregulating its expression. Given that no SARS-CoV-2 protein capable of controlling the expression of SERINC5 has been described so far and considering the emerging evidence pointing to the existence of miRNAs encoded in the genome of the SARS-CoV-2, as occurs in other viruses, we wanted to address the hypothesis that SERINC5 expression can be regulated by svRNAs. Using two different *in silico* approaches, we identified two svRNAs, as putative miRNA-like regulators of SERINC5. We found an anti-correlative expression between these two svRNAs and SERINC5 in different biological samples, including samples from COVID-19 patients. Furthermore, we proved that silencing of both svRNAs during the course of infection of Vero E6 cells restores SERINC5 expression and enhances the levels of its direct interacting partner, MAVS, a master protein involved in antiviral response. We also showed that these molecular changes were accompanied by a reduction in the expression of the viral proteins N and S.

2. Materials and methods

2.1. Human samples and ethics statement

Swabs and saliva samples were provided by Hospital Universitario de la Ribera (Valencia, Spain). All samples were collected from COVID-19

patients or healthy subjects and written informed consent was obtained from the participants. All procedures were approved by the Ethics Committee of Hospital Universitario de la Ribera (Valencia, Spain) and performed under the guidelines set forth by the Declaration of Helsinki.

2.2. Biosafety

All the experiments with SARS-CoV-2 were approved by the National Centre for Biotechnology (CNB-CSIC) Institutional Biosafety Committee (IBC) and were carried out in an appropriate biosafety level 3 (BSL3) laboratory at CNB following the safety guidelines and procedures approved for this kind of laboratory.

2.3. Cells and viruses

Vero E6 cells (African green monkey kidney epithelial cells) were obtained from the American Type Culture Collection (ATCC; CRL-1586). HEK293T-hACE2 cells, expressing the human angiotensin I converting enzyme 2 (ACE2), were kindly provided by Dr. Martinez-Sobrido (Texas Biomedical Research Institute, San Antonio, United States).

Vero E6 negative control cells and Vero E6 cells overexpressing SERINC5 were obtained by transfection of Vero E6 cells with 1 μg/mL of the empty plasmid pIRES2 ZsGreen1 or the plasmid pIRES2 ZsGreen1 containing the *Chlorocebus* SERINC5 cDNA, using Lipofectamine 2000 reagent (Invitrogen) and Opti-MEM medium according to manufacturer's instructions. Forty-eight hours after transfection, cells were sorted by ZsGreen signal using SONY sorter and selected with 1 mg/mL G-418 for 48 h and then grown with 0.5 mg/mL G-418.

In all cases, cells were cultured in high glucose Dulbecco's modified Eagle medium (DMEM, Gibco) supplemented with 25 mM HEPES, 10% Fetal Bovine Serum (FBS), 1 mM sodium pyruvate, 100 U/mL penicillin, 100 μg/mL streptomycin, 2 mM glutamine and 1 mM non-essential amino acids (growth medium). They were kept at 37°C in a humidified atmosphere with 5% CO_2.

SARS-CoV-2 MAD6 isolate was kindly provided by Dr. Luis Enjuanes (CNB-CSIC, Madrid, Spain). This virus was obtained in March 2020 from the nasal sample of a COVID-19 patient hospitalized in Hospital 12 de Octubre (Madrid, Spain), after obtaining the patient's informed consent and Regional Government permits. The genome sequence is identical to that of Wuhan-Hu-1 (GenBank MN908947) except for three mutations: C3037T (silent), C14408T (P214L in Nsp12), and A234303G (D614G in S). From the nasal sample, the virus was cloned by plaque assay and amplified in confluent Vero E6 cells to generate a working virus stock. This virus stock was used to infect Vero E6 and HEK293T-hACE2 cells using virus growth medium (growth medium containing 2% FBS). A multiplicity of infection (MOI) of 1 plaque forming unit (PFU) per cell was used in most of the experiments.

2.4. Virus titration

Confluent monolayers of Vero E6 cells seeded in 12-well plates were infected with 300 μL of serial 10-fold dilutions of the virus in virus growth medium for 1 h at 37°C. After viral adsorption, the viral inoculum was removed and the cells overlaid with 2 mL virus growth medium containing 1% DEAE-Dextran (Sigma-Aldrich) and 0.6% low-melting-point agarose. After 3 days of incubation at 37°C, the cells were fixed with 10% formaldehyde for 1 h at room temperature, the overlaid removed, and the viral plaques visualized by staining with 0.1% crystal violet in 20% methanol. Visible plaques were counted and virus titer was calculated as PFU/mL.

2.5. Plasmids construction

The plasmid pIRES2-ZsGreen 1 (PT3824–5, Clontech) was used to insert the *Chlorocebus* SERINC5 cDNA into its NheI and EcoRI sites. On the other hand, to clone the 3′ end of the 3′UTR of SERINC5 gene, a 1Kb PCR product insert was purified using the PCR Clean-Up kit. Linearization of pMir was performed with MluI according to the manufacturer's instructions. The purified PCR insert was cloned into linearized pMir with the In-Fusion HD Cloning Plus enzyme mix and then transformed into the provided Stellar Competent Cells. Both plasmid constructs were verified by DNA sequencing. The oligonucleotides used to amplify the full cDNA and the 3'UTR of SERINC5 are indicated in Table 1.

2.6. Cell transfections

We used two classes of oligonucleotides in transfection experiments. mirVana miRNA mimics are oligonucleotides designed for their use in *in vitro* and *in vivo* gain-of-function experiments. mirVana miRNA mimics are small, double-stranded RNAs that mimic endogenous precursor miRNAs (pre-miRNAs). One strand is identical to and effectively mimics a known mature miRNA. The manufacturer's design of these oligonucleotides and their chemical modifications optimize selection of the active strand for uptake and activation by the RNA-induced silencing complex (RISC). On the other hand, mirVana miRNA inhibitors are designed for their use in *in vitro* and *in vivo* loss-of-function experiments. mirVana miRNA inhibitors are single-stranded RNA-based oligonucleotides that are designed to bind to, and inhibit the activity of endogenous miRNAs when introduced into cells. The design coupled to chemical modifications improves potency and specificity for miRNA inhibition.

In particular, we used the custom version of mirVana miRNA mimics and inhibitors since they are synthesized by the manufacturer basing on the unpublished mature miRNA sequences provided by the customer (svRNA 1: ACTCATGCAGACCACACAAGGCAG; svRNA2: CAAAACATTCCCACCAACAGAGCC) (Table 1). Previously, the sequence input passes the design requirements established by manufacturer's design tool (GeneAssist™ miRNA Workflow Builder). Both, custom mimics and inhibitors, incorporates the same chemical modifications as the manufacturer's predesigned mirVana mimics and inhibitors. The complete sequences from custom mirVana miRNA mimics, inhibitors or their respective controls require a confidential disclosure agreement. 1–100 nM is the concentration range recommended by the manufacturer for optimization experiments. We observed maximum effects at 60 nM.

For the transfections with the above oligonucleotides, Vero E6 or HEK293T-hACE2 cells were seeded at 500,000 cells/well in 6 well plates. After 24 h, transfection mix for each well was prepared by adding drop by drop with a 100 μL-pipette a mix containing 2.4 μL of 50 μM of one of the above oligonucleotides [mimic molecules (custom mirVana miRNA mimic; Thermofisher) of svRNA 1 (pre-svRNA 1), svRNA 2 (pre-svRNA 2), or antisense oligonucleotides (custom mirVana miRNA

inhibitor; Thermofisher) targeting svRNA 1 (anti-svRNA 1), svRNA 2 (anti-svRNA 2) or their respective negative controls (NC) [mirVana miRNA Mimic Negative Control #1 (NC-pre-svRNA; 4,464,058, Thermofisher) and mirVana™ miRNA Inhibitor Negative Control #1 (NC-anti-svRNA; 4,464,076, Thermofisher)]] and 250 µL of Opti-MEM medium to a mix containing 4 µL of Lipofectamine 2000 reagent (Invitrogen) and 250 µL of Opti-MEM medium. After 30 min of incubation, the 500 µL-transfection mix was added to the cells from the well in which the growth medium was previously replaced by 1.5 mL of Opti-MEM medium. The medium was replaced by fresh growth medium 6 h after transfection and cells were infected 24 h after transfection with SARS-CoV-2 at a MOI of 1 UFP/cell.

The same conditions were used for the transfection of HEK293T-hACE2 cells with Sigma siRNAs targeting Dicer (SASI-Hs01-00160748, SASI_Hs01_00130221) or Ago2 (SASI-Hs01-00343736, SASI_Hs01_00161740) or with negative control (NC) siRNA (SIC001).

2.7. RNA isolation and RT-qPCR

Total RNA from saliva, from preservation solution in contact with the swab or from cell pellet was isolated using TRI reagent (Sigma) following the manufacturer's protocol.

To quantify mRNA levels, one-step RT-qPCRs were performed in an Applied Biosystems Step-One Real-Time PCR System. To that end, 25 ng of total RNA were reverse-transcribed and amplified by qPCR in a 12 µL total volume reaction containing specific primers (Table 1), Power SYBR Green PCR Master Mix, MultiScribe Reverse Transcriptase, and RNase Inhibitor (all from Applied Biosystems), according to the manufacturer's instructions. The amplification efficiency values were very close to 100%. Relative quantitation of mRNA levels was calculated using the ΔΔCt method and ribonuclease P/MRP subunit p30 (RPP30) mRNAs as endogenous control. The viral titer of each sample was estimated by determining the viral E mRNA copies/mL. They were calculated by interpolation in a standard curve (Ct vs. amount) prepared from a serial dilution of a SARS-CoV-2 genome standard [1.05×10^8 genome equivalents/mL (NR-52285, bei Resources)].

For svRNA quantification, 10 ng of total RNA were reverse-transcribed in 15 µL total reaction volume using the MultiScribe reverse transcriptase and custom miRNA-specific stem-loop RT primers (Table 1). Then, 1.33 µL of the reverse transcription reaction was subjected to a custom TaqMan miRNA assay (Table 1), in a total reaction volume of 12 µL, using specific primers and probes for the svRNAs and U6 snRNA (Table 1), according to the manufacturer's protocol. Expression values were calculated using the ΔΔCt method and U6 snRNA, the most commonly used endogenous control gene in miRNA

TABLE 1 Oligonucleotides used in the study.

Oligonucleotides used for mRNA level quantitation (RT-qPCR)				
Name	Sequence	Gene	Provider	
IFNβ Fwd	CATGAGCTACAACTTGCTTGG	IFNβ	IDT	
IFNβ Rev	TCCTCCTTCTGGAACTGCTG			
ISG20 Fwd	TGACAAGTTTGCCCTGAGTG	ISG20	IDT	
ISG20 Rev	ATGCTTTAACTGGCGTCACC			
CCL20 Fwd	GCTTTGATGTCAGTGCTGCTAC	CCL20	IDT	
CCL20 Rev	TTGGATTTGCGCACACAG			
SERINC5 Fwd	ATCGAGTTCTGACGCTCTGC	SERINC5	IDT	
SERINC5 Rev	GCTCTTCAGTGTCCTCTCCAC			
RPP30 Fwd	CTATTAATGTGGCGATTGACCGA	RPP30	IDT	
RPP30 Rev	TGAGGGCACTGGAAATTGTAT			
Sequences used to order the custom TaqMan miRNA assays				
Name	Target sequence	Gene	Provider	
svRNA 1	ACTCATGCAGACCACACAAGGCAG	svRNA 1	Thermo Fisher Scientific	
svRNA 2	CAAAACATTCCCACCAACAGAGCC	svRNA 2	Thermo Fisher Scientific	
TaqMan miRNA control assay				
Name	Assay ID	Gene	Provider	
U6 snRNA	001973	U6 snRNA	Thermo Fisher Scientific	
Oligonucleotides used for the cloning of the 3′ UTR of SERINC5 into pMIR				
Name	Sequence	Restriction enzyme	Gene	Provider
SERINC5_3UTR_F	GAAacgcgtTGATATCGGCGGTCCCCT	*MluI*	SERINC5	IDT
SERINC5_3UTR_R	GAAacgcgtTTGCACACCACAGATATATATCT	*MluI*		
Oligonucleotides used for the cloning of SERINC5 cDNA into pIRES2 ZsGreen1 plasmid				
Name	Sequence	Restriction enzyme	Gene	Provider
mSERINC5 Fwd	GGACGAgctagcATGTCAGCTCAGTGCTGTGCAGGCCAGCT	*NheI*	SERINC5	IDT
mSERINC5 Rev	GTATTAgaattcTCACACAGAGAACTCCCGGGTGGGGCAGCAGA	*EcoRI*	SERINC5	

The lowercase letters indicate restriction enzyme sites introduced for cloning.

RT-qPCR assays. When the expression value was calculated with respect to uninfected samples (reference or control), we used the Ct value of the product detected in the PCR reaction (non-specific product) as the Ct value for the reference sample.

2.8. Western blot analysis

Cell extracts were prepared in Laemmli sample buffer (2% SDS, 10% glycerol, 5% 2-mercaptoethanol, 0.004% bromophenol blue and 0.0625 M Tris HCl pH 6.8) containing 0.1 mM leupeptin and 1 mM phenylmethanesulphonyl fluoride, and boiled at 95°C for 10 min. Then, 15 µL of lysates were resolved by SDS/PAGE (12% polyacrylamide) and transferred to PVDF membranes (GE Healthcare, Amersham Biosciences) following the manufacturer's recommendations. Membranes were blocked for 1 h at room temperature with 5% dried skimmed milk in TBS (20 mM Tris–HCl pH 7.5, 150 mM NaCl) and then probed overnight at 4°C with specific antibodies diluted in TTBS (TBS containing 0.1% Tween 20) containing 3% dried skimmed milk. We used the following primary antibodies: 1:5,000-diluted anti-SARS-CoV-2 N protein (40143-MM05, Sino Biological), 1:1,000-diluted anti-SARS-CoV-2 S protein (GTX632604, GeneTex), 1:500-diluted anti-SERINC5 (ab204400), 1:500-diluted anti-MAVS (24,930, Cell Signaling), and 1:10,000-diluted anti-Tubulin (ab6160). The blots were then incubated with the secondary antibodies anti-rabbit (A0545) or anti-mouse (A9044) IgG-horseradish peroxidase-conjugated (Sigma-Aldrich) diluted in TTBS-3% dried skimmed milk for 1 h at room temperature, and the immune complexes were detected using Lumi-light Western Blotting substrate (Roche) or ECL prime western blotting detection system (Amersham), according to the manufacturer's instructions. Protein bands were quantified by densitometric analysis with an Image Quant ECL (GE Healthcare).

2.9. Fluorescence microscopy

Vero E6 cells were cultured on coverslips in 24-well plates. Twenty-four hours post-seeding, cells were rinsed with PBS, fixed with 4% paraformaldehyde in PBS for 20 min at room temperature, washed with PBS, permeabilized with 0.5% Triton X-100 in PBS for 10 min and washed twice with PBS. Then, they were blocked with a solution containing 4% FBS in PBS for 30 min at room temperature, and incubated with 1:100-diluted anti-SERINC5 (ab204400), rabbit anti-MAVS (24,930, Cell Signaling) or mouse anti-MAVS (sc-166,583) in blocking solution for 1 h at room temperature. After three washes with PBS, bound antibodies were detected by incubation, as appropriate, with AlexaFluor 594-conjugated anti-mouse (A11020, Invitrogen) or AlexaFluor 633-conjugated anti-rabbit (A21072, Invitrogen) secondary antibodies in blocking solution for 1 h at 37°C. Slides were mounted in Prolong Gold antifade reagent with DAPI (Molecular Probes, 936,576) and images were obtained with an Apotome-equipped Axio Observer Z1 microscope (Carl Zeiss AG).

2.10. Luciferase reporter assay

Vero E6 cells were seeded in 24-well plates at 50,000 cells/well. After 24 h, transfection mix for each well was prepared by adding, drop by drop with a 100 µL-pipette, a mix containing 500 ng of a Firefly Luciferase reporter plasmid, 25 ng of Renilla Luciferase control vector (Promega; internal control), 0.5 µL of 50 µM of one of the svRNA mimics (pre-svRNA 1, pre-svRNA 2) or NC-pre-miR and 50 µL of Opti-MEM medium to a mix containing 1 µL of Lipofectamine 2000 reagent (Invitrogen) and 50 µL of Opti-MEM medium. After 30 min of incubation, the 100 µL-transfection mix was added to the cells from the well in which the growth medium was previously replaced by 400 µL of Opti-MEM medium. The medium was replaced by fresh growth medium 6 h after transfection. 48 h post-transfection, cells were washed with PBS and lysed by shaking the plate/s during 20 min at room temperature with 100 µL of 1X Passive Lysis buffer per well. 20 µL of each cell lysate were transferred into the luminometer plate. Firefly and Renilla luciferase activities from the cell extracts were respectively measured in the luminometer (settings: a 2-s premeasurement delay, followed by a 10-s measurement period for each reporter assay) after sequential addition of 100 µL of Luciferse Assay reagent II and 100 µL of Stop and Glo reagent from the Dual-luciferase Reporter Assay System (Promega).

2.11. Reanalysis of deposited sequencing data and selection of svRNA candidates

To analyze SERINC5 expression in Calu3 and Caco2 cells, SRA files were downloaded from GSE148729. We used for this study SRA files from the sequencing of polyA RNA from Calu3 cells and Caco2 cells, infected or not with SARS-CoV and SARS-CoV-2. Normalized read counts from the SRA files were rescaled to avoid negative values and subsequently logarithmic transformed. Expression levels of SERINC5 at the different time points were plotted for each sample collection.

Data from small RNA were collected from GSE148729 and fastq files were downloaded using SRA-Toolkit. Sequences from these files were trimmed with cutadapt. We removed (i) the Truseq adapter for small RNA (TGGAATTCTCGGGTGCCAAGG), (ii) the first three 5′ nucleotides from the reads, (iii) the reads with a phred below 30, (iv) polyA tails and (v) the very short reads. Then, the DEUS tool for R was used to detect unique reads (human and virus) and to perform differential expression (only reads with zero values in the non-infected condition). Sequence annotation [Homo sapiens (human) GRCh38 (hg38)] and SARS-CoV-2 isolate Wuhan-Hu-1 (NC_045512.2) genomes were used as a reference for the blast and clustering of selected similar sequences. svRNA 2 was one of the most represented in number of counts and also one of the most differentially expressed svRNAs (Supplementary Table S1).

svRNA 1 was selected after exploring the intergenic regions of the SARS-CoV-2 isolate Wuhan-Hu-1 (NC_045512.2) genome with RNA central to find similar non-coding RNA sequences in the human genome. A region from pre-miR-431 was found to be highly similar to the region between N and Orf10 genes from the SARS-CoV-2 genome. This result was also confirmed by searching for similarity with miRBase (search sequences: stem-loop sequences, search method: BLASTN, E-value cutoff: 100, maximum number of hits: 100).

Binding sites for svRNA 1 and 2 were found in the 3'UTR of SERINC5 mRNA using the Diana MR-microT tool.

2.12. Statistical analysis

Statistical analysis was performed using Student's *t*-test and was conducted using GraphPad Prism 8 (GraphPad Software, Inc., San Diego, CA). The statistically significant differences between the means were indicated by asterisks (*$p < 0.05$, **$p < 0.01$, or ***$p < 0.001$), and non-significant differences by ns.

3. Results

3.1. Levels of SERINC5 mRNA are reduced in COVID-19 patients and this reduction is inversely proportional to the level of two svRNAs predicted to bind SERINC5 mRNA

SERINC5 was identified as a critical restriction factor for the infectivity of certain viruses such as HIV-1 (Ahi et al., 2016; Chande et al., 2016; Trautz et al., 2017). To explore whether the expression of SERINC5 is affected during SARS-CoV-2 infection, the level of SERINC5 mRNA was analyzed from transcriptomic data of Calu3 cells infected with SARS-CoV-2 deposited in GEO (GSE148729) and from nasopharyngeal and saliva samples from COVID-19 patients. The analysis of GSE148729 data (Supplementary Figure S1) showed that SERINC5 mRNA levels progressively decrease with the time of infection in Calu3 cells. Similar results were obtained with Caco2 cells (data not shown). Then, we evaluated the level of SERINC5 mRNA in nasopharyngeal (swabs) and saliva samples from patients with COVID-19 and controls. RT-qPCR analysis of SERINC5 mRNA levels showed a significant reduction in both types of samples from patients compared to controls (Figure 1A). When the correlation between SERINC5 expression and viral titer (assessed in terms of subgenomic E mRNA expression) was analyzed (Figure 1B), we found a clear inverse correlation in the swabs samples. However, in saliva this correlation was not significant, likely due to the complex nature of this sample type, with many contaminants (proteins, complex organic molecules, and bacteria) and RNAses that may affect the quality of RNA. Altogether, these data indicated that the infection of SARS-CoV-2 induced a reduction in the levels of SERINC5 mRNA.

In SARS-CoV-2 no viral protein capable of repressing the expression of SERINC5 in host cells has been identified. Therefore, we investigated the hypothesis that the genome of the virus harbors small RNA regulators of host gene expression, similar to miRNAs, that could be responsible for the reduction of SERINC5 levels during infection. Through an *in silico* study, we identified two svRNAs (svRNAs 1 and 2) with predicted binding sites in the 3'UTR region of the SERINC5 gene (Figure 2). svRNA 1 was identified from the analysis of the intergenic regions of the SARS-CoV-2 genome with the RNA central program. RNA Central Resources can identify, in a sequence query, any small non-coding RNA (sncRNA) sequence similar to those deposited in the database. This database houses all types of ncRNA from a wide range of organisms. RNA central provided a 24 nt sequence, located in the intergenic sequence between N and ORF10 genes at the 3'-end of the SARS-CoV-2 genome (29,534 nt–29,557 nt; Figure 2A), which was similar to the cellular microRNA precursor pre-miRNA-431. This

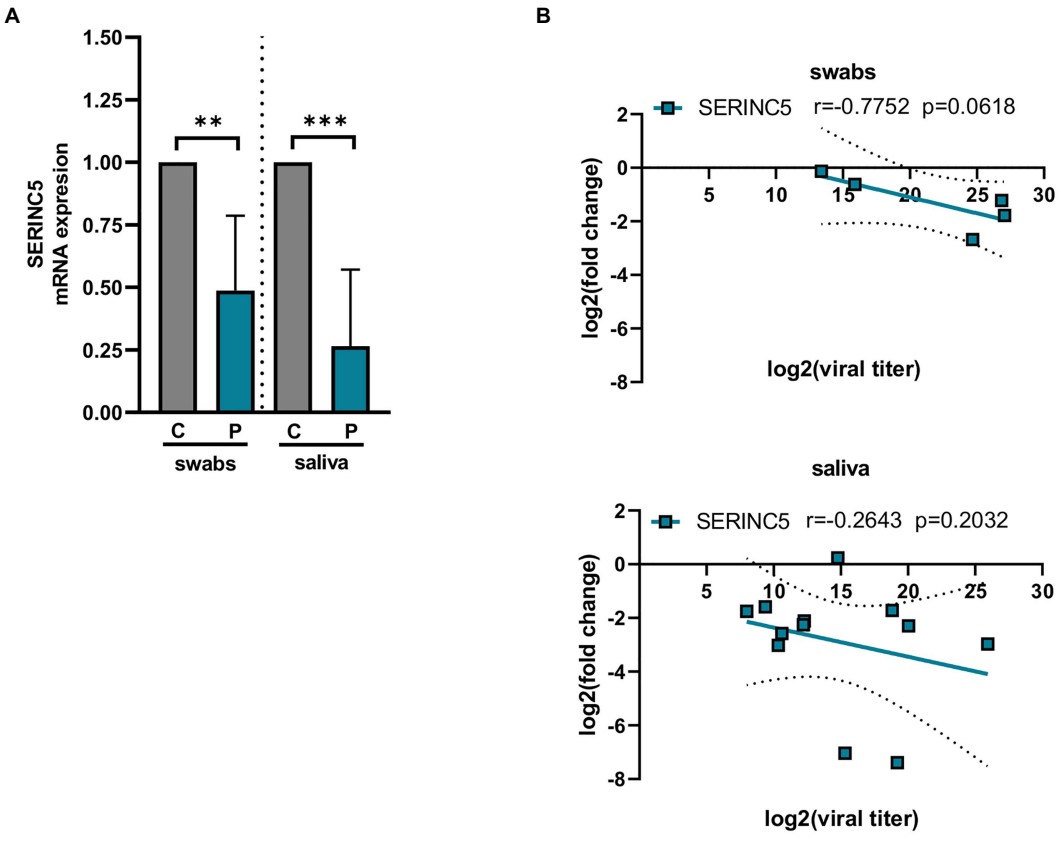

FIGURE 1
Analysis of the levels of SERINC5 mRNA in nasopharyngeal and saliva samples of COVID-19 patients. **(A)** RT-qPCR analysis of the expression of SERINC5 mRNA in nasopharyngeal (swabs) and saliva samples from COVID-19 patients (P) with respect to healthy patients (C). The control value represents the mean of all control samples. The ΔΔCt method was used for relative quantification using RPP30 mRNA as an endogenous control. Data are represented as log2 fold change with respect to control samples. **(B)** Correlation analysis between log2 fold changes obtained for SERINC5 mRNA and log2 viral titers in swabs (top) and saliva (bottom) samples. Viral titer was expressed as E mRNA copies/mL sample. Differences from control values were found to be statistically significant at *p<0.05, **p<0.01, and ***p<0.001.

10.3389/fmicb.2023.1066493

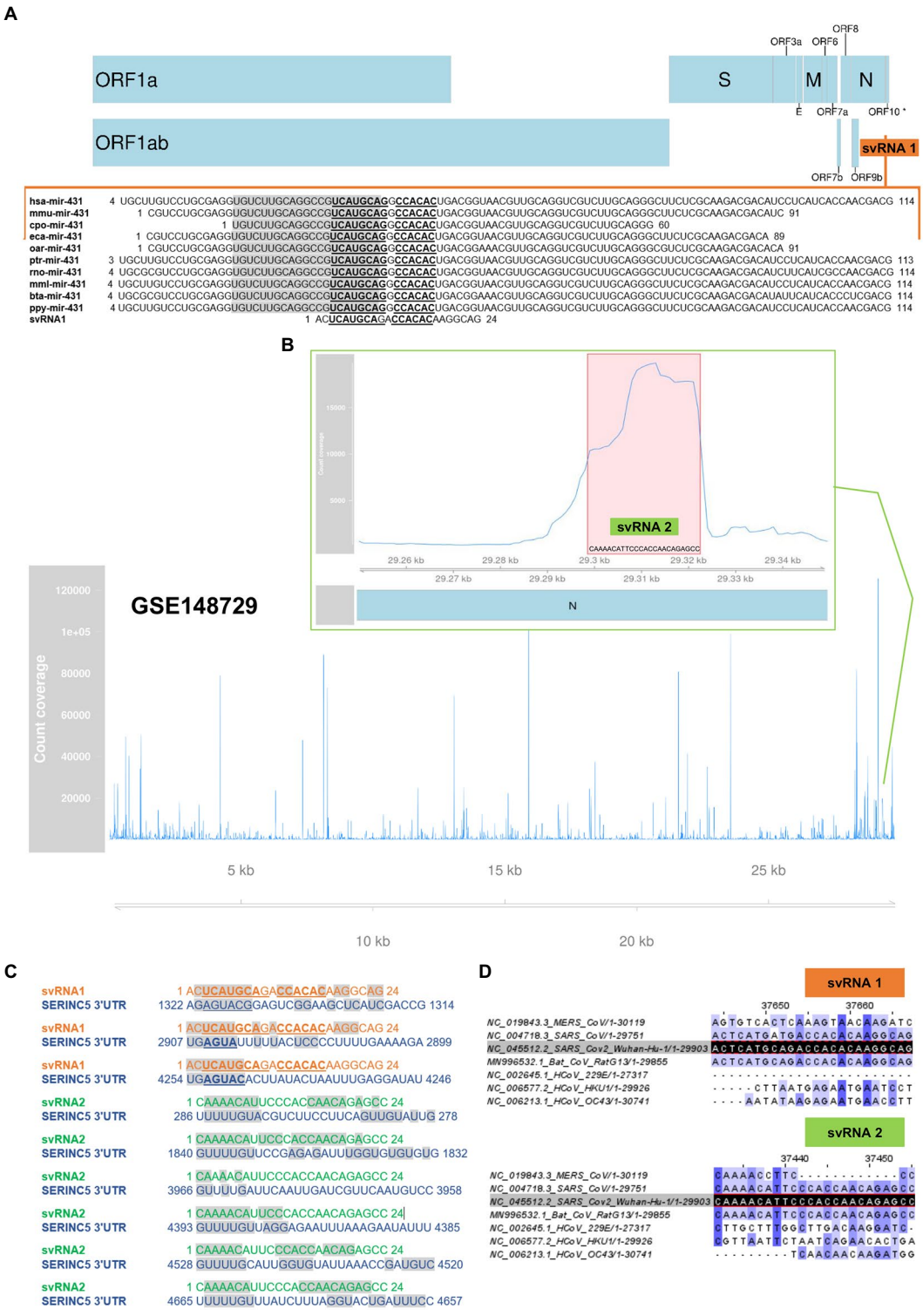

FIGURE 2
In silico prediction of SARS-CoV-2 svRNAs interacting with SERINC5 mRNA. **(A)** Identification of svRNA 1 using RNA Central Resources. Sequence and genomic location of svRNA 1 and alignment of svRNA 1 sequence with those of pre-miRNA-431 from different species are shown. The mature miRNA sequences are in grey shadow and the conserved nucleotides among species are in bold letters. (*) ORF10 has so far little experimental support as a protein-coding gene **(B)** Identification of svRNA 2 by reanalysis of GSE148729 dataset. Count coverage of small RNA sequences from SARS-CoV-2-infected Calu3 cells aligning with the SARS-CoV-2 genome is indicated. The top panel shows the region's count coverage containing the svRNA 2 at 24 hpi. The red shadow indicates the svRNA 2 sequence. **(C)** Predicted interaction of svRNAs 1 and 2 with the 3'UTR of SERINC5 mRNA according to the Diana MR-microT tool. Grey shadow indicates nucleotides involved in the interaction. **(D)** Alignment of SARS-CoV-2 genome-encoded svRNA 1 and 2 sequences (dark shadow) with the genomes of other coronaviruses: MERS-CoV, SARS-CoV, HCoV-229E, HCoV-HKU1, HCoV-OC43, and the SARS-like betacoronavirus Bat coronavirus RaTG13. A higher intensity of the blue shade denotes higher conservation.

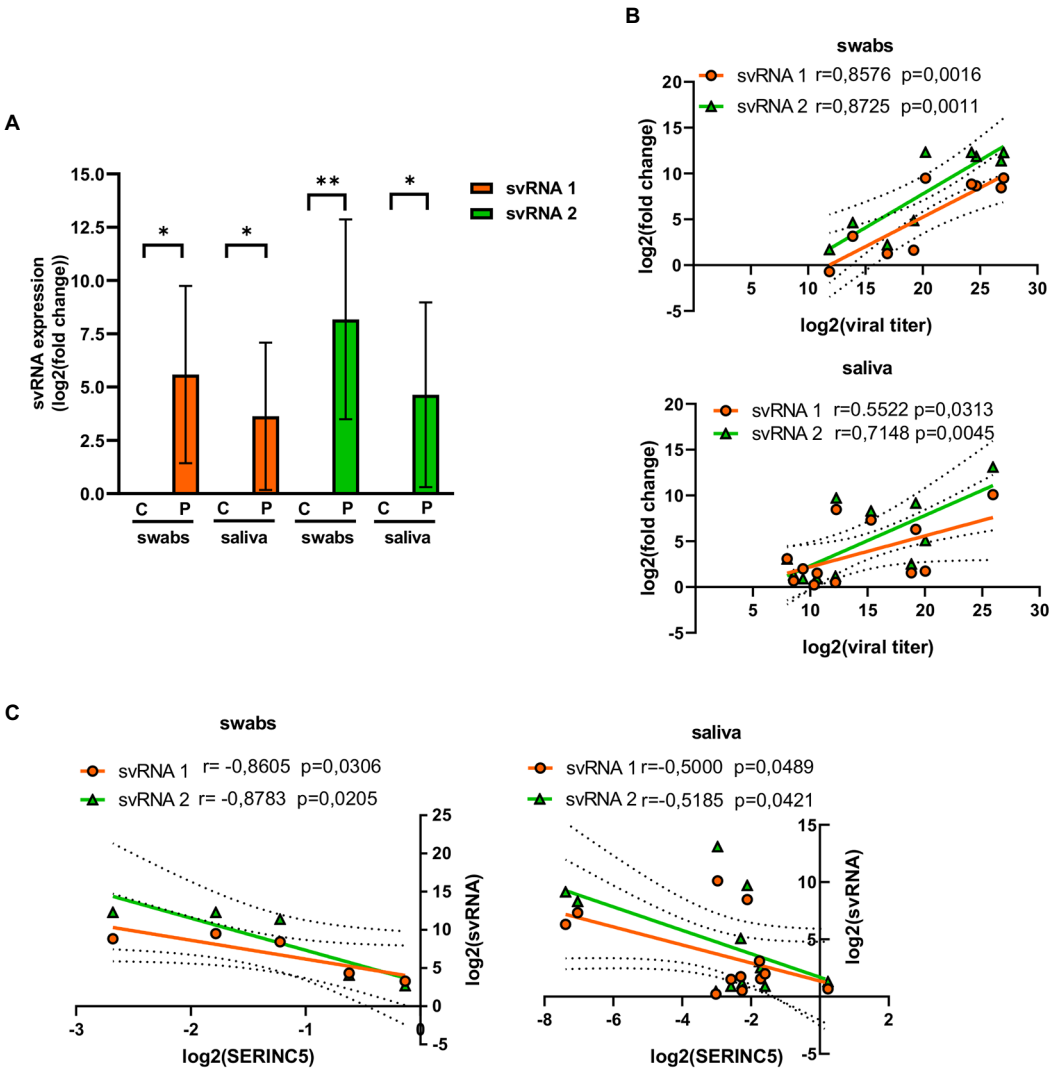

FIGURE 3
Analysis of the levels of svRNA 1 and 2 in nasopharyngeal and saliva samples of COVID-19 patients. **(A)** RT-qPCR analysis of the expression of svRNA 1 and svRNA 2 in nasopharyngeal (swabs) and saliva samples from COVID-19 patients (P) with respect to control samples (C). The control value represents the mean of all control samples. The ΔΔCt method was used for relative quantification with U6 snRNA as an endogenous control. Data are represented as log2 fold change with respect to control samples. **(B)** Correlation analysis between log2 fold changes obtained for svRNA 1 or svRNA 2 and log 2 viral titers in swabs (top) and saliva (bottom) samples. **(C)** Correlation analysis of log2 fold changes obtained for svRNA 1 or svRNA 2 and SERINC5 mRNA in swabs (left) and saliva (right) samples. Differences from control values were found to be statistically significant at *p<0.05, **p<0.01, and ***p<0.001.

sequence was conserved among several mammalian species, including humans, and showed a binding capacity to the 3'UTR region of SERINC5 mRNA according to the Diana MR-microT tool (Figure 2C). On the other hand, svRNA 2 was selected as one of the most expressed small RNAs from the reanalysis of a small RNA dataset deposited in GEO (GSE148729) that was generated from Calu3 cells infected with SARS-CoV-2 (Figure 2B; Supplementary Table S1). This 24 nt long svRNA mapped in the N gene (29,353 nt–29,376 nt) and its sequence also showed binding sites to the 3'UTR region of SERINC5 mRNA (Figure 2C). Both svRNA candidates were confirmed by the miRNA fold tool, which allows the prediction of microRNA hairpin structures using a genome sequence as Input (Supplementary Table S2). Moreover, the conservation of svRNA sequences among different classes of coronavirus was also analyzed, showing that svRNA 1 and 2 exhibited high conservation grades among coronaviruses SARS-CoV, SARS-CoV-2 and the SARS-like betacoronavirus Bat coronavirus RaTG13, known as the closest relative of SARS-CoV-2 (Figure 2D). Altogether, these *in silico* studies suggested the existence of two SARS-CoV-2 svRNAs predicted to interact with the 3'UTR region of SERINC5 mRNA.

To confirm the existence of svRNA 1 and svRNA 2 in COVID-19 patients, the presence of both svRNAs was analyzed in both nasopharyngeal and saliva samples by RT-qPCR, using specific TaqMan probes (Table 1). Both svRNAs were detected in both types of samples (Figure 3A). Although their levels among the samples were heterogeneous, they showed a significant correlation with the viral titer (Figure 3B). Interestingly, when we studied the correlation between svRNA 1 and 2 levels and SERINC5 mRNA levels, we found an inverse correlation that was significant for svRNA 1 and svRNA 2 in both sample types (Figure 3C).

Altogether, these data indicated that in SARS-CoV-2-infected patients, the level of SERINC5 mRNA was reduced and this reduction was inversely proportional to the viral titer and the level of svRNA 1 and svRNA 2.

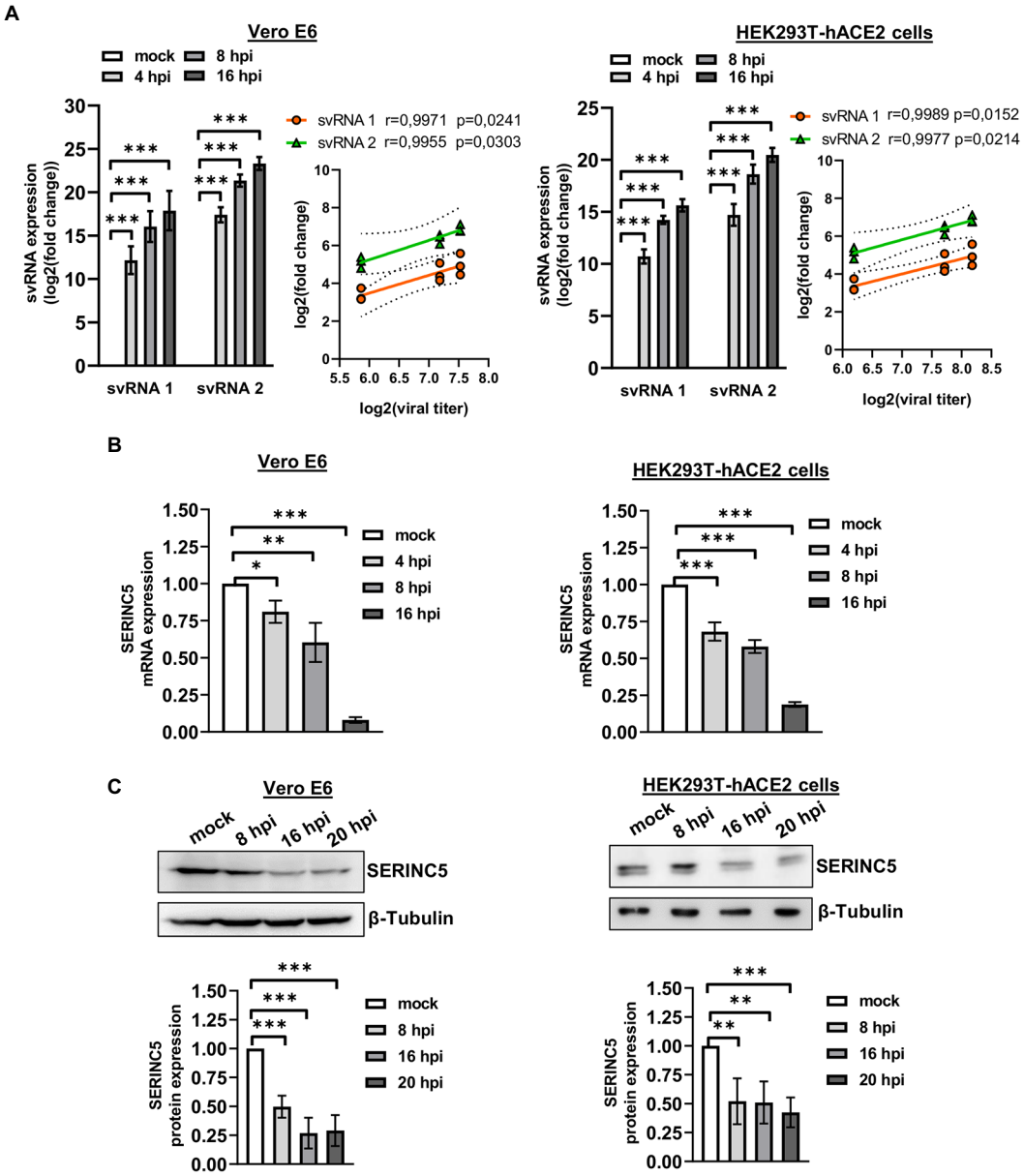

FIGURE 4
Analysis of the expression of svRNAs 1 and 2 and SERINC5 in Vero E6 and HEK293T-hACE2 infected cells. **(A)** RT-qPCR analysis of svRNAs 1 and 2 expression and correlation analysis between log2 fold changes obtained for svRNA 1 and svRNA 2 and log 2 viral titers in SARS-CoV-2-infected (MOI, 1 PFU/cell) Vero E6 (left panels) and HEK293T-hACE2 (right panels) cells at 4, 8, and 16 hpi. The ΔΔCt method was used for relative quantification, with U6 snRNA as an endogenous control. Data are represented as log2 fold change with respect to mock values and are the mean±SD of at least three independent experiments. Viral titer was expressed as E mRNA copies/mL sample. **(B)** RT-qPCR analysis of SERINC5 mRNA expression in SARS-CoV-2-infected (MOI, 1 PFU/cell) Vero E6 (left panel) and HEK293T-hACE2 (right panel) cells at 4, 8, and 16 hpi. The ΔΔCt method was used for relative quantification with RPP30 mRNA as an endogenous control. Data are represented in logarithmic scale as fold change with respect to mock values and are the mean±SD of at least three independent experiments. **(C)** Western blot analysis of SERINC5 protein in SARS-CoV-2-infected (MOI, 1 PFU/cell) Vero E6 (left panels) and HEK293T-hACE2 (right panels) cells at 8, 16, and 20hpi. Blots are representative of at least three independent experiments. The scatter plot shows the densitometric analysis of the protein normalized to β-tubulin and represented as fold change relative to mock. Differences from mock values were found to be statistically significant at *p<0.05, **p<0.01, and ***p<0.001.

3.2. Levels of SARS-CoV-2 svRNAs 1 and 2 are inversely correlated with the levels of SERINC5 in Vero E6 and HEK293T-hACE2 infected cells

After the identification of SARS-CoV-2 svRNAs in patient samples and demonstrating an inverse correlation with SERINC5 expression, we performed similar studies *in vitro* using the cell lines Vero E6 and HEK293T-hACE2 (Figure 4). To that end, Vero E6 and HEK293T-hACE2 cells were infected with SARS-CoV-2 with a MOI of 1 PFU/cell and at 4, 8, and 16 h post-infection (hpi) the expression of svRNAs 1 y 2 and SERINC5 mRNA was analyzed by RT-qPCR. Based on the RT-qPCR data, we found that both svRNAs progressively accumulated in both cell lines and this accumulation directly correlated with the viral titer (Figure 4A). Interestingly, when the levels of SERINC5 mRNA were analyzed, we detected a progressive reduction throughout the infection until extremely low values at 16 hpi in both cell lines (Figure 4B), which was inversely correlated with the virus titer. To confirm this reduction, the

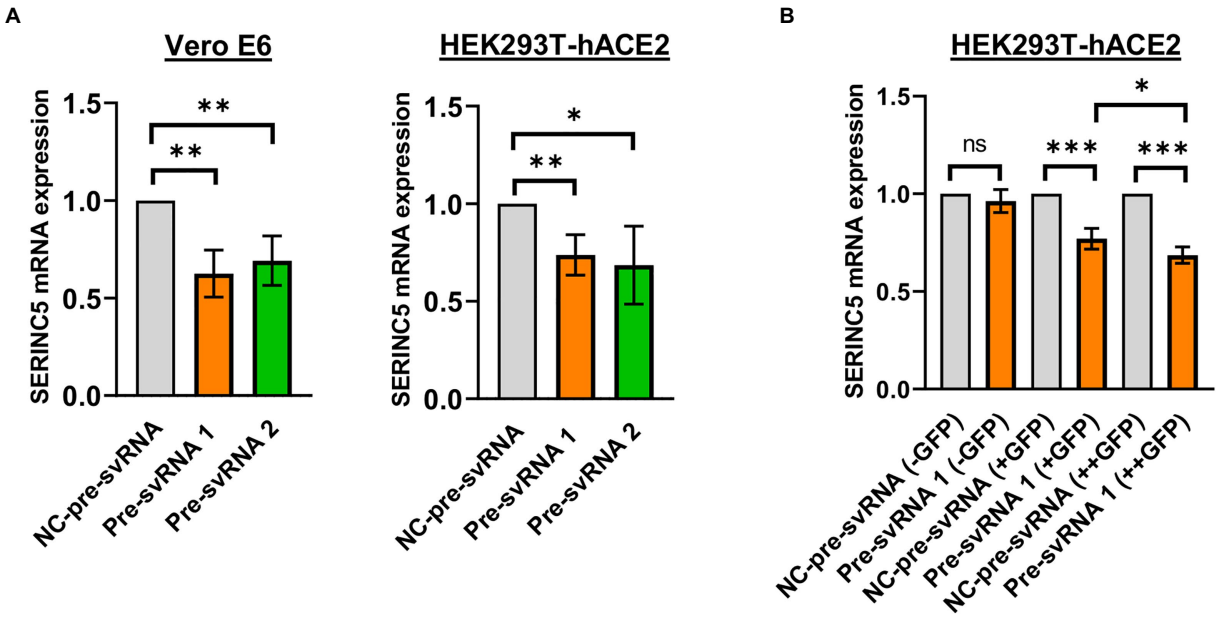

FIGURE 5
Analysis of the levels of SERINC5 mRNA in Vero E6 and HEK293T-hACE2 cells transfected with svRNAs 1 and 2 mimics. **(A)** RT-qPCR analysis of SERINC5 mRNA level in Vero E6 (left panel) and HEK293T-hACE2 (right panel) cells transfected with an oligonucleotide that mimics the precursor of svRNA 1 or 2 (Pre-svRNA 1 and 2, respectively) or an irrelevant precursor svRNA (NC-pre-svRNA) as a negative control. Data are represented as fold change with respect to values from control samples. **(B)** RT-qPCR analysis of SERINC5 mRNA level in HEK293T-hACE2 cells co-transfected with Pre-svRNA 1 and a GFP-expressing plasmid. The study was performed on these cells after sorting them into three populations, non-expressing (−GFP), intermediate expressing (+GFP), and highly expressing (++GFP) GFP cells. Data are represented as fold change with respect to values from negative control-transfected cells.

expression of SERINC5 at the protein level was also analyzed by western blot. A clear reduction in the levels of SERINC5 protein throughout the infection was detected, with their lowest values at 16 and 20 hpi in both cell lines (Figure 4C). These results indicated that the infection of SARS-CoV-2 reduces the level of SERINC5, that this reduction is inversely proportional to the levels of SARS-CoV-2 svRNAs 1 and 2, and that this effect is independent of the cell type and species.

3.3. svRNAs 1 and 2 can bind the 3′UTR of SERINC5 mRNA and reduce SERINC5 expression *in vitro*

Once the existence of svRNA 1 and 2 during SARS-CoV-2 infection was demonstrated and the levels of these svRNAs inversely correlated with the level of SERINC5, we explored the ability of these svRNAs to post-transcriptionally regulate endogenous SERINC5 expression. To that end, Vero E6 and HEK293T-hACE2 cells were transfected with svRNA 1 or svRNA 2 mimic molecules (Pre-svRNA 1 and 2) and the levels of SERINC5 mRNA were determined by RT-qPCR. As shown in Figure 5A, a clear reduction in SERINC5 mRNA levels was observed in both Vero E6 and HEK293T-hACE2 cells transfected with either of the two Pre-svRNAs, confirming that both svRNAs are responsible for the downregulation of SERINC5 observed during SARS-CoV-2 infection. Then, we analyzed whether the svRNAs effect was dose-dependent. To this end, we co-transfected HEK293T-hACE2 cells with a GFP-expressing plasmid and the svRNA 1 mimic, and then sorted the cells into three populations: non-expressing, moderately expressing, and highly expressing GFP. The analysis of these three populations showed that the expression of SERINC5 was inversely proportional to the expression of GFP, confirming that, at least for svRNA 1, the level of expression of this svRNA mimic within the cell influences the expression of SERINC5 in a dose-dependent way (Figure 5B).

Finally, we evaluated the ability of svRNAs 1 and 2 to bind to the 3′UTR of SERINC5 mRNA target using a luciferase reporter assay. To this end, we cloned a portion of the 3′UTR of SERINC5 mRNA downstream of the Firefly Luciferase reporter gene in the pMIR plasmid in direct (+) or reverse (−) direction [pMIR-Luc-SERINC5-3′UTR(+) and pMIR-Luc-SERINC5-3′UTR(−), respectively]. Then, we co-transfected each plasmid into Vero E6 cells together with the control plasmid expressing Renila Luciferase and the respective svRNA mimic or its negative control. As shown in Figure 6, co-transfection of the wild-type SERINC5 3′UTR reporter [pMIR-Luc-SERINC5-3′UTR(+)] with svRNAs 1 or 2 mimics reduced significantly the luciferase activity when compared with the mimic control transfected cells (Figure 6, left panel), whereas no effect was observed when the reporter carried the 3′UTR cloned in the reverse direction [pMIR-Luc-SERINC5-3′UTR(−)] (Figure 6, right panel). Altogether, these data indicate that svRNAs 1 and 2 function as a miRNA-like regulators of SERINC5, directly targeting the 3′UTR of the SERINC5 mRNA.

3.4. Treatment with antisense oligonucleotides against svRNA 1 and 2 recovers SERINC5 expression and reduces the levels of SARS-CoV-2 N and S viral proteins

To explore the biological function of svRNAs 1 and 2, we performed overexpression or silencing experiments. To that end,

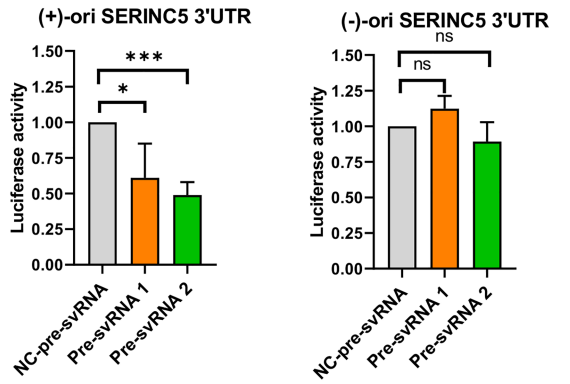

FIGURE 6
Study of the binding capacity of svRNA 1 and 2 to the 3'UTR of SERINC5 mRNA. Vero E6 cells were co-transfected with a negative control oligonucleotide (NC-pre-svRNA), the oligonucleotide mimic of svRNA 1 or 2 (pre-svRNA 1 and 2) together with the reporter constructs containing the Firefly Luciferase gene fused with the SERINC5-3'UTR in the direct (+) (left panel) or reverse (–) direction (right panel), and the Renilla Luciferase control vector. At 48h post-transfection the luciferase activity was analyzed and the data obtained were normalized to the levels of Renilla Luciferase (Control of transfection). Differences from control values were found to be statistically significant at *p<0.05, **p<0.01, and ***p<0.001.

Vero E6 cells were transfected with specific mimic (overexpression) or anti-svRNA (silencing) oligonucleotides (Table 1). At 36 h post-transfection, the cells were infected with SARS-CoV-2 at a MOI of 1 PFU/cell and at 20 hpi the levels of svRNAs, viral N and S proteins, and SERINC5 were analyzed. Previously, we confirmed the overexpression and silencing of svRNAs 1 and 2 by RT-qPCR. Levels of svRNA 1 and 2 were increased 4- and 2-fold, respectively, in pre-svRNA 1 or 2-transfected cells compared to cells transfected with a non-related mimic sequence [negative control (NC-Pre-svRNA)] (Figure 7A, left panel). Conversely, they were reduced by almost 75% in anti-svRNA 1 and 2-transfected cells compared to cells transfected with a non-related sequence inhibitor [negative control (NC) anti-miR] (Figure 7A, right panel). Interestingly, in cells where svRNA 1 had been silenced we also noted a moderate reduction of svRNA 2 level, suggesting that svRNA 1 biogenesis positively regulates the generation of svRNA 2. After that, we analyzed the effect of the mimic svRNAs and anti-svRNAs on virus replication by analyzing the expression of N and S proteins by western blot (Figure 7B). No significant differences were found in the levels of S and N proteins when cells were treated with mimic molecules. In contrast, when cells were treated with the anti-svRNAs a significant reduction in the levels of S and N proteins was detected, being more evident in the case of N protein (40% reduction; Figure 7B). In addition, we also analyzed the effect of the mimic svRNA and anti-svRNA molecules on virus production (24 hpi). No significant differences were detected between cells treated or untreated with the mimic molecules. In contrast, a very moderate reduction was observed in cells treated with anti-svRNA 1 (1.50 fold decrease) or 2 (1.75 fold decrease), which could be in concordance with the reduction observed in the levels of N and S proteins (Figure 7C). Although these differences are very low, they are statistically significant.

Finally, we explored by Western-blot whether the overexpression or silencing of SARS-CoV-2 svRNAs affected the levels of SERINC5 protein (Figure 7D). As expected, we observed that the treatment with either svRNA 1 or svRNA 2 mimics reduced SERINC5 expression while anti-svRNA 1 and 2 treatments achieved a moderate increase in SERINC5 levels compared to NC-transfected cells.

Altogether, these data confirm the regulation of SERINC5 by the SARS-CoV-2 svRNAs and indicate that anti-svRNA 1 and 2 have only a moderate effect on virus production, possibly by increasing the levels of SERINC5, the target of the viral svRNAs.

3.5. Anti-svRNAs treatment modifies the levels of MAVS in SARS-CoV-2 infected cells

A novel antiviral activity of SERINC5 has been recently described (Zeng et al., 2021). SERINC5 has been shown to translocate to the mitochondrial membrane after viral infection, where it associates with MAVS and promotes its oligomerization. Aggregated MAVS acts as a central hub for signal transduction, leading to changes in the expression of several genes involved in inflammation, apoptosis and cell cycle as part of the cellular response against viral infection (Zhang et al., 2020; Zeng et al., 2021). However, there are several viruses, including SARS-CoV-2, that are capable of controlling the MAVS cascade by establishing interactions between the elements of this cascade and several viral proteins. This strategy allows them to escape and over-activate the innate immune response during the course of infection (Fu et al., 2021; Fung et al., 2021; Han et al., 2021; Liu et al., 2021; Zotta et al., 2021; Li et al., 2022; Thorne et al., 2022; Zheng et al., 2022).

In a first approach, we evaluated the control of SERINC5 on the levels of endogenous MAVS protein in uninfected Vero E6 cells, by examining its levels in cells that overexpress SERINC5. We found that these cells exhibited a 5-fold increase of endogenous MAVS protein (Supplementary Figure S2). Furthermore, we observed, as described before (Zeng et al., 2021), that SERINC5 partially co-localized with mitochondria (Supplementary Figure S3) and with MAVS (Supplementary Figure S4) in Vero E6 cells.

Based on this regulation and considering that SARS-CoV-2 infection of Vero E6 and HEK293T-hACE2 cells triggers a decrease in SERINC5 protein levels, a reduction in MAVS protein levels would be expected under these conditions. To verify this, Vero E6 and HEK293T-hACE2 cells were infected with SARS-CoV-2 (MOI of 1 PFU/cell) and the expression of SERINC5 and MAVS was analyzed at 8, 16, and 20 hpi by Western blot. Surprisingly, in both cell types the levels of MAVS protein increased when those of SERINC5 decreased during viral infection (Figure 8A), suggesting the involvement of a SERINC5-independent and positive regulatory mechanism of MAVS. In this line, it has been reported that the viral protein nsp5 increases the stability of MAVS by promoting its SUMOylation and, consequently, increasing its levels (Li et al., 2021). Based on our findings, although both SERINC5-dependent and -independent mechanisms coexist during the infection, positive regulation of MAVS by the SERINC5-independent mechanism apparently has a greater effect on MAVS expression than the negative effect of reducing SERINC5 (SERINC5-dependent mechanism).

Then we explored whether anti-svRNA 1 and 2 treatments had any effect on MAVS expression. In particular, we examined the levels of MAVS protein after SARS-CoV-2 infection of Vero E6 cells transfected

10.3389/fmicb.2023.1066493

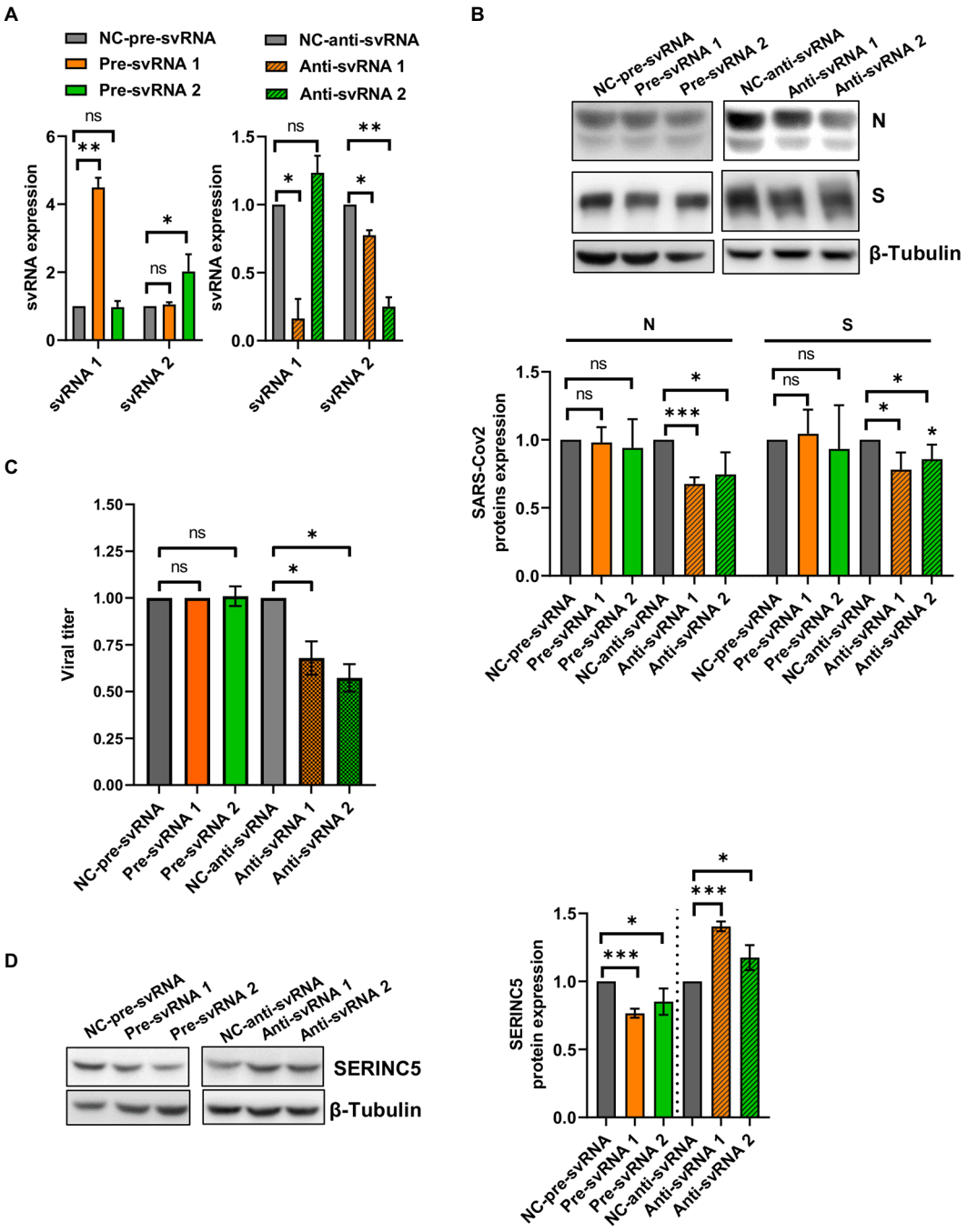

FIGURE 7
Expression levels of svRNAs 1 and 2, viral proteins and cellular SERINC5 in Vero E6 cells treated with mimic or anti-sense molecules for svRNA 1 and 2 and infected with SARS-CoV-2. Vero E6 cells were transfected with specific oligonucleotides mimic for svRNA 1 or svRNA 2 (Pre-svRNA 1 and 2), or specific antisense oligonucleotides for svRNA 1 or svRNA 2 (Anti-svRNA 1 and 2), and at 36h post-transfection the cells were infected with SARS-CoV-2 (1 PFU/cell). The levels of svRNAs, N, S and SERINC5 proteins were analyzed at 20hpi and the virus production in the cell supernatants at 24 hpi. **(A)** RT-qPCR analysis of svRNAs 1 and 2 levels in cells transfected with Pre-svRNA 1 and 2 (left panel), or Anti-svRNA 1 and 2 (right panel). Data are represented as fold change respect to the negative control (NC-pre-svRNA or NC-anti-svRNA)-transfected and SARS-CoV-2-infected cells (control samples). The control value represents the mean of all control samples. **(B)** Western blot analysis of viral N and S proteins. The scatter plot shows the densitometric analysis of N and S proteins normalized to β-tubulin and represented as fold change relative to negative control-transfected cells. The control value represents the mean of all control samples. **(C)** Virus production. The viral titers in the cell supernatants were determined at 24 hpi by plaque assay. Data are represented as fold change respect to the negative control (NC-pre-svRNA or NC-anti-svRNA)-transfected and SARS-CoV-2-infected cells (control samples). **(D)** Western blot analysis of SERINC5. The scatter plot shows the densitometric analysis of SERINC5 protein normalized to β-tubulin and represented as fold change relative to SARS-CoV-2-infected, negative control-transfected cells. The control value represents the mean of all control samples. Differences from negative control values were found to be statistically significant at *p<0.05, **p<0.01 and ***p<0.001.

with the anti-svRNA 1 or 2 and we compared them with those of NC-anti-svRNA-transfected cells. As shown in Figure 8B, the increase in MAVS levels after SARS-CoV-2 infection was significantly reinforced by the anti-svRNA treatments. This reflects an accumulative effect on MAVS by the SERINC5-dependent pathway when SERINC5 is recovered.

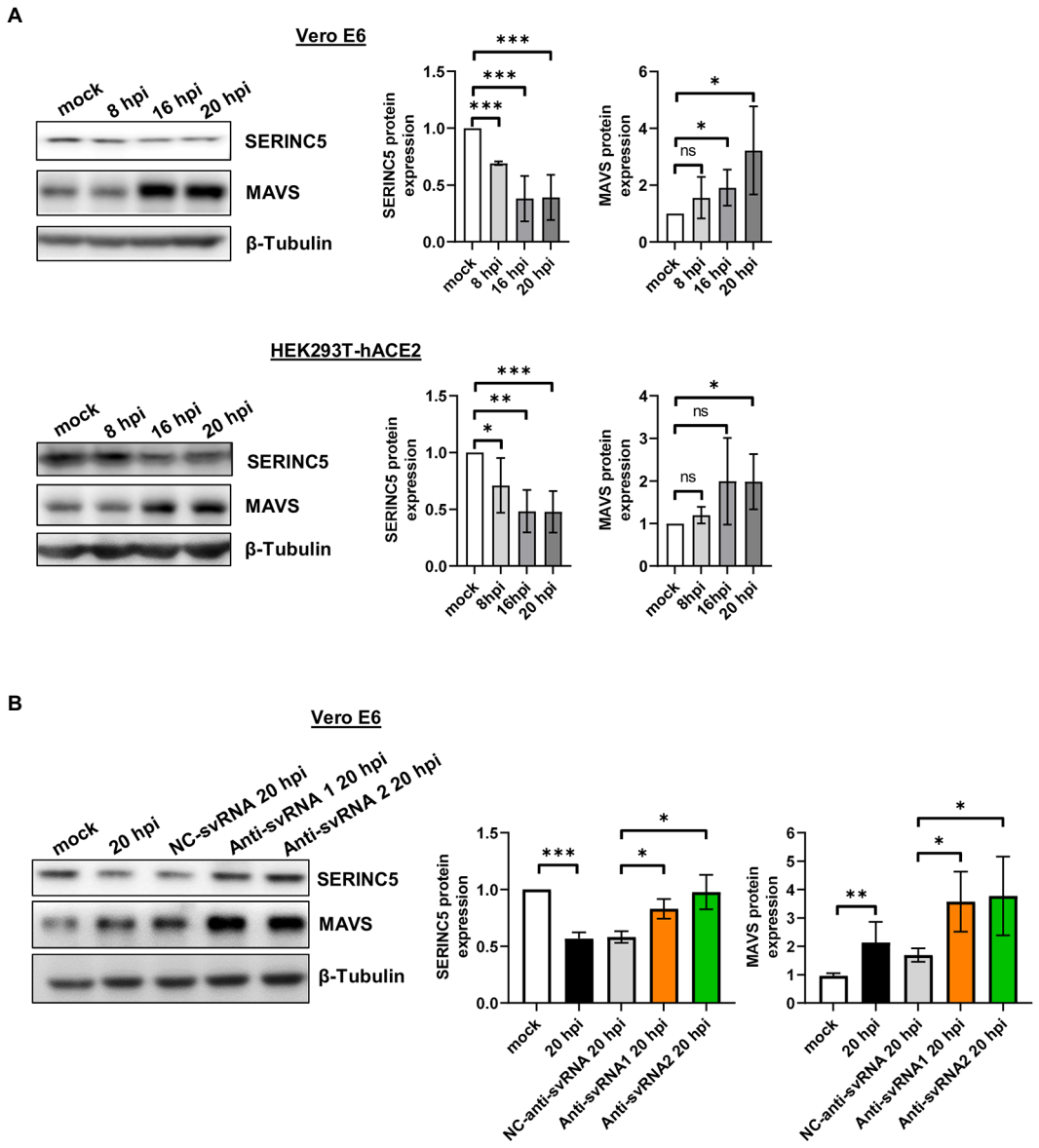

FIGURE 8
Analysis of MAVS expression during SARS-CoV-2 infection of Vero E6 and HEK293T-hACE2 cells treated or not with anti-sense molecules for svRNA 1 and 2. **(A)** Western blot analysis of SERINC5 and MAVS in Vero E6 (left) or HEK293T-hACE2 cells (right) mock-infected or infected with SARS-CoV-2 (MOI of 1 PFU/cell) at 8, 16, and 20hpi. The scatter plot shows the densitometric analysis of MAVS protein normalized to β-tubulin and represented as fold change relative to non-infected (mock) cells. **(B)** Western blot analysis of MAVS in Vero E6 cells mock-transfected or transfected with anti-svRNA 1, anti-svRNA 2, or NC-anti-svRNA for 36h and then infected with SARS-CoV-2 with a MOI of 1PFU/cell for 20h. The scatter plot shows the densitometric analysis of MAVS and SERINC5 proteins normalized to β-tubulin, represented as fold change relative to non-transfected mock-infected (mock) cells. Differences from control values were found to be statistically significant at *p<0.05, **p<0.01, and ***p<0.001.

3.6. Anti-svRNA 1 treatment lowers the induction of innate immune-related genes

SERINC5 has recently been considered as a key factor in the innate immune response (Firrito et al., 2018; Li et al., 2020; Zeng et al., 2021). Since we observed that the anti-svRNA treatment recovers the expression of SERINC5 in Vero E6 cells infected with SARS-CoV-2 (Figure 7D), we evaluate the expression of certain innate immune related genes under these conditions. In particular, we analyzed by RT-qPCR the mRNA levels of interferon β (IFNβ), an interferon-stimulated gene [interferon stimulated exonuclease gene 20 (ISG20)] and a chemokine [chemokine (C-C motif) ligand 20 (CCL20)] after the SARS-CoV-2 infection of VeroE6 cells previously transfected with anti-svRNA 1, the most efficient svRNA inhibitor recovering SERINC5 (Figure 7D), or with the negative control (NC) anti-svRNA The oligonucleotides used are described in Table 1. We found that SARS-CoV-2 infection induced the mRNA expression of IFNβ, ISG20, and CCL20 and that this induction was partially counteracted when the cells recover SERINC5 expression by treatment with anti-svRNA 1 (Figure 9). These data suggests that SERINC5 is a negative regulator of the innate immune response. To confirm this negative role of SERINC5, the expression of IFNβ, ISG20, and CCL20 was evaluate in VeroE6 cells over-expressing SERINC5 in comparison to control cells. We found that VeroE6 cells over-expressing SERINC5 showed reduced levels of IFNβ, ISG20, and CCL20 mRNAs when compared to control cells (Supplementary Figure S5).

Overall, our results suggest that recovery of SERINC5 by anti-svRNA treatment lowers the host innate response triggered by the virus.

4. Discussion

SERINC5 is an unconventional restriction and cell-associated innate immunity factor required to restrict the infectivity of certain viruses such as HIV-1, MLV, simian immunodeficiency virus (SIV), EIAV, vesicular stomatitis virus (VSV), and Zika virus (ZIKV) (Rosa et al., 2015; Chande et al., 2016; Heigele et al., 2016; Timilsina et al., 2020; Zeng et al., 2021). These studies have shown that when SERINC5 is over-expressed within the cell, it effectively suppresses the viral particle infectivity. It incorporates into nascent viral particles and compromises the formation of the virus-cell fusion pore for viral entry into new target cells. Recent work has demonstrated that SERINC5 operates in the same way during SARS-CoV-2 infection of Calu3 cells (Timilsina et al., 2022). SERINC5 inhibits SARS-CoV-2 infection by binding to SARS-CoV-2 S protein, thus blocking the fusion step during virus entry. Furthermore, two additional roles have recently been attributed to this protein. In the case of the Hepatitis B virus (HBV), SERINC5 inhibits virion secretion by interfering with the glycosylation of HBV envelope proteins (10). In contrast, in HIV-1, VSV, and ZIKV, SERINC5 inhibits virus infection by interacting with the outer mitochondrial membrane protein MAVS facilitating its aggregation and, consequently, triggering the activation of downstream signaling pathways (Zeng et al., 2021).

In many of the viruses described above, different mechanisms to counteract the antiviral effect of SERINC5 have been described. HIV-1, MLV, and EIA encode viral proteins to counteract SERINC5 activities (Usami et al., 2015; Ahi et al., 2016; Chande et al., 2016). In SARS-CoV-2 (Timilsina et al., 2022), it has been demonstrated that protein 7a counteracts SERINC5 by blocking SERINC5 incorporation in budding virions and by forming a complex with SERINC5 and SARS-CoV-2 S protein, hindering the activity of the SERINC5 molecules incorporated in budding virions. Interestingly, these studies with SARS-CoV-2 were performed in Calu3 cells at 2 and 6 hpi, a period in which authors did not observed changes in SERINC5 mRNA levels. A similar result was also obtained here at 4 hpi in the *in silico* study using GSE148729 data for that cell line, where no major changes in the mRNA level were detected (Supplementary Figure S1). However, we revealed in the *in silico* study that levels of SERINC5 mRNA started to decline from 12hpi. Moreover, we have confirmed that reduction of SERINC5 mRNA levels during SARS-Cov2 infection also occurred in VeroE6 and HEK293T-hACE2 cells (Figure 4), mainly at late stage, and in COVID-19 patient samples (Figure 1).Therefore, these data suggest that SARS-CoV-2 infection counteracts SERINC5 protein activity by protein 7a in the first stage and SERINC5 mRNA/protein levels at late stage by repression in the expression of this gene, highlighting the importance of the host factor in virus restriction.

Here, we demonstrated that levels of SERINC5 were reduced during the infection by SARS-CoV-2 both in cell cultures and in COVID-19 patients. Since no viral protein capable of repressing the expression of SERINC5 in host cells was identified, we hypothesized that svRNAs encoded in the SARS-CoV-2 genome could be responsible for this repression during infection. Through an *in silico* study, we identified two viral small RNAs (svRNAs 1 and 2) with predicted binding sites in the 3'UTR region of the SERINC5 gene. svRNA 1 is a 24 nt-long RNA, located in the intergenic sequence between N and ORF10 genes at the

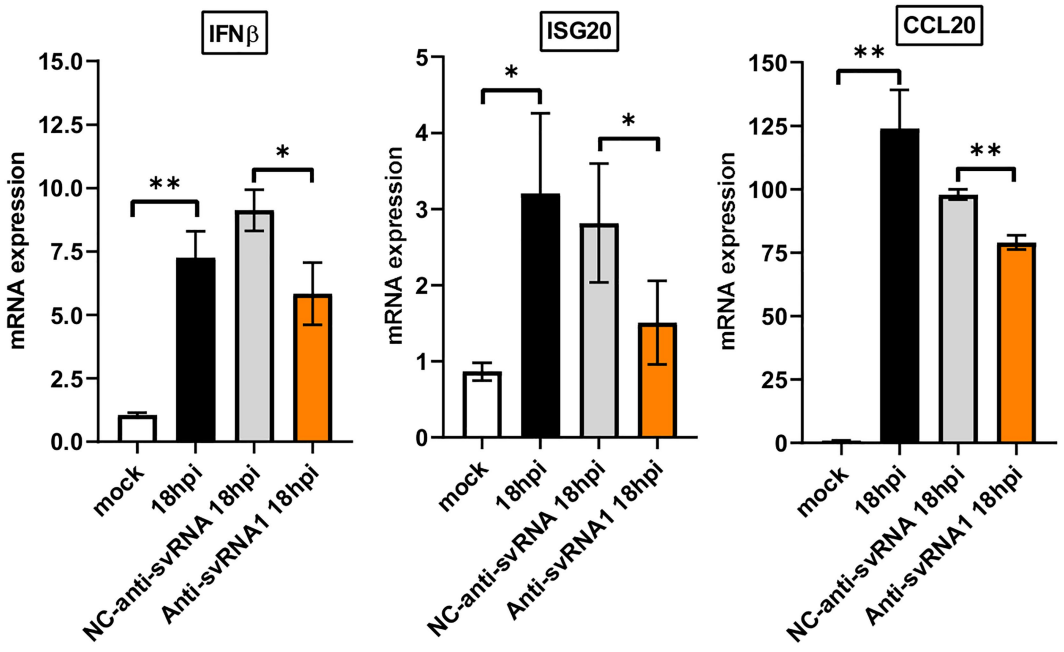

FIGURE 9
Expression levels of IFNβ, ISG20, and CCL20 mRNAs in Vero E6 cells treated or not with anti-sense molecules for svRNA 1. Vero E6 cells were mock transfected or transfected with either a specific antisense oligonucleotide for svRNA 1 (Anti-svRNA1) or an irrelevant oligonucleotide (NC-anti-svRNA) as a negative control. At 36h post-transfection the cells were infected with SARS-CoV-2 (1 PFU/cell) and the levels of IFNβ, ISG20 and CCL20 mRNAs were analyzed at 18 hpi by RT-qPCR. The ΔΔCt method was used for relative quantification with RPP30 mRNA as an endogenous control. Data are represented as fold change relative to non-transfected mock-infected (mock) cells and are the mean±SD of at least three independent experiments. Differences from control values were found to be statistically significant at *p<0.05 and **p<0.01.

3'end of the SARS-CoV-2 genome, that showed a sequence similar to a region of the cellular microRNA precursor pre-miRNA-431. Interestingly, this conservation is maintained among several mammalian species, including humans. As described for other viral miRNAs with high homologies to host miRNAs in seed sequence, this strategy could allow the virus to mislead host cells or take control of pre-existing regulatory pathways of host miRNAs (Gottwein et al., 2007; Skalsky et al., 2007; Kincaid et al., 2012). On the other hand, svRNA 2 is a 24 nt-long RNA located in the N gene. Both svRNAs exhibited high conservation grades among different coronaviruses and showed *in silico*-binding capacity to the 3'UTR of SERINC5 mRNA.

First, we proved the existence of both svRNAs in nasopharyngeal and saliva samples from COVID-19 patients and SARS-CoV-2-infected cell lines. In both cases, the level of SERINC5 mRNA was reduced and this reduction was inversely proportional to the viral titer and to the level of svRNA 1 and svRNA 2. This effect was independent of the cell type and species according to the experiments with Vero E6 and HEK293T-hACE2 cells. Moreover, we explored whether SARS-CoV-2 svRNA production was dependent on the cellular miRNA pathway by the analysis of svRNAs expression in HEK293T-hACE2 cells, in which Dicer and Argonaute 2 (Ago2) proteins were silenced (Supplementary Figure S6). We found that knocking down the expression of Dicer and Ago2 did not significantly affect the expression of either svRNA in infected cells (Supplementary Figure S6). These data are consistent with the previous results reported in SARS-CoV (Morales et al., 2017) and suggest that svRNAs are generated by alternative pathway/s.

Then we demonstrated that both svRNAs down-regulate the levels of endogenous SERINC5 mRNA and that this regulation occurs directly through the binding of the svRNAs to the 3'UTR. This regulation was demonstrated by overexpression and silencing experiments. Overexpression of svRNA 1 or svRNA 2 in cells infected with SARS-CoV-2, promoted the reduction of SERINC5 protein levels, and their partial silencing with antisense oligonucleotide against these svRNAs, partially recovers SERINC5 expression. In these conditions, SERINC5 recovery was accompanied by a reduction in the levels of SARS-CoV-2 N and S proteins and by a very moderate decrease in virus production. This slight impact on viral production is possible because the anti-svRNAs effect on viral proteins did not reach compromised levels in these cell lines in which virus infection and replication are very favorable.

Then we showed that SERINC5 controlled the levels of MAVS in uninfected Vero E6 cells, as SERINC5 overexpression (~2-fold) triggered a marked increase in MAVS protein (~5-fold). This phenomenon was previously observed in the HEK293T cells (Zeng et al., 2021). However, during infection in Vero E6 and HEK293T-hACE2 cells, even though SERINC5 levels were reduced by the action of svRNAs, the levels of MAVS did not decrease in parallel. On the contrary, they progressively increased, suggesting that a SERINC5-independent mechanism would be responsible for the augmentation in MAVS during infection. In this line, recent work has shown that the SARS-CoV-2 nsp5 protein increases the stability of MAVS by promoting its SUMOylation (Li et al., 2021). As MAVS increases during infection, the positive regulation by this SERINC5-independent mechanism apparently prevails over the negative effect of reducing SERINC5 (SERINC5-dependent mechanism). On the other hand, we have observed that the recovery of SERINC5 by anti-svRNA treatment during infection was accompanied by a greater increase in MAVS than that normally induced by SARS-CoV-2 infection alone, thus showing an accumulative effect. Altogether, these data suggest that SARS-CoV-2 expresses svRNAs to block host control over MAVS by reducing SERINC5 expression and favoring control of MAVS by viral proteins such as nsp5. Through treatment with anti-svRNAs, we were able to restore the SERINC5-dependent regulation of MAVS and reduce the levels of SARS-CoV-2 viral proteins N and S.

Different studies have described how SARS-CoV-2 proteins nsp5, N, M, ORF6, ORF9b, and ORF10 interfere with IFN production by targeting components of RIG1/MDA5-MAVS-IFN signaling pathways (Fu et al., 2021; Fung et al., 2021; Han et al., 2021; Liu et al., 2021; Zotta et al., 2021; Li et al., 2022; Thorne et al., 2022; Zheng et al., 2022). These findings suggest that SARS-CoV-2 proteins exert important control over the MAVS cascade. The interactions between those viral proteins and components of the MAVS cascade could condition the activity of MAVS in different pathways during the course of the infection, facilitating the evasion of the virus from the innate immune response and favoring its pathogenicity (Mattoo et al., 2022).

The innate immune system functions as the first line of defense against SARS-CoV-2; however, dysregulated innate immune responses can induce aberrant inflammation, cytokine storm, tissue damage, and acute respiratory distress syndrome in the host (Karki and Kanneganti, 2022). We found that anti-svRNA 1 treatment, which recovers SERINC5, lowers the induction of innate immune-related genes (IFNβ, ISG20 and CCL20; Figure 9; Supplementary Figure S5), indicating that SERINC5 acts as a negative regulator of these genes during SARS-CoV-2 infection. Overall, our data suggest that anti-svRNA treatment partially mitigates the innate immune response and promotes the reestablishment of basal levels of these immune signals. Although we still need further experiments to assess the therapeutic role of the use of antisense oligonucleotides against these svRNAs, our findings highlight potential therapeutic targets based on their action on key genes of the innate immune response.

Finally, considering that svRNAs 1 and 2 were easily detected in COVID-19 patient samples and that their levels correlated well with SARS-CoV-2 viral titer, svRNAs could be good candidate biomarkers in the diagnosis of the disease. A higher cohort of COVID-19 patient samples will allow testing of this possibility.

Data availability statement

The datasets presented in this study can be found in online repositories. The names of the repository/repositories and accession number(s) can be found in the article/Supplementary material.

Ethics statement

The studies involving human participants were reviewed and approved by Ethics Committee of Hospital Universitario de la Ribera (Valencia, Spain) and performed under the guidelines set forth by the Declaration of Helsinki. The patients/participants provided their written informed consent to participate in this study.

Author contributions

SM, EE, FA, and FI designed the study. SM, FA, M-PR, OC-R, and BP-B performed the experiments. BL constructed the Luciferase

reporter plasmids. RP-M, SR-G, and FG-G performed the in silico reanalysis of deposited sequencing data. OM-M and AC provided the samples of COVID-19 patients. SM, FA, and EE wrote the paper. All authors reviewed the manuscript.

Funding

This work has been supported by grant CSIC-COV19-106 (202020 E164) from the Spanish National Research Council (CSIC) to FA and FI, and grant from RTI2018-101291-B-I00 to EE from the Spanish Ministry of Science and Innovation.

Acknowledgments

The authors thank all patients for their contributions to the study. We also thank the staff at Hospital Universitario de la Ribera (Valencia, Spain) for collecting and providing the samples for the study.

Conflict of interest

The authors declare that the research was conducted in the absence of any commercial or financial relationships that could be construed as a potential conflict of interest.

Publisher's note

All claims expressed in this article are solely those of the authors and do not necessarily represent those of their affiliated organizations, or those of the publisher, the editors and the reviewers. Any product that may be evaluated in this article, or claim that may be made by its manufacturer, is not guaranteed or endorsed by the publisher.

Supplementary material

The Supplementary material for this article can be found online at: https://www.frontiersin.org/articles/10.3389/fmicb.2023.1066493/full#supplementary-material

References

Abedi, F., Rezaee, R., Hayes, A. W., Nasiripour, S., and Karimi, G. (2021). MicroRNAs and SARS-CoV-2 life cycle, pathogenesis, and mutations: biomarkers or therapeutic agents? *Cell Cycle* 20, 143–153. doi: 10.1080/15384101.2020.1867792

Ahi, Y. S., Zhang, S., Thappeta, Y., Denman, A., Feizpour, A., Gummuluru, S., et al. (2016). Functional interplay between murine leukemia virus Glycogag, SERINC5, and surface glycoprotein governs virus entry, with opposite effects on Gammaretroviral and ebolavirus glycoproteins. *MBio* 7:e01985. doi: 10.1128/mBio.01985-16

Becher, P., Avalos Ramirez, R., Orlich, M., Cedillo Rosales, S., König, M., Schweizer, M., et al. (2003). Genetic and antigenic characterization of novel pestivirus genotypes: implications for classification. *Virology* 311, 96–104. doi: 10.1016/S0042-6822(03)00192-2

Beitari, S., Ding, S., Pan, Q., Finzi, A., and Liang, C. (2017). Effect of Hiv-1 Env on SERINC5 antagonism. *J. Virol.* 91:e02214. doi: 10.1128/JVI.02214-16

Chande, A., Cuccurullo, E. C., Rosa, A., Ziglio, S., Carpenter, S., and Pizzato, M. (2016). S2 from equine infectious anemia virus is an infectivity factor which counteracts the retroviral inhibitors SERINC5 and SERINC3. *Proc. Natl. Acad. Sci. U. S. A.* 113, 13197–13202. doi: 10.1073/pnas.1612044113

Colomer-Lluch, M., Ruiz, A., Moris, A., and Prado, J. G. (2018). Restriction factors: from intrinsic viral restriction to shaping cellular immunity against Hiv-1. *Front. Immunol.* 9:2876. doi: 10.3389/fimmu.2018.02876

Coronaviridae Study Group of the International Committee on Taxonomy of Viruses (2020). The species severe acute respiratory syndrome-related coronavirus: classifying 2019-nCoV and naming it SARS-CoV-2. *Nat. Microbiol.* 5, 536–544. doi: 10.1038/s41564-020-0695-z

Firrito, C., Bertelli, C., Vanzo, T., Chande, A., and Pizzato, M. (2018). SERINC5 as a new restriction factor for human immunodeficiency virus and murine leukemia virus. *Ann. Rev. Virol.* 5, 323–340. doi: 10.1146/annurev-virology-092917-043308

Fu, Y. Z., Wang, S. Y., Zheng, Z. Q., Huang, Y., Li, W. W., Xu, Z. S., et al. (2021). SARS-CoV-2 membrane glycoprotein M antagonizes the Mavs-mediated innate antiviral response. *Cell. Mol. Immunol.* 18, 613–620. doi: 10.1038/s41423-020-00571-x

Fung, S. Y., Siu, K. L., Lin, H., Yeung, M. L., and Jin, D. Y. (2021). SARS-CoV-2 main protease suppresses type I interferon production by preventing nuclear translocation of phosphorylated Irf3. *Int. J. Biol. Sci.* 17, 1547–1554. doi: 10.7150/ijbs.59943

Ghimire, D., Rai, M., and Gaur, R. (2018). Novel host restriction factors implicated in Hiv-1 replication. *J. Gen. Virol.* 99, 435–446. doi: 10.1099/jgv.0.001026

Gottwein, E., Mukherjee, N., Sachse, C., Frenzel, C., Majoros, W. H., Chi, J. T., et al. (2007). A viral microRNA functions as an orthologue of cellular miR-155. *Nature* 450, 1096–1099. doi: 10.1038/nature05992

Goujon, C., Moncorgé, O., Bauby, H., Doyle, T., Ward, C. C., Schaller, T., et al. (2013). Human Mx2 is an interferon-induced post-entry inhibitor of Hiv-1 infection. *Nature* 502, 559–562. doi: 10.1038/nature12542

Grehl, C., Schultheiß, C., Hoffmann, K., Binder, M., Altmann, T., Grosse, I., et al. (2021). Detection of SARS-CoV-2 derived small RNAs and changes in circulating small RNAs associated with Covid-19. *Viruses* 13:1593. doi: 10.3390/v13081593

Han, L., Zhuang, M. W., Deng, J., Zheng, Y., Zhang, J., Nan, M. L., et al. (2021). SARS-CoV-2 Orf9b antagonizes type I and iii interferons by targeting multiple components of the rig-I/Mda-5-Mavs, Tlr3-Trif, and cgas-sting signaling pathways. *J. Med. Virol.* 93, 5376–5389. doi: 10.1002/jmv.27050

Hartenian, E., Nandakumar, D., Lari, A., Ly, M., Tucker, J. M., and Glaunsinger, B. A. (2020). The molecular virology of coronaviruses. *J. Biol. Chem.* 295, 12910–12934. doi: 10.1074/jbc.REV120.013930

Heigele, A., Kmiec, D., Regensburger, K., Langer, S., Peiffer, L., Stürzel, C. M., et al. (2016). The potency of Nef-mediated SERINC5 antagonism correlates with the prevalence of primate lentiviruses in the wild. *Cell Host Microbe* 20, 381–391. doi: 10.1016/j.chom.2016.08.004

Inuzuka, M., Hayakawa, M., and Ingi, T. (2005). SERINC, an activity-regulated protein family, incorporates serine into membrane lipid synthesis. *J. Biol. Chem.* 280, 35776–35783. doi: 10.1074/jbc.M505712200

Kane, M., Yadav, S. S., Bitzegeio, J., Kutluay, S. B., Zang, T., Wilson, S. J., et al. (2013). Mx2 is an interferon-induced inhibitor of HIV-1 infection. *Nature* 502, 563–566. doi: 10.1038/nature12653

Karki, R. P., and Kanneganti, T. D. (2022). Innate immunity, cytokine storm, and inflammatory cell death in COVID-19. *J Transl Med.* 22, 542. doi: 10.1186/s12967-022-03767-z

Kincaid, R. P., Burke, J. M., and Sullivan, C. S. (2012). RNA virus microRNA that mimics a B-cell oncomiR. *Proc. Natl. Acad. Sci. U. S. A.* 109, 3077–3082. doi: 10.1073/pnas.1116107109

Kincaid, R. P., and Sullivan, C. S. (2012). Virus-encoded microRNAs: an overview and a look to the future. *PLoS Pathog.* 8:e1003018. doi: 10.1371/journal.ppat.1003018

Li, X., Hou, P., Ma, W., Wang, X., Wang, H., Yu, Z., et al. (2022). SARS-CoV-2 Orf10 suppresses the antiviral innate immune response by degrading Mavs through mitophagy. *Cell. Mol. Immunol.* 19, 67–78. doi: 10.1038/s41423-021-00807-4

Li, W., Qiao, J., You, Q., Zong, S., Peng, Q., Liu, Y., et al. (2021). SARS-CoV-2 Nsp5 activates Nf-κB pathway by upregulating Sumoylation of Mavs. *Front. Immunol.* 12:750969. doi: 10.3389/fimmu.2021.750969

Li, W., Zhang, Z., Zhang, L., Li, H., Fan, S., Zhu, E., et al. (2020). Antiviral role of serine incorporator 5 (SERINC5) proteins in classical swine fever virus infection. *Front. Microbiol.* 11:580233. doi: 10.3389/fmicb.2020.580233

Liu, Y., Qin, C., Rao, Y., Ngo, C., Feng, J. J., Zhao, J., et al. (2021). SARS-CoV-2 Nsp5 demonstrates two distinct mechanisms targeting rig-I and Mavs to evade the innate immune response. *MBio* 12:e0233521. doi: 10.1128/mBio.02335-21

Liu, Y., Wang, H., Zhang, J., Yang, J., Bai, L., Zheng, B., et al. (2020). SERINC5 inhibits the secretion of complete and genome-free hepatitis B Virions through interfering with the glycosylation of the Hbv envelope. *Front. Microbiol.* 11:697. doi: 10.3389/fmicb.2020.00697

Matheson, N. J., Sumner, J., Wals, K., Rapiteanu, R., Weekes, M. P., Vigan, R., et al. (2015). Cell surface proteomic map of Hiv infection reveals antagonism of amino acid metabolism by Vpu and Nef. *Cell Host Microbe* 18, 409–423. doi: 10.1016/j.chom.2015.09.003

Mattoo, S. U., Kim, S. J., Ahn, D. G., and Myoung, J. (2022). Escape and over-activation of innate immune responses by SARS-CoV-2: two faces of a coin. *Viruses* 14:530. doi: 10.3390/v14030530

Mishra, R., Kumar, A., Ingle, H., and Kumar, H. (2019). The interplay between viral-derived miRNAs and host immunity during infection. *Front. Immunol.* 10:3079. doi: 10.3389/fimmu.2019.03079

Mittal, A., Manjunath, K., Ranjan, R. K., Kaushik, S., Kumar, S., and Verma, V. (2020). Covid-19 pandemic: insights into structure, function, and hace2 receptor recognition by SARS-CoV-2. *PLoS Pathog.* 16:e1008762. doi: 10.1371/journal.ppat.1008762

Morales, L., Oliveros, J. C., Fernandez-Delgado, R., Tenoever, B. R., Enjuanes, L., and Sola, I. (2017). SARS-CoV-encoded small Rnas contribute to infection-associated lung pathology. *Cell Host Microbe* 21, 344–355. doi: 10.1016/j.chom.2017.01.015

Nanbo, A., Furuyama, W., and Lin, Z. (2021). RNA virus-encoded miRNAs: current insights and future challenges. *Front. Microbiol.* 12:679210. doi: 10.3389/fmicb.2021.679210

Pawlica, P., Yario, T. A., White, S., Wang, J., Moss, W. N., Hui, P., et al. (2021). SARS-CoV-2 expresses a microRNA-like small Rna able to selectively repress host genes. *Proc. Natl. Acad. Sci. U. S. A.* 118:e2116668118. doi: 10.1073/pnas.2116668118

Redd, W. D., Zhou, J. C., Hathorn, K. E., Mccarty, T. R., Bazarbashi, A. N., Thompson, C. C., et al. (2020). Prevalence and characteristics of gastrointestinal symptoms in patients with severe acute respiratory syndrome coronavirus 2 infection in the United States: A multicenter cohort study. *Gastroenterology* 159, 765–767.e2. doi: 10.1053/j.gastro.2020.04.045

Rosa, A., Chande, A., Ziglio, S., De Sanctis, V., Bertorelli, R., Goh, S. L., et al. (2015). HIV-1 Nef promotes infection by excluding SERINC5 from virion incorporation. *Nature* 526, 212–217. doi: 10.1038/nature15399

Shi, J., Sun, J., Wang, B., Wu, M., Zhang, J., Duan, Z., et al. (2014). Novel microRNA-like viral small regulatory RNAs arising during human hepatitis A virus infection. *FASEB J.* 28, 4381–4393. doi: 10.1096/fj.14-253534

Simon, V., Bloch, N., and Landau, N. R. (2015). Intrinsic host restrictions to HIV-1 and mechanisms of viral escape. *Nat. Immunol.* 16, 546–553. doi: 10.1038/ni.3156

Singh, M., Chazal, M., Quarato, P., Bourdon, L., Malabat, C., Vallet, T., et al. (2022). A virus-derived microRNA targets immune response genes during SARS-CoV-2 infection. *EMBO Rep.* 23:e54341. doi: 10.15252/embr.202154341

Skalsky, R. L., and Cullen, B. R. (2010). Viruses, microRNAs, and host interactions. *Annu. Rev. Microbiol.* 64, 123–141. doi: 10.1146/annurev.micro.112408.134243

Skalsky, R. L., Samols, M. A., Plaisance, K. B., Boss, I. W., Riva, A., Lopez, M. C., et al. (2007). Kaposi's sarcoma-associated herpesvirus encodes an ortholog of miR-155. *J. Virol.* 81, 12836–12845. doi: 10.1128/JVI.01804-07

Thorne, L. G., Bouhaddou, M., Reuschl, A. K., Zuliani-Alvarez, L., Polacco, B., Pelin, A., et al. (2022). Evolution of enhanced innate immune evasion by SARS-CoV-2. *Nature* 602, 487–495. doi: 10.1038/s41586-021-04352-y

Timilsina, U., Umthong, S., Ivey, E. B., Waxman, B., and Stavrou, S. (2022). SARS-CoV-2 Orf7a potently inhibits the antiviral effect of the host factor SERINC5. *Nat. Commun.* 13:2935. doi: 10.1038/s41467-022-30609-9

Timilsina, U., Umthong, S., Lynch, B., Stablewski, A., and Stavrou, S. (2020). SERINC5 potently restricts retrovirus infection. *mBio* 11:e00588. doi: 10.1128/mBio.00588-20

Trautz, B., Wiedemann, H., Lüchtenborg, C., Pierini, V., Kranich, J., Glass, B., et al. (2017). The host-cell restriction factor SERINC5 restricts HIV-1 infectivity without altering the lipid composition and organization of viral particles. *J. Biol. Chem.* 292, 13702–13713. doi: 10.1074/jbc.M117.797332

Usami, Y., Wu, Y., and Göttlinger, H. G. (2015). SERINC3 and SERINC5 restrict Hiv-1 infectivity and are counteracted by Nef. *Nature* 526, 218–223. doi: 10.1038/nature15400

Varble, A., and Ten Oever, B. R. (2011). Implications of RNA virus-produced miRNAs. *RNA Biol.* 8, 190–194. doi: 10.4161/RNA.8.2.13983

Wu, F., Zhao, S., Yu, B., Chen, Y. M., Wang, W., Song, Z. G., et al. (2020). A new coronavirus associated with human respiratory disease in China. *Nature* 579, 265–269. doi: 10.1038/s41586-020-2008-3

Yang, Y., Xiao, Z., Ye, K., He, X., Sun, B., Qin, Z., et al. (2020). SARS-CoV-2: characteristics and current advances in research. *Virol. J.* 17:117. doi: 10.1186/s12985-020-01369-z

Zeng, C., Waheed, A. A., Li, T., Yu, J., Zheng, Y. M., Yount, J. S., et al. (2021). Serinc proteins potentiate antiviral type I IFN production and proinflammatory signaling pathways. *Sci. Signal.* 14:eabc7611. doi: 10.1126/scisignal.abc7611

Zhang, W., Gong, J., Yang, H., Wan, L., Peng, Y., Wang, X., et al. (2020). The mitochondrial protein MAVS stabilizes p53 to suppress tumorigenesis. *Cell Rep.* 30, 725–738.e4. doi: 10.1016/j.celrep.2019.12.051

Zheng, Y., Deng, J., Han, L., Zhuang, M. W., Xu, Y., Zhang, J., et al. (2022). SARS-CoV-2 NSP5 and N protein counteract the RIG-I signaling pathway by suppressing the formation of stress granules. *Signal Transduct. Target. Ther.* 7:22. doi: 10.1038/s41392-022-00878-3

Zhu, N., Zhang, D., Wang, W., Li, X., Yang, B., Song, J., et al. (2020). A novel coronavirus from patients with pneumonia in China, 2019. *N. Engl. J. Med.* 382, 727–733. doi: 10.1056/NEJMoa2001017

Zotta, A., Hooftman, A., and O'neill, L. A. J. (2021). SARS-CoV-2 targets MAVS for immune evasion. *Nat. Cell Biol.* 23, 682–683. doi: 10.1038/s41556-021-00712-y

Frontiers in Microbiology

Explores the habitable world and the potential of microbial life

The largest and most cited microbiology journal which advances our understanding of the role microbes play in addressing global challenges such as healthcare, food security, and climate change.

Discover the latest Research Topics

See more →

Frontiers

Avenue du Tribunal-Fédéral 34
1005 Lausanne, Switzerland
frontiersin.org

Contact us

+41 (0)21 510 17 00
frontiersin.org/about/contact